New Concepts, Catalysts, and Methods for Enantioselective Synthesis of C-B and C-C Bonds

Author: Suttipol Radomkit

NEW CONCEPTS, CATALYSTS, AND METHODS FOR ENANTIOSELECTIVE SYNTHESIS OF C–B AND C–C BONDS

SUTTIPOL RADOMKIT

A dissertation

submitted to the department of chemistry

in partial fulfillment

of the requirements for the degree of

Doctor of Philosophy

Boston College
Morrissey College of Arts and Sciences
Graduate School

December 2016

NEW CONCEPTS, CATALYSTS, AND METHODS FOR ENANTIOSELECTIVE SYNTHESIS OF C–B AND C–C BONDS

Suttipol Radomkit

Dissertation advisor: Prof. Amir H. Hoveyda

Abstract

Chapter 1. Part A: *N*-Heterocyclic Carbenes Catalyzed Enantioselective Boryl Conjugate Additions to α,β-Unsaturated Ketones, Esters, Weinreb Amides and Aldehydes. The first broadly applicable enantioselective boryl conjugate addition reactions to a variety of α,β-unsaturated carbonyls are reported. Transformations are promoted by 5.0 mol % of a chiral Lewis basic *N*-heterocyclic carbene. The distinctive feature of the reactions in chemoselectivity of the method compared to the Cu-catalyzed variants has been illustrated.

Part B: Enantioselective Synthesis of Boron-Substituted Quaternary Carbon Stereogenic Centers through *N*-Heterocyclic Carbenes Catalyzed Boryl Conjugate Additions to Cyclic and Acyclic Enones The first examples of Lewis base catalyzed enantioselective boryl conjugate additions that afford products containing boron-substituted quaternary carbon stereogenic centers are presented. The carbon–boron bond forming reactions are promoted by 1.0–5.0 mol % of a chiral *N*–hererocyclic carbene. Cyclic or linear α,β–unsaturated ketones can be used as suitable substrates and the desired products are obtained in 63–95% yield and 91:9 to >99:1 enantiomeric ratio. The utility of the Lewis base-catalyzed approach is demonstrated in the context of an enantioselective formal synthesis of antifungal natural product crassinervic acid.

Chapter 2. Enantioselectivity Fluctuations in Phosphine–Cu-Catalyzed Enantioselective Boron-Allyl Addition to Aryl-Substituted Olefins. Catalytic enantioselective multicomponent processes involving $B_2(pin)_2$, aryl or heteroaryl monosubstituted olefins, and allylic phosphates or carbonates are disclosed. Transformations promoted by a chiral Cu–phosphine complex afford products that contain a primary C–B(pin) bond and an allyl-substituted tertiary carbon stereogenic center in up to 84% yield and 98:2 enantiomeric ratio. The utility of the approach is showcased in the enantioselective formal synthesis of biologically active heliespirones A and C. Based on mechanistic and computational studies, we show that enantioselectivities variations can depend on electronic and/or steric factors of the alkene substrate and the allyl electrophile as well as their concentration. In most cases, selectivity loss can be minimized and that the resulting insights are also applicable to reactions involving Cu–H species.

Chapter 3. Synthesis of Vicinal Diboronate Compounds through Practical Phosphine–Copper Catalyzed Three-Component Processes. The phosphine–Cu-catalyzed multicomponent processes have been developed for a practical and direct synthesis of vicinal diboronate compounds. Reactions of alkenyl–boronates, allylic phosphates, and diboron reagents are promoted by 2.5–10 mol % of a Cy_3P–Cu complex affording a wide range of desirable vicinal diboronate products. The ability for easy access to either regioisomers of the products with a C–B(pin) and an adjacent C–B(dan) bond that can be site-selectively functionalized is a noteworthy feature of the method.

Table of Contents

Chapter 1

Part A: *N*-Heterocyclic Carbenes Catalyzed Enantioselective Boryl Conjugate Additions to α,β-Unsaturated Ketones, Esters, Weinreb Amides and Aldehydes

1A.1. Introduction

Organoboron compounds are versatile intermediates in organic synthesis.[1] Development of catalytic methods to efficiently and selectively access these entities are thus of considerable interest especially in the pharmaceutical industry; for example, the antidepressant Prozac® (fluoxetine)[2] and the cholesterol-lowering drug Lipitor® (atorvastatin).[3] In addition, Velcade® (bortezomib)[4] and Kerydin® (tavaborole)[5] are examples of boron-containing pharmaceuticals approved by FDA for treatment of people with multiple myeloma (a cancer of the plasma cells) and onychomycosis of the toenails (a fungal infection), respectively.

One important approach to obtain boron-containing compounds is catalytic enantioselective boryl conjugate additions (BCAs) to α,β-unsaturated carbonyls. The product of such method contains a boron-substituted carbon stereogenic center at the β-

(1) For representative reviews on organoboron chemistry, see: (a) Lappert, M. F. *Chem. Rev.* **1956**, *56*, 959–1064. (b) Thomas, S. E. *Organic Synthesis: The Roles of Boron and Silicon* (*Oxford Chemistry*

(2) Robertson, D. W.; Krushinski J. H.; Fuller R. W.; Leander J. D. *J. Med. Chem.* **1988**, *31*, 1412–1417.

(3) Roth, B. D. *Progress in Medicinal Chemistry* **2002**, *40*, 1–22.

(4) Curran, M. P.; McKeage, K. *Drugs* **2009**, *69*, 859–888.

(5) Elewski, B. E.; Aly, R.; Baldwin, S. L.; González Soto, R. F.; Rich, P.; Weisfeld, M.; Wiltz, H.; Zane, L. T.; Pollak, R. *J. Am. Acad. Dermatol.* **2015**, *73*, 62–69.

position of the carbonyl group. The corresponding C–B bond can be readily converted into C–O[6], C–N[7], C–C[8] as well as C–F bond.[9] Catalytic BCAs have only been reported with a catalyst derived from a transition-metal complex until our report in 2009, in which the reaction is catalyzed by a *N*-heterocyclic carbene (NHC).[10] This method not only offers complementary reactivities and selectivities to the metal-catalyzed variants, but proceeds through a different pathway that relates to other Lewis base-catalyzed transformations.

In this chapter, development of Lewis base promoted BCAs will be outlined including our disclosures on enantioselective BCAs catalyzed by a chiral NHC to access products containing B-substituted tertiary (Part A) and quaternary (Part B) carbon stereogenic centers.

1A.2. Background

1A.2.1. Initial Evidence of B–B Bonds Activation by a Lewis Base

Activation of B–B bond by a Lewis base has been shown in the reaction of NHC- or phosphine-Cu-alkoxide with bis(pinacolato)diboron [$B_2(pin)_2$] affording the corresponding Cu–B(pin) complex **1.3** (Scheme 1.1).[11] The oxygen of the copper alkoxide complex interacts with one of the boron atoms in $B_2(pin)_2$. The B–B bond is

(6) Carboni, B.; Ollivault, M.; Bouguenec, F. L.; Carrié, R.; Jazouli, M. *Tetrahedron Lett.* **1997**, *38*, 6665–6668.

(7) (a) Moran, W. J.; Morken, J. P. *Org. Lett.* **2006**, *8*, 2413–2415. (b) Mlynarski, S. N.; Karns, A. S.; Morken, J. P. *J. Am. Chem. Soc.* **2012**, *134*, 16449–16451.

(8) (a) Imao, D.; Glasspoole, B. W.; Laberge, V. S.; Crudden, C. M. *J. Am. Chem. Soc.* **2009**, *131*, 5024–5025. (b) Ohmura, T.; Awano, T.; Suginome, M. *J. Am. Chem. Soc.* **2010**, *132*, 13191–13193. (c) Sandrock, D.; Jean-Gérard, L.; Chen, C. Y.; Dreher, S. D.; Molander, G. A. *J. Am. Chem. Soc.* **2010**, *132*, 17108–17110.

(9) Li, Z.; Wang, Z.; Zhu, L.; Tan, X.; Li, C. *J. Am. Chem. Soc.* **2014**, *136*, 16439–16443.

(10) (a) Lee, K.-S.; Zhugralin, A. R.; Hoveyda, A. H. *J. Am. Chem. Soc.* **2009**, *131*, 7253–7255. (b) Lee, K.-S.; Zhugralin, A. R.; Hoveyda, A. H. *J. Am. Chem. Soc.* **2010**, *132*, 12766.

(11) Laitar, D.S.; Müller, P.; Sadighi, J. P. *J. Am. Chem. Soc.* **2005**, *127*, 17196–17197.

polarized/weaken and the Cu–B(pin) complex is generated upon formation of RO–B(pin) through σ–bond metathesis. A Lewis basic ligand on Cu plays a crucial role in donating its electron density to the metal center, rendering Cu more Lewis acidic and the alkoxide oxygen more Lewis basic based on the principle of Lewis base activation of Lewis acid.[12]

Scheme 1.1. B–B bond activation by a Cu–alkoxide complex

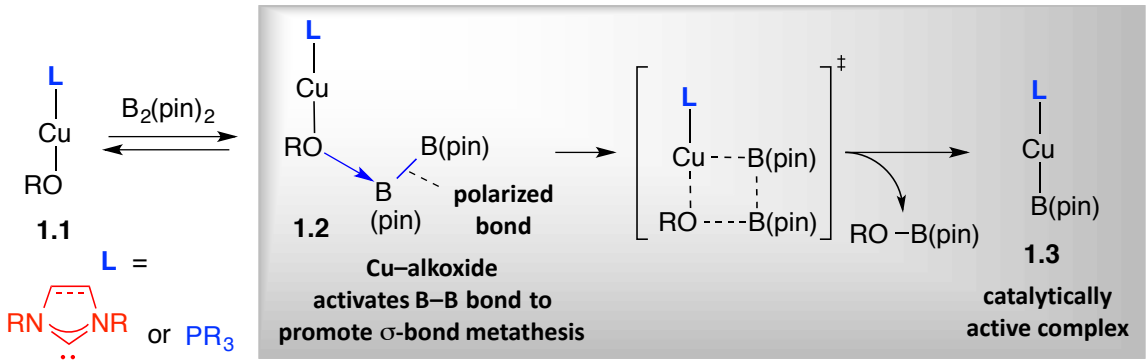

X-ray crystallographic data shown in Scheme 1.2 support the idea that the B–B bond can be elongated and weakened by donation of electron density by a Lewis base. Complex **1.4** formed from binding of 4-methylpyridine with bis(catecholato)diboron, disclosed in 1995 by Marder and Norman shows significant lengthening of the B–B bond.[13] Later in 1997, they also showed that a phosphine can donate a pair of electrons to cause the stretching of a B–B bond from 1.673 to 1.689 Å (**1.5**, Scheme 1.2). [14]

(12) For discussions on Lewis base activations of Lewis acids, see: (a) Guttmann, V. *The Donor–Acceptor Approach to Molecular Interactions*; Plenum Press, New York, 1978. (b) Denmark, S. E.; Beutner, G. L. *Angew. Chem., Int. Ed.* **2008**, *47*, 1560–1638.

(13) Nguyen, P.; Dai, C.; Taylor, N. J.; Power, W. P.; Marder, T. B. *Inorg. Chem.* **1995**, 34, 4290–4291.

(14) Clegg, W.; Dai, C.; Lawlor, F. J.; Marder, T. B.; Nguyen, P.; Norman, N. C.; Pickett, N. L.; Power, W. P.; Scott, A. J. *J. Chem. Soc., Dalton Trans.* **1997**, 839–846.

Scheme 1.2. Elongation of B–B bonds by a Lewis base evidenced by X-Ray crystallography data

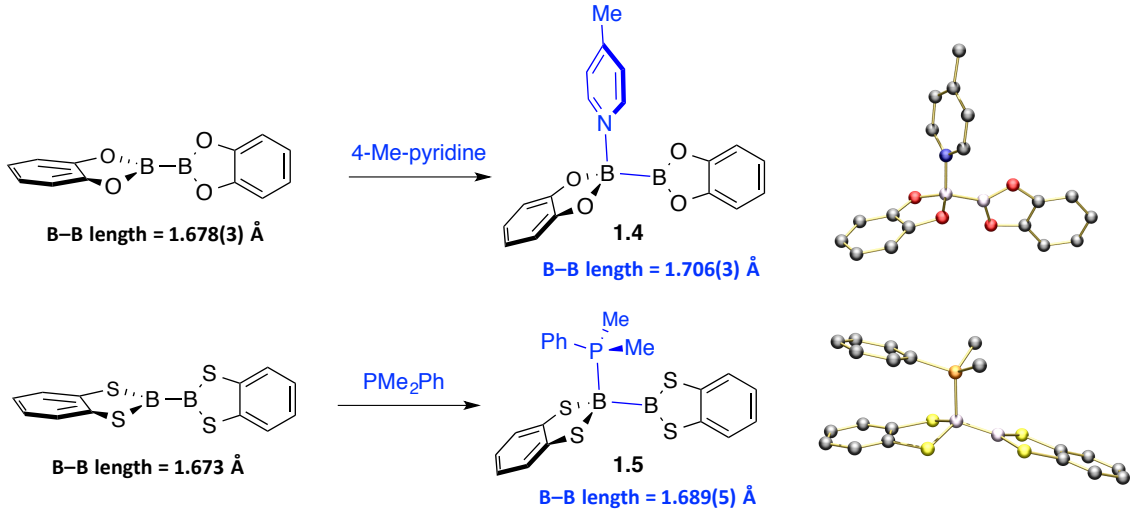

1A.2.2. Boryl Conjugate Additions Catalyzed by Achiral NHCs

In 2009, our laboratories investigated a possibility for an NHC to activate a diboron reagent. We selected an NHC as a representative for a Lewis base due to its unique electronic nature: a strong σ-donor and weak π-acceptor. We found that when $B_2(pin)_2$ is treated with 1,3-biscyclohexylimidazolylidene **1.6** in thf-d_8 at –10 ºC, within 5 min, an NHC•$B_2(pin)_2$ complex **1.7** is formed and characterized by ^{11}B NMR spectra (Scheme 1.3).[10] The ^{11}B NMR signal of $B_2(pin)_2$ (30.1 ppm) disappears [>98% conv of $B_2(pin)_2$], and two signals at 1.8 and 36.3 ppm appear instead. The signal at 1.8 ppm likely corresponds to an sp^3-hybridized boron indicating the coordination of the NHC **1.6**. Interestingly, the sp^2-hybridized boron shows a more downfield signal at 36.3 ppm compared to a signal of $B_2(pin)_2$ at 30.1 ppm. As the NHC coordinates to $B_2(pin)_2$, it polarizes the B–B bond and the net accumulation of electron density resides on the two more electronegative oxygen atoms. Because of this Lewis base activation of Lewis acid scenario, the sp^2-hybridized boron becomes more electrophilic and results in a downfield shift in ^{11}B NMR spectra.

DFT calculations were performed and an increased bond length was observed from $B_2(pin)_2$ (1.703 Å) to NHC•diboron complex **1.7** (1.749 Å). This is consistent with a report in 2012 by Marder and co-workers on the X-ray crystal structure of complex **1.7**. The B–B length in the crystal structure is 1.743(2) Å, very similar to our calculated value (1.749 Å).

Scheme 1.3. B–B bond activation by an NHC serving as the Lewis base

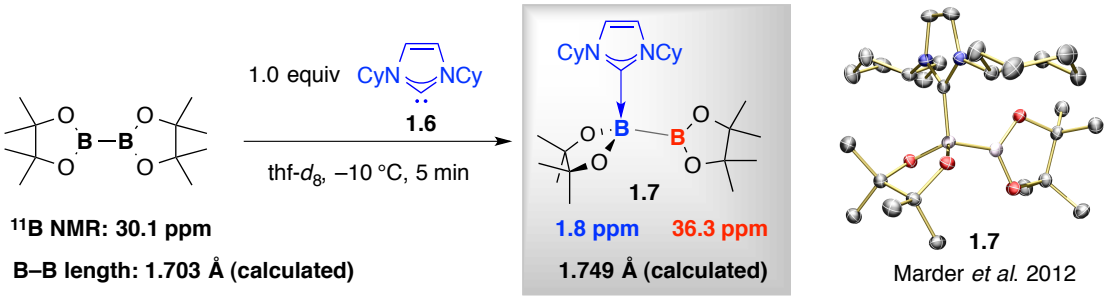

^{11}B NMR: 30.1 ppm

B–B length: 1.703 Å (calculated)

We then began to investigate whether the BCA process can occur in the presence of NHC as a Lewis base. Cyclohexenone **1.8a** was used as a representative substrate and treated with a mixture of 1.1 equiv $B_2(pin)_2$ and 10 mol % of an NHC (generated *in situ* from deprotonation of the corresponding imidazolium/imidazolinium salt) (Scheme 1.4).[10] When an NHC derived from imidazolium salt **im-1** was used, there was 66% conv to the desired product (**1.9a**) at room temperature after 12 h. With **im-2**, the efficiency improved (92% conv). However, reactivity suffered when a more sizable NHC precursor (**im-3**) was used (45% conv). With the more electron-donating bis-cyclohexyl imidazolium salt **im-4**, the reaction proceeded to >98% conv to afford **1.9a**. The BCA reaction does not proceed in the absence of an *N*-heterocyclic salt, or with less Lewis basic PPh_3 or PCy_3. However, 50% conv was observed with $OPPh_3$ present indicating it as a potential catalyst for Lewis base catalyzed transformations as well.

Scheme 1.4. Examination of different Lewis bases as catalysts for metal-free BCA reactions

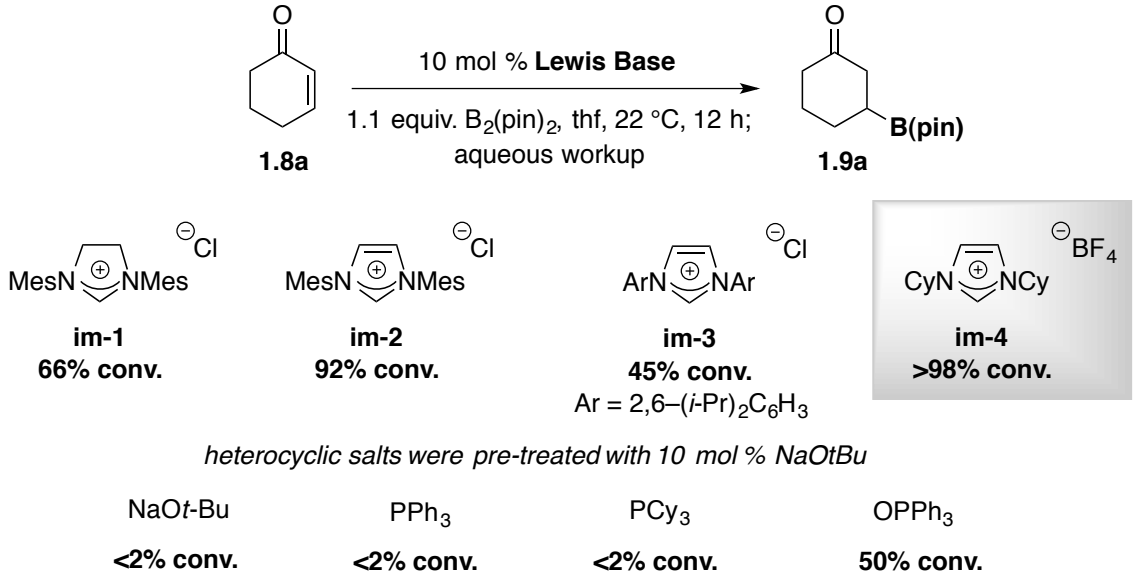

As shown in Scheme 1.5, the NHC-catalyzed boryl conjugate additions to α,β-unsaturated carbonyls proved to be efficient and general. A variety of cyclic and acyclic enones and enoates are suitable substrates. Cyclic enones with different ring sizes are generally effective (**1.9b**, **1.9c** and **1.9d**). Cyclic or acyclic enoates are also suitable substrates, although a slightly higher catalyst loading (5 mol %) and longer reaction time (24 h) are required for a complete transformation (**1.9e** and **1.12**). Reaction to produce **1.9f** indicates that the NHC-catalyzed protocol can be scalable.

In NHC-catalyzed BCAs, boryl enolate **1.13** can be isolated without aqueous workup (Scheme 1.6). Moreover, the reaction proceeds with high efficiency in the presence of 1-hexyne (Scheme 1.6). This is in contrast to the Cu-catalyzed reaction. There is <2% conv when 2.5 mol % CuO*t*-Bu is present. In another example, when benzaldehyde is added, the NHC-catalyzed BCA proceeds to afford the β-boryl aldol product **1.14** cleanly with high diastereoselectivity (85% yield, >98:2 dr). The Cu-

catalyzed reaction; however, results in only 31% of the desired product with 19% conv to benzaldehyde diboration.

Scheme 1.5. Efficient BCA reactions catalyzed by achiral NHC

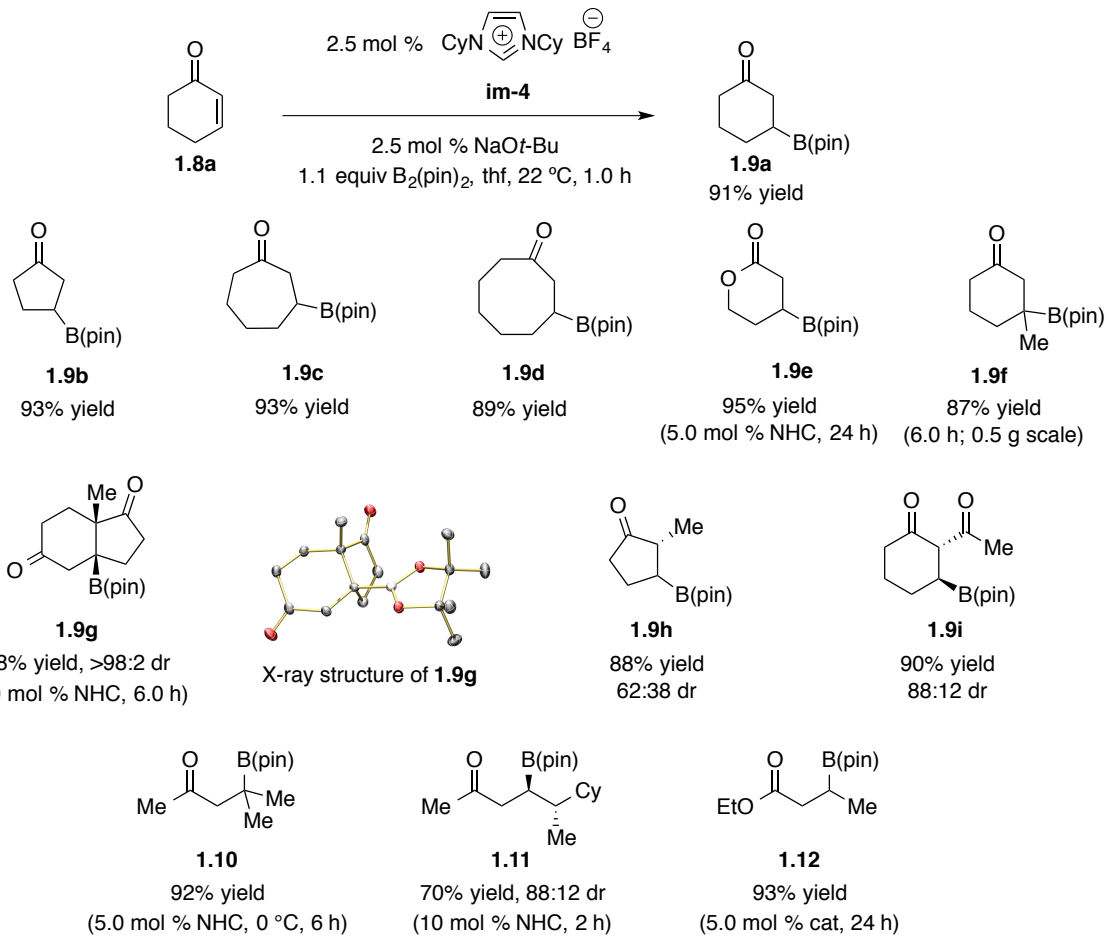

Our initial proposed mechanism was based on the formation of NHC•diboron complex **i** (Scheme 1.7). The B–B bond in **i** is polarized and the electron density is accumulated at the uncoordinated B(pin) unit enhancing its nucleophilicity. The B(pin) group transfers to the β-carbon of the enone, resulting in formation of **iii** and **iv** which probably are in equilibrium favoring of **iv** due to a stronger B–O bond. Upon release of the NHC, product **v** is generated.

Scheme 1.6. High efficiency and chemoselectivity in NHC catalyzed BCA reactions

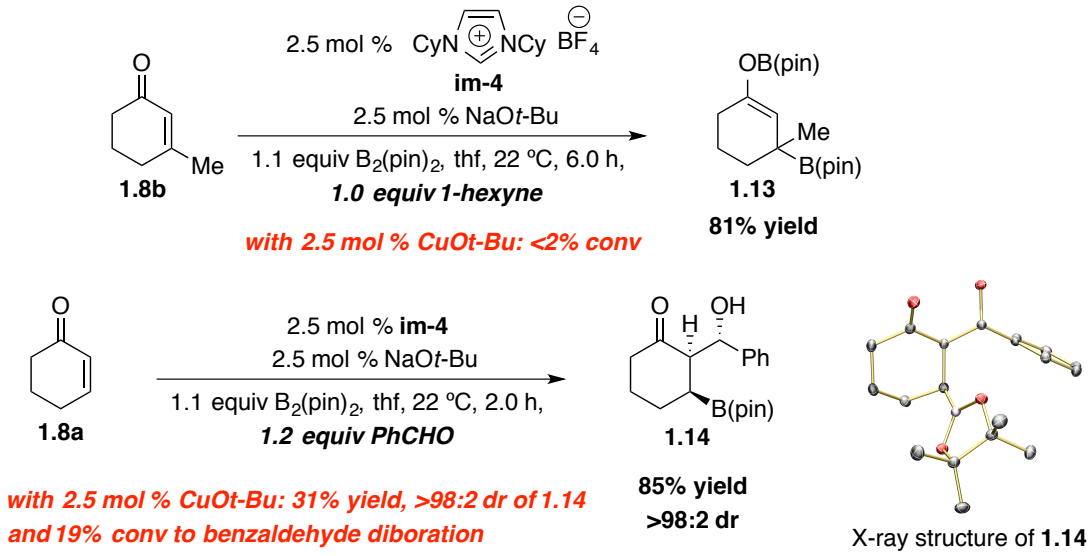

The NHC-catalyzed boryl conjugate addition to a variety of α,β-unsaturated carbonyls unveils an entirely new avenue in the realm of catalysis. It is the first transition metal-free catalytic transformation to form C–B bonds. A number of Lewis base catalyzed protocols to construct C–B, C–Si and C–C bonds were discovered after this report. In the next section, focus will be placed on the development of an enantioselective version of this transformation and illustrate the knowledge we learned during our studies.

Scheme 1.7. The proposed mechanism for NHC-catalyzed BCA reaction reported in 2009

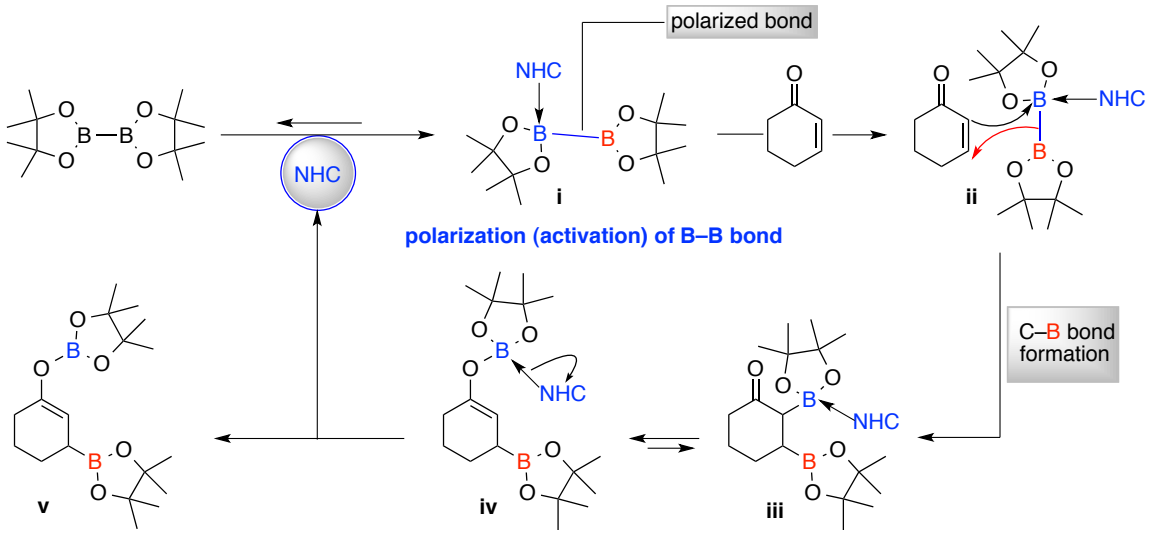

1A.2.3. Boryl Conjugate Additions Catalyzed by Phosphine/alkoxide

In 2010, Fernández and co-workers reported the first phosphine-promoted boron conjugate additions to α,β-unsaturated ketones and esters.[15] As shown in Scheme 1.8, PPh_3 or dppf is used to promote the reaction at 70 ºC. Excess methanol and base (Cs_2CO_3) prove to be essential for high efficiency similar to the report from our group.[10] PPh_3 is more effective than the more sizable dppf. Cyclohexenone, a single case of a cyclic enone, requires a longer reaction time (16 h) for high conversion (**1.9a**, Scheme 1.8).

Scheme 1.8. Boryl conjugate additions performed with achiral phosphines

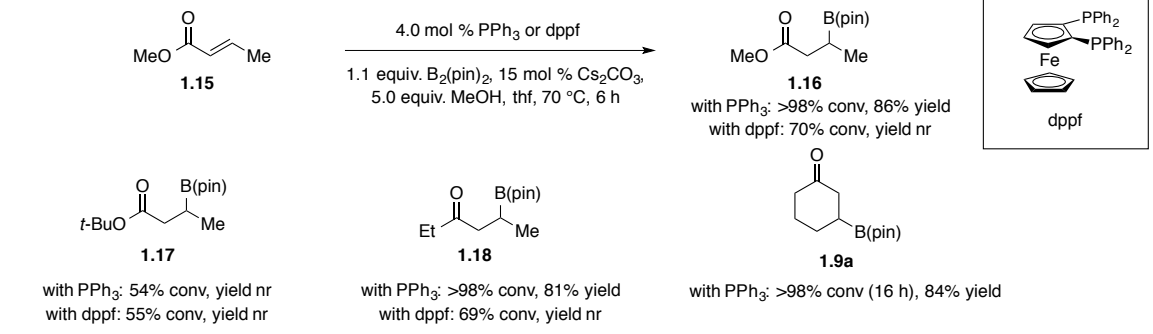

(15) Bonet, A.; Gulyás, H.; Fernández, E. *Angew. Chem., Int. Ed.* **2010**, *49*, 5130–5134.

In the same study, a variety of chiral phosphines were examined and (*R*)-binap or (*R*)-(*S*)-josiphos **1.20** was found to be optimal. However, the method usually delivered products with low enantioselectivity (Scheme 1.9).

Scheme 1.9. Boryl conjugate additions performed with chiral phosphines

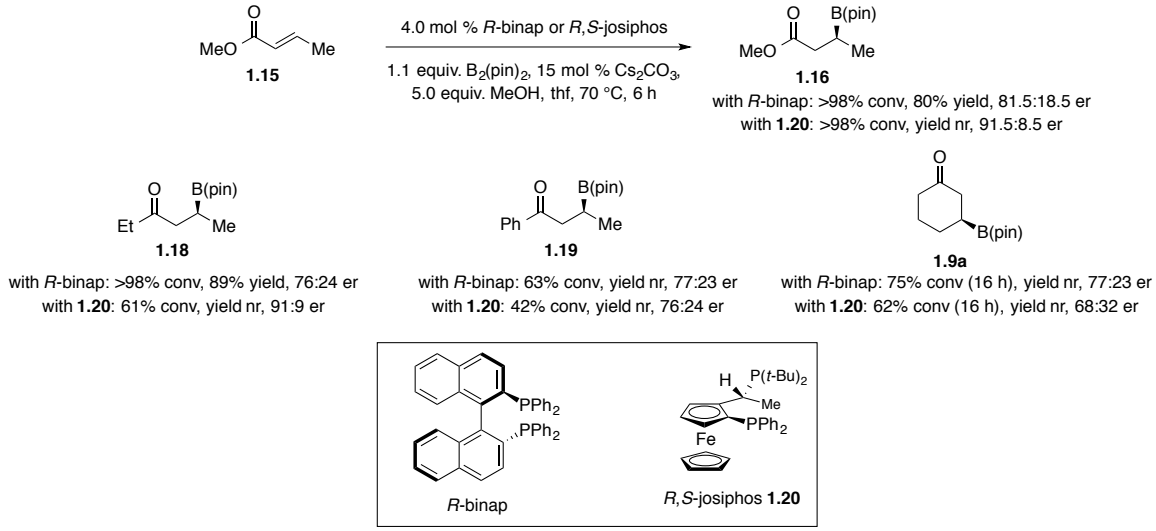

A mechanistic study by the same group showed that ion pair **1.21** derived from addition of a methoxy group to $B_2(pin)_2$ and conjugate addition of PMe_3 to an enone can be detected spectroscopically (Scheme 1.10).[16] DFT calculations of the reaction were carried out subsequently. As shown in Scheme 1.10, a transition structure was proposed, in which an α-carbonyl proton serves as a connector for a four-component ensemble.

(16) Pubill-Ulldemolins, C.; Bonet, A.; Gulyás, H.; Bo, C.; Fernández, E. *Org. Biomol. Chem.* **2012**, *10*, 9677–9682.

Scheme 1.10. Spectroscopic data and proposed transition state for phosphine-catalyzed BCAs

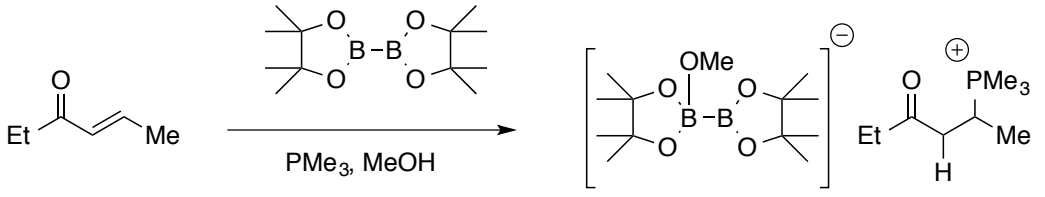

transition state proposed by Bo, Gulyás and Fernández:

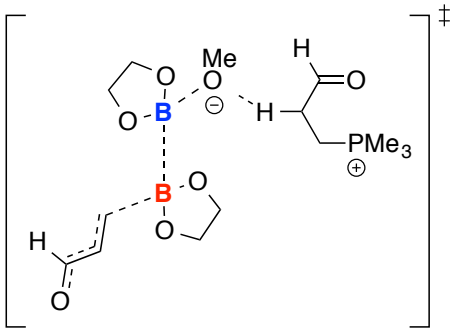

Based on the proposed mechanism, Fernández and co-workers in the same report developed phosphine promoted base-free BCAs to α,β-unsaturated carbonyls (Scheme 1.11). In the presence of PCy_3 and MeOH without any additional base such as Cs_2CO_3, the BCA reactions are efficient delivering β-boryl ketones and esters in high yields, except the acyclic one bearing a quaternary carbon center (**1.23**).

Scheme 1.11. Phosphine-catalyzed boryl conjugate additions performed in methanol

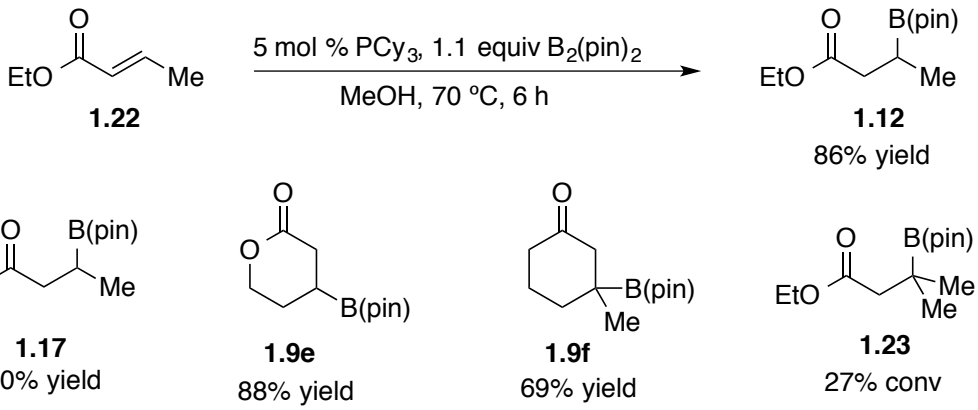

In a follow-up report in the same year, the same group also reported another

methoxide catalyzed BCA. Verkade's base was employed instead of phosphine, as shown in Scheme 1.12.[17] The reactions, however, require 15 mol % catalyst loading (vs 5 mol % PCy_3) and longer reaction time (24 h vs 6 h). In addition to $B_2(pin)_2$, $B_2(cat)_2$ (cat = catechol) can be used as a diboron reagent delivering the corresponding product in high conversion (**1.24**, Scheme 1.12). This report shows that the Lewis base catalyst in the phosphine assisted BCAs mentioned above is the methoxide anion rather than the phosphine itself.

Scheme 1.12. Verkade base-promoted boryl conjugate additions

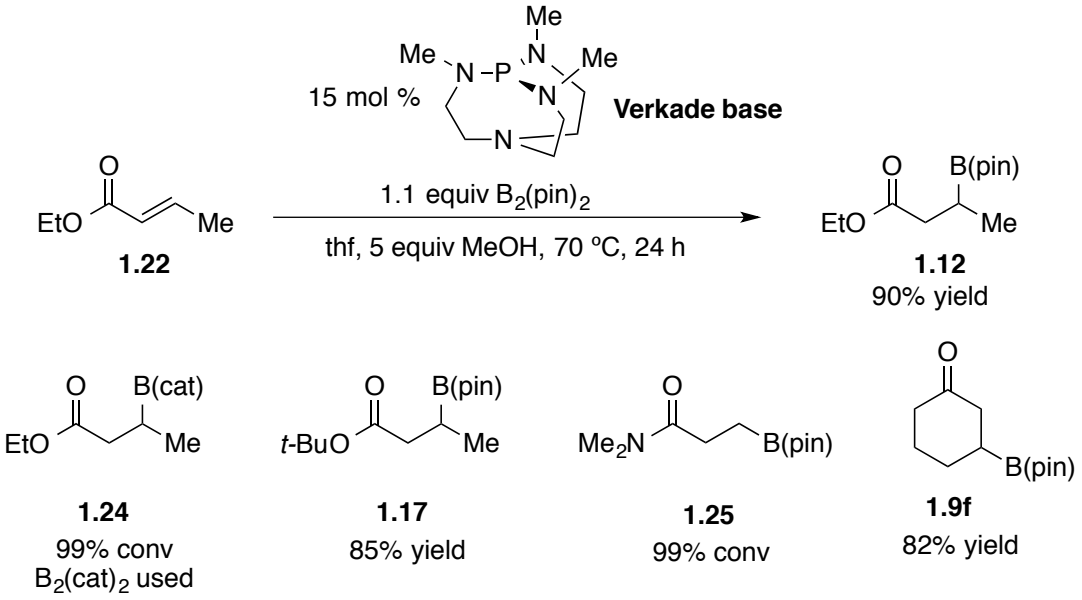

Fernández and co-workers have shown that methoxide can promote diboron additions to unactivated alkyl-substituted alkenes.[18] As shown in Scheme 1.13, in addition to monosubstituted alkenes, disubstituted alkenes (*E* and *Z* isomers) as well as an allene are suitable substrates. When styrene was employed, the reaction suffered from

(17) Pubill-Ulldemolins, C.; Bonet, A.; Bo, C.; Gulyás, H.; Fernández, E. *Chem. Eur. J.* **2012**, *18*, 1121–1126.

(18) Bonet, A., Pubill-Ulldemolins, C.; Bo, C.; Gulyás, H.; Fernández, E. *Angew. Chem., Int. Ed.* **2011**, *50*, 7158–7161.

competitive protoboration reaction.

Scheme 1.13. Alkoxide-catalyzed diboration reactions with non-activated olefins and an allene

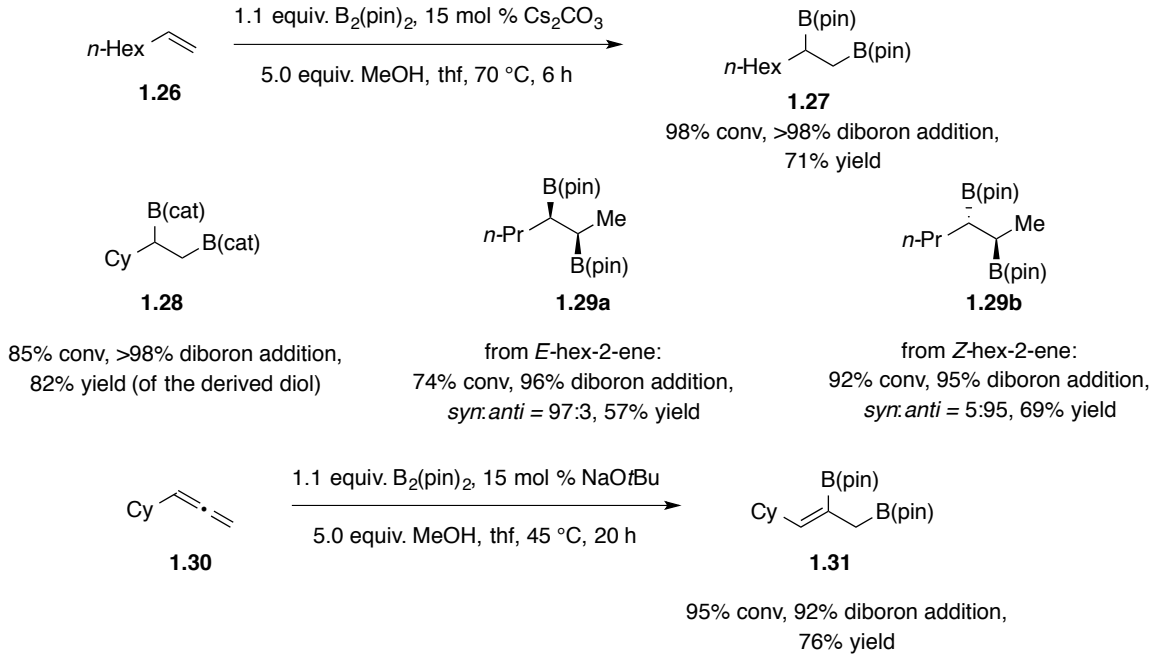

In addition to reactions of diboron reagent with unsaturated carbonyls and alkenes, Fernández and co-workers reported that phosphine can catalyze the reaction of $B_2(pin)_2$ with aryl- and alkyl-substituted *N*-tosylimines to produce α-amino boronic esters, as shown in Scheme 1.14.[19] Reactions with PPh_3 were carried out at 70 ºC, while (*R*)-(*R*)-Walphos (CF_3) can be used to deliver products with 62:38 er to 95:5 er (at 45 ºC). Both Cs_2CO_3 and MeOH were required for high efficiency of reactions as well as the phosphine (the reaction proceeds to 70% conv without PPh_3).

(19) Solé, C.; Gulyás, H.; Fernández, E. *Chem. Commun.* **2012**, *48*, 3769–3771.

Scheme 1.14. Alkoxide catalyzed boron additions to tosylimines

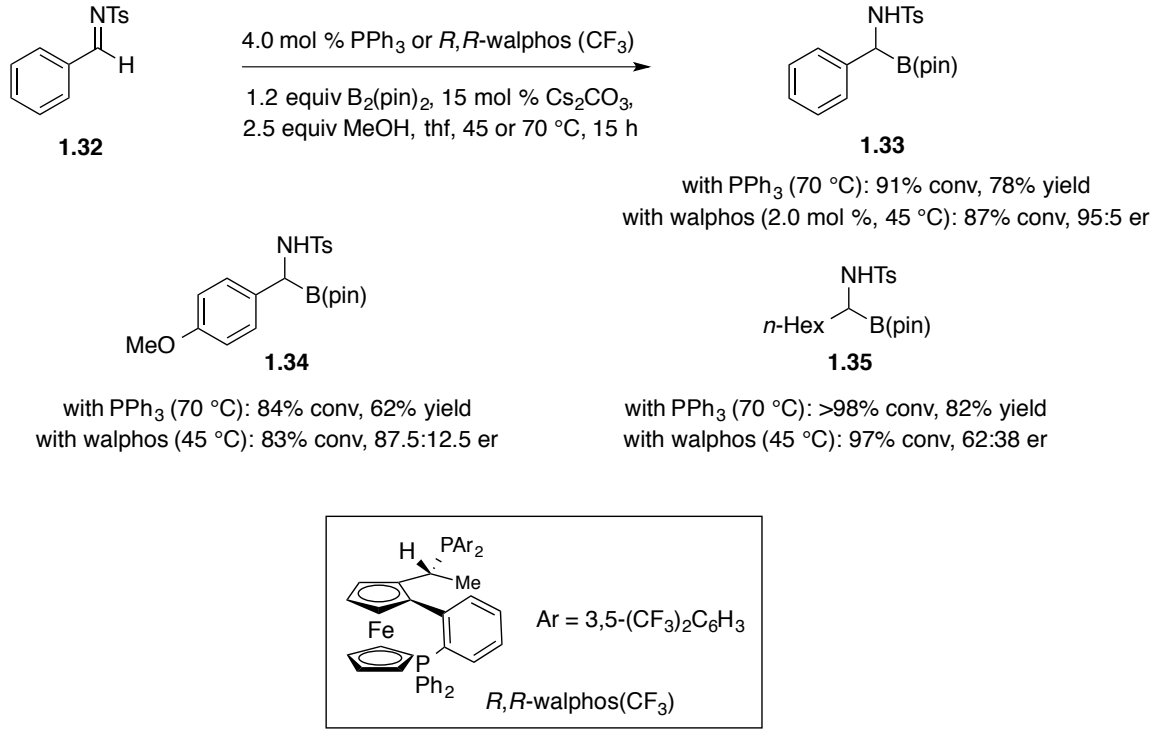

1A.2.4. Reactions Promoted by Other Lewis Bases

Ohmura, Suginome and co-workers reported in 2012 a method for 1,4-diboron additions of pyrazines, as shown in Scheme 1.15.[20] The reactions proceed without any additional base and products were isolated in 77–96% yield. The mechanism begins with a pyrazine nitrogen coordinating to one of the boron atoms in $B_2(pin)_2$. Subsequent nucleophilic addition of the uncoordinated B(pin) unit to the C_2 carbon of pyrazine followed by an intramolecular rearrangement produces the 1,4-diboron pyrazine.

(20) Oshima, K.; Ohmura, T.; Suginome, M. *Chem. Commun.* **2012**, *48*, 8571–8573.

Scheme 1.15. 1,4-Diboration of pyrazine

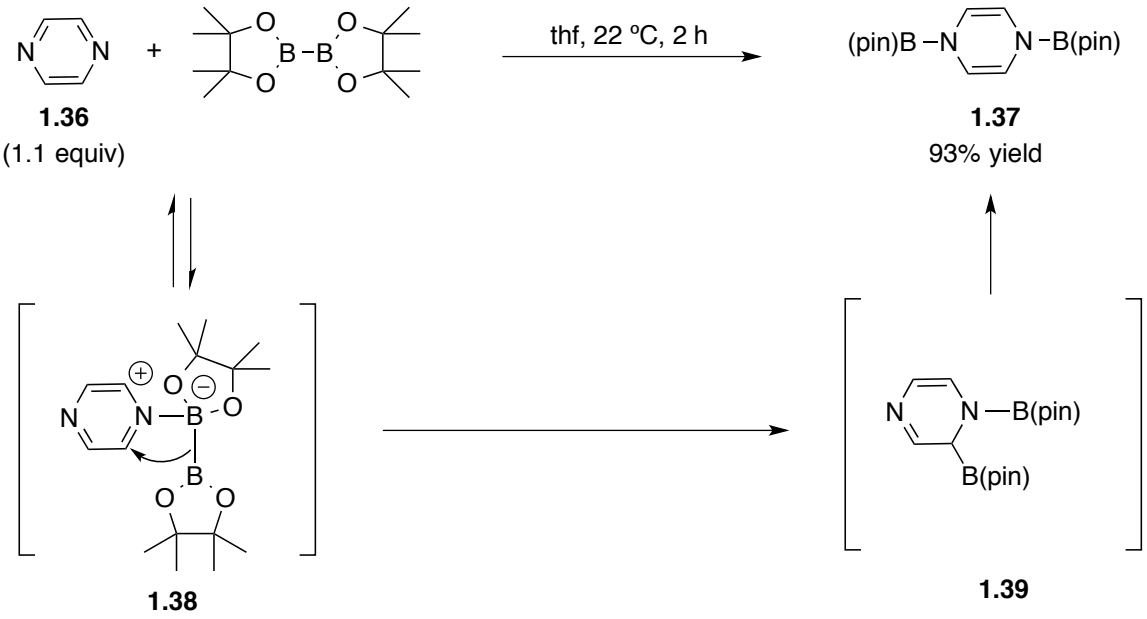

In 2013, Zhang and co-workers used a Lewis base activation of a B–B bond strategy to effect borylation of aryl iodides (Scheme 1.16).[21] In the presence of 2.0 equiv of Cs_2CO_3 in refluxing methanol after 20–48 h, the desired aryl-B(pin) compounds with an electron-withdrawing or donating can be isolated in moderate to good yields. The mechanism of the reaction is unclear; however, preliminary mechanistic study shows that the reaction is not copper-catalyzed or proceeds through a radical pathway.

Morken and co-workers reported an alkoxide-catalyzed directed diboron addition to homoallylic alcohols (Scheme 1.17a).[22] In the presence of Cs_2CO_3 and methanol, the reactions are efficient delivering a variety of triol products (products after oxidation) after 6–12 hours at 70 ºC and with high diastereoselectivity. The diborylation reaction is scalable. For example, compound **1.46** can be isolated with similarly high efficiency and

(21) Zhang, J.; Wu, H.-H.; Zhang, J. *Eur. J. Org. Chem.* **2013**, 6263–6266.
(22) Blaisdell, T. P.; Caya, T. C.; Zhang, L.; Sanz-Marco, A.; Morken, J. P. *J. Am. Chem. Soc.* **2014**, *136*, 9264–9267.

stereoselectivity on a 5 gram scale. Low diastereoselectivity when a trishomoallylic alcohol (**1.52**, 1:1 dr) was used suggests that the hydroxyl unit is too far to be able to direct diboron addition effectively.

A mechanism was proposed based on several experimental supports that the alkoxide in the substrate activates $B_2(pin)_2$ to initiate diboron addition. A stereochemical model also explains the observed *syn* selectivity of the diborylation (Scheme 1.17b).

Scheme 1.16. Base-mediated borylations of aryl iodides

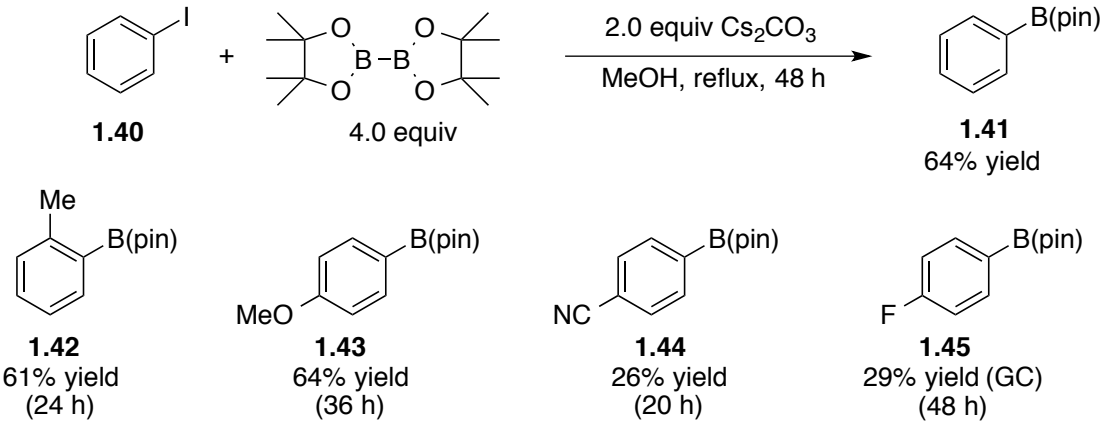

Hirano, Uchiyama, and co-workers disclosed *trans*-diboryl additions to propargylic alcohols (Scheme 1.18).[23] Treatment of a propargylic alcohol with one equivalent of *n*-BuLi followed by the addition of $B_2(pin)_2$ allows the formation of the corresponding *trans*-diborylated products after 24 h at 75 °C. A range of propargylic alcohols can be used as substrates. In addition, a dissymmetrical diboron [(pin)B–B(dan), (dan) = naphthalene-1,8-diaminato] could be employed in the reaction as well, delivering the product bearing the B(dan) unit selectively (Scheme 1.18a).

(23) Nagashima, Y.; Hirano, K.; Takita, R.; Uchiyama, M. *J. Am. Chem. Soc.* **2014**, *136*, 8532–8535.

Scheme 1.17. Hydroxyl-directed diastereoselective diboron additions to alkenes

a) Hydroxyl-directed stereoselective diboron additions to alkenes

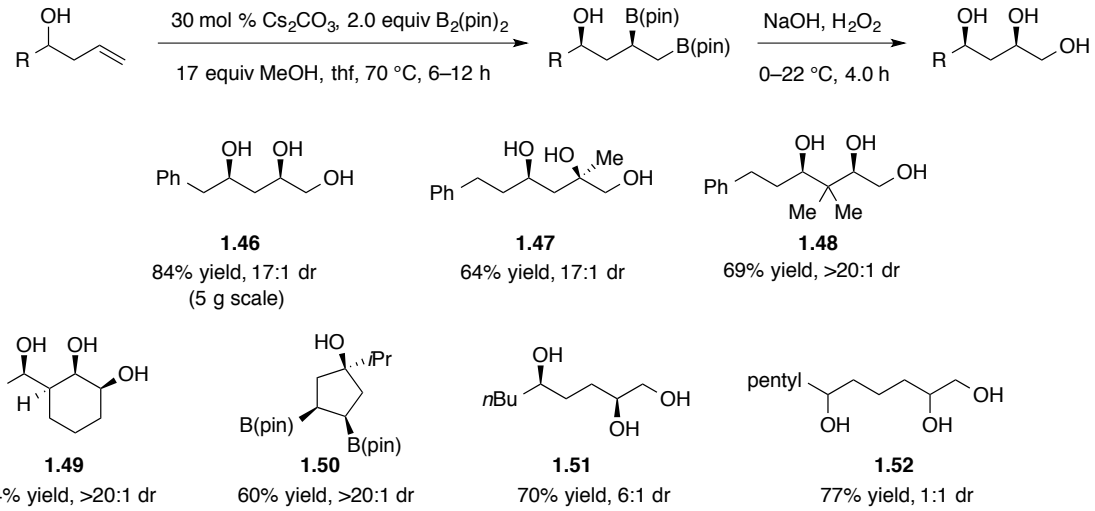

b) Proposed stereochemical model

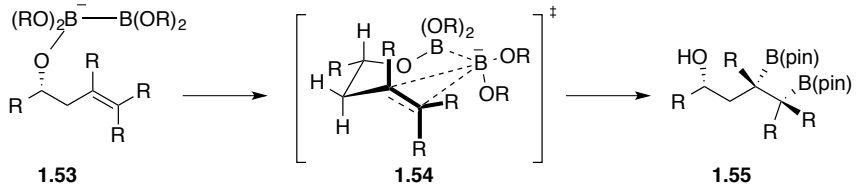

DFT calculations were performed to provide insight into mechanism of the reaction (Scheme 1.18b). The initial complexation of diboron reagent and lithium propargylic alkoxide is likely to occur prior to the first C–B bond formation (activation energy = +23.2 kcal/mol). The second C–B bond formation is proposed to be more energetically favored (activation barrier = +2.1 kcal/mol) leading to the observed *trans* diboron addition product.

Scheme 1.18. Alkoxide-activated trans-diboron additions to propargylic alcohols

a) *trans*-Diborylation of propargylic alcohols

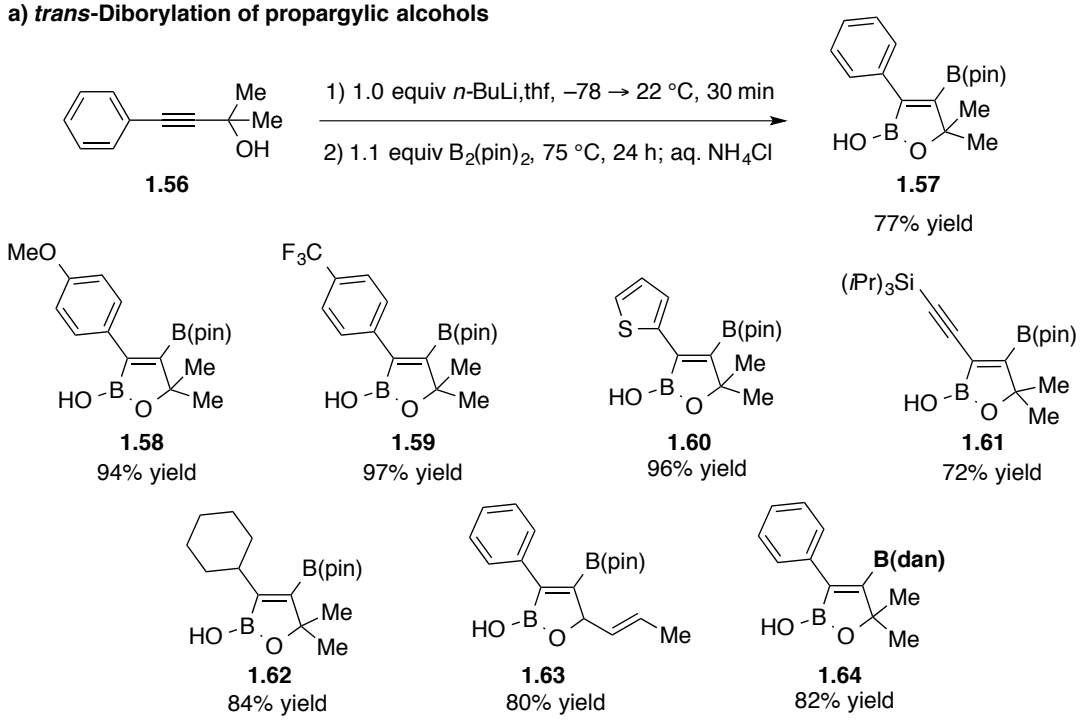

b) Proposed mechanism based on DFT calculations

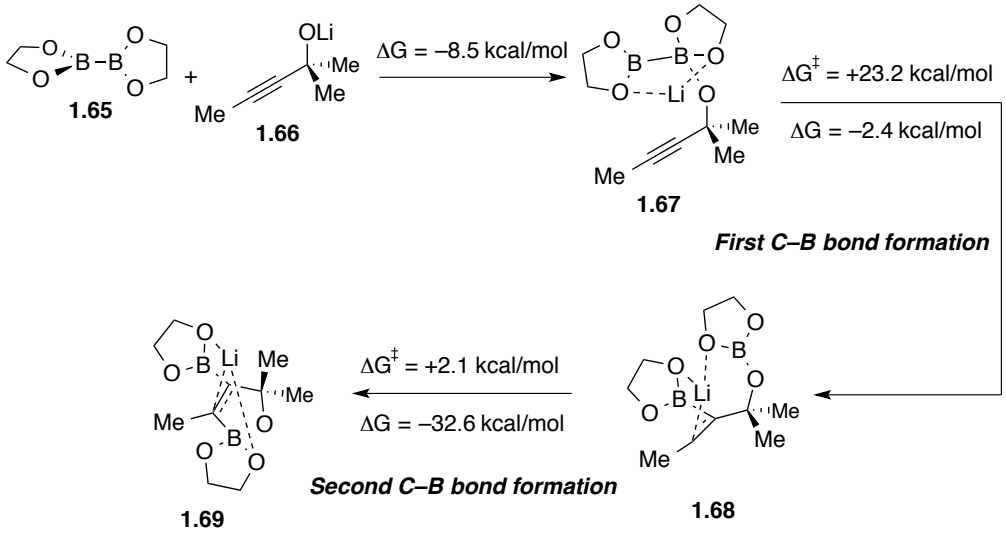

Another set of transformations involves the activation of a B–B bond by a diazo intermediate reported by Wang and co-workers (Scheme 1.19).[24] Tosylhydrazones can be converted to alkyl–B(pin) through reactions with $B_2(pin)_2$. Aryl-substituted

(24) Li, H.; Wang, L.; Zhang, Y.; Wang, J. *Angew. Chem., Int. Ed.* **2012**, *51*, 2943–2946.

tosylhydrazones, including those with an electron-rich, electron-poor or B(pin) substituent, as well as alkyl tosylhydrazones can serve as suitable substrates (Scheme 1.19a). There is, however, minimal conversion to the desired products with the ketone-derived substrates under the same conditions. Based on the hypothesis that the lower reactivity of ketones might be due to the sizeable $B_2(pin)_2$, reactions with the smaller HB(pin) were examined and indeed proceeded to generate products with a secondary C–B bond more efficiently. It was proposed that the transformation starts with in situ generation of a diazo compound, which then coordinates to $B_2(pin)_2$ followed by a 1,2-migration (Scheme 1.19b). The diboron intermediate would then be converted to the alkyl–B(pin) product by a proto-deboration process in the presence of NaOMe and MeOH. Reaction with HB(pin), 1,2-migration would then generate the product directly.

Scheme 1.19. Alkoxide-promoted reactions of tosylhydrazones and $B_2(pin)_2$ or HB(pin)

a) Synthesis of alkylboronates from tosylhydrazones

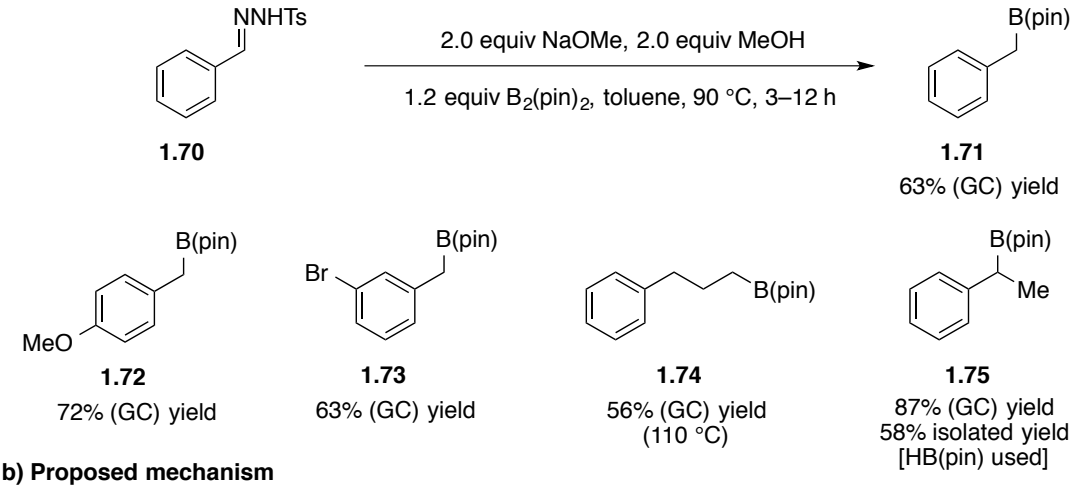

b) Proposed mechanism

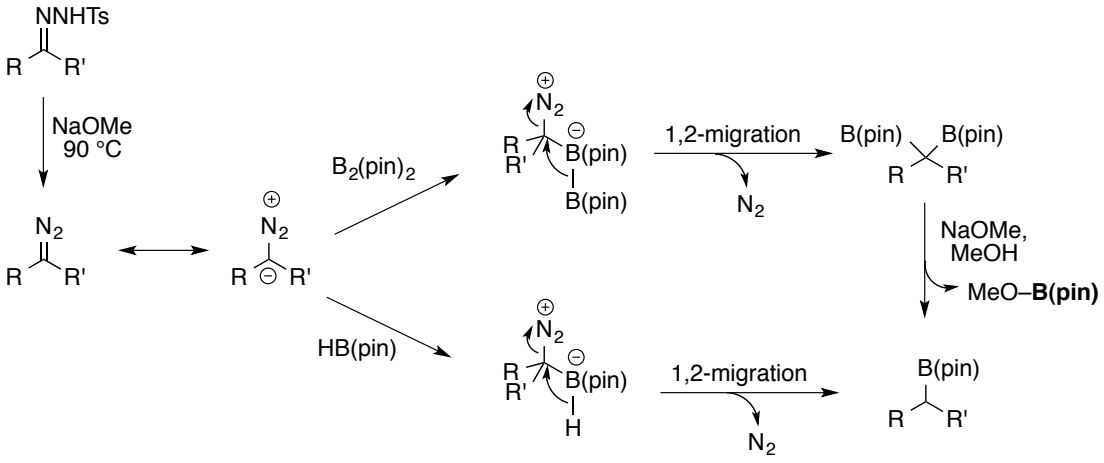

1A.3. NHC-catalyzed Enantioselective Boryl Conjugate Additions to Generate Boron Substituted Tertiary Carbon Stereogenic Centers

1A.3.1. Initial Studies

We began by employing similar conditions used for non-enantioselective BCAs with enone **1.76** except a chiral imidazolinium salt (**im-5**) was used.[10] There was hardly any product formation after 14 h (Scheme 1.20a). We reasoned that it might be because the sterically hindered chiral NHC cannot coordinate effectively with $B_2(pin)_2$. As shown in Scheme 1.20b, we proposed that if one of the sizable pinacol units is replaced to a

smaller alkoxide group such as methoxide, the boron center would become more accessible and allow effective association of the chiral NHC. We then added 20 equiv of MeOH into the reaction mixture (Scheme 1.20c). Indeed, there was 24% conv to the desired product, which was formed with appreciable enantioselectivity (87:13 er). When we switched the base to dbu (1,8-diazabicyclo[5.4.0]-undec-7-ene), higher conversion was observed with slightly increased er value (47% conv, 92:8 er) indicating that in the reaction with NaO*t*-Bu, there was some catalysis by an achiral Lewis base (likely the methoxide) causing lower enantioselectivity. We found that increasing the amount of MeOH to 60 equiv gave 82% yield of the product with 92:8 er. [25]

(25) Wu, H.; Radomkit, S.; O'Brien, J. M.; Hoveyda, A. H. *J. Am. Chem. Soc.* **2012**, *134*, 8277–8285.

Scheme 1.20. Development of an enantioselective NHC-catalyzed BCAs

a) Initial observation

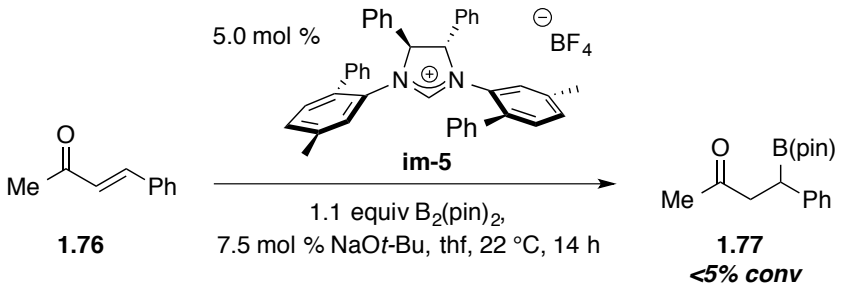

b) Hypothesis: Enhanced reaction rate through addition of MeOH

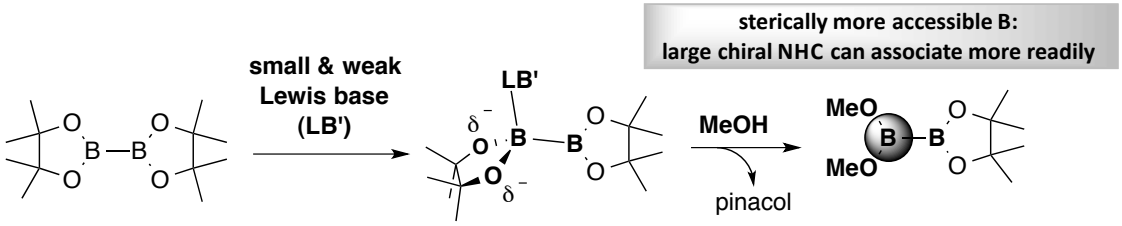

c) Validation of hypothesis

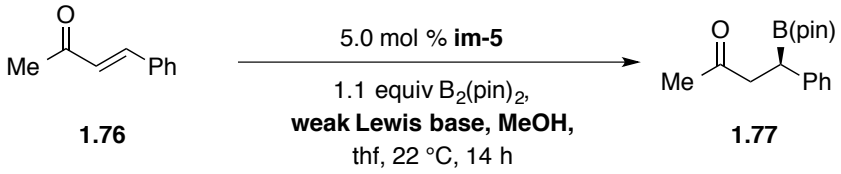

with 7.5 mol % **NaO*t*-Bu** + 20 equiv. **MeOH**: **24% conv, 87:13 er**
with 20 mol % **dbu** + 20 equiv. **MeOH**: **47% conv, 92:8 er**
with 20 mol % **dbu** + 60 equiv. **MeOH**: ***87% conv, 82% yield, 92:8 er***

1A.3.2. NHC Screening for Catalytic Enantioselective BCA Reactions

With similar reaction conditions (use of dbu and MeOH), we have tried a variety of chiral imidazolinium salts, the results are summarized in Table 1.1. The sulfonate-containing NHC (derived from **im-6**, entry 1) promotes the BCA reaction generating the product in 48% conv, but with low enantioselectivity (47:53 er). We turned our attention to using a monodentate NHC as a catalyst. With the monophenyl backbone NHC derived from **im-7**, only 30% conv is observed with 31:69 er. When we switched to monodentate NHCs that contain a biphenyl backbone, there was dramatic improvement in

enantioselectivity (up to 81:19 er, entries 4–5) although the conversions are still low. A methyl substituent at the ortho position of the unsymmetric N-aryl motif (**im-11**, entry 6) diminishes both efficiency and selectivity. However, reactions with NHCs that contain a meta-substituent proceed with higher conversion (82% and 78% conv, entries 7 and 8, respectively). After modifications of the NHCs structure, we found that the NHC-derived from **im-16** promotes the BCA reaction efficiently and selectively (81% conv and 95:5 er, entry 11). Again, increasing the amount of MeOH (60 equiv) improves reaction efficiency (>98% conv, 96:4 er, entry 15).

Table 1.1. Examination on various chiral NHC catalysts[a]

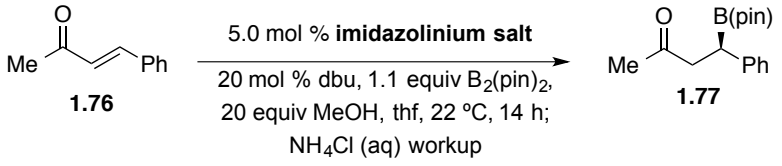

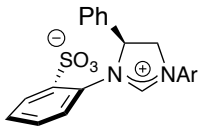

im-6 Ar = 2,6-$(Et)_2C_6H_3$

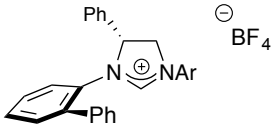

im-7 Ar = 2,6-$(Et)_2C_6H_3$

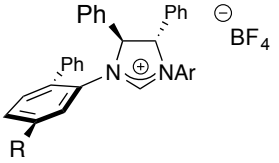

im-8 R = H, Ar = Mes
im-9 R = H, Ar = 2,6-$(Et)_2C_6H_3$
im-10 R = H, Ar = 2,6-$(i\text{-}Pr)_2C_6H_3$

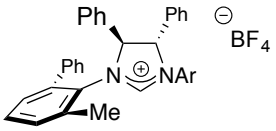

im-11 Ar = 2,6-$(Et)_2C_6H_3$

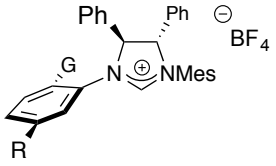

im-12 R = Me, G = Ph
im-13 R = *i*-Pr, G = Ph
im-14 R = H, G = Cy
im-15 R = H, G = Mes
im-16 R = *i*-Pr, G = Mes

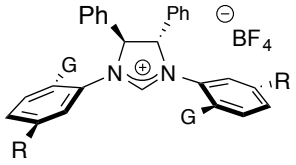

im-17 R = H, G = Ph
im-5 R = Me, G = Ph
im-18 R = H, G = Cy

entry	imidazolinium salt	conv (%)[b]	er[c]
1	**im-6**	48	47:53
2	**im-7**	30	31:69
3	**im-8**	10	56:44
4	**im-9**	37	81:19
5	**im-10**	24	80:20
6	**im-11**	25	72:28
7	**im-12**	82	80.5:19.5
8	**im-13**	78	76:24
9	**im-14**	37	72:28
10	**im-15**	30	94:6
11	**im-16**	81	95:5
12	**im-17**	35	82:18
13	**im-5**	87	92:8
14	**im-18**	14	35:65
15[d]	**im-16**	>98	96:4

[a] Reactions were performed under N_2 atmosphere. [b] Conversions to the desired product were determined by analysis of 400 MHz ^1H NMR spectra of unpurified mixtures. [c] Determined by HPLC analysis. [d] 60 equiv MeOH was used. Mes = 2,4,6-$(Me)_3C_6H_2$.

1A.3.3. Catalytic Enantioselective BCA Reactions to α,β-Unsaturated Acyclic Ketones

With the optimized reaction conditions in hand, various acyclic α,β-unsaturated ketones were examined (Scheme 1.21). The BCA reactions are quite general delivering good yield and enantioselectivity of products containing electron-donating or electron-withdrawing groups on the aryl substituent as well as a hetero-aryl substituent. Reaction with a substrate bearing an ortho-methyl phenyl substituent requires higher temperature (50 ºC) to proceed to 95% conv (~15% conv at 22 ºC), but with diminished enantioselectivity (**1.81**, 90% yield, 85.5:14.5 er). The NHC-catalyzed enantioselective BCA reaction accommodates enones with alkyl substituents with high efficiencies (**1.82–1.83**) and enantioselectivities (up to 94.5:5.5 er). The reaction with *trans*-chalcone is slightly slower; however, with a higher amount of dbu, the reaction proceeds to complete conversion (vs 82% conv with 20 mol% dbu). The reason why increasing the amount of dbu facilitate BCA processes is that deprotonation of the imidazolinium salt as well as MeOH hydrolysis of $B_2(pin)_2$ requires an excess amount of base, therefore more dbu means higher efficiency of the processes that will result in higher conversion.

Scheme 1.21. NHC-catalyzed enantioselective BCA to acyclic enones

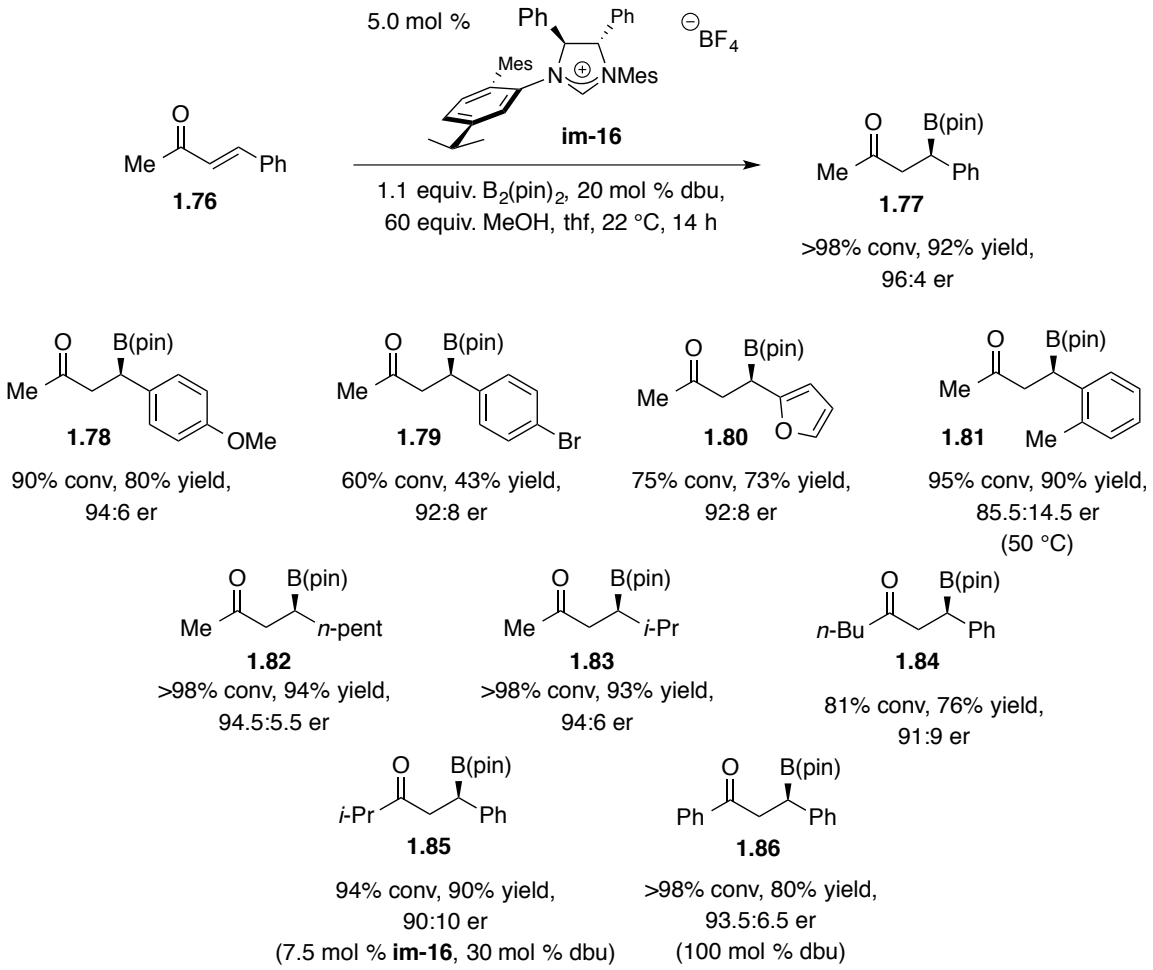

The strategy of using higher amount of dbu can be applied to other substrates that are not effective. As shown in Scheme 1.22, with 1.0 equiv of dbu, the desired products are generated in much higher yields and in some cases, with higher enantioselectivity. The enhancement in selectivity suggests that at a lower concentration of dbu, there is probably incomplete deprotonation of imidazolinium salt to form NHC as well as a lower concentration of a partially methanolyzed diboron species [$(MeO)_2B$–B(pin)]. The background reaction promoted by a methoxide is then more competitive causing lower enantioselectivity of the products.

Scheme 1.22. Influence of dbu on NHC-catalyzed enantioselective BCA reactions

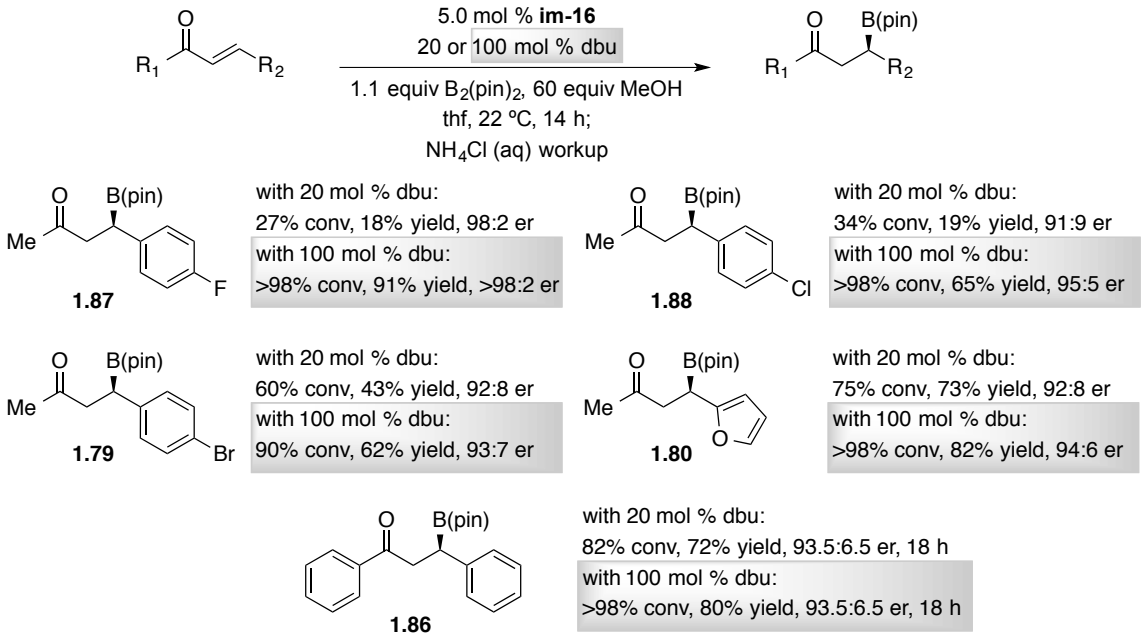

1A.3.4. Catalytic Enantioselective BCA Reactions to α,β-Unsaturated Acyclic Esters

α,β-Unsaturated esters or enoates are as well suitable substrates in the NHC-catalyzed enantioselective BCA reactions. As shown in Scheme 1.23, methyl esters (**1.90–1.92**) as well as a more sizable *tert*-butyl ester (**1.93**) proceed to generate β-boryl esters in 62–87% yield and 94:6 to 98:2 er. Although, in some cases (**1.91** and **1.93**), a higher temperature is required for high reactivity. For **1.91**, we used 7.5 mol % of **im-16** and quenched the reaction after 10 h to minimize the proto-deboration of the product.

Scheme 1.23. NHC-catalyzed enantioselective BCA reactions to enoates

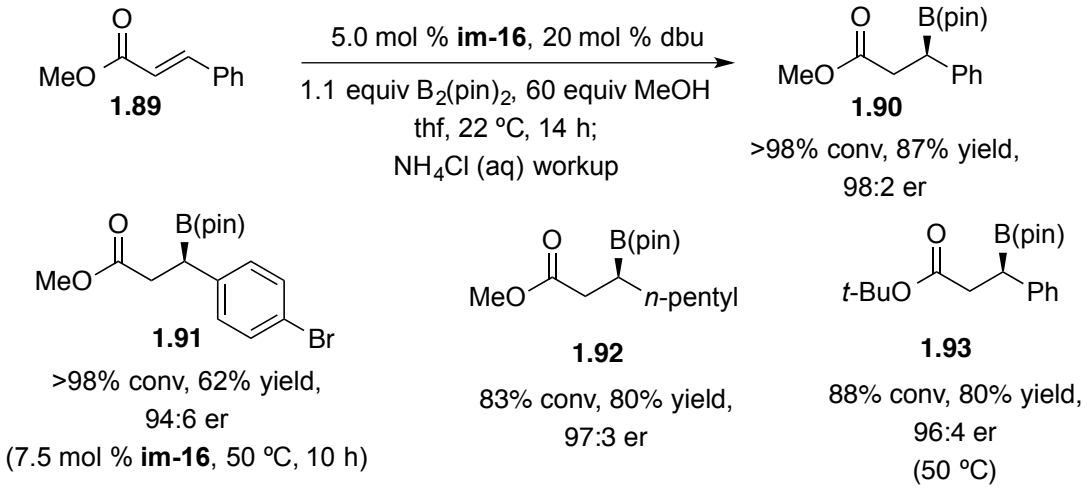

1A.3.5. Catalytic Enantioselective BCA Reactions to α,β-Unsaturated Weinreb Amides

We examined our BCA reactions with α,β-unsaturated Weinreb amides[26] to obtain synthetically useful β-boryl amides. Weinreb amides are generally less effective substrates. Thus, higher reaction temperatures and/or longer reaction times are required. The scope of the reactions is shown in Scheme 1.24. Substrates bearing aryl- or alkyl-substituent are both effective and proceed to afford the desired products in 60–92% yield and 86.5:13.5–95:5 er. In certain cases, less MeOH (30 equiv) was used to minimize proto-deboration and/or formation of β-boryl methyl esters (**1.95–1.96**).

To the best of our knowledge, there is only one example of enantioselective BCA reaction to a Weinreb amide.[27] However, this method is Cu-catalyzed rendering our metal-free protocol an attractive strategy to access these versatile entities.

(26) Nahm, S.; Weinreb, S. M. *Tetrahedron Lett.* **1981**, *22*, 3815–3818.
(27) Hirsch-Weil, D.; Abboud, K. A.; Hong, S. *Chem. Commun.* **2010**, *46*, 7525–7527.

Scheme 1.24. NHC-catalyzed enantioselective BCA reactions to unsaturated Weinreb amides

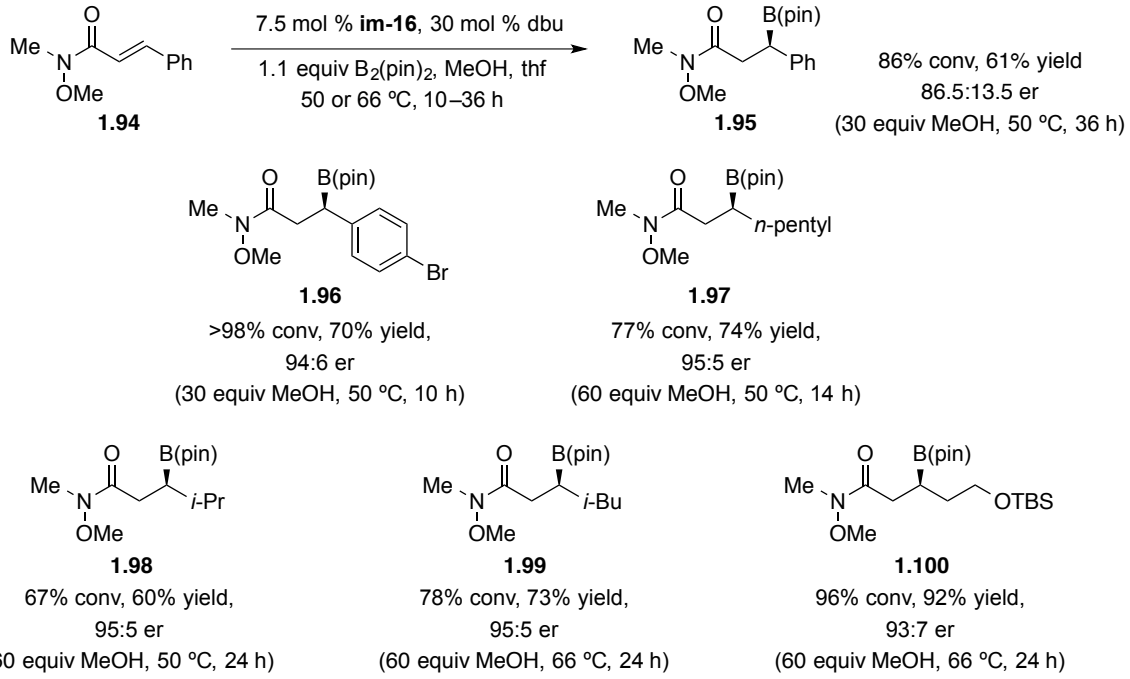

1A.3.6. Catalytic Enantioselective BCA Reactions to α,β-Unsaturated Aldehydes

As discussed earlier in the context of reactions with achiral NHC, chemoselectivity is problematic with Cu-catalyzed variants in the presence of aldehydes (1,2- vs 1,4-addition). However, there has been a single example on an enantioselective NHC–Cu-catalyzed BCA reaction of cinnamaldehyde although the desired product was obtained in low enantioselectivity (86% conv, yield not reported, 70:30 er).[28] In addition, a report by Ibrahem and co-workers on a Cu-catalyzed protocol to *in situ* generated unsaturated iminiums, an important strategy to access β-boryl aldehyde enantioselectively appeared in 2011.[29] However, the use of an air- and moisture-sensitive $Cu(OTf)_2$ and a Brønsted acid (o-$FC_6H_4CO_2H$) is required. With these limitations, we

(28) Lillo, V.; Prieto, A.; Bonet, A.; Díaz-Requejo, M. M.; Ramírez, J.; Pérez, P. J.; Fernández, E. *Organometallics,* **2009**, *28*, 659–662.

(29) Ibrahem, I.; Breistein, P.; Córdova, A. *Angew. Chem., Int. Ed.* **2011**, *50*, 12036–12041.

then pursued our NHC-catalyzed enantioselective BCA reactions with α,β-unsaturated aldehydes.

Scheme 1.25. NHC-catalyzed enantioselective BCA reactions to enals

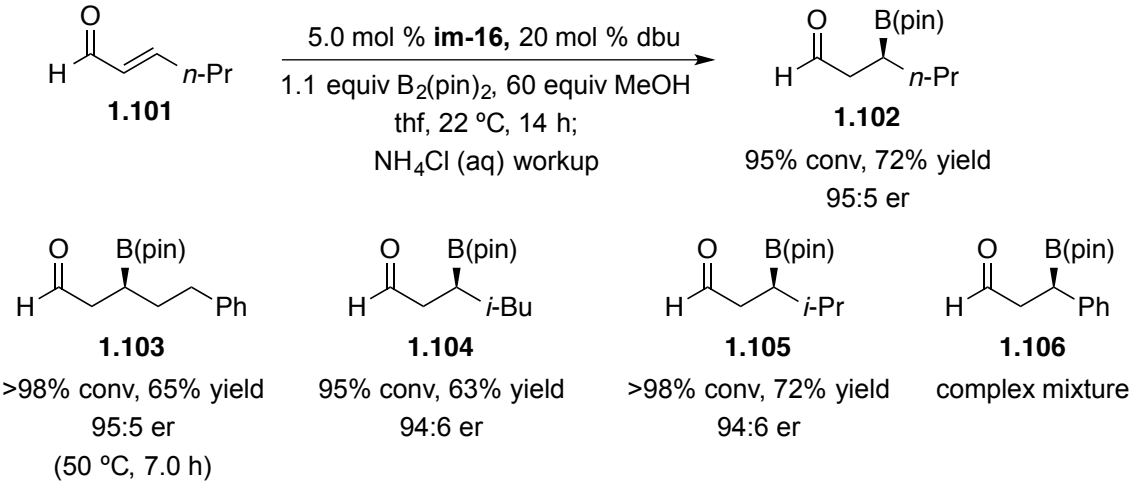

As shown in Scheme 1.25, the BCA reactions with alkyl-substituted enals are highly efficient (≥95% conv) and enantioselective (94:6–95:5 er). Due to the instability of β-boryl aldehydes on silica gel, there was discrepancy between conversions and yields after isolation (63–72% yield). Reaction with aryl-substituted unsaturated aldehydes (for example, cinnamaldehyde) results in a complex mixture probably due to reaction of an NHC with carbonyl unit forming a Breslow intermediate, as well as methoxide conjugate additions to unsaturated aldehydes (a byproduct also observed in the BCA reactions to alkyl-substituted enals).

1A.3.7. Functional Group Compatibilities of NHC-catalyzed Enantioselective BCA Reactions

In the Scheme 1.26, NHC-catalyzed enantioselective BCA reactions and the previously reported phosphine–Cu-catalyzed protocols[30] were tested in comparison in the presence of an equivalent of an additive. For the reaction with **1.76** without any additive, both methods are equally effective (>98% conv, 92–93% yield), although the enantioselectivity of the Cu-catalyzed reaction is slightly lower (85:15 er) likely because the optimal ligand is not Josiphos for this particular substrate. Addition of phenol does not affect the NHC-catalyzed protocol; however, the reaction is significantly slower in the phosphine–Cu-catalyzed reaction. This is probably due to inefficient reaction of phosphine–Cu-OPh with $B_2(pin)_2$ compared to phosphine-Cu-O*t*-Bu complex.

Scheme 1.26. NHC- or Cu-catalyzed enantioselective BCA reactions with a variety of additives

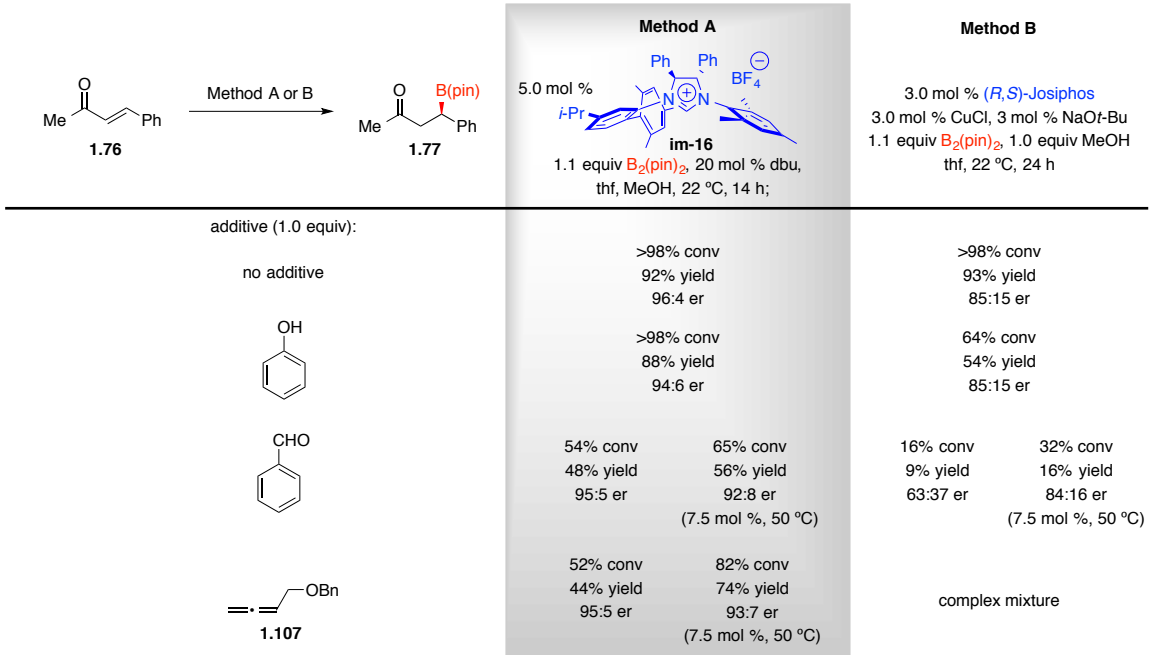

In the presence of benzaldehyde, both protocols proceeded with diminished efficiency. However, the NHC-catalyzed one proceeded to 54% conv (65% conv with higher catalyst loading and temperature), while the Cu-catalyzed alternative suffered

(30) (a) Lee, J.-E.; Yun, J. *Angew. Chem., Int. Ed.* **2008**, *47*, 145−147. (b) Sim, H.-S.; Feng, X.; Yun, J. *Chem. Eur. J.* **2009**, *15*, 1939−1943. (c) Feng, X.; Yun, J. *Chem.Eur. J.* **2010**, *16*, 13609−13612.

much more (only 16% conv). As mentioned before, NHC may reversibly react with benzaldehyde, forming a Breslow-type intermediate, but the Cu–B(pin) addition to the carbonyl moiety of the aldehyde is very efficient. Perhaps the most obvious example of chemoselectivity obtained from the NHC-catalyzed BCAs is when an equivalent of allene **1.107** was added. The reaction promoted by a chiral NHC proceeded to afford the desired product (74% yield, 93:7 er with 7.5 mol % catalyst at 50 °C). In contrast, the Cu-catalyzed reaction led to a complex mixture without any detectable product formation. This is probably because the Cu–B(pin) reacts efficiently with an allene.[31]

Scheme 1.27. NHC- or Cu-catalyzed enantioselective BCA reactions with enones containing an alkyne

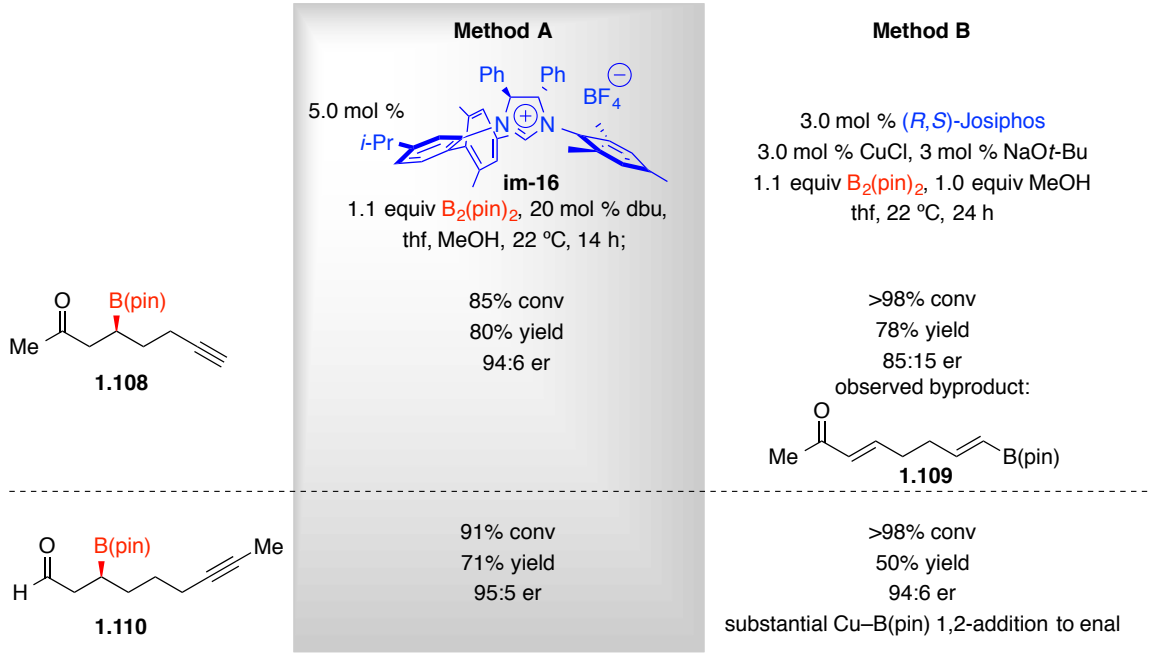

Another set of examples for demonstration of the functional group compatibility, we prepared substrates bearing an alkyne group. The NHC-catalyzed reactions proceed with high efficiency and enantioselectivity (71–80% yield, 94:6–95:5 er). While in the

(31) Jung, B.; Hoveyda, A. H. *J. Am. Chem. Soc.* **2012**, *134*, 1490−1493.

Cu-catalyzed protocol again suffers from reaction of the Cu–B(pin) with alkyne or aldehyde moiety.[32]

1A.4. Conclusions

The enantioselective NHC-catalyzed boryl conjugate addition reactions can be used to access a range of β-boryl carbonyls including ketones, esters, Weinreb amides and aldehydes. The metal-free strategy offers complementary reactivity and selectivity profiles to the previously reported Cu-catalyzed alternatives and thus rendering its potential utility in chemical synthesis. In addition, the finding relates to the critical role of methanol in the enantioselective BCAs (vs reactions with achiral NHCs) will be beneficial for other methods involving diboron reagents and sterically hindered chiral catalysts.

1A.5. Experimental Section

General. Infrared (IR) spectra were recorded on a Bruker FT-IR Alpha (ATR mode) spectrophotometer, ν_{max} in cm^{-1}. Bands are characterized as broad (br), strong (s), medium (m), and weak (w). ^{1}H NMR spectra were recorded on a Varian Unity INOVA 400 (400 MHz) spectrometer. Chemical shifts are reported in ppm from tetramethylsilane with the solvent resonance as the internal standard ($CDCl_3$: 7.26 ppm). Data are reported as follows: chemical shift, integration, multiplicity (s = singlet, d = doublet, t = triplet, q = quartet, m = multiplet), and coupling constants (Hz). ^{13}C NMR spectra were recorded on a Varian Unity INOVA 400 (100 MHz) spectrometer with complete proton

(32) For catalytic hydroborations of alkynes, which involve Cu−B additions, see: (a) Takahashi, K.; Ishiyama, T.; Miayura, N. *J. Organomet. Chem.* **2001**, *625*, 47−52. (b) Lee, J.-E.; Kwon, J.; Yun, J. *Chem. Commun.* **2008**, *44*, 733−734. (c) Kim, H. R.; Jung, I. G.; Yoo, K.; Jang, K.; Lee, E. S.; Yun, J.; Son, S. U. *Chem. Commun.* **2010**, *46*, 758−760. (d) Kim, H. R.; Yun, J. *Chem. Commun.* **2011**, *47*, 2943− 2945. (e) Jang, H.; Zhugralin, A. R.; Lee, Y.; Hoveyda, A. H. *J. Am. Chem. Soc.* **2011**, *133*, 7859−7871.

decoupling. Chemical shifts are reported in ppm from tetramethylsilane with the solvent resonance as the internal standard ($CDCl_3$: 77.16 ppm). ^{11}B NMR were recorded on a Varian Unity INOVA 500 (128 MHz) with $BF_3 \bullet OEt_2$ resonance as the external reference (d_8-thf: 0.0 ppm). High-resolution mass spectrometry was performed on a Micromass LCT ESI-MS (positive mode) at the Mass Spectrometry Facility, Boston College. Enantiomeric ratios were determined by GLC analysis (Alltech Associated Chiraldex GTA column (30 m x 0.25 mm), Chiraldex B-DM (30 m x 0.25 mm) and Chiraldex aTA (30 m x 0.25 mm)) and HPLC analysis (high-performance liquid chromatography) with a Shimadzu chromatograph (Chiral Technologies Chiralcel OJ-H (4.6 x 250 mm), Chiral Technologies Chiralcel OD-H (4.6 x 250 mm), Chiral Technologies Chiralpak AS-H (4.6 x 250 mm) or Chiral Technologies Chiralpak AD-H (4.6 x 250 mm)) in comparison with authentic racemic materials. Specific rotations were measured on a Rudolph Research Analytical Autopol IV Polarimeter.

Unless otherwise noted, reactions were carried out with distilled and degassed solvents under an atmosphere of dry N_2 in oven- (135 ºC) or flame-dried glassware with standard dry box or vacuum-line techniques. Tetrahydrofuran (Aldrich Chemical Co.) was purified by distillation from sodium benzophenone ketyl immediately prior to use. Methanol (Acros Organics 99.9% Extra Dry, AcroSeal$^{@}$) was used as received. All work-up and purification procedures were carried out with reagent grade solvents (purchased from Fisher Scientific) under air.

■ **Reagents:**

Bis(pinacolato)diboron [$B_2(pin)_2$]: gifts from Frontier Scientific Inc., recrystallized from pentane and dried under vacuum prior to use.

1,8-Diazabicyclo[5.4.0]undec-7-ene (dbu): purchased from Aldrich Chemical Co. and purified by distillation from CaH_2 prior to use.

(*E*)-4-Phenylbut-3-en-2-one (1.76): purchased from Aldrich Chemical Co., purified by recrystallization in pentane and dried under vacuum prior to use.

(*E*)-4-(4-Methoxyphenyl)but-3-en-2-one (substrate for 1.78): purchased from Aldrich Chemical Co. and used as received.

(*E*)-4-(Furan-2-yl)but-3-en-2-one (substrate for 1.80): purchased from Aldrich Chemical Co., purified by chromatography and dried under vacuum prior to use.

(*E*)-Non-3-en-2-one (substrate for 1.82): purchased from Aldrich Chemical Co. and purified by distillation from CaH_2 prior to use.

(*E*)-5-Methylhex-3-en-2-one (substrate for 1.83): purchased from Aldrich Chemical Co. and purified by distillation from CaH_2 prior to use.

(*E*)-Chalcone (substrate for 1.86): purchased from Aldrich Chemical Co., purified by chromatography and dried under vacuum prior to use.

Methyl cinnamate (1.89): purchased from Aldrich Chemical Co., purified by chromatography and dried under vacuum prior to use.

(*E*)-Methyl 3-(4-bromophenyl)acrylate (substrate for 1.91): purchased from Aldrich Chemical Co., purified by chromatography and dried under vacuum prior to use.

(*E*)-Methyl oct-2-enoate (substrate for 1.92): purchased from Aldrich Chemical Co. and purified by distillation from CaH_2 prior to use.

***tert*-Butyl cinnamate (1.82d):** purchased from Aldrich Chemical Co., purified by chromatography and dried under vacuum prior to use.

(*E*)-Hex-2-enal (1.101): purchased from Aldrich Chemical Co. and purified by distillation from CaH_2 prior to use.

(*E*)-4-Methylpent-2-enal (substrate for 1.105): purchased from Acros Organics and purified by distillation from CaH_2 prior to use.

Other α,β-unsaturated carbonyls: prepared according to Wittig olefinations of the corresponding aldehydes, which were purchased from Aldrich Chemical Co. and used as received.

■ **Representative Experimental Procedure for NHC–Catalyzed Enantioselective (Pinacolato)boron Conjugate Addition:** In a glovebox, an oven-dried vial (8 x 1 cm) equipped with a stir bar was charged with a solution of NHC, which was prepared from **im-16** (11 mg, 0.017 mmol), dbu (10 mg, 0.066 mmol), and thf (0.47 mL, 0.036 M solution of catalyst) for 30 min at 22 °C under a dry N_2 atmosphere. Bis(pinacolato)diboron (93 mg, 0.37 mmol), (*E*)-4-phenylbut-3-en-2-one (**1.76**) (49 mg, 0.33 mmol) and methanol (0.80 mL) were added to the vial (0.26 M solution of substrate), which was sealed with a cap before removal from the glovebox. The mixture was allowed to stir at 22 °C for 14 h, after which the reaction was quenched by the addition of an aqueous solution of NH_4Cl (1.0 mL, 0.7 M) and the mixture was allowed to stir for an additional 20 min. The aqueous layer was washed with diethyl ether (3 x 5 mL). The combined organic layers were dried over anhydrous $MgSO_4$ and filtered. The volatiles were removed under vacuum and the resulting light yellow oil was purified by silica gel chromatography (hexanes:Et_2O = 10:1) to afford 84 mg (0.31 mmol, 92% yield) of (*R*)-4-phenyl-4-(4,4,5,5-tetramethyl-1,3,2-dioxaborolan-2-yl)butan-2-one (**1.77**) as a colorless oil. **(*R*)-4-Phenyl-4-(4,4,5,5-tetramethyl-1,3,2-dioxaborolan-2-yl)butan-2-**

one (1.77): The spectroscopic data match those reported previously.[33] ^{1}H NMR (400 MHz, $CDCl_3$): δ 7.26–7.18 (4H, m), 7.14–7.10 (1H, m), 3.02 (1H, dd, *J* = 18.4, 10.8 Hz), 2.82 (1H, dd, *J* = 18.4, 5.6 Hz), 2.62 (1H, dd, *J* = 10.8, 5.6 Hz), 2.12 (3H, s), 1.20 (6H, s), 1.14 (6H, s); Specific Rotation: $[\alpha]_D^{20}$ –34.2 (*c* 1.06, $CHCl_3$) for an enantiomerically enriched sample of 96:4 er. Enantiomeric purity was determined by HPLC analysis in comparison with authentic racemic material (96:4 er shown; Chiralpak AS-H column, 98/2 hexanes/*i*-PrOH, 0.3 mL/min, 220 nm).

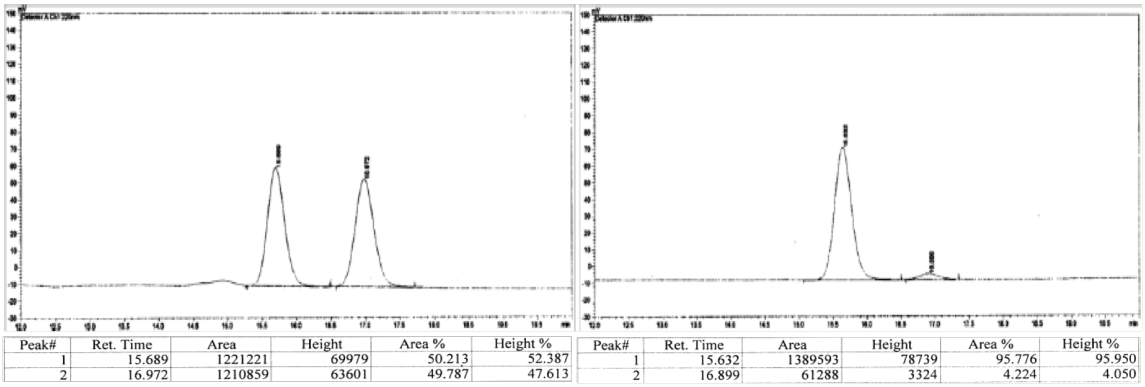

Peak#	Ret. Time	Area	Height	Area %	Height %
1	15.689	1221221	69979	50.213	52.387
2	16.972	1210859	63601	49.787	47.613

Peak#	Ret. Time	Area	Height	Area %	Height %
1	15.632	1389593	78739	95.776	95.950
2	16.899	61288	3324	4.224	4.050

Peak #	Time (min)	Area (%)	Peak #	Time (min)	Area (%)
1	15.689	50.213	1	15.632	95.776
2	16.972	49.787	2	16.899	4.224

Proof of Stereochemistry: The corresponding (*R*)-4-hydroxy-4-phenylbutan-2-one was obtained after oxidation of **1.77**, the spectroscopic data match those reported previously.[33] Specific Rotation of (*R*)-4-hydroxy-4-phenylbutan-2-one: $[\alpha]_D^{20}$ +64.3 (*c* 0.83, $CHCl_3$). Literature value ($[\alpha]_D^{20}$ –49.0 (*c* 0.52, $CHCl_3$), 89.5:10.5 er) is assigned to the (*S*) enantiomer.[33]

(33) Sim, H.-S.; Feng, X.; Yun, J. *Chem. Eur. J.* **2009**, *15*, 1939–1943

(*E*)-4-(*o*-Tolyl)but-3-en-2-one (substrate for 1.81): The spectroscopic data match those reported previously.[34] ^{1}H NMR (400 MHz, $CDCl_3$): δ 7.79 (1H, d, *J* = 16.4 Hz), 7.55–7.53 (1H, m), 7.28–7.17 (3H, m), 6.62 (1H, d, *J* = 16.4 Hz), 2.42 (3H, s), 2.36 (3H, s).

(*R*)-4-(4,4,5,5-Tetramethyl-1,3,2-dioxaborolan-2-yl)-4-(*o*-tolyl)butan-2-one (1.81): IR (neat): 2976 (m), 1713 (s), 1356 (s), 1318 (s), 1259 (m), 1214 (m), 1165 (m), 1140 (s), 1012 (w), 966 (m), 852 (m), 771 (m), 754 (m) cm^{-1}; ^{1}H NMR (400 MHz, $CDCl_3$): δ 7.17–7.00 (4H, m), 3.00 (1H, dd, *J* = 17.6, 10.4 Hz), 2.85 (1H, dd, *J* = 10.4, 4.8 Hz), 2.74 (1H, dd, *J* = 17.6, 4.8 Hz), 2.33 (3H, s), 2.12 (3H, s), 1.20 (6H, s), 1.14 (6H, s); ^{13}C NMR (100 MHz, $CDCl_3$): δ 208.5, 140.1, 136.2, 130.4, 127.6, 126.0, 125.4, 83.3, 46.9, 29.6, 24.5, 24.5, 20.0; HRMS (ESI+): Calcd for $C_{17}H_{26}B_1O_3$ $[M+H]^+$: 289.1975, Found: 289.1977. Specific Rotation: $[\alpha]_D^{20}$ –18.7 (*c* 1.07, $CHCl_3$) for an enantiomerically enriched sample of 85.5:14.5 er. Enantiomeric purity was determined by HPLC analysis in comparison with authentic racemic material (85.5:14.5 er shown; Chiralcel OD-H column, 99/1 hexanes/*i*-PrOH, 0.3 mL/min, 220 nm).

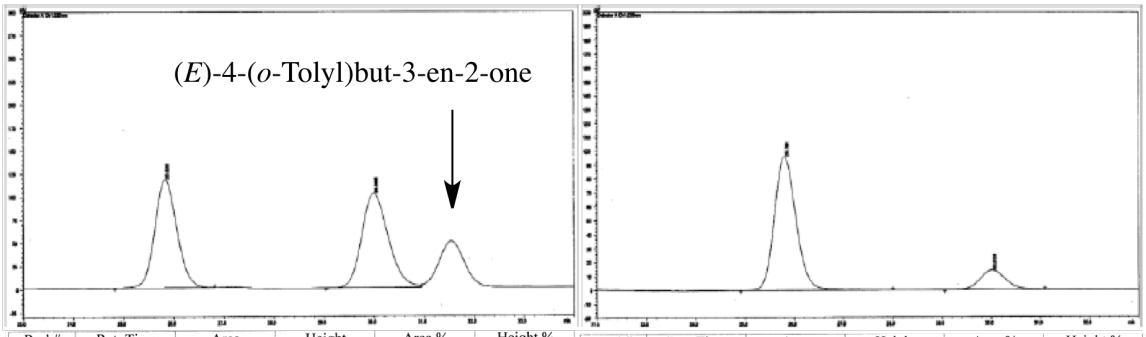

Peak#	Ret. Time	Area	Height	Area %	Height %
1	25.820	3598601	117051	48.956	53.448
2	29.986	3752098	101947	51.044	46.552

Peak#	Ret. Time	Area	Height	Area %	Height %
1	25.791	2938186	96094	85.556	87.335
2	30.010	496027	13936	14.444	12.665

Peak #	Time (min)	Area (%)	Peak #	Time (min)	Area (%)
1	25.820	48.956	1	25.791	85.556
2	29.986	51.044	2	30.010	14.444

(34) Cá, N. D.; Motti, E.; Mega, A.; Catellani, M. *Adv. Synth. Catal.* **2010**, *352*, 1451–1454.

(*R*)-4-(4-Methoxyphenyl)-4-(4,4,5,5-tetramethyl-1,3,2-dioxaborolan-2-yl)butan-2-one (1.78): The spectroscopic data match those reported previously.[35] ^{1}H NMR (400 MHz, $CDCl_3$): δ 7.13–7.09 (2H, m), 6.80–6.76 (2H, m), 3.75 (3H, s), 2.96 (1H, dd, *J* = 18.2, 10.6 Hz), 2.78 (1H, dd, *J* = 18.2, 5.6 Hz), 2.56 (1H, dd, *J* = 10.6, 5.6 Hz), 2.11 (3H, s), 1.20 (6H, s), 1.15 (6H, s); Specific Rotation: $[\alpha]_D^{20}$ –29.1 (*c* 1.07, $CHCl_3$) for an enantiomerically enriched sample of 94:6 er. Enantiomeric purity was determined by HPLC analysis in comparison with authentic racemic material (94:6 er shown; Chiralcel OD-H column, 98/2 hexanes/*i*-PrOH, 0.3 mL/min, 220 nm).

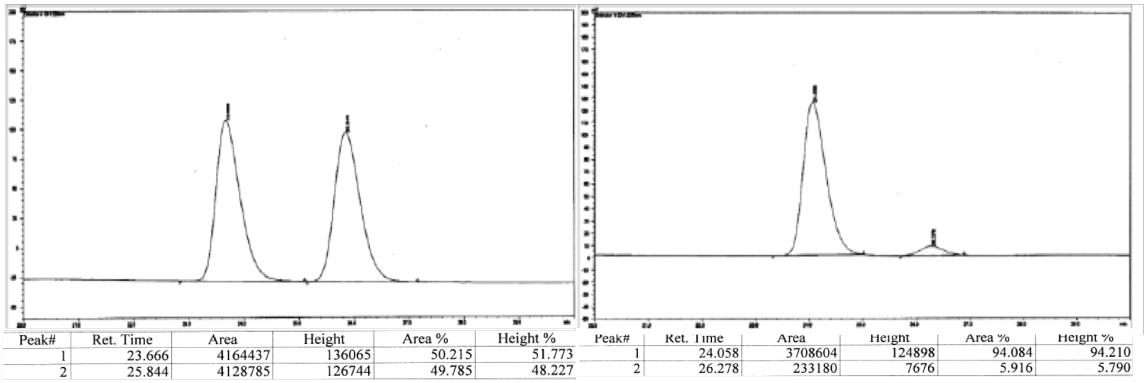

Peak#	Ret. Time	Area	Height	Area %	Height %
1	23.666	4164437	136065	50.215	51.773
2	25.844	4128785	126744	49.785	48.227

Peak#	Ret. Time	Area	Height	Area %	Height %
1	24.058	3708604	124898	94.084	94.210
2	26.278	233180	7676	5.916	5.790

Peak #	Time (min)	Area (%)	Peak #	Time (min)	Area (%)
1	23.666	50.215	1	24.058	94.084
2	25.844	49.785	2	26.278	5.916

(*E*)-4-(4-Bromophenyl)but-3-en-2-one (substrate for 1.79): The spectroscopic data match those reported previously.[36] ^{1}H NMR (400 MHz, $CDCl_3$): δ 7.52 (2H, d, *J* = 8.4 Hz), 7.43 (1H, d, *J* = 16.4 Hz), 7.39 (2H, d, *J* = 8.4 Hz), 6.68 (1H, d, *J* = 16.4 Hz), 2.36 (3H, s).

(*R*)-4-(4-Bromophenyl)-4-(4,4,5,5-tetramethyl-1,3,2-dioxaborolan-2-yl)butan-2-one (1.79): IR (neat): 2957 (m), 2922 (s), 2853 (m), 1707 (m), 1362 (m), 1327 (m), 1142 (m)

(35) Shiomi, T.; Adachi, T.; Toribatake, K.; Zhou, L.; Nishiyama, H. *Chem. Commun.* **2009**, 5987–5989.
(36) Stern, T.; Rückbrod, S.; Czekelius, C.; Donner, C.; Brunner, H. *Adv. Synth. Catal.* **2010**, *352*, 1983–1992.

cm^{-1}; ^{1}H NMR (400 MHz, $CDCl_3$): δ 7.36 (2H, d, *J* = 8.4 Hz), 7.09 (2H, d, *J* = 8.4 Hz), 2.99 (1H, dd, *J* = 18.4, 10.4 Hz), 2.81 (1H, dd, *J* = 18.4, 5.6 Hz), 2.60 (1H, dd, *J* = 10.4, 5.6 Hz), 2.14 (3H, s), 1.21 (6H, s), 1.16 (6H, s); ^{13}C NMR (100 MHz, $CDCl_3$): δ 208.1, 141.0, 131.6, 130.1, 119.5, 83.7, 47.4, 29.8, 24.7; HRMS (ESI+): Calcd for $C_{16}H_{23}B_1Br_1O_3$ $[M+H]^+$: 353.0924, Found: 353.0908. Specific Rotation: $[\alpha]_D^{20}$ –7.2 (*c* 0.33, $CHCl_3$) for an enantiomerically enriched sample of 92:8 er. Enantiomeric purity was determined by HPLC analysis in comparison with authentic racemic material (92:8 er shown; Chiralpak AS-H column, 99/1 hexanes/*i*-PrOH, 0.3 mL/min, 220 nm).

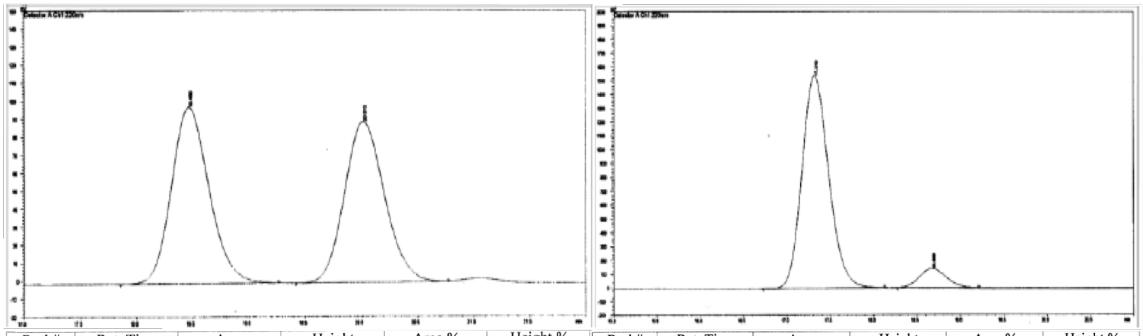

Peak#	Ret. Time	Area	Height	Area %	Height %
1	18.460	2283801	98020	50.801	52.269
2	20.013	2211799	89509	49.199	47.731

Peak#	Ret. Time	Area	Height	Area %	Height %
1	17.310	33200851	1540116	91.628	91.682
2	18.669	3033602	139724	8.372	8.318

Peak #	Time (min)	Area (%)	Peak #	Time (min)	Area (%)
1	18.460	50.801	1	17.310	91.628
2	20.013	49.199	2	18.669	8.372

(*R*)-4-(Furan-2-yl)-4-(4,4,5,5-tetramethyl-1,3,2-dioxaborolan-2-yl)butan-2-one (1.80): IR (neat): 2978 (m), 2928 (m), 1714 (s), 1359 (s), 1324 (s), 1165 (s), 1124 (s), 1008 (m), 850 (m), 727 (m), 799 (m) cm^{-1}; ^{1}H NMR (400 MHz, $CDCl_3$): δ 7.21–7.19 (1H, m), 6.19–6.18 (1H, m), 5.95–5.94 (1H, m), 2.95–2.81 (2H, m), 2.70–2.66 (1H, m), 2.08 (3H, s), 1.19 (6H, s), 1.16 (6H, s); ^{13}C NMR (100 MHz, $CDCl_3$): δ 207.8, 155.1, 140.9, 110.2, 104.9, 83.7, 44.5, 29.5, 24.6, 24.5; HRMS (ESI+): Calcd for $C_{14}H_{22}B_1O_4$ $[M+H]^+$: 265.1611, Found: 265.1616. Specific Rotation: $[\alpha]_D^{20}$ –2.7 (*c* 1.10, $CHCl_3$) for an enantiomerically enriched sample of 92:8 er. Enantiomeric purity was determined by

HPLC analysis in comparison with authentic racemic material (92:8 er shown; Chiralpak AS-H column, 99.5/0.5 hexanes/*i*-PrOH, 0.3 mL/min, 220 nm).

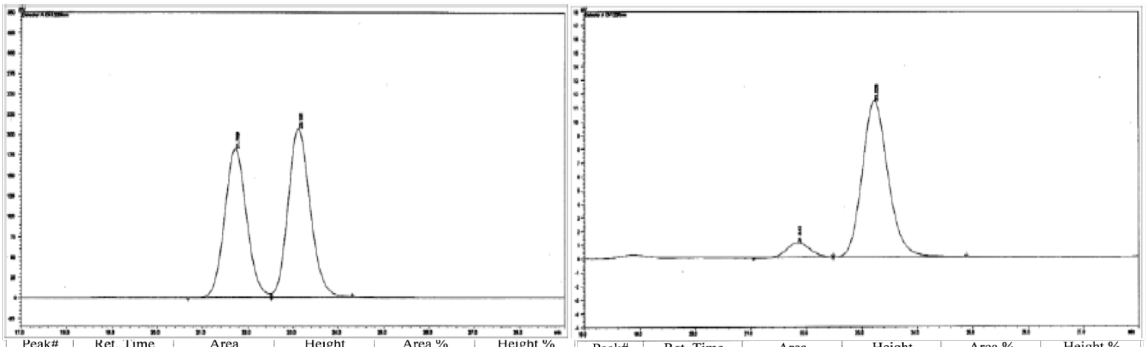

Peak#	Ret. Time	Area	Height	Area %	Height %
1	21.709	6139232	181902	46.698	46.835
2	23.101	7007475	206483	53.302	53.165

Peak#	Ret. Time	Area	Height	Area %	Height %
1	21.842	30843	1066	7.711	8.572
2	23.223	369153	11366	92.289	91.428

Peak #	Time (min)	Area (%)	Peak #	Time (min)	Area (%)
1	21.709	46.698	1	21.842	7.711
2	23.101	53.302	2	23.223	92.289

(*S*)-4-(4,4,5,5-Tetramethyl-1,3,2-dioxaborolan-2-yl)nonan-2-one (1.82): IR (neat): 2976 (w), 2958 (m), 2925 (m), 1715 (s), 1410 (s), 1379 (s), 1312 (s), 1266 (w), 1244 (w), 1214 (w), 1143 (s), 968 (m), 857 (m), 670 (m) cm^{-1}; ^{1}H NMR (400 MHz, $CDCl_3$): δ 2.53 (2H, apparent d), 2.08 (3H, s), 1.40–1.34 (1H m), 1.29–1.19 (20H, m), 0.83 (3H, apparent t); ^{13}C NMR (100 MHz, $CDCl_3$): δ 209.2, 82.9, 45.8, 31.9, 30.3, 29.6, 28.5, 24.7, 24.6, 22.5, 14.0; HRMS (ESI+): Calcd for $C_{15}H_{30}B_1O_3$ $[M+H]^+$: 269.2288, Found: 269.2279. Specific Rotation: $[\alpha]_D^{20}$ +0.8 (*c* 1.00, $CHCl_3$) for an enantiomerically enriched sample of 94:6 er. Enantiomeric purity was determined by HPLC analysis in comparison with authentic racemic material (94:6 er shown; Chiralpak AD-H column, 99.8/0.2 hexanes/*i*-PrOH, 0.3 mL/min, 300 nm).

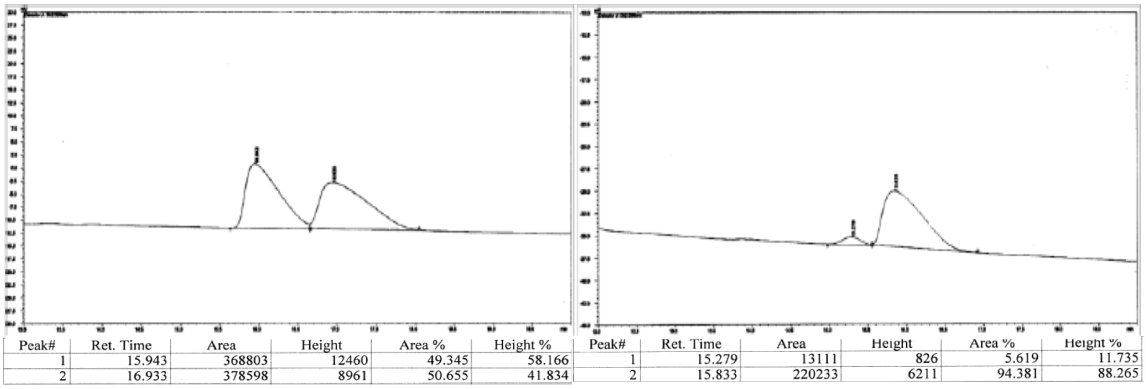

Peak#	Ret. Time	Area	Height	Area %	Height %
1	15.943	368803	12460	49.345	58.166
2	16.933	378598	8961	50.655	41.834

Peak#	Ret. Time	Area	Height	Area %	Height %
1	15.279	13111	826	5.619	11.735
2	15.833	220233	6211	94.381	88.265

Peak #	Time (min)	Area (%)	Peak #	Time (min)	Area (%)
1	15.943	49.343	1	15.279	5.619
2	16.933	50.635	2	15.833	94.387

(*R*)-5-Methyl-4-(4,4,5,5-tetramethyl-1,3,2-dioxaborolan-2-yl)hexan-2-one (1.83): IR (neat): 2976 (m), 2958 (m), 1715 (s), 1412 (w), 1371 (s), 1310 (s), 1279 (s), 1214 (m), 1165 (m), 1142 (s), 1123 (s), 969 (w), 850 (m) cm^{-1}; ^{1}H NMR (400 MHz, $CDCl_3$): δ 2.59 (1H, dd, *J* = 18.4, 11.2 Hz), 2.48 (1H, dd, *J* = 18.4, 4.8 Hz), 2.09 (3H, s), 1.71–1.63 (1H, m), 1.23–1.13 (13H, m), 0.91–0.88 (6H, m); ^{13}C NMR (100 MHz, $CDCl_3$): δ 209.5, 82.9, 43.8, 29.7, 28.9, 25.0, 24.9, 24.7, 22.1, 21.6; HRMS (ESI+): Calcd for $C_{13}H_{26}B_1O_3$ $[M+H]^+$: 241.1975, Found: 241.1984. Specific Rotation: $[\alpha]_D^{20}$ +1.2 (*c* 1.80, $CHCl_3$) for an enantiomerically enriched sample of 94:6 er. Enantiomeric purity was determined by HPLC analysis in comparison with authentic racemic material (94:6 er shown; Chiralcel OD-H column, 99.9/0.1 hexanes/*i*-PrOH, 0.3 mL/min, 300 nm).

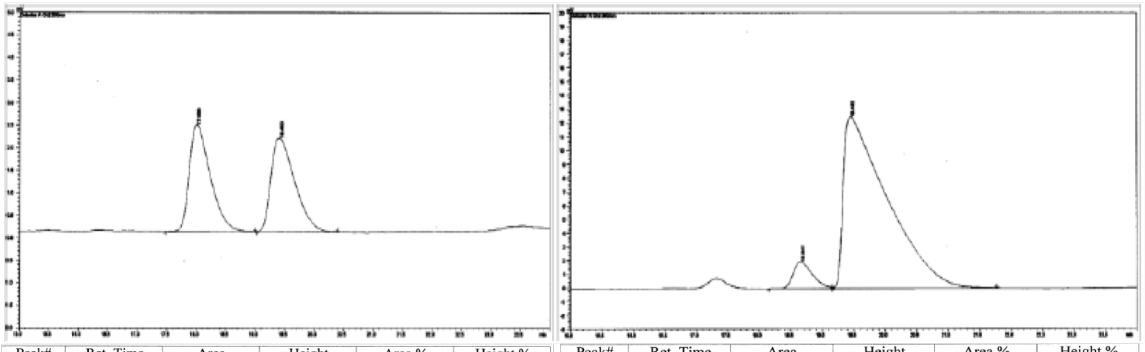

Peak#	Ret. Time	Area	Height	Area %	Height %
1	17.999	59414	2379	50.558	53.289
2	19.403	58102	2085	49.442	46.711

Peak#	Ret. Time	Area	Height	Area %	Height %
1	18.647	41086	1953	6.344	13.555
2	19.442	606515	12457	93.656	86.445

Peak #	Time (min)	Area (%)	Peak #	Time (min)	Area (%)
1	17.999	50.558	1	18.647	6.344
2	19.403	49.442	2	19.442	93.656

(*E*)-1-Phenylhept-1-en-3-one (substrate for 1.84): The spectroscopic data match those reported previously.[37] ^{1}H NMR (400 MHz, $CDCl_3$): δ 7.55–7.51 (3H, m), 7.39–7.37 (3H, m), 6.73 (1H, d, J = 16.4 Hz), 2.65 (2H, t, J = 7.2 Hz), 1.69–1.61 (2H, m), 1.42–1.33 (2H, m), 0.93 (3H, t, J = 7.2 Hz).

(*R*)-1-Phenyl-1-(4,4,5,5-tetramethyl-1,3,2-dioxaborolan-2-yl)heptan-3-one (1.84): IR (neat): 2976 (m), 2931 (m), 1709 (s), 1369 (s), 1319 (s), 1280 (m), 1261 (w), 1214 (w), 1141 (s), 1124 (s), 968 (m), 850 (m), 701 (s) cm^{-1}; ^{1}H NMR (400 MHz, $CDCl_3$): δ 7.25–7.18 (4H, m), 7.14–7.10 (1H, m), 2.99 (1H, dd, J = 18.2, 10.8 Hz), 2.78 (1H, dd, J = 18.2, 5.2 Hz), 2.63 (1H, dd, J = 10.8, 5.2 Hz), 2.44–2.25 (2H, m), 1.58–1.50 (2H, m), 1.33–1.24 (2H, m), 1.20 (6H, s), 1.14 (6H, s), 0.87 (3H, apparent t); ^{13}C NMR (100 MHz, $CDCl_3$): δ 210.8, 141.8, 128.4, 128.2, 125.5, 83.3, 46.6, 42.2, 26.2, 24.5, 24.5, 22.3, 13.8; HRMS (ESI+): Calcd for $C_{19}H_{30}B_1O_3$ $[M+H]^+$: 317.2288, Found: 317.2297. Specific Rotation: $[\alpha]_D^{20}$ –21.0 (*c* 1.34, $CHCl_3$) for an enantiomerically enriched sample of 91:9 er. Enantiomeric purity was determined by HPLC analysis in comparison with authentic racemic material (91:9 er shown; Chiralcel OJ-H column, 98/2 hexanes/*i*-PrOH, 0.3 mL/min, 220 nm).

(37) Badioli, M.; Ballini, R.; Bartolacci, M.; Bosica, G.; Torregiani, E.; Marcantoni, E. *J. Org. Chem.* **2002**, *67*, 8938–8942.

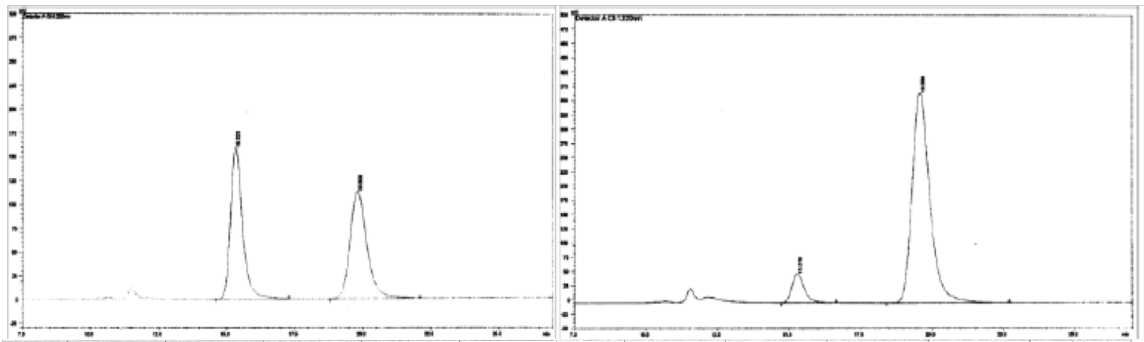

Peak#	Ret. Time	Area	Height	Area %	Height %
1	15.323	4859526	159419	49.918	58.619
2	19.806	4875440	112537	50.082	41.381

Peak#	Ret. Time	Area	Height	Area %	Height %
1	15.278	1492188	50800	8.601	12.089
2	19.556	15857595	369410	91.399	87.911

Peak #	Time (min)	Area (%)	Peak #	Time (min)	Area (%)
1	15.323	49.918	1	15.278	8.601
2	19.806	50.082	2	19.556	91.399

(*E*)-4-Methyl-1-phenylpent-1-en-3-one (substrate for 1.85): The spectroscopic data match those reported previously.[38] ^{1}H NMR (400 MHz, $CDCl_3$): δ 7.60 (1H, d, J = 16.0 Hz), 7.56–7.53 (2H, m), 7.40–7.36 (3H, m), 6.80 (1H, d, J = 16.4 Hz), 2.97–2.87 (1H, m), 1.18 (3H, s), 1.16 (3H, s).

(*R*)-4-Methyl-1-phenyl-1-(4,4,5,5-tetramethyl-1,3,2-dioxaborolan-2-yl)pentan-3-one (1.85): The spectroscopic data match those reported previously.[33] ^{1}H NMR (400 MHz, $CDCl_3$): δ 7.25–7.19 (4H, m), 7.14–7.10 (1H, m), 3.03 (1H, dd, J = 18.2, 11.2 Hz), 2.82 (1H, dd, J = 18.2, 4.8 Hz), 2.63 (1H, dd, J = 11.2, 4.8 Hz), 2.59–2.53 (1H, m), 1.20 (6H, s), 1.13 (6H, s), 1.09–1.04 (6H, m); Specific Rotation: $[\alpha]_D^{20}$ –20.3 (*c* 1.07, $CHCl_3$) for an enantiomerically enriched sample of 90:10 er. Enantiomeric purity was determined by HPLC analysis in comparison with authentic racemic material (90:10 er shown; Chiralpak AS-H column, 98/2 hexanes/*i*-PrOH, 0.3 mL/min, 220 nm).

(38) Gillmore, A.; Lauret, C.; Roberts, S. M. *Tetrahedron,* **2003**, *59*, 4363–4375.

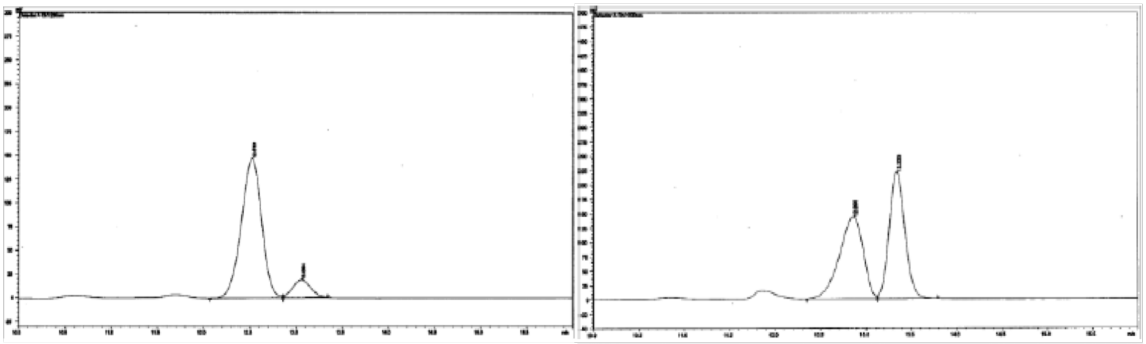

Peak#	Ret. Time	Area	Height	Area %	Height %
1	12.855	2577826	142585	49.099	39.254
2	13.333	2672412	220656	50.901	60.746

Peak#	Ret. Time	Area	Height	Area %	Height %
1	12.519	2250201	147162	89.879	88.721
2	13.054	253385	18708	10.121	11.279

Peak #	Time (min)	Area (%)	Peak #	Time (min)	Area (%)
1	12.855	49.099	1	12.519	89.879
2	13.333	50.901	2	13.054	10.121

(*R*)-1,3-Diphenyl-3-(4,4,5,5-tetramethyl-1,3,2-dioxaborolan-2-yl)propan-1-one (1.86): The spectroscopic data match those reported previously.[36] ^{1}H NMR (400 MHz, $CDCl_3$): δ 7.97–7.94 (2H, m), 7.55–7.50 (1H, m), 7.44–7.40 (2H, m), 7.31–7.24 (4H, m), 7.17–7.13 (1H, m), 3.54 (1H, dd, J = 18.4, 10.8 Hz), 3.41 (1H, dd, J = 18.4, 5.2 Hz), 2.79 (1H, dd, J = 10.8, 5.2 Hz), 1.23 (6H, s), 1.15 (6H, s); Specific Rotation: $[\alpha]_D^{20}$ –18.7 (*c* 1.10, $CHCl_3$) for an enantiomerically enriched sample of 94:6 er. Enantiomeric purity was determined by HPLC analysis in comparison with authentic racemic material (94:6 er shown; Chiralcel OJ-H column, 98/2 hexanes/*i*-PrOH, 0.3 mL/min, 220 nm).

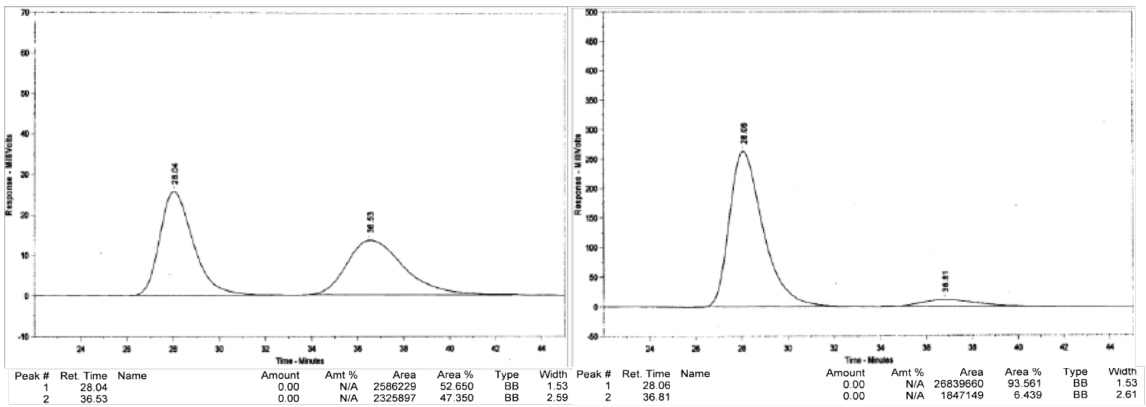

Peak #	Ret. Time	Name	Amount	Amt %	Area	Area %	Type	Width
1	28.04		0.00	N/A	2586229	52.650	BB	1.53
2	36.53		0.00	N/A	2325897	47.350	BB	2.59

Peak #	Ret. Time	Name	Amount	Amt %	Area	Area %	Type	Width
1	28.06		0.00	N/A	26839660	93.561	BB	1.53
2	36.81		0.00	N/A	1847149	6.439	BB	2.61

Peak #	Time (min)	Area (%)	Peak #	Time (min)	Area (%)
1	28.04	52.650	1	28.06	93.561
2	36.53	47.350	2	36.81	6.439

(*E*)-4-(4-Fluorophenyl)but-3-en-2-one (substrate for 1.87): The compound has been previously reported and spectra data match those previously described.[38] ^{1}H NMR (400 MHz, $CDCl_3$): δ 7.56–7.50 (2H, m), 7.48 (1H, d, *J* = 16.4 Hz), 7.12–7.06 (2H, m), 6.65 (1H, d, *J* = 16.4 Hz), 2.37 (3H, s).

(*R*)-4-(4-Fluorophenyl)-4-(4,4,5,5-tetramethyl-1,3,2-dioxaborolan-2-yl)butan-2-one (1.87): IR (neat): 2977 (m), 2926 (m), 2854 (w), 1714 (m), 1508 (s), 1362 (s), 1322 (s), 1261 (m), 1220 (m), 1166 (m), 1142 (s) cm^{-1}; ^{1}H NMR (400 MHz, $CDCl_3$): δ 7.19–7.14 (2H, m), 7.98–6.91 (2H, m), 2.99 (1H, dd, *J* = 18.4, 10.4 Hz), 2.81 (1H, dd, *J* = 18.2, 5.4 Hz), 2.61 (1H, dd, *J* = 10.4, 5.2 Hz), 2.13 (3H, s), 1.22 (6H, s), 1.16 (6H, s); ^{13}C NMR (100 MHz, $CDCl_3$): δ 208.3, 161.2 (d, *J* = 241.8 Hz), 137.4 (d, *J* = 3 Hz), 129.7 (d, *J* = 8.2 Hz), 115.3 (d, *J* = 20.9 Hz), 83.6, 47.7, 29.8, 29.7, 24.7; HRMS (ESI+): Calcd for $C_{16}H_{23}B_1F_1O_3$ $[M+H]^+$: 293.1724, Found: 293.1719. Specific Rotation: $[\alpha]_D^{20}$ –26.5 (*c* 0.25, $CHCl_3$) for an enantiomerically enriched sample of >99:1 er. Enantiomeric purity was determined by HPLC analysis in comparison with authentic racemic material (>99:1 er shown; Chiralpak AD-H column, 99/1 hexanes/*i*-PrOH, 0.3 mL/min, 220 nm).

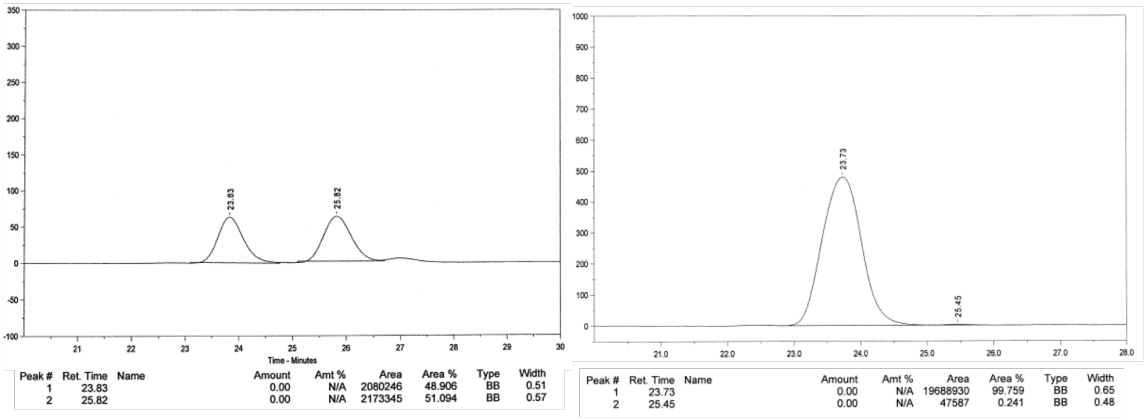

Peak #	Time (min)	Area (%)	Peak #	Time (min)	Area (%)
1	23.83	48.906	1	23.73	99.759
2	25.82	51.094	2	25.45	0.241

(*E*)-4-(4-Chlorophenyl)but-3-en-2-one (substrate for 1.88): The compound has been previously reported and spectra data match those previously described.[36] ^{1}H NMR (400 MHz, $CDCl_3$): δ 7.50–7.44 (3H, m), 7.39–7.36 (2H, m), 6.69 (1H, d, J = 16.4 Hz), 2.38 (3H, s).

(*R*)-4-(4-Chlorophenyl)-4-(4,4,5,5-tetramethyl-1,3,2-dioxaborolan-2-yl)butan-2-one (1.88): IR (neat): 2975 (m), 2925 (m), 2851 (w), 1707 (s), 1491 (w), 1418 (w), 1359 (s), 1325 (s), 1312 (m), 1141 (s) cm^{-1}; ^{1}H NMR (400 MHz, $CDCl_3$): δ 7.22 (2H, d, J = 8.4 Hz), 7.14 (2H, d, J = 8.4 Hz), 2.99 (1H, dd, J = 18.4, 10.4 Hz), 2.82 (1H, dd, J = 18.4, 5.6 Hz), 2.61 (1H, dd, J = 10.2, 5.4 Hz), 2.14 (3H, s), 1.21 (6H, s), 1.16 (6H, s); ^{13}C NMR (100 MHz, $CDCl_3$): δ 208.2, 140.4, 131.4, 129.7, 128.7, 83.7, 47.4, 29.9, 29.7, 24.7; HRMS (ESI+): Calcd for $C_{16}H_{23}B_1Cl_1O_3$ $[M+H]^+$: 309.1429, Found: 309.1429. Specific Rotation: $[\alpha]_D^{20}$ –12.0 (*c* 0.12, $CHCl_3$) for an enantiomerically enriched sample of 95:5 er. Enantiomeric purity is determined by HPLC analysis in comparison with authentic racemic material (95:5 er shown; Chiralpak AS-H column, 99.5/0.5 hexanes/*i*-PrOH, 0.3 mL/min, 220 nm).

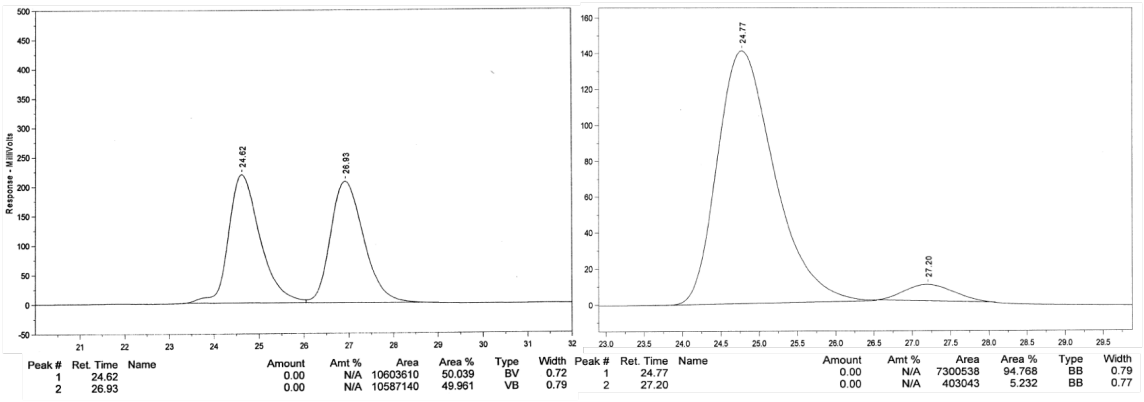

Peak #	Time (min)	Area (%)	Peak #	Time (min)	Area (%)
1	24.62	50.039	1	24.77	94.768
2	26.93	49.961	2	27.20	5.232

(*R*)-Methyl-3-phenyl-3-(4,4,5,5-tetramethyl-1,3,2-dioxaborolan-2-yl)propanoate (1.90): The spectroscopic data match those reported previously.[39] ^{1}H NMR (400 MHz, $CDCl_3$): δ 7.26–7.18 (4H, m), 7.15–7.11 (1H, m), 3.63 (3H, s), 2.88 (1H, dd, J = 15.8, 9.6 Hz), 2.74–2.61 (2H, m), 1.24 (6H, s), 1.15 (6H, s); Specific Rotation: $[\alpha]_D^{20}$ –20.3 (*c* 1.05, $CHCl_3$) for an enantiomerically enriched sample of 98:2 er. Enantiomeric purity was determined by HPLC analysis in comparison with authentic racemic material (98:2 er shown; Chiralcel OJ-H column, 98/2 hexanes/*i*-PrOH, 0.3 mL/min, 220 nm).

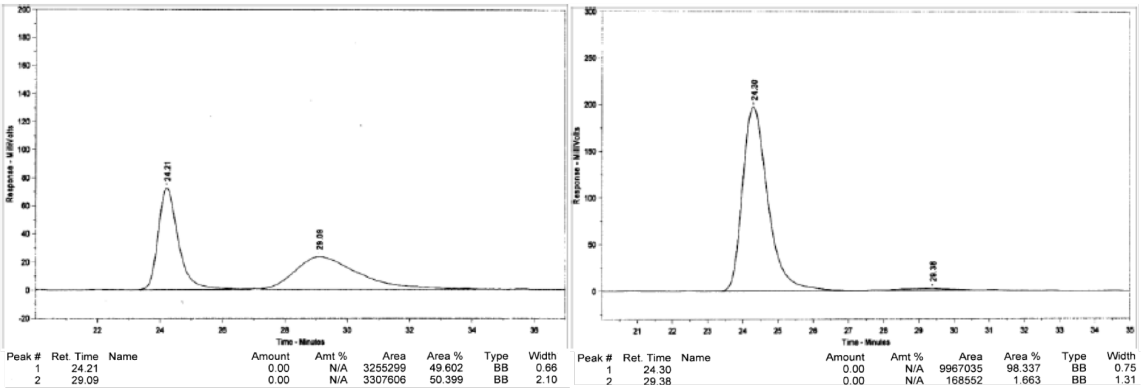

Peak #	Time (min)	Area (%)	Peak #	Time (min)	Area (%)
1	24.21	49.602	1	24.30	98.337
2	29.09	50.399	2	29.38	1.663

(*R*)-Methyl-3-(4-bromophenyl)-3-(4,4,5,5-tetramethyl-1,3,2-dioxaborolan-2-yl)propanoate (1.91): IR (neat): 2976 (m), 2953 (m), 2924 (m), 2853 (w), 1736 (s), 1487 (m), 1437 (m), 1370 (s), 1327 (s), 1169 (m), 1141 (s), 1011 (m), 847 (m) cm^{-1}; ^{1}H NMR (400 MHz, $CDCl_3$): δ 7.37 (2H, d, J = 8.4 Hz), 7.09 (2H, d, J = 8.4 Hz), 3.64 (3H, s), 2.85 (1H, dd, J = 15.4, 8.6 Hz), 2.71–2.61 (2H, m), 1.21 (6H, s), 1.17 (6H, s); ^{13}C NMR (100 MHz, $CDCl_3$): δ 173.9, 140.8, 131.9, 130.3, 119.9, 84.1, 52.0, 37.2, 30.1, 30.5, 24.9,

(39) Park, J. K.; Lackey, H. H.; Rexford, M. D.; Kovnir, K.; Shatruk, M.; McQuade, D. T. *Org. Lett.* **2010**, *12*, 5008–5011.

24.8; HRMS (ESI+): Calcd for $C_{16}H_{23}B_1Br_1O_4$ $[M+H]^+$: 369.0873, Found: 369.0872. Specific Rotation: $[\alpha]_D^{20}$ –10.2 (*c* 0.32, $CHCl_3$) for an enantiomerically enriched sample of 94:6 er. Enantiomeric purity was determined by HPLC analysis in comparison with authentic racemic material (94:6 er shown; Chiralcel OJ-H column, 99/1 hexanes/*i*-PrOH, 0.3 mL/min, 220 nm).

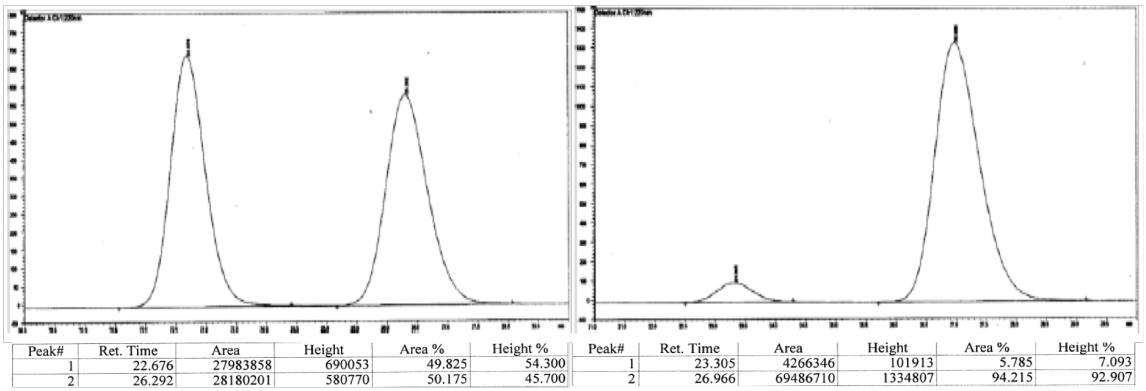

Peak#	Ret. Time	Area	Height	Area %	Height %
1	22.676	27983858	690053	49.825	54.300
2	26.292	28180201	580770	50.175	45.700

Peak#	Ret. Time	Area	Height	Area %	Height %
1	23.305	4266346	101913	5.785	7.093
2	26.966	69486710	1334807	94.215	92.907

Peak #	Time (min)	Area (%)	Peak #	Time (min)	Area (%)
1	22.676	49.825	1	23.305	5.785
2	26.292	50.175	2	26.966	94.215

(*S*)-Methyl-3-(4,4,5,5-tetramethyl-1,3,2-dioxaborolan-2-yl)octanoate (1.92): IR (neat): 2978 (m), 2927 (m), 2857 (w), 1737 (s), 1371 (m), 1318 (m), 1280 (s), 1168 (m), 1143 (s), 1124 (s), 850 (s) cm^{-1}; ^1H NMR (400 MHz, $CDCl_3$): δ 3.61 (3H, s), 2.44–2.32 (2H, m), 1.44–1.37 (1H, m), 1.32–1.20 (20H, m), 0.84 (3H, apparent t); ^{13}C NMR (100 MHz, $CDCl_3$): δ 174.4, 83.1, 51.3, 35.6, 31.9, 30.5, 28.3, 24.7, 24.6, 22.5, 14.0; HRMS (ESI+): Calcd for $C_{15}H_{30}B_1O_4$ $[M+H]^+$: 285.2237, Found: 285.2236. Specific Rotation: $[\alpha]_D^{20}$ +2.5 (*c* 0.85, $CHCl_3$) for an enantiomerically enriched sample of 95:5 er. Enantiomeric purity was determined by GLC analysis in comparison with authentic racemic material (95:5 er shown; Chiraldex B-DM column, 15 psi, 90 ºC).

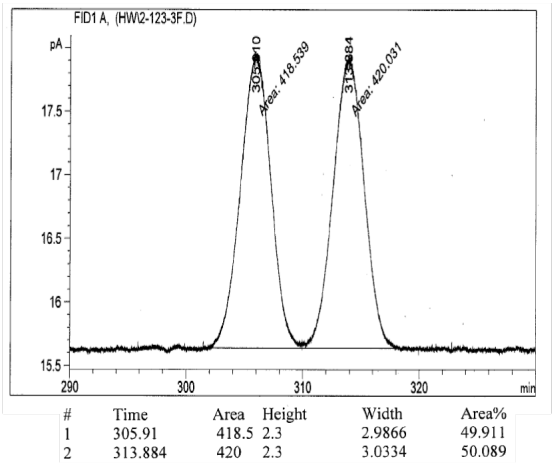

#	Time	Area	Height	Width	Area%
1	305.91	418.5	2.3	2.9866	49.911
2	313.884	420	2.3	3.0334	50.089

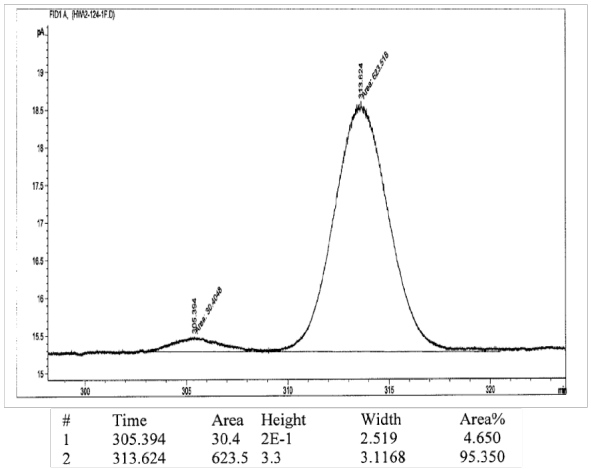

#	Time	Area	Height	Width	Area%
1	305.394	30.4	2E-1	2.519	4.650
2	313.624	623.5	3.3	3.1168	95.350

Peak #	Time (min)	Area (%)	Peak #	Time (min)	Area (%)
1	305.910	49.911	1	305.394	4.650
2	313.884	50.089	2	313.624	95.350

(*R*)-*tert*-Butyl-3-phenyl-3-(4,4,5,5-tetramethyl-1,3,2-dioxaborolan-2-yl)propanoate (1.93): The spectroscopic data match those reported previously.[35] ^{1}H NMR (400 MHz, $CDCl_3$): δ 7.25–7.18 (4H, m), 7.14–7.09 (1H, m), 2.78 (1H, dd, J = 15.6, 10.0 Hz), 2.68 (1H, dd, J = 10.0, 5.6 Hz), 2.56 (1H, dd, J = 15.6, 5.6 Hz), 1.39 (9H, s), 1.20 (6H, s), 1.15 (6H, s); Specific Rotation: $[\alpha]_D^{20}$ –19.6 (*c* 1.20, $CHCl_3$) for an enantiomerically enriched sample of 98:2 er. Enantiomeric purity was determined by HPLC analysis in comparison with authentic racemic material (98:2 er shown; Chiralcel OD-H column, 99.9/0.1 hexanes/*i*-PrOH, 0.3 mL/min, 220 nm).

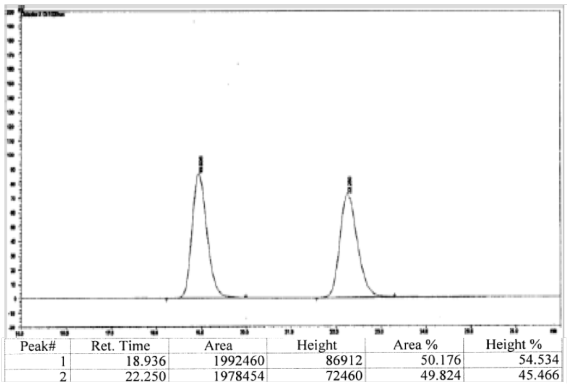

Peak#	Ret. Time	Area	Height	Area %	Height %
1	18.936	1992460	86912	50.176	54.534
2	22.250	1978454	72460	49.824	45.466

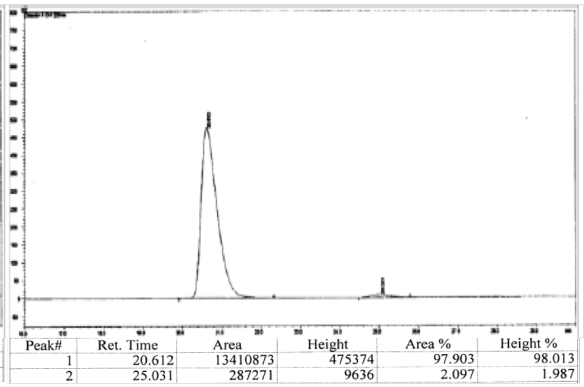

Peak#	Ret. Time	Area	Height	Area %	Height %
1	20.612	13410873	475374	97.903	98.013
2	25.031	287271	9636	2.097	1.987

Peak #	Time (min)	Area (%)	Peak #	Time (min)	Area (%)
1	18.936	50.176	1	20.612	97.903

2	22.250	49.824	2	25.031	2.097

***N*-Methoxy-*N*-methylcinnamamide (1.94):** The spectroscopic data match those reported previously.[40] ^{1}H NMR (400 MHz, $CDCl_3$): δ 7.72 (1H, d, J = 15.6 Hz), 7.57–7.54 (2H, m), 7.40–7.24 (3H, m), 7.02 (1H, d, J = 15.6 Hz), 3.75 (3H, s), 3.30 (3H, s).

(*R*)-*N*-Methoxy-*N*-methyl-3-phenyl-3-(4,4,5,5-tetramethyl-1,3,2-dioxaborolan-2-yl)propanamide (1.95): IR (neat): 2975 (w), 2931 (w), 1657 (s), 1359 (s), 1319 (s), 1248 (m), 1140 (s), 1109 (m), 996 (m), 969 (w), 701 (s) cm^{-1}; ^{1}H NMR (400 MHz, $CDCl_3$): δ 7.27–7.21 (4H, m), 7.16–7.10 (1H, m), 3.61 (3H, s), 3.14 (3H, s), 2.98–2.81 (2H, m), 2.69 (1H, dd, J = 11.2, 5.6 Hz), 1.20 (6H, s), 1.15 (6H, s); ^{13}C NMR (100 MHz, $CDCl_3$): δ 174.3, 142.1, 128.4, 128.4, 125.5, 83.2, 61.1, 35.9, 32.3, 24.6, 24.5; HRMS (ESI+): Calcd for $C_{16}H_{33}B_1N_1O_4$ $[M+H]^+$: 320.2033, Found: 320.2032. Specific Rotation: $[\alpha]_D^{20}$ – 65.3 (*c* 0.73, $CHCl_3$) for an enantiomerically enriched sample of 86.5:13.5 er. Enantiomeric purity was determined by HPLC analysis in comparison with authentic racemic material (86.5:13.5 er shown; Chiralcel OJ-H column, 99/1 hexanes/*i*-PrOH, 0.3 mL/min, 220 nm).

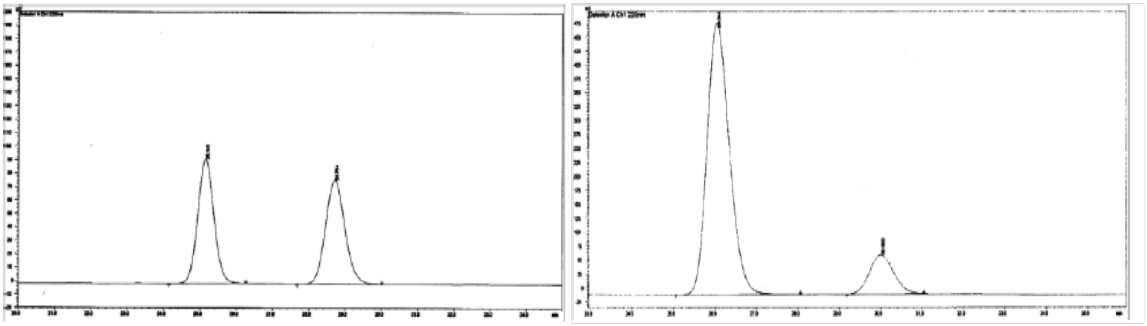

Peak#	Ret. Time	Area	Height	Area %	Height %
1	25.141	2874969	92232	49.901	54.451
2	28.704	2886371	77153	50.099	45.549

Peak#	Ret. Time	Area	Height	Area %	Height %
1	26.044	18287171	487358	86.472	87.461
2	30.000	2860809	69871	13.528	12.539

Peak #	Time (mins)	Area (%)	Peak #	Time (mins)	Area (%)
1	25.141	49.901	1	26.044	86.472

(40) Murphy, J. A.; Commeureuc, A. G. J.; Snaddon, T. N.; McGuire, T. M.; Khan, T. A.; Hisler, K.; Dewis, M. L.; Carling, R. *Org. Lett.* **2005**, *7*, 1427–1429.

2	28.704	50.099	2	30.000	13.528

(*E*)-3-(4-Bromophenyl)-*N*-methoxy-*N*-methylacrylamide (substrate for 1.96): IR (neat): 2964 (w), 2935 (w), 1656 (s), 1619 (s), 1488 (s), 1461 (s), 1379 (s), 1199 (m), 1071 (s), 1008 (s), 815 (s), 789 (m), cm^{-1}; ^1H NMR (400 MHz, $CDCl_3$): δ 7.65 (1H, d, *J* = 16.0 Hz), 7.50 (2H, d, *J* = 6.8 Hz), 7.42 (2H, d, *J* = 6.8 Hz), 7.01 (1H, d, *J* = 16.0 Hz), 3.76 (3H, s), 3.30 (3H, s); ^{13}C NMR (100 MHz, $CDCl_3$): δ 166.7, 142.2, 134.2, 132.1, 129.6, 124.1, 116.6, 62.0, 32.6; HRMS (ESI+): Calcd for $C_{11}H_{13}Br_1N_1O_2$ $[M+H]^+$: 272.0109, Found: 272.0114.

(*R*)-3-(4-Bromophenyl)-*N*-methoxy-*N*-methyl-3-(4,4,5,5-tetramethyl-1,3,2-dioxaborolan-2-yl)propanamide (1.96): IR (neat): 2973 (w), 2922 (m), 2852 (w), 1725 (w), 1659 (s), 1486 (m), 1361 (s), 1324 (s), 1108 (s) cm^{-1}; ^1H NMR (400 MHz, $CDCl_3$): δ 7.37 (2H, d, *J* = 8.4 Hz), 7.15 (2H, d, *J* = 8.4 Hz), 3.64 (3H, s), 3.15 (3H, s), 2.98–2.82 (2H, m), 2.66 (1H, dd, *J* = 10.0, 6.0 Hz), 1.21 (6H, s), 1.17 (6H, s); ^{13}C NMR (100 MHz, $CDCl_3$): δ 174.0, 141.4, 131.5, 130.3, 119.4, 83.5, 61.3, 35.8, 32.5, 29.8, 24.7, 24.7; HRMS (ESI+): Calcd for $C_{17}H_{26}B_1Br_1N_1O_4$ $[M+H]^+$: 398.1138, Found: 398.1139. Specific Rotation: $[\alpha]_D^{20}$ –15.6 (*c* 0.81, $CHCl_3$) for an enantiomerically enriched sample of 94:6 er. Enantiomeric purity was determined by HPLC analysis in comparison with authentic racemic material (94:6 er shown; Chiralcel OD-H column, 99/1 hexanes/*i*-PrOH, 0.3 mL/min, 220 nm).

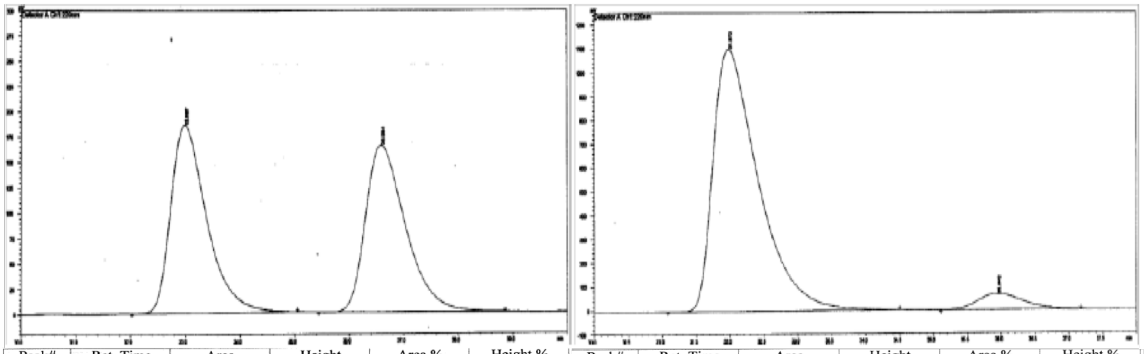

Peak#	Ret. Time	Area	Height	Area %	Height %
1	32.987	8439612	184976	50.132	52.944
2	36.584	8395168	164405	49.868	47.056

Peak#	Ret. Time	Area	Height	Area %	Height %
1	31.973	50884394	1100553	94.229	94.382
2	35.942	3116450	65507	5.771	5.618

Peak #	Time (min)	Area (%)	Peak #	Time (min)	Area (%)
1	32.987	50.132	1	31.973	94.229
2	36.584	49.868	2	35.942	5.771

(*E*)-*N*-Methoxy-*N*-methyloct-2-enamide (substrate for 1.97): IR (neat): 2957 (m), 2928 (m), 2858 (w), 1665 (s), 1635 (s), 1462 (m), 1442 (m), 1411 (m), 1378 (s), 1177 (w), 993 (m), 967 (w) cm^{-1}; ^1H NMR (400 MHz, $CDCl_3$): δ 6.96 (1H, dt, J = 15.6, 6.8 Hz), 6.37 (1H, dt, J = 14.0, 1.2 Hz), 3.68 (3H, s), 3.22 (3H, s), 2.24–2.18 (2H, m), 1.49–1.41 (2H, m), 1.32–1.25 (4H, m), 0.89–0.84 (3H, m); ^{13}C NMR (100 MHz, $CDCl_3$): δ 166.9, 147.7, 118.5, 61.5, 32.3, 32.1, 31.2, 27.9, 22.3, 13.8; HRMS (ESI+): Calcd for $C_{10}H_{20}N_1O_2$ $[M+H]^+$:186.1494, Found: 186.1480.

(*S*)-*N*-Methoxy-*N*-methyl-3-(4,4,5,5-tetramethyl-1,3,2-dioxaborolan-2-yl)octanamide (1.97): IR (neat): 2958 (w), 2925 (m), 2856 (w), 1664 (s), 1462 (w), 1414 (m), 1379 (s), 1315 (s), 1242 (w), 1215 (w), 1145 (s), 1003 (m), 968 (w), 867 (w) cm^{-1}; ^1H NMR (400 MHz, $CDCl_3$): δ 3.64 (3H, s), 3.12 (3H, s), 2.55–2.43 (2H, m), 1.45–1.20 (21H, m), 0.83 (3H, apparent t); ^{13}C NMR (100 MHz, $CDCl_3$): δ 174.9, 82.7, 61.1, 33.7, 32.3, 32.0, 30.7, 28.6, 24.8, 24.7, 22.5, 14.0; HRMS (ESI+): Calcd for $C_{16}H_{33}B_1N_1O_4$ $[M+H]^+$: 314.2503, Found: 314.2509. Specific Rotation: $[\alpha]_D^{20}$ –1.1 (*c* 1.08, $CHCl_3$) for an enantiomerically enriched sample of 95:5 er. Enantiomeric purity was determined by HPLC analysis in

comparison with authentic racemic material (95:5 er shown; Chiralcel OD-H column, 99.9/0.1 hexanes/*i*-PrOH, 0.3 mL/min, 220 nm).

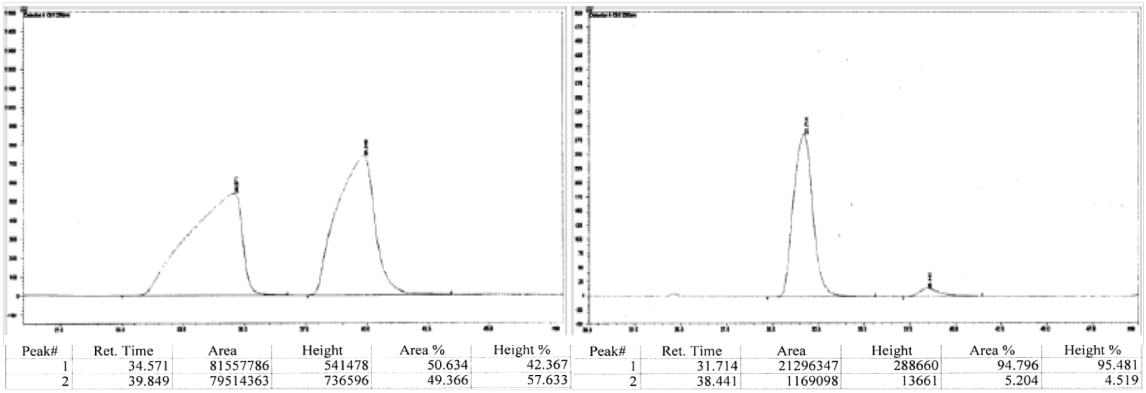

Peak#	Ret. Time	Area	Height	Area %	Height %
1	34.571	81557786	541478	50.634	42.367
2	39.849	79514363	736596	49.366	57.633

Peak#	Ret. Time	Area	Height	Area %	Height %
1	31.714	21296347	288660	94.796	95.481
2	38.441	1169098	13661	5.204	4.519

Peak #	Time (min)	Area (%)	Peak #	Time (min)	Area (%)
1	34.571	50.634	1	31.714	94.796
2	39.849	49.366	2	38.441	5.204

(*E*)-*N*-Methoxy-*N*,4-dimethylpent-2-enamide (substrate 1.98): The spectroscopic data match those reported previously.[41] ^{1}H NMR (400 MHz, $CDCl_3$): δ 6.95 (1H, dd, J = 15.6, 6.8 Hz), 6.34 (1H, d, J = 15.8 Hz), 3.70 (3H, s), 3.24 (3H, s), 2.52–2.47 (1H, m), 1.07 (6H, overlapping d, J = 8.0 Hz).

(*R*)-*N*-Methoxy-*N*,4-dimethyl-3-(4,4,5,5-tetramethyl-1,3,2-dioxaborolan-2-yl)pentanamide (1.98): IR (neat): 2957 (m), 2872 (w), 1662 (s), 1464 (w), 1444 (m), 1378 (s), 1317 (s), 1255 (m), 1215 (m), 1165 (m), 1144 (s), 1112 (w), 1099 (w), 1002 (m), 976 (m), 870 (w) cm^{-1}; ^{1}H NMR (400 MHz, $CDCl_3$): δ 3.66 (3H, s), 3.12 (3H, s), 2.52–2.50 (2H, m), 1.78–1.66 (1H, m), 1.26–1.23 (7H, m), 1.20 (6H, s), 0.95–0.92 (6H, m); ^{13}C NMR (100 MHz, $CDCl_3$): δ 175.3, 82.8, 61.1, 32.2, 31.7, 29.2, 25.0, 24.8, 22.2, 21.7; HRMS (ESI+): Calcd for $C_{14}H_{29}B_1N_1O_4$ $[M+H]^+$: 286.2190, Found: 286.2187. Specific Rotation: $[\alpha]_D^{20}$ –2.0 (*c* 1.30, $CHCl_3$) for an enantiomerically enriched sample of 95:5 er. Enantiomeric purity was determined by HPLC analysis in comparison with authentic

(41) Shintani, R.; Kimura, T.; Hayashi, T. *Chem. Commun.* **2005**, *41*, 3213–3214.

racemic material (95:5 er shown; Chiralcel OD-H column, 99.9/0.1 hexanes/*i*-PrOH, 0.3 mL/min, 220 nm).

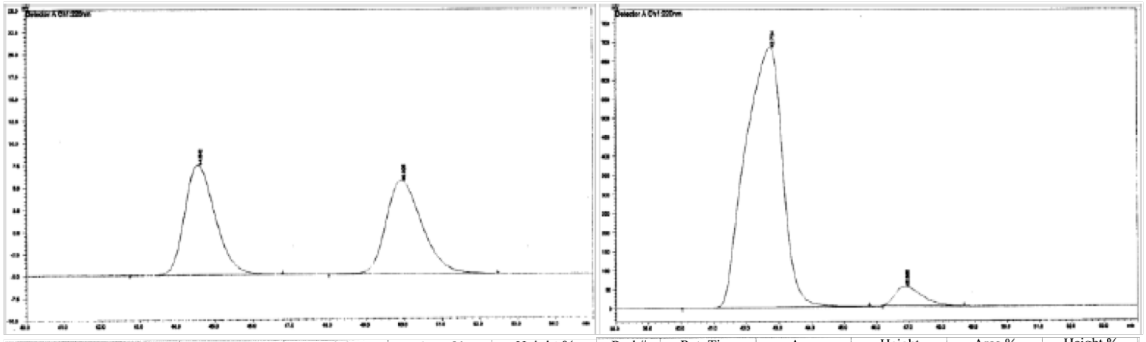

Peak#	Ret. Time	Area	Height	Area %	Height %
1	44.542	700008	12417	50.003	54.078
2	49.925	699936	10545	49.997	45.922

Peak#	Ret. Time	Area	Height	Area %	Height %
1	42.734	54101785	684104	94.812	93.046
2	46.866	2960643	51129	5.188	6.954

Peak #	Time (mins)	Area (%)	Peak #	Time (mins)	Area (%)
1	44.542	50.003	1	42.734	94.812
2	49.925	49.997	2	46.866	5.188

(*E*)-*N*-Methoxy-*N*,5-dimethylhex-2-enamide (substrate for 1.99): IR (neat): 2956 (m), 2925 (m), 2871 (w), 1664 (s), 1634 (s), 1464 (m), 1411 (m), 1378 (s), 1176 (m), 1152 (w), 1114 (w), 1095 (w), 996 (s), 984 (s) cm^{-1}; ^1H NMR (400 MHz, $CDCl_3$): δ 6.93 (1H, dt, J = 12.0, 6.0 Hz), 6.36 (1H, d, J = 12.0 Hz), 3.67 (3H, s), 3.21 (3H, s), 2.10 (2H, td, J = 5.2, 1.2 Hz), 1.78–1.70 (1H, m), 0.90 (6H, overlapping d, J = 5.6 Hz); ^{13}C NMR (100 MHz, $CDCl_3$): δ 167.3, 147.0, 120.0, 61.9, 42.1, 32.6, 28.2, 22.6; HRMS (ESI+): Calcd for $C_9H_{18}N_1O_2$ $[M+H]^+$: 172.1338, Found: 172.1342.

(*S*)-*N*-Methoxy-*N*,5-dimethyl-3-(4,4,5,5-tetramethyl-1,3,2-dioxaborolan-2-yl)hexanamide (1.99): IR (neat): 2955 (m), 2921 (s), 2852 (m), 1666 (m), 1463 (m), 1378 (s), 1319 (m), 1146 (s) cm^{-1}; ^1H NMR (400 MHz, $CDCl_3$): δ 3.67 (3H, s), 3.15 (3H, s), 2.57–2.43 (2H, m), 1.67–1.57 (1H, m), 1.41–1.32 (2H, m), 1.24–1.14 (13H, m), 0.89 (3H, d, J = 6.8 Hz), 0.86 (3H, d, J = 6.8 Hz); ^{13}C NMR (100 MHz, $CDCl_3$): δ 174.9, 82.7, 61.1, 39.9, 33.8, 30.3, 26.7, 24.8, 24.7, 22.8, 22.6; HRMS (ESI+): Calcd for $C_{15}H_{31}B_1N_1O_4$ $[M+H]^+$: 300.2346, Found: 300.2362. Specific Rotation: $[\alpha]_D^{20}$ +2.8 (*c*

0.67, $CHCl_3$) for an enantiomerically enriched sample of 95:5 er. Enantiomeric purity was determined by HPLC analysis in comparison with authentic racemic material (95:5 er shown; Chiralpak AS-H column, 99.8/0.2 hexanes/*i*-PrOH, 0.3 mL/min, 220 nm).

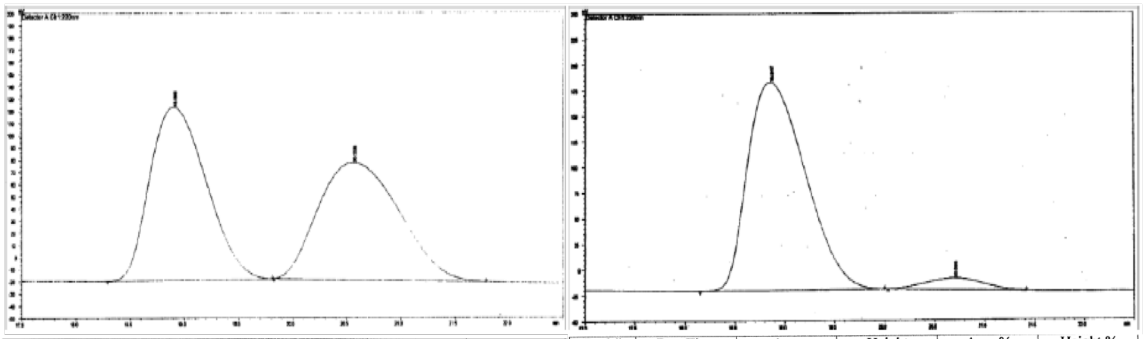

Peak#	Ret. Time	Area	Height	Area %	Height %
1	18.899	5143401	142102	50.664	59.555
2	20.558	5008624	96505	49.336	40.445

Peak#	Ret. Time	Area	Height	Area %	Height %
1	18.847	8185682	203240	94.706	94.675
2	20.688	457548	11432	5.294	5.325

Peak #	Time (min)	Area (%)	Peak #	Time (min)	Area (%)
1	18.899	50.664	1	18.847	94.706
2	20.558	49.336	2	20.688	5.294

(*E*)-5-[(*tert*-Butyldimethylsilyl)oxy]-*N*-methoxy-*N*-methylpent-2-enamide (substrate for 1.100): IR (neat): 2954 (m), 2930 (m), 2857 (m), 1667 (s), 1637 (s), 1463 (w), 1411 (w), 1379 (s), 1254 (m), 1098 (s), 998 (m), 981 (m), 836 (s), 776 (s) cm^{-1}; ^1H NMR (400 MHz, $CDCl_3$): δ 6.95 (1H, dt, J = 15.6, 7.2 Hz), 6.46 (1H, dt, J = 15.6, 1.2 Hz), 3.73 (2H, t, J = 6.8 Hz), 3.69 (3H, s), 3.23 (3H, s), 2.48–2.45 (2H, m), 0.88 (9H, s), 0.05 (6H, s); ^{13}C NMR (100 MHz, $CDCl_3$): δ 167.1, 144.5, 120.7, 62.0, 61.9, 36.3, 32.6, 26.2, 18.6, –5.0; HRMS (ESI+): Calcd for $C_{13}H_{28}N_1O_3Si_1$ $[M+H]^+$: 274.1838, Found: 274.1848.

(*S*)-5-[(*tert*-Butyldimethylsilyl)oxy]-*N*-methoxy-*N*-methyl-3-(4,4,5,5-tetramethyl-1,3,2-dioxaborolan-2-yl)pentanamide (1.100): IR (neat): 2956 (m), 2926 (s), 2855 (m), 1665 (s), 1463 (w), 1414 (m), 1378 (s), 1316 (m), 1252 (m), 1146 (s), 1097 (s), 1006 (w), 835 (s), 775 (m) cm^{-1}; ^1H NMR (400 MHz, $CDCl_3$): δ 3.60–3.70 (5H, m), 3.15 (3H, s), 2.67–2.52 (2H, m), 1.79–1.70 (1H, m), 1.58–1.50 (1H, m), 1.38–1.31 (1H, m), 1.24 (6H, s), 1.23 (6H, s), 0.88 (9H, s), 0.04 (6H, s); ^{13}C NMR (100 MHz, $CDCl_3$): δ 174.9, 82.8,

62.8, 61.1, 33.7, 30.3, 26.0, 25.0, 24.8, 24.8, 18.3, –5.3; HRMS (ESI+): Calcd for $C_{19}H_{41}B_1N_1O_5Si_1$ $[M+H]^+$: 402.2847, Found: 402.2862. Specific Rotation: $[\alpha]_D^{20}$ –1.8 (*c* 1.28, $CHCl_3$) for an enantiomerically enriched sample of 93:7 er. Enantiomeric purity was determined by HPLC analysis in comparison with authentic racemic material (93:7 er shown; Chiralpak AS-H column, 99.8/0.2 hexanes/*i*-PrOH, 0.3 mL/min, 220 nm).

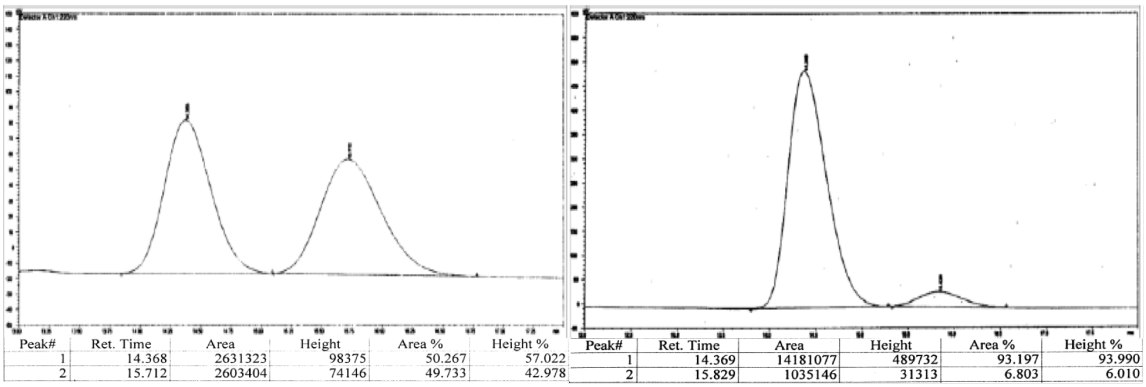

Peak#	Ret. Time	Area	Height	Area %	Height %
1	14.368	2631323	98375	50.267	57.022
2	15.712	2603404	74146	49.733	42.978

Peak#	Ret. Time	Area	Height	Area %	Height %
1	14.369	14181077	489732	93.197	93.990
2	15.829	1035146	31313	6.803	6.010

Peak #	Time (min)	Area (%)	Peak #	Time (min)	Area (%)
1	14.368	50.267	1	14.369	93.197
2	15.712	49.733	2	15.829	6.803

(*S*)-3-(4,4,5,5-Tetramethyl-1,3,2-dioxaborolan-2-yl)hexanal (1.102): The spectroscopic data match those reported previously.[42] ^{1}H NMR (400 MHz, $CDCl_3$): δ 9.74–9.74 (1H, m), 2.59–2.39 (2H, m), 1.47–1.40 (1H, m), 1.36–1.26 (4H, m), 1.22 (6H, s), 1.21 (6H, s), 0.87 (3H, t, J = 7.2 Hz); Specific Rotation: $[\alpha]_D^{20}$ +3.6 (*c* 1.11, $CHCl_3$) for an enantiomerically enriched sample of 95:5 er. Enantiomeric purity was determined by GLC analysis in comparison with authentic racemic material (95:5 er shown; Chiraldex GTA column, 15 psi, 70 ºC).

(42) Bonet, A.; Lillo, V.; Ramírez, J.; Mar Díaz-Requejo, M.; Fernández, E. *Org. Biomol. Chem.* **2009**, *7*, 1533–1535.

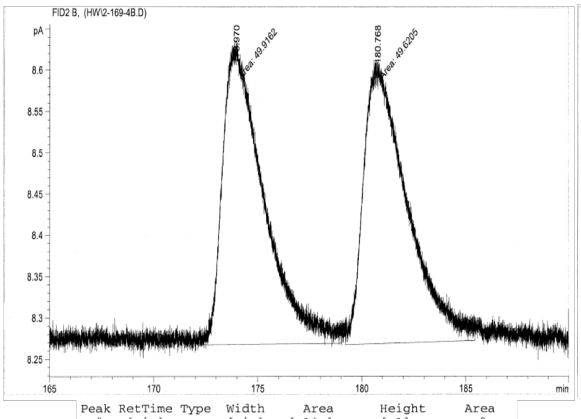

Peak #	RetTime [min]	Type	Width [min]	Area [pA*s]	Height [pA]	Area %
1	173.970	MM	2.2612	49.91620	3.67922e-1	50.14852
2	180.768	MM	2.4142	49.62053	3.42553e-1	49.85148

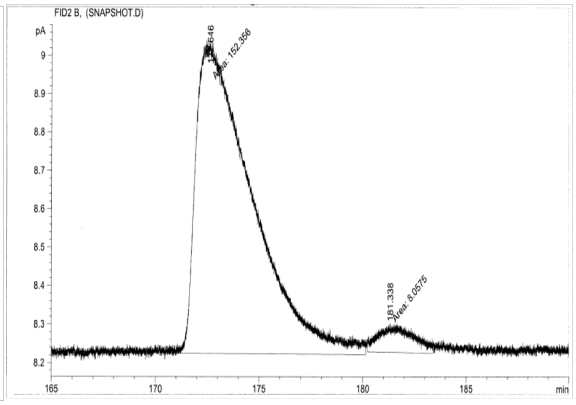

Peak #	RetTime [min]	Type	Width [min]	Area [pA*s]	Height [pA]	Area %
1	172.646	MM	3.1155	152.35625	8.15038e-1	94.97705
2	181.338	MM	1.8548	8.05750	7.24024e-2	5.02295

Peak #	Time (min)	Area (%)	Peak #	Time (min)	Area (%)
1	173.970	50.14852	1	172.646	94.97705
2	180.768	49.85148	2	181.338	5.02295

(*E*)-5-Phenylpent-2-enal (substrate for 1.103): The spectroscopic data match those reported previously.[43] ^{1}H NMR (400 MHz, $CDCl_3$): δ 9.50 (1H, d, *J* = 8.0 Hz), 7.33–7.29 (2H, m), 7.24–7.18 (3H, m), 6.86 (1H, dt, *J* = 16.0, 6.6 Hz), 6.17–6.11 (1H, m), 2.84 (2H, t, *J* = 7.6 Hz), 2.70–2.64 (2H, m).

(*S*)-5-Phenyl-3-(4,4,5,5-tetramethyl-1,3,2-dioxaborolan-2-yl)pentanal (1.103): IR (neat): 2976 (m), 2924 (m), 2855 (w), 2713 (w), 1723 (s), 1380 (s), 1318 (s), 1144 (s), 701 (m) cm^{-1}; ^{1}H NMR (400 MHz, $CDCl_3$): δ 9.74 (1H, t, *J* = 1.0 Hz), 7.26–7.23 (2H, m), 7.16–7.14 (3H, m), 2.67–2.53 (4H, m), 1.83–1.75 (1H, m), 1.65–1.58 (1H, m), 1.40–1.35 (1H, m), 1.24 (6H, s), 1.23 (6H, s); ^{13}C NMR (100 MHz, $CDCl_3$): δ 202.7, 142.5, 128.5, 128.47, 125.9, 83.5, 46.0, 35.3, 32.7, 30.5, 25.0, 24.9; HRMS (ESI+): Calcd for $C_{17}H_{26}B_1O_3$ $[M+H]^+$: 289.1975, Found: 289.2002. Specific Rotation: $[\alpha]_D^{20}$ –9.6 (*c* 0.37, $CHCl_3$) for an enantiomerically enriched sample of 95:5 er. Enantiomeric purity was

(43) Palais, L.; Babel, L.; Quintard, A.; Belot, S.; Alexakis, A. *Org. Lett.* **2010**, *12*, 1988–1991.

determined by HPLC analysis in comparison with authentic racemic material (95:5 er shown; Chiralcel OJ-H column, 99/1 hexanes/*i*-PrOH, 0.3 mL/min, 220 nm).

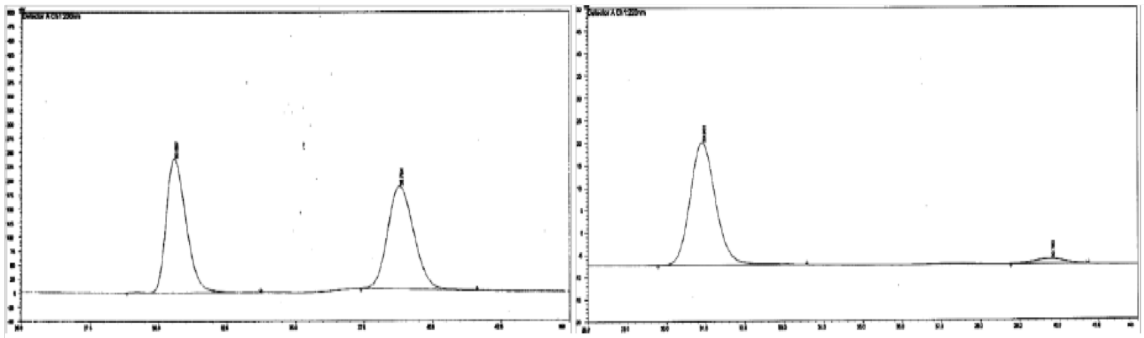

Peak#	Ret. Time	Area	Height	Area %	Height %	Peak#	Ret. Time	Area	Height	Area %	Height %
1	30.557	12024437	237330	49.690	56.442	1	30.903	1256604	27405	95.192	96.110
2	38.784	12174228	183157	50.310	43.558	2	39.780	63468	1109	4.808	3.890

Peak #	Time (min)	Area (%)	Peak #	Time (min)	Area (%)
1	30.557	49.690	1	30.903	95.192
2	38.784	50.310	2	39.780	4.808

(*E*)-5-Methylhex-2-enal (substrate for 1.104): IR (neat): 2930 (m), 2871 (w), 2811 (w), 1686 (s), 1638 (m), 1466 (w), 1153 (m), 1112 (m), 1091 (m), 1012 (w), 977 (m), 885 (w) cm^{-1}; ^{1}H NMR (400 MHz, $CDCl_3$): δ 9.49 (1H, d, J = 8.0 Hz), 6.80 (1H, dt, J = 15.6, 7.2 Hz), 6.12–6.05 (1H, m), 2.23–2.18 (2H, m), 1.85–1.75 (1H, m), 0.93 (6H, overlapping d, J = 7.2 Hz); ^{13}C NMR (100 MHz, $CDCl_3$): δ 194.1, 157.7, 134.1, 41.9, 27.8, 22.3; HRMS (ESI+): Calcd for $C_7H_{13}O_1$ $[M+H]^+$: 113.0966, Found: 113.0961.

(*S*)-5-Methyl-3-(4,4,5,5-tetramethyl-1,3,2-dioxaborolan-2-yl)hexanal (1.104): IR (neat): 2977 (m), 2956 (m), 2926 (m), 2869 (w), 2716 (w), 1725 (s), 1467 (w), 1379 (s), 1372 (s), 1317 (m), 1280 (m), 1168 (w), 1145 (s), 1125 (s), 850 (m) cm^{-1}; ^{1}H NMR (400 MHz, $CDCl_3$): δ 9.75 (1H, m), 2.53–2.51 (2H, m), 1.62–1.55 (1H, m), 1.40–1.33 (2H, m), 1.23–1.14 (13H, m), 0.88 (3H, d, J = 6.4 Hz), 0.85 (3H, d, J = 6.4 Hz); ^{13}C NMR (100 MHz, $CDCl_3$): δ 202.9, 83.3, 46.0, 39.6, 26.7, 25.1, 24.8, 22.7, 22.5; HRMS (ESI+): Calcd for $C_{13}H_{26}B_1O_3$ $[M+H]^+$: 241.1975, Found: 241.1964. Specific Rotation: $[\alpha]_D^{20}$ – 3.8 (*c* 0.94, $CHCl_3$) for an enantiomerically enriched sample of 94:6 er. Enantiomeric

purity was determined by GLC analysis in comparison with authentic racemic material (94:6 er shown; Chiraldex GTA column, 15 psi, 70 ºC).

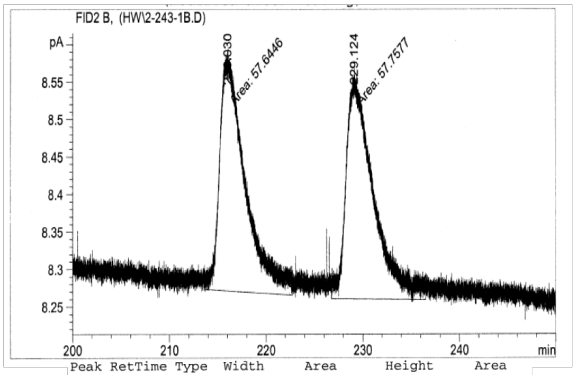

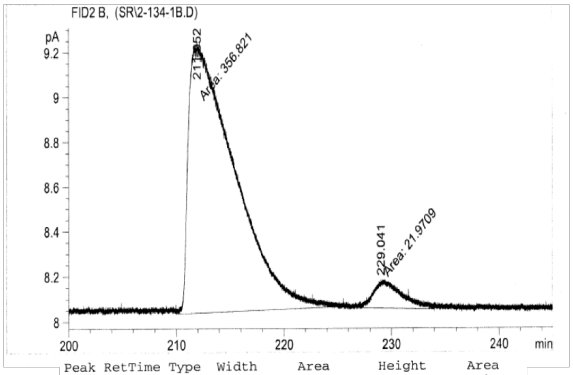

Peak #	Time (min)	Area (%)	Peak #	Time (min)	Area (%)
1	216.030	49.95908	1	211.952	94.19974
2	229.124	50.04902	2	229.041	5.80026

(*S*)-4-Methyl-3-(4,4,5,5-tetramethyl-1,3,2-dioxaborolan-2-yl)pentanal (1.105): IR (neat): 2977 (m), 2931 (m), 2873 (w), 2716 (w), 1721 (s), 1372 (s), 1310 (s), 1279 (s), 1214 (w), 1143 (s), 1124 (s), 967 (w), 849 (s) cm^{-1}; ^{1}H NMR (400 MHz, $CDCl_3$): δ 9.72 (1H, m), 2.56 (1H, dd, J = 18.2, 10.0 Hz), 2.43 (1H, dd, J = 18.2, 4.2 Hz), 1.74–1.66 (1H, m), 1.24–1.14 (13H, m), 0.89–0.83 (6H, m); ^{13}C NMR (100 MHz, $CDCl_3$): δ 203.1, 83.2, 43.9, 28.9, 24.9, 24.7, 21.9, 21.5; HRMS (ESI+): Calcd for $C_{12}H_{24}B_1O_3$ $[M+H]^+$: 227.1819, Found: 227.1829. Specific Rotation: $[\alpha]_D^{20}$ +2.4 (*c* 1.43, $CHCl_3$) for an enantiomerically enriched sample of 91:9 er. Enantiomeric purity was determined by GLC analysis in comparison with authentic racemic material (91:9 er shown; Chiraldex GTA column, 15 psi, 70 ºC).

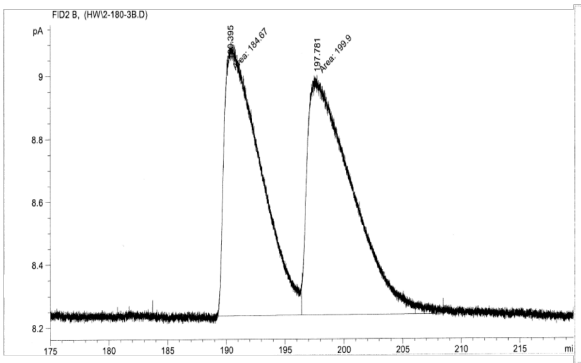

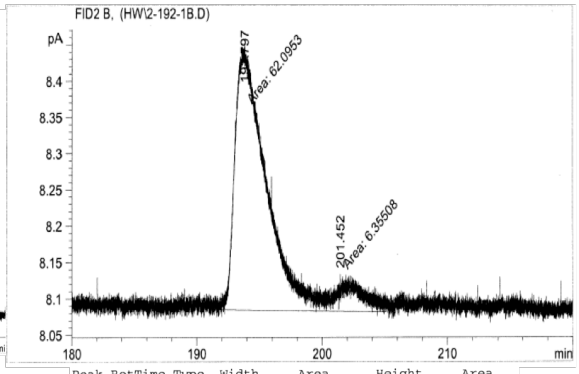

Peak #	Time (min)	Area (%)	Peak #	Time (min)	Area (%)
1	190.395	48.01977	1	193.797	90.71579
2	197.781	51.98023	2	201.452	9.28421

(*E*)-Oct-3-en-7-yn-2-one (substrate for 1.108): IR (neat): 3291 (br), 2962 (m), 2919 (m), 2850 (m), 1697 (m), 1672 (s), 1627 (m), 1432 (m), 1361 (m), 1255 (s), 1018 (m), 972 (m), 798 (m) 638 (br) cm^{-1}; ^{1}H NMR (400 MHz, $CDCl_3$): δ 6.82 (1H, dt, J = 16.0, 6.8 Hz), 6.13 (1H, d, J = 16.0 Hz), 2.48–2.43 (2H, m), 2.39–2.35 (2H, m), 2.26 (3H, s), 2.01 (1H, t, J = 2.4 Hz); ^{13}C NMR (100 MHz, $CDCl_3$): δ 198.4, 145.3, 132.2, 82.6, 69.6, 31.2, 27.0, 17.5; HRMS (ESI+): Calcd for $C_8H_{11}O_1$ $[M+H]^+$: 123.0810, Found: 123.0790.

(*S*)-4-(4,4,5,5-Tetramethyl-1,3,2-dioxaborolan-2-yl)oct-7-yn-2-one (1.108): IR (neat): 3291 (br), 2977 (m), 2922 (m), 2852 (m), 1714 (m), 1380 (s), 1372 (s), 1315 (s), 1166 (s), 1143 (s), 1125 (s), 967 (m), 851 (m), 671 (m), 632 (m) cm^{-1}; ^{1}H NMR (400 MHz, $CDCl_3$): δ 2.66–2.54 (2H, m), 2.24–2.19 (2H, m), 2.11 (3H, s), 1.93–1.92 (1H, m), 1.76–1.67 (1H, m), 1.55–1.46 (1H, m), 1.39–1.30 (1H, m), 1.23 (6H, s), 1.22 (6H, s); ^{13}C NMR (100 MHz, $CDCl_3$): δ 208.8, 84.6, 83.3, 68.5, 45.3, 29.8, 29.3, 24.9, 24.8, 17.9; HRMS (ESI+): Calcd for $C_{14}H_{24}B_1O_3$ $[M+H]^+$: 251.1819, Found: 251.1813. Specific Rotation: $[\alpha]_D^{20}$ –3.0 (*c* 0.87, $CHCl_3$) for an enantiomerically enriched sample of 94:6 er.

Enantiomeric purity was determined by GLC analysis in comparison with authentic racemic material (94:6 er shown; Chiraldex aTA column, 15 psi, 90 ºC).

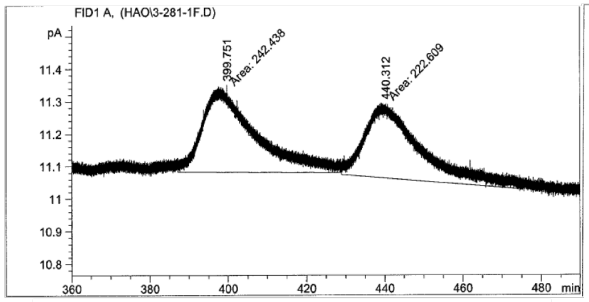

Peak #	RetTime [min]	Type	Width [min]	Area [pA*s]	Height [pA]	Area %
1	399.751	MM	14.9662	242.43753	2.69983e-1	52.13187
2	440.312	MM	15.9993	222.60918	2.31895e-1	47.86813

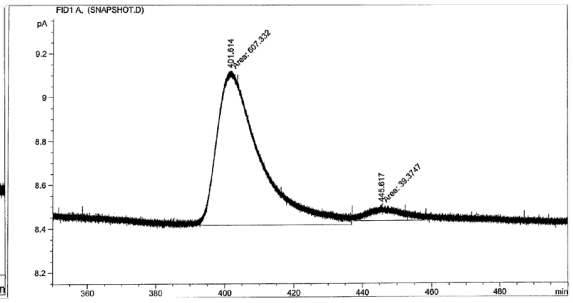

Peak #	RetTime [min]	Type	Width [min]	Area [pA*s]	Height [pA]	Area %
1	401.614	MM	14.2804	607.33191	7.08815e-1	93.91151
2	445.617	MM	8.8193	39.37469	7.44098e-2	6.08849

Peak #	Time (min)	Area (%)	Peak #	Time (min)	Area (%)
1	399.751	52.13187	1	401.614	93.91151
2	440.312	47.86813	2	445.617	6.08849

(*E*)-Non-2-en-7-ynal (substrate for 1.110): IR (neat): 2939 (m), 2918 (m), 2712 (m), 1691 (s), 1638 (m), 1434 (m), 1167 (m), 1124 (m), 975 (m) cm^{-1}; ^{1}H NMR (400 MHz, $CDCl_3$): δ 9.50 (1H, d, *J* = 8.0 Hz), 6.84 (1H, dt, *J* = 15.6, 6.8 Hz), 6.14 (1H, dd, *J* = 15.6, 8 Hz), 2.47–2.42 (2H, m), 2.22–2.17 (2H, m), 1.78–1.76 (3H, m), 1.76–1.64 (2H, m); ^{13}C NMR (100 MHz, $CDCl_3$): δ 194.1, 157.9, 133.4, 78.0, 76.7, 31.8, 27.2, 18.3, 3.5; HRMS (ESI+): Calcd for $C_9H_{13}O_2$ $[M+OH]^+$: 153.0916, Found: 153.0922.

(*S*)-3-(4,4,5,5-Tetramethyl-1,3,2-dioxaborolan-2-yl)non-7-ynal (1.110): IR (neat): 2977 (m), 2924 (s), 2857 (m), 2712 (m), 1723 (m), 1458 (m), 1380 (s), 1372 (s), 1318 (s), 1280 (m), 1166 (m), 1144 (s), 1125 (s), 967 (m), 850 (m) cm^{-1}; ^{1}H NMR (400 MHz, $CDCl_3$): δ 9.76 (1H, s), 2.64–2.51 (2H, m), 2.13–2.09 (2H, m), 1.77–1.76 (3H, m), 1.56–1.40 (4H, m), 1.36–1.30 (1H, m), 1.24 (6H, s), 1.23 (6H, s); ^{13}C NMR (100 MHz, $CDCl_3$): δ 202.8, 83.5, 79.2, 75.7, 46.0, 29.9, 28.5, 24.9, 24.8, 19.0, 3.6; HRMS (ESI+): Calcd for $C_{15}H_{26}B_1O_3$ $[M+H]^+$: 265.1975, Found: 265.1975. Specific Rotation: $[\alpha]_D^{20}$ +11.0 (*c* 0.25, $CHCl_3$) for an enantiomerically enriched sample of 95:5 er.

Enantiomeric purity was determined by GLC analysis in comparison with authentic racemic material (95:5 er shown; Chiraldex GTA column, 15 psi, 90 ºC).

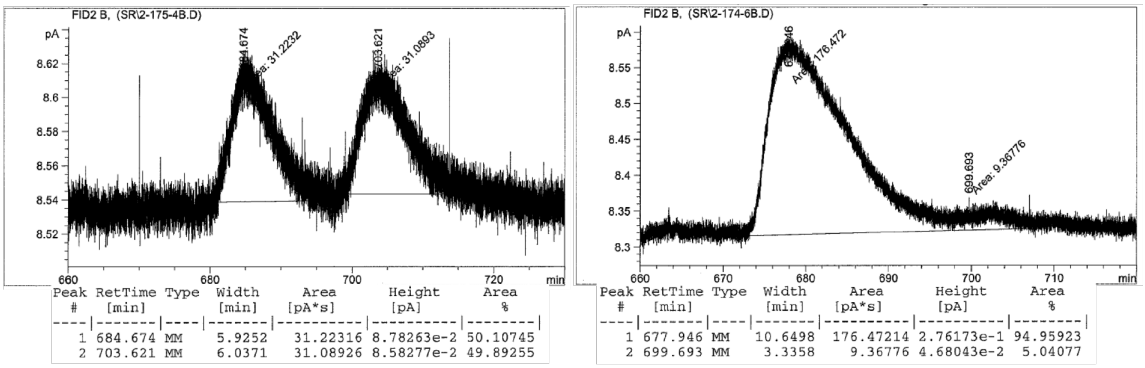

Peak #	Time (min)	Area (%)	Peak #	Time (min)	Area (%)
1	684.674	50.10745	1	677.946	94.95923
2	703.621	49.89255	2	699.693	5.04077

Imidazolinium Tetrafluoroborate Salt (im-16): Prepared according to a reported procedure and the spectroscopic data match those reported previously.[44] ^{1}H NMR (400 MHz, $CDCl_3$): δ 8.76 (1H, s), 7.89 (1H, d, *J* = 1.6 Hz), 7.46–7.25 (7H, m), 7.19–7.02 (4H, m), 7.01 (1H, d, *J* = 8.0 Hz), 6.91 (1H, s), 6.59 (1H, s), 6.43–6.41 (2H, m), 5.35 (1H, d, *J* = 7.6 Hz), 5.21 (1H, d, *J* = 7.6 Hz), 3.08–3.01 (1H, m), 2.52 (3H, s), 2.50 (3H, s), 2.17 (3H, s), 2.05 (3H, s), 1.93 (3H, s), 1.58 (3H, s), 1.25 (6H, d, *J* = 8.4 Hz).

■ **^{1}H NMR Spectra**

(44) Vieira, E. M.; Snapper, M. L.; Hoveyda, A. H. *J. Am. Chem. Soc.* **2011**, *133*, 3332–3335.

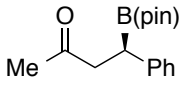
O
B(pin)
Me
Ph

1.77

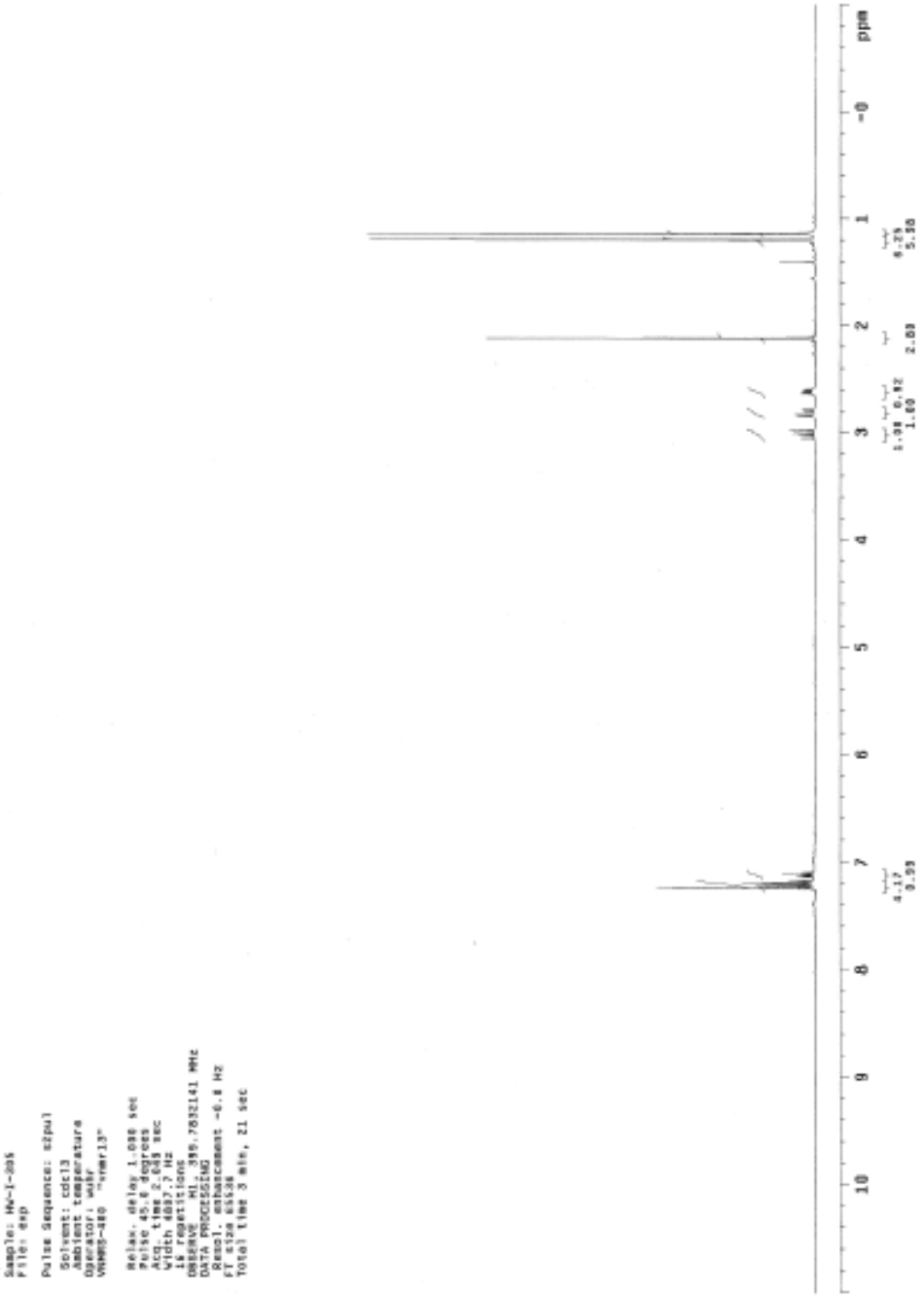
Sample: HW-I-205
File: exp
Pulse Sequence: s2pul
Solvent: cdcl3
Ambient temperature
Operator: wshr
VNMRS-400 "vnmr13"
Relax. delay 1.000 sec
Pulse 45.0 degrees
Acq. time 2.849 sec
Width 4807.7 Hz
16 repetitions
OBSERVE H1, 399.7832141 MHz
DATA PROCESSING
Resol. enhancement -0.8 Hz
FT size 65536
Total time 3 min, 21 sec
ppm
4.17
3.99
1.98
6.92
1.00
2.00
9.79
5.98

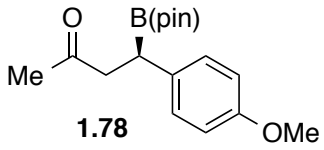

1.78

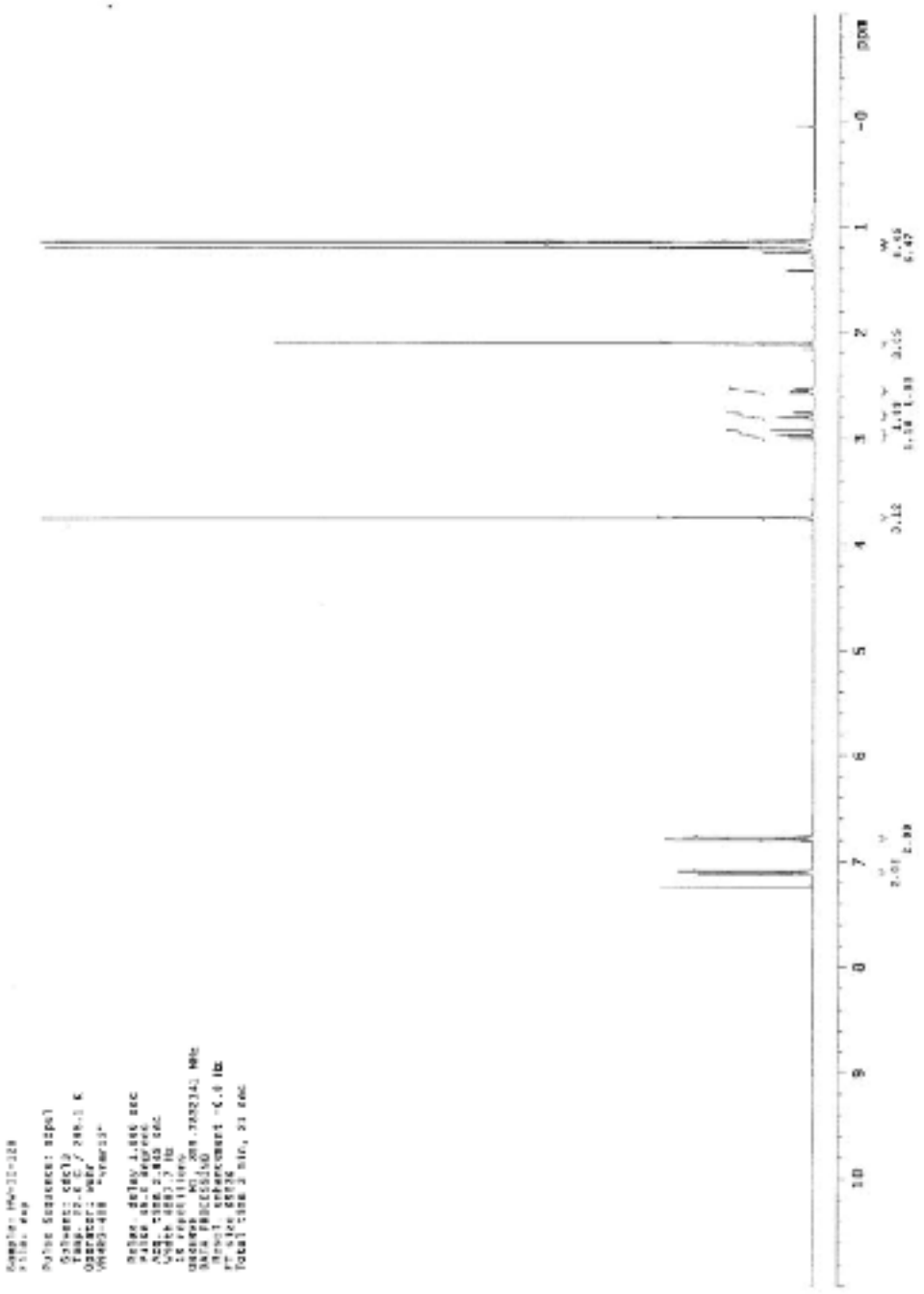

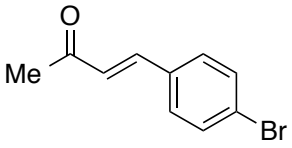

substrate for 1.79

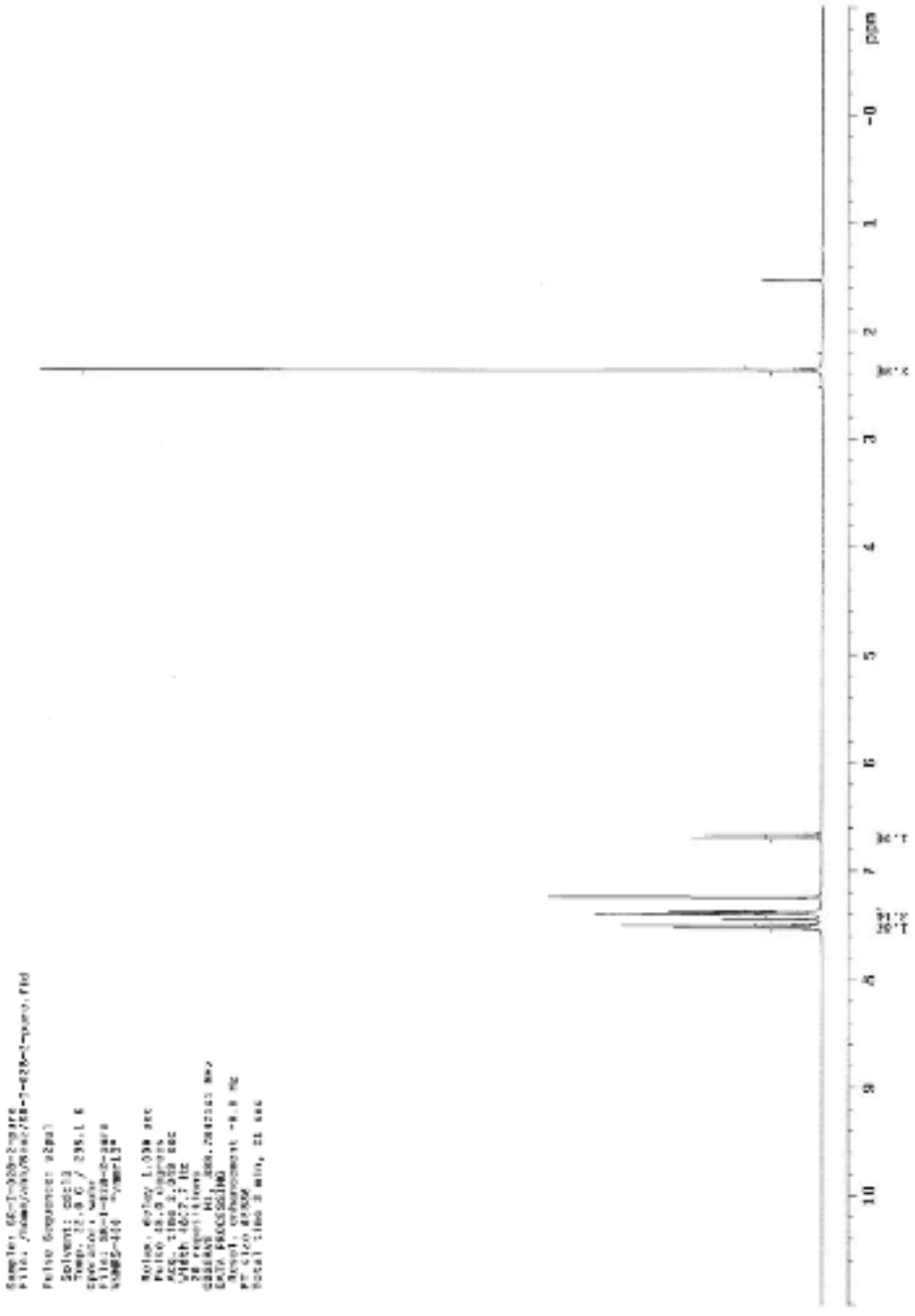

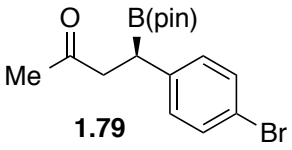

1.79

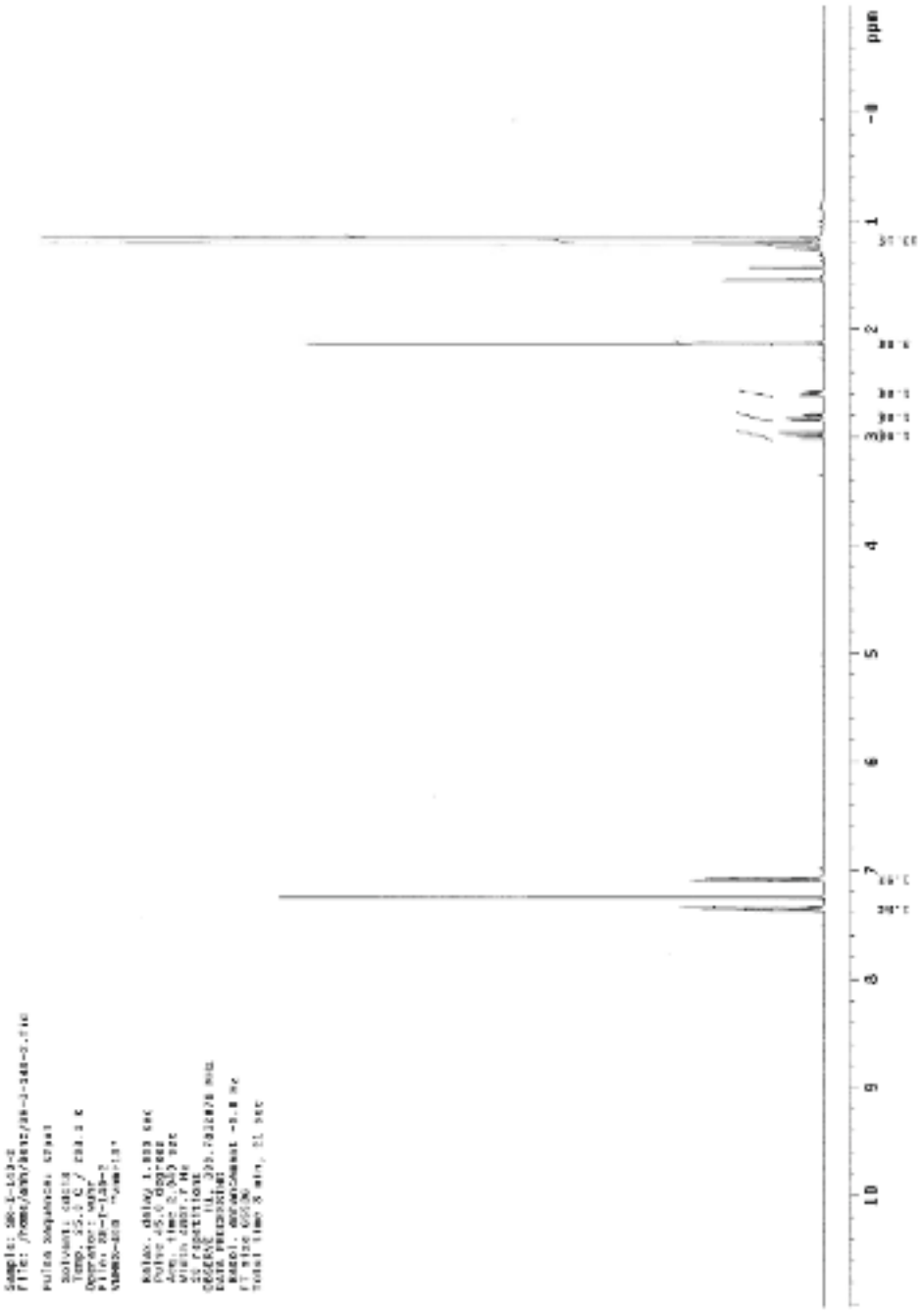

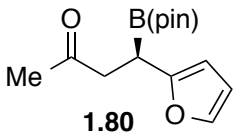

1.80

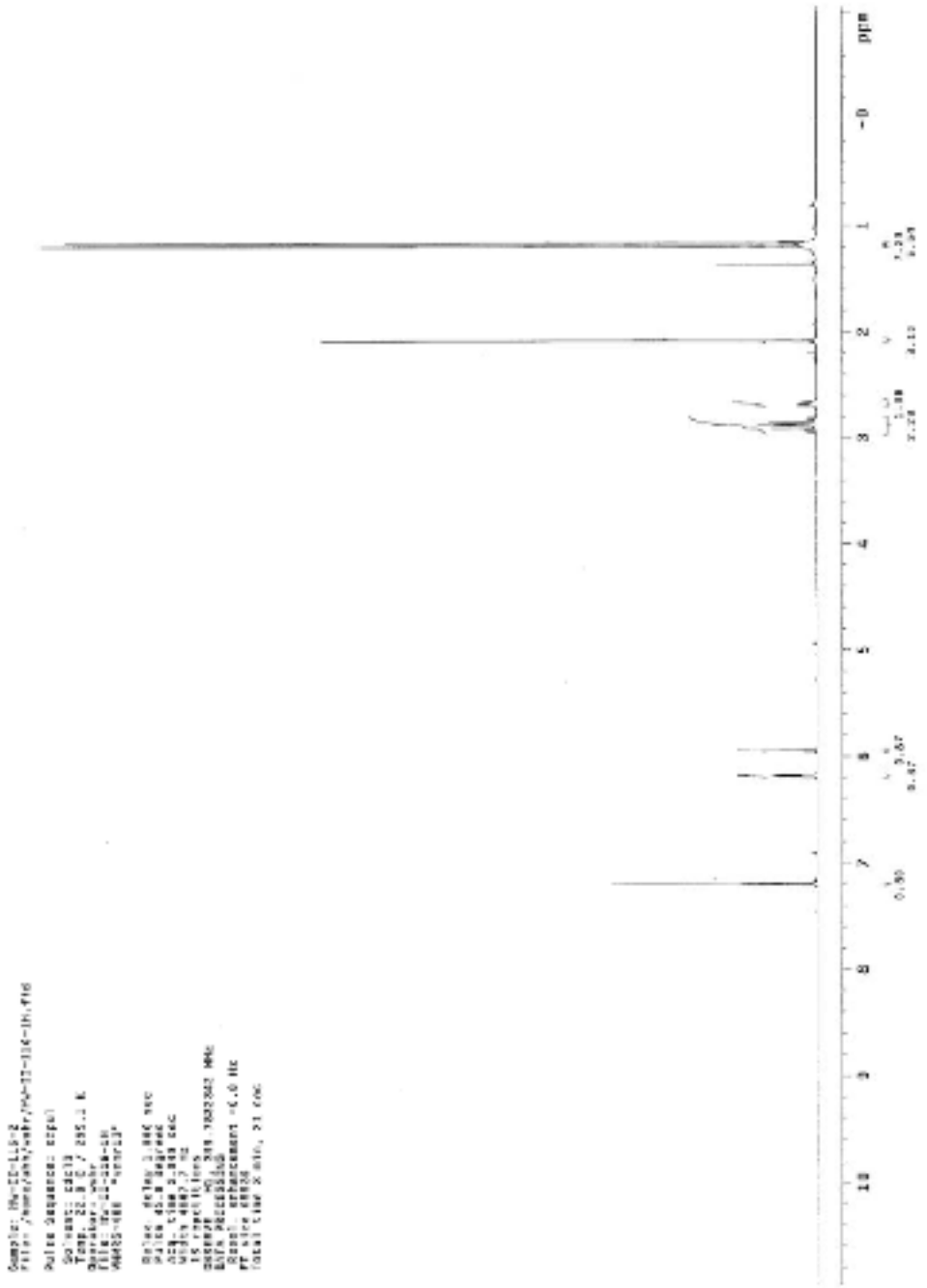

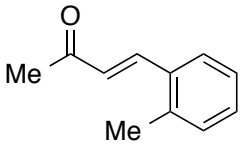

substrate for 1.81

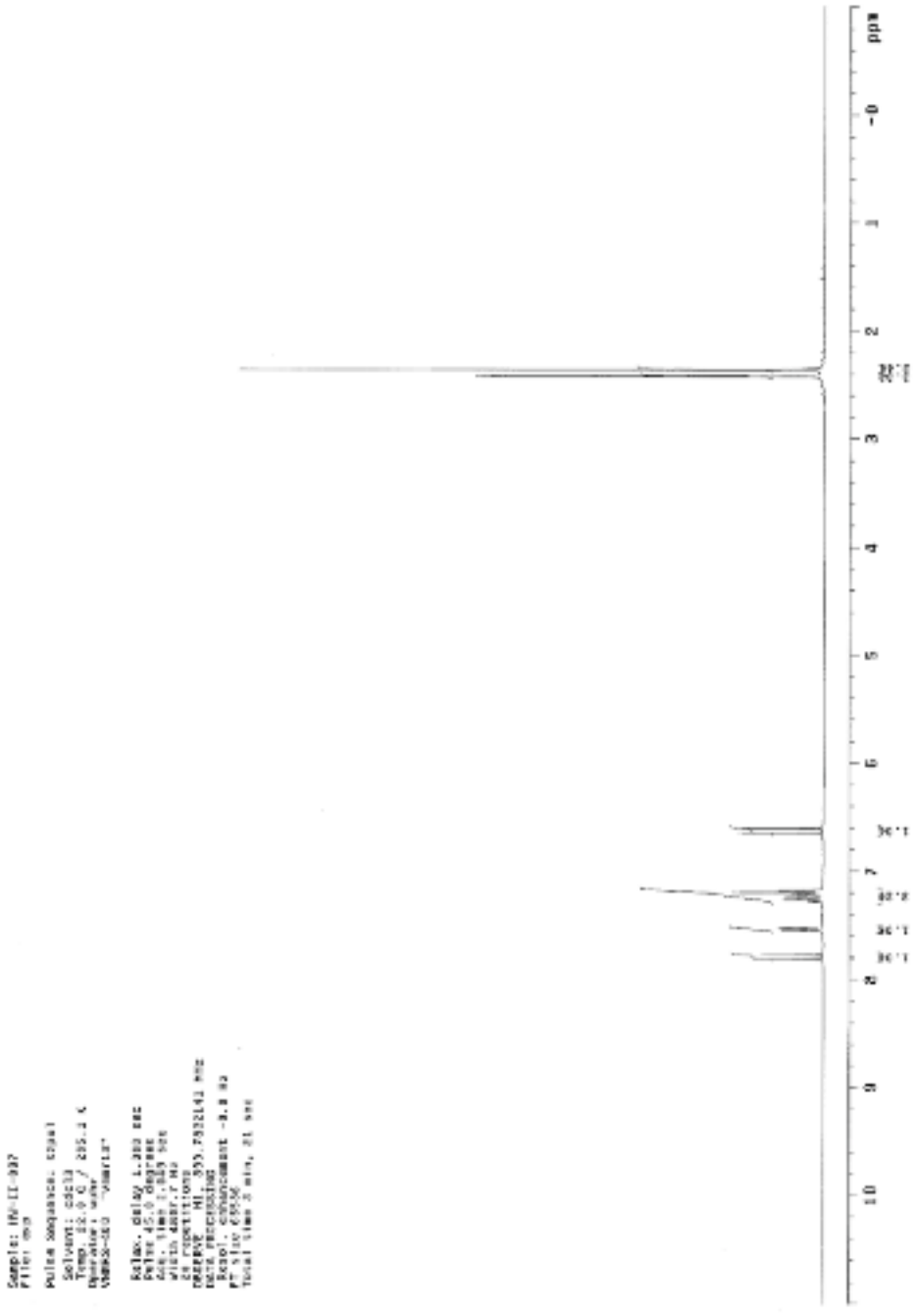

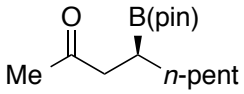

1.82

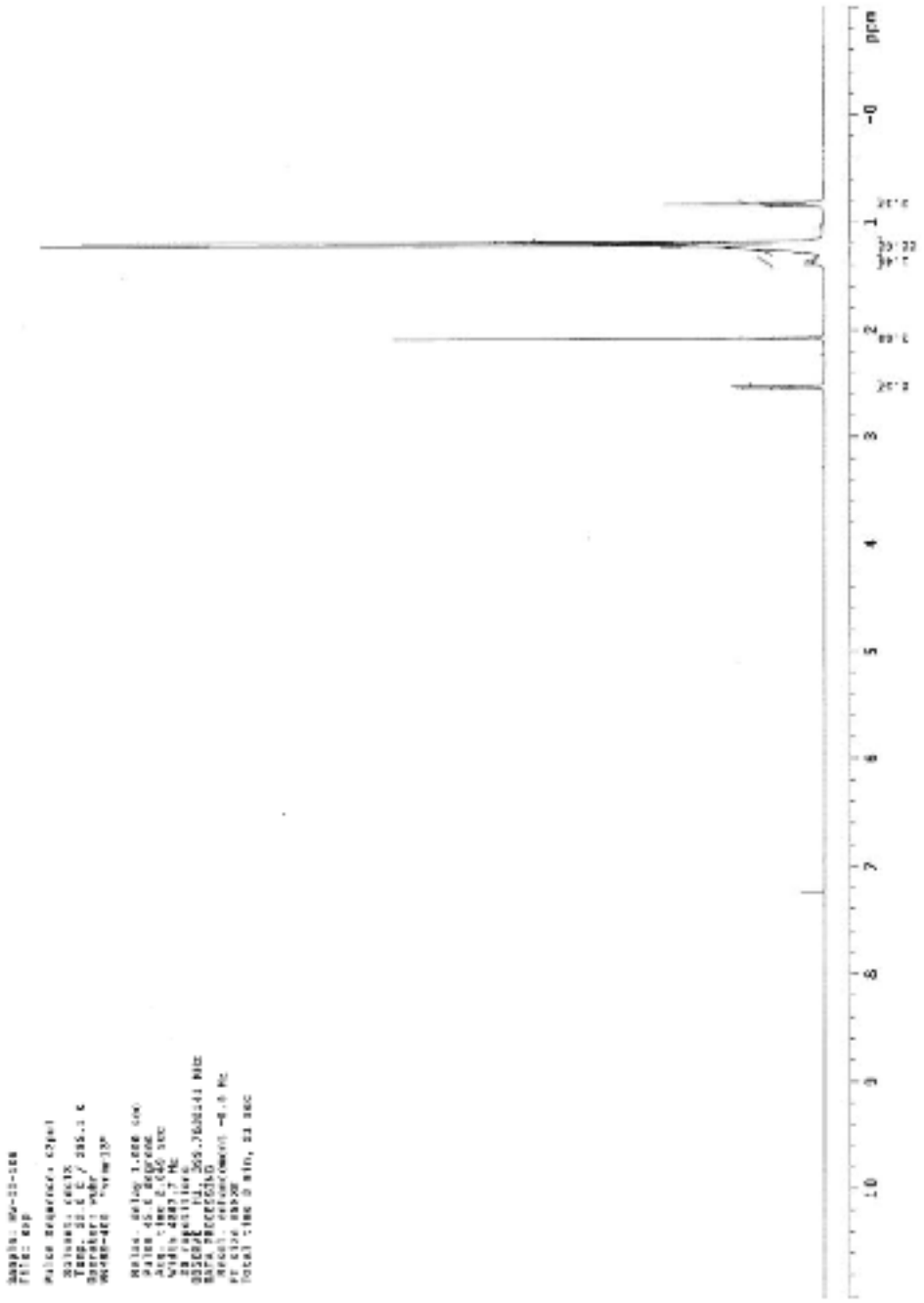

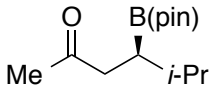

1.83

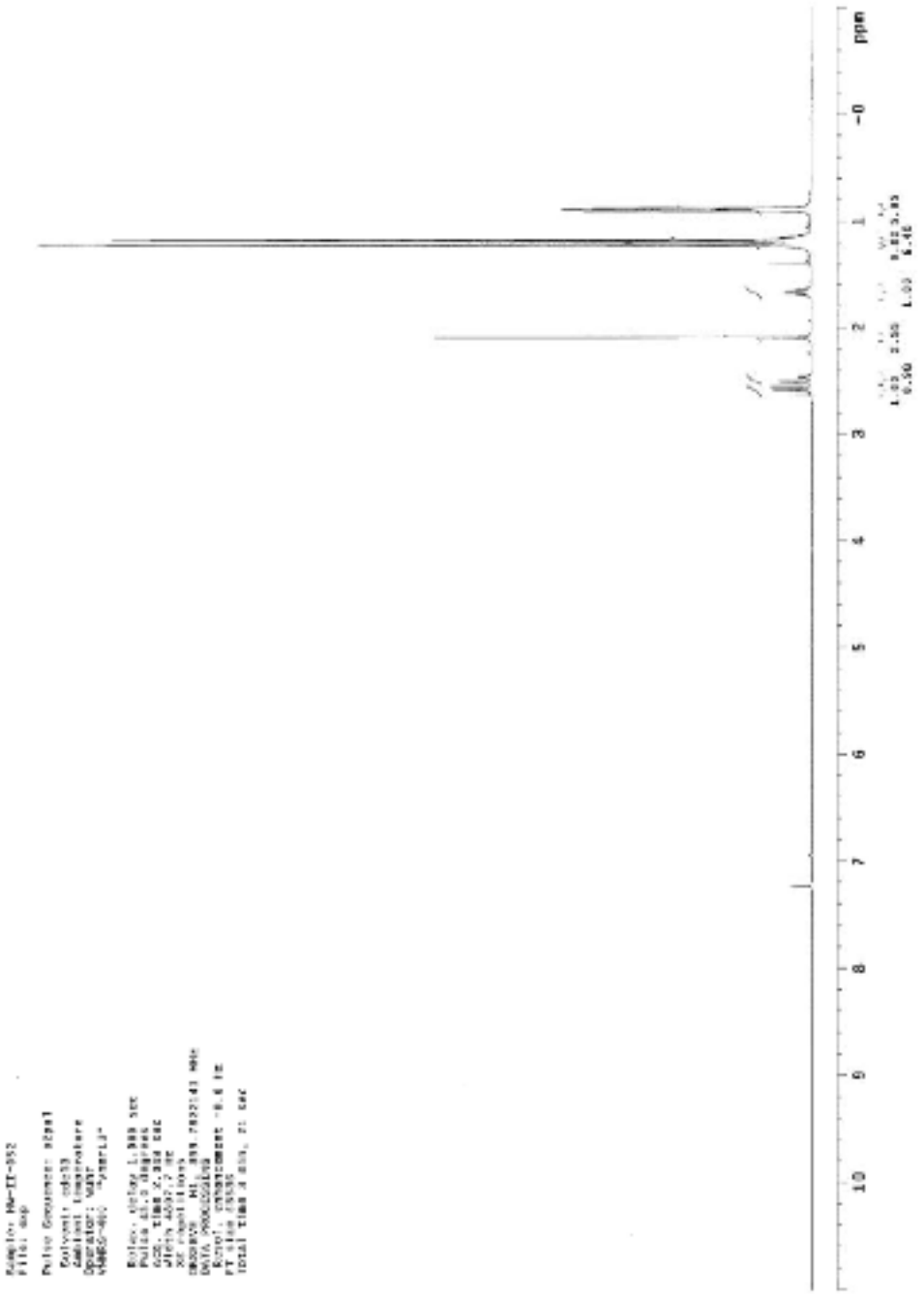

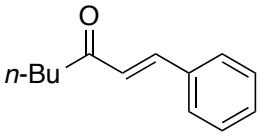

substrate for 1.84

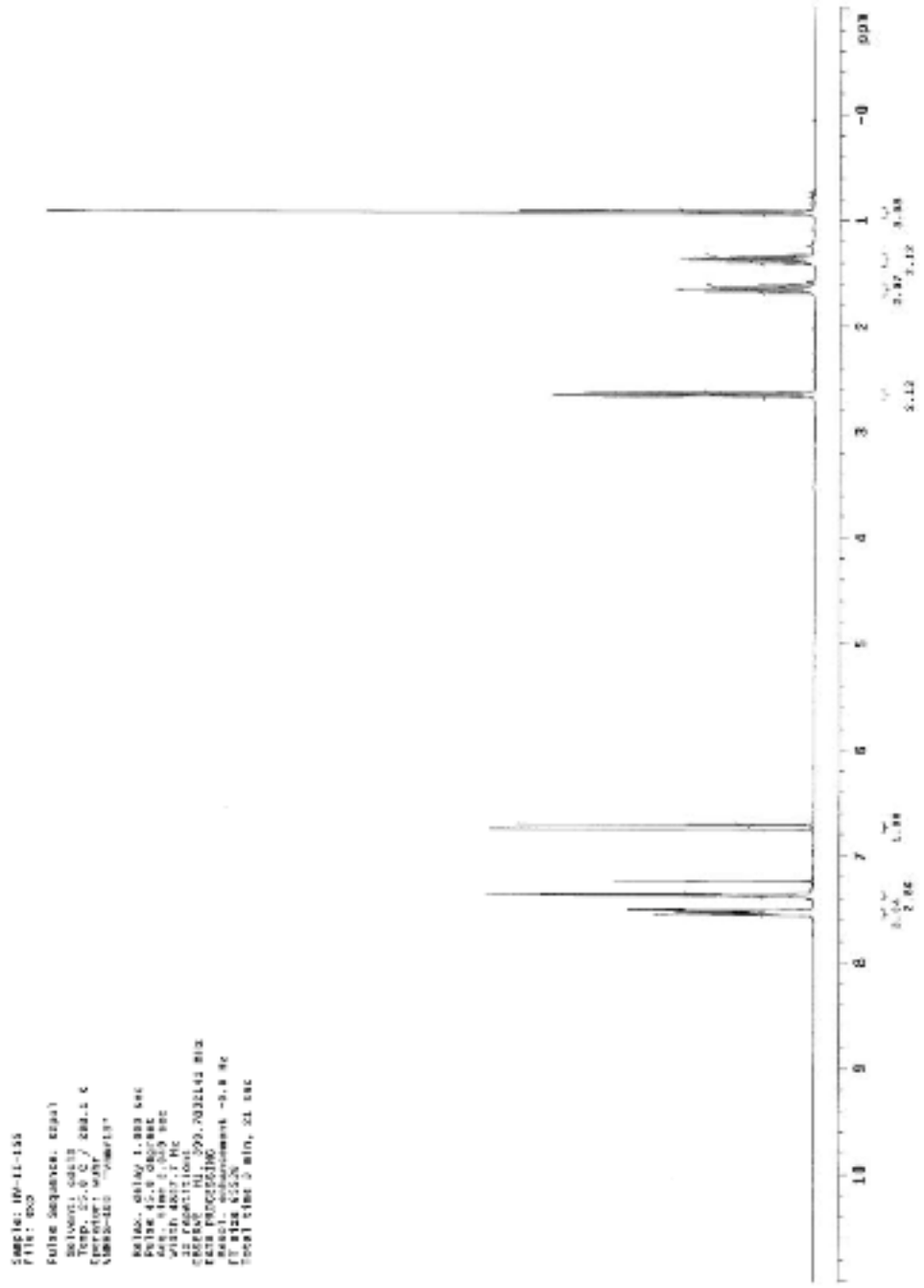

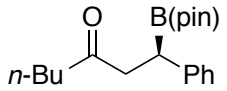

1.84

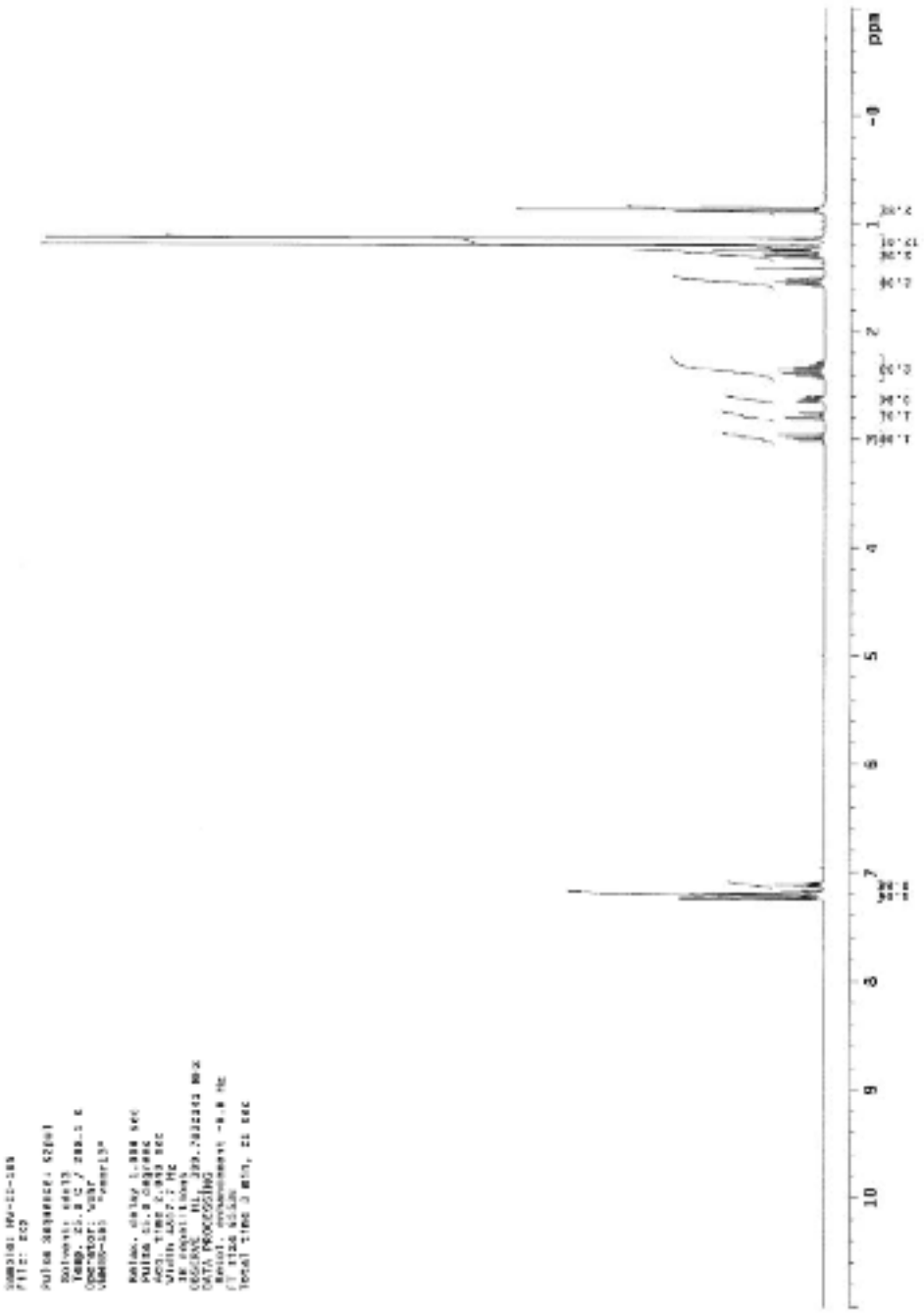

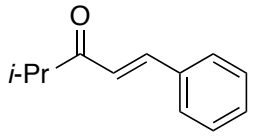

substrate for 1.85

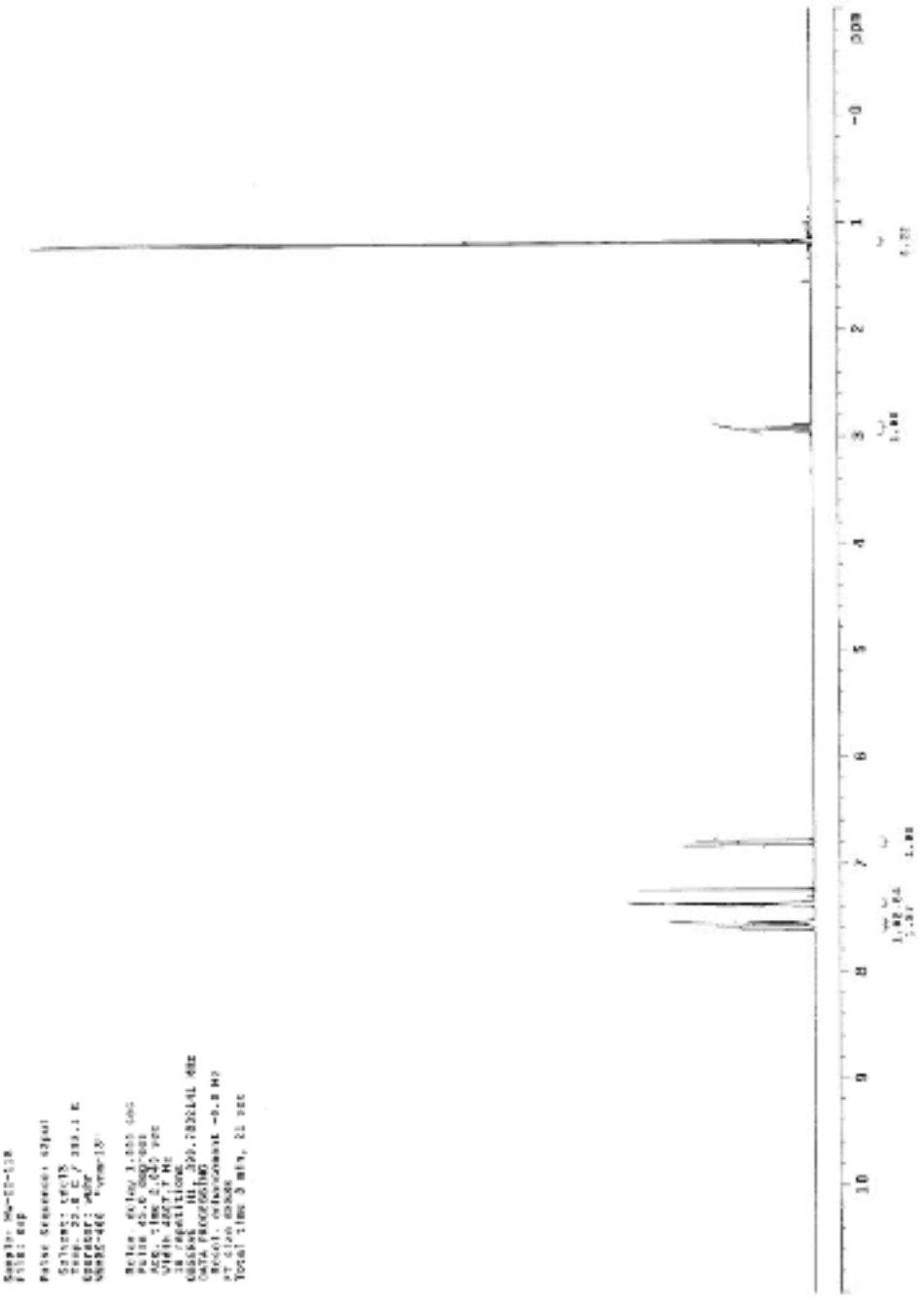

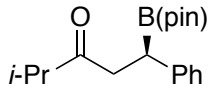

1.85

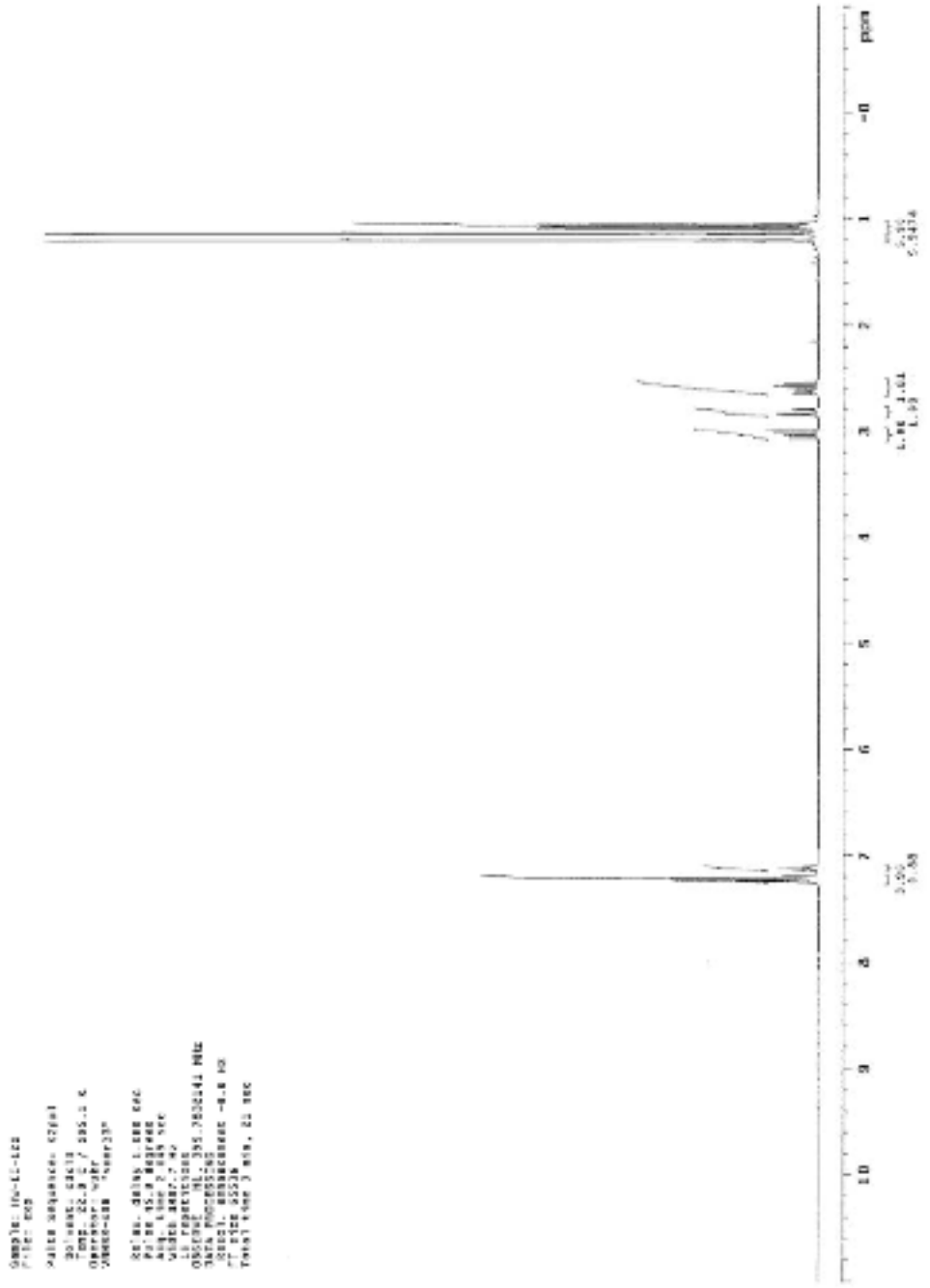

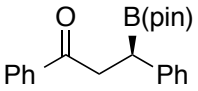

1.86

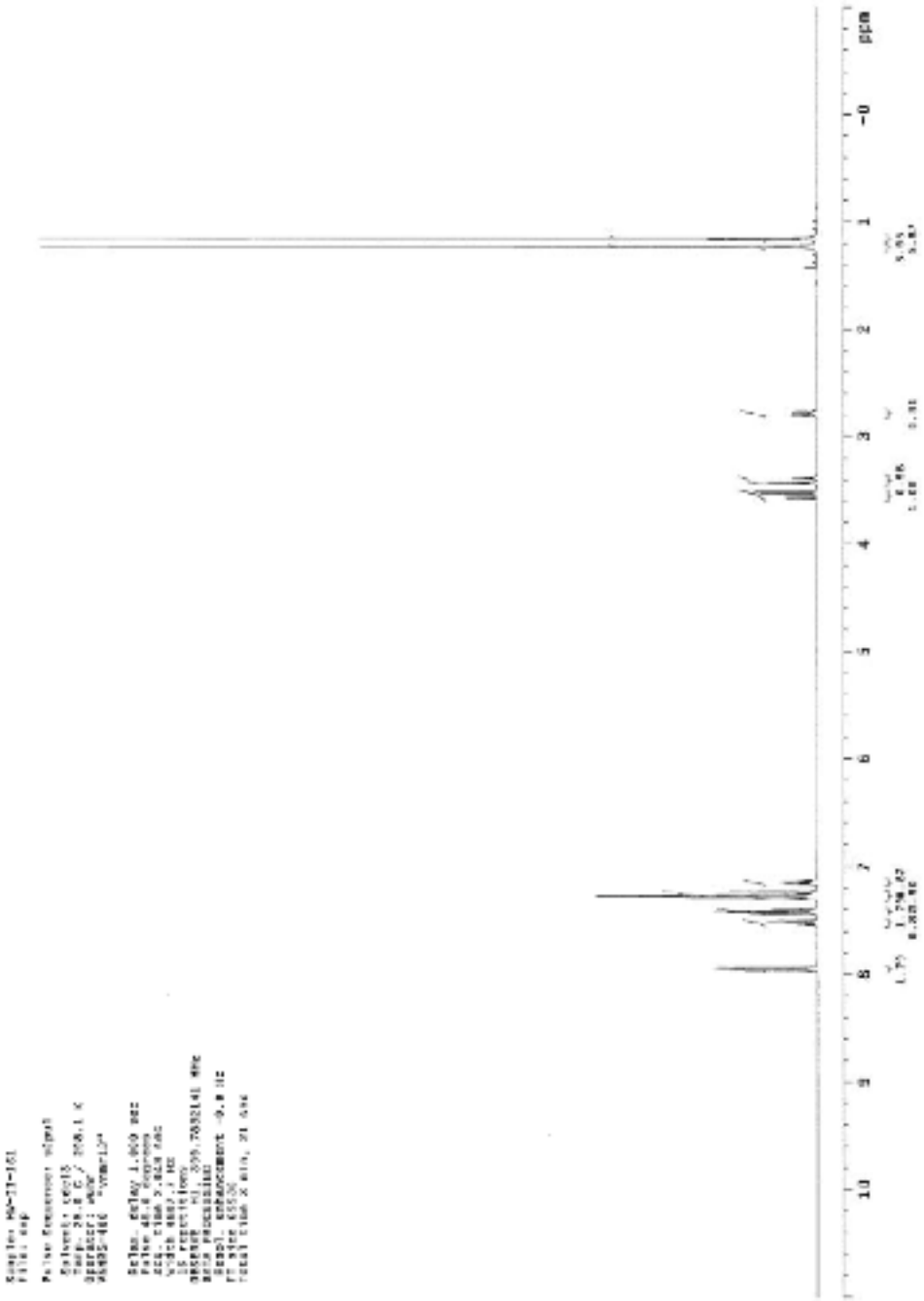

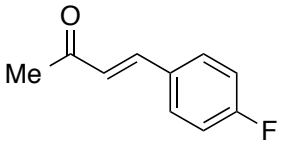

substrate for 1.87

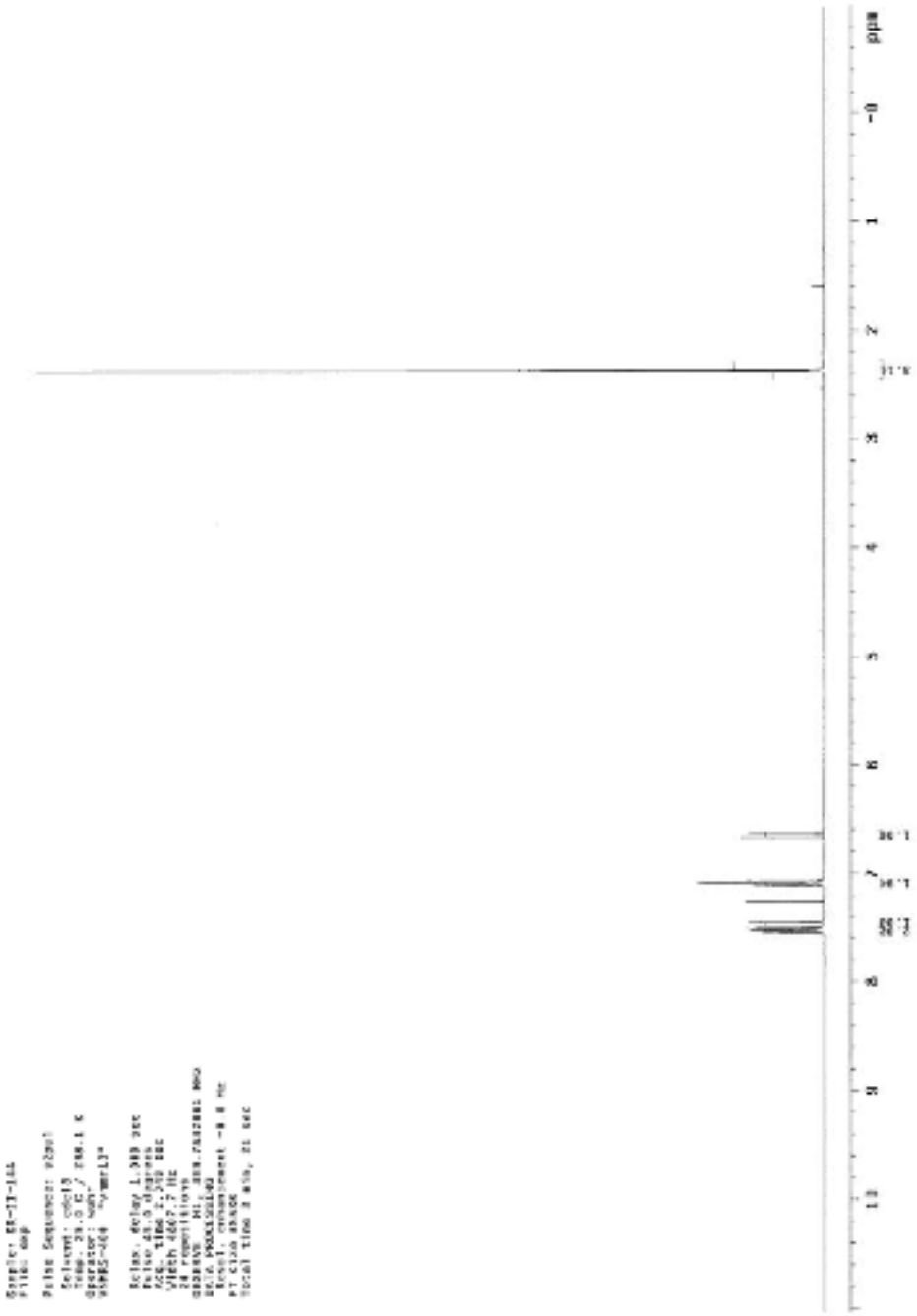

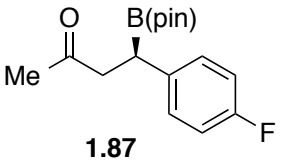

1.87

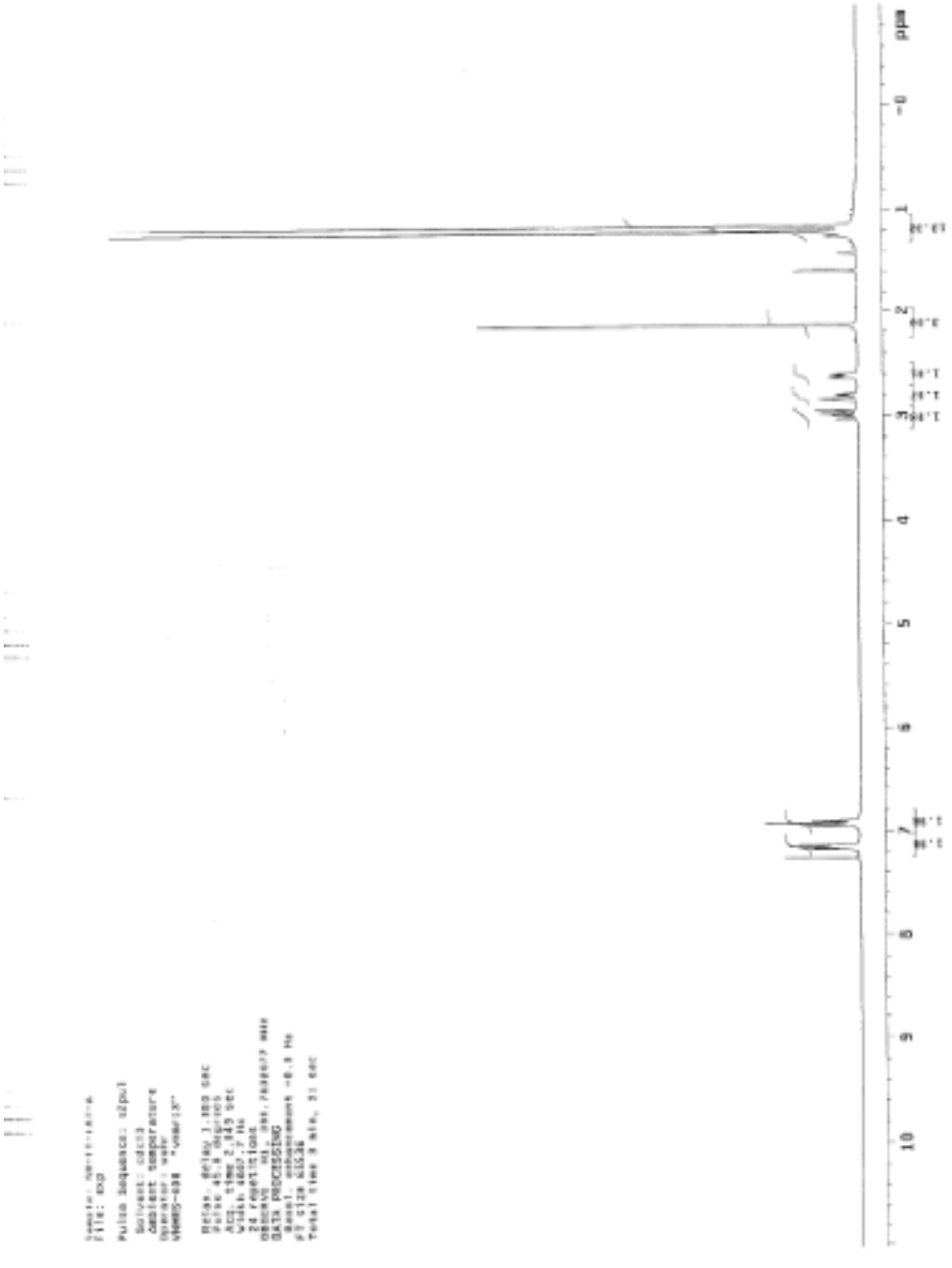

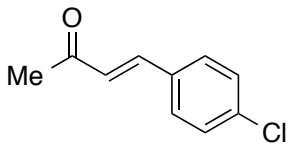

substrate for 1.88

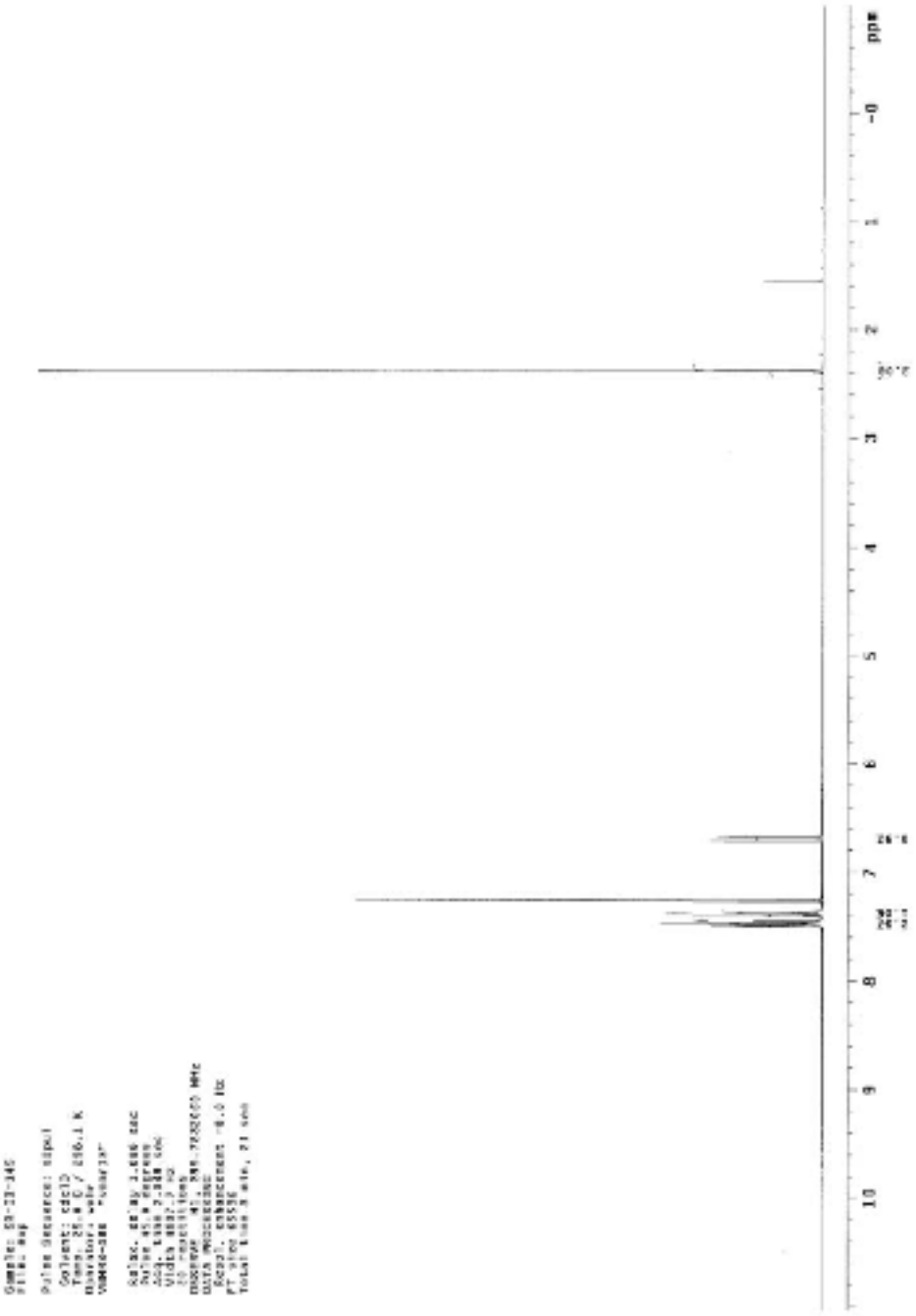

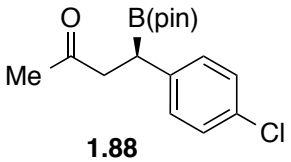

1.88

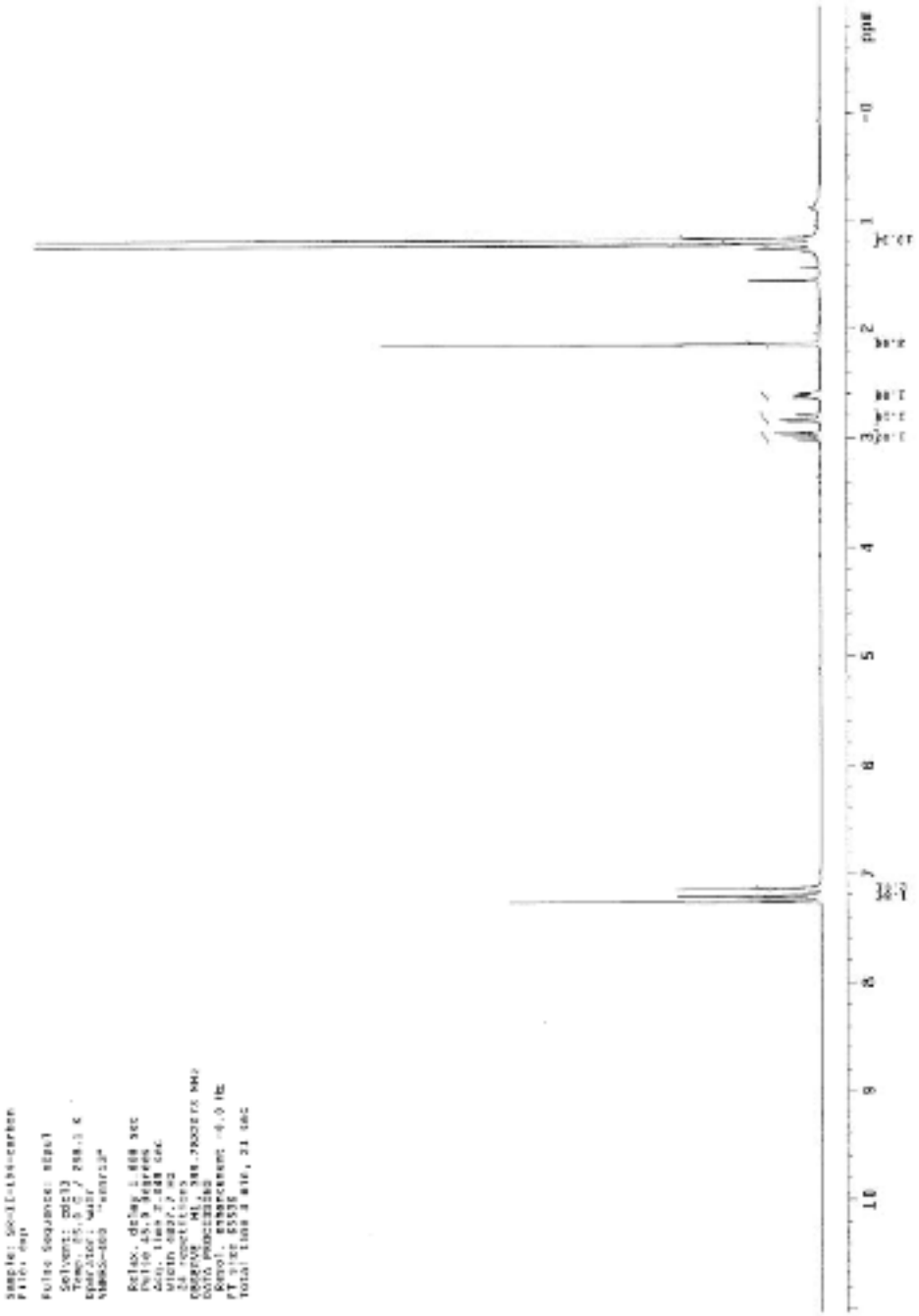

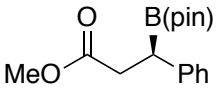

1.90

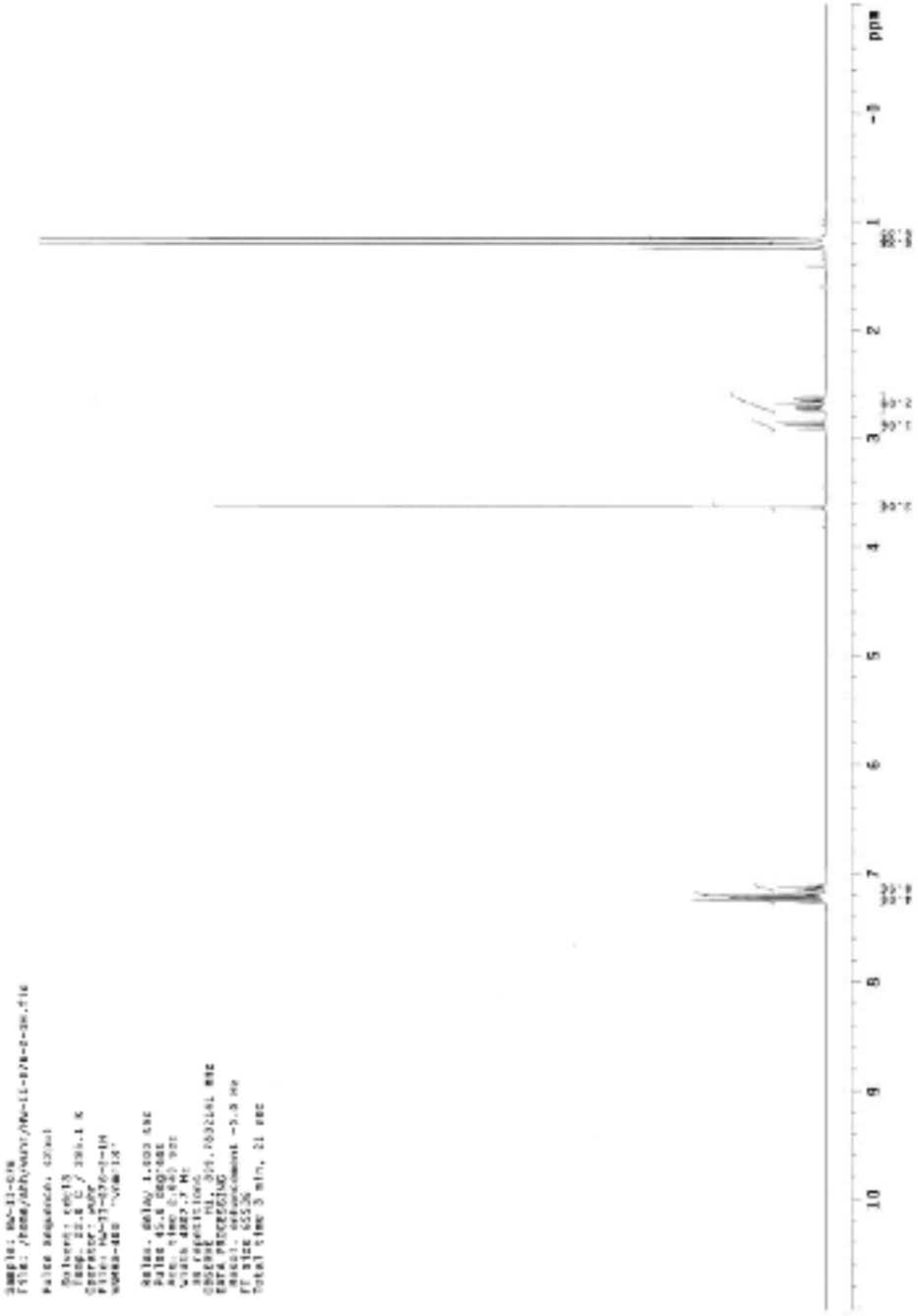

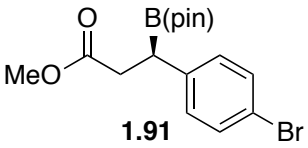

1.91

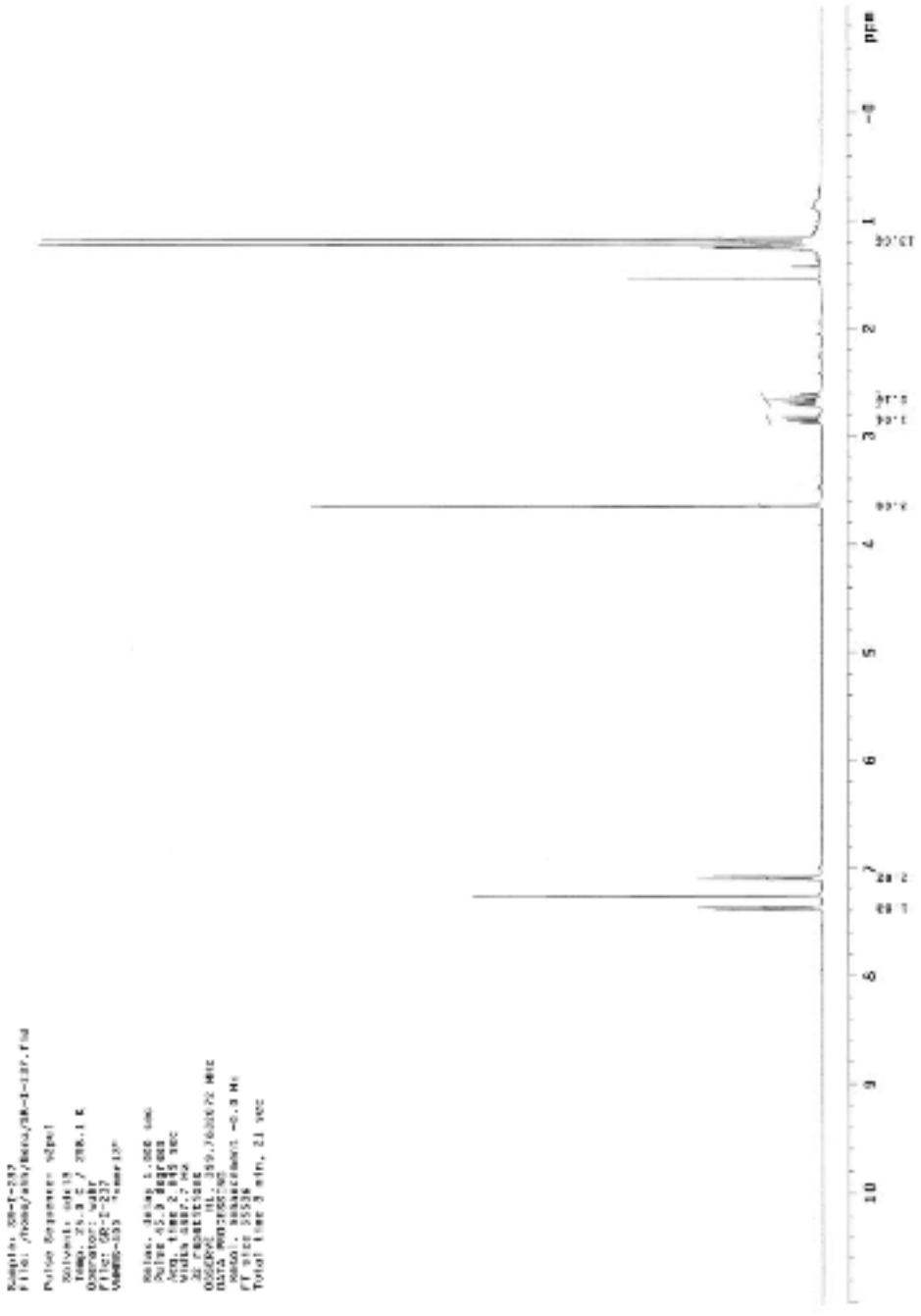

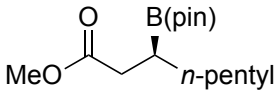

1.92

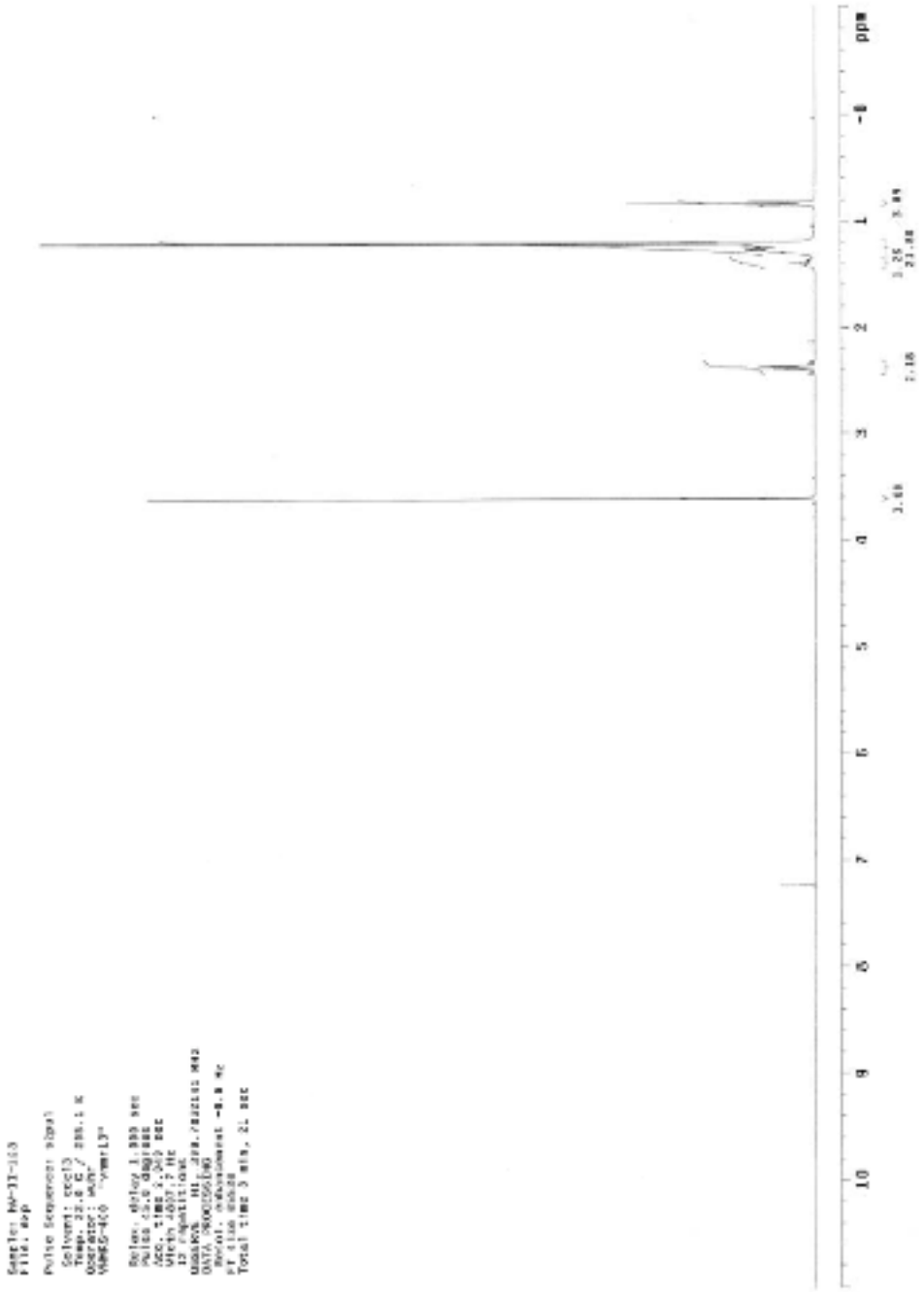

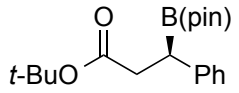

1.93

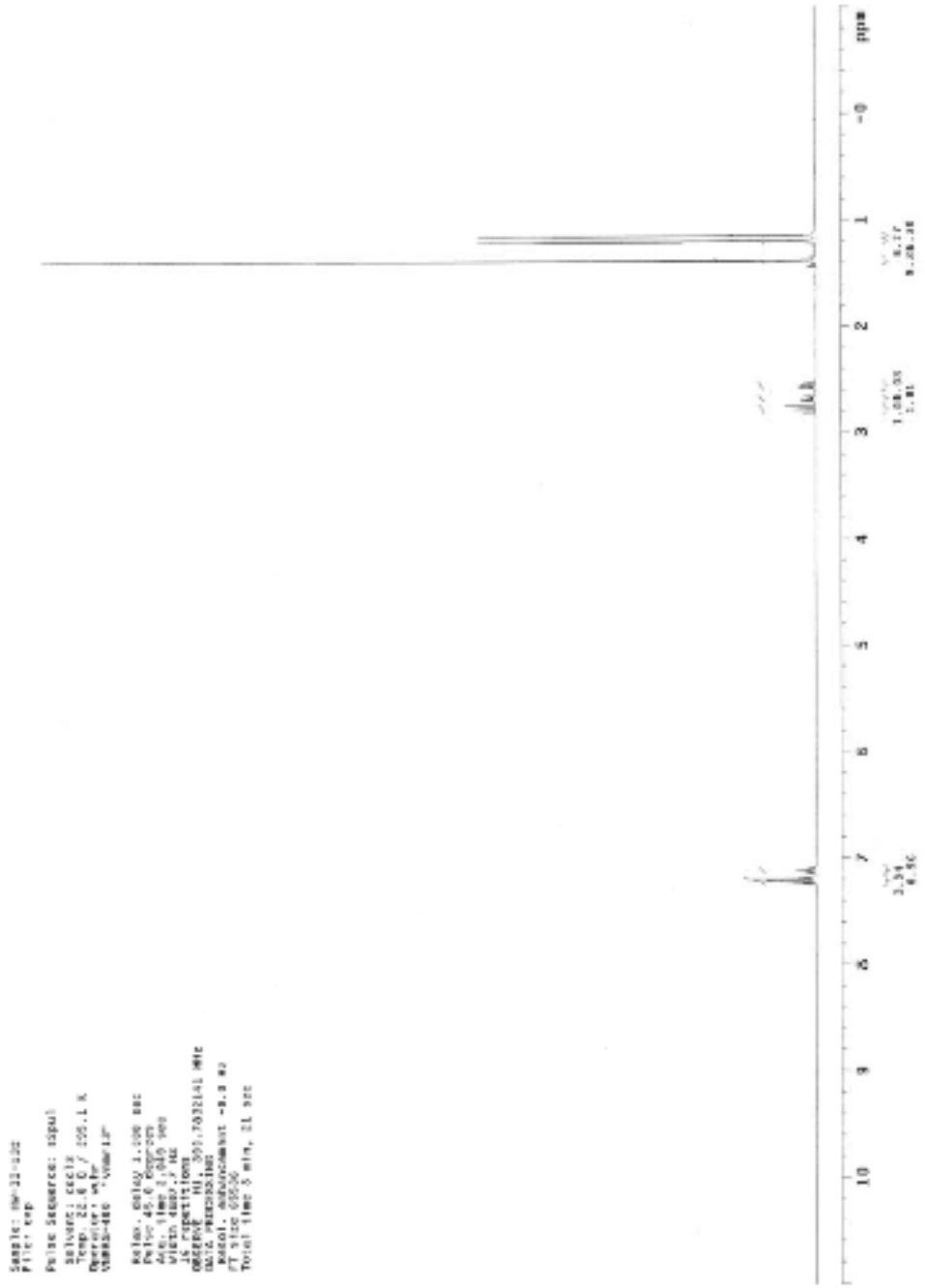

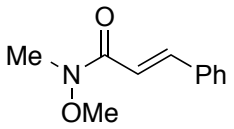

1.94

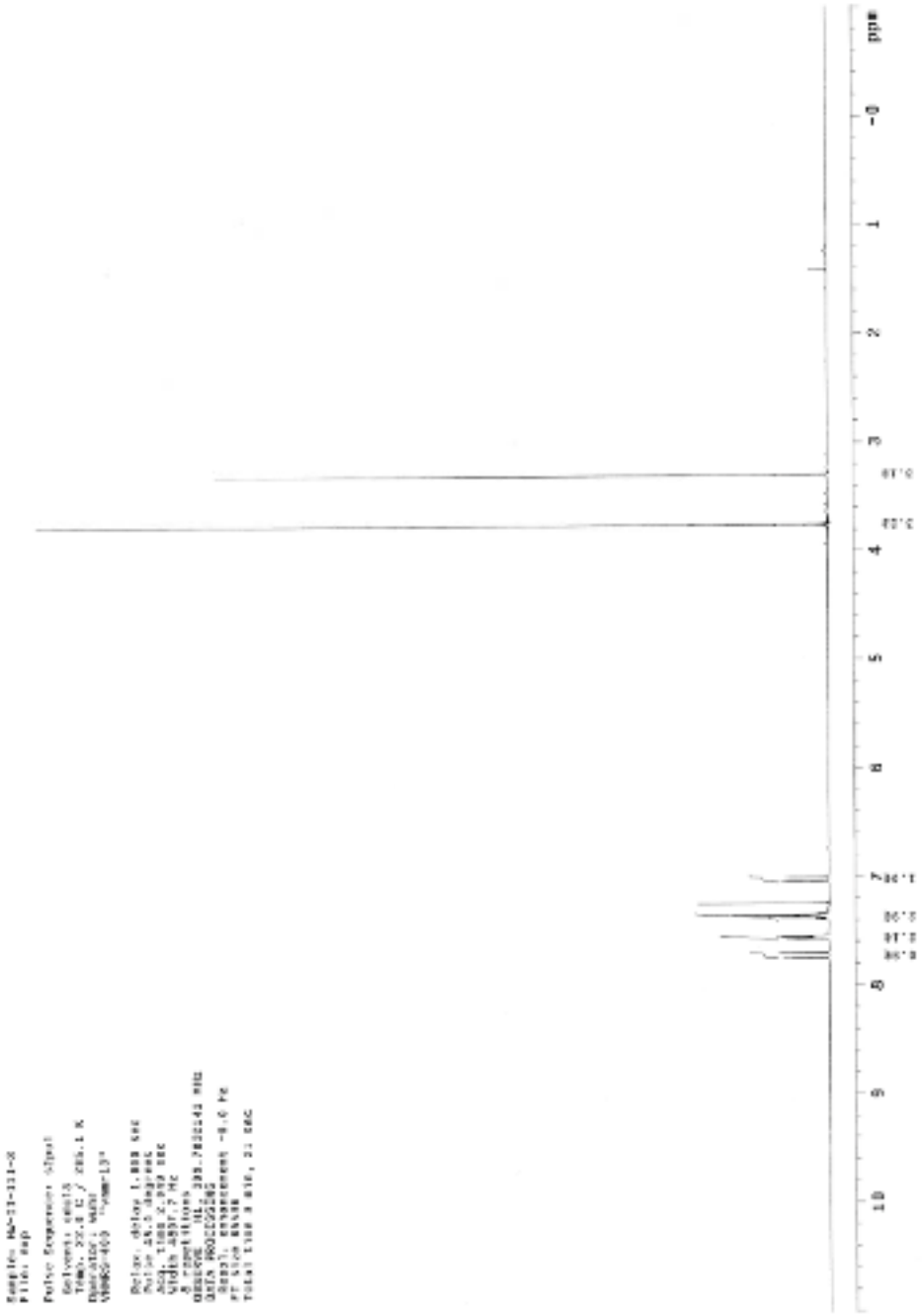

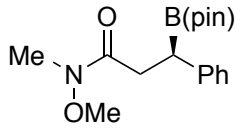

1.95

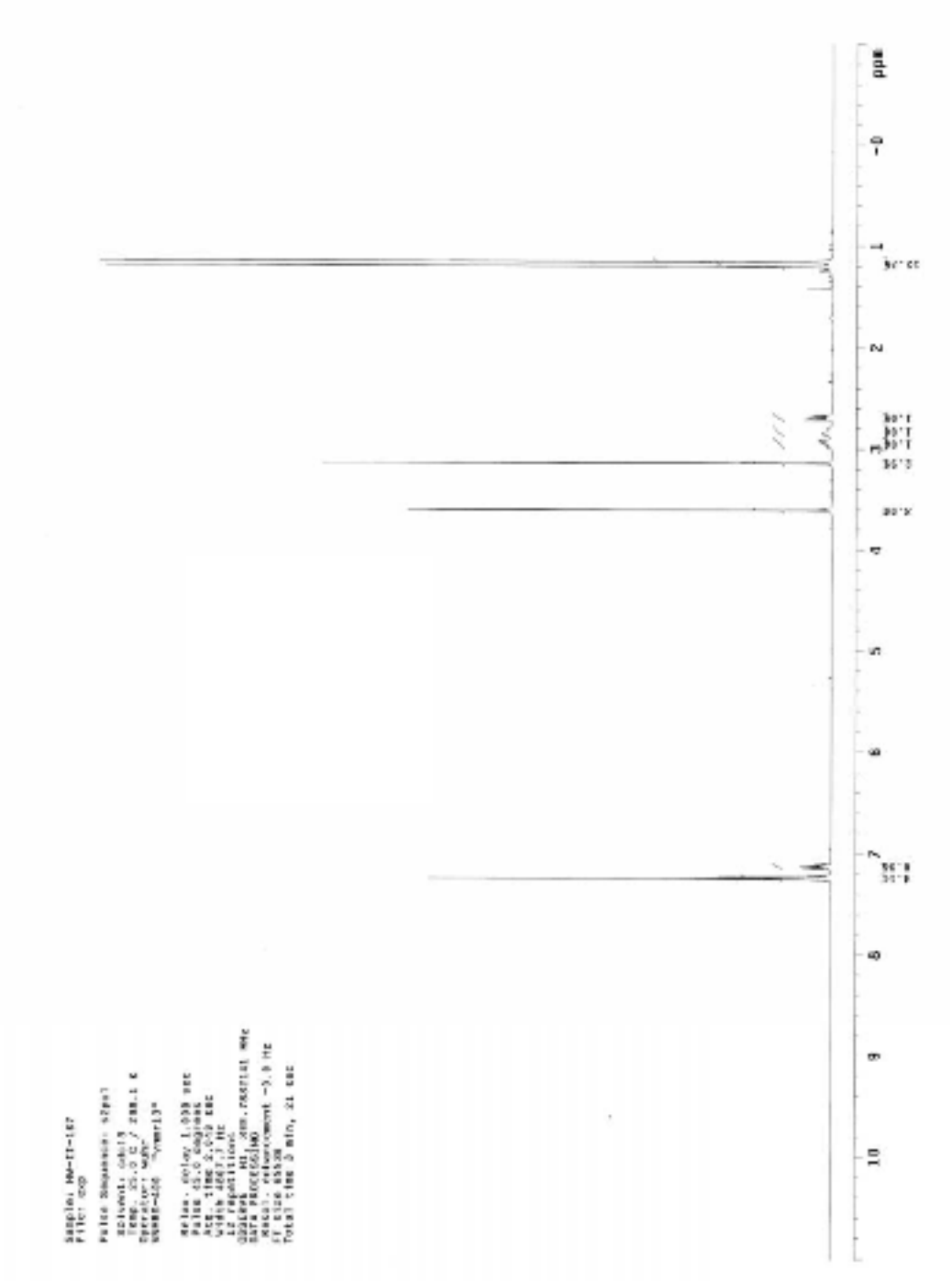

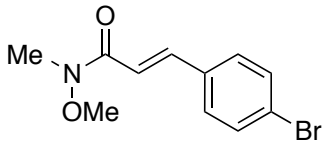

substrate for 1.96

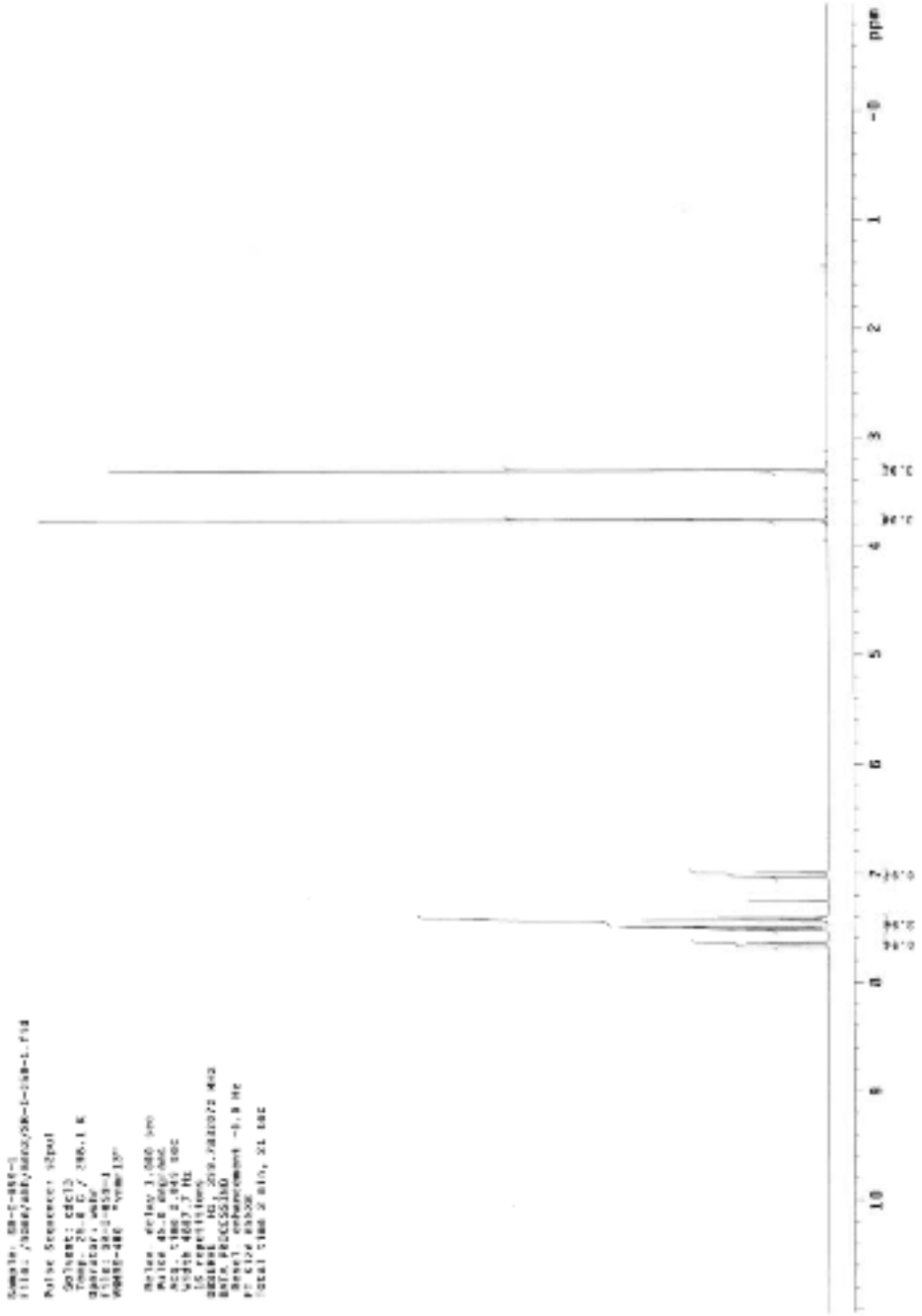

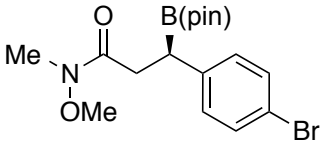

1.96

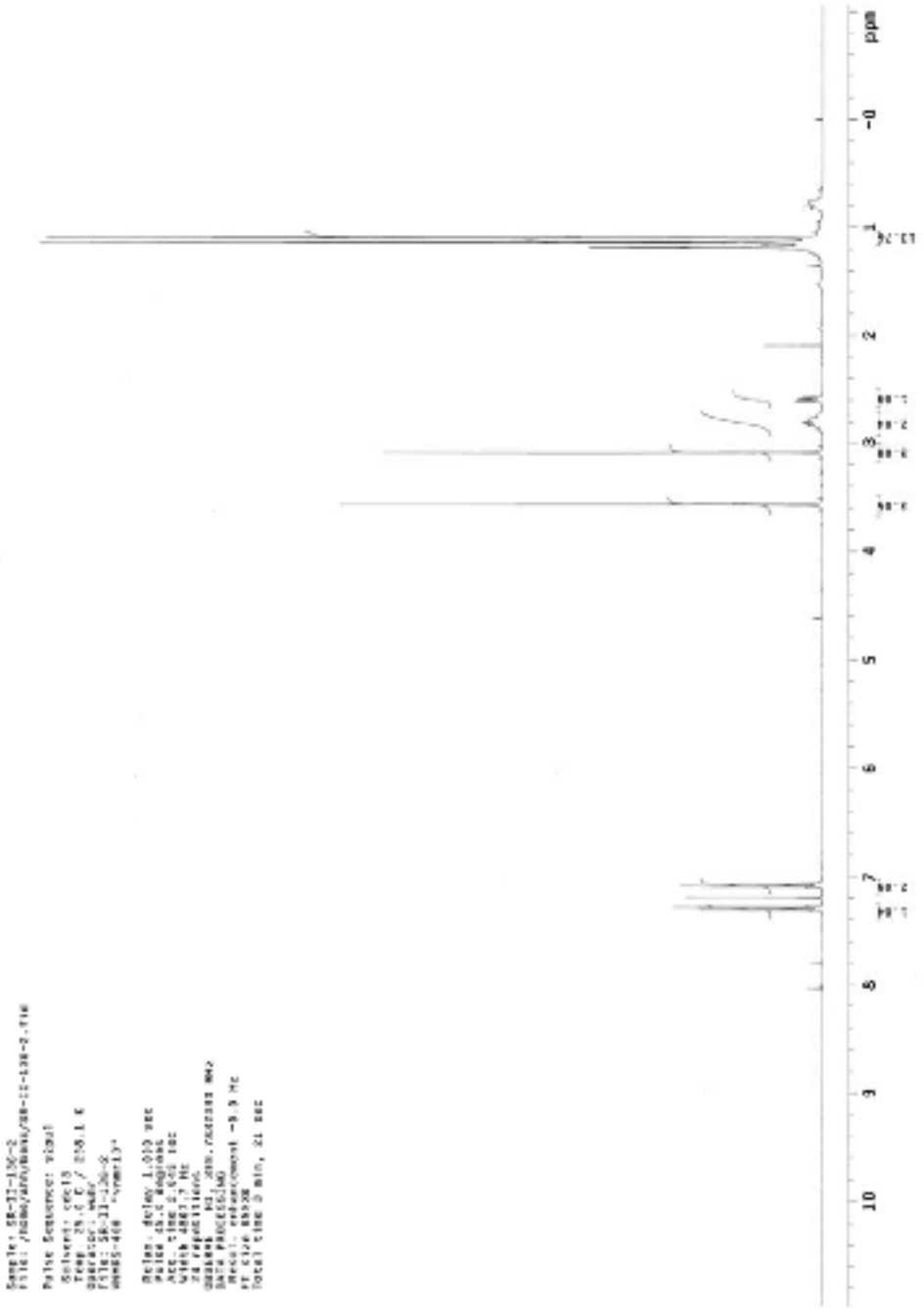

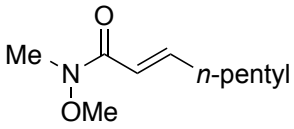

substrate for 1.97

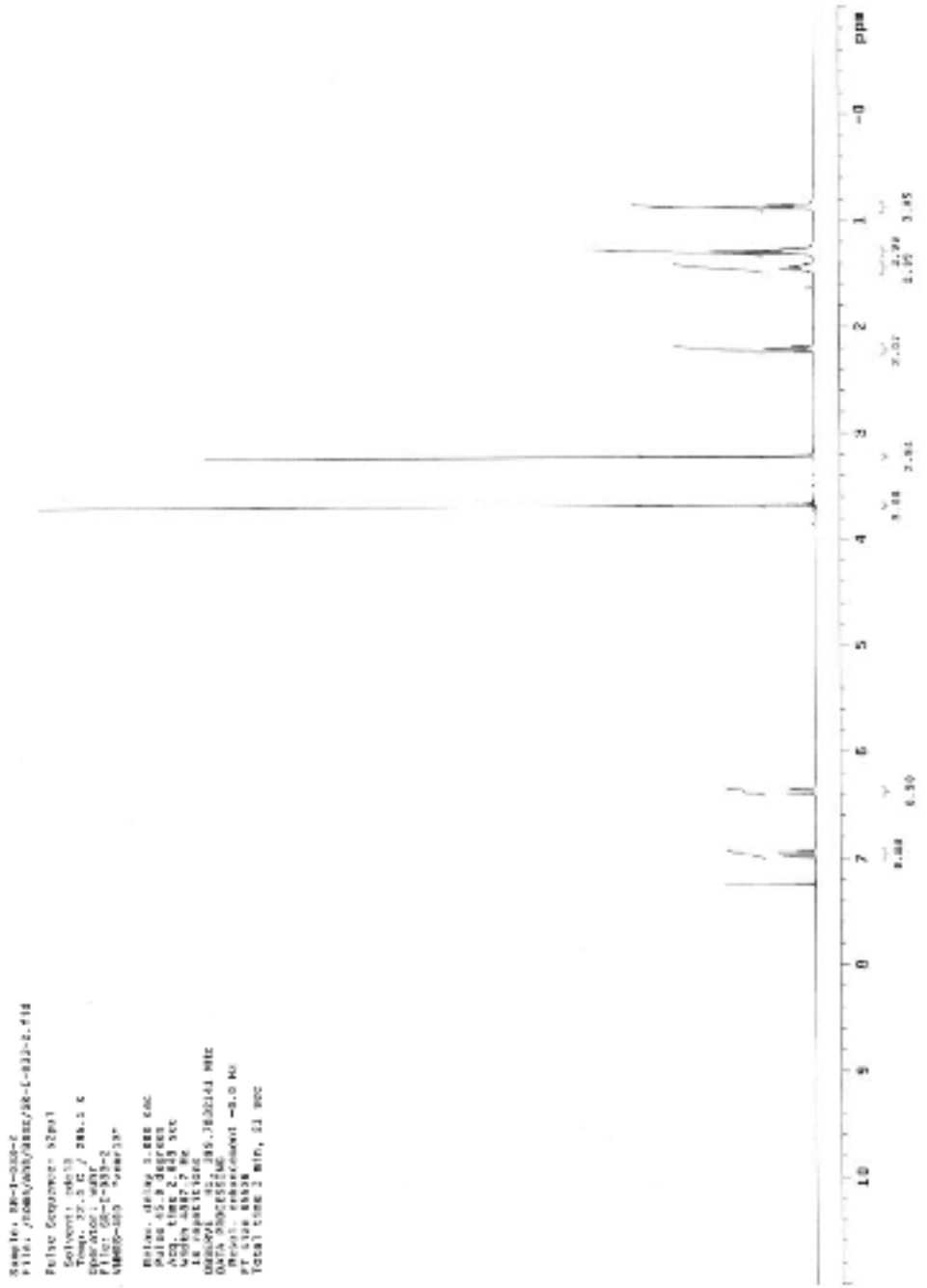

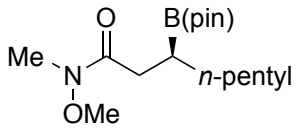

1.97

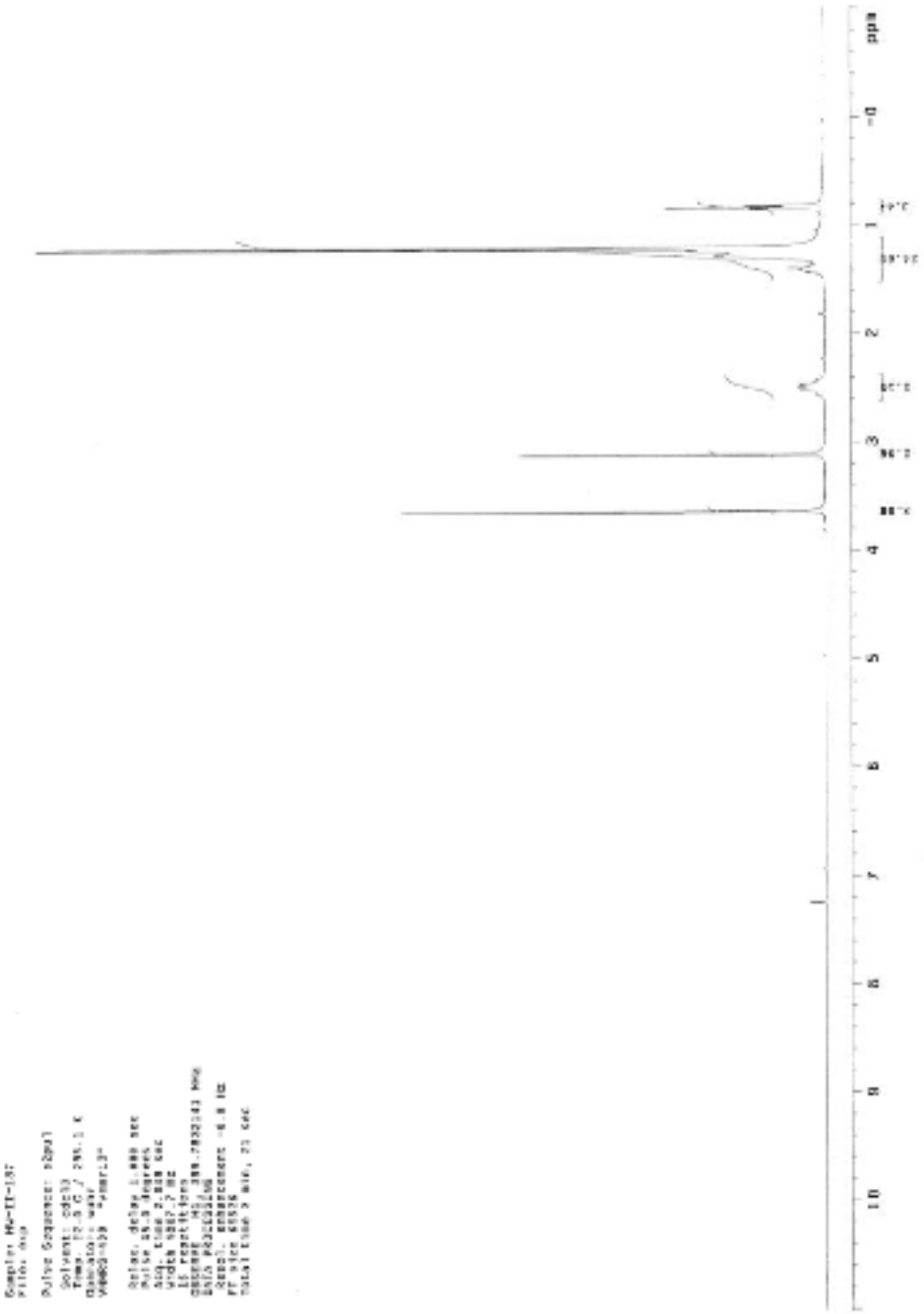

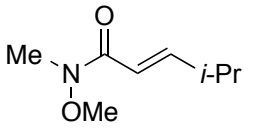

substrate for 1.98

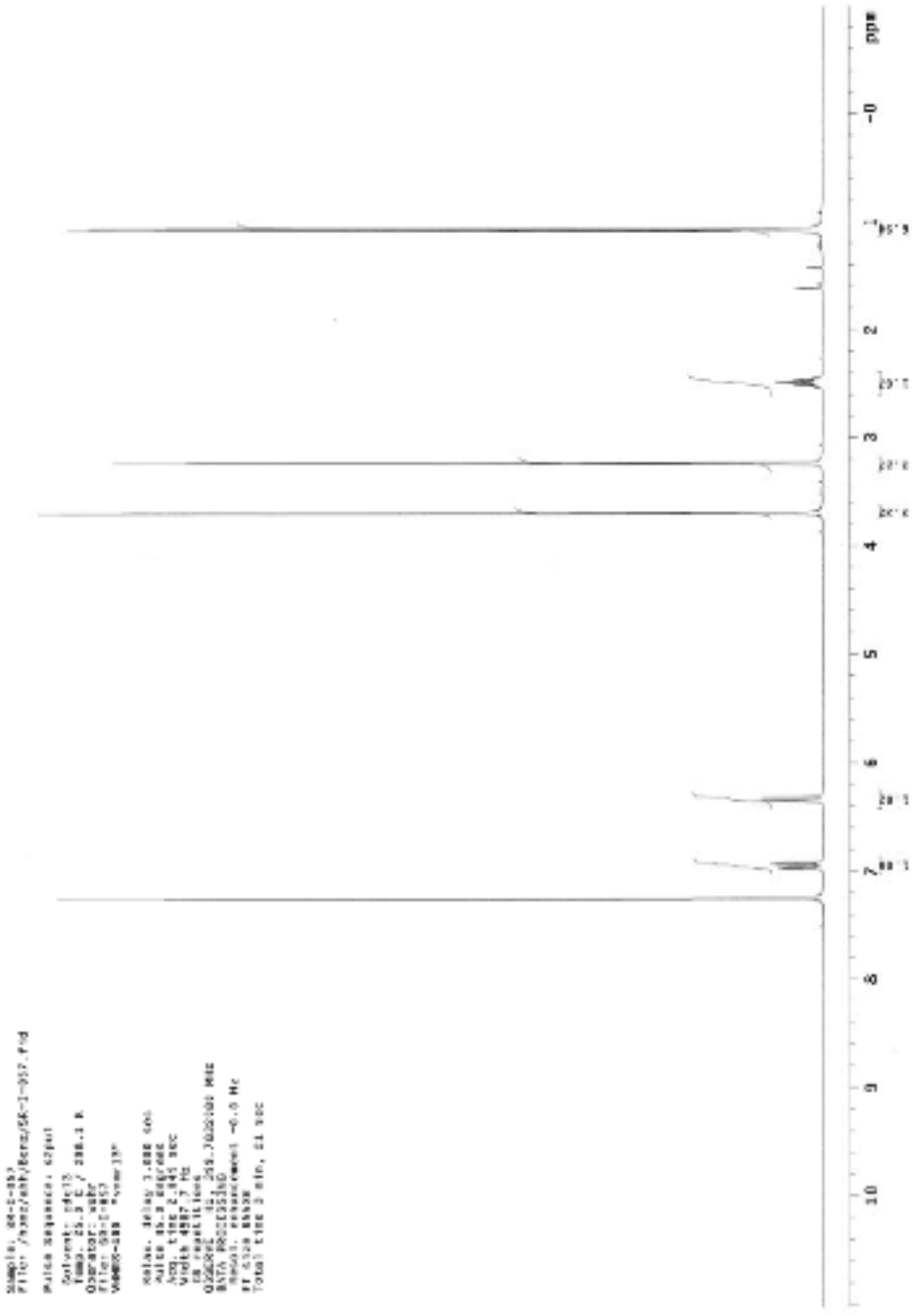

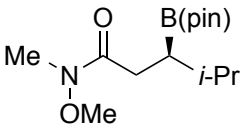

1.98

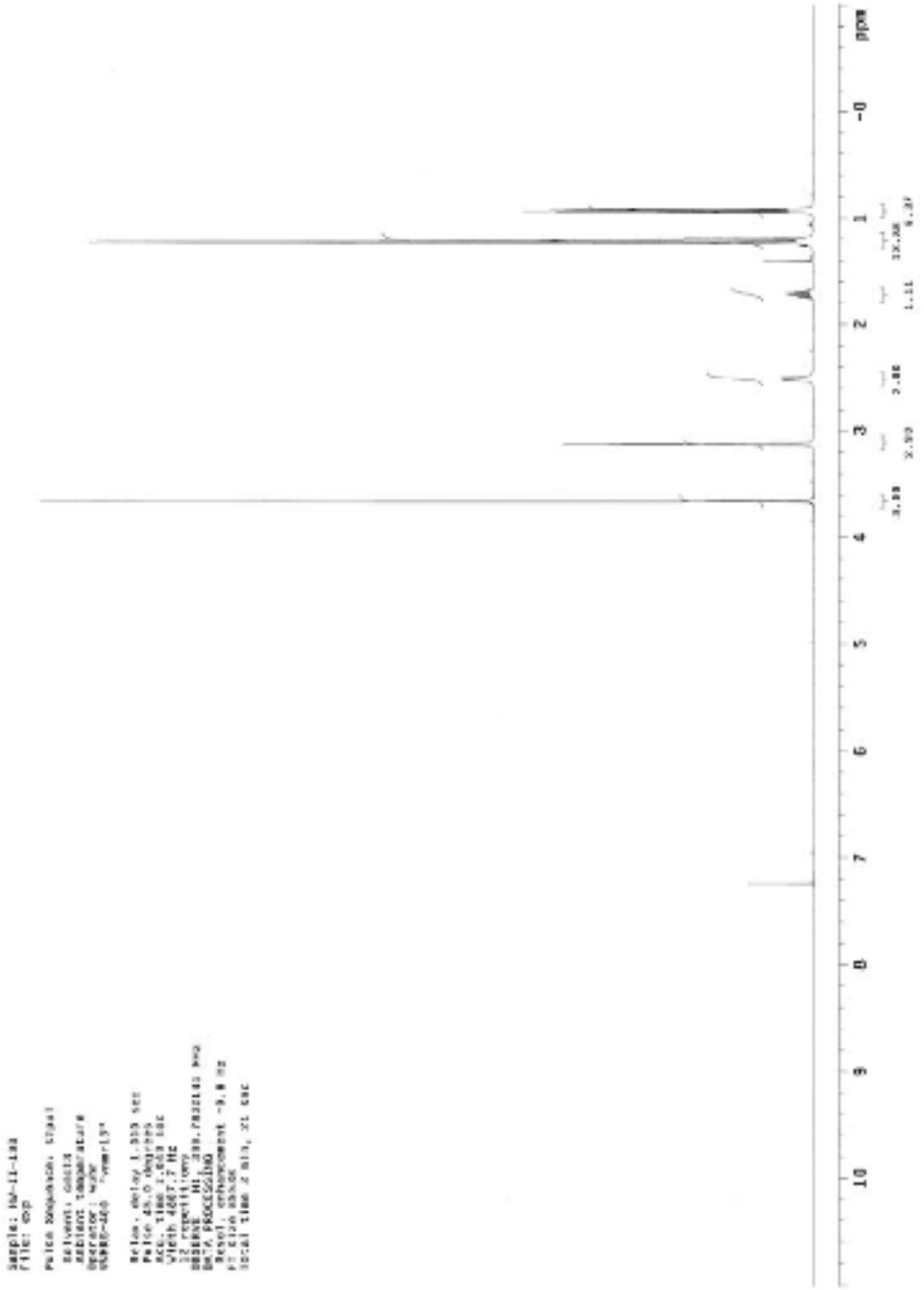

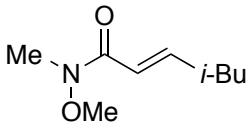

substrate for 1.99

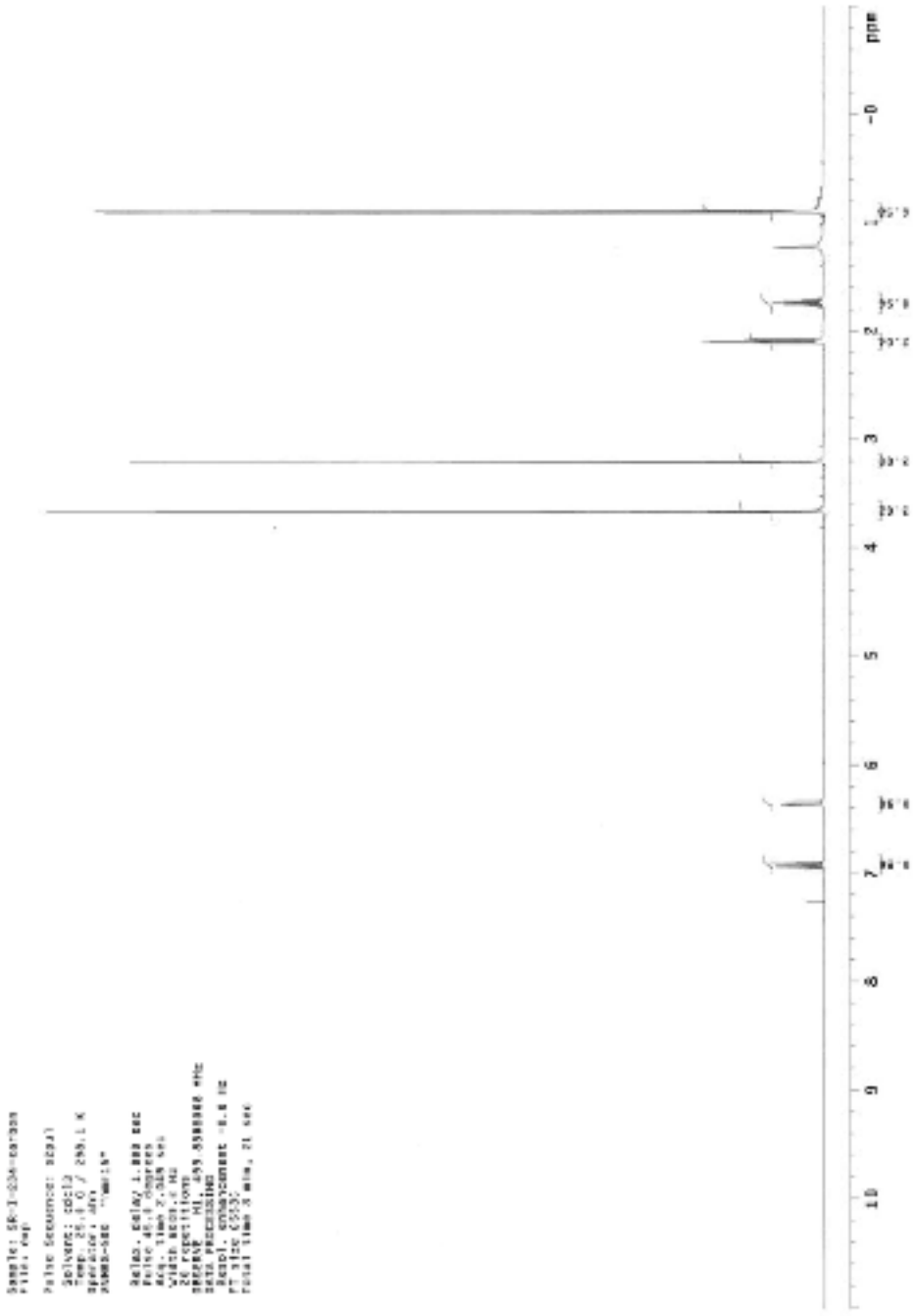

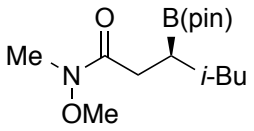

1.99

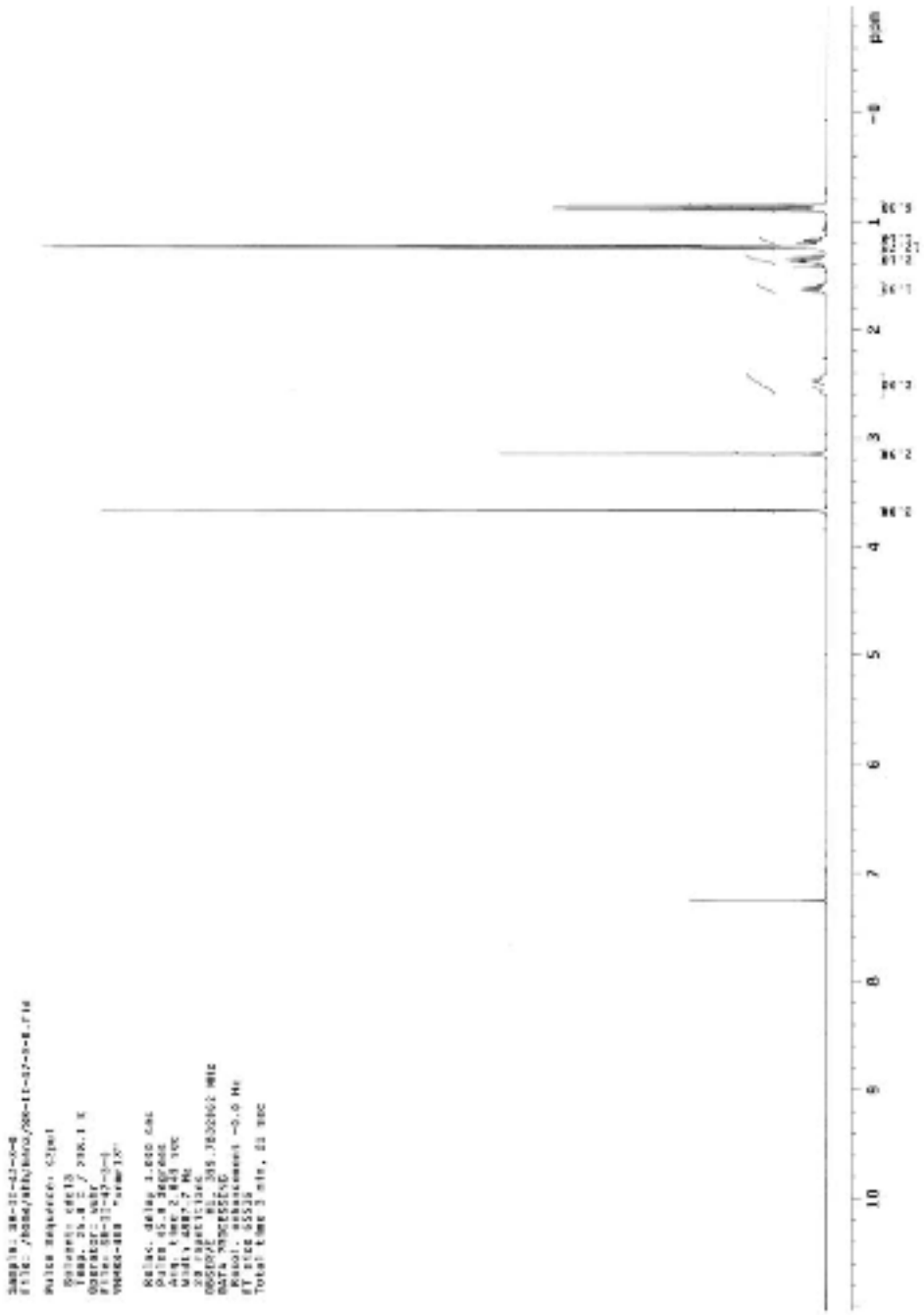

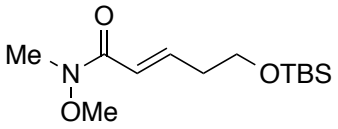

substrate for 1.100

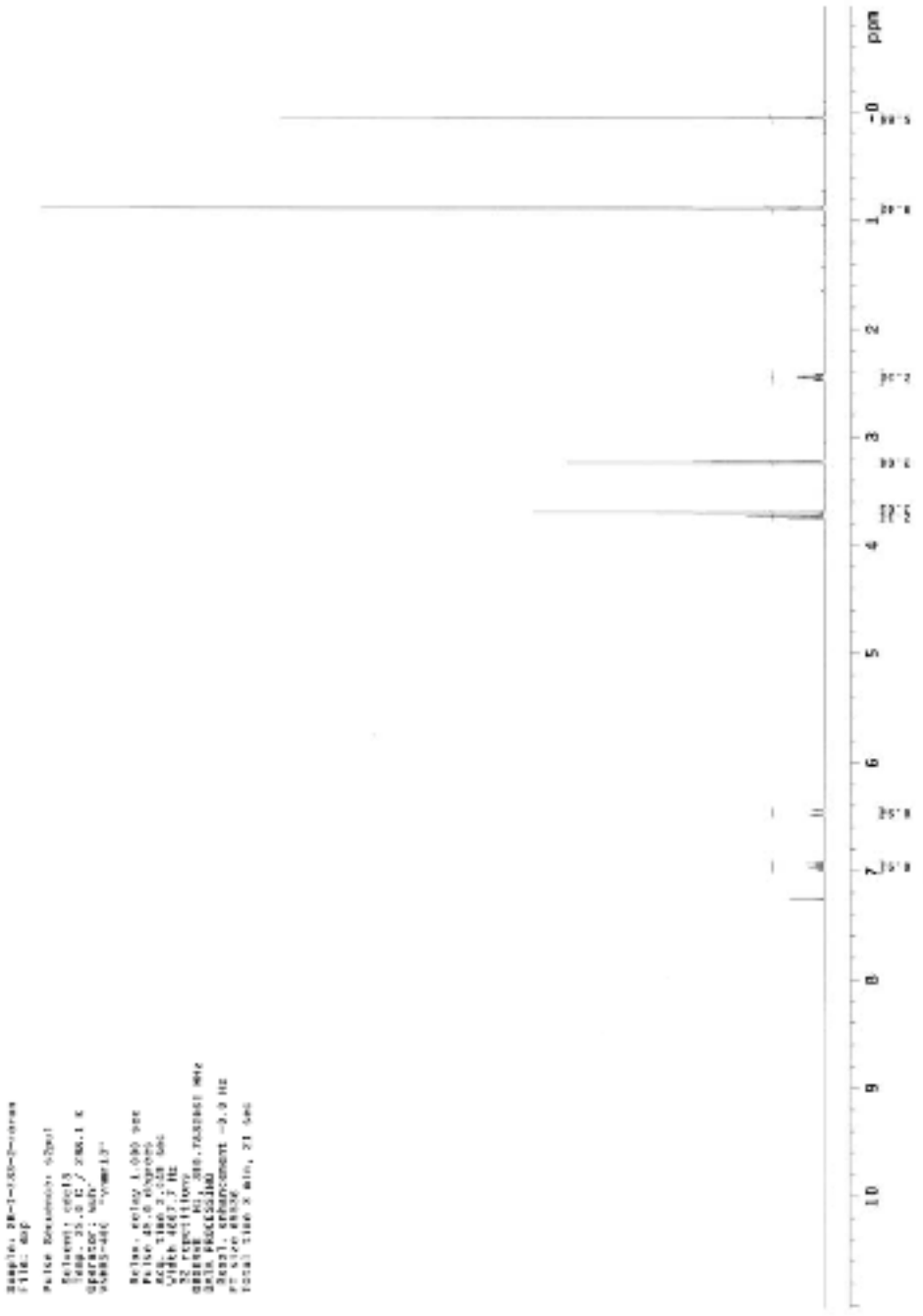

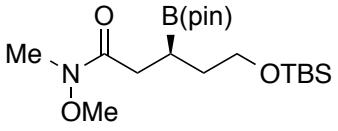

1.100

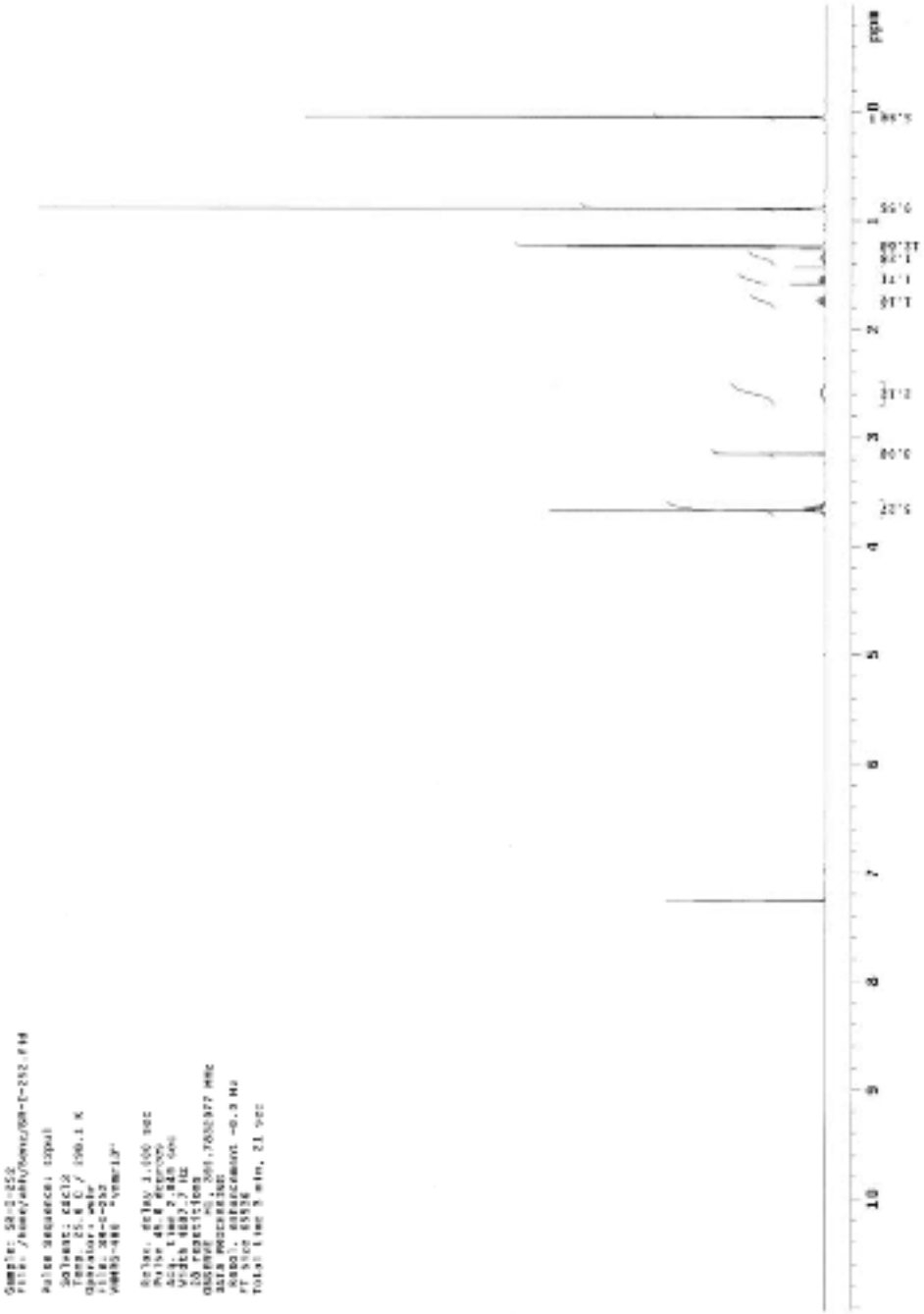

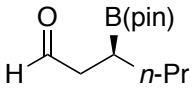

1.102

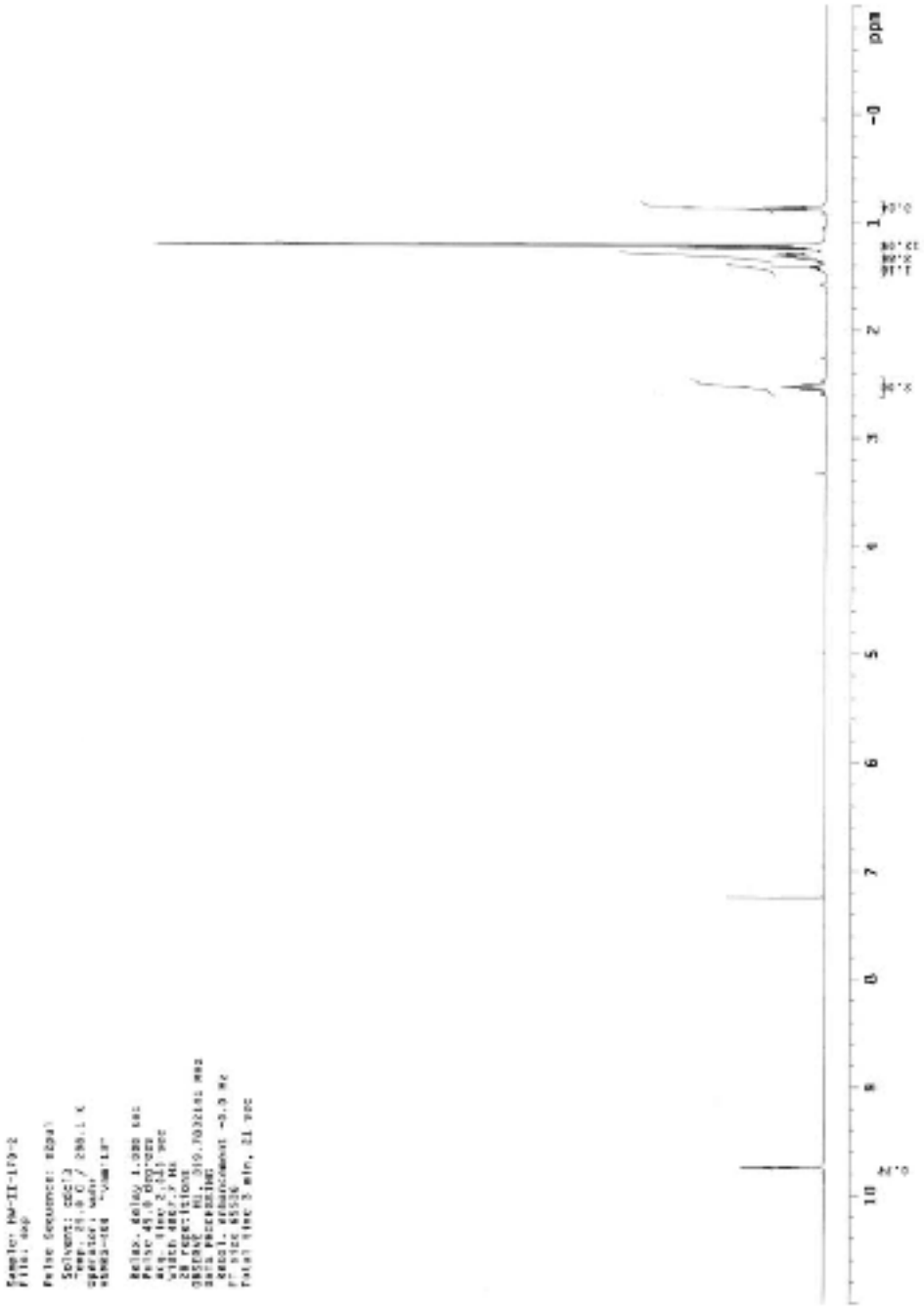

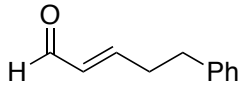

substrate for 1.103

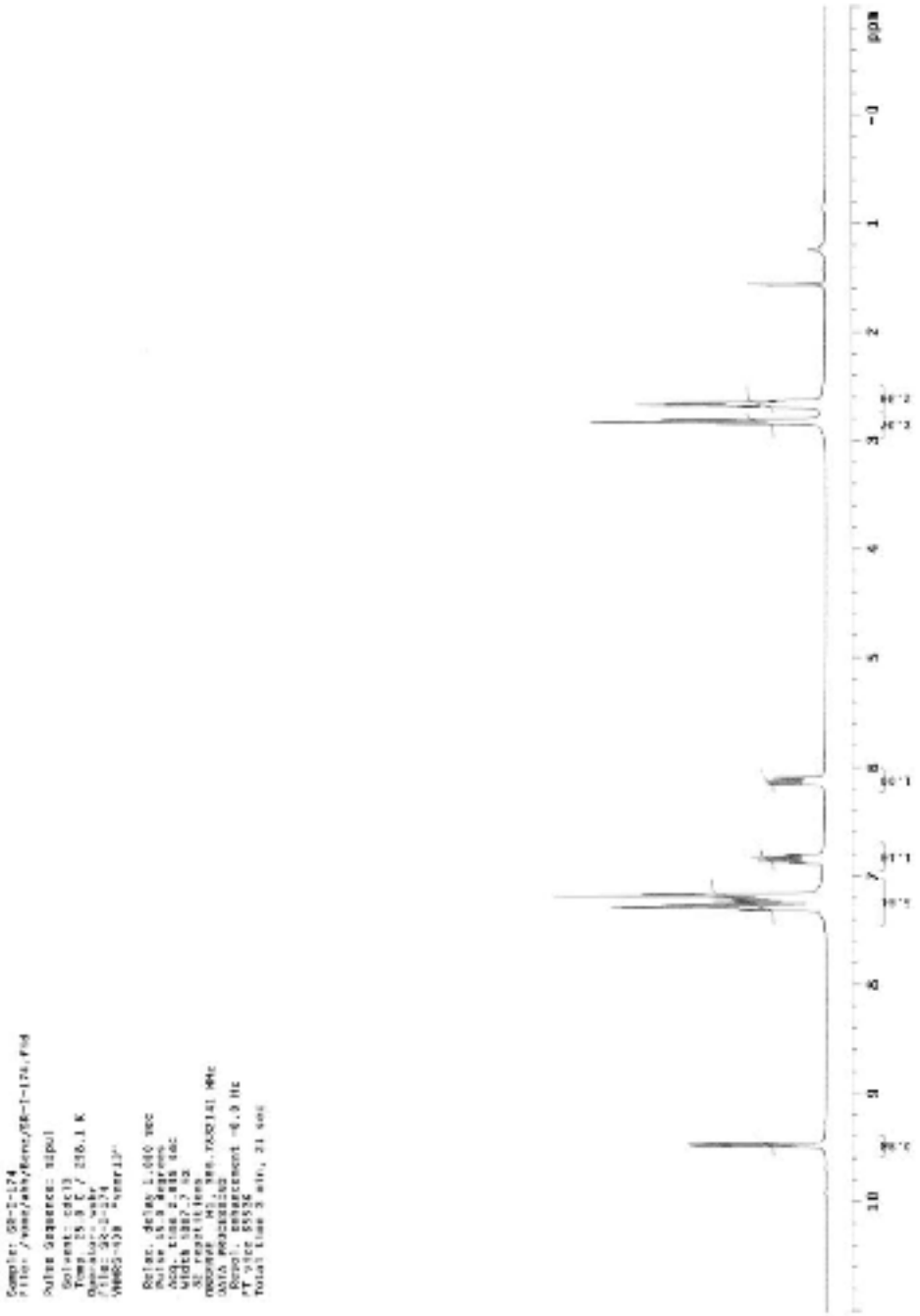

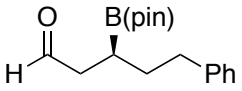

1.103

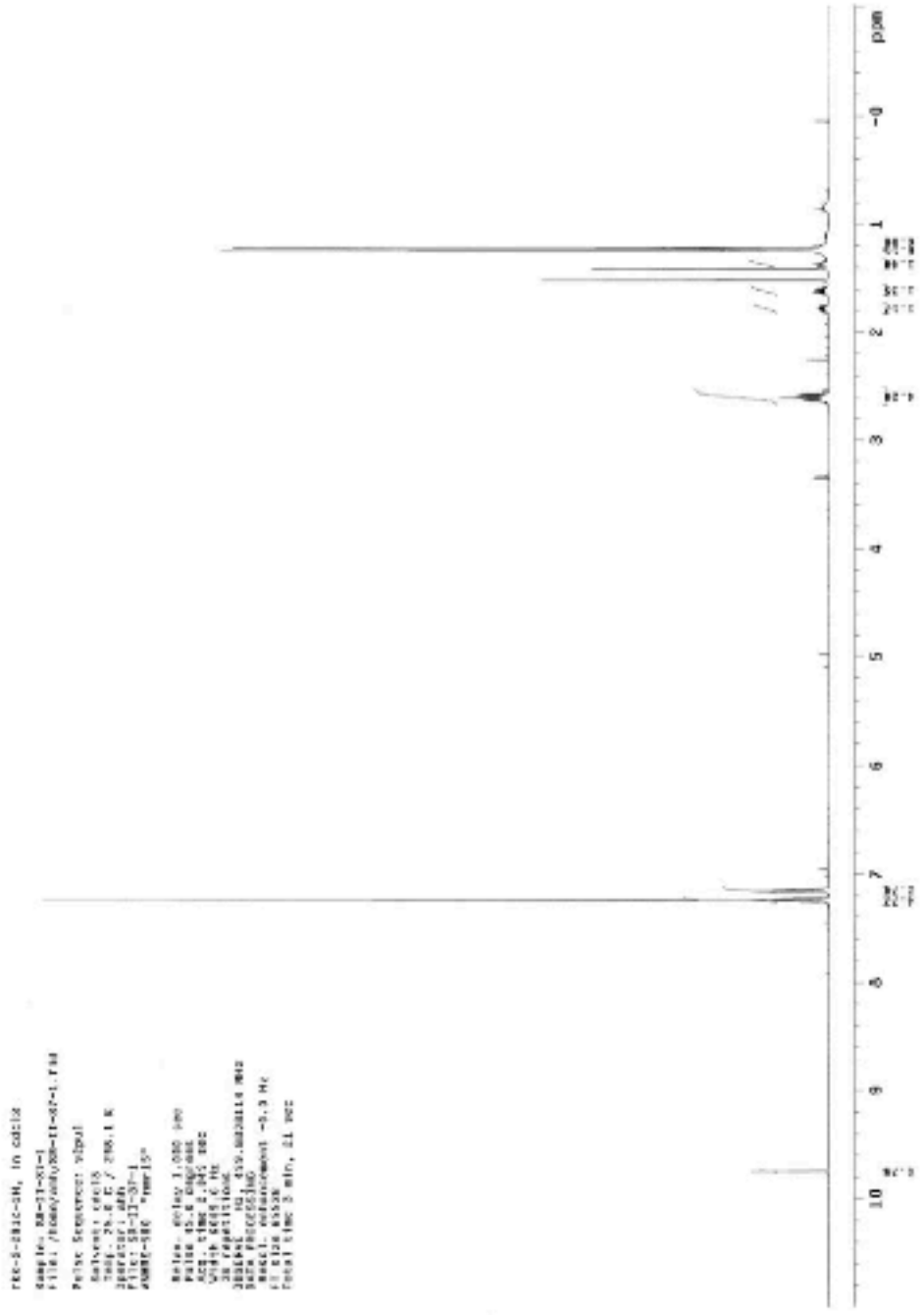

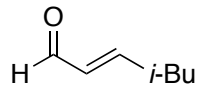

substrate for 1.104

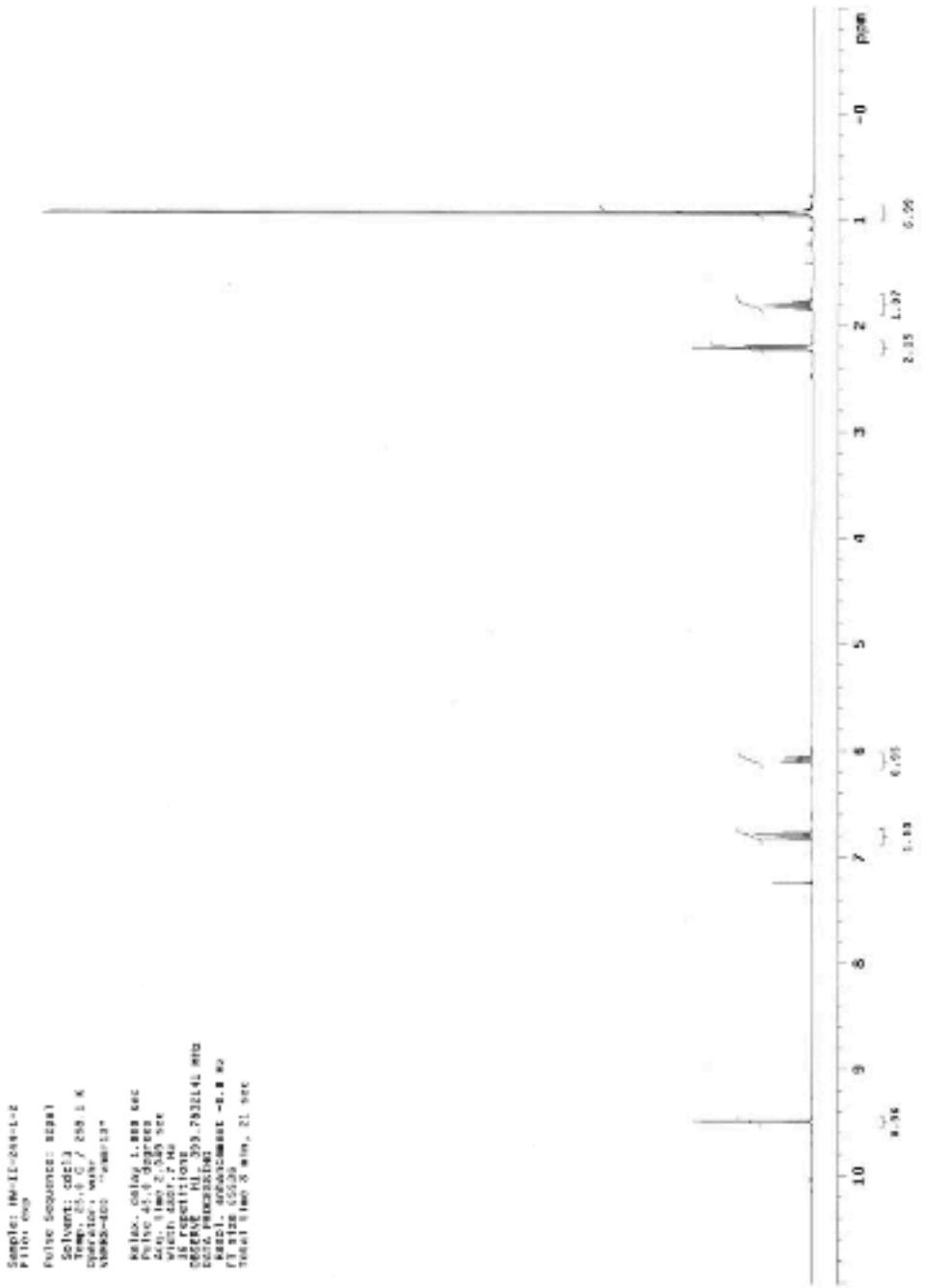

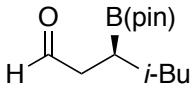

1.104

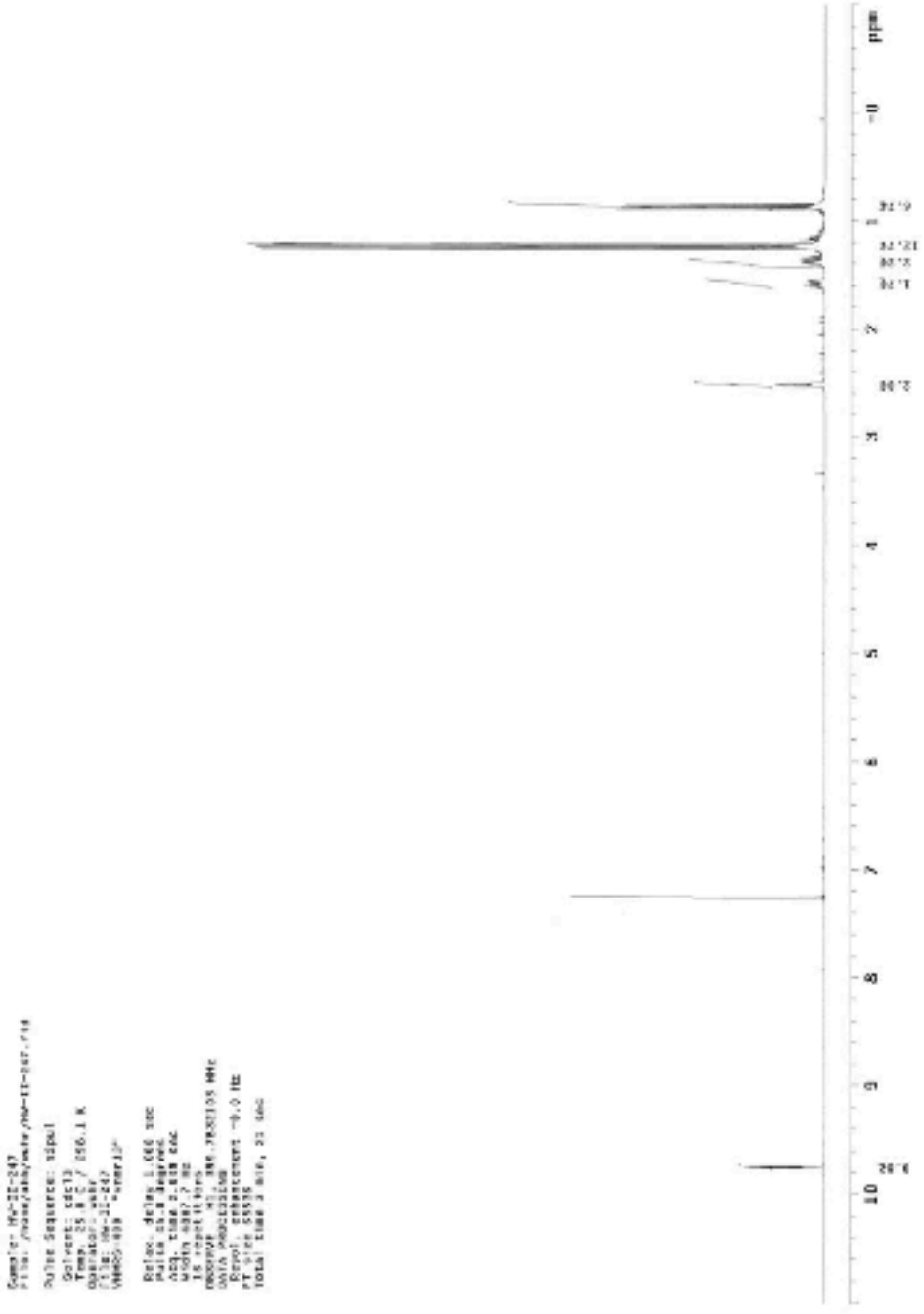

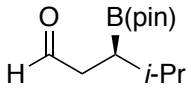

1.105

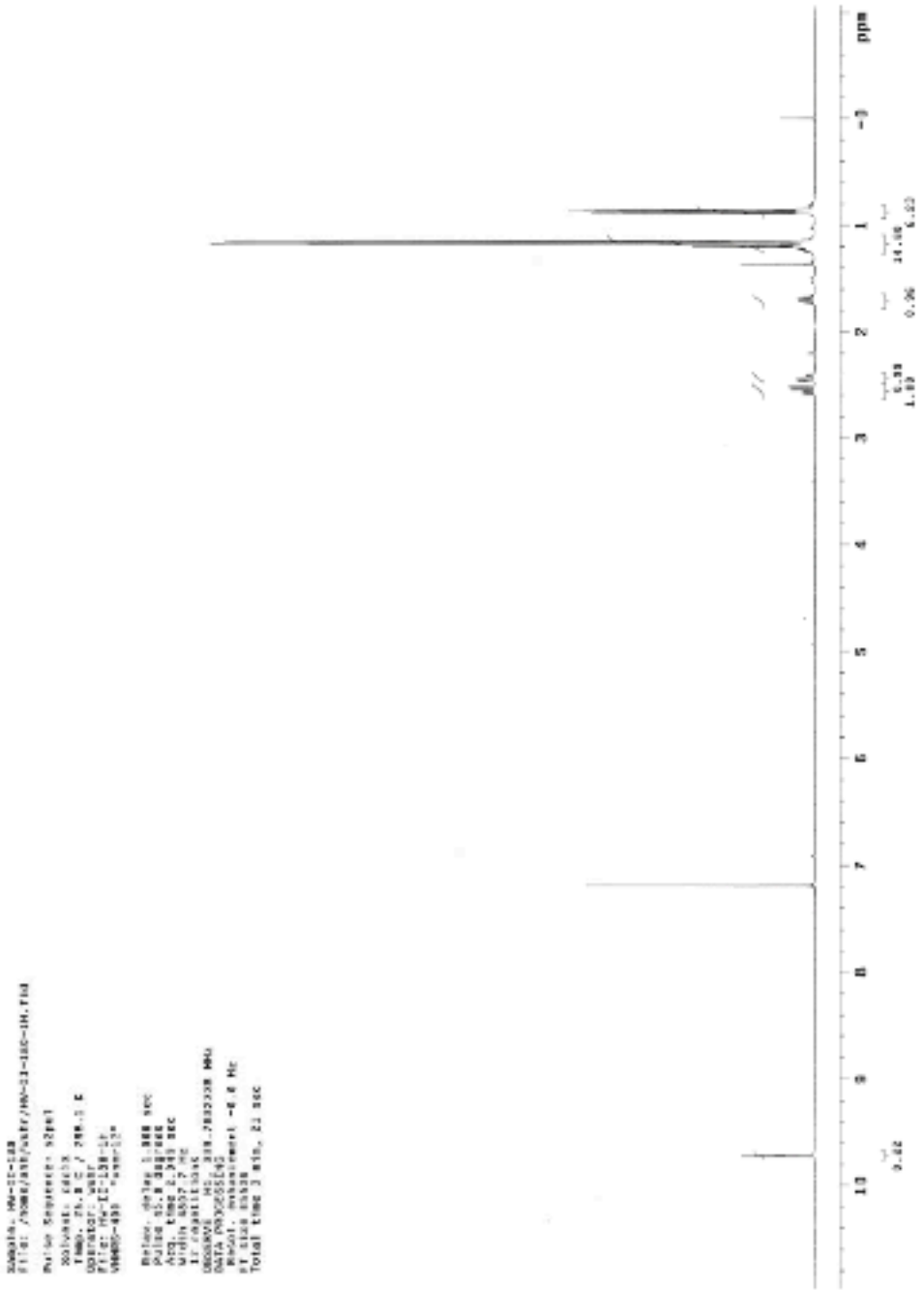

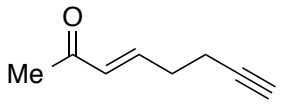

substrate for 1.108

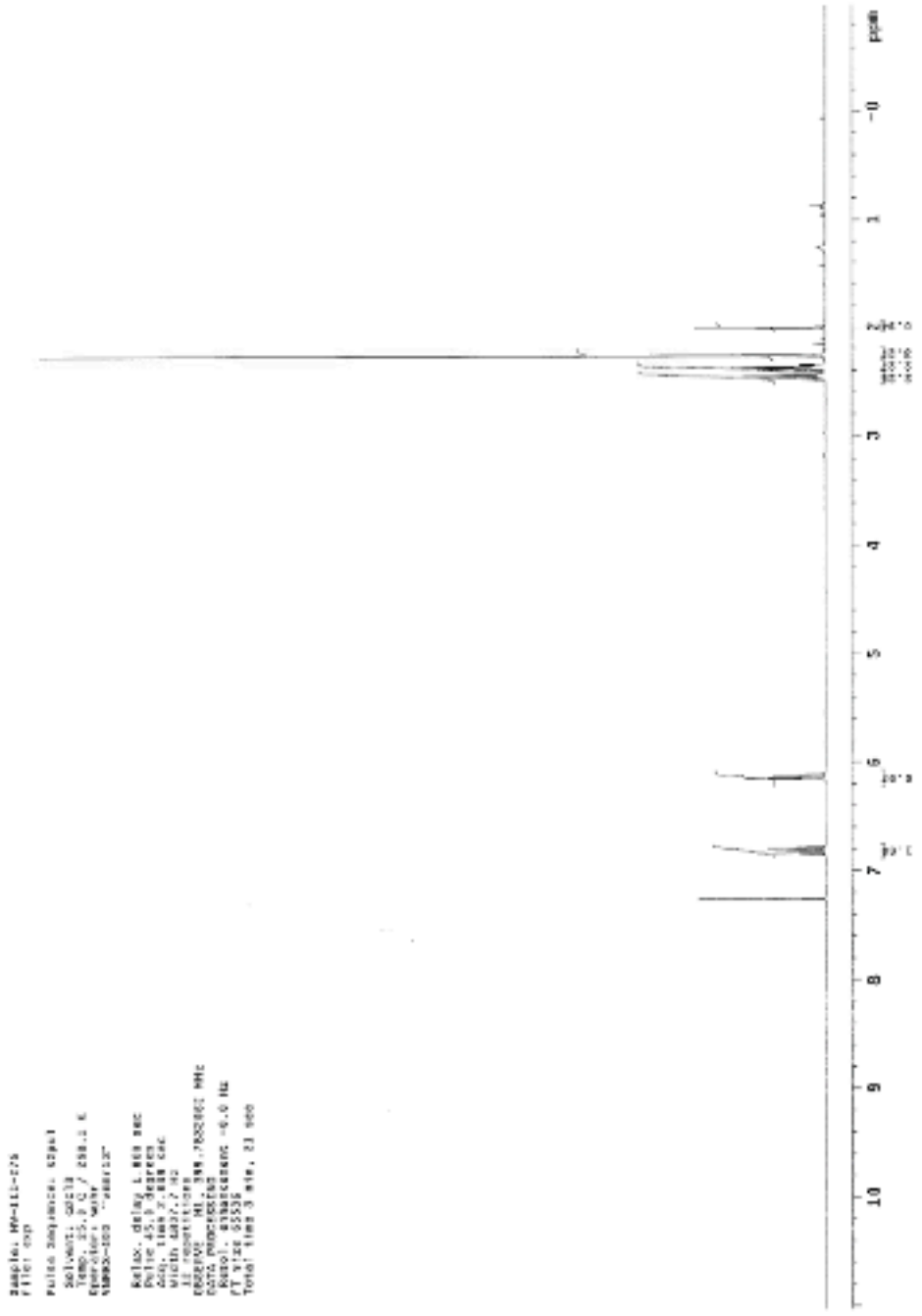

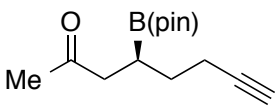

1.108

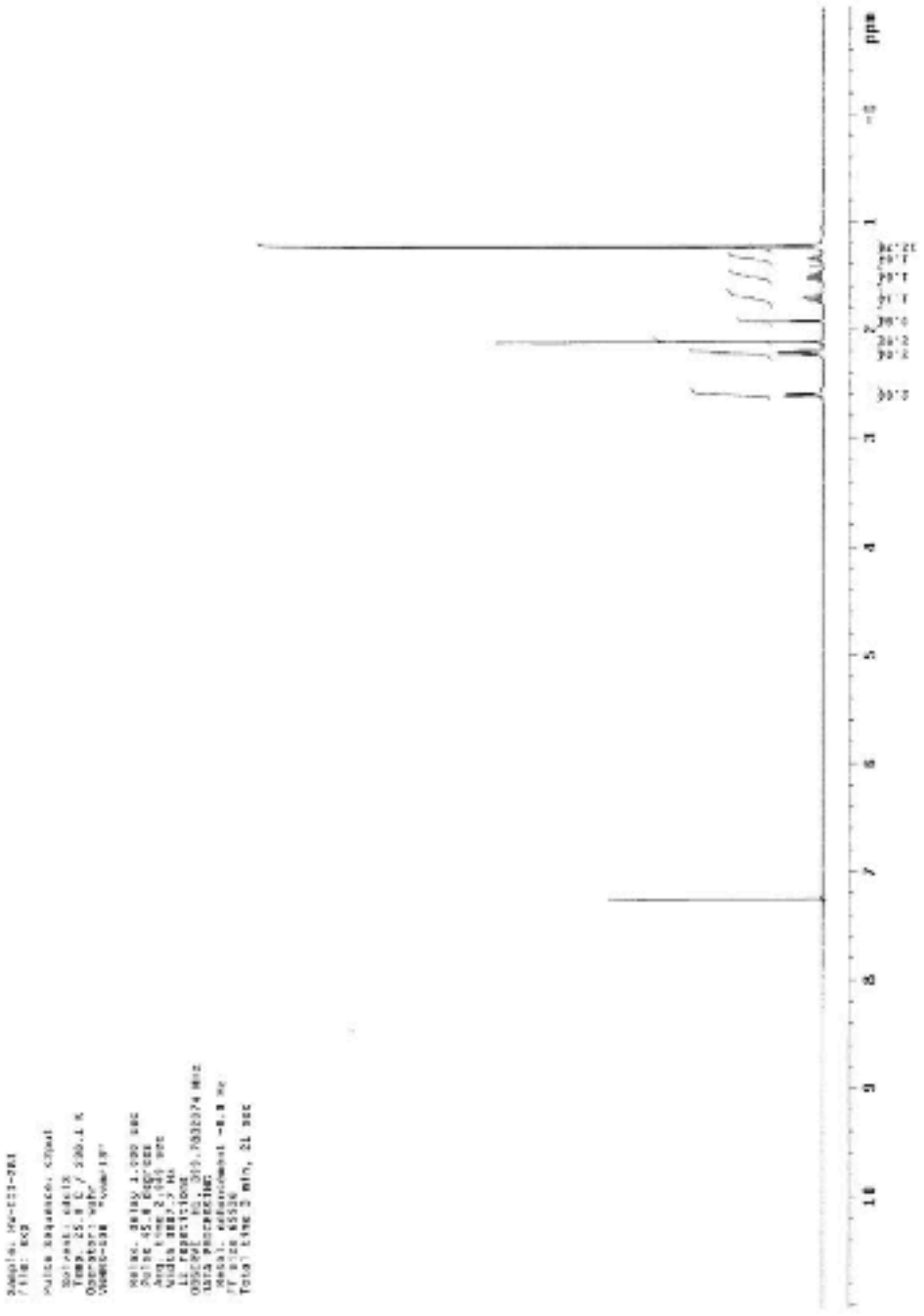

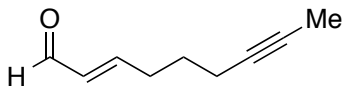

substrate for 1.110

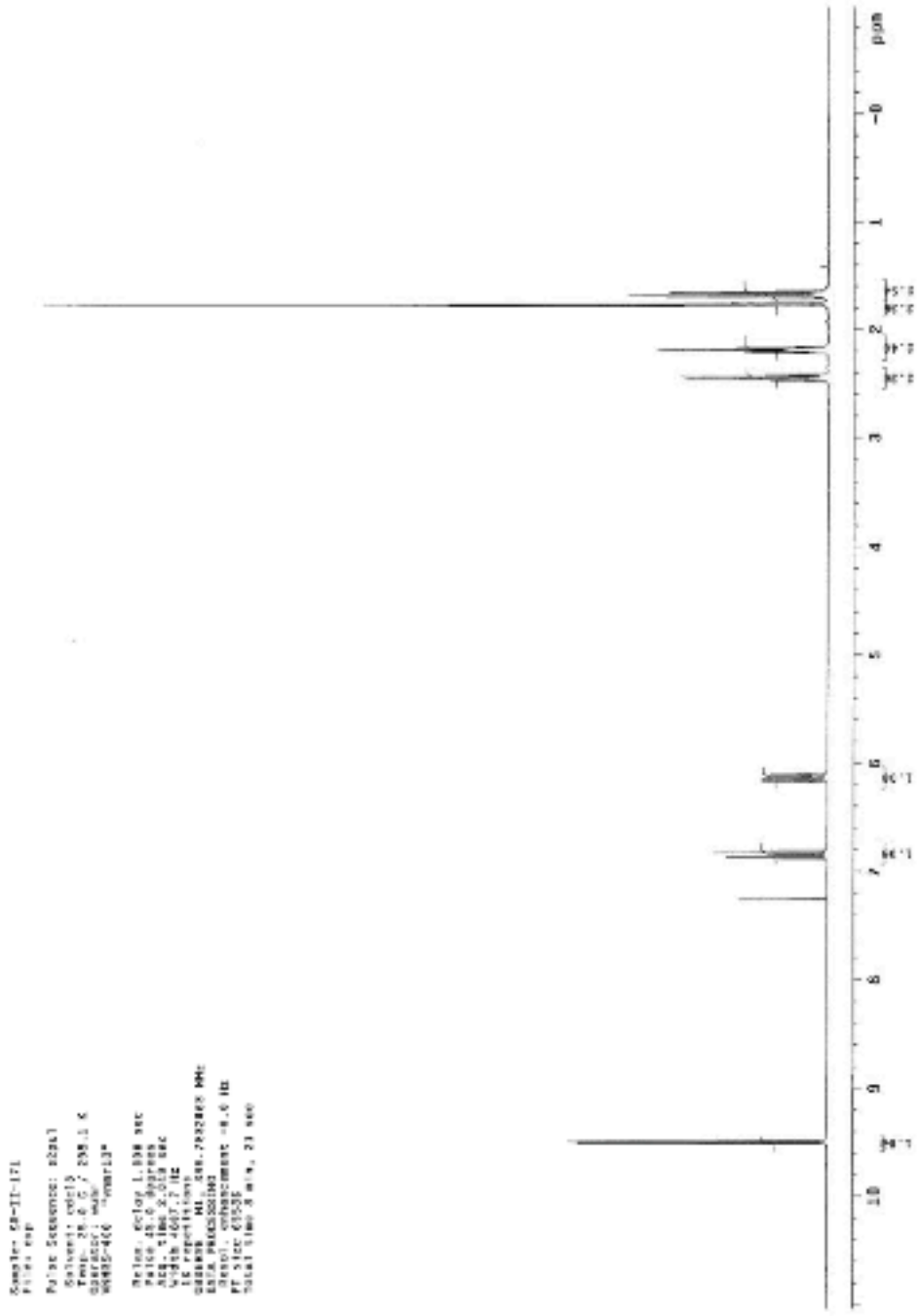

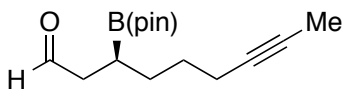

1.110

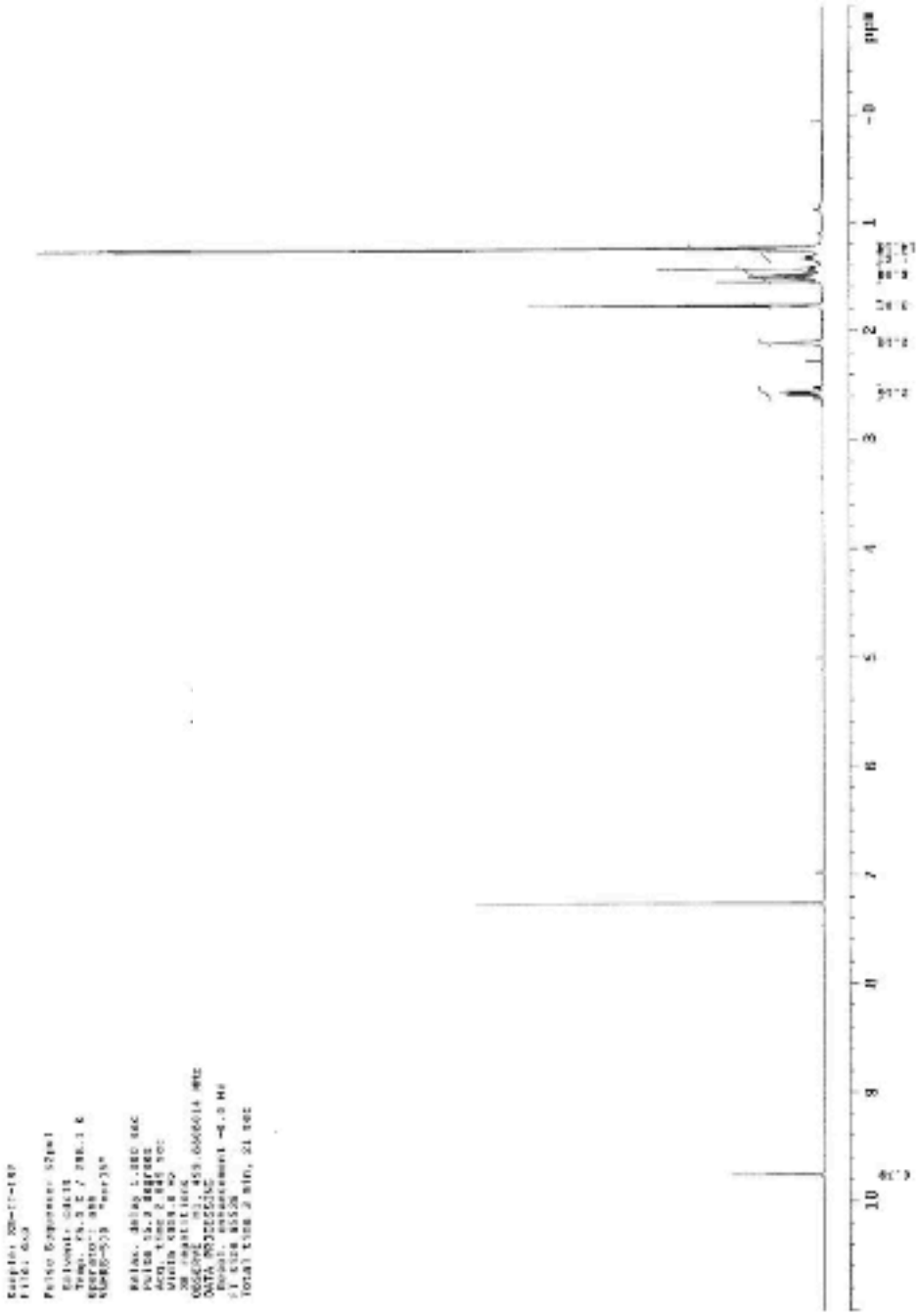

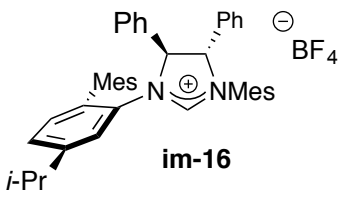

im-16

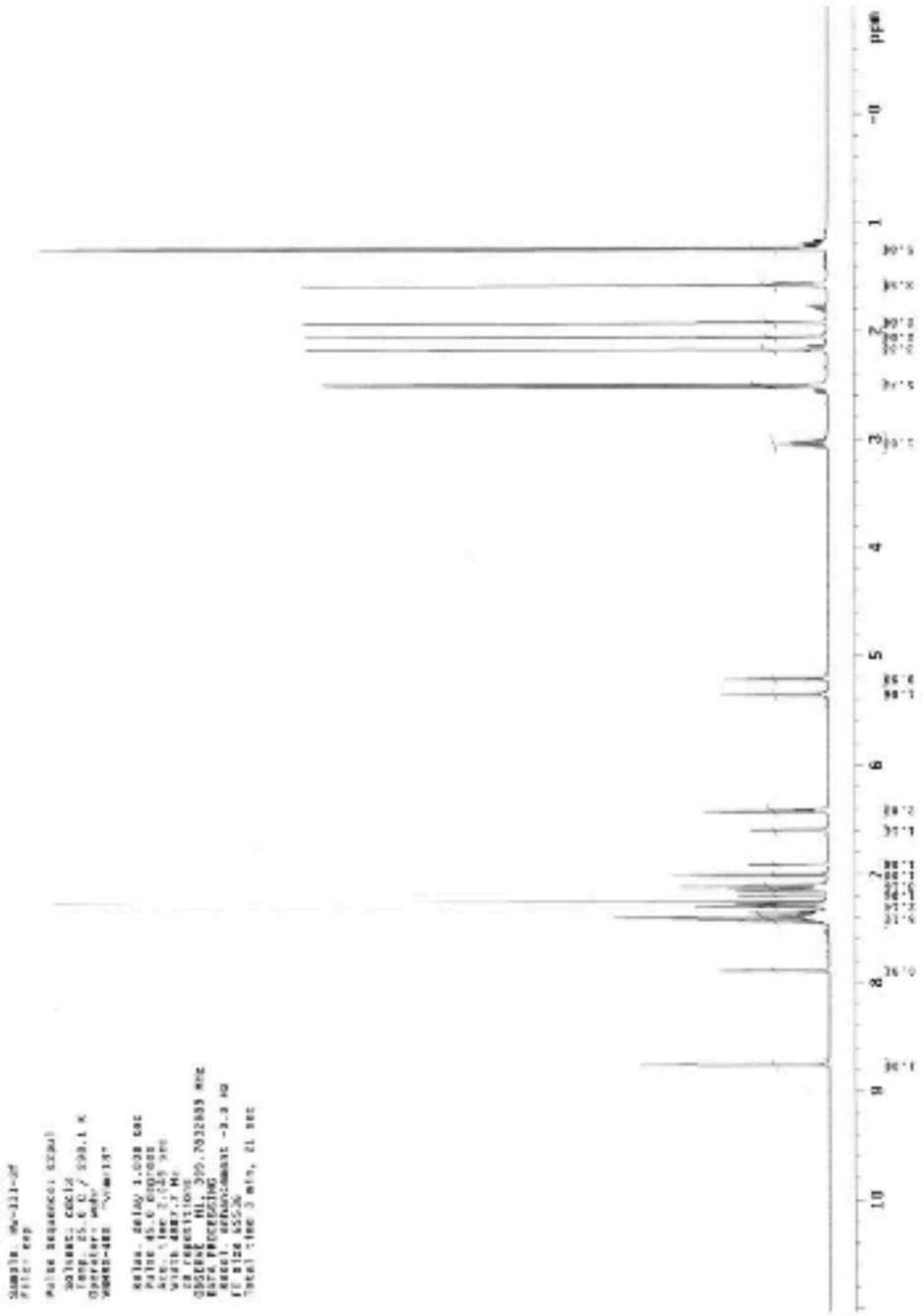

Chapter 1

Part B: Enantioselective Synthesis of Boron-Substituted Quaternary Carbon Stereogenic Centers through *N*-Heterocyclic Carbenes Catalyzed Boryl Conjugate Additions to Cyclic and Acyclic Enones

1B.1. Introduction

In recent years, development of an efficient and enantioselective synthesis of boron-containing molecules, which are versatile intermediates in chemical synthesis,[45] has exceedingly become the subject of current research interest. Despite several reports on the utility of C–B bonds,[46] an efficient and selective synthetic strategy to furnish enantiomerically enriched boron-substituted quaternary stereogenic centers remains scarce. Two existing catalytic enantioselective approaches to those tertiary boronic esters

(45) For representative reviews and articles regarding organoboron in synthesis, see: (a) Miyaura, N.; Suzuki, A. *Chem. Rev.* **1995**, *95*, 2457–2483. (b) Miyaura, N. *Cross-Coupling Reactions*; Springer-Verlag Berlin; Berlin, Germany, 2002; Vol. 219, pp 11–59. (c) Suzuki, A. *J. Organomet. Chem.* **1999**, *576*, 147–168. (d) Darses, S.; Genet, J. P. *Eur. J. Org. Chem.* **2003**, 4313–4327. (e) Sato, M.; Miyaura, N.; Suzuki, A.; *Chem. Lett.* **1989**, 1405–1408. (f) Lee, J.-E.; Yun, J. *Angew. Chem., Int. Ed.* **2008**, *47*, 145–147. (g) Ohmura, T.; Taniguchi, H.; Kondo, Y.; Suginome, M. *J. Am. Chem. Soc.* **2007**, *129*, 3518–3519. (h) Morrill, C.; Funk, T. W.; Grubbs, R. H. *Tetrahedron Lett.* **2004**, *45*, 7733–7736. (i) Hall, D. G. *Boronic Acids. Preparation, Applications in Organic Synthesis and Medicine*, Wiley-VCH, Weinheim, **2005**.

(46) For representative examples of converting C–B to C–O, see: (a) Tortosa, M. *Angew. Chem., Int. Ed.* **2011**, *50*, 3950–3953. (b) Stymiest, J. L.; Bagutski, V.; French, R. M.; Aggarwal, V. K. *Nature* **2008**, *456*, 778–782. For C–B to C–C, see: (c) Imao, D.; Glasspoole, B.W.; Laberge, V. S.; Crudden, C. M. *J. Am. Chem. Soc.* **2009**, *131*, 5024–5025. (d) Hupe, E.; Marek, I.; Knochel, P. *Org. Lett.* **2002**, *4*, 2861–2863. For C–B to C–N, see: (e) Moran, W. J.; Morken, J. P. *Org. Lett.* **2006**, *8*, 2413–2415. (f) Mlynarski, S. N.; Karns, A. S.; Morken, J. P. *J. Am. Chem. Soc.* **2012**, *134,* 16449–16451. For C–B to C–halogen, see: (g) Larouche-Gauthier, R.; Elford, T. G.; Aggarwal, V. K. *J. Am. Chem. Soc.* **2011**, *133*, 16794–16797. For C–B to C–H, see: (h) Nave, S.; Sonawane, R. P.; Elford, T. G.; Aggarwal, V. K. *J. Am. Chem. Soc.* **2010**, *132*, 17096–17098.

are outlined in Scheme 1.28: conjugate addition[47] and allylic substitution.[48, 49] Enantioselective BCA reactions to α,β-unsaturated carbonyls provide access to invaluable β-boryl carbonyls.[50,51, 52] However, the reported procedures are promoted by organocopper complexes that are known to promote Cu–B addition reactions to other functional groups (i.e. alkyne,[53] allene,[54] and aldehyde[55]) besides unsaturated carbonyls, thus the reaction could suffer from chemoselectivity issues in cases where substrates contain the aforementioned functional groups. In addition, use of transition-metal salts could cause complication in pharmaceutical industry; for example, removal of metal impurities from therapeutic agents as well as waste stream and toxicity issues associated

---

(47) For a single report on Cu-catalyzed enantioselective BCAs to β-substituted cyclic enones, see: (a) Chen, I.-H.; Yin, L.; Itano, W.; Kanai, M.; Shibasaki, M. *J. Am. Chem. Soc.* **2009**, *131*, 11664–11665. For Cu-catalyzed enantioselective BCAs to β-substituted acyclic enoates and enones, see: (b) O'Brien, J. M.; Lee, K.-s.; Hoveyda, A. H. *J. Am. Chem. Soc.* **2010**, *132*, 10630–10633**.** (c) Feng, X.; Yun, J. *Chem. Eur. J.* **2010**, *16*, 13609–13612**.** (d) Chen, I.-H.; Kanai, M.; Shibasaki, M. *Org. Lett.* **2010**, *12*, 4098–4101**.** (e) Kobayashi, S.; Xu, P.; Endo, T.; Ueno, M.; Kitanosono, T. *Angew. Chem., Int. Ed.* **2012**, *51*, 12763–12766.

(48) For a report on Cu-catalyzed enantioselective (pinacolato)boron allylic substitution, see: A. Guzman-Martinez, A. H. Hoveyda, *J. Am. Chem. Soc.* **2010**, *132*, 10634–10637.

(49) For a non-catalytic enantioselective synthesis of boron-substituted quaternary carbons, see: (a) ref. 34b. (b) Bagutski, V.; French, R. M.; Aggarwal, V. K. *Angew. Chem., Int. Ed.* **2010**, *49*, 5142–5145. (c) Sonawane, R. P.; Jheengut, V.; Rabalakos, C.; Larouche-Gauthier, R.; Scott, H. K.; Aggarwal, V. K. *Angew. Chem., Int. Ed.* **2011**, *50*, 3760–3763.

(50) For a review regarding the significance of enantioselective conjugate additions with B- and Si-based nucleophiles, see: Hartmann, E.; Vyas, D. J.; Oestreich, M. *Chem. Commun.* **2011**, *47*, 7917–7932.

(51) For an application of enantioselective Cu-catalyzed BCA to synthesis of a biologically active molecule, see: (a) Chea, H.; Sim, H.-S.; Yun, J. *Adv. Synth. Catal.* **2009**, *351*, 855–858. (b) Stavber, G.; Časar, Z. *Appl. Organometal. Chem.* **2013**, *27*, 159–165. For a related non-enantioselective example, see: (c) Marcus, A. P.; Sarpong, R. *Org. Lett.* **2010**, *12*, 4560–4563.

(52) For an application of enantioselective NHC-catalyzed BCA to synthesis of neopeltolide, see; Yu, M.; Hoveyda, A.H. *Angew. Chem., Int. Ed.* **2015***, 54*, 215–220.

(53) For representative Cu–B additions to alkynes, see: (a) Lee, Y.; Jang, H.; Hoveyda, A. H. *J. Am. Chem. Soc.* **2009**, *131*, 18234–18235. (b) Jang, H.; Zhugralin, A. R.; Lee, Y.; Hoveyda, A. H. *J. Am. Chem. Soc.* **2011**, *133*, 7859–7871. (c) Liu, P.; Fukui, Y.; Tian, P.; He, Z.-T.; Sun, C.-Y.; Wu, N.-Y.; Lin, G.-Q. *J. Am. Chem. Soc.* **2013**, *135*, 11700–11703. (d) Moure, A. L.; Mauleon, P.; Arrayas, R. G.; Carretero, J. C. *Org. Lett.* **2013**, *15*, 2054–2057.

(54) For representative Cu–B additions to allenes, see: (a) Jung, B.; Hoveyda, A. H. *J. Am. Chem. Soc.* **2012**, *134*, 1490–1493. (b) Yuan, W.; Ma, S. *Adv. Synth. Catal.* **2012**, *354*, 1867–1872. (c) Meng, F.; Jung, B.; Haeffner, F.; Hoveyda, A. H. *Org. Lett.* **2013**, *15*, 1414–1417; d) Meng, F.; Jang, H.; Jung, B.; Hoveyda, A. H. *Angew. Chem., Int. Ed.* **2013**, *52*, 5046–5051. (e) Semba, K.; Shinomiya, M.; Fujihara, T.; Terao, J.; Tsuji, Y. *Chem. Eur. J.* **2013**, *19*, 7125–7132.

(55) Laitar, D. S.; Tsui, E. Y.; Sadighi, J. P. *J. Am. Chem. Soc.* **2006**, *128*, 11036–11037.

with metal complexes.[56] A metal-free alternative that is complementary to Cu-catalyzed variants and offers chemoselective BCA reactions is thus compelling.

Scheme 1.28. Catalytic enantioselective synthesis of boron-substituted quaternary carbons

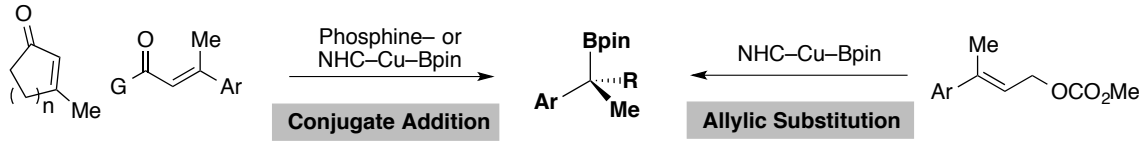

1B.2. NHC-catalyzed Enantioselective Boryl Conjugate Additions to Generate Boron-Substituted Quaternary Carbon Stereogenic Centers

1B.2.1. Reaction conditions optimization and catalyst screening

We began our investigation with a representative enone **1.111** and imidazolinium salt **im-5**. Based on reaction conditions identified for NHC-catalyzed enantioselective BCA reactions (Chapter 1, Part A), we chose dbu as a base and MeOH as an additive. As data in Table 1.2 indicate, use of 20 mol % dbu and 60 equiv of MeOH results in high conversion and appreciable enantioselectivity (96% conv, 85% yield, 84:16 er, entry 2). The results improve slightly with higher amount of dbu (>98% conv, 92% yield, 86:14 er, entry 4). Use of other amine bases such as Et_3N gives only 12% yield of the desired product suggesting Et_3N being an inefficient base to deprotonate **im-5** to generate an NHC (entry 5). With a sizable alcohol additive isopropanol, the BCA reaction proceeds to only 16% conv (entry 7). This is in agreement with the previously discussed role of alcohol to generate a more accessible diboron reagent. Reactions in the presence of polar aprotic additive did not give any product **1.112** (<2% conv, entries 8–9). In the presence of H_2O as an additive, although the reaction is very efficient, the product is formed with

(56) For selected reports on the significance of non-metal catalysis, see: (a) Gaunt, M. J.; Johansson, C. C. C.; McNally, A.; Vo, N. T. *Drug Discovery Today* **2007**, *12*, 8–27. (b) MacMillan, D. W. C. *Nature* **2008**, *455*, 304–308.

much lower er value (85% yield, 68:32 er, entry 10). This can be contributed to more background reaction (a hydroxide catalyzed BCA reaction) compared to when MeOH is used.

Without an alcohol additive, there is no product formation (<2% conv, entry 11). Results in entries 13–14 suggest that the NHC-catalyzed reaction proceeds with a distinct mechanism and without the presence of Cu salt because much lower er values were obtained from addition of CuCl (65:35 er, entry 13 and 64:36 er, entry 14 vs 84:16 er without CuCl, entry 2).

Table 1.2. Optimization of reaction conditions with **im-5** as the chiral NHC precursor[a]

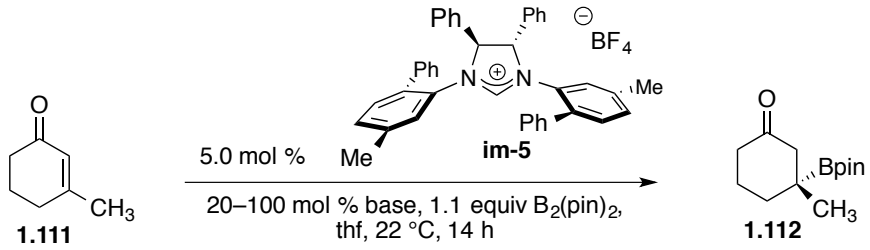

1.111 **1.112**

entry	base; mol%	additive; equiv	solvent	conv (%)[b]	yield (%)[c]	er[d]
1	dbu; 10	MeOH; 60	thf	62	51	82:18
2	dbu; 20	MeOH; 60	thf	96	85	84:16
3	dbu; 20	MeOH; 30	thf	71	63	86:14
4	dbu; 100	MeOH; 60	thf	>98	92	86:14
5	Et_3N; 20	MeOH; 60	thf	19	12	85:15
6	dbu; 100	EtOH; 60	thf	>98	90	83:17
7	dbu; 100	*i*-PrOH; 60	thf	16	nd	nd
8	dbu; 100	dmso; 60	thf	<2	na	na
9	dbu; 100	dmf; 60	thf	<2	na	na
10	dbu; 100	H_2O; 60	thf	>98	85	68:32
11	dbu; 100	-	thf	<2	na	na
12	dbu; 100	-	MeOH	71	65	85:15
13	dbu; 100	CuCl, MeOH; 0.01, 60	thf	93	81	65:35
14	dbu; 100	CuCl, MeOH; 0.05, 60	thf	>98	90	64:36

[a] All reactions were performed under N_2 atm. [b] Determined by analysis of 400 MHz ^{1}H NMR spectra of unpurified mixtures. [c] Yields of purified products. [d] Determined by HPLC analysis. nd = not determined. na = not available.

After having identified suitable reaction conditions, we turned to search for the most selective chiral NHC. As shown in Table 1.3, we started with C_2-symmetric imidazolinium salts because **im-5** gave promising results. Removing methyl substituents on the *meta* positions of the N-aryl motifs did not improve enantioselectivity (84:16 er, entry 1). While increasing the size of the substituents to *i*-Pr and *t*-Bu groups, the enantioselectivities decrease (79:21 er and 69:31 er, entries 2–3, respectively).

We then examined the BCA reaction with C_1-symmetric imidazolinium salts as NHC precursors. Reaction with **im-8** proceeds with low efficiency although the enantioselectivity is similar to **im-5** (21% yield, and 82:18 er, entry 4). Modification of its structure by changing the substituent at the *meta* position did not improve enantioselectivity, on the other hand the er values decrease with larger group (entries 5–7). A very promising result was obtained when **im-22** was employed. The BCA product was formed in 74% yield and 91.5:8.5 er (entry 10). Further modification of the imidazolinium salts' structure gave **im-25** as the optimal NHC precursor for reactions with cyclic enones (90% yield, and 96:4 er, entry 13).

Table 1.3. Examination on various chiral NHC catalysts[a]

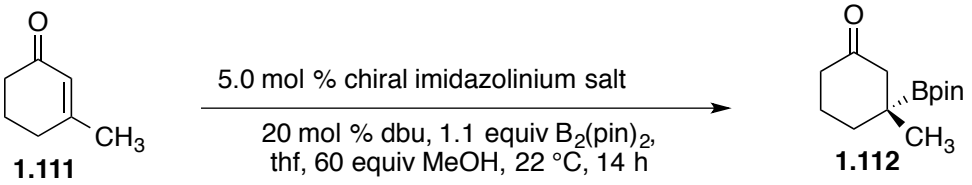

1.111 **1.112**

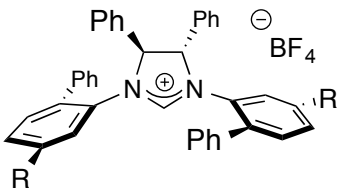

im-17 R = H
im-19 R = *i*-Pr
im-20 R = *t*-Bu

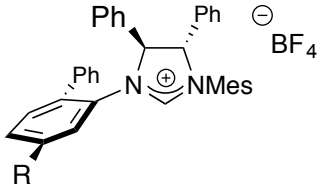

im-8 R = H
im-12 R = Me
im-13 R = *i*-Pr
im-21 R = *t*-Bu

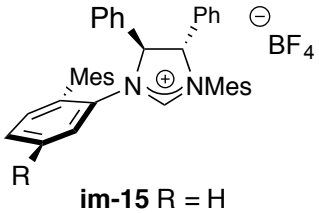

im-15 R = H
im-16 R = *i*-Pr

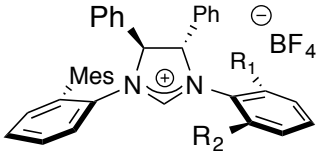

im-22 R_1,R_2 = Et
im-23 R_1,R_2 = *n*-Pr
im-24 R_1 = *i*-Pr,R_2 = H
im-25 R_1 = *i*-Pr,R_2 = Me
im-26 R_1 = Ph,R_2 = Me

entry	imidazolinium salt	conv (%)[a]	yield (%)[a]	er[a]
1	**im-17**	53	46	84:16
2	**im-19**	81	75	79:21
3	**im-20**	91	83	69:31
4	**im-8**	27	21	82:18
5	**im-12**	82	75	79:21
6	**im-13**	72	66	70:30
7	**im-21**	78	75	47:53
8	**im-15**	>98	79	88:12
9	**im-16**	68	54	67:33
10	**im-22**	>98	74	91.5:8.5
11	**im-23**	>98	91	90:10
12	**im-24**	91	82	90:10
13	**im-25**	>98	90	96:4
14	**im-26**	52	50	90:10

[a] See Table 1.2. Mes = 2,4,6-$(Me)_3C_6H_2$.

1B.2.2. NHC-catalyzed enantioselective BCAs to β-substituted cyclic enones

We probe the generality of the NHC-catalyzed enantioselective BCA reaction. A variety of cyclic enones, ranging from five-, six-, seven-, and eight-membered rings, are suitable substrates and proceed to generate β-boryl ketones in 63–95% yield and in 92:8–>98:2 er (Table 1.4). The transformations to produce boron-substituted cyclopentanone **1.113–1.116** are usually efficient (>98% conv in all cases, entries 1–4). Reaction to afford product **1.113** is exceedingly enantioselective (entry 1, >98:2 er). Reactions with relatively larger aryl-substituted cyclopentenones are also efficient; however, somewhat lower enantioselectivities are obtained (entries 2–4, 92:8–95:5 er).

Catalytic BCAs with cyclohexenones tolerate towards substituents bearing electron-donating (entries 6 and 9) and electron-withdrawing groups (entries 7–8) and proceed efficiently and enantioselectively to deliver the corresponding products in 63–93% yield and 92.5:7.5–97:3 er. In case of the strongly electron-withdrawing *p*-CF_3 substituted substrate, there is formation of proto-deboration product resulting in the diminished yield of **1.120** after isolation; however, the enantioselectivity remains high (>98% conv, 63% yield, 96:4 er, entry 8). Notably, the sterically-demanding naphthyl-substituted cyclohexenone proceeds in BCA efficiently and enantioselectively at 4 °C after 14 h affording compound **1.122** in 93% yield and 96:4 er (entry 10). In addition to reactions with aryl-substituted cyclohexenones, BCA reactions of alkyl-substituted cyclohexenones afford a range of β-boryl products bearing a substituent ranging from *n*-Bu **1.123**, phenethyl **1.124**, and silylprotected alkyne **1.125** in 80–91% yield and 94:6–96:4 er. Large ring sizes including 7- and 8-membered substrates are effective in metal-free BCA affording the products in 77–78% yield and 95:5 er (entries 14–15); it is worth

to mention that this is the first example of enantioselective BCA to a large ring-size substrate such as cyclooctenone.

Table 1.4. NHC-catalyzed enantioselective BCAs to β-substituted cyclic enones[a]

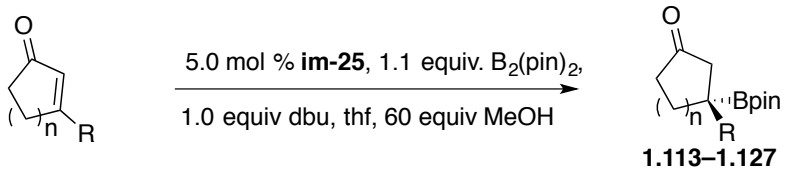

1.113–1.127

entry	n	R	temp (°C); time (h)	conv (%)	yield (%)	er
1	1	Me; **1.113**	4; 14	>98	90	>98:2
2	1	Ph; **1.114**	4; 14	>98	89	93:7
3	1	*p*-FC_6H_4; **1.115**	22; 14	>98	91	92:8
4	1	*m*-$OMeC_6H_4$; **1.116**	–5; 14	>98	91	95:5
5	2	Ph; **1.117**	4; 14	>98	91	96:4
6	2	*p*-$OMeC_6H_4$; **1.118**	–15; 14	>98	91	97:3
7	2	*p*-FC_6H_4; **1.119**	4; 14	>98	93	96.5:3.5
8[b]	2	*p*-$CF_3C_6H_4$; **1.120**	4; 24	>98	63	96:4
9	2	*m*-$OMeC_6H_4$; **1.121**	–5; 14	>98	92	92.5:7.5
10	2	2-naphthyl; **1.122**	4; 14	>98	93	96:4
11	2	*n*-Bu; **1.123**	4; 24	92	85	94:6
12	2	CH_2CH_2Ph; **1.124**	4; 24	>98	91	96:4
13	2	$(CH_2)_3C{\equiv}CTMS$; **1.125**	22; 14	87	80	94:6
14	3	Me; **1.126**	–5; 14	82	77	95:5
15	4	Me; **1.127**	4; 14	95	89	95:5

[a] See Table 1.2. [b] ~30% proto-deboration product is formed (determined by analysis of 400 MHz ^{1}H NMR spectrum of the unpurified mixture).

As shown in Scheme 1.29, facile enantioselective BCAs of relatively reactive substrates proceed efficiently with only 1.0 mol % of NHC precursor **im-25** to afford the corresponding products without loss of efficiency and enantioselectivity compared to results obtained with higher loading (78–95% yield and 95:5–97:3 er).

Scheme 1.29. NHC-catalyzed enantioselective BCAs to β-substituted cyclic enones on low catalyst loading

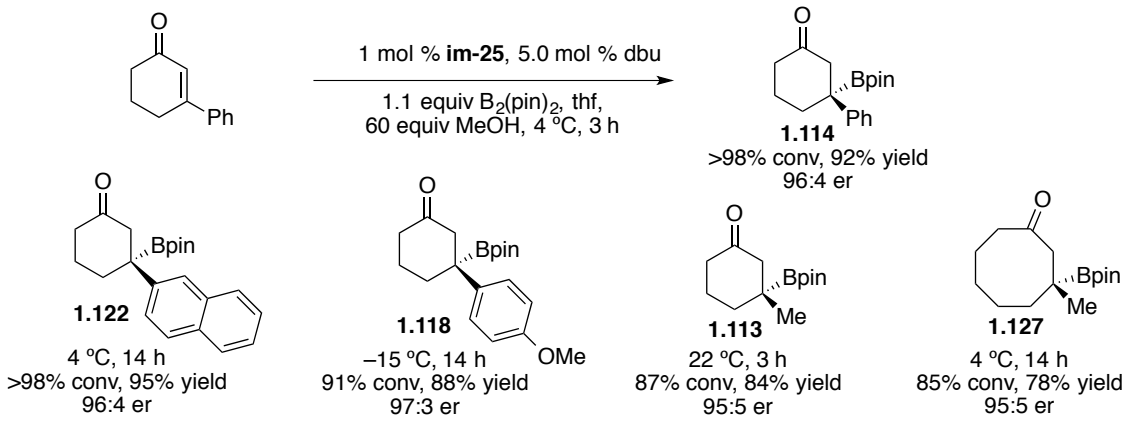

1B.2.3. NHC-catalyzed enantioselective BCAs to β,β-disubstituted acyclic enones

We began searching for an optimal NHC catalyst for enantioselective BCAs of acyclic enones with **im-25**, the optimal NHC precursor in reactions with cyclic enones (Scheme 1.30). Reaction of acyclic enone **1.128** proceeds to give the desired product in 69% yield and 89:11 er. Removing the *ortho* methyl substituent of the NHC derived from **im-24** results in higher efficiency, but lower selectivity (89% yield, 79:21 er). Increasing the size to *i*-Pr group almost inhibits the reaction (**im-27**, 5% conv, 54:46 er). However, putting *t*-Bu substituents at the *meta* positions does not improve the result (**im-28**, 59% yield, 72:28 er). Imidazolinium salt **im-15** bearing a N–Mes unit proves to be optimal generating the desired product in 90% yield and 91:9 er.

Scheme 1.30. Examination on different chiral NHCs for acyclic substrates

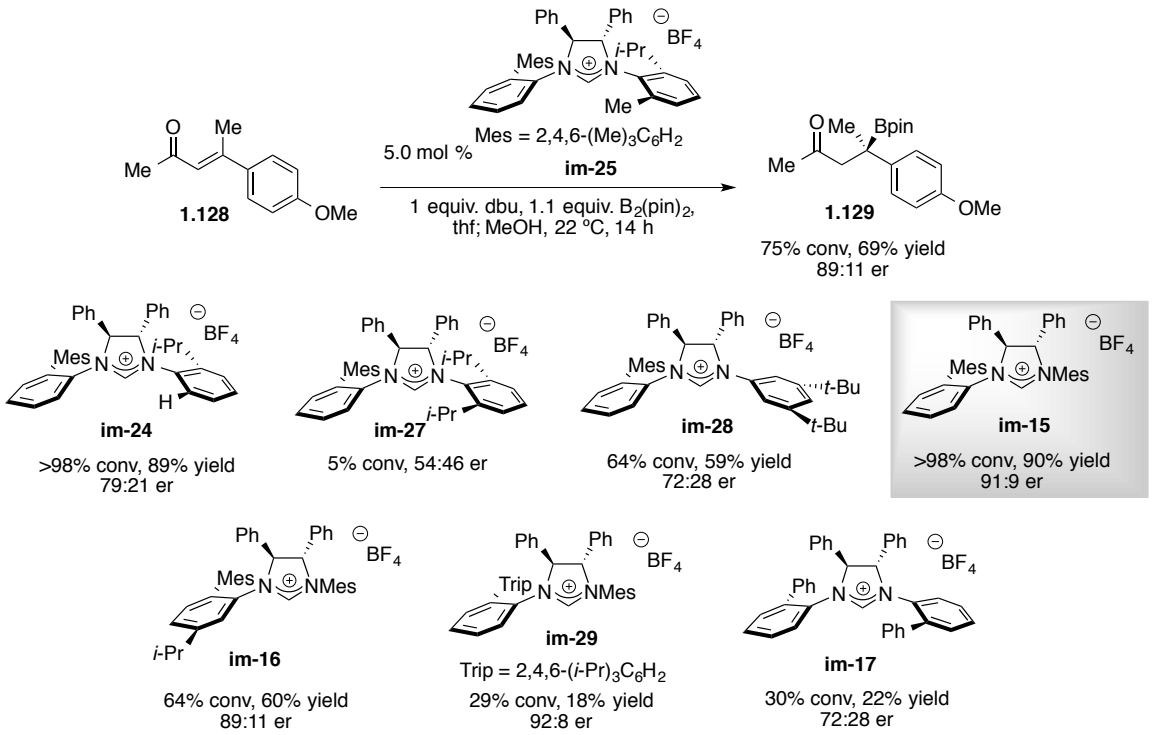

As the results in Scheme 1.31 illustrate, an array of β-substituted acyclic enones can be used as substrates. A range of products bearing aryl- or alkyl-substituted enones are suitable substrates in BCA affording the corresponding β-boryl compounds in 69–94% yield and 91:9–98:2 er. It is worth mentioning that in certain cases, due to crystallinity gained from addition of the B(pin) unit, products can be recrystallized to obtain a higher enantiopurity. For example, compound **1.129–1.130** and **1.132** are obtained after recrystallization in 56–70% yield and >98:2 er (vs 90:10–92:8 er before recrystallization). Phenyl ketones, which prove to be difficult and less explored in Cu-catalyzed variants,[35b–e] are shown to be effective in the NHC-catalyzed BCA; β-boryl ketone **1.138** and **1.139** are generated in 90–92% yield and 97:3–98:2 er. The reaction that delivers *n*-hexyl **1.140** is; however, somewhat less efficient and enantioselective

(69% yield and 91:9 er) presumably due to lack of conjugation to lower the LUMO of the enone.

In terms of practicality of the method, catalytic enantioselective BCA reactions can be performed without strictly-inert atmosphere conditions. For example, ketone **1.112** was obtained in 92% yield, 95:5 er when the reaction was performed outside of the glovebox (vs 90% yield, 96:4 er with glovebox techniques, entry 13, Table 1.2). One limitation of our metal-free method is that unsaturated esters as well as Weinreb amides are not suitable substrates and did not proceed in the BCA reactions.

Scheme 1.31. NHC-Catalyzed enantioselective BCAs to β-substituted acyclic enones

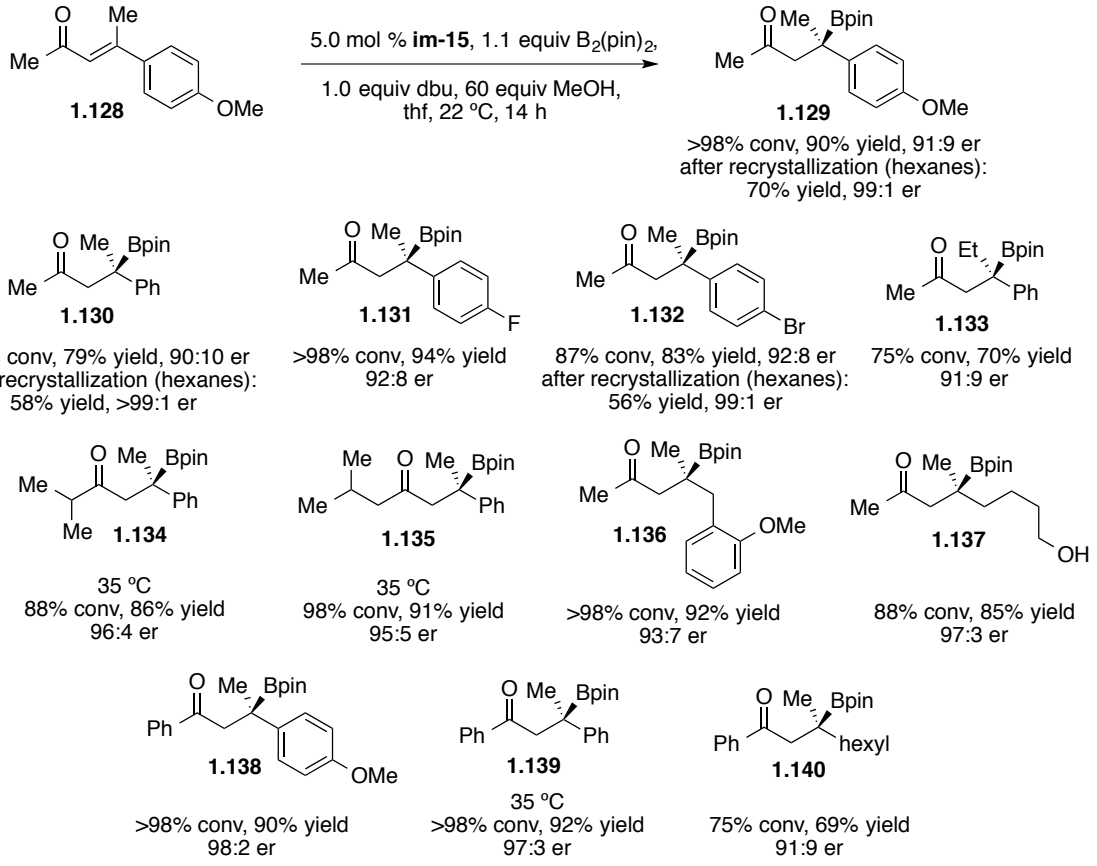

Transformations in Scheme 1.32 illustrate the utility of the resulting BCA product; β-hydroxy carbonyl **1.141** can be efficiently obtained from oxidation by bleach

at ambient temperature in two hours and with complete enantiospecificity (es) (95% yield, >98% es).[39b] Notably, at elevated temperature (70 °C), double-oxidation of boron-containing compound **1.130** delivers β-hydroxy carboxylic acid **1.142** in 63% yield and >98% es.[57,58]

Scheme 1.32. Synthesis of the ketone aldol product and the derived β-hydroxy carboxylic acid

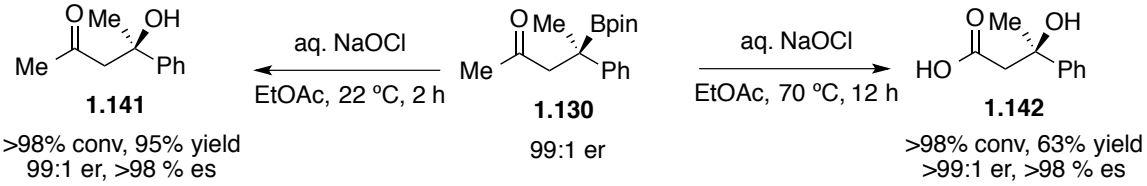

Additionally, the absolute stereochemistry of the β-boryl products was unambiguously confirmed by X-ray structures of **1.124** (for cyclic) and **1.129** (for acyclic) as depicted in Scheme 1.33.

Scheme 1.33. Absolute configurations confirmed by X-ray crystallography

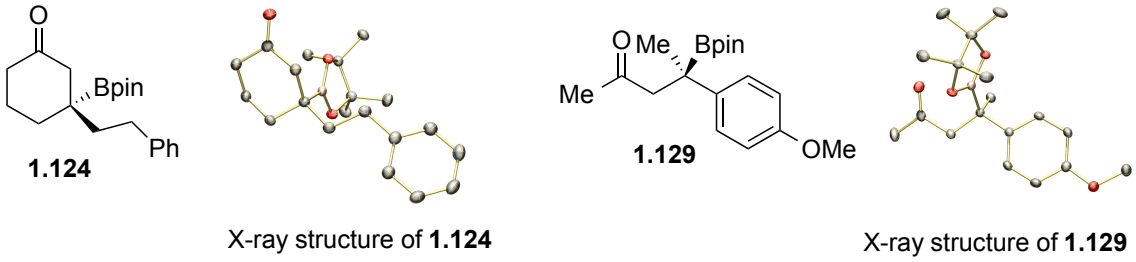

1B.2.4. Functional group compatibilities and application in natural product synthesis

The next phase of our studies is to illustrate the utility of the metal-free approach in comparison to Cu catalysis. As shown in Scheme 1.34, whereas NHC-catalyzed BCA

(57) Liskin, D. V.; Valente, E. J. *J. Mol. Struct.* **2008**, 878, 149–159.

(58) There is ~30% conversion to benzoic acid presumably through retro-aldol of the resulting β-hydroxy ketone (determined by analysis of ^{1}H NMR of the unpurified mixture). For a recent example of oxidation of ketone to carboxylic acid, see: Dabrowski, J. A.; Villaume, M. T.; Hoveyda, A. H. *Angew. Chem., Int. Ed.* **2013**, *52*, 8156–8159.

to alkyne-containing cyclohexenone **1.143** proceeds with high chemoselectivity to obtain product **1.144** in 75% yield and 94.5:5.5 er, under Cu-catalyzed conditions, compound **1.144** is isolated in 45% yield and approximately 40% of Cu–B addition to alkyne is observed in the ^{1}H NMR of the unpurified mixture. A more distinct example of chemoselectivity obtained from the NHC-catalyzed reaction is illustrated by reaction to generate allene-substituted **1.145**. The reaction promoted by NHC offers a higher degree of chemoselectivity and delivers the product in 71% yield and 95:5 er although ~10% protoboration is detected. The Cu-catalyzed reaction significantly suffers from the Cu–B addition to allene (>98% reaction with allene moiety); allylcopper species formed in situ can further react with ketone moiety resulting in a complex mixture.

Scheme 1.34. NHC-Catalyzed enantioselective BCAa to polyfunctional substrates

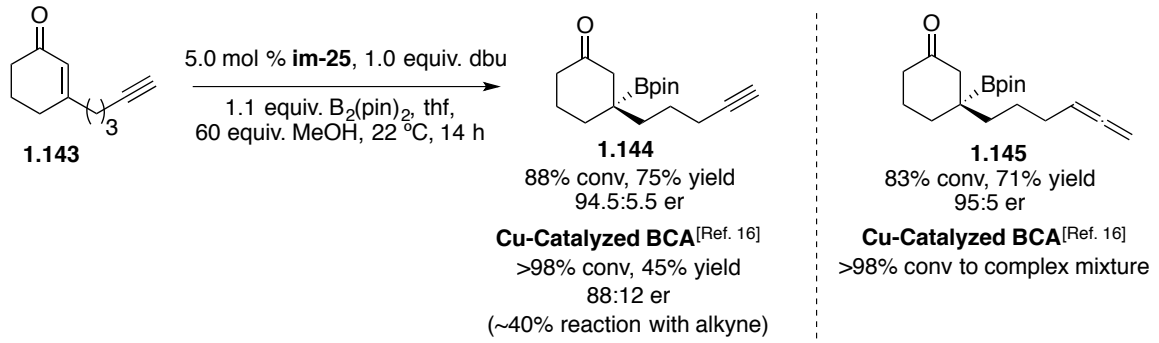

Finally, as shown in Scheme 1.35, we demonstrate the utility of the NHC-catalyzed BCA through the enantioselective formal synthesis of natural product (–)-crassinervic acid, an antifungal agent, that contains a hydroxyl-substituted quaternary carbon at the β postion of the carbonyl.[59] Highly functionalized ketone **1.146** proceeds efficiently and selectively in the NHC-catalyzed BCA reaction affording β-boryl ketone

(59) Lago, J. H. G.; Ramos, C. S.; Casanova, D. C. C.; Morandim, A. A.; Bergamo, D. C. B.; Cavalheiro, A. J.; Bolzani, V. S.; Furlan, M.; Guimaraes, E. F.; Young, M. C. M.; Kato, M. J. *J. Nat. Prod.* **2004**, *67*, 1783–1788.

1.147 in 72% yield and 95:5 er; however, less dbu (40 mol % vs 100 mol %) is used to minimize the reversible intramolecular cyclization of phenol to enone and the reaction was performed at slightly elevated temperature (35 °C) to regenerate the substrate for BCA from the cyclized byproduct. Oxidation of the C–B bond in **1.147** cleanly affords β-hydroxy derivative in 93% yield, which can be converted to natural product (–)-crassinervic acid, in one step by Pinnick oxidation.[60]

Scheme 1.35. Application in the synthesis of (–)-crassinervic acid

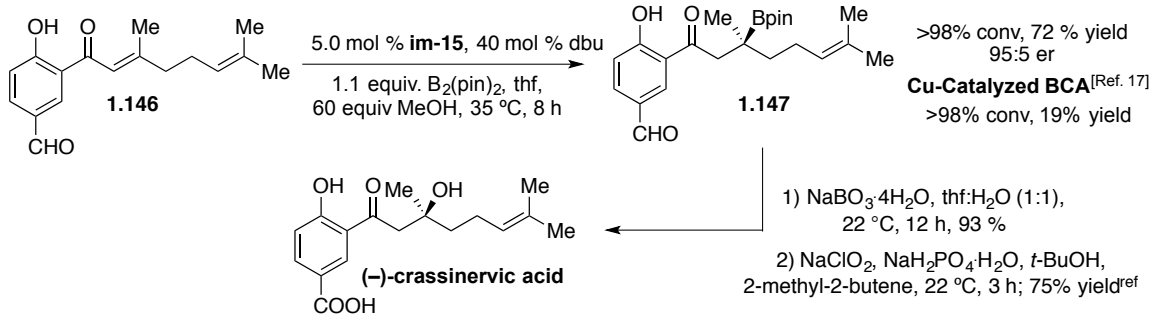

1B.3. Conclusions

We have demonstrated the first NHC-catalyzed enantioselective BCAs to β-substituted cyclic and acyclic enones.[61] A wide range of B-substituted quaternary stereogenic centers are produced in up to 95% yield and >98:2 er. The described method is complementary to the more examined Cu-catalyzed alternatives. Moreover, the unique profiles in chemoselectivity of the metal-free approach are illustrated through cases involving polyfunctional molecules and in the formal synthesis of natural product (–)-crassinervic acid. All above attributes from the NHC-catalyzed BCA should render the present study of useful in chemical synthesis.

(60) Chakor, J. N.; Merlini, L.; Dallavalle, S. *Tetrahedron* **2011**, *67*, 6300–6307.
(61) Radomkit, S.; Hoveyda, A. H. *Angew. Chem., Int. Ed.* **2014**, *53*, 3387–3391.

1B.4. Experimental Section

General. Infrared (IR) spectra were recorded on a Bruker FT-IR Alpha (ATR mode) spectrophotometer, ν_{max} in cm^{-1}. Bands are characterized as broad (br), strong (s), medium (m), and weak (w). ^{1}H NMR spectra were recorded on a Varian Unity INOVA 400 (400 MHz) spectrometer. Chemical shifts are reported in ppm from tetramethylsilane with the solvent resonance as the internal standard ($CDCl_3$: δ 7.26 ppm). Data are reported as follows: chemical shift, integration, multiplicity (s = singlet, d = doublet, t = triplet, q = quartet, quint = quintet, sept = septet, m = multiplet), and coupling constants (Hz). ^{13}C NMR spectra were recorded on a Varian Unity INOVA 400 (100 MHz) spectrometer with complete proton decoupling. Chemical shifts are reported in ppm from tetramethylsilane with the solvent resonance as the internal standard ($CDCl_3$: δ 77.16 ppm). High-resolution mass spectrometry was performed on a Micromass LCT ESI-MS (positive mode) at the Mass Spectrometry Facility, Boston College. Enantiomeric ratios were determined by GC analysis (Alltech Associated Chiraldex B-DM (30 m x 0.25 mm)) and HPLC analysis (high-performance liquid chromatography) with a Shimadzu chromatograph [Chiral Technologies Chiralcel OJ-H (4.6 x 250 mm), Chiral Technologies Chiralcel OD-H (4.6 x 250 mm), Chiral Technologies Chiralpak AS-H (4.6 x 250 mm) or Chiral Technologies Chiralpak AD-H (4.6 x 250 mm)] in comparison with authentic racemic materials. Specific rotations were measured on a Rudolph Research Analytical Autopol IV Polarimeter. Melting points were measured on a Thomas Hoover capillary melting point apparatus and are uncorrected. X-ray structures were obtained with a Microfocus sealed Cu tube from Incote. It is well established that that

aforementioned detector allows for the determination of absolute configuration of molecules that do not have a heavy atom.

Unless otherwise noted, reactions were carried out with distilled and degassed solvents under an atmosphere of dry N_2 in oven- (135 ºC) or flame-dried glassware with standard dry box or vacuum-line techniques. Tetrahydrofuran (Aldrich Chemical Co.) was purified by distillation from sodium benzophenone ketyl immediately prior to use. Methanol (Acros Organics 99.9% Extra Dry, AcroSeal$^{@}$) was used as received. All work-up and purification procedures were carried out with reagent grade solvents (purchased from Fisher Scientific) under an atmosphere of air.

■ **Reagents:**

Acetyl chloride: purchased from Aldrich and used as received.

Alkyne substrates for preparation of acyclic enones: purchased from Aldrich and distilled over CaH_2 prior to use, except 4'-bromophenylacetylene, which was used as received.

Bis(pinacolato)diboron [$B_2(pin)_2$]: gifts/purchased from Frontier Scientific, Inc., recrystallized from pentane and dried under vacuum prior to use.

3-Bromo-4-hydroxybenzaldehyde (S1): purchased from Aldrich and used as received.

***tert*-Buthanol:** purchased from Aldrich and used as received.

***tert*-Butyllithium:** purchased from Aldrich and titrated before use.

Tetrakis(acetonitrile)copper (I) hexafluorophosphate: purchased from Aldrich and used as received.

Copper (II) chloride: purchased from Strem and used as received.

***bis*-(Cyclopentadienyl)zirconium dichloride:** purchased from Strem and recrystallized from toluene prior to use.

1,8-Diazabicyclo[5.4.0]undec-7-ene (dbu): purchased from Aldrich and purified by distillation from CaH_2 prior to use.

Dimethyl sulfoxide: purchased from Aldrich and purified by distillation from CaH_2 prior to use.

Dimethoxyethane: purchased from Aldrich and purified by distillation from Na prior to use.

Ethylene glycol: purchased from Aldrich and used as received.

Geranial: prepared from oxidation of geraniol according to a previously reported procedure.[62]

Geraniol: purchased from Aldrich and used as received.

Imidazolinium salt im-15: prepared according to a previously reported procedure.[63]

Imidazolinium salt im-25: prepared according to a previously reported procedure.[64]

Isopropanol: purchased from Fisher Scientific and and purified by distillation from Mg prior to use.

Lithium *tert*-butoxide: purchased from Strem and used as received.

2-Methyl-2-butene: purchased from TCI and used as received.

---

(62) Fontán, N.; Vaz, B.; Álvarez, R.; de Lera, A. R. *Chem. Commun*. **2013**, *49*, 2694–2696.

(63) Lee, K.-s.; Hoveyda, A. H. *J. Org. Chem.* **2009,** *74*, 4455–4462.

(64) Vieira, E. M.; Snapper, M. L.; Hoveyda, A. H. *J. Am. Chem. Soc.* **2011**, *133*, 3332–3335.

3-Methyl-2-cyclohexen-1-one: purchased from Aldrich and purified by distillation from CaH_2 prior to use.

3-Methyl-2-cyclopenten-1-one: purchased from Aldrich and purified by distillation from CaH_2 prior to use.

N-Methylmorpholine N-oxide: purchased from Aldrich and used as received.

(*R*,*R*)-QuinoxP*: purchased from Aldrich and used as received.

Tetrapropylammonium perruthenate: purchased from TCI and used as received.

***p*-Toluenesulfonic acid monohydrate:** purchased from Aldrich and used as received.

Trimethylaluminum: purchased from Aldrich (neat) and used as received.

Triethylaluminum: purchased from Aldrich (neat) and used as received.

Sodium chlorite: purchased from Alfa Aesar and used as received.

Sodium hypochlorite (10–15%): purchased from Aldrich and used as received.

Sodium phosphate monobasic monohydrate: purchased from Alfa Aesar and used as received.

Sodium *tert*-butoxide: purchased from Strem and used as received.

■ **Representative Experimental Procedure for the Synthesis of Enone Substrates**

Cyclic enones were prepared according to a reported protocol.[65] Acyclic enone substrates were synthesized according to a modified reported precedure[66] for zirconocene-catalyzed carboalumination reactions.

---

(65) Moritani, Y.; Appella, D. H.; Jurkauskas, V.; Buchwald, S. L. *J. Am. Chem. Soc.* **2000**, *122*, 6797–6798.

(66) Wipf, P.; Lim, S. *Angew. Chem., Int. Ed.* **1993**, *32*, 1068–1071.

To a flame-dried round bottom flask equipped with a stir bar was added Cp_2ZrCl_2 (643 mg, 2.20 mmol) and CH_2Cl_2 (50 mL) under N_2 after which Me_3Al (2.9 mL, 30 mmol, USE CAUTION, PYROPHORIC) was added by syringe. The resulting mixture was allowed to cool to –22 °C (dry ice/acetone bath) and H_2O (0.27 ml, 15 mmol) was added by syringe drop-wise (reaction is extremely vigorous, use vent needle). After allowing the mixture to stir for 10 min, phenylacetylene (1.1 ml, 10 mmol) was added by syringe. The mixture was allowed to stir for an additional 10 minutes, after which, acetyl chloride (0.85 ml, 12 mmol) was added. The mixture was allowed to stir for 10 min at –22 ºC and then warm to 22 ºC and stir for an additional 10 min. The reaction was quenched upon drop-wise addition of a saturated aqueous solution of K_2CO_3 (1.0 mL, reaction is vigorous, use of a vent needle is recommended) until evolution of gas ceases. The mixture was transferred to a separatory funnel, Rochelle's salt was added (20 mL) and the layers separated. The aqueous layer was washed with Et_2O (3 x 20 mL). The combined organic layers were dried over $MgSO_4$ and concentrated. The resulting yellow oil was purified by silica gel chromatography (100% hexanes → 20:1 Hexanes/Et_2O) to afford **(*E*)-4-phenylpent-3-en-2-one (substrate for 1.130)** as a light yellow solid (1.3 g, 8.0 mmol, 80%).

(*E*)-4-(4-Fluorophenyl)pent-3-en-2-one (substrate for 1.131): IR (neat): 3051 (w), 2919 (w), 1680 (s), 1598 (s), 1584 (s), 1507 (s), 1234 (m), 1178 (s), 1162 (s), 824 (m) cm^{-1}; ^1H NMR (400 MHz, $CDCl_3$): δ 7.42–7.39 (2H, m), 7.02–6.97 (2H, m), 6.41 (1H, s), 2.45 (3H, s), 2.22 (3H, s); ^{13}C NMR (100 MHz, $CDCl_3$): δ 198.8, 163.4, (d, J = 248.1 Hz), 162.1, 152.6, 138.6 (d, J = 3.1 Hz), 128.4 (d, J = 8.4 Hz), 124.4, 115.6 (d, J = 21.3

Hz), 32.3, 18.4; HRMS (ESI+): Calcd for $C_{11}H_{12}F_1O_1$ $[M+H]^+$: 179.0872, Found: 179.0877.

(*E*)-8-Hydroxy-4-methyloct-3-en-2-one (substrate for 1.137): IR (neat): 3425 (br), 2938 (m), 2866 (m), 1685 (s), 1612 (s), 1423 (m), 1357 (m), 1217 (m), 1064 (m) cm^{-1}; ^1H NMR (400 MHz, $CDCl_3$): δ 6.06 (1H, s), 3.67–3.63 (2H, m), 2.16–2.11 (8H, m), 1.58–1.53 (5H, m); ^{13}C NMR (100 MHz, $CDCl_3$): δ 199.1, 158.6, 123.7, 62.5, 40.9, 32.3, 31.8, 23.8, 19.3; HRMS (ESI+): Calcd for $C_9H_{17}O_2$ $[M+H]^+$: 157.1229, Found: 157.1231.

(*E*)-5-(2-Methoxyphenyl)-4-methylpent-3-en-2-one (substrate for 1.136): IR (neat): 3002 (m), 2938 (m), 2837 (m), 1686 (s), 1616 (s), 1493 (s), 1245 (s), 754 (s) cm^{-1}; ^1H NMR (400 MHz, $CDCl_3$): δ 7.26–7.22 (1H, m), 7.08 (1H, d, J = 7.6, 2.0 Hz), 6.93–6.87 (2H, m), 5.98 (1H, s), 3.81 (3H, s), 3.44 (2H, s), 2.14 (3H, s), 2.13 (3H, s); ^{13}C NMR (100 MHz, $CDCl_3$): δ 199.1, 157.7, 157.3, 130.8, 128.2, 126.4, 124.5, 120.6, 110.7, 55.5, 40.9, 32.0, 19.6; HRMS (ESI+): Calcd for $C_{13}H_{17}O_2$ $[M+H]^+$: 205.1229, Found: 205.1226.

(*E*)-3-(4-Methoxyphenyl)-1-phenylbut-2-en-1-one (substrate for 1.138): IR (neat): 3056 (m), 3002 (m), 2956 (m), 2837 (m), 1650 (s), 1585 (s), 1566 (s), 1447 (m), 1250 (m), 1211 (s), 1177 (s), 1026 (s), 828 (s) cm^{-1}; ^1H NMR (400 MHz, $CDCl_3$): δ 8.01–7.98 (2H, m), 7.58–7.45 (5H, m), 7.17 (1H, s), 6.97–6.93 (2H, m), 3.85 (3H, s), 2.61 (3H, s); ^{13}C NMR (100 MHz, $CDCl_3$): δ 191.9, 160.7, 154.9, 139.8, 135.0, 132.5, 128.6, 128.3, 128.0, 120.5, 114.1, 55.5, 18.8; HRMS (ESI+): Calcd for $C_{17}H_{17}O_2$ $[M+H]^+$: 253.1229, Found: 253.1229.

(*E*)-6-Methyl-2-phenylhept-2-en-4-one (substrate for 1.135): IR (neat): 2955 (m), 2870 (m), 1678 (s), 1598 (s), 1446 (m), 1364 (m), 1174 (m), 1064 (m), 756 (s), 695 (s)

cm^{-1}; ^{1}H NMR (400 MHz, $CDCl_3$): δ 7.49–7.45 (2H, m), 7.39–7.34 (3H, m), 6.48 (1H, s), 2.54 (3H, s), 2.41 (2H, d, *J* = 7.2 Hz), 2.21 (1H, sept, *J* = 5.8 Hz), 0.97 (6H, d, *J* = 6.8 Hz); ^{13}C NMR (100 MHz, $CDCl_3$): δ 201.3, 153.4, 142.7, 129.0, 128.5, 126.5, 124.6, 54.0, 25.3, 25.3, 22.7, 18.3; HRMS (ESI+): Calcd for $C_{14}H_{19}O_1$ $[M+H]^+$: 203.1436, Found: 203.1436.

■ **Experimental Procedure for the Synthesis of 1.146**

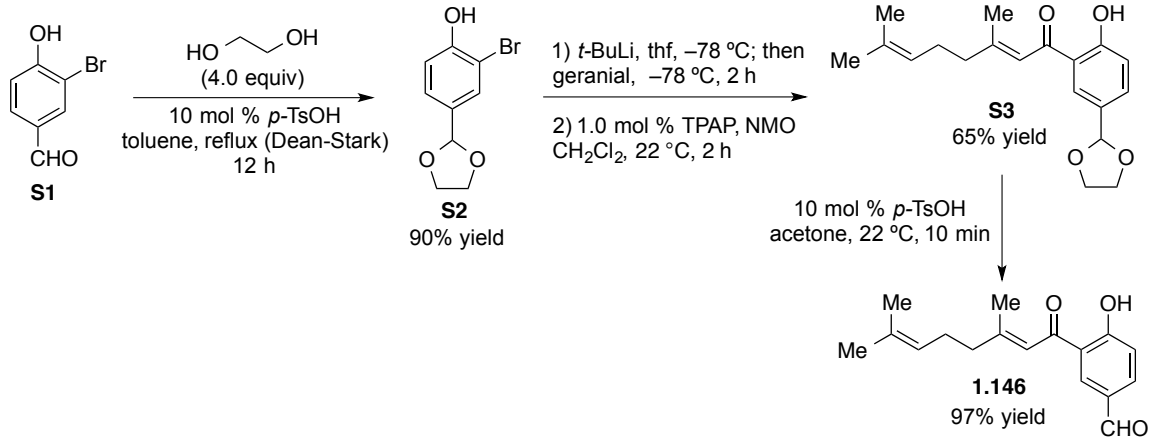

(*E*)-1-(5-(1,3-Dioxolan-2-yl)-2-hydroxyphenyl)-3,7-dimethylocta-2,6-dien-1-one (S2): A flame-dried 100 mL round-bottom flask equipped with a Dean-Stark trap, reflux condenser, and a stir bar was charged with benzaldehyde **S1** (2.00 g, 9.95 mmol), ethylene glycol (2.20 mL, 39.8 mmol), *p*-TsOH (189 mg, 0.995 mmol) and toluene (50 mL). The mixture was allowed to reflux for 12 h. After allowing the solution to cool to 22 °C, toluene was removed *in vacuo*. The resulting residue was passed through a short plug of neutralized silica gel with Et_2O as eluent. All volatiles were removed under reduced pressure to afford 2.19 g (8.95 mmol, 90%) of **S2**, which was used in the next step without further purification.

To a solution of **S2** (1.00 g, 4.08 mmol) in thf (20 mL) was added 1.7 M *t*-BuLi (7.20 mL, 12.2 mmol) at –78 °C under an N_2 atmosphere. After 10 min, geranial (1.05 mL, 6.12 mmol) was added and the reaction mixture was allowed to stir for 2 h at –78 °C. After allowing the solution to warm to 22 ºC, water (10 mL) was added. The layers were separated and the aqueous segment was washed with Et_2O (3 x 15 mL). The combined organic layer was dried over anhydrous Na_2SO_4, filtered, and concentrated *in vacuo*. The residue was dissolved in CH_2Cl_2 and N-methylmorpholine N-oxide (718 mg, 6.12 mmol) and tetrapropylammonium perruthenate (14.0 mg, 0.0408 mmol) were added. The solution was allowed to stir at 22 ºC for 2 h, after which it was filtered through a short plug of neutralized (flushed with 2 % Et_3N in Et_2O) silica gel with Et_2O as eluent. All volatiles were removed *in vacuo* and the resulting brown oil was purified by neutralized (flushed with 2 % Et_3N in 10:1 hexanes: Et_2O) silica gel chromatography (10:1 hexanes: Et_2O) to afford 839 mg (2.65 mmol, 65%) of **S3** as light yellow solid. Melting point: 56–58 °C. IR (neat): 2963 (m), 2922 (m), 2887 (m), 1638 (s), 1583 (s), 1490 (m), 1364 (m), 1289 (m), 1206 (m), 1088 (m) cm^{-1}; ^1H NMR (400 MHz, $CDCl_3$): δ 12.9 (1H, s), 7.86 (1H, d, J = 2.0 Hz), 7.56 (1H, dd, J = 2.0, 8.4 Hz), 6.99 (1H, d, J = 8.8 Hz), 6.78 (1H, s), 5.74 (1H, s), 5.15–5.12 (1H, m), 4.16–4.02 (4H, m), 2.34–2.23 (4H, m), 2.20 (3H, s), 1.72 (3H, s), 1.64 (3H, s). ^{13}C NMR (100 MHz, $CDCl_3$): δ 196.4, 164.2, 161.8, 134.1, 133.0, 128.3, 128.1, 123.0, 120.4, 119.6, 118.8, 103.4, 65.4, 41.8, 26.3, 25.8, 20.2, 17.9; HRMS (ESI+): Calcd for $C_{19}H_{25}O_4$ $[M+H]^+$: 317.1753, Found: 317.1762.

(*E*)-3-(3,7-Dimethylocta-2,6-dienoyl)-4-hydroxybenzaldehyde (1.146). To a solution of **S3** (500 mg, 1.58 mmol) in acetone (5 mL) was added *p*-TsOH•H_2O (30.1 mg, 0.158 mmol). The mixture was allowed to stir at 22 ºC for 10 min. Water (5 mL) and Et_2O (5

mL) were added. The organic layer was separated and the aqueous layer was washed with Et_2O (3 x 10 mL). The combined organic layer was dried over Na_2SO_4, filtered, and concentrated *in vacuo*. The resulting yellow oil was purified by silica gel chromatography (10:1 hexanes: Et_2O) to afford 417 mg (1.53 mmol, 97%) of **1.146** as light yellow oil. IR (neat): 2966 (m), 2918 (m), 2856 (m), 2732 (w), 1693 (s), 1634 (s), 1577 (s), 1485 (m), 1297 (m), 1214 (m), 838 (m) cm^{-1}; ^1H NMR (400 MHz, $CDCl_3$): δ 13.5 (1H, s), 9.89 (1H, s), 8.31 (1H, d, J = 2.0 Hz), 7.96 (1H, dd, J = 6.8, 1.6 Hz), 7.09 (1H, d, J = 7.2 Hz), 6.86 (1H, s), 5.15–5.12 (1H, m), 2.37–2.16 (7H, m), 1.72 (3H, s), 1.60 (3H, s); ^{13}C NMR (100 MHz, $CDCl_3$): δ 195.8, 190.1, 168.6, 164.5, 136.4, 133.2, 132.9, 128.1, 122.8, 120.6, 119.7, 118.8, 42.1, 26.4, 25.9, 20.6, 18.0; HRMS (ESI+): Calcd for $C_{17}H_{21}O_3$ $[M+H]^+$: 273.1491, Found: 273.1483.

■ **Representative Procedure for NHC–Catalyzed Enantioselective (Pinacolato)boron Conjugate Addition (Table 1.3, Entry 13):** In a glove-box, an oven-dried 1 dram vial equipped with a stir bar was charged with imidazolinium salt **im-25** (3.2 mg, 0.005 mmol), dbu (3.0 mg, 0.02 mmol) and thf (0.15 mL, 0.033 M solution of catalyst) for 30 min at 22 °C under a dry N_2 atm. Bis(pinacolato)diboron (27.9 mg, 0.11 mmol), 3-methyl-2-cyclohexen-1-one (11.0 mg, 0.10 mmol) and methanol (0.24 mL) were added to the vial (0.26 M solution of substrate), which was sealed with a cap before removal from the glove-box. The solution was allowed to stir at 22 °C for 14 h, after which the reaction was quenched by the addition of an aqueous solution of NH_4Cl (0.5 mL, 1.0 M) and the mixture was allowed to stir for an additional 20 min. The aqueous layer was washed with diethyl ether (3 x 2 mL). The combined organic layers were dried over anhydrous $MgSO_4$ and filtered. The volatiles were removed under vacuum and the

resulting light yellow oil was purified by silica gel chromatography (hexanes:Et_2O = 10:1) to afford 21.4 mg (0.09 mmol, 90% yield) of **1.112**. *For the representative procedure carried out in a typical fume hood, see below.*

(*S*)-3-Methyl-3-(4,4,5,5-tetramethyl-1,3,2-dioxaborolan-2-yl)cyclohexan-1-one (1.112): The spectroscopic data are consistent with those reported previously.[67] ^{1}H NMR (400 MHz, $CDCl_3$): δ 2.48 (1H, d, *J* = 13.6 Hz), 2.31–2.15 (2H, m), 2.01–1.90 (3H, m), 1.82–1.71 (1H, m), 1.43–1.34 (1H, m), 1.19 (12H, s), 1.01 (3H, s). Specific Rotation: $[\alpha]_D^{20}$ –11.5 (*c* 1.01, $CHCl_3$) for an enantiomerically enriched sample of 96:4 er. Enantiomeric purity was determined by GC analysis in comparison with authentic racemic material (96:4 er shown; Chiraldex B-DM column, 15 psi, 100 °C).

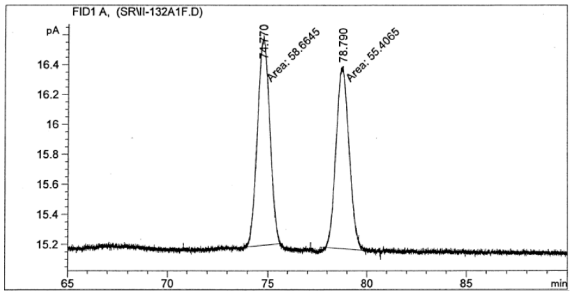

Peak #	RetTime [min]	Type	Width [min]	Area [pA*s]	Height [pA]	Area %
1	74.770	MM	0.6970	58.66451	1.40273	51.42808
2	78.790	MM	0.7557	55.40647	1.22204	48.57192

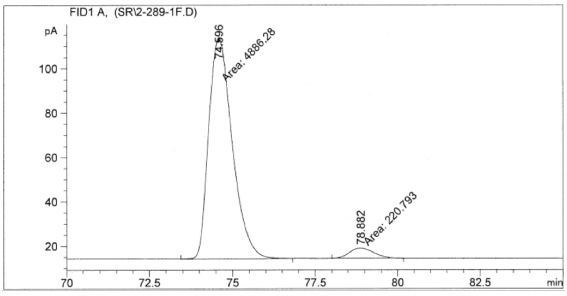

Peak #	RetTime [min]	Type	Width [min]	Area [pA*s]	Height [pA]	Area %
1	74.596	MM	0.8097	4886.27783	100.57249	95.67673
2	78.882	MM	0.8087	220.79254	4.55016	4.32327

Peak #	Time (min)	Area (%)	Peak #	Time (min)	Area (%)
1	74.770	51.428	1	74.596	95.677
2	78.790	48.573	2	78.882	4.323

(*S*)-3-Butyl-3-(4,4,5,5-tetramethyl-1,3,2-dioxaborolan-2-yl)cyclohexan-1-one (1.123): IR (neat): 2976 (m), 2960 (m), 2930 (s), 2873 (m), 1714 (s), 1409 (m), 1313 (s), 1144 (s) cm^{-1}; ^{1}H NMR (400 MHz, $CDCl_3$): δ 2.52 (1H, dt, *J* = 13.6, 1.5 Hz), 2.34–2.18 (2H, d, m), 2.01–1.92 (3H, m), 1.81–1.71 (1H, m), 1.48–1.21 (19H, m), 0.88 (3H, t, *J* = 7.0 Hz); ^{13}C NMR (100 MHz, $CDCl_3$): δ 212.3, 83.7, 49.3, 41.5, 38.6, 32.9, 28.1, 25.0, 24.8, 24.2,

(67) Chen, I.–H.; Yin, L.; Itano, W.; Kanai, M.; Shibasaki, M. *J. Am. Chem. Soc.* **2009**, *131*, 11664–11665.

23.5, 14.1; HRMS (ESI+): Calcd for $C_{16}H_{30}B_1O_3$ $[M+H]^+$: 281.2288, Found: 281.2294. Specific Rotation: $[\alpha]_D^{20}$ –9.1 (*c* 0.37, $CHCl_3$) for an enantiomerically enriched sample of 94:6 er. Enantiomeric purity is determined by GC analysis in comparison with authentic racemic material (94:6 er shown; Chiraldex B-DM column, 15 psi, 100 °C).

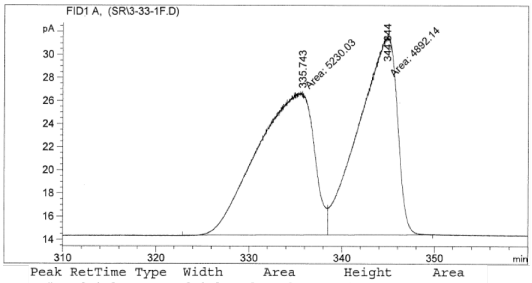

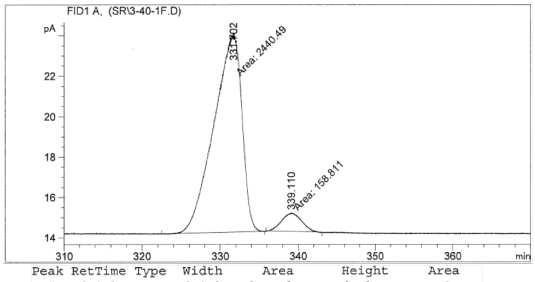

Peak #	Time (min)	Area (%)	Peak #	Time (min)	Area (%)
1	335.743	51.669	1	331.702	93.890
2	344.844	48.331	2	339.110	6.110

(*R*)-3-Phenethyl-3-(4,4,5,5-tetramethyl-1,3,2-dioxaborolan-2-yl)cyclohexan-1-one (1.124): Melting point: 90–91°C. IR (neat): 2977 (m), 2932 (m), 2866 (w), 1711 (s), 1454 (m), 1383 (m), 1314 (m), 1143 (s) cm^{-1}; ^1H NMR (400 MHz, $CDCl_3$): δ 7.29–7.24 (2H, m), 7.19–7.15 (3H, m), 2.63–2.49 (3H, m), 2.37–2.21 (2H, m), 2.09–1.96 (3H, m), 1.87–1.62 (3H, m), 1.55–1.48 (1H, m), 1.25 (12H, s); ^{13}C NMR (100 MHz, $CDCl_3$): δ 211.8, 142.3, 128.5, 128.4, 125.9, 83.8, 49.1, 41.5, 41.2, 32.8, 32.5, 25.0, 24.9, 24.1; HRMS (ESI+): Calcd for $C_{20}H_{30}B_1O_3$ $[M+H]^+$: 329.2293, Found: 329.2288. Specific Rotation: $[\alpha]_D^{20}$ –8.6 (*c* 1.20, $CHCl_3$) for an enantiomerically enriched sample of 96:4 er. Enantiomeric purity was determined by HPLC analysis in comparison with authentic racemic material (96:4 er shown; Chiralcel OD-H column, 99/1 hexanes/*i*-PrOH, 0.3 mL/min, 220 nm).

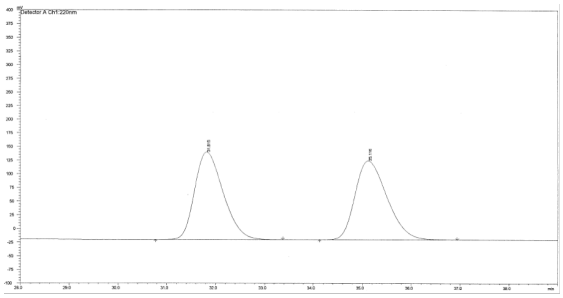

Peak#	Ret. Time	Area	Height	Area %
1	31.815	6451565	159870	49.734
2	35.116	6520477	144287	50.266
Total		12972042	304157	100.000

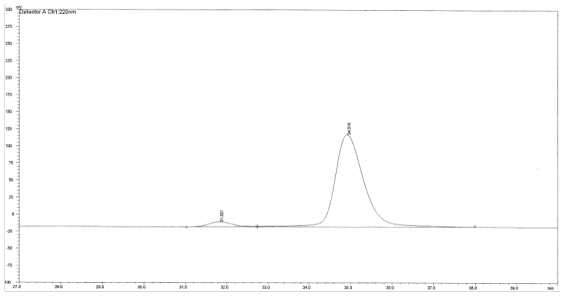

Peak#	Ret. Time	Area	Height	Area %
1	31.821	279414	7180	4.136
2	34.916	6476241	135241	95.864
Total		6755655	142422	100.000

Peak #	Time (min)	Area (%)	Peak #	Time (min)	Area (%)
1	31.815	49.734	1	31.821	4.136
2	35.116	50.266	2	34.916	95.864

(***S*)-3-(Pent-4-yn-1-yl)-3-(4,4,5,5-tetramethyl-1,3,2-dioxaborolan-2-yl)cyclohexan-1-one (1.144)**: IR (neat): 3283 (m), 2977 (m), 2933 (m), 2870 (m), 2116 (w), 1710 (s), 1386 (m), 1312 (s), 1143 (s), 892 (m) cm^{-1}; ^{1}H NMR (400 MHz, $CDCl_3$): δ 2.53 (1H, d, *J* = 14.0 Hz), 2.34–2.14 (4H, m), 2.02–1.93 (4H, m), 1.82–1.72 (1H, m), 1.54–1.42 (5H, m), 1.21 (12H, s); ^{13}C NMR (100 MHz, $CDCl_3$): δ 211.8, 84.4, 83.8, 68.6, 49.2, 41.5, 38.0, 32.8, 25.0, 24.97, 24.9, 24.1, 19.2; HRMS (ESI+): Calcd for $C_{17}H_{28}B_1O_3$ $[M+H]^+$: 291.2132, Found: 291.2134. Specific Rotation: $[\alpha]_D^{20}$ –10.6 (*c* 0.50, $CHCl_3$) for an enantiomerically enriched sample of 94.5:5.5 er. Enantiomeric purity was determined by HPLC analysis in comparison with authentic racemic material (94.5:5.5 er shown; Chiralcel OD-H column, 99/1 hexanes/*i*-PrOH, 0.3 mL/min, 300 nm).

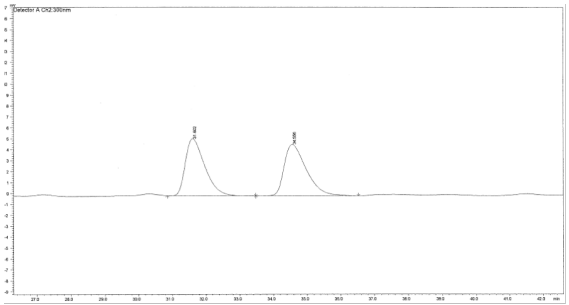

Peak#	Ret. Time	Area	Height	Area %
1	31.602	209161	5228	49.431
2	34.556	213975	4706	50.569
Total		423136	9934	100.000

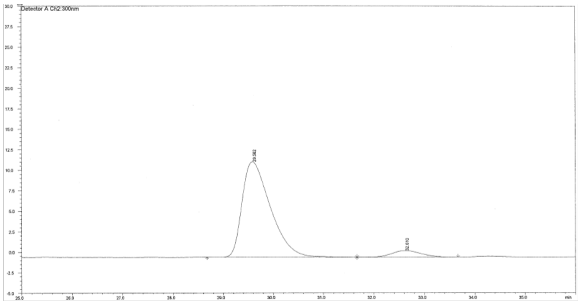

Peak#	Ret. Time	Area	Height	Area %
1	29.582	454676	11620	94.500
2	32.610	26464	735	5.500
Total		481139	12355	100.000

Peak #	Time (mins)	Area (%)	Peak #	Time (mins)	Area (%)
1	31.602	49.431	1	29.582	94.500

2	34.556	50.569	2	32.610	5.500

(***S*)-3-(Hexa-4,5-dien-1-yl)-3-(4,4,5,5-tetramethyl-1,3,2-dioxaborolan-2-yl)cyclohexan-1-one (1.145)**: IR (neat): 2976 (m), 2934 (m), 2871 (m), 1955 (m), 1703 (m), 1665 (s), 1454 (s), 1327 (s), 1145 (s), 852 (m) cm^{-1}; ^{1}H NMR (400 MHz, $CDCl_3$): δ 5.07 (1H, quin, J = 6.7 Hz), 4.66–4.63 (2H, m), 2.54 (1H, d, J = 13.6 Hz), 2.33–2.18 (2H, m), 2.01–1.92 (5H, m), 1.82–1.72 (1H, m), 1.49–1.34 (5H, m), 1.21 (12H, s); ^{13}C NMR (100 MHz, $CDCl_3$): δ 212.1, 208.7, 89.9, 83.7, 75.0, 49.3, 41.5, 38.4, 32.9, 28.9, 25.5, 25.0, 24.9, 24.2; HRMS (ESI+): Calcd for $C_{18}H_{30}B_1O_3$ $[M+H]^+$: 305.2301, Found: 305.2288. Specific Rotation: $[\alpha]_D^{20}$ –33.0 (*c* 0.50, $CHCl_3$) for an enantiomerically enriched sample of 95:5 er. Enantiomeric purity was determined by HPLC analysis in comparison with authentic racemic material (95:5 er shown; Chiralpak AS-H column, 99/1 hexanes/*i*-PrOH, 0.3 mL/min, 220 nm).

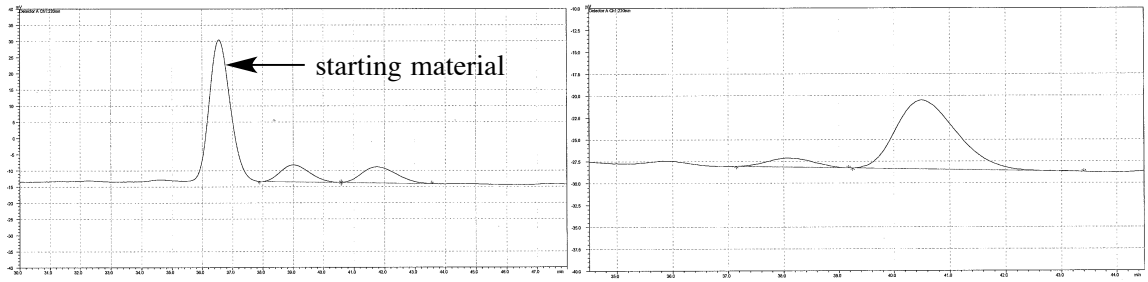

Peak#	Ret. Time	Area	Height	Area %
1	38.999	345217	5199	48.502
2	41.746	366542	4816	51.498
Total		711759	10014	100.000

Peak#	Ret. Time	Area	Height	Area %
1	38.054	33093	746	5.321
2	40.493	588839	7872	94.679
Total		621932	8618	100.000

Peak #	Time (min)	Area (%)	Peak #	Time (min)	Area (%)
1	38.999	48.502	1	38.054	5.321
2	41.746	51.498	2	40.493	94.679

(***S*)-3-Phenyl-3-(4,4,5,5-tetramethyl-1,3,2-dioxaborolan-2-yl)cyclohexan-1-one (1.117)**: The spectroscopic data match those reported previously.[67] ^{1}H NMR (400 MHz, $CDCl_3$): δ 7.32–7.28 (4H, m), 7.19–7.14 (1H, m), 2.87 (1H, d, J = 14.0 Hz), 2.59 (1H, d, J = 14.4 Hz), 2.40–2.24 (3H, m), 2.01–1.75 (3H, m) 1.15 (6H, s), 1.146 (6H, s); Specific Rotation: $[\alpha]_D^{20}$ +15.2 (*c* 1.01, $CHCl_3$) for an enantiomerically enriched sample of 96:4 er.

Enantiomeric purity was determined by HPLC analysis in comparison with authentic racemic material (96:4 er shown; Chiralpak AD-H column, 99/1 hexanes/*i*-PrOH, 0.3 mL/min, 220 nm).

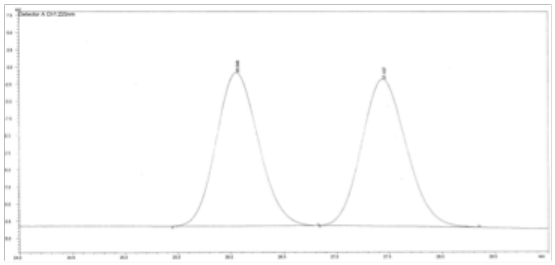

Peak#	Ret. Time	Area	Height	Area %
1	26.048	627233	22449	49.830
2	27.437	631501	21551	50.170
Total		1258733	44000	100.000

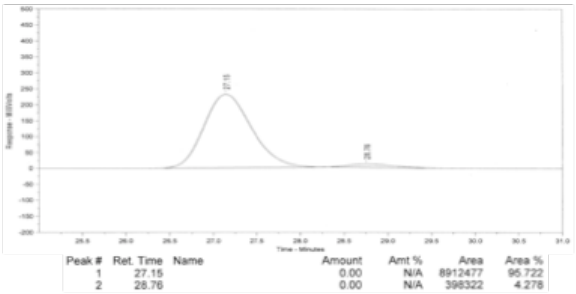

Peak #	Ret. Time	Name	Amount	Amt %	Area	Area %
1	27.15		0.00	N/A	8912477	95.722
2	28.76		0.00	N/A	398322	4.278

Peak #	Time (min)	Area (%)	Peak #	Time (min)	Area (%)
1	26.048	49.830	1	27.150	95.722
2	27.437	50.170	2	28.760	4.278

(*S*)-3-(4-Methoxyphenyl)-3-(4,4,5,5-tetramethyl-1,3,2-dioxaborolan-2-yl)cyclohexan-1-one (1.118): The spectroscopic data match those reported previously.[67] ^{1}H NMR (400 MHz, $CDCl_3$): δ 7.20 (2H, d, *J* = 8.8 Hz), 6.84 (2H, d, *J* = 8.8 Hz), 3.78 (3H, s), 2.84 (1H, d, *J* = 14.4 Hz), 2.55 (1H, d, *J* = 14.0 Hz), 2.39–2.23 (3H, m), 1.96–1.87 (2H, m), 1.84–1.73 (1H, m), 1.15 (6H, s), 1.14 (6H, s); Specific Rotation: $[\alpha]_D^{20}$ +13.6 (*c* 1.01, $CHCl_3$) for an enantiomerically enriched sample of 97:3 er. Enantiomeric purity was determined by HPLC analysis in comparison with authentic racemic material (97:3 er shown; Chiraldex AD-H column, 99/1 hexanes/*i*-PrOH, 0.3 mL/min, 220 nm).

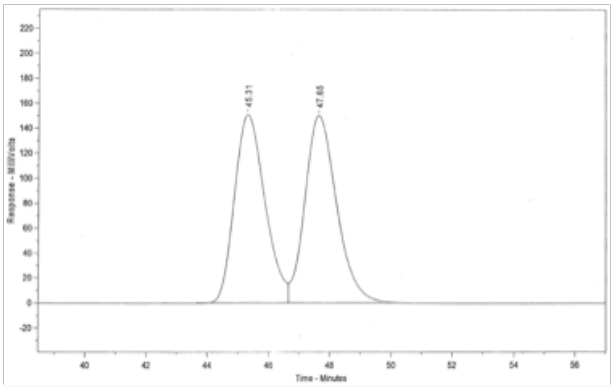

Peak #	Ret. Time	Name	Amount	Amt %	Area	Area %
1	45.31		0.00	N/A	10354300	48.898
2	47.65		0.00	N/A	10821210	51.102

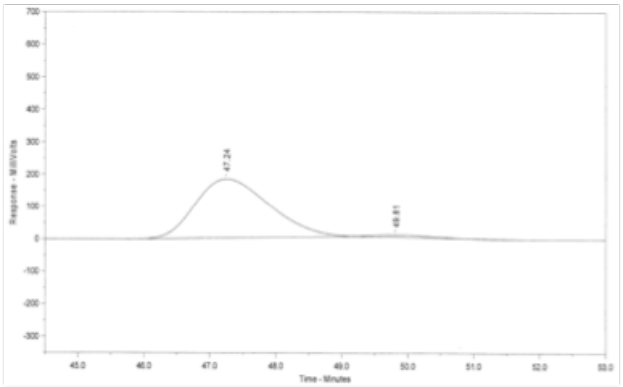

Peak #	Ret. Time	Name	Amount	Amt %	Area	Area %
1	47.24		0.00	N/A	14138840	97.333
2	49.81		0.00	N/A	387354	2.667

Peak #	Time (min)	Area (%)	Peak #	Time (min)	Area (%)
1	45.310	48.898	1	47.240	97.333
2	47.650	51.102	2	49.810	2.667

(*S*)-3-(4,4,5,5-Tetramethyl-1,3,2-dioxaborolan-2-yl)-3-(4-(trifluoromethyl)phenyl)cyclohexan-1-one (1.120): IR (neat): 2956 (m), 2926 (s), 2855 (m), 2853 (w), 1717 (m), 1326 (s), 1166 (m), 1126 (m) cm^{-1}; ^{1}H NMR (400 MHz, $CDCl_3$): δ 7.55 (2H, d, J = 8.4 Hz), 7.40 (2H, d, J = 8.4 Hz), 2.88 (1H, d, J = 14.0 Hz), 2.60 (1H, d, J = 14.0 Hz), 2.41–2.24 (3H, m), 2.04–1.79 (3H, m), 1.16 (6H, s), 1.15 (6H, s); ^{13}C NMR (100 MHz, $CDCl_3$): δ 210.7, 148.9, 128.1 (q, J = 31.9 Hz), 126.9, 125.5 (q, J = 3.8 Hz), 124.4 (q, J = 272.1 Hz), 84.3, 48.2, 41.2, 33.2, 25.0, 24.7, 24.5, 23.7; HRMS (ESI+): Calcd for $C_{19}H_{24}B_1F_3NaO_3$ $[M+Na]^+$: 391.1668, Found: 391.1672. Specific Rotation: $[\alpha]_D^{20}$ +6.2 (*c* 0.63, $CHCl_3$) for an enantiomerically enriched sample of 96:4 er. Enantiomeric purity was determined by HPLC analysis in comparison with authentic racemic material (96:4 er shown; Chiralpak AS-H column, 99/1 hexanes/*i*-PrOH, 0.3 mL/min, 220 nm).

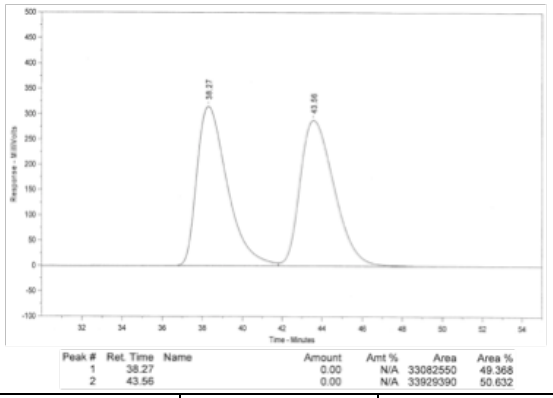

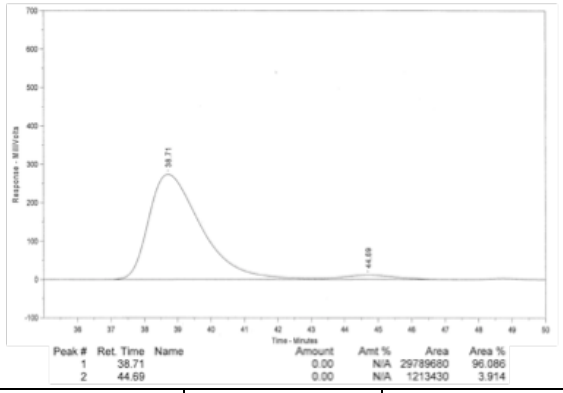

Peak #	Time (min)	Area (%)	Peak #	Time (min)	Area (%)
1	38.270	49.368	1	38.710	96.086
2	43.560	50.632	2	44.690	3.914

(*S*)-3-(3-Methoxyphenyl)-3-(4,4,5,5-tetramethyl-1,3,2-dioxaborolan-2-yl)cyclohexan-1-one (1.121): The spectroscopic data match those reported previously.[67] ^{1}H NMR (400 MHz, $CDCl_3$): δ 7.21 (1H, t, J = 8.2 Hz), 6.88–6.84 (2H, m), 6.71 (1H, ddd, J = 8.5, 2.7,

0.9 Hz), 3.79 (3H, s), 2.85 (1H, dt, J = 14.0, 1.5 Hz), 2.57 (1H, d, J = 14.0 Hz), 2.39–2.24 (3H, m), 2.00–1.89 (2H, m), 1.88–1.74 (1H, m), 1.16 (6H, s), 1.155 (6H, s); Specific Rotation: $[\alpha]_D^{20}$ +15.9 (*c* 0.49, $CHCl_3$) for an enantiomerically enriched sample of 93:7 er. Enantiomeric purity was determined by HPLC analysis in comparison with authentic racemic material (93:7 er shown; Chiralcel OC-H column, 98/2 hexanes/*i*-PrOH, 0.3 mL/min, 220 nm).

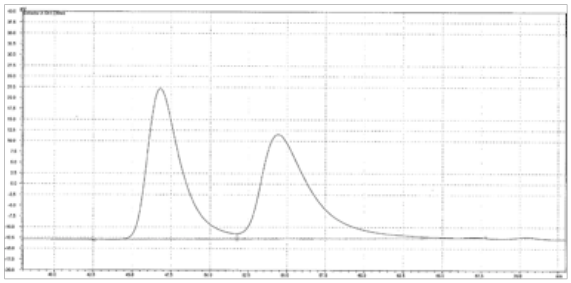

Peak#	Ret. Time	Area	Height	Area %
1	46.798	5267322	34984	49.065
2	54.404	5468019	24254	50.935
Total		10735342	59238	100.000

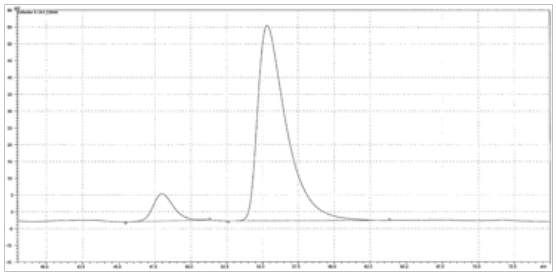

Peak#	Ret. Time	Area	Height	Area %
1	47.971	615342	7243	7.035
2	55.322	8131134	58205	92.965
Total		8746476	65448	100.000

Peak #	Time (min)	Area (%)	Peak #	Time (min)	Area (%)
1	46.789	49.065	1	47.971	7.035
2	54.404	50.935	2	55.322	92.965

(***S*)-3-(Naphthalen-2-yl)-3-(4,4,5,5-tetramethyl-1,3,2-dioxaborolan-2-yl)cyclohexan-1-one (1.122)**: Melting point: 146–147°C. IR (neat): 2975 (m), 2929 (m), 2866 (w), 2853 (w), 1712 (s), 1448 (w), 1370 (s), 1326 (s), 1142 (s), 856 (m) cm^{-1}; ^1H NMR (400 MHz, $CDCl_3$): δ 7.81–7.77 (3H, m), 7.67 (1H, s), 7.48–7.40 (3H, m), 2.96 (1H, d, J = 14.0 Hz), 2.72 (1H, d, J = 14.4 Hz), 2.47–2.27 (3H, m), 2.13–2.07 (1H, m), 1.93–1.81 (2H, m), 1.16 (12H, s); ^{13}C NMR (100 MHz, $CDCl_3$): δ 211.4, 142.2, 133.8, 131.9, 128.1, 128.0, 127.5, 126.1, 125.6, 125.5, 124.7, 84.1, 48.5, 41.4, 33.2, 24.7, 24.5, 23.8; HRMS (ESI+): Calcd for $C_{22}H_{28}B_1O_3$ $[M+H]^+$: 351.2132, Found: 351.2136. Specific Rotation: $[\alpha]_D^{20}$ +32.9 (*c* 0.34, $CHCl_3$) for an enantiomerically enriched sample of 96:4 er. Enantiomeric

purity was determined by HPLC analysis in comparison with authentic racemic material (96:4 er shown; Chiralpak AD-H column, 99/1 hexanes/*i*-PrOH, 0.3 mL/min, 220 nm).

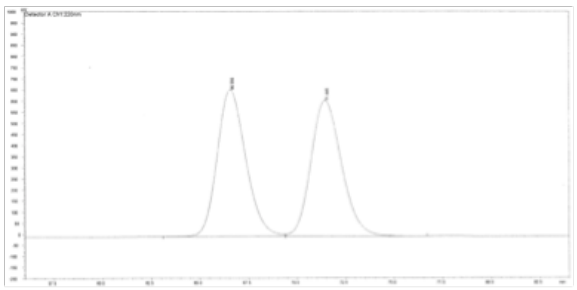

Peak#	Ret. Time	Area	Height	Area %
1	66.555	67116963	659931	50.121
2	71.445	66792280	611870	49.879
Total		133909242	1271801	100.000

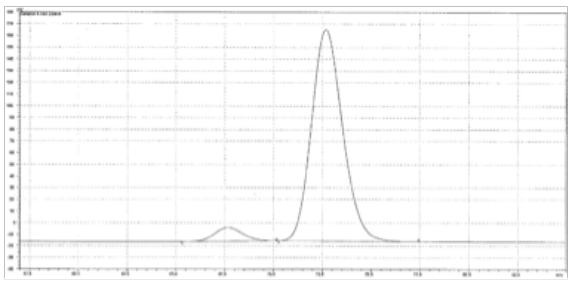

Peak#	Ret. Time	Area	Height	Area %
1	67.656	811030	9899	3.900
2	72.684	19983307	181242	96.100
Total		20794337	191141	100.000

Peak #	Time (min)	Area (%)	Peak #	Time (min)	Area (%)
1	66.555	50.121	1	67.656	3.900
2	71.445	51.094	2	72.684	96.100

(***S*)-3-Methyl-3-(4,4,5,5-tetramethyl-1,3,2-dioxaborolan-2-yl)cyclopentan-1-one (1.113)**: The spectroscopic data match those reported previously.[68] ^{1}H NMR (400 MHz, $CDCl_3$): δ 2.42 (1H, d, *J* = 18.0 Hz), 2.32–2.11 (3H, m), 1.87 (1H, d, *J* = 18.0 Hz), 1.68–1.60 (1H, m), 1.23 (12H, s), 1.12 (3H, s); Specific Rotation: $[\alpha]_D^{20}$ –14.0 (*c* 0.20, $CHCl_3$) for an enantiomerically enriched sample of >98:2 er. Enantiomeric purity was determined by GC analysis in comparison with authentic racemic material (>98:2 er shown; Chiraldex B-DM column, 15 psi, 100 °C).

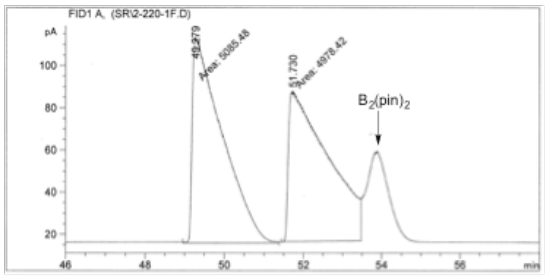

Peak #	RetTime [min]	Type	Width [min]	Area [pA*s]	Height [pA]	Area %
1	49.279	MM	0.8635	5085.48438	98.16087	50.53191
2	51.730	MF	1.1575	4978.42236	71.68157	49.46809

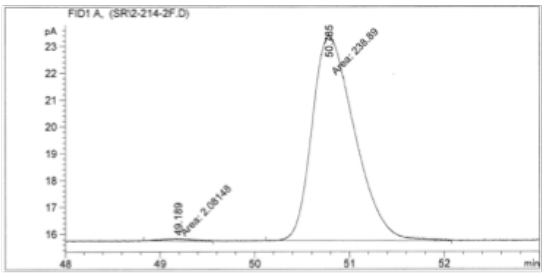

Peak #	RetTime [min]	Type	Width [min]	Area [pA*s]	Height [pA]	Area %
1	49.189	MM	0.3592	2.08148	9.65808e-2	0.86378
2	50.785	MM	0.5197	238.89021	7.66098	99.13622

Peak #	Time (min)	Area (%)	Peak #	Time (min)	Area (%)
1	49.279	50.532	1	49.189	0.864
2	51.730	49.468	2	50.785	99.136

(68) Lee, K–s.; Zhugralin, A. R.; Hoveyda, A. H. *J. Am. Chem. Soc.* **2009**, *131*, 7253–7255.

(***S***)**-3-Phenyl-3-(4,4,5,5-tetramethyl-1,3,2-dioxaborolan-2-yl)cyclopentan-1-one (1.114)**: The spectroscopic data match those reported previously.[67] ^{1}H NMR (400 MHz, $CDCl_3$): δ 7.33–7.16 (5H, m), 2.91 (1H, d, *J* = 18.0 Hz), 2.73–2.67 (1H, m), 2.42 (1H, d, *J* = 17.6 Hz), 2.37–2.18 (2H, m), 2.11–2.03 (1H, m), 1.14 (12H, s). Specific Rotation: $[\alpha]_D^{20}$ –25.7 (*c* 0.80, $CHCl_3$) for an enantiomerically enriched sample of 93:7 er. Enantiomeric purity was determined by GC analysis in comparison with authentic racemic material (93:7 er shown; Chiraldex B-DM column, 15 psi, 130 °C).

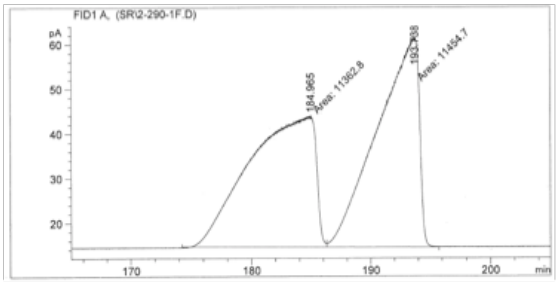

Peak #	RetTime [min]	Type	Width [min]	Area [pA*s]	Height [pA]	Area %
1	184.965	MF	6.4566	1.13628e4	29.33108	49.79863
2	193.738	FM	4.0444	1.14547e4	47.20415	50.20137

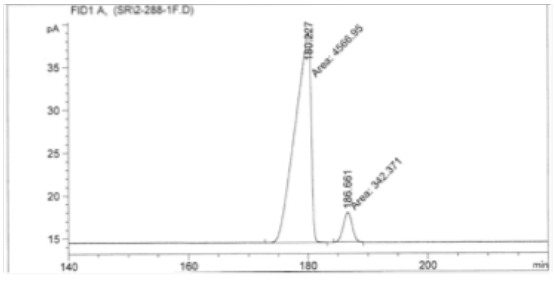

Peak #	RetTime [min]	Type	Width [min]	Area [pA*s]	Height [pA]	Area %
1	180.227	MM	3.0938	4566.94971	24.60283	93.02611
2	186.661	MM	1.6430	342.37076	3.47293	6.97389

Peak #	Time (min)	Area (%)	Peak #	Time (min)	Area (%)
1	184.965	49.799	1	180.227	93.026
2	193.738	50.201	2	186.661	6.974

(***S***)**-3-(4-Fluorophenyl)-3-(4,4,5,5-tetramethyl-1,3,2-dioxaborolan-2-yl)cyclopentan-1-one (1.115)**: Melting point: 106–108°C. IR (neat): 2980 (m), 2963 (m), 2928 (m), 2858 (m), 1743 (s), 1507 (s), 1406 (s), 1374 (s), 1325 (s), 1221 (m), 1137 (s), 851 (m), 836 (m) cm^{-1}; ^{1}H NMR (400 MHz, $CDCl_3$): δ 7.22–7.17 (2H, m), 7.02–6.96 (2H, m), 2.89 (1H, d, *J* = 17.6 Hz), 2.71–2.65 (1H, m), 2.36 (1H, d, *J* = 18.4 Hz), 2.36–2.18 (2H, m), 2.06–1.99 (1H, m), 1.34 (12H, s); ^{13}C NMR (100 MHz, $CDCl_3$): δ 218.6, 161.2 (d, *J* = 242.8 Hz), 140.6 (d, *J* = 3.8 Hz), 128.0 (d, *J* = 7.6 Hz), 115.3 (d, *J* = 20.5 Hz), 84.3, 47.5, 38.3, 32.3, 29.7, 24.6, 24.5; HRMS (ESI+): Calcd for $C_{17}H_{23}B_1F_1O_3$ $[M+H]^+$: 305.1724, Found: 305.1720. Specific Rotation: $[\alpha]_D^{20}$ –27.9 (*c* 0.60, $CHCl_3$) for an enantiomerically

enriched sample of 95:5 er. Enantiomeric purity was determined by HPLC analysis in comparison with authentic racemic material (95:5 er shown; Chiralpak AS-H column, 99/1 hexanes/*i*-PrOH, 0.3 mL/min, 220 nm).

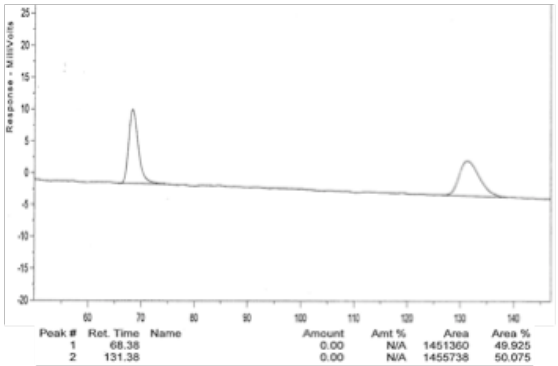

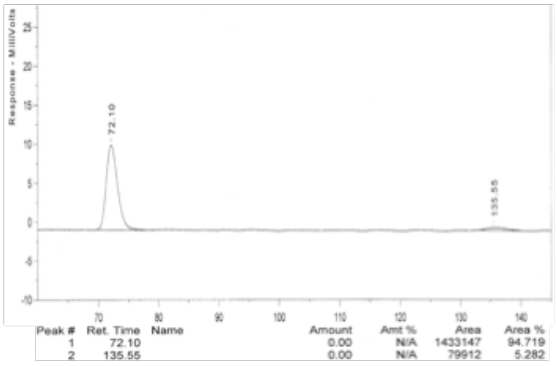

Peak #	Time (min)	Area (%)	Peak #	Time (min)	Area (%)
1	68.380	49.925	1	72.100	94.719
2	131.38	50.075	2	135.55	5.282

(*S*)-3-(3-Methoxyphenyl)-3-(4,4,5,5-tetramethyl-1,3,2-dioxaborolan-2-yl)cyclopentan-1-one (1.116): Melting point: 78–79 °C. IR (neat): 2976 (m), 2932 (m), 1742 (s), 1600 (m), 1581 (s), 1352 (m), 1322 (m), 1139 (s) cm^{-1}; ^{1}H NMR (400 MHz, $CDCl_3$): δ 7.24–7.20 (1H, m), 6.84–6.79 (2H, m), 6.74–6.71 (1H, m), 3.80 (3H, s), 2.87 (1H, d, *J* = 17.6 Hz), 2.69–2.63 (1H, m), 2.41 (1H, d, *J* = 18.0 Hz), 2.36–2.17 (2H, m), 2.10–2.02 (1H, m), 1.15 (12H, s); ^{13}C NMR (100 MHz, $CDCl_3$): δ 218.9, 159.8, 146.6, 129.5, 119.1, 112.8, 110.9, 84.2, 55.3, 47.4, 38.3, 32.1, 24.6, 24.5 HRMS (ESI+): Calcd for $C_{18}H_{26}B_1O_4$ $[M+H]^+$: 317.1924, Found: 317.1931. Specific Rotation: $[\alpha]_D^{20}$ –24.4 (*c* 0.56, $CHCl_3$) for an enantiomerically enriched sample of 95:5 er. Enantiomeric purity was determined by HPLC analysis in comparison with authentic racemic material (95:5 er shown; Chiralpak AD-H column, 99/1 hexanes/*i*-PrOH, 0.3 mL/min, 220 nm).

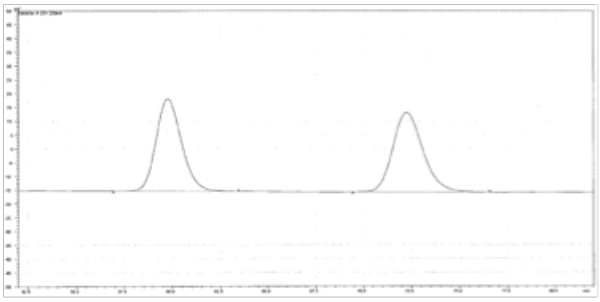

Peak#	Ret. Time	Area	Height	Area %
1	59.770	3078435	33459	49.476
2	72.253	3143631	28879	50.524
Total		6222066	62338	100.000

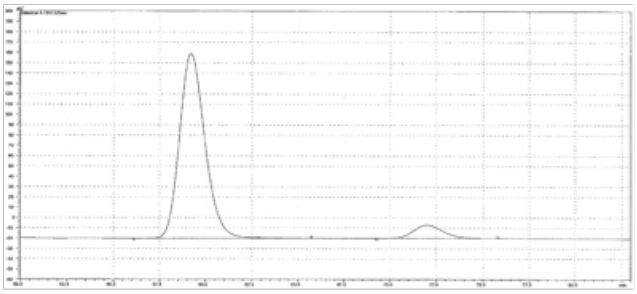

Peak#	Ret. Time	Area	Height	Area %
1	59.201	17120511	179084	94.834
2	72.006	932619	10406	5.166
Total		18053130	189490	100.000

Peak #	Time (min)	Area (%)	Peak #	Time (min)	Area (%)
1	59.770	49.476	1	59.201	94.834
2	72.253	53.302	2	72.006	5.166

(***S*)-3-Methyl-3-(4,4,5,5-tetramethyl-1,3,2-dioxaborolan-2-yl)cycloheptan-1-one (1.126)**: IR (neat): 2977 (m), 2926 (m), 2863 (m), 1698 (s), 1462 (m), 1371 (m), 1317 (s), 1142 (s), 851 (m) cm^{-1}; ^1H NMR (400 MHz, $CDCl_3$): δ 2.66 (1H, dd, J = 14.8, 1.2 Hz), 2.46–2.42 (2H, m), 2.28 (1H, d, J = 14.8 Hz), 1.96–1.91 (1H, m), 1.84–1.73 (2H, m), 1.68–1.54 (2H, m), 1.41–1.34 (1H, m), 1.22 (12H, s), 0.97 (3H, s); ^{13}C NMR (100 MHz, $CDCl_3$): δ 214.8, 83.6, 53.1, 44.6, 40.8, 27.7, 25.5, 24.8, 24.3; HRMS (ESI+): Calcd for $C_{14}H_{26}B_1O_3$ $[M+H]^+$: 253.1984, Found: 253.1975. Specific Rotation: $[\alpha]_D^{20}$ –31.1 (*c* 0.78, $CHCl_3$) for an enantiomerically enriched sample of 95:5 er. Enantiomeric purity was determined by HPLC analysis in comparison with authentic racemic material (95:5 er shown; Chiraldex B-DM column, 15 psi, 100 °C).

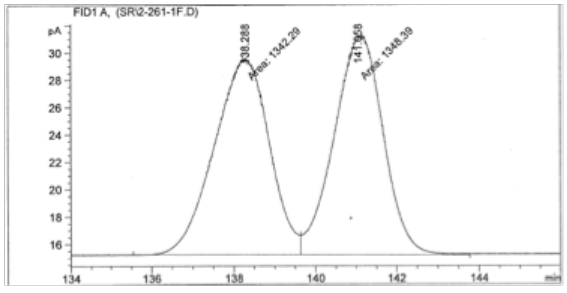

Peak #	RetTime [min]	Type	Width [min]	Area [pA*s]	Height [pA]	Area %
1	138.288	MF	1.5532	1342.28857	14.40388	49.88669
2	141.058	FM	1.3963	1348.38635	16.09432	50.11331

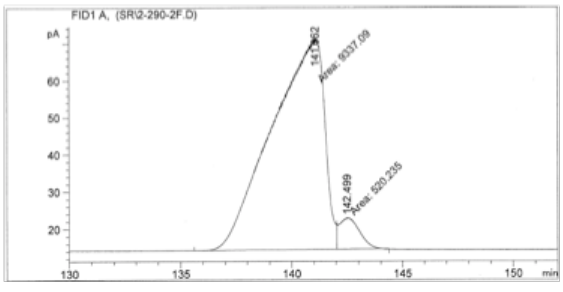

Peak #	RetTime [min]	Type	Width [min]	Area [pA*s]	Height [pA]	Area %
1	141.062	MF	2.7214	9337.09082	57.18342	94.72235
2	142.499	FM	1.0321	520.23468	8.40080	5.27765

Peak #	Time (min)	Area (%)	Peak #	Time (min)	Area (%)
1	138.288	49.887	1	141.062	94.722

2	141.058	50.113	2	142.499	5.278

(*S*)-3-Methyl-3-(4,4,5,5-tetramethyl-1,3,2-dioxaborolan-2-yl)cyclooctan-1-one (1.127): IR (neat): 2975 (m), 2928 (m), 2855 (m), 1698 (s), 1468 (m), 1381 (m), 1371 (m), 1313 (s), 1146 (s), 1113 (s), 844 (m) cm^{-1}; ^1H NMR (400 MHz, $CDCl_3$): δ 2.64 (1H, d, *J* = 11.6 Hz), 2.32–2.28 (3H, m), 2.01–1.82 (2H, m), 1.74–1.68 (1H, m), 1.60–1.46 (3H, m), 1.41–1.29 (1H, m), 1.26–1.24 (13H, m), 1.01 (3H, s); ^{13}C NMR (100 MHz, $CDCl_3$): δ 216.8, 83.4, 46.6, 45.4, 35.0, 29.3, 24.9, 24.7, 24.4, 23.0, 22.7; HRMS (ESI+): Calcd for $C_{15}H_{28}B_1O_3$ $[M+H]^+$: 267.2132, Found: 267.2136. Specific Rotation: $[\alpha]_D^{20}$ +49.6 (*c* 1.00, $CHCl_3$) for an enantiomerically enriched sample of 95:5 er. Enantiomeric purity was determined by GC analysis in comparison with authentic racemic material (95:5 er shown; Chiraldex B-DM column, 15 psi, 100 ºC).

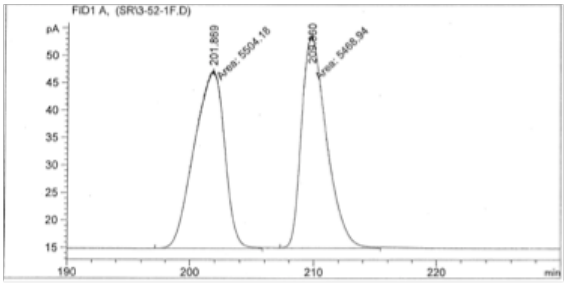

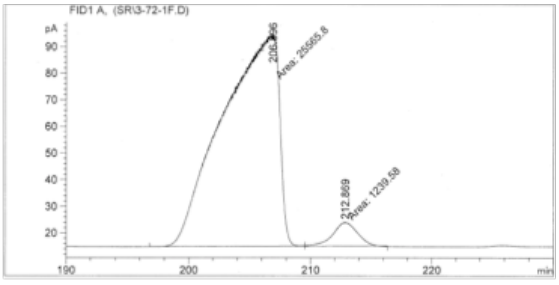

Peak #	RetTime [min]	Type	Width [min]	Area [pA*s]	Height [pA]	Area %
1	201.869	MM	2.8012	5504.17529	32.74893	50.16053
2	209.860	MM	2.3365	5468.94482	39.01094	49.83947

Peak #	RetTime [min]	Type	Width [min]	Area [pA*s]	Height [pA]	Area %
1	206.896	MF	5.3256	2.55657e4	80.00931	95.37562
2	212.869	FM	2.3173	1239.57959	8.91559	4.62438

Peak #	Time (min)	Area (%)	Peak #	Time (min)	Area (%)
1	201.869	50.161	1	206.896	95.376
2	209.860	49.839	2	212.869	4.624

(*S*)-4-Phenyl-4-(4,4,5,5-tetramethyl-1,3,2-dioxaborolan-2-yl)pentan-2-one (1.130): The spectroscopic data match those reported previously.[69] ^1H NMR (400 MHz, $CDCl_3$): δ 7.38–7.35 (2H, m), 7.30–7.26 (2H, m), 7.17–7.12 (1H, m), 3.18 (1H, d, *J* = 18.4 Hz), 2.76 (1H, d, *J* = 18.0 Hz), 2.14 (3H, s), 1.34 (3H, s), 1.21 (6H, s), 1.19 (6H, s). Specific Rotation: $[\alpha]_D^{20}$ –36.2 (*c* 0.60, $CHCl_3$) for an enantiomerically enriched sample of 92:8 er.

(69) O'Brien, J. M.; Lee, K–s.; Hoveyda, A. H. *J. Am. Chem. Soc.* **2010**, *132*, 10630–10633.

Enantiomeric purity was determined by HPLC analysis in comparison with authentic racemic material (>99:1 er shown; Chiraldex AD-H column, 99/1 hexanes/*i*-PrOH, 0.3 mL/min, 220 nm)

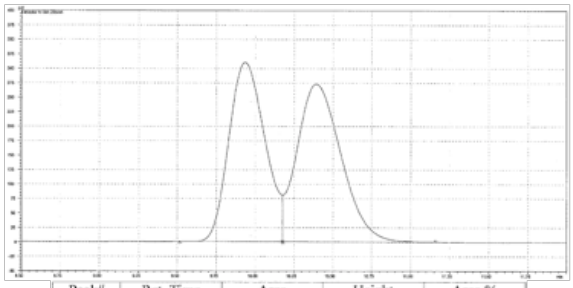

Peak#	Ret. Time	Area	Height	Area %
1	9.930	5002921	309968	48.156
2	10.389	5386173	272714	51.844
Total		10389095	582682	100.000

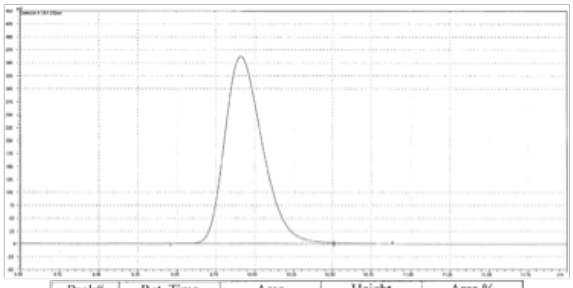

Peak#	Ret. Time	Area	Height	Area %
1	9.907	6074933	362129	99.712
2	10.392	17549	3465	0.288
Total		6092481	365593	100.000

Peak #	Time (mins)	Area (%)	Peak #	Time (mins)	Area (%)
1	9.930	48.156	1	9.907	99.712
2	10.389	51.844	2	10.392	0.288

(*S*)-4-(4-Methoxyphenyl)-4-(4,4,5,5-tetramethyl-1,3,2-dioxaborolan-2-yl)pentan-2-one (1.129): Melting point: 82–83 °C. IR (neat): 2975 (m), 2927 (s), 2855 (m), 1715 (m), 1511 (s), 1345 (s), 1464 (m), 1372 (m), 1348 (m), 1250 (s) cm^{-1}; ^{1}H NMR (400 MHz, $CDCl_3$): δ 7.30–7.60 (2H, m), 6.85–6.81 (2H, m), 3.78 (3H, s), 3.13 (1H, d, J = 18.0 Hz), 2.72 (1H, d, J = 18.0 Hz), 2.12 (3H, s), 1.31 (3H, s), 1.21 (6H, s), 1.18 (6H, s); ^{13}C NMR (100 MHz, $CDCl_3$): δ 208.3, 157.5, 138.4, 127.6, 113.7, 83.5, 55.3, 54.5, 30.4, 24.8, 24.7, 23.0; HRMS (ESI+): Calcd for $C_{18}H_{28}B_1O_4$ $[M+H]^+$: 319.2081, Found: 319.2090. Specific Rotation: $[\alpha]_D^{20}$ –32.3 (*c* 0.56, $CHCl_3$) for an enantiomerically enriched sample of 91:9 er. Enantiomeric purity was determined by HPLC analysis in comparison with authentic racemic material (99:1 er shown; Chiralcel OD-H column, 99.5/0.5 hexanes/*i*-PrOH, 0.3 mL/min, 220 nm).

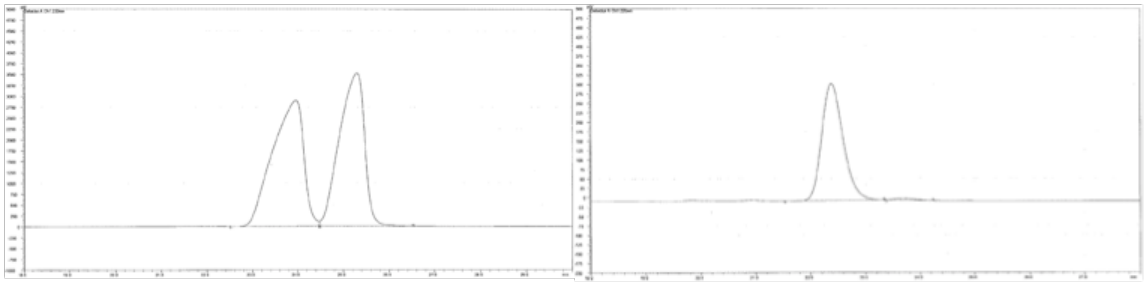

Peak#	Ret. Time	Area	Height	Area %
1	23.958	139363286	2900160	50.846
2	25.295	134724706	3517065	49.154
Total		274087992	6417225	100.000

Peak#	Ret. Time	Area	Height	Area %
1	22.371	8416611	310328	98.697
2	23.683	111093	4619	1.303
Total		8527704	314947	100.000

Peak #	Time (min)	Area (%)	Peak #	Time (min)	Area (%)
1	23.958	50.846	1	22.371	98.697
2	25.295	49.154	2	23.683	1.303

(***S***)**-4-(4-Fluorophenyl)-4-(4,4,5,5-tetramethyl-1,3,2-dioxaborolan-2-yl)pentan-2-one (1.131)**: Melting point: 81–83 °C. IR (neat): 2976 (m), 2927 (m), 1715 (s), 1509 (s), 1372 (m), 1347 (s), 1315 (s), 1228 (s), 1144 (s), 859 (m), 835 (m) cm^{-1}; ^{1}H NMR (400 MHz, $CDCl_3$): δ 7.34–7.30 (2H, m), 6.98–6.94 (2H, m), 3.12 (1H, d, *J* = 18.0 Hz), 2.74 (1H, d, *J* = 18.0 Hz), 2.13 (3H, s), 1.32 (3H, s), 1.20 (6H, s), 1.18 (6H, s); ^{13}C NMR (100 MHz, $CDCl_3$): δ 208.0, 161.0 (d, *J* = 241.8 Hz), 142.0 (d, *J* = 3.0 Hz), 128.1 (d, *J* = 8.2 Hz), 115.0 (d, *J* = 20.9 Hz), 83.6, 54.5, 30.3, 29.9, 24.7, 24.65, 23.1; HRMS (ESI+): Calcd for $C_{17}H_{25}B_1F_1O_3$ $[M+H]^+$: 307.1881, Found: 305.1881. Specific Rotation: $[\alpha]_D^{20}$ –68.4 (*c* 0.50, $CHCl_3$) for an enantiomerically enriched sample of 92:8 er. Enantiomeric purity was determined by HPLC analysis in comparison with authentic racemic material (92:8 er shown; Chiralcel AZ-H column, 99/1 hexanes/*i*-PrOH, 0.3 mL/min, 220 nm).

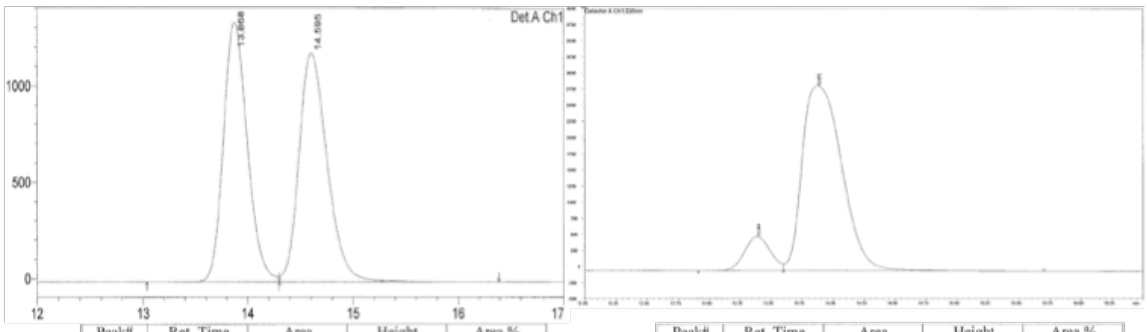

Peak#	Ret. Time	Area	Height	Area %
1	13.868	21372374	1343619	49.426
2	14.595	21869045	1185230	50.574
Total		43241420	2528849	100.000

Peak#	Ret. Time	Area	Height	Area %
1	13.384	5229756	437481	8.095
2	13.870	59377181	2778160	91.905
Total		64606937	3215641	100.000

Peak #	Time (min)	Area (%)	Peak #	Time (min)	Area (%)
1	13.868	49.426	1	13.384	8.095
2	14.595	50.574	2	13.870	91.905

(*S*)-4-(4-Bromophenyl)-4-(4,4,5,5-tetramethyl-1,3,2-dioxaborolan-2-yl)pentan-2-one (1.132): Melting point: 125–127 °C. IR (neat): 2977 (m), 2928 (m), 1716 (s), 1490 (m), 1371 (m), 1345 (s), 1316 (s), 1143 (s) cm^{-1}; ^1H NMR (400 MHz, $CDCl_3$): δ 7.39 (2H, d, *J* = 8.8 Hz), 7.23 (2H, d, *J* = 8.8 Hz), 3.11 (1H, d, *J* = 18.0 Hz), 2.73 (1H, d, *J* = 18.4 Hz), 2.14 (3H, s), 1.34 (3H, s), 1.20 (6H, s), 1.18 (6H, s); ^{13}C NMR (100 MHz, $CDCl_3$): δ 207.9, 145.6, 131.3, 128.6, 119.4, 83.7, 54.2, 30.3, 24.7, 24.67, 22.8; HRMS (ESI+): Calcd for $C_{17}H_{25}B_1Br_1O_3$ $[M+H]^+$: 367.1080, Found: 367.1076. Specific Rotation: $[\alpha]_D^{20}$ –39.2 (*c* 0.65, $CHCl_3$) for an enantiomerically enriched sample of 92:8 er. Enantiomeric purity was determined by HPLC analysis in comparison with authentic racemic material (99:1 er shown; Chiralcel AZ-H column, 99/1 hexanes/*i*-PrOH, 0.3 mL/min, 220 nm).

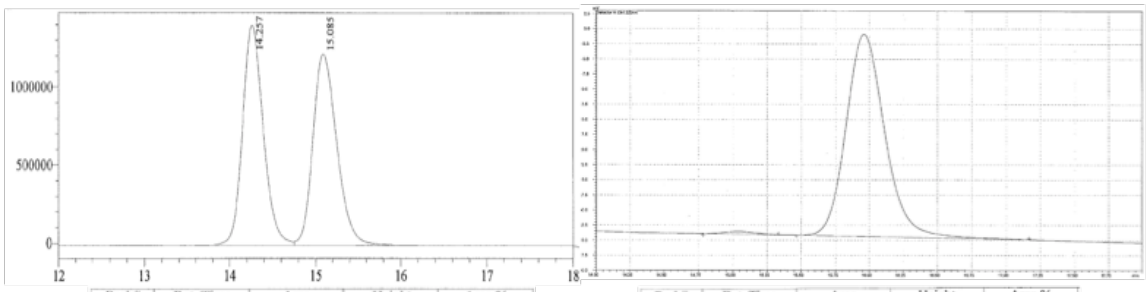

Peak#	Ret. Time	Area	Height	Area %
1	14.257	23917872	1409813	49.860
2	15.085	24051851	1224601	50.140
Total		47969723	2634414	100.000

Peak#	Ret. Time	Area	Height	Area %
1	15.027	6869	443	1.017
2	15.956	668872	33512	98.983
Total		675741	33955	100.000

Peak #	Time (min)	Area (%)	Peak #	Time (min)	Area (%)
1	14.257	49.860	1	15.027	1.017
2	15.085	50.140	2	15.956	98.983

(*S*)-4-Phenyl-4-(4,4,5,5-tetramethyl-1,3,2-dioxaborolan-2-yl)hexan-2-one (1.133): IR (neat): 2970 (m), 2936 (m), 1715 (s), 1347 (s), 1309 (s), 1316 (s), 1144 (s) cm^{-1}; ^1H NMR (400 MHz, $CDCl_3$): δ 7.31–7.25 (4H, m), 7.15–7.11 (1H, m), 3.04 (2H, s), 2.14 (3H, s), 2.99–1.81 (2H, m), 1.22 (6H, s), 1.20 (6H, s), 0.57 (3H, t, *J* = 7.4 Hz); ^{13}C NMR (100 MHz, $CDCl_3$): δ 208.3, 144.3, 128.2, 127.4, 125.4, 83.4, 48.4, 30.5, 28.1, 24.8, 24.78, 8.5; HRMS (ESI+): Calcd for $C_{18}H_{28}B_1O_3$ $[M+H]^+$: 303.2132, Found: 303.2128.

Specific Rotation: $[\alpha]_D^{20}$ –26.3 (*c* 0.22, $CHCl_3$) for an enantiomerically enriched sample of 91:9 er. Enantiomeric purity was determined by HPLC analysis in comparison with authentic racemic material (91:9 er shown; Chiralcel OD-H column, 100% hexanes, 0.3 mL/min, 220 nm).

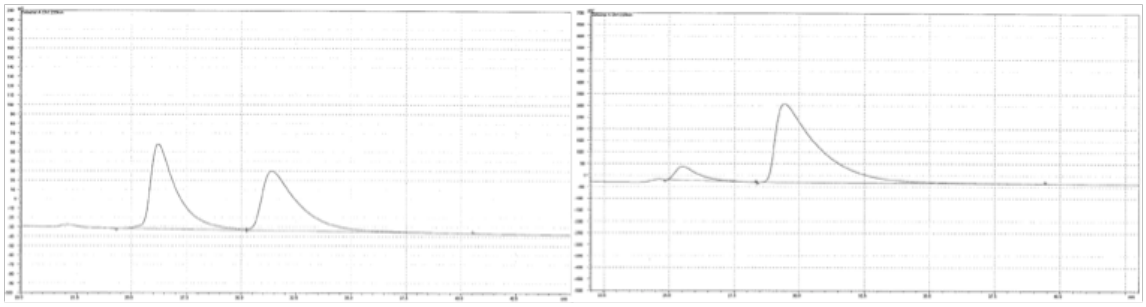

Peak#	Ret. Time	Area	Height	Area %
1	26.212	7381446	90342	50.172
2	31.390	7330932	63640	49.828
Total		14712379	153982	100.000

Peak#	Ret. Time	Area	Height	Area %
1	25.513	3576114	58372	8.591
2	29.431	38049535	338653	91.409
Total		41625650	397026	100.000

Peak #	Time (min)	Area (%)	Peak #	Time (min)	Area (%)
1	26.212	50.172	1	25.513	8.591
2	31.390	49.828	2	29.431	91.409

(*R*)-8-Hydroxy-4-methyl-4-(4,4,5,5-tetramethyl-1,3,2-dioxaborolan-2-yl)octan-2-one (1.137): IR (neat): 3449 (br), 2975 (m), 2933 (m), 2867 (m), 1714 (s), 1469 (m), 1371 (s), 1307 (s), 1145 (s) cm^{-1}; ^1H NMR (400 MHz, $CDCl_3$): δ 3.63 (2H, q, *J* = 6.0 Hz), 2.62 (1H, d, *J* = 18.0 Hz), 2.39 (1H, d, *J* = 18.0 Hz), 2.08 (3H, s), 1.54–1.46 (3H, m), 1.39–1.28 (3H, m), 1.25 (6H, s), 1.23 (6H, s), 0.92 (3H, s); ^{13}C NMR (100 MHz, $CDCl_3$): δ 208.9, 83.2, 62.8, 54.2, 38.1, 35.0, 33.4, 30.3, 24.93, 24.91, 21.5, 21.3; HRMS (ESI+): Calcd for $C_{15}H_{30}B_1O_4$ $[M+H]^+$: 285.2237, Found: 285.2247. Specific Rotation: $[\alpha]_D^{20}$ –11.2 (*c* 0.30, $CHCl_3$) for an enantiomerically enriched sample of 97:3 er. Enantiomeric purity was determined by HPLC analysis in comparison with authentic racemic material (97:3 er shown; Chiralcel OJ-H column, 98/2 hexanes/*i*-PrOH, 0.3 mL/min, 300 nm).

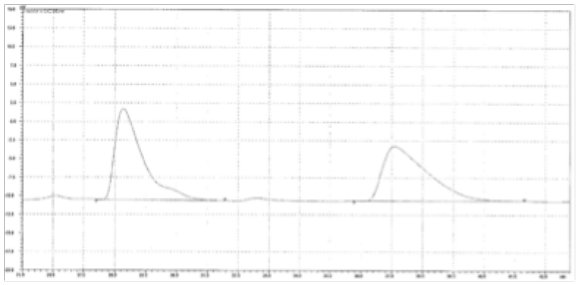

Peak#	Ret. Time	Area	Height	Area %
1	28.257	766694	12208	50.953
2	37.087	738003	7385	49.047
Total		1504696	19593	100.000

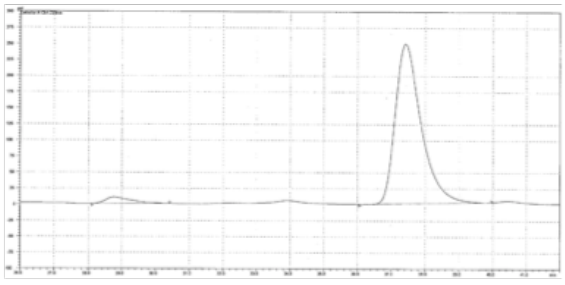

Peak#	Ret. Time	Area	Height	Area %
1	28.236	4387	92	3.428
2	37.415	123603	1978	96.572
Total		127990	2070	100.000

Peak #	Time (min)	Area (%)	Peak #	Time (min)	Area (%)
1	28.257	50.953	1	28.236	3.428
2	37.087	49.047	2	37.415	96.572

(***R*)-5-(2-Methoxyphenyl)-4-methyl-4-(4,4,5,5-tetramethyl-1,3,2-dioxaborolan-2-yl)pentan-2-one (1.136)**: IR (neat): 2974 (m), 2874 (m), 2835 (m) 1713 (s), 1492 (m), 1460 (m), 1361 (s), 1305 (s), 1169 (s), 1146 (s), 1105 (m) cm^{-1}; ^{1}H NMR (400 MHz, $CDCl_3$): δ 7.20–7.15 (1H, m), 7.05 (1H, dd, *J* = 7.2, 1.6 Hz), 6.88–6.83 (2H, m), 3.74 (3H, s), 2.99 (1H, d, *J* = 13.2 Hz), 2.54 (1H, d, *J* = 13.2 Hz), 2.51 (1H, d, *J* = 18.8 Hz), 2.27 (1H, d, *J* = 18.8 Hz), 2.05 (3H, s), 1.28 (12H, s), 0.87 (3H, s); ^{13}C NMR (100 MHz, $CDCl_3$): δ 208.6, 158.3, 133.0, 127.5, 127.5, 127.3, 120.0, 110.6, 103.9, 83.1, 55.3, 51.7, 34.7, 29.7, 24.9, 24.8, 21.3; HRMS (ESI+): Calcd for $C_{19}H_{30}B_1O_4$ $[M+H]^+$: 333.2237, Found: 333.2251. Specific Rotation: $[\alpha]_D^{20}$ –16.8 (*c* 0.45, $CHCl_3$) for an enantiomerically enriched sample of 93:7 er. Enantiomeric purity was determined by HPLC analysis in comparison with authentic racemic material (93:7 er shown; Chiralcel OC-H column, 99/1 hexanes/*i*-PrOH, 0.3 mL/min, 220 nm).

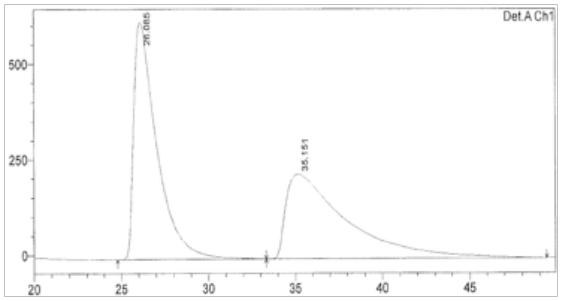

Peak#	Ret. Time	Area	Height	Area %
1	26.085	57304431	620115	51.742
2	35.151	53445929	221360	48.258
Total		110750360	841475	100.000

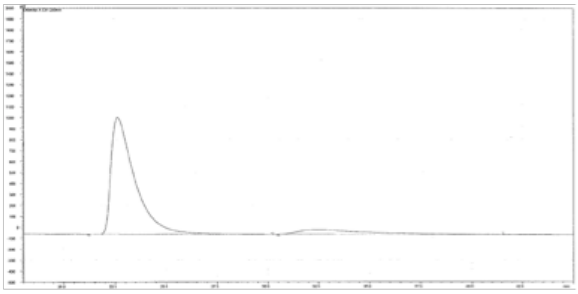

Peak#	Ret. Time	Area	Height	Area %
1	22.613	85086583	1062924	92.956
2	32.533	6448064	37480	7.044
Total		91534647	1100404	100.000

Peak #	Time (min)	Area (%)	Peak #	Time (min)	Area (%)
1	26.085	51.742	1	22.613	92.956
2	35.151	48.258	2	32.533	7.044

(*S*)-1,3-Diphenyl-3-(4,4,5,5-tetramethyl-1,3,2-dioxaborolan-2-yl)butan-1-one (1.139): The spectroscopic data match those reported previously.[10] Melting point: 89–91 °C. ^{1}H NMR (400 MHz, $CDCl_3$): δ 8.00–7.98 (2H, m), 7.57–7.53 (1H, m), 7.48–7.43 (4H, m), 7.33–7.29 (2H, m), 7.19–7.15 (1H, m), 3.67 (1H, d, J = 18.4 Hz), 3.36 (1H, d, J = 18.0 Hz), 1.43 (3H, s), 1.24 (6H, s), 1.20 (6H, s). Specific Rotation: $[\alpha]_D^{20}$ –55.7 (*c* 0.69, $CHCl_3$) for an enantiomerically enriched sample of 97:3 er. Enantiomeric purity was determined by HPLC analysis in comparison with authentic racemic material (97:3 er shown; Chiralpak AD-H column, 100% hexanes, 0.3 mL/min, 220 nm).

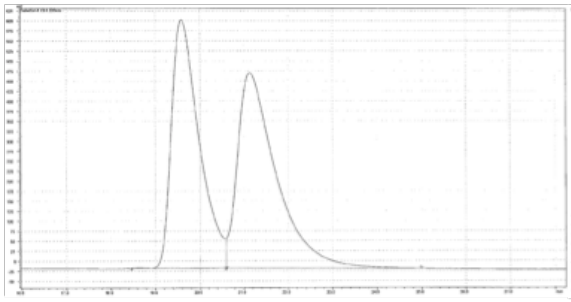

Peak#	Ret. Time	Area	Height	Area %
1	19.579	26917963	620350	47.613
2	21.136	29616732	488422	52.387
Total		56534695	1108772	100.000

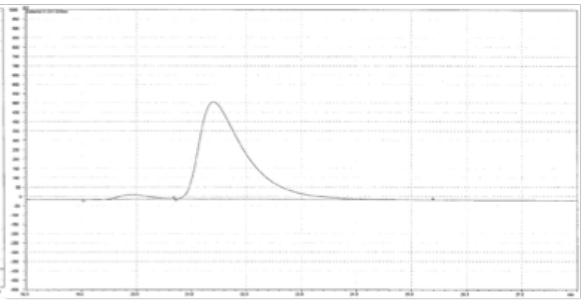

Peak#	Ret. Time	Area	Height	Area %
1	19.908	904777	25234	2.903
2	21.394	30263984	519494	97.097
Total		31168762	544728	100.000

Peak #	Time (min)	Area (%)	Peak #	Time (min)	Area (%)
1	19.579	47.613	1	19.908	2.903
2	21.136	52.387	2	21.394	97.097

(*S*)-3-(4-Methoxyphenyl)-1-phenyl-3-(4,4,5,5-tetramethyl-1,3,2-dioxaborolan-2-yl)butan-1-one (1.138): IR (neat): 2977 (m), 1683 (s), 1511 (m), 1340 (m), 1307 (m),

1249 (s), 1144 (s) cm^{-1}; ^1H NMR (400 MHz, $CDCl_3$): δ 7.99–7.97 (2H, m), 7.55–7.38 (5H, m), 6.88–6.86 (2H, m), 3.80 (3H, s), 3.63 (1H, d, *J* = 18.0 Hz), 3.33 (1H, d, *J* = 18.4 Hz), 1.42 (3H, s), 1.25 (6H, s), 1.21 (6H, s); ^{13}C NMR (100 MHz, $CDCl_3$): δ 199.4, 157.5, 138.7, 137.3, 133.0, 128.6, 128.2, 127.8, 113.7, 83.4, 55.3, 50.1, 24.79, 24.77, 23.3; HRMS (ESI+): Calcd for $C_{23}H_{30}B_1O_4$ $[M+H]^+$: 381.2237, Found: 381.2236. Specific Rotation: $[\alpha]_D^{20}$ –52.8 (*c* 0.36, $CHCl_3$) for an enantiomerically enriched sample of 98:2 er. Enantiomeric purity was determined by HPLC analysis in comparison with authentic racemic material (98:2 er shown; Chiraldex AD-H column, 99/1 hexanes/*i*-PrOH, 0.3 mL/min, 220 nm).

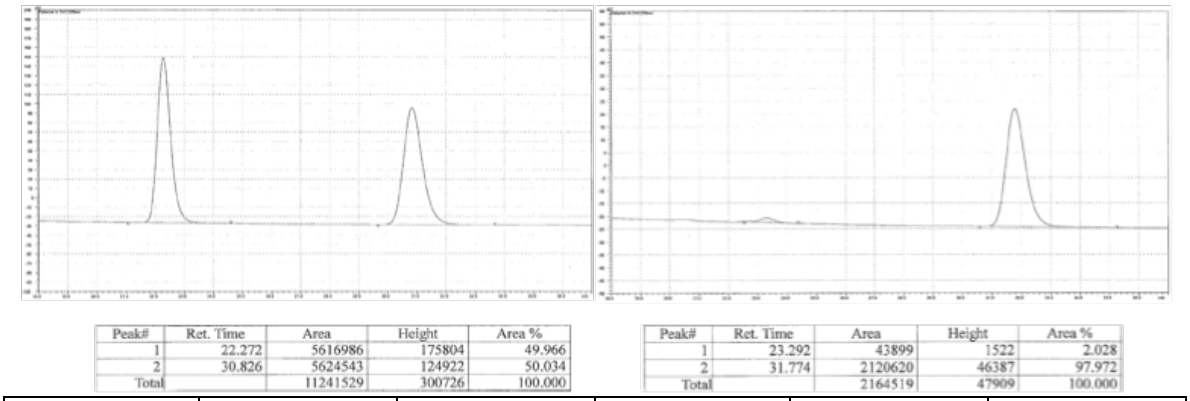

Peak#	Ret. Time	Area	Height	Area %
1	22.272	5616986	175804	49.966
2	30.826	5624543	124922	50.034
Total		11241529	300726	100.000

Peak#	Ret. Time	Area	Height	Area %
1	23.292	43899	1522	2.028
2	31.774	2120620	46387	97.972
Total		2164519	47909	100.000

Peak #	Time (min)	Area (%)	Peak #	Time (min)	Area (%)
1	22.272	49.966	1	23.292	2.028
2	30.826	50.034	2	31.774	97.972

(*S*)-6-Methyl-2-phenyl-2-(4,4,5,5-tetramethyl-1,3,2-dioxaborolan-2-yl)heptan-4-one (1.135): IR (neat): 2973 (m), 2957 (m), 2925 (m), 2871 (m), 1709 (m), 1465 (m), 1370 (m), 1311 (s), 1310 (s), 1140 (s), 699 (s) cm^{-1}; ^1H NMR (400 MHz, $CDCl_3$): δ 7.38–7.35 (2H, m), 7.30–7.25 (2H, m), 7.16–7.12 (1H, m), 3.14 (1H, d, *J* = 18.4 Hz), 2.72 (1H, d, *J* = 18.4 Hz), 2.31–2.10 (3H, m), 1.34 (3H, s), 1.21 (6H, s), 1.18 (6H, s), 0.92 (6H, d, *J* = 6.4 Hz); ^{13}C NMR (100 MHz, $CDCl_3$): δ 210.3, 146.6, 128.3, 126.7, 125.4, 83.4, 54.1, 51.9, 29.8, 25.3, 24.8, 23.1, 22.7, 22.6; HRMS (ESI+): Calcd for $C_{20}H_{32}B_1O_3$ $[M+H]^+$:

331.2445, Found: 331.2454. Specific Rotation: $[\alpha]_D^{20}$ –38.7 (*c* 0.63, $CHCl_3$) for an enantiomerically enriched sample of 95:5 er. Enantiomeric purity was determined by HPLC analysis in comparison with authentic racemic material (95:5 er shown; Chiralcel OJ-H column, 100% hexanes, 0.3 mL/min, 220 nm).

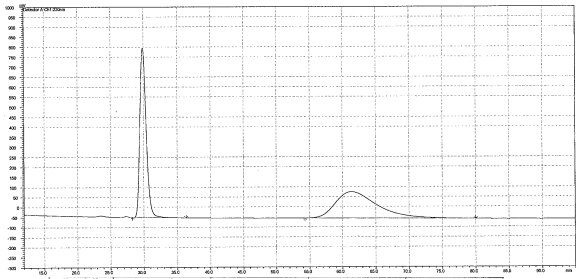

Peak#	Ret. Time	Area	Height	Area %
1	29.890	55933419	845938	49.269
2	61.372	57592643	131860	50.731
Total		113526062	977798	100.000

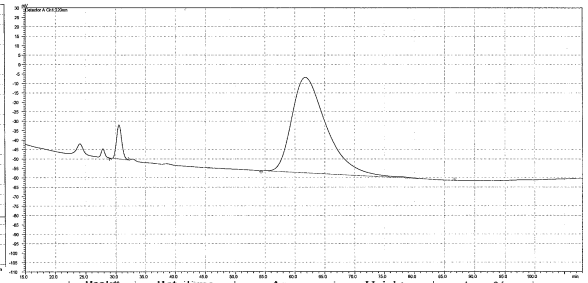

Peak#	Ret. Time	Area	Height	Area %
1	30.511	1123805	18124	5.216
2	61.773	20419689	50637	94.784
Total		21543494	68761	100.000

Peak #	Time (min)	Area (%)	Peak #	Time (min)	Area (%)
1	29.890	49.269	1	30.511	5.216
2	61.372	50.731	2	61.773	94.784

(***S*)-2-Methyl-5-phenyl-5-(4,4,5,5-tetramethyl-1,3,2-dioxaborolan-2-yl)hexan-3-one (1.134)**: IR (neat): 2973 (m), 2931 (m), 2873 (m), 1709 (s), 1466 (m), 1372 (s), 1346 (s), 1310 (s), 1142 (s), 700 (m) cm^{-1}; ^1H NMR (400 MHz, $CDCl_3$): δ 7.39–7.36 (2H, m), 7.30–7.25 (2H, m), 7.16–7.12 (1H, m), 3.16 (1H, d, *J* = 18.0 Hz), 2.79 (1H, d, *J* = 17.6 Hz), 2.58 (1H, sept, *J* = 5.9 Hz), 1.33 (3H, s), 1.21 (6H, s), 1.18 (6H, s), 1.10 (3H, d, *J* = 2.4 Hz), 1.08 (3H, d, *J* = 2.0 Hz); ^{13}C NMR (100 MHz, $CDCl_3$): δ 214.2, 146.7, 128.3, 126.7, 125.4, 83.4, 51.2, 40.7, 24.8, 24.7, 23.0, 18.4, 18.3; HRMS (ESI+): Calcd for $C_{19}H_{30}B_1O_3$ $[M+H]^+$: 317.2288, Found: 317.2291. Specific Rotation: $[\alpha]_D^{20}$ –32.5 (*c* 0.64, $CHCl_3$) for an enantiomerically enriched sample of 96:4 er. Enantiomeric purity was determined by HPLC analysis in comparison with authentic racemic material (96:4 er shown; Chiralcel OJ-H column, 100/0 hexanes/*i*-PrOH, 0.3 mL/min, 220 nm).

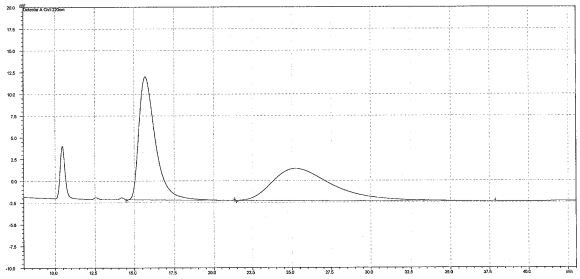

Peak#	Ret. Time	Area	Height	Area %
1	15.695	1010735	14154	51.341
2	25.333	957929	3679	48.659
Total		1968664	17833	100.000

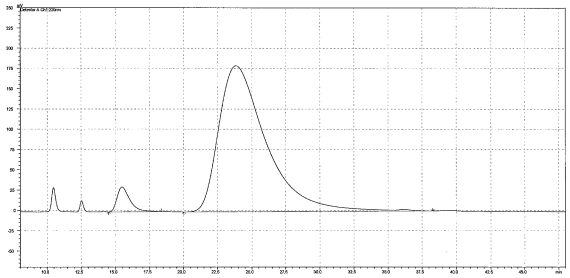

Peak#	Ret. Time	Area	Height	Area %
1	15.462	1966340	30623	4.300
2	23.839	43765941	180076	95.700
Total		45732282	210699	100.000

Peak #	Time (min)	Area (%)	Peak #	Time (min)	Area (%)
1	15.695	51.341	1	15.462	4.300
2	25.333	48.659	2	23.839	95.700

(*R*)-3-Hydroxy-3-phenylbutanoic acid (1.142): IR (neat): 3409 (br), 2978 (m), 2931 (m), 1705 (s), 1399 (m), 1208 (s), 700 (m) cm^{-1}; ^1H NMR (400 MHz, $CDCl_3$): δ 7.45–7.43 (2H, m), 7.37–7.33 (2H, m), 7.28–7.24 (1H, m), 3.03 (1H, d, J = 16.4 Hz), 2.85 (1H, d, J = 16.4 Hz), 1.57 (3H, s). ^{13}C NMR (100 MHz, $CDCl_3$): δ 177.0, 146.5, 128.6, 127.3, 124.5, 72.9, 46.2, 30.8; HRMS (ESI+): Calcd for $C_{10}H_{16}N_1O_3$ $[M+NH_4]^+$: 198.1130, Found: 198.1130. Specific Rotation: $[\alpha]_D^{20}$ –5.9 (*c* 0.28, EtOH) for an enantiomerically enriched sample of >99:1 er. Enantiomeric purity was determined by HPLC analysis in comparison with authentic racemic material (>99:1 er shown; Chiralcel OD-H column, 99/1 hexanes/*i*-PrOH, 0.3 mL/min, 220 nm).

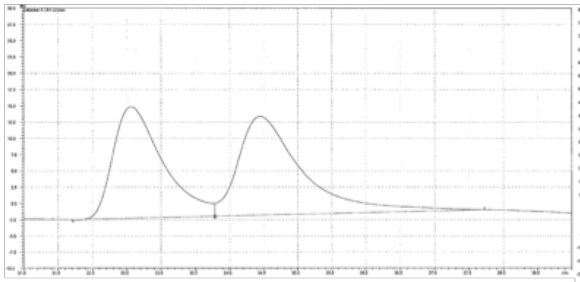

Peak#	Ret. Time	Area	Height	Area %
1	32.561	849598	17012	48.105
2	34.444	916524	14930	51.895
Total		1766122	31942	100.000

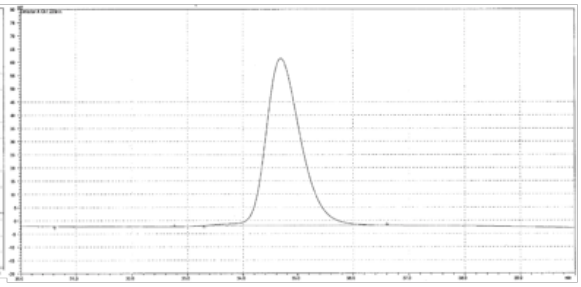

Peak#	Ret. Time	Area	Height	Area %
1	32.042	1808	66	0.065
2	34.686	2788142	63284	99.935
Total		2789949	63349	100.000

Peak #	Time (min)	Area (%)	Peak #	Time (min)	Area (%)
1	32.561	48.105	1	32.042	0.065
2	34.444	51.895	2	34.686	99.935

(*R*)-4-Hydroxy-4-phenylpentan-2-one (1.141): The spectroscopic data match those reported previously.[70] ^{1}H NMR (400 MHz, $CDCl_3$): δ 7.44–7.41 (2H, m), 7.35–7.31 (2H, m), 7.25–7.21 (1H, m), 4.50 (1H, s), 3.19 (1H, d, *J* = 16.8 Hz), 2.85 (1H, d, *J* = 17.2 Hz), 2.08 (3H, s), 1.52 (3H, s). Specific Rotation: $[\alpha]_D^{20}$ +25.1 (*c* 0.75, $CHCl_3$) for an enantiomerically enriched sample of 99:1 er. Enantiomeric purity was determined by HPLC analysis in comparison with authentic racemic material (99:1 er shown; Chiralcel OD-H column, 99/1 hexanes/*i*-PrOH, 0.3 mL/min, 220 nm).

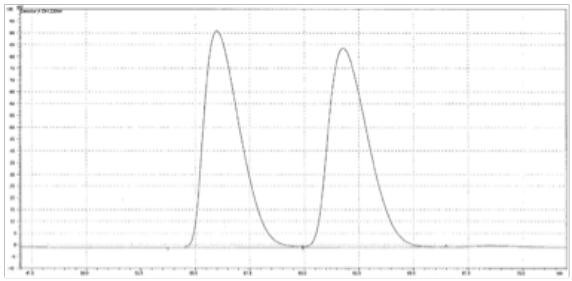

Peak#	Ret. Time	Area	Height	Area %
1	55.999	10535262	92021	49.829
2	61.778	10607491	84657	50.171
Total		21142753	176678	100.000

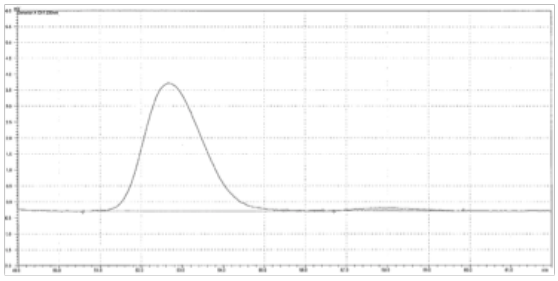

Peak#	Ret. Time	Area	Height	Area %
1	52.663	391600	4007	98.644
2	58.152	5382	70	1.356
Total		396981	4077	100.000

Peak #	Time (min)	Area (%)	Peak #	Time (min)	Area (%)
1	55.999	49.829	1	52.663	98.644
2	61.778	50.171	2	58.152	1.356

(*R*)-3-(3,7-Dimethyl-3-(4,4,5,5-tetramethyl-1,3,2-dioxaborolan-2-yl)oct-6-enoyl)-4-hydroxybenzaldehyde (1.147): IR (neat): 2975 (m), 2926 (m), 2725 (w), 1699 (m), 1640 (s), 1591 (m), 1482 (m), 1370 (s), 1310 (m), 1144 (s), 881 (m) cm^{-1}; ^{1}H NMR (400 MHz, $CDCl_3$): δ 12.8 (1H, s), 9.90 (1H, s), 8.33 (1H, d, *J* = 2.0 Hz), 7.98 (1H, dd, *J* = 8.4, 1.6 Hz), 7.09 (1H, d, *J* = 8.8 Hz), 5.09 (1H, t, *J* = 7.2 Hz), 3.29 (1H, d, *J* = 18.4 Hz), 3.06 (1H, d, *J* = 18.4 Hz), 2.08–1.95 (2H, m), 1.66 (3H, s), 1.60 (3H, s), 1.54–1.36 (2H, m), 1.27 (6H, s), 1.24 (6H, s), 1.06 (3H, s); ^{13}C NMR (100 MHz, $CDCl_3$): δ 206.5, 190.0, 167.3, 145.5, 136.7, 133.3, 131.5, 128.3, 124.9, 119.6, 119.57, 83.4, 48.6, 39.0, 25.8,

(70) Kobayashi, S.; Xu, P.; Endo, T.; Ueno, M.; Kitanosono, T. *Angew. Chem., Int. Ed.* **2012**, *51*, 12763–12766.

25.0, 24.9, 23.96, 21.7, 17.8; HRMS (ESI+): Calcd for $C_{23}H_{34}B_1O_5$ $[M+H]^+$: 401.2499, Found: 401.2517. Specific Rotation: $[\alpha]_D^{20}$ –20.3 (*c* 0.23 $CHCl_3$) for an enantiomerically enriched sample of 95:5 er. Enantiomeric purity was determined by HPLC analysis in comparison with authentic racemic material (95:5 er shown; Chiraldex AD-H column, 99/1 hexanes/*i*-PrOH, 0.3 mL/min, 220 nm).

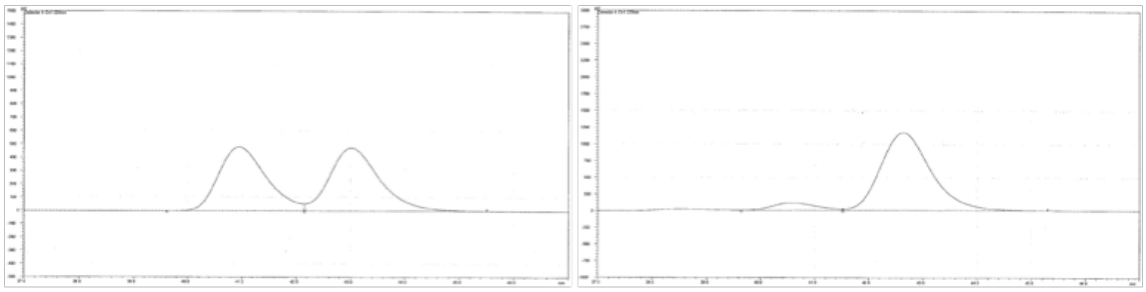

Peak#	Ret. Time	Area	Height	Area %
1	40.946	29237664	480967	48.962
2	43.008	30477906	475301	51.038
Total		59715571	956268	100.000

Peak#	Ret. Time	Area	Height	Area %
1	40.570	4106972	90509	5.357
2	42.637	72561346	1151210	94.643
Total		76668318	1241719	100.000

Peak #	Time (min)	Area (%)	Peak #	Time (min)	Area (%)
1	40.946	48.962	1	40.570	5.357
2	43.008	51.038	2	42.637	94.643

(*S*)-4-Hydroxy-3-(3-hydroxy-3,7-dimethyloct-6-enoyl)benzaldehyde (product after oxidation of 1.147): The spectroscopic data match those reported previously.[71] ^{1}H NMR (400 MHz, $CDCl_3$): δ 12.7 (1H, s), 9.91 (1H, s), 8.32 (1H, d, *J* = 1.6 Hz), 8.02 (1H, dd, *J* = 8.4, 1.6 Hz), 7.13 (1H, d, *J* = 9.2 Hz), 5.09 (1H, t, *J* = 7.2 Hz), 3.30 (1H, d, *J* = 16.4 Hz), 3.27 (1H, s), 3.19 (1H, d, *J* = 16.8 Hz), 2.16–2.05 (2H, m), 1.74–1.57 (8H, m), 1.36 (3H, s). Specific Rotation: $[\alpha]_D^{20}$ –11.3 (*c* 0.21, $CHCl_3$).

■ **Experimental Procedure for NHC–Catalyzed Enantioselective (Pinacolato)boron Conjugate Addition (*performed in a typical fume hood*):** To a flame-dried 1 dram vial equipped with a stir bar was added imidazolinium salt **im-25** (3.2 mg, 0.005 mmol) and dbu (3.0 mg, 0.02 mmol). The vial was sealed with a cap with a septum and purged with

(71) Chakor, J. N.; Merlini, L.; Dallavalle, S. *Tetrahedron* **2011**, *67* , 6300–6307.

dry N_2 for 20 min before addition of thf (0.15 mL) and the resulting mixture was allowed to stir for 30 min at 22 °C under a dry N_2 atmosphere. Bis(pinacolato)diboron (27.9 mg, 0.11 mmol) and 3-methyl-2-cyclohexen-1-one (11.0 mg, 0.10 mmol) were weighed into a separate flame-dried 1 dram vial. The vial was sealed with a cap with a septum and purged with dry N_2 for 20 min before addition of methanol (0.24 mL) and the solution was transferred via syringe to the NHC solution (minimal addition of thf was used to ensure complete transfer). The mixture was allowed to stir at 22 °C for 14 h, after which the reaction was quenched upon addition of an aqueous solution of NH_4Cl (0.5 mL, 1.0 M) and the mixture was allowed to stir for an additional 20 min. The aqueous layer was washed with diethyl ether (3 x 2 mL). The combined organic layers were dried over anhydrous $MgSO_4$ and filtered. The volatiles were removed under vacuum and the resulting light yellow oil was purified by silica gel chromatography (hexanes:Et_2O = 10:1) to afford 21.9 mg (0.09 mmol, 92% yield) of **(*S*)-3-methyl-3-(4,4,5,5-tetramethyl-1,3,2-dioxaborolan-2-yl)cyclohexan-1-one (1.112)**. Enantiomeric purity was determined by GC analysis in comparison with authentic racemic material (95:5 er shown; Chiraldex B-DM column, 15 psi, 100 °C).

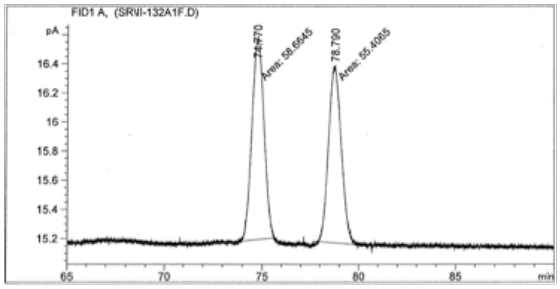

Peak #	RetTime Type	Width [min]	Area [pA*s]	Height [pA]	Area %
1	74.770 MM	0.6970	58.66451	1.40273	51.42808
2	78.790 MM	0.7557	55.40647	1.22204	48.57192

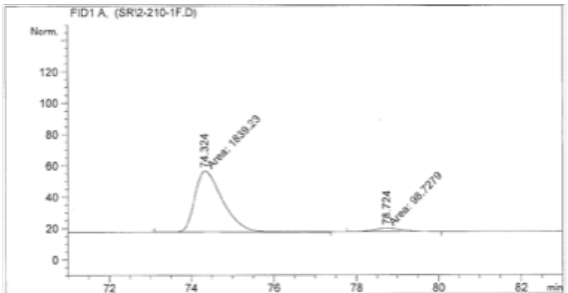

Peak #	RetTime Type	Width [min]	Area [pA*s]	Height [pA]	Area %
1	74.324 MM	0.7858	1839.22913	39.00990	94.90557
2	78.724 MM	0.7635	98.72794	2.15519	5.09443

Peak #	Time (min)	Area (%)	Peak #	Time (min)	Area (%)
1	74.770	51.428	1	74.324	94.906
2	78.790	48.573	2	78.724	5.094

■ **Experimental Procedures for Cu–Catalyzed Enantioselective (Pinacolato)boron Conjugate Additions with Previously Reported Catalyst Systems**

Reactions with (R,R)–QuinoxP* reported by Shibasaki **(Scheme 1.34).** Transformations were performed according to the reported procedure.[68] Dimethyl sulfoxide (125 μL) was added to a mixture of bis(pinacolato)diboron (38.1 mg, 0.15 mmol), cyclic enone substrate (**1.143**: 16.2 mg, 0.10 mmol, for **1.145**: 17.6 mg, 0.10 mmol), $CuPF_6(CH_3CN)_4$ (3.7 mg, 0.010 mmol), and QuinoxP* (4.0 mg, 0.012 mmol), and the mixture was stirred for 10 minutes at 22 ºC. A thf solution of 1 M lithium *tert*-butoxide (15 μL, 0.015 mmol) was then added, and the solution was allowed to stir for 12 hours. The reaction mixture was diluted with EtOAc (1 mL), water (1 mL) was added, and the mixture was allowed to stir for 5 minutes. The aqueous layer was then washed with EtOAc (2 x 1 mL). The combined organic layers were dried over Na_2SO_4, filter, and concentrated under reduce pressure. The resulting yellow oil was purified by silica gel column chromatography.

Reactions with diamine–Cu reported by Shibasaki **(Scheme 1.35).** Transformations were performed according to the reported procedure.[72] To a mixture of acyclic enone substrate (**1.146**: 31.6 mg, 0.1 mmol), bis(pinacolato)diboron (38.1 mg, 0.15 mmol), $CuPF_6(CH_3CN)_4$ (3.7 mg, 0.010 mmol), and diamine catalyst (3.2 mg, 0.012 mmol), dme (33 μL) was added. The resulting solution was allowed to stir for 5 minutes at 22 ºC. Additional dme (167 μL) was then added, and the solution was allowed to stir for 5 min. Followed by adding a 1 M thf solution of lithium *tert*-butoxide (15 μL, 0.015 mmol) and isopropanol (15 μL, 0.2 mmol), the solution was stirred for 24 h. The solution was diluted

(72) Chen, I.–H.; Kanai, M.; Shibasaki, M. *Org. Lett.* **2010**, *12*, 4098–4101.

with EtOAc (1 mL) and water (0.5 mL) was added. The aqueous layer was washed with EtOAc (2 x 1 mL). The combined organic layers were dried over Na_2SO_4, filter, and concentrated under reduce pressure. The resulting yellow oil was purified by silica gel column chromatography.

Reactions with NHC–Cu reported by Hoveyda **(Scheme 1.35).** Transformations were performed according to the reported procedure.[69] In an oven-dried 1 dram vial equipped with a stir bar, imidazolinium salt (3.3 mg, 0.005 mmol), NaO*t*-Bu (1.2 mg, 0.013 mmol), and CuCl (0.5 mg, 0.005 mmol) were placed and thf (0.5 mL) was added in the glove-box. After the solution was allowed to stir for two hours at 22 ºC, the resulting solution was charged with $B_2(pin)_2$ (27.9 mg , 0.11 mmol). The vessel was sealed with a cap with a septum, removed from the glovebox, placed in a fume hood and allowed to cool to –30 °C. Acyclic enone substrate (**1.146**: 31.6 mg, 0.1 mmol), and MeOH (4.8 μL, 0.12 mmol) were added and the mixture was allowed to stir for 24 hours at –30 °C, after which the reaction was quenched by the addition of 30% HCl in MeOH (0.5 mL). The resulting mixture was subsequently allowed to warm to 22 ºC, H_2O (1 mL) was added, and the solution was neutralized through addition of a saturated solution of $NaHCO_3$. The layers were separated, and the aqueous portion was washed with Et_2O (3 x 1 mL). The combined organic layers were dried over Na_2SO_4 and filtered. The volatiles were removed *in vacuo* and the resulting yellow oil was purified by silica gel chromatography.

■ **Data for X-ray Crystallography of 1.124**

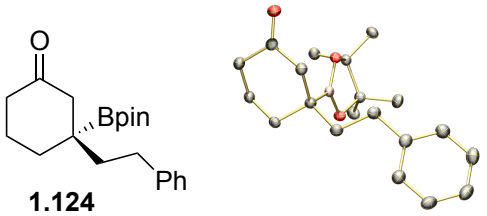

1.124

X-ray structure of **1.124**

Table 1. **Crystal data and structure refinement for $C_{20}H_{29}BO_3$**

Identification code	C20H29BO3	
Empirical formula	C20 H29 B O3	
Formula weight	328.24	
Temperature	100(2) K	
Wavelength	1.54178 Å	
Crystal system	Orthorhombic	
Space group	P 21 21 21	
Unit cell dimensions	a = 6.1291(5) Å	α= 90 °.
	b = 9.8899(9) Å	β= 90 °.
	c = 29.990(3) Å	γ = 90 °.
Volume	1817.9(3) Å ^{3}	
Z	4	
Density (calculated)	1.199 Mg/m^3	
Absorption coefficient	0.610 mm^{-1}	
F(000)	712	
Crystal size	0.400 x 0.150 x 0.080 mm^3	
Theta range for data collection	2.947 to 70.063 °.	
Index ranges	-5<=h<=7, -11<=k<=11, -36<=l<=36	
Reflections collected	22781	
Independent reflections	3393 [R(int) = 0.0317]	
Completeness to theta = 67.679 °	99.7 %	
Absorption correction	Semi-empirical from equivalents	
Max. and min. transmission	0.7533 and 0.5897	
Refinement method	Full-matrix least-squares on F^2	
Data / restraints / parameters	3393 / 0 / 217	
Goodness-of-fit on F^2	1.053	

Final R indices [I>2sigma(I)]	R1 = 0.0282, wR2 = 0.0764
R indices (all data)	R1 = 0.0283, wR2 = 0.0765
Absolute structure parameter	0.01(3)
Extinction coefficient	na
Largest diff. peak and hole	0.188 and -0.149 e. $Å^{-3}$

Table 2. **Atomic coordinates (x 10^4) and equivalent isotropic displacement parameters ($Å^2$ x 10^3) for $C_{20}H_{29}BO_3$. U(eq) is defined as one third of the trace of the orthogonalized U^{ij} tensor**

	x	y	z	U(eq)
O(1)	9129(2)	218(1)	1623(1)	27(1)
O(2)	9235(2)	3770(1)	1679(1)	18(1)
O(3)	6701(2)	5312(1)	1443(1)	20(1)
B(1)	7547(3)	4040(2)	1395(1)	17(1)
C(1)	7602(3)	815(2)	1456(1)	20(1)
C(2)	5322(3)	705(2)	1640(1)	23(1)
C(3)	4044(3)	2038(2)	1626(1)	21(1)
C(4)	4214(3)	2707(2)	1167(1)	20(1)
C(5)	6602(3)	3002(2)	1041(1)	18(1)
C(6)	7880(3)	1652(2)	1036(1)	19(1)
C(7)	6682(3)	3673(2)	576(1)	21(1)
C(8)	9002(3)	3975(2)	414(1)	23(1)
C(9)	9168(3)	4968(2)	30(1)	22(1)
C(10)	10999(3)	5801(2)	-6(1)	26(1)
C(11)	11194(3)	6728(2)	-351(1)	31(1)
C(12)	9558(3)	6835(2)	-670(1)	29(1)
C(13)	7736(3)	6005(2)	-640(1)	27(1)
C(14)	7540(3)	5083(2)	-292(1)	24(1)
C(15)	9321(3)	4891(2)	2000(1)	18(1)
C(16)	8197(3)	6057(2)	1735(1)	21(1)
C(17)	8054(3)	4437(2)	2409(1)	24(1)

C(18)	11681(3)	5157(2)	2122(1)	23(1)
C(19)	6893(3)	7033(2)	2020(1)	28(1)
C(20)	9748(3)	6827(2)	1432(1)	28(1)

Table 3. **Bond lengths [Å] and angles [º] for $C_{20}H_{29}BO_3$**

O(1)-C(1)	1.214(2)
O(2)-B(1)	1.367(2)
O(2)-C(15)	1.4692(17)
O(3)-B(1)	1.368(2)
O(3)-C(16)	1.4663(18)
B(1)-C(5)	1.585(2)
C(1)-C(2)	1.506(2)
C(1)-C(6)	1.517(2)
C(2)-C(3)	1.534(2)
C(2)-H(2A)	0.9900
C(2)-H(2B)	0.9900
C(3)-C(4)	1.529(2)
C(3)-H(3A)	0.9900
C(3)-H(3B)	0.9900
C(4)-C(5)	1.539(2)
C(4)-H(4A)	0.9900
C(4)-H(4B)	0.9900
C(5)-C(7)	1.545(2)
C(5)-C(6)	1.548(2)
C(6)-H(6A)	0.9900
C(6)-H(6B)	0.9900
C(7)-C(8)	1.532(2)
C(7)-H(7A)	0.9900
C(7)-H(7B)	0.9900
C(8)-C(9)	1.518(2)
C(8)-H(8A)	0.9900
C(8)-H(8B)	0.9900
C(9)-C(14)	1.392(2)

C(9)-C(10)	1.396(2)
C(10)-C(11)	1.389(2)
C(10)-H(10)	0.9500
C(11)-C(12)	1.389(3)
C(11)-H(11)	0.9500
C(12)-C(13)	1.389(3)
C(12)-H(12)	0.9500
C(13)-C(14)	1.392(2)
C(13)-H(13)	0.9500
C(14)-H(14)	0.9500
C(15)-C(18)	1.515(2)
C(15)-C(17)	1.519(2)
C(15)-C(16)	1.561(2)
C(16)-C(19)	1.517(2)
C(16)-C(20)	1.521(2)
C(17)-H(17A)	0.9800
C(17)-H(17B)	0.9800
C(17)-H(17C)	0.9800
C(18)-H(18A)	0.9800
C(18)-H(18B)	0.9800
C(18)-H(18C)	0.9800
C(19)-H(19A)	0.9800
C(19)-H(19B)	0.9800
C(19)-H(19C)	0.9800
C(20)-H(20A)	0.9800
C(20)-H(20B)	0.9800
C(20)-H(20C)	0.9800

B(1)-O(2)-C(15)	106.78(11)
B(1)-O(3)-C(16)	106.76(12)
O(2)-B(1)-O(3)	113.59(13)
O(2)-B(1)-C(5)	124.56(14)
O(3)-B(1)-C(5)	121.85(14)
O(1)-C(1)-C(2)	121.99(14)
O(1)-C(1)-C(6)	121.34(15)

C(2)-C(1)-C(6)	116.59(13)
C(1)-C(2)-C(3)	113.63(13)
C(1)-C(2)-H(2A)	108.8
C(3)-C(2)-H(2A)	108.8
C(1)-C(2)-H(2B)	108.8
C(3)-C(2)-H(2B)	108.8
H(2A)-C(2)-H(2B)	107.7
C(4)-C(3)-C(2)	111.27(12)
C(4)-C(3)-H(3A)	109.4
C(2)-C(3)-H(3A)	109.4
C(4)-C(3)-H(3B)	109.4
C(2)-C(3)-H(3B)	109.4
H(3A)-C(3)-H(3B)	108.0
C(3)-C(4)-C(5)	111.56(12)
C(3)-C(4)-H(4A)	109.3
C(5)-C(4)-H(4A)	109.3
C(3)-C(4)-H(4B)	109.3
C(5)-C(4)-H(4B)	109.3
H(4A)-C(4)-H(4B)	108.0
C(4)-C(5)-C(7)	109.45(12)
C(4)-C(5)-C(6)	108.66(12)
C(7)-C(5)-C(6)	110.19(12)
C(4)-C(5)-B(1)	107.83(12)
C(7)-C(5)-B(1)	108.28(12)
C(6)-C(5)-B(1)	112.38(12)
C(1)-C(6)-C(5)	113.89(12)
C(1)-C(6)-H(6A)	108.8
C(5)-C(6)-H(6A)	108.8
C(1)-C(6)-H(6B)	108.8
C(5)-C(6)-H(6B)	108.8
H(6A)-C(6)-H(6B)	107.7
C(8)-C(7)-C(5)	113.54(13)
C(8)-C(7)-H(7A)	108.9
C(5)-C(7)-H(7A)	108.9
C(8)-C(7)-H(7B)	108.9

C(5)-C(7)-H(7B)	108.9
H(7A)-C(7)-H(7B)	107.7
C(9)-C(8)-C(7)	115.41(13)
C(9)-C(8)-H(8A)	108.4
C(7)-C(8)-H(8A)	108.4
C(9)-C(8)-H(8B)	108.4
C(7)-C(8)-H(8B)	108.4
H(8A)-C(8)-H(8B)	107.5
C(14)-C(9)-C(10)	118.32(15)
C(14)-C(9)-C(8)	122.05(15)
C(10)-C(9)-C(8)	119.63(15)
C(11)-C(10)-C(9)	121.07(16)
C(11)-C(10)-H(10)	119.5
C(9)-C(10)-H(10)	119.5
C(12)-C(11)-C(10)	120.10(17)
C(12)-C(11)-H(11)	119.9
C(10)-C(11)-H(11)	119.9
C(11)-C(12)-C(13)	119.41(15)
C(11)-C(12)-H(12)	120.3
C(13)-C(12)-H(12)	120.3
C(12)-C(13)-C(14)	120.32(16)
C(12)-C(13)-H(13)	119.8
C(14)-C(13)-H(13)	119.8
C(13)-C(14)-C(9)	120.78(16)
C(13)-C(14)-H(14)	119.6
C(9)-C(14)-H(14)	119.6
O(2)-C(15)-C(18)	108.88(12)
O(2)-C(15)-C(17)	106.68(12)
C(18)-C(15)-C(17)	110.17(13)
O(2)-C(15)-C(16)	101.99(11)
C(18)-C(15)-C(16)	114.59(13)
C(17)-C(15)-C(16)	113.81(13)
O(3)-C(16)-C(19)	109.04(13)
O(3)-C(16)-C(20)	106.59(13)
C(19)-C(16)-C(20)	110.37(13)

O(3)-C(16)-C(15)	102.04(11)
C(19)-C(16)-C(15)	114.56(13)
C(20)-C(16)-C(15)	113.52(14)
C(15)-C(17)-H(17A)	109.5
C(15)-C(17)-H(17B)	109.5
H(17A)-C(17)-H(17B)	109.5
C(15)-C(17)-H(17C)	109.5
H(17A)-C(17)-H(17C)	109.5
H(17B)-C(17)-H(17C)	109.5
C(15)-C(18)-H(18A)	109.5
C(15)-C(18)-H(18B)	109.5
H(18A)-C(18)-H(18B)	109.5
C(15)-C(18)-H(18C)	109.5
H(18A)-C(18)-H(18C)	109.5
H(18B)-C(18)-H(18C)	109.5
C(16)-C(19)-H(19A)	109.5
C(16)-C(19)-H(19B)	109.5
H(19A)-C(19)-H(19B)	109.5
C(16)-C(19)-H(19C)	109.5
H(19A)-C(19)-H(19C)	109.5
H(19B)-C(19)-H(19C)	109.5
C(16)-C(20)-H(20A)	109.5
C(16)-C(20)-H(20B)	109.5
H(20A)-C(20)-H(20B)	109.5
C(16)-C(20)-H(20C)	109.5
H(20A)-C(20)-H(20C)	109.5
H(20B)-C(20)-H(20C)	109.5

Symmetry transformations used to generate equivalent atoms:

Table 4. **Anisotropic displacement parameters ($Å^2$ x 10^3) for sad. The anisotropic displacement factor exponent takes the form: $-2\pi^2[h^2 a^{*2} U^{11} + ... + 2 h k a^* b^* U^{12}]$**

	U^{11}	U^{22}	U^{33}	U^{23}	U^{13}	U^{12}

O(1)	25(1)	24(1)	33(1)	4(1)	-2(1)	3(1)
O(2)	19(1)	16(1)	19(1)	-3(1)	-2(1)	1(1)
O(3)	21(1)	17(1)	23(1)	-2(1)	-6(1)	1(1)
B(1)	16(1)	17(1)	17(1)	2(1)	2(1)	-1(1)
C(1)	24(1)	14(1)	22(1)	-3(1)	-2(1)	0(1)
C(2)	23(1)	20(1)	25(1)	2(1)	1(1)	-2(1)
C(3)	19(1)	21(1)	24(1)	0(1)	2(1)	-2(1)
C(4)	17(1)	20(1)	22(1)	-1(1)	-3(1)	-1(1)
C(5)	18(1)	18(1)	18(1)	-1(1)	0(1)	1(1)
C(6)	21(1)	18(1)	19(1)	-3(1)	1(1)	0(1)
C(7)	22(1)	22(1)	18(1)	-1(1)	-2(1)	1(1)
C(8)	24(1)	27(1)	19(1)	1(1)	1(1)	2(1)
C(9)	26(1)	20(1)	18(1)	-4(1)	3(1)	2(1)
C(10)	28(1)	27(1)	23(1)	-4(1)	0(1)	-1(1)
C(11)	35(1)	25(1)	34(1)	-2(1)	7(1)	-6(1)
C(12)	39(1)	23(1)	25(1)	4(1)	7(1)	4(1)
C(13)	32(1)	28(1)	21(1)	2(1)	-1(1)	6(1)
C(14)	27(1)	23(1)	22(1)	-1(1)	2(1)	0(1)
C(15)	19(1)	18(1)	19(1)	-4(1)	0(1)	-1(1)
C(16)	21(1)	17(1)	23(1)	-2(1)	-2(1)	-2(1)
C(17)	23(1)	28(1)	20(1)	0(1)	-1(1)	-3(1)
C(18)	18(1)	24(1)	27(1)	-4(1)	-3(1)	-1(1)
C(19)	25(1)	20(1)	37(1)	-10(1)	-2(1)	1(1)
C(20)	32(1)	21(1)	30(1)	2(1)	1(1)	-5(1)

Table 5. **Hydrogen coordinates (x 10^4) and isotropic displacement parameters (Å^2 x 10^3) for $C_{20}H_{29}BO_3$**

	x	y	z	U(eq)

H(2A)	5403	390	1953	27
H(2B)	4514	14	1467	27
H(3A)	2492	1860	1695	25
H(3B)	4624	2661	1855	25
H(4A)	3379	3564	1169	24
H(4B)	3559	2105	940	24
H(6A)	7390	1109	777	23
H(6B)	9450	1850	994	23
H(7A)	5959	3070	358	25
H(7B)	5847	4529	586	25
H(8A)	9855	4334	668	28
H(8B)	9688	3113	322	28
H(10)	12129	5733	210	31
H(11)	12449	7289	-370	37
H(12)	9684	7471	-906	35
H(13)	6618	6067	-858	33
H(14)	6281	4525	-273	29
H(17A)	6531	4268	2326	36
H(17B)	8111	5146	2637	36
H(17C)	8701	3605	2527	36
H(18A)	12482	5450	1856	35
H(18B)	12338	4327	2239	35
H(18C)	11750	5867	2350	35
H(19A)	5903	6523	2214	41
H(19B)	6042	7634	1827	41
H(19C)	7890	7572	2203	41
H(20A)	10581	6185	1250	41
H(20B)	10755	7366	1613	41
H(20C)	8909	7427	1236	41

Table 6. **Torsion angles [º] for $C_{20}H_{29}BO_3$**

C(15)-O(2)-B(1)-O(3)	9.61(17)
C(15)-O(2)-B(1)-C(5)	-169.85(14)
C(16)-O(3)-B(1)-O(2)	10.53(17)
C(16)-O(3)-B(1)-C(5)	-169.99(13)
O(1)-C(1)-C(2)-C(3)	141.86(15)
C(6)-C(1)-C(2)-C(3)	-41.42(18)
C(1)-C(2)-C(3)-C(4)	48.21(18)
C(2)-C(3)-C(4)-C(5)	-58.82(17)
C(3)-C(4)-C(5)-C(7)	179.87(12)
C(3)-C(4)-C(5)-C(6)	59.51(15)
C(3)-C(4)-C(5)-B(1)	-62.55(16)
O(2)-B(1)-C(5)-C(4)	116.97(16)
O(3)-B(1)-C(5)-C(4)	-62.45(17)
O(2)-B(1)-C(5)-C(7)	-124.69(15)
O(3)-B(1)-C(5)-C(7)	55.89(18)
O(2)-B(1)-C(5)-C(6)	-2.8(2)
O(3)-B(1)-C(5)-C(6)	177.82(13)
O(1)-C(1)-C(6)-C(5)	-139.62(15)
C(2)-C(1)-C(6)-C(5)	43.63(18)
C(4)-C(5)-C(6)-C(1)	-51.15(16)
C(7)-C(5)-C(6)-C(1)	-171.06(13)
B(1)-C(5)-C(6)-C(1)	68.09(16)
C(4)-C(5)-C(7)-C(8)	-178.46(13)
C(6)-C(5)-C(7)-C(8)	-59.03(17)
B(1)-C(5)-C(7)-C(8)	64.24(17)
C(5)-C(7)-C(8)-C(9)	-163.48(13)
C(7)-C(8)-C(9)-C(14)	-30.9(2)
C(7)-C(8)-C(9)-C(10)	149.01(15)
C(14)-C(9)-C(10)-C(11)	0.4(2)
C(8)-C(9)-C(10)-C(11)	-179.55(15)

C(9)-C(10)-C(11)-C(12)	-0.2(3)
C(10)-C(11)-C(12)-C(13)	-0.3(3)
C(11)-C(12)-C(13)-C(14)	0.7(3)
C(12)-C(13)-C(14)-C(9)	-0.5(2)
C(10)-C(9)-C(14)-C(13)	0.0(2)
C(8)-C(9)-C(14)-C(13)	179.93(14)
B(1)-O(2)-C(15)-C(18)	-145.41(13)
B(1)-O(2)-C(15)-C(17)	95.72(14)
B(1)-O(2)-C(15)-C(16)	-23.92(15)
B(1)-O(3)-C(16)-C(19)	-146.01(13)
B(1)-O(3)-C(16)-C(20)	94.83(14)
B(1)-O(3)-C(16)-C(15)	-24.46(14)
O(2)-C(15)-C(16)-O(3)	29.06(14)
C(18)-C(15)-C(16)-O(3)	146.51(12)
C(17)-C(15)-C(16)-O(3)	-85.43(14)
O(2)-C(15)-C(16)-C(19)	146.73(13)
C(18)-C(15)-C(16)-C(19)	-95.82(16)
C(17)-C(15)-C(16)-C(19)	32.24(18)
O(2)-C(15)-C(16)-C(20)	-85.22(15)
C(18)-C(15)-C(16)-C(20)	32.23(17)
C(17)-C(15)-C(16)-C(20)	160.29(13)

Symmetry transformations used to generate equivalent atoms:

■ **Data for X-ray Crystallography of 1.129**

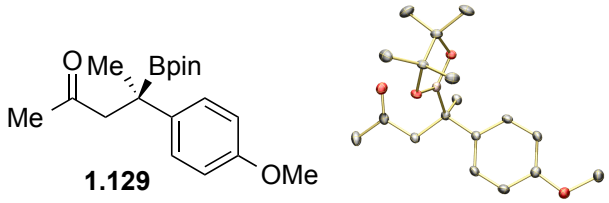

1.129

X-ray structure of **1.129**

Table 1. **Crystal data and structure refinement for $C_{18}H_{27}BO_4$**

Identification code	C18H27BO4
Empirical formula	C18 H27 B O4

Formula weight	318.20	
Temperature	100(2) K	
Wavelength	1.54178 Å	
Crystal system	Monoclinic	
Space group	P 21	
Unit cell dimensions	a = 6.4661(3) Å	α= 90 º.
	b = 22.7367(11) Å	β= 99.0710(10) º.
	c = 12.2957(6) Å	γ = 90 º.
Volume	1785.08(15) $Å^3$	
Z	4	
Density (calculated)	1.184 Mg/m^3	
Absorption coefficient	0.648 mm^{-1}	
F(000)	688	
Crystal size	0.600 x 0.160 x 0.100 mm^3	
Theta range for data collection	3.640 to 70.154 º.	
Index ranges	-7<=h<=7, 0<=k<=27, 0<=l<=14	
Reflections collected	6613	
Independent reflections	6613 [R(int) = ?]	
Completeness to theta = 67.679∞	99.7 %	
Absorption correction	Semi-empirical from equivalents	
Max. and min. transmission	0.7533 and 0.6403	
Refinement method	Full-matrix least-squares on F^2	
Data / restraints / parameters	6613 / 1 / 420	
Goodness-of-fit on F^2	1.049	
Final R indices [I>2sigma(I)]	R1 = 0.0291, wR2 = 0.0832	
R indices (all data)	R1 = 0.0293, wR2 = 0.0833	
Absolute structure parameter	0.07(4)	
Extinction coefficient	na	
Largest diff. peak and hole	0.256 and -0.166 e. $Å^{-3}$	

Table 2. **Atomic coordinates (x 10^4) and equivalent isotropic displacement parameters ($Å^2$ x 10^3) for $C_{18}H_{27}BO_4$. U(eq) is defined as one third of the trace of the orthogonalized U^{ij} tensor**

	x	y	z	U(eq)
B(1)	5335(4)	1121(1)	418(2)	15(1)
O(1)	3839(2)	808(1)	-1666(1)	24(1)
O(2)	4182(2)	1626(1)	312(1)	16(1)
O(3)	7446(2)	1212(1)	541(1)	16(1)
O(4)	3517(2)	380(1)	5139(1)	22(1)
C(1)	394(4)	423(1)	-2207(2)	27(1)
C(2)	2301(3)	579(1)	-1384(2)	18(1)
C(3)	2193(3)	453(1)	-191(2)	17(1)
C(4)	4309(3)	498(1)	564(2)	15(1)
C(5)	4069(3)	471(1)	1791(2)	14(1)
C(6)	5851(3)	488(1)	2591(2)	18(1)
C(7)	5753(3)	458(1)	3713(2)	18(1)
C(8)	3818(3)	418(1)	4059(2)	17(1)
C(9)	2015(3)	408(1)	3276(2)	20(1)
C(10)	2136(3)	435(1)	2162(2)	18(1)
C(11)	5651(3)	2114(1)	578(2)	16(1)
C(12)	7772(3)	1840(1)	372(2)	17(1)
C(13)	5619(3)	2271(1)	1781(2)	22(1)
C(14)	4880(4)	2628(1)	-167(2)	24(1)
C(15)	8175(4)	1909(1)	-808(2)	27(1)
C(16)	9660(3)	2035(1)	1182(2)	25(1)
C(17)	5750(3)	-6(1)	310(2)	18(1)
C(18)	5344(3)	374(1)	5956(2)	23(1)
B(2)	-298(3)	8107(1)	4778(2)	14(1)
O(5)	864(2)	8425(1)	2948(1)	23(1)
O(6)	858(2)	7600(1)	4832(1)	15(1)
O(7)	-2416(2)	8007(1)	4569(1)	16(1)
O(8)	1646(2)	8885(1)	9797(1)	20(1)
C(19)	4213(3)	8821(1)	2792(2)	20(1)
C(20)	2461(3)	8659(1)	3403(2)	17(1)
C(21)	2762(3)	8789(1)	4631(1)	16(1)
C(22)	710(3)	8731(1)	5099(2)	16(1)

C(23)	1024(3)	8762(1)	6358(2)	15(1)
C(24)	-694(3)	8665(1)	6894(2)	18(1)
C(25)	-564(3)	8699(1)	8029(2)	18(1)
C(26)	1339(3)	8835(1)	8672(2)	16(1)
C(27)	3080(3)	8930(1)	8161(2)	18(1)
C(28)	2922(3)	8892(1)	7023(2)	17(1)
C(29)	-577(3)	7123(1)	4430(2)	16(1)
C(30)	-2730(3)	7371(1)	4629(2)	15(1)
C(31)	-456(3)	7033(1)	3214(2)	21(1)
C(32)	151(4)	6573(1)	5084(2)	23(1)
C(33)	-4575(3)	7205(1)	3755(2)	23(1)
C(34)	-3238(4)	7243(1)	5771(2)	24(1)
C(35)	-772(3)	9240(1)	4654(2)	19(1)
C(36)	-149(3)	8822(1)	10324(2)	27(1)

Table 3. **Bond lengths [Å] and angles [º] for $C_{18}H_{27}BO_4$**

B(1)-O(2)	1.364(3)
B(1)-O(3)	1.365(3)
B(1)-C(4)	1.588(3)
O(1)-C(2)	1.221(3)
O(2)-C(11)	1.464(2)
O(3)-C(12)	1.465(2)
O(4)-C(8)	1.375(2)
O(4)-C(18)	1.425(2)
C(1)-C(2)	1.509(3)
C(1)-H(1A)	0.9800
C(1)-H(1B)	0.9800
C(1)-H(1C)	0.9800
C(2)-C(3)	1.507(3)
C(3)-C(4)	1.531(3)
C(3)-H(3A)	0.9900
C(3)-H(3B)	0.9900

C(4)-C(17)	1.540(3)
C(4)-C(5)	1.542(2)
C(5)-C(6)	1.393(3)
C(5)-C(10)	1.399(3)
C(6)-C(7)	1.392(3)
C(6)-H(6)	0.9500
C(7)-C(8)	1.386(3)
C(7)-H(7)	0.9500
C(8)-C(9)	1.390(3)
C(9)-C(10)	1.386(3)
C(9)-H(9)	0.9500
C(10)-H(10)	0.9500
C(11)-C(14)	1.520(3)
C(11)-C(13)	1.525(3)
C(11)-C(12)	1.563(3)
C(12)-C(16)	1.516(3)
C(12)-C(15)	1.521(3)
C(13)-H(13A)	0.9800
C(13)-H(13B)	0.9800
C(13)-H(13C)	0.9800
C(14)-H(14A)	0.9800
C(14)-H(14B)	0.9800
C(14)-H(14C)	0.9800
C(15)-H(15A)	0.9800
C(15)-H(15B)	0.9800
C(15)-H(15C)	0.9800
C(16)-H(16A)	0.9800
C(16)-H(16B)	0.9800
C(16)-H(16C)	0.9800
C(17)-H(17A)	0.9800
C(17)-H(17B)	0.9800
C(17)-H(17C)	0.9800
C(18)-H(18A)	0.9800
C(18)-H(18B)	0.9800
C(18)-H(18C)	0.9800

B(2)-O(6)	1.370(3)
B(2)-O(7)	1.372(3)
B(2)-C(22)	1.586(3)
O(5)-C(20)	1.216(2)
O(6)-C(29)	1.461(2)
O(7)-C(30)	1.464(2)
O(8)-C(26)	1.370(2)
O(8)-C(36)	1.424(3)
C(19)-C(20)	1.501(3)
C(19)-H(19A)	0.9800
C(19)-H(19B)	0.9800
C(19)-H(19C)	0.9800
C(20)-C(21)	1.520(2)
C(21)-C(22)	1.534(3)
C(21)-H(21A)	0.9900
C(21)-H(21B)	0.9900
C(22)-C(23)	1.530(2)
C(22)-C(35)	1.546(3)
C(23)-C(28)	1.394(3)
C(23)-C(24)	1.395(3)
C(24)-C(25)	1.388(3)
C(24)-H(24)	0.9500
C(25)-C(26)	1.388(3)
C(25)-H(25)	0.9500
C(26)-C(27)	1.389(3)
C(27)-C(28)	1.390(3)
C(27)-H(27)	0.9500
C(28)-H(28)	0.9500
C(29)-C(32)	1.520(3)
C(29)-C(31)	1.524(3)
C(29)-C(30)	1.556(3)
C(30)-C(34)	1.521(2)
C(30)-C(33)	1.521(3)
C(31)-H(31A)	0.9800
C(31)-H(31B)	0.9800

C(31)-H(31C)	0.9800
C(32)-H(32A)	0.9800
C(32)-H(32B)	0.9800
C(32)-H(32C)	0.9800
C(33)-H(33A)	0.9800
C(33)-H(33B)	0.9800
C(33)-H(33C)	0.9800
C(34)-H(34A)	0.9800
C(34)-H(34B)	0.9800
C(34)-H(34C)	0.9800
C(35)-H(35A)	0.9800
C(35)-H(35B)	0.9800
C(35)-H(35C)	0.9800
C(36)-H(36A)	0.9800
C(36)-H(36B)	0.9800
C(36)-H(36C)	0.9800

O(2)-B(1)-O(3)	113.98(17)
O(2)-B(1)-C(4)	122.07(18)
O(3)-B(1)-C(4)	123.36(17)
B(1)-O(2)-C(11)	106.90(14)
B(1)-O(3)-C(12)	107.12(15)
C(8)-O(4)-C(18)	116.98(15)
C(2)-C(1)-H(1A)	109.5
C(2)-C(1)-H(1B)	109.5
H(1A)-C(1)-H(1B)	109.5
C(2)-C(1)-H(1C)	109.5
H(1A)-C(1)-H(1C)	109.5
H(1B)-C(1)-H(1C)	109.5
O(1)-C(2)-C(3)	121.50(17)
O(1)-C(2)-C(1)	121.73(17)
C(3)-C(2)-C(1)	116.75(17)
C(2)-C(3)-C(4)	113.78(16)
C(2)-C(3)-H(3A)	108.8
C(4)-C(3)-H(3A)	108.8

C(2)-C(3)-H(3B)	108.8
C(4)-C(3)-H(3B)	108.8
H(3A)-C(3)-H(3B)	107.7
C(3)-C(4)-C(17)	109.82(15)
C(3)-C(4)-C(5)	111.84(15)
C(17)-C(4)-C(5)	109.08(15)
C(3)-C(4)-B(1)	109.91(15)
C(17)-C(4)-B(1)	111.42(16)
C(5)-C(4)-B(1)	104.69(14)
C(6)-C(5)-C(10)	116.98(17)
C(6)-C(5)-C(4)	119.35(16)
C(10)-C(5)-C(4)	123.67(16)
C(7)-C(6)-C(5)	122.44(18)
C(7)-C(6)-H(6)	118.8
C(5)-C(6)-H(6)	118.8
C(8)-C(7)-C(6)	119.46(17)
C(8)-C(7)-H(7)	120.3
C(6)-C(7)-H(7)	120.3
O(4)-C(8)-C(7)	124.94(17)
O(4)-C(8)-C(9)	115.91(17)
C(7)-C(8)-C(9)	119.15(17)
C(10)-C(9)-C(8)	120.79(18)
C(10)-C(9)-H(9)	119.6
C(8)-C(9)-H(9)	119.6
C(9)-C(10)-C(5)	121.17(17)
C(9)-C(10)-H(10)	119.4
C(5)-C(10)-H(10)	119.4
O(2)-C(11)-C(14)	107.97(15)
O(2)-C(11)-C(13)	106.69(15)
C(14)-C(11)-C(13)	110.57(16)
O(2)-C(11)-C(12)	102.51(15)
C(14)-C(11)-C(12)	114.90(16)
C(13)-C(11)-C(12)	113.42(16)
O(3)-C(12)-C(16)	108.12(17)
O(3)-C(12)-C(15)	106.64(15)

C(16)-C(12)-C(15)	110.79(18)
O(3)-C(12)-C(11)	102.50(15)
C(16)-C(12)-C(11)	114.41(16)
C(15)-C(12)-C(11)	113.60(17)
C(11)-C(13)-H(13A)	109.5
C(11)-C(13)-H(13B)	109.5
H(13A)-C(13)-H(13B)	109.5
C(11)-C(13)-H(13C)	109.5
H(13A)-C(13)-H(13C)	109.5
H(13B)-C(13)-H(13C)	109.5
C(11)-C(14)-H(14A)	109.5
C(11)-C(14)-H(14B)	109.5
H(14A)-C(14)-H(14B)	109.5
C(11)-C(14)-H(14C)	109.5
H(14A)-C(14)-H(14C)	109.5
H(14B)-C(14)-H(14C)	109.5
C(12)-C(15)-H(15A)	109.5
C(12)-C(15)-H(15B)	109.5
H(15A)-C(15)-H(15B)	109.5
C(12)-C(15)-H(15C)	109.5
H(15A)-C(15)-H(15C)	109.5
H(15B)-C(15)-H(15C)	109.5
C(12)-C(16)-H(16A)	109.5
C(12)-C(16)-H(16B)	109.5
H(16A)-C(16)-H(16B)	109.5
C(12)-C(16)-H(16C)	109.5
H(16A)-C(16)-H(16C)	109.5
H(16B)-C(16)-H(16C)	109.5
C(4)-C(17)-H(17A)	109.5
C(4)-C(17)-H(17B)	109.5
H(17A)-C(17)-H(17B)	109.5
C(4)-C(17)-H(17C)	109.5
H(17A)-C(17)-H(17C)	109.5
H(17B)-C(17)-H(17C)	109.5
O(4)-C(18)-H(18A)	109.5

O(4)-C(18)-H(18B)	109.5
H(18A)-C(18)-H(18B)	109.5
O(4)-C(18)-H(18C)	109.5
H(18A)-C(18)-H(18C)	109.5
H(18B)-C(18)-H(18C)	109.5
O(6)-B(2)-O(7)	113.00(17)
O(6)-B(2)-C(22)	122.77(17)
O(7)-B(2)-C(22)	123.63(17)
B(2)-O(6)-C(29)	107.17(15)
B(2)-O(7)-C(30)	107.25(15)
C(26)-O(8)-C(36)	116.93(15)
C(20)-C(19)-H(19A)	109.5
C(20)-C(19)-H(19B)	109.5
H(19A)-C(19)-H(19B)	109.5
C(20)-C(19)-H(19C)	109.5
H(19A)-C(19)-H(19C)	109.5
H(19B)-C(19)-H(19C)	109.5
O(5)-C(20)-C(19)	121.98(17)
O(5)-C(20)-C(21)	120.57(17)
C(19)-C(20)-C(21)	117.44(17)
C(20)-C(21)-C(22)	111.93(16)
C(20)-C(21)-H(21A)	109.2
C(22)-C(21)-H(21A)	109.2
C(20)-C(21)-H(21B)	109.2
C(22)-C(21)-H(21B)	109.2
H(21A)-C(21)-H(21B)	107.9
C(23)-C(22)-C(21)	113.03(16)
C(23)-C(22)-C(35)	107.48(15)
C(21)-C(22)-C(35)	109.08(16)
C(23)-C(22)-B(2)	106.11(14)
C(21)-C(22)-B(2)	109.21(16)
C(35)-C(22)-B(2)	111.95(15)
C(28)-C(23)-C(24)	116.71(17)
C(28)-C(23)-C(22)	124.52(17)
C(24)-C(23)-C(22)	118.76(17)

C(25)-C(24)-C(23)	122.64(18)
C(25)-C(24)-H(24)	118.7
C(23)-C(24)-H(24)	118.7
C(24)-C(25)-C(26)	119.54(18)
C(24)-C(25)-H(25)	120.2
C(26)-C(25)-H(25)	120.2
O(8)-C(26)-C(25)	124.54(18)
O(8)-C(26)-C(27)	116.41(17)
C(25)-C(26)-C(27)	119.06(17)
C(26)-C(27)-C(28)	120.61(17)
C(26)-C(27)-H(27)	119.7
C(28)-C(27)-H(27)	119.7
C(27)-C(28)-C(23)	121.44(18)
C(27)-C(28)-H(28)	119.3
C(23)-C(28)-H(28)	119.3
O(6)-C(29)-C(32)	107.71(16)
O(6)-C(29)-C(31)	107.64(15)
C(32)-C(29)-C(31)	110.43(17)
O(6)-C(29)-C(30)	102.40(15)
C(32)-C(29)-C(30)	115.14(16)
C(31)-C(29)-C(30)	112.82(16)
O(7)-C(30)-C(34)	106.71(15)
O(7)-C(30)-C(33)	107.93(15)
C(34)-C(30)-C(33)	110.22(17)
O(7)-C(30)-C(29)	102.40(15)
C(34)-C(30)-C(29)	113.87(16)
C(33)-C(30)-C(29)	114.92(16)
C(29)-C(31)-H(31A)	109.5
C(29)-C(31)-H(31B)	109.5
H(31A)-C(31)-H(31B)	109.5
C(29)-C(31)-H(31C)	109.5
H(31A)-C(31)-H(31C)	109.5
H(31B)-C(31)-H(31C)	109.5
C(29)-C(32)-H(32A)	109.5
C(29)-C(32)-H(32B)	109.5

H(32A)-C(32)-H(32B)	109.5
C(29)-C(32)-H(32C)	109.5
H(32A)-C(32)-H(32C)	109.5
H(32B)-C(32)-H(32C)	109.5
C(30)-C(33)-H(33A)	109.5
C(30)-C(33)-H(33B)	109.5
H(33A)-C(33)-H(33B)	109.5
C(30)-C(33)-H(33C)	109.5
H(33A)-C(33)-H(33C)	109.5
H(33B)-C(33)-H(33C)	109.5
C(30)-C(34)-H(34A)	109.5
C(30)-C(34)-H(34B)	109.5
H(34A)-C(34)-H(34B)	109.5
C(30)-C(34)-H(34C)	109.5
H(34A)-C(34)-H(34C)	109.5
H(34B)-C(34)-H(34C)	109.5
C(22)-C(35)-H(35A)	109.5
C(22)-C(35)-H(35B)	109.5
H(35A)-C(35)-H(35B)	109.5
C(22)-C(35)-H(35C)	109.5
H(35A)-C(35)-H(35C)	109.5
H(35B)-C(35)-H(35C)	109.5
O(8)-C(36)-H(36A)	109.5
O(8)-C(36)-H(36B)	109.5
H(36A)-C(36)-H(36B)	109.5
O(8)-C(36)-H(36C)	109.5
H(36A)-C(36)-H(36C)	109.5
H(36B)-C(36)-H(36C)	109.5

Symmetry transformations used to generate equivalent atoms:

Table 4. **Anisotropic displacement parameters ($Å^2$ x 10^3) for $C_{18}H_{27}BO_4$. The anisotropic**

displacement factor exponent takes the form: $-2\pi^2[h^2 a^{*2}U^{11} + ... + 2 h k a^* b^* U^{12}]$

	U^{11}	U^{22}	U^{33}	U^{23}	U^{13}	U^{12}
B(1)	16(1)	17(1)	11(1)	-1(1)	2(1)	0(1)
O(1)	27(1)	26(1)	19(1)	0(1)	4(1)	-2(1)
O(2)	13(1)	14(1)	21(1)	-1(1)	3(1)	-2(1)
O(3)	14(1)	14(1)	20(1)	1(1)	3(1)	0(1)
O(4)	20(1)	30(1)	17(1)	-1(1)	4(1)	1(1)
C(1)	31(1)	22(1)	24(1)	0(1)	-8(1)	-2(1)
C(2)	21(1)	14(1)	19(1)	-2(1)	-1(1)	2(1)
C(3)	16(1)	16(1)	18(1)	-1(1)	0(1)	-2(1)
C(4)	15(1)	15(1)	15(1)	0(1)	2(1)	1(1)
C(5)	15(1)	11(1)	17(1)	1(1)	2(1)	-1(1)
C(6)	13(1)	19(1)	22(1)	1(1)	3(1)	-1(1)
C(7)	15(1)	18(1)	18(1)	1(1)	-1(1)	0(1)
C(8)	21(1)	14(1)	16(1)	-1(1)	3(1)	1(1)
C(9)	14(1)	24(1)	23(1)	1(1)	5(1)	0(1)
C(10)	13(1)	20(1)	20(1)	1(1)	-1(1)	0(1)
C(11)	13(1)	15(1)	21(1)	-1(1)	3(1)	-3(1)
C(12)	16(1)	14(1)	21(1)	-1(1)	6(1)	-1(1)
C(13)	21(1)	23(1)	24(1)	-6(1)	8(1)	-2(1)
C(14)	21(1)	16(1)	33(1)	2(1)	3(1)	1(1)
C(15)	32(1)	24(1)	27(1)	3(1)	16(1)	0(1)
C(16)	15(1)	24(1)	36(1)	-5(1)	4(1)	-4(1)
C(17)	18(1)	17(1)	20(1)	-2(1)	1(1)	2(1)
C(18)	23(1)	29(1)	17(1)	-1(1)	1(1)	2(1)
B(2)	14(1)	18(1)	10(1)	0(1)	1(1)	1(1)
O(5)	22(1)	28(1)	18(1)	0(1)	0(1)	-7(1)
O(6)	12(1)	14(1)	17(1)	-2(1)	1(1)	0(1)
O(7)	13(1)	15(1)	19(1)	0(1)	2(1)	-1(1)
O(8)	21(1)	24(1)	15(1)	-1(1)	1(1)	0(1)
C(19)	18(1)	24(1)	18(1)	2(1)	4(1)	0(1)

C(20)	16(1)	17(1)	18(1)	3(1)	2(1)	1(1)
C(21)	18(1)	15(1)	16(1)	0(1)	3(1)	-1(1)
C(22)	15(1)	15(1)	16(1)	0(1)	0(1)	-1(1)
C(23)	16(1)	12(1)	17(1)	-1(1)	2(1)	1(1)
C(24)	13(1)	20(1)	20(1)	-4(1)	0(1)	-1(1)
C(25)	15(1)	18(1)	22(1)	-3(1)	5(1)	-2(1)
C(26)	22(1)	11(1)	17(1)	-1(1)	2(1)	2(1)
C(27)	15(1)	18(1)	20(1)	-2(1)	-1(1)	0(1)
C(28)	16(1)	15(1)	19(1)	-1(1)	3(1)	-1(1)
C(29)	12(1)	16(1)	20(1)	-2(1)	2(1)	-3(1)
C(30)	14(1)	15(1)	18(1)	-1(1)	5(1)	-2(1)
C(31)	19(1)	24(1)	22(1)	-9(1)	7(1)	-5(1)
C(32)	22(1)	16(1)	31(1)	1(1)	3(1)	1(1)
C(33)	12(1)	25(1)	31(1)	-6(1)	2(1)	-4(1)
C(34)	26(1)	25(1)	23(1)	3(1)	12(1)	2(1)
C(35)	17(1)	17(1)	23(1)	2(1)	1(1)	1(1)
C(36)	23(1)	43(1)	17(1)	0(1)	5(1)	1(1)

Table 5. **Hydrogen coordinates (x 10^4) and isotropic displacement parameters (Å^2 x 10^3) for $C_{18}H_{27}BO_4$**

	x	y	z	U(eq)
H(1A)	556	578	-2933	40
H(1B)	-854	596	-1974	40
H(1C)	242	-6	-2250	40
H(3A)	1625	52	-131	21

H(3B)	1205	733	68	21
H(6)	7183	522	2363	21
H(7)	7001	465	4236	21
H(9)	684	383	3507	24
H(10)	884	428	1641	22
H(13A)	6113	1935	2249	33
H(13B)	4186	2371	1881	33
H(13C)	6538	2610	1986	33
H(14A)	4900	2519	-937	35
H(14B)	5797	2968	24	35
H(14C)	3448	2730	-70	35
H(15A)	6936	1782	-1317	40
H(15B)	9379	1668	-918	40
H(15C)	8470	2323	-947	40
H(16A)	9367	1988	1935	38
H(16B)	9960	2450	1052	38
H(16C)	10874	1795	1084	38
H(17A)	5913	9	-469	28
H(17B)	5130	-384	466	28
H(17C)	7125	35	770	28
H(18A)	6209	33	5838	35
H(18B)	4932	348	6688	35
H(18C)	6146	735	5903	35
H(19A)	3898	8676	2033	30
H(19B)	5521	8643	3158	30
H(19C)	4366	9250	2785	30
H(21A)	3314	9193	4763	19
H(21B)	3809	8513	5021	19
H(24)	-2005	8571	6464	21
H(25)	-1769	8631	8364	22
H(27)	4391	9021	8594	22
H(28)	4133	8956	6690	20
H(31A)	-936	7390	2804	32
H(31B)	-1350	6702	2931	32
H(31C)	995	6950	3125	32

H(32A)	67	6638	5864	35
H(32B)	1602	6486	5001	35
H(32C)	-747	6241	4808	35
H(33A)	-4228	7289	3023	34
H(33B)	-5806	7435	3866	34
H(33C)	-4880	6785	3813	34
H(34A)	-2043	7353	6327	35
H(34B)	-3527	6822	5836	35
H(34C)	-4472	7470	5888	35
H(35A)	-1011	9230	3847	29
H(35B)	-132	9616	4908	29
H(35C)	-2110	9195	4923	29
H(36A)	-1222	9106	10012	41
H(36B)	243	8895	11115	41
H(36C)	-705	8422	10208	41

Table 6. **Torsion angles [º] for $C_{18}H_{27}BO_4$**

O(3)-B(1)-O(2)-C(11)	-10.68(19)
C(4)-B(1)-O(2)-C(11)	160.75(17)
O(2)-B(1)-O(3)-C(12)	-7.3(2)
C(4)-B(1)-O(3)-C(12)	-178.57(16)
O(1)-C(2)-C(3)-C(4)	-13.9(3)
C(1)-C(2)-C(3)-C(4)	167.75(17)
C(2)-C(3)-C(4)-C(17)	-68.5(2)
C(2)-C(3)-C(4)-C(5)	170.24(15)
C(2)-C(3)-C(4)-B(1)	54.4(2)
O(2)-B(1)-C(4)-C(3)	40.5(2)
O(3)-B(1)-C(4)-C(3)	-148.91(17)
O(2)-B(1)-C(4)-C(17)	162.44(16)
O(3)-B(1)-C(4)-C(17)	-26.9(2)
O(2)-B(1)-C(4)-C(5)	-79.8(2)
O(3)-B(1)-C(4)-C(5)	90.8(2)

C(3)-C(4)-C(5)-C(6)	178.10(16)
C(17)-C(4)-C(5)-C(6)	56.4(2)
B(1)-C(4)-C(5)-C(6)	-62.9(2)
C(3)-C(4)-C(5)-C(10)	-2.5(3)
C(17)-C(4)-C(5)-C(10)	-124.15(19)
B(1)-C(4)-C(5)-C(10)	116.5(2)
C(10)-C(5)-C(6)-C(7)	1.4(3)
C(4)-C(5)-C(6)-C(7)	-179.12(17)
C(5)-C(6)-C(7)-C(8)	-1.0(3)
C(18)-O(4)-C(8)-C(7)	-1.0(3)
C(18)-O(4)-C(8)-C(9)	178.41(17)
C(6)-C(7)-C(8)-O(4)	179.43(18)
C(6)-C(7)-C(8)-C(9)	0.0(3)
O(4)-C(8)-C(9)-C(10)	-179.06(18)
C(7)-C(8)-C(9)-C(10)	0.4(3)
C(8)-C(9)-C(10)-C(5)	0.1(3)
C(6)-C(5)-C(10)-C(9)	-1.0(3)
C(4)-C(5)-C(10)-C(9)	179.59(18)
B(1)-O(2)-C(11)-C(14)	144.16(16)
B(1)-O(2)-C(11)-C(13)	-96.98(17)
B(1)-O(2)-C(11)-C(12)	22.46(17)
B(1)-O(3)-C(12)-C(16)	141.73(16)
B(1)-O(3)-C(12)-C(15)	-99.09(18)
B(1)-O(3)-C(12)-C(11)	20.54(18)
O(2)-C(11)-C(12)-O(3)	-25.86(17)
C(14)-C(11)-C(12)-O(3)	-142.70(16)
C(13)-C(11)-C(12)-O(3)	88.76(18)
O(2)-C(11)-C(12)-C(16)	-142.63(16)
C(14)-C(11)-C(12)-C(16)	100.5(2)
C(13)-C(11)-C(12)-C(16)	-28.0(2)
O(2)-C(11)-C(12)-C(15)	88.78(18)
C(14)-C(11)-C(12)-C(15)	-28.1(2)
C(13)-C(11)-C(12)-C(15)	-156.60(18)
O(7)-B(2)-O(6)-C(29)	11.0(2)
C(22)-B(2)-O(6)-C(29)	-177.57(16)

O(6)-B(2)-O(7)-C(30)	7.9(2)
C(22)-B(2)-O(7)-C(30)	-163.45(16)
O(5)-C(20)-C(21)-C(22)	-13.6(3)
C(19)-C(20)-C(21)-C(22)	167.42(16)
C(20)-C(21)-C(22)-C(23)	170.82(15)
C(20)-C(21)-C(22)-C(35)	-69.69(19)
C(20)-C(21)-C(22)-B(2)	52.9(2)
O(6)-B(2)-C(22)-C(23)	-79.6(2)
O(7)-B(2)-C(22)-C(23)	90.93(19)
O(6)-B(2)-C(22)-C(21)	42.5(2)
O(7)-B(2)-C(22)-C(21)	-146.95(17)
O(6)-B(2)-C(22)-C(35)	163.41(17)
O(7)-B(2)-C(22)-C(35)	-26.0(2)
C(21)-C(22)-C(23)-C(28)	6.6(3)
C(35)-C(22)-C(23)-C(28)	-113.9(2)
B(2)-C(22)-C(23)-C(28)	126.21(19)
C(21)-C(22)-C(23)-C(24)	-174.58(17)
C(35)-C(22)-C(23)-C(24)	65.0(2)
B(2)-C(22)-C(23)-C(24)	-54.9(2)
C(28)-C(23)-C(24)-C(25)	0.7(3)
C(22)-C(23)-C(24)-C(25)	-178.24(17)
C(23)-C(24)-C(25)-C(26)	-0.1(3)
C(36)-O(8)-C(26)-C(25)	-3.4(3)
C(36)-O(8)-C(26)-C(27)	176.51(18)
C(24)-C(25)-C(26)-O(8)	179.57(18)
C(24)-C(25)-C(26)-C(27)	-0.4(3)
O(8)-C(26)-C(27)-C(28)	-179.71(17)
C(25)-C(26)-C(27)-C(28)	0.2(3)
C(26)-C(27)-C(28)-C(23)	0.4(3)
C(24)-C(23)-C(28)-C(27)	-0.8(3)
C(22)-C(23)-C(28)-C(27)	178.04(17)
B(2)-O(6)-C(29)-C(32)	-145.40(16)
B(2)-O(6)-C(29)-C(31)	95.51(18)
B(2)-O(6)-C(29)-C(30)	-23.61(17)
B(2)-O(7)-C(30)-C(34)	98.05(17)

B(2)-O(7)-C(30)-C(33)	-143.50(16)
B(2)-O(7)-C(30)-C(29)	-21.85(17)
O(6)-C(29)-C(30)-O(7)	27.29(16)
C(32)-C(29)-C(30)-O(7)	143.86(16)
C(31)-C(29)-C(30)-O(7)	-88.13(18)
O(6)-C(29)-C(30)-C(34)	-87.49(18)
C(32)-C(29)-C(30)-C(34)	29.1(2)
C(31)-C(29)-C(30)-C(34)	157.09(17)
O(6)-C(29)-C(30)-C(33)	144.02(16)
C(32)-C(29)-C(30)-C(33)	-99.4(2)
C(31)-C(29)-C(30)-C(33)	28.6(2)

Symmetry transformations used to generate equivalent atoms:

■ **NMR Spectra**

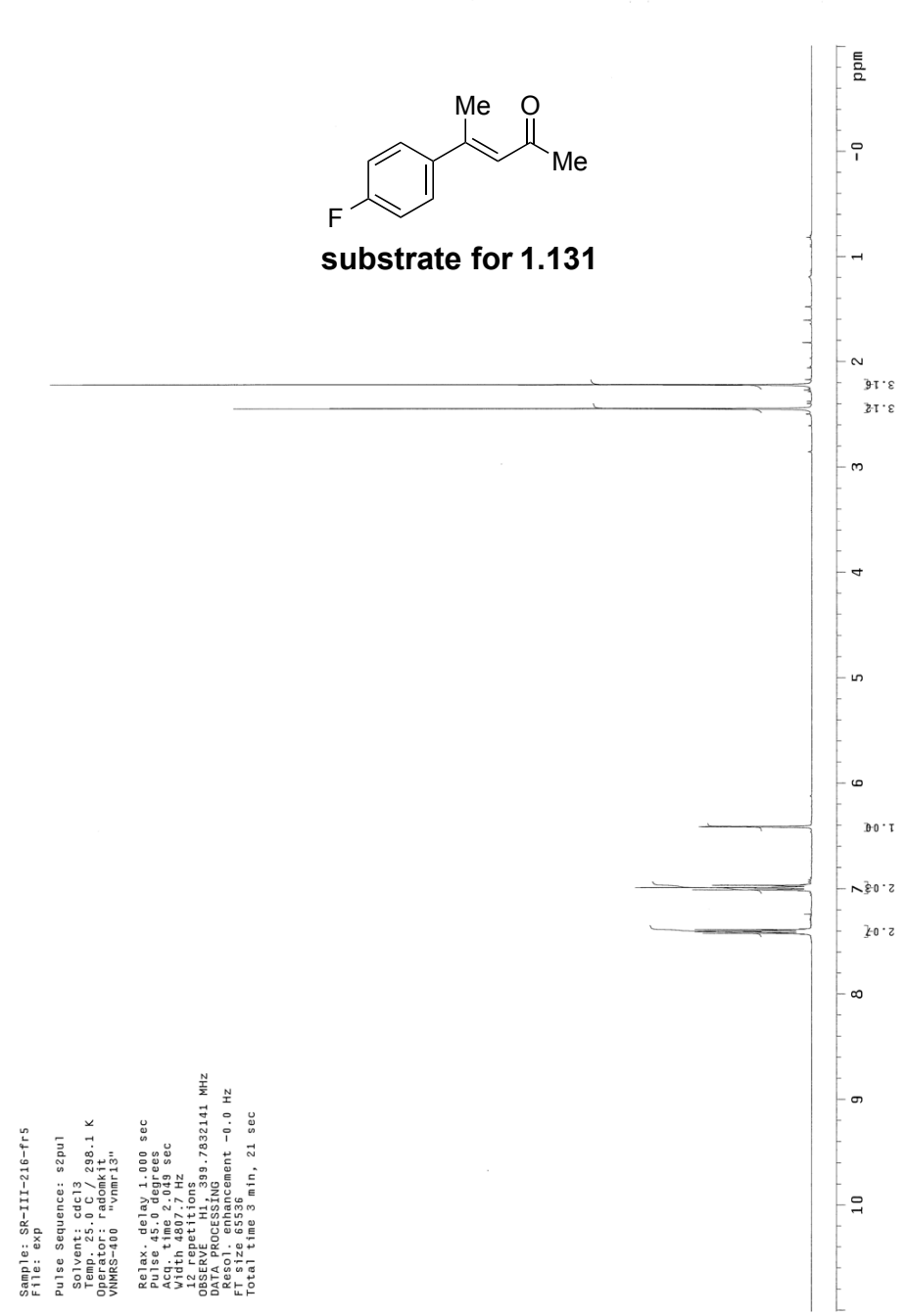
Me
O
Me
F
substrate for 1.131
Sample: SR-III-216-fr5
File: exp
Pulse Sequence: s2pul
Solvent: cdcl3
Temp. 25.0 C / 298.1 K
Operator: radomkit
VNMRS-400 "vnmr13"
Relax. delay 1.000 sec
Pulse 45.0 degrees
Acq. time 2.049 sec
Width 4807.7 Hz
32 repetitions
OBSERVE H1, 399.7832141 MHz
DATA PROCESSING
Resol. enhancement -0.0 Hz
FT size 65536
Total time 3 min, 21 sec
ppm
3.16
3.12
1.04
2.03
2.07

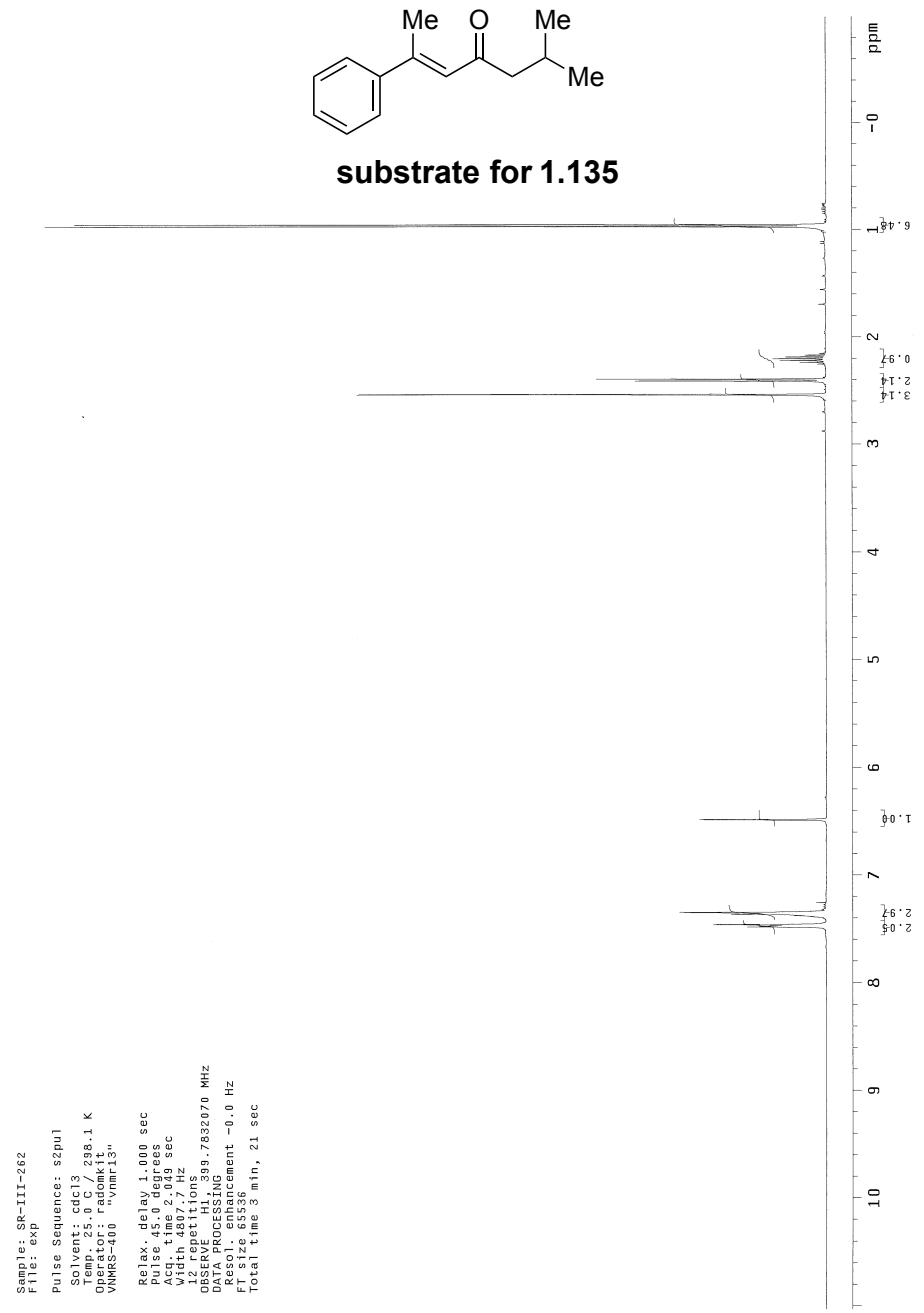
Me
O
Me
Me
substrate for 1.135
Sample: SR-III-262
File: exp
Pulse Sequence: s2pul
Solvent: cdcl3
Temp. 25.0 C / 298.1 K
Operator: radomkit
VNMRS-400 "vnmr13"
Relax. delay 1.000 sec
Pulse 45.0 degrees
Acq. time 2.049 sec
Width 4807.7 Hz
12 repetitions
OBSERVE H1, 399.7832070 MHz
DATA PROCESSING
Resol enhancement -0.0 Hz
FT size 65536
Total time 3 min, 21 sec
ppm
6.48
0.97
2.14
3.14
1.00
2.97
2.05

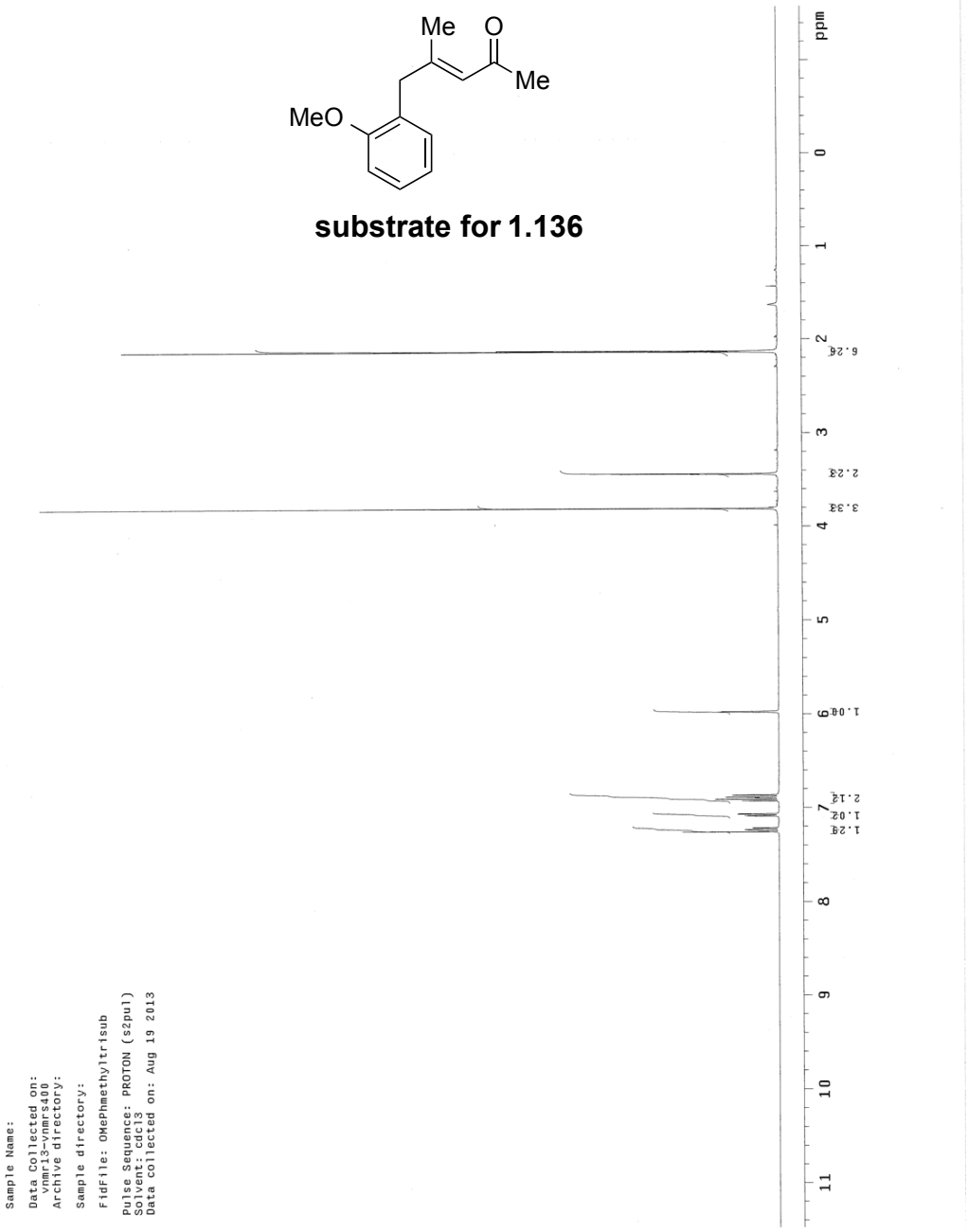
Me
O
Me
MeO
substrate for 1.136
ppm
6.26
2.23
3.33
1.00
2.14
1.02
1.29
Sample Name:
Data Collected on:
vnmr13-vnmrs400
Archive directory:
Sample directory:
FidFile: OMePhmethyltrisub
Pulse Sequence: PROTON (s2pul)
Solvent: cdcl3
Data collected on: Aug 19 2013

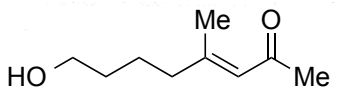

substrate for 1.137

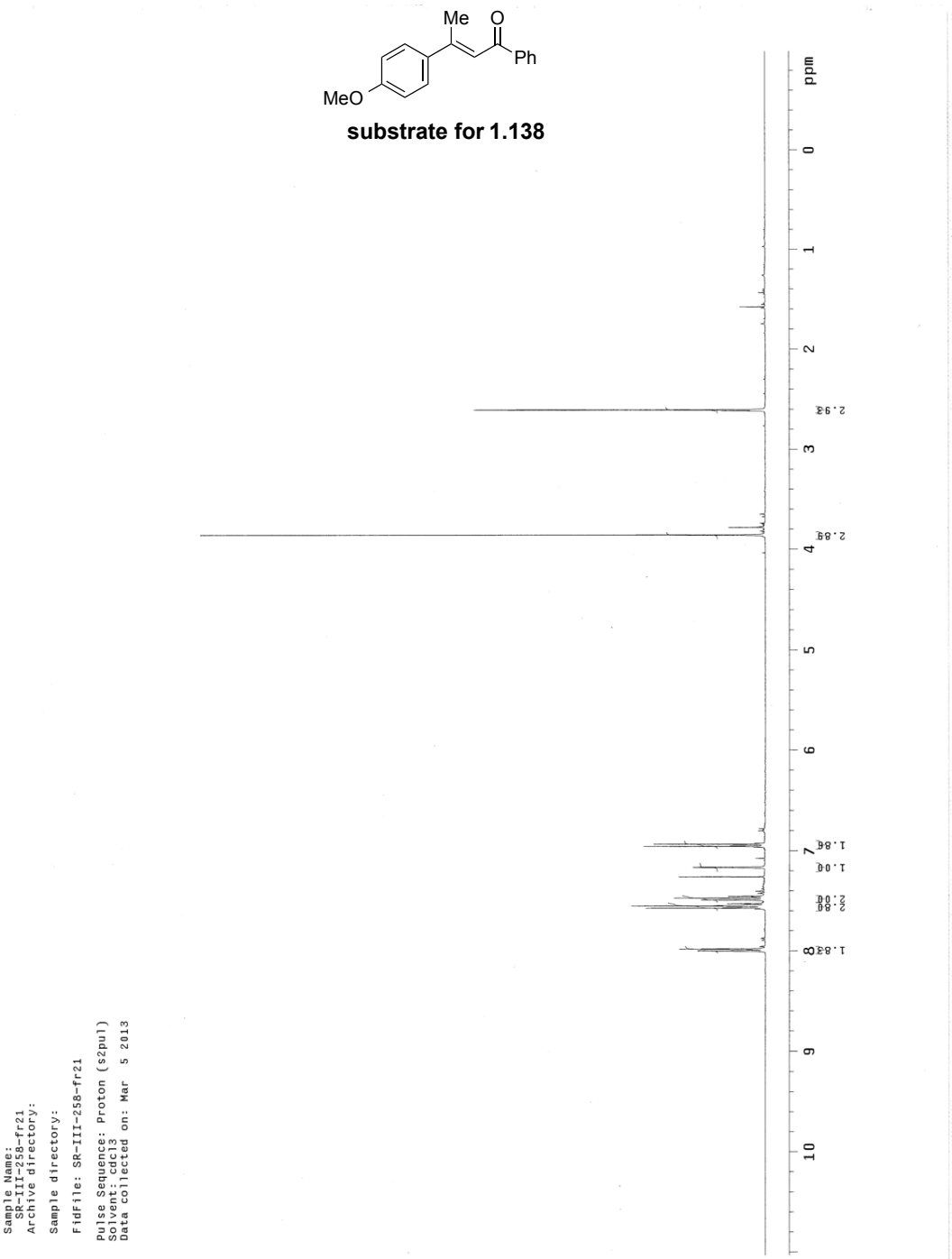
Me
O
Ph
MeO
substrate for 1.138
ppm
0
1
2
3
4
5
6
7
8
9
10
2.93
2.89
1.86
1.00
2.00
2.00
1.83
Sample Name:
SR-III-258-fr21
Archive directory:
Sample directory:
FidFile: SR-III-258-fr21
Pulse Sequence: Proton (s2pul)
Solvent: cdcl3
Data collected on: Mar 5 2013

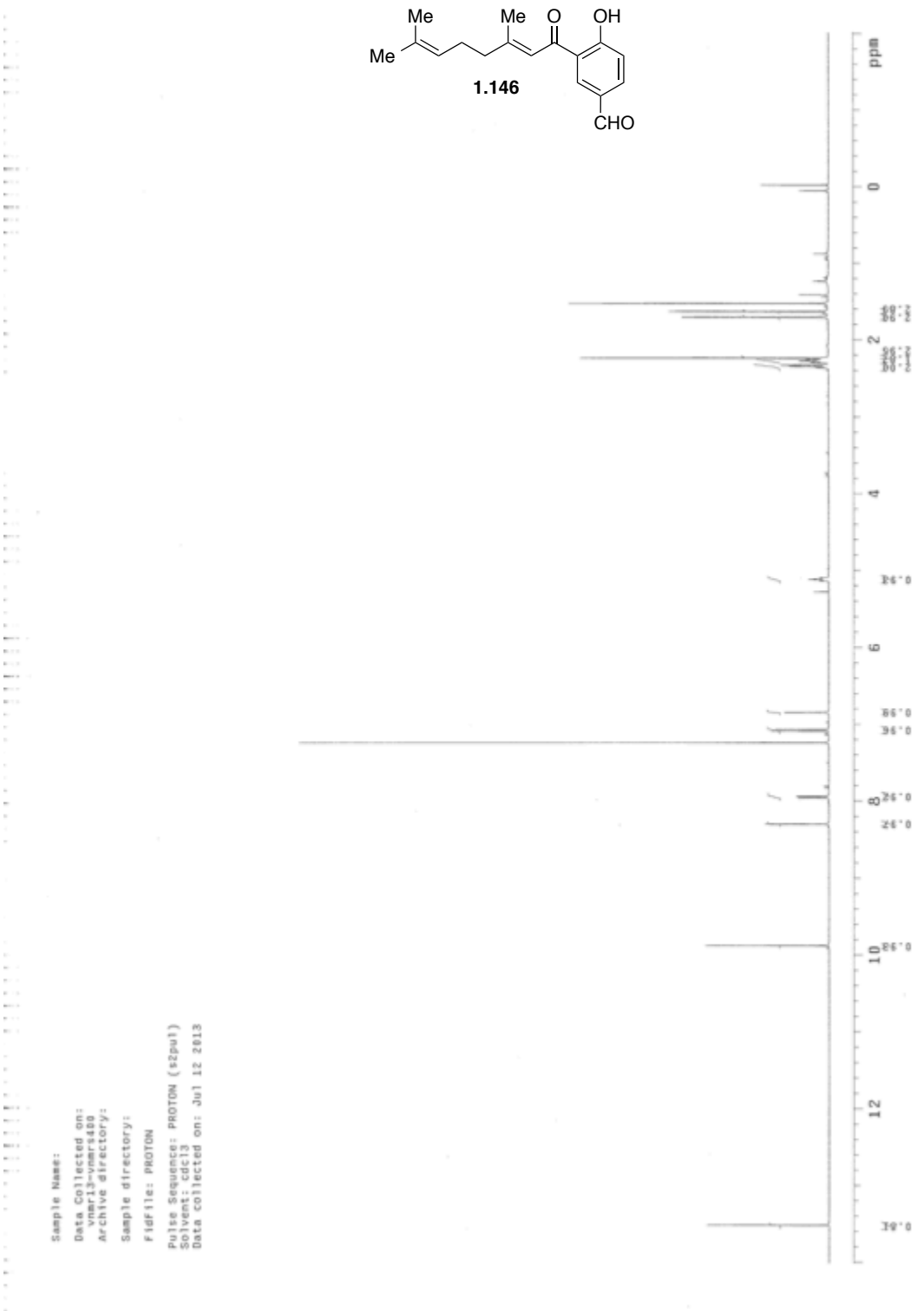
Me
Me
Me
O
OH
CHO
1.146
Sample Name:
Data Collected on:
vnmr13-vnmrs400
Archive directory:
Sample directory:
FidFile: PROTON
Pulse Sequence: PROTON (s2pul)
Solvent: cdcl3
Data collected on: Jul 12 2013
ppm
0
2
4
6
8
10
12

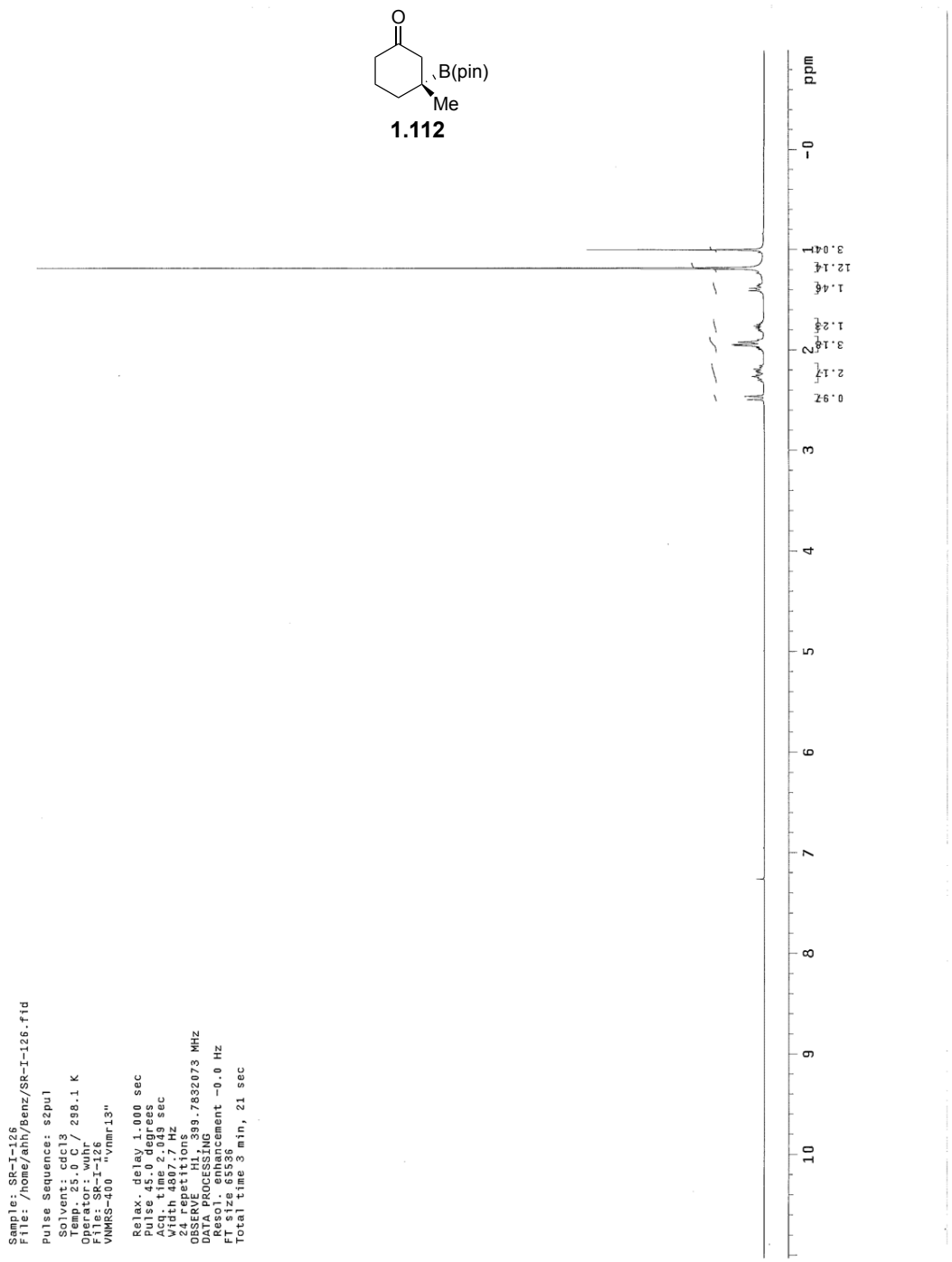
O
B(pin)
Me
1.112
Sample: SR-I-126
File: /home/anh/Benz/SR-I-126.fid
Pulse Sequence: s2pul
Solvent: cdcl3
Temp: 25.0 C / 298.1 K
Operator: whhr
File: SR-I-126
VNMRS-400 "vnmr13"
Relax. delay 1.000 sec
Pulse 45.0 degrees
Acq. time 2.048 sec
Width 4807.7 Hz
24 repetitions
OBSERVE H1, 399.7832073 MHz
DATA PROCESSING
Resol. enhancement -0.0 Hz
FT size 65536
Total time 3 min, 21 sec
ppm
10
9
8
7
6
5
4
3
2
1
-0
3.041
12.14
1.46
1.24
3.14
2.17
0.92

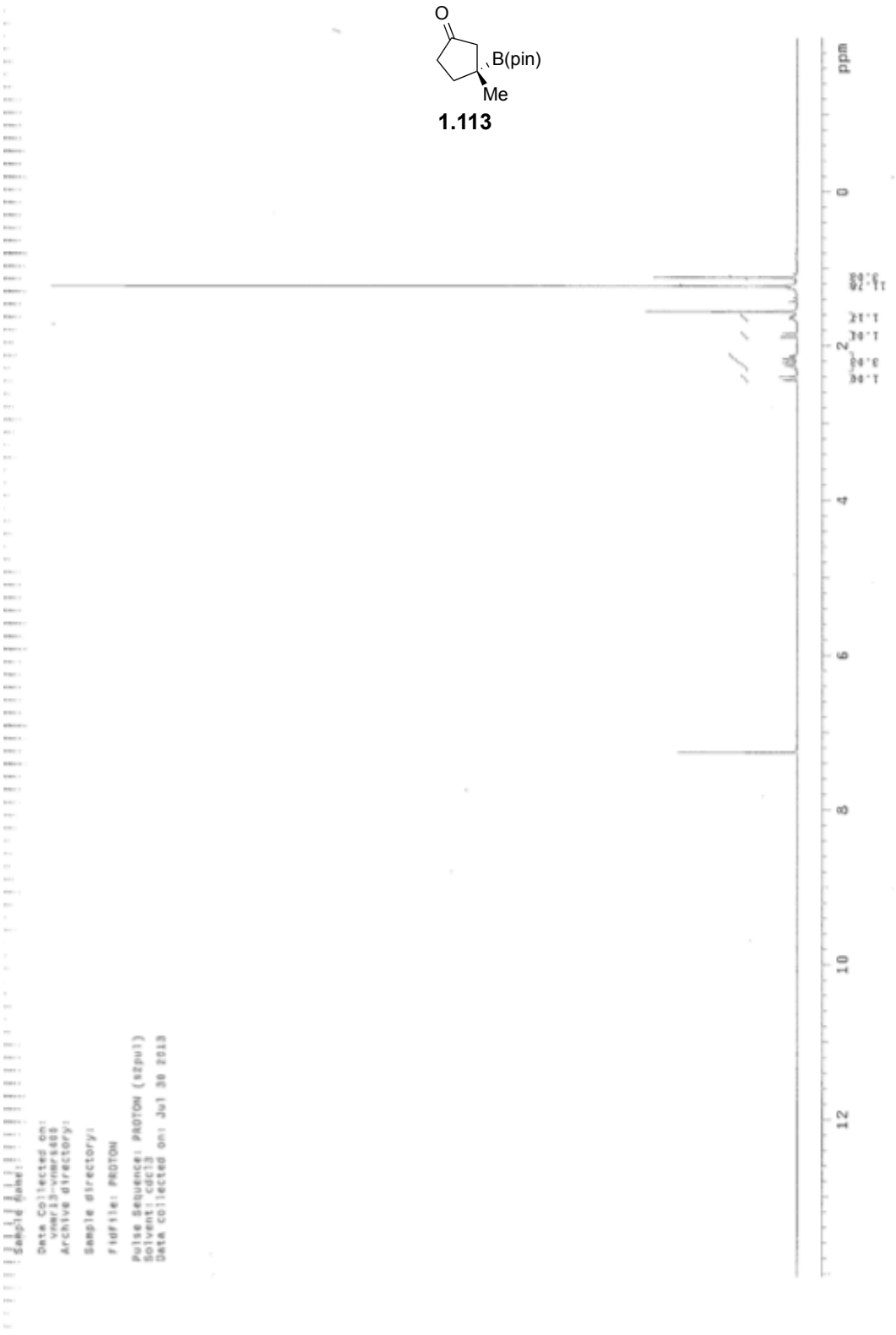
O
B(pin)
Me
1.113
ppm
0
2
4
6
8
10
12
Sample Name:
Data Collected on:
vnmrj3-vnmrs600
Archive directory:
Sample directory:
FidFile: PROTON
Pulse Sequence: PROTON (s2pul)
Solvent: cdcl3
Data collected on: Jul 30 2018

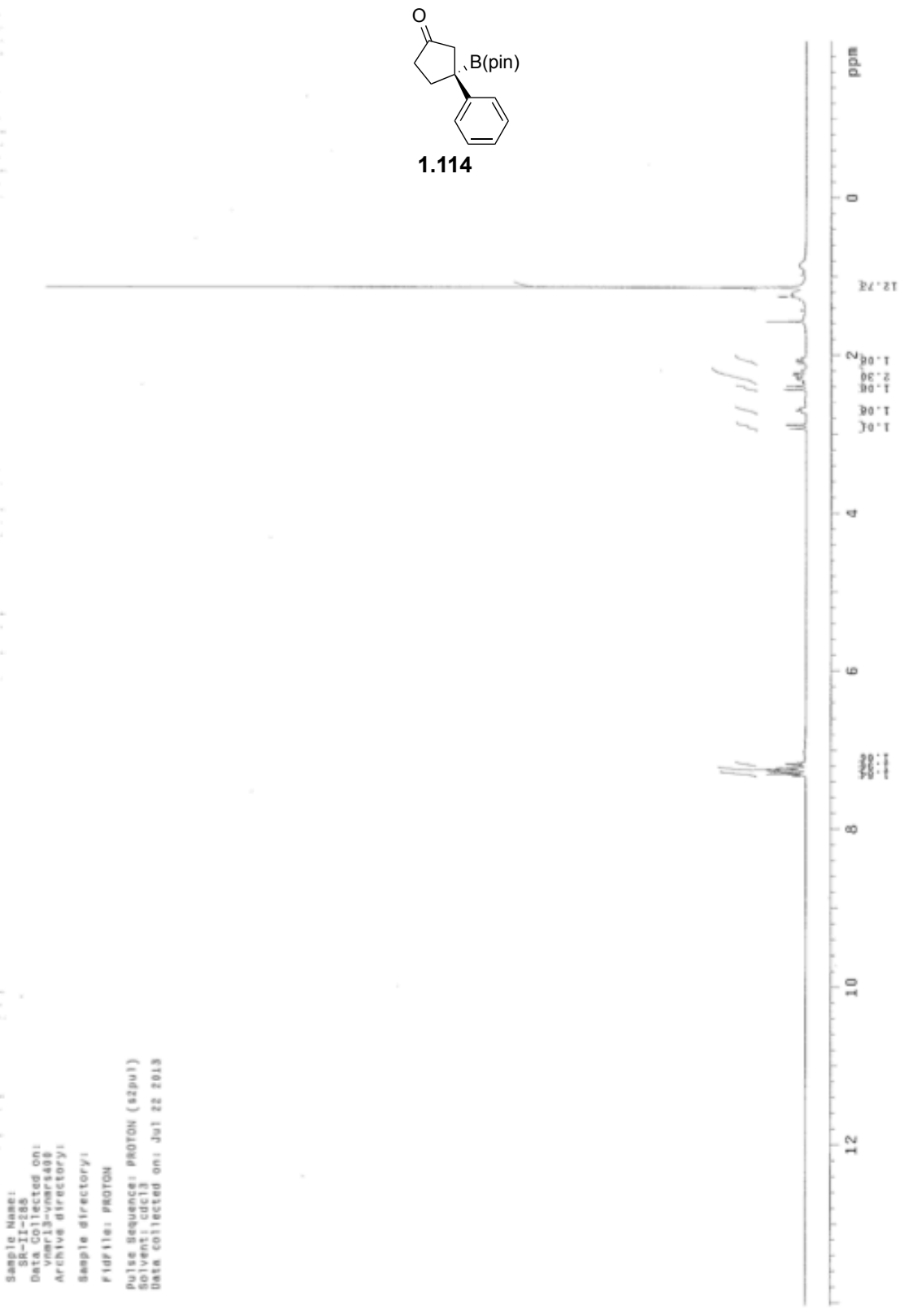
O
B(pin)
1.114
Sample Name:
SR-II-288
Data Collected on:
vnmr13-vnmrs400
Archive directory:
Sample directory:
Fidfile: PROTON
Pulse Sequence: PROTON (s2pul)
Solvent: cdcl3
Data collected on: Jul 22 2013
ppm
12.74
2.30
1.08
1.06

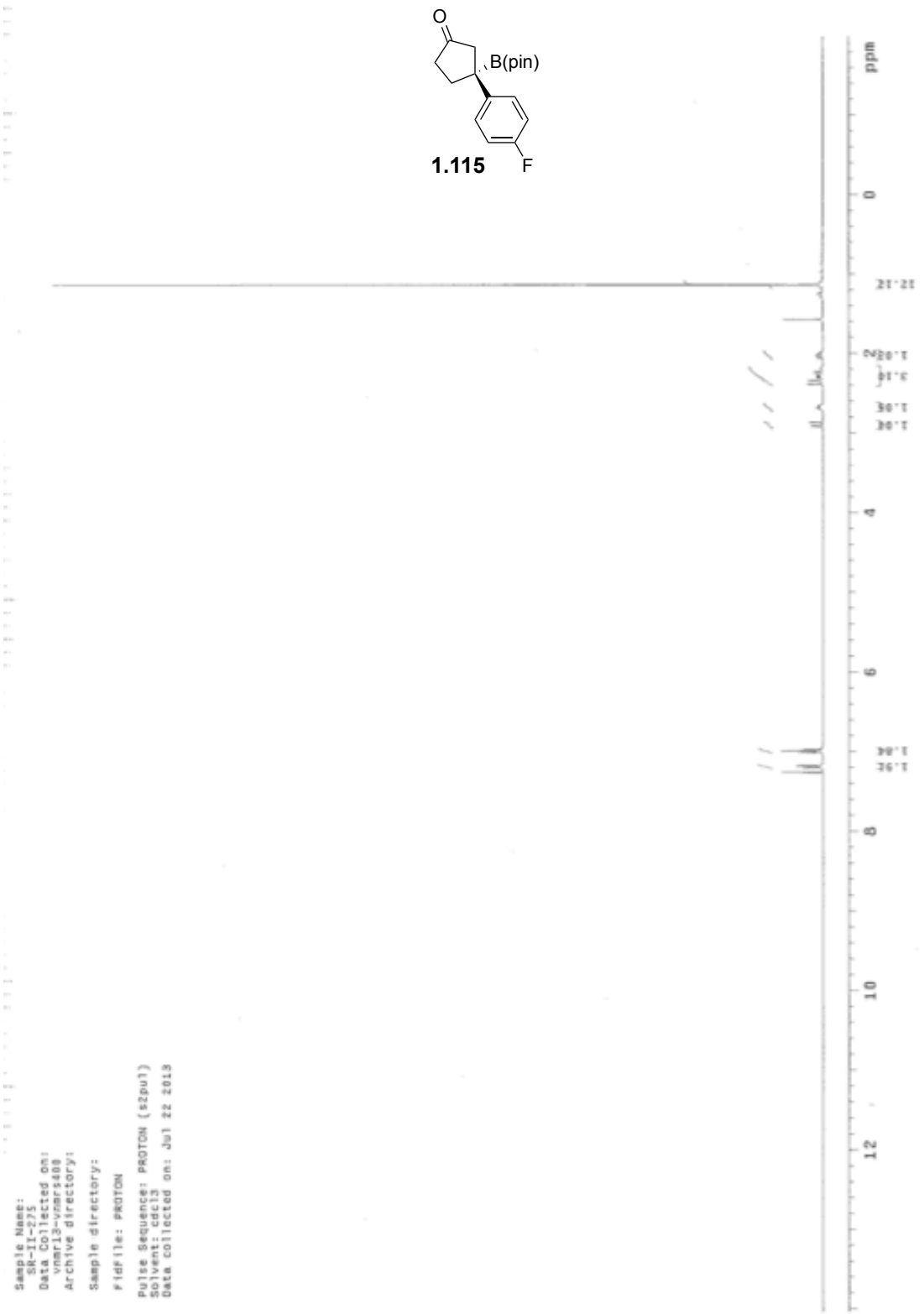
O
B(pin)
F
1.115
ppm
0
2
4
6
8
10
12
Sample Name:
SR-II-275
Data Collected on:
vnmr13-vmars400
Archive directory:
Sample directory:
Fidfile: PROTON
Pulse Sequence: PROTON (s2pul)
Solvent: cdcl3
Data collected on: Jul 22 2013

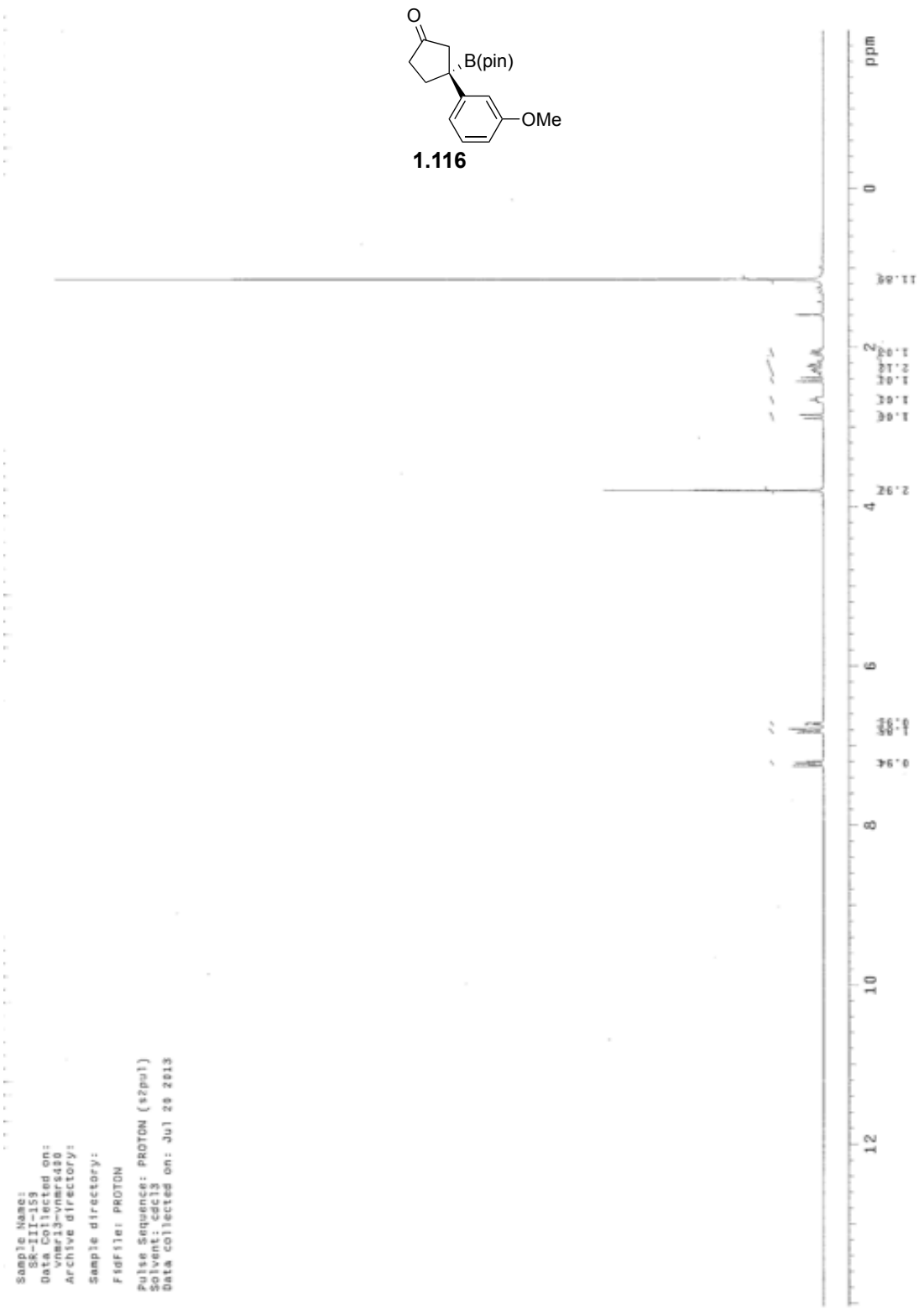
O
B(pin)
OMe
1.116
Sample Name:
SR-III-159
Data Collected on:
vnmr13-vnmrs400
Archive directory:
Sample directory:
FidFile: PROTON
Pulse Sequence: PROTON (s2pul)
Solvent: cdcl3
Data collected on: Jul 29 2013
ppm
0
2
4
6
8
10
12

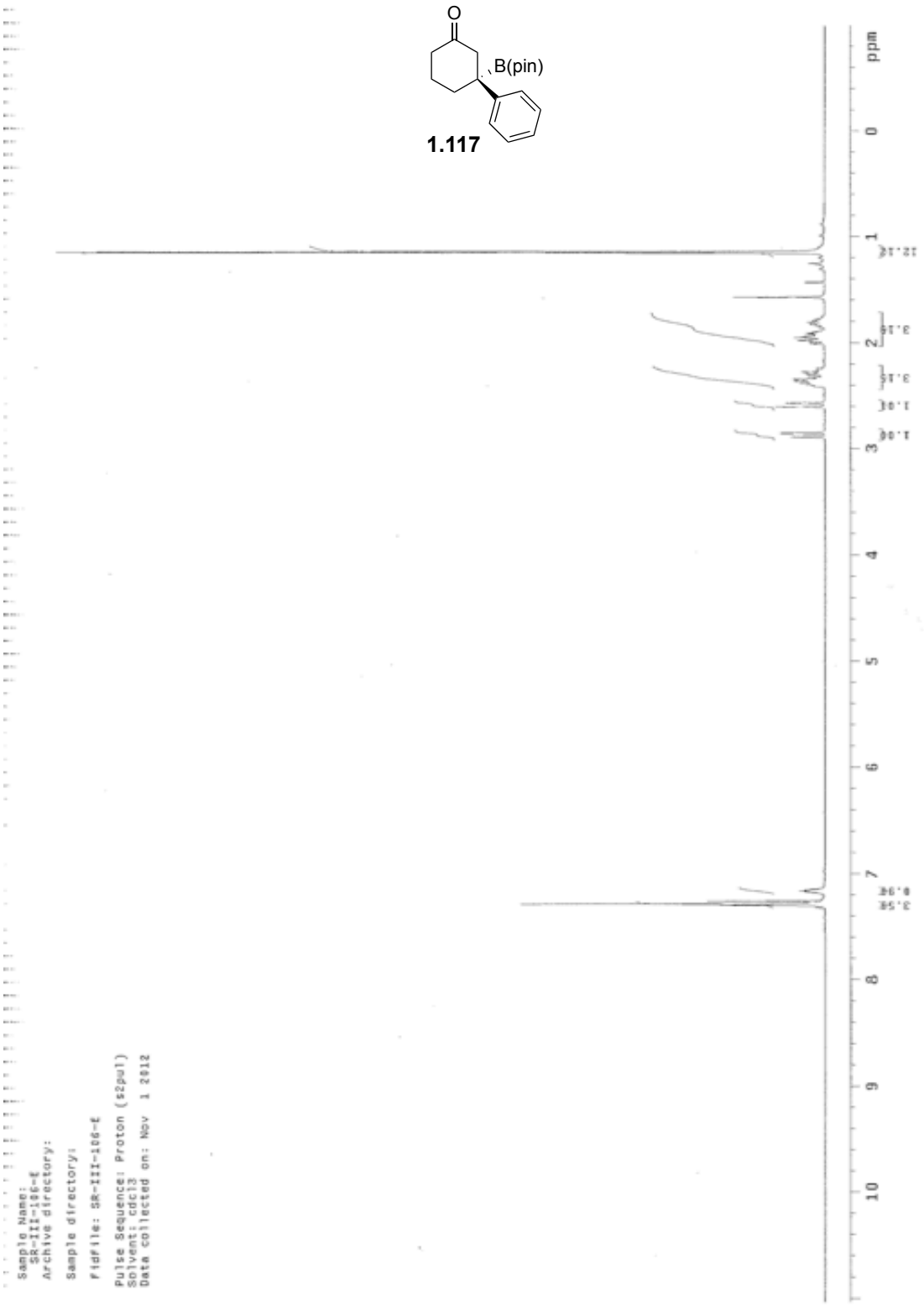
O
B(pin)
1.117
Sample Name:
SR-III-186-E
Archive directory:
Sample directory:
Fidfile: SR-III-186-E
Pulse Sequence: Proton (s2pul)
Solvent: cdcl3
Data collected on: Nov 1 2012
ppm

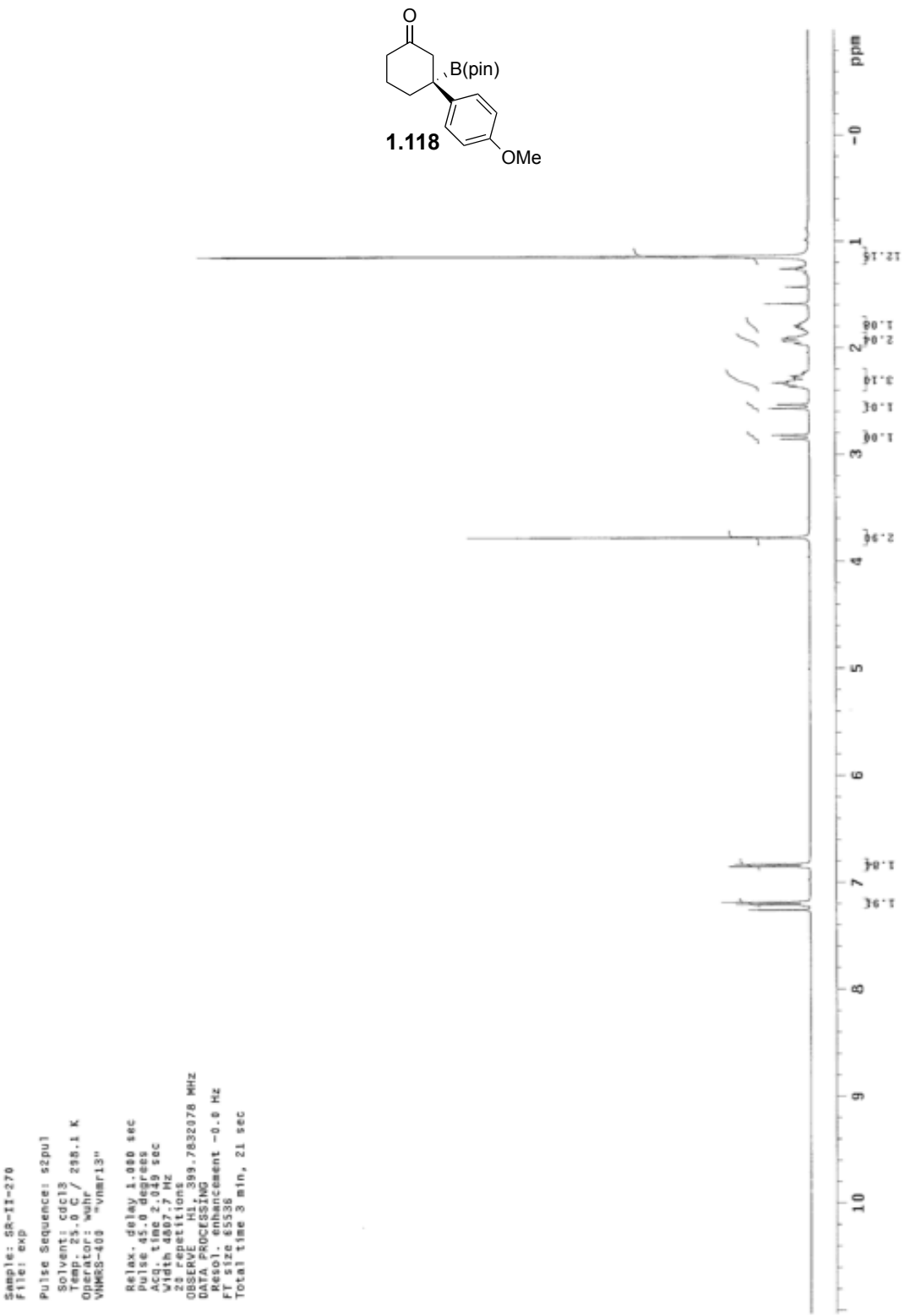
O
B(pin)
1.118
OMe
Sample: SR-II-270
File: exp
Pulse Sequence: s2pul
Solvent: cdcl3
Temp: 25.0 C / 298.1 K
Operator: wuhr
VNMRS-400 "vnmr13"
Relax. delay 1.000 sec
Pulse 45.0 degrees
Acq. time 2.049 sec
Width 4807.7 Hz
28 repetitions
OBSERVE H1, 399.7832078 MHz
DATA PROCESSING
Resol. enhancement -0.0 Hz
FT size 65536
Total time 3 min, 21 sec
ppm

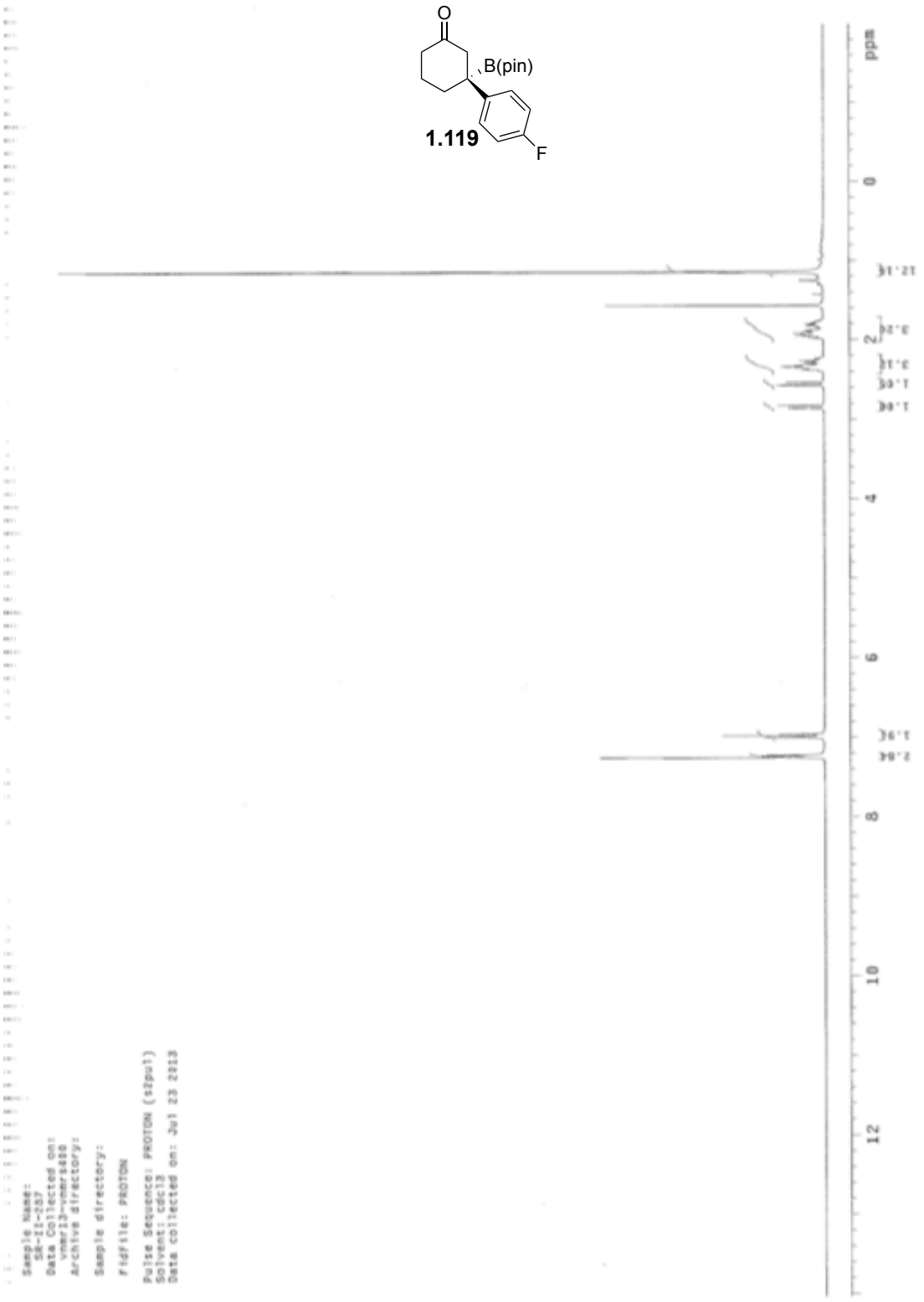
O
B(pin)
F
1.119
ppm
0
2
4
6
8
10
12
31.21
3.26
3.16
3.01
3.00
1.96
2.04
Sample Name:
SR-11-207
Data Collected on:
vnmr13-nmrs400
Archive directory:
Sample directory:
Fidfile: PROTON
Pulse Sequence: PROTON (s2pul)
Solvent: cdcl3
Data collected on: Jul 23 2018

O
B(pin)
CF3

1.120

Sample Name:
Data Collected on:
vnmrj3-vnmr1400
Archive directory:
Sample directory:
FidFile: PROTON
Pulse Sequence: PROTON (s2pul)
Solvent: cdcl3
Data collected on: Aug 7 2013
ppm
0
2
4
6
8
10
12

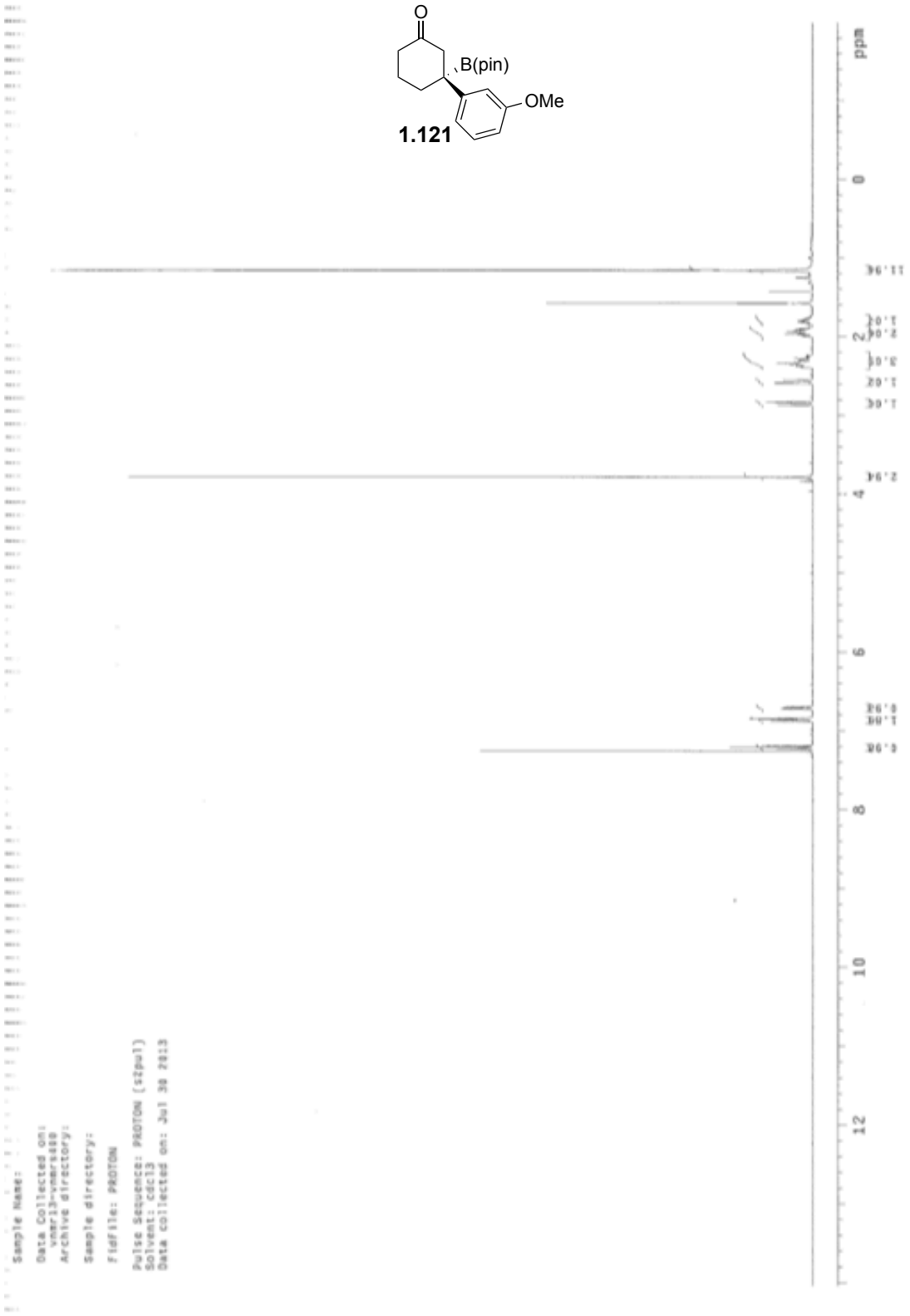
O
B(pin)
OMe
1.121
ppm
0
2
4
6
8
10
12
Sample Name:
Data Collected on:
vnmrj3-vnmrs400
Archive directory:
Sample directory:
FidFile: PROTON
Pulse Sequence: PROTON (s2pul)
Solvent: cdcl3
Data collected on: Jul 30 2013

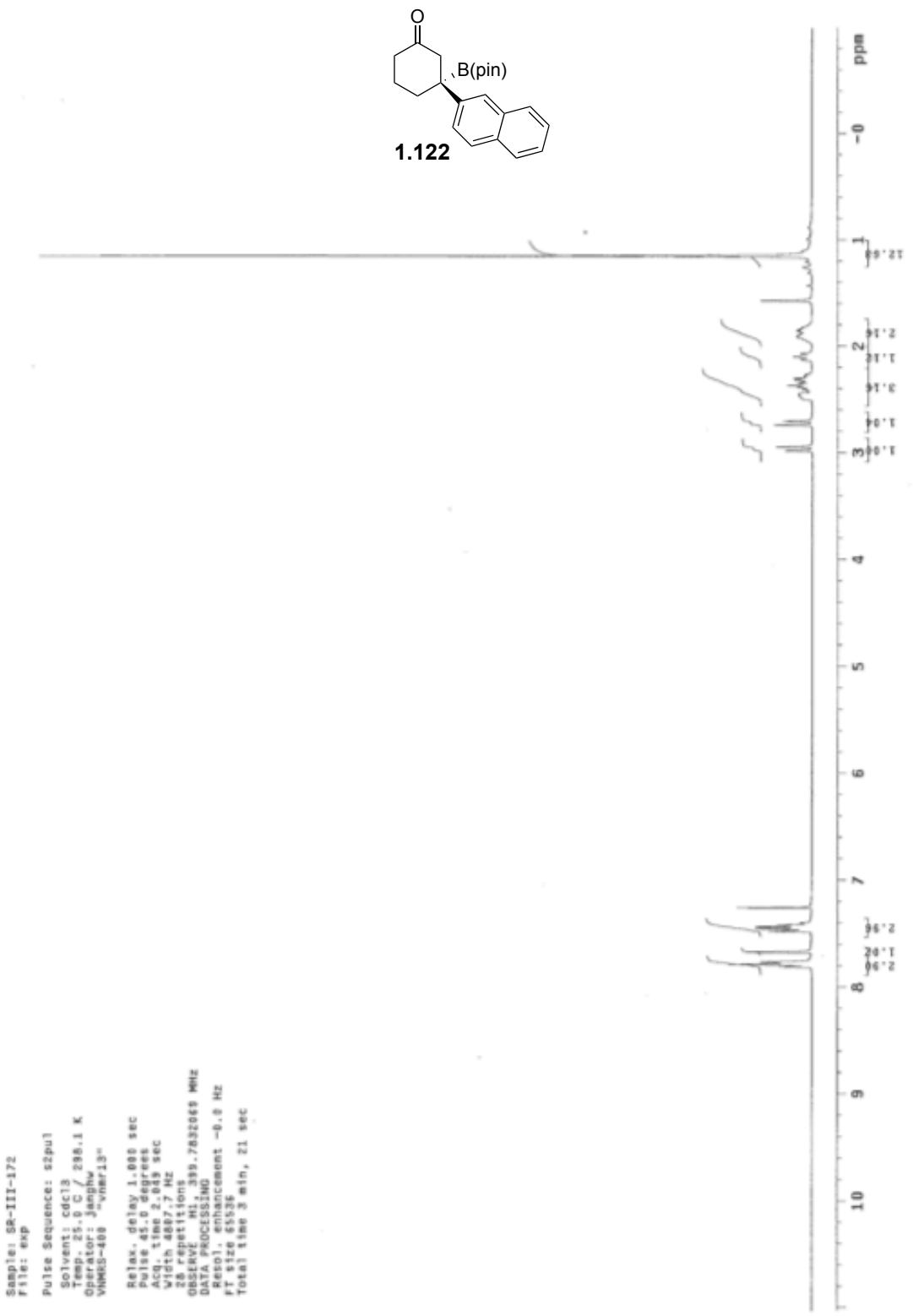
O
B(pin)
1.122
Sample: SR-III-172
File: exp
Pulse Sequence: s2pul
Solvent: cdcl3
Temp. 25.0 C / 298.1 K
Operator: Jamphw
VNMRS-400 "vmr13"
Relax. delay 1.000 sec
Pulse 45.0 degrees
Acq. time 2.049 sec
Width 4807.7 Hz
28 repetitions
OBSERVE H1, 399.7832069 MHz
DATA PROCESSING
Resol. enhancement -0.0 Hz
FT size 65536
Total time 3 min, 21 sec
ppm

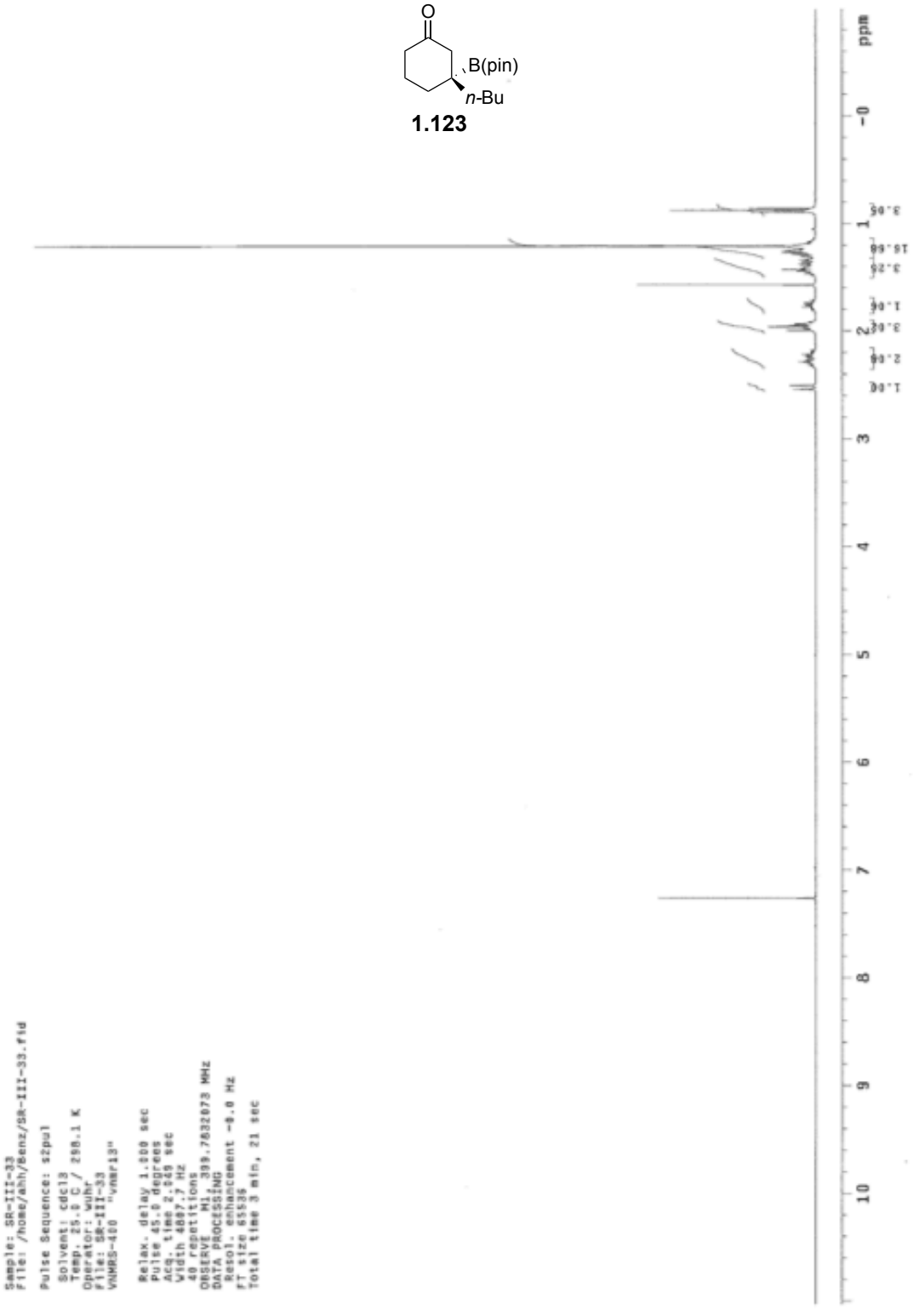
O
B(pin)
n-Bu
1.123
Sample: SR-III-33
File: /home/ahh/Benz/SR-III-33.fid
Pulse Sequence: s2pul
Solvent: cdcl3
Temp. 25.0 C / 298.1 K
Operator: wuhr
File: SR-III-33
VNMRS-400 "vmar13"
Relax. delay 1.800 sec
Pulse 45.0 degrees
Acq. time 2.849 sec
Width 4887.7 Hz
40 repetitions
OBSERVE H1, 399.7832673 MHz
DATA PROCESSING
Resol. enhancement -0.0 Hz
FT size 65536
Total time 3 min, 21 sec
ppm
3.06
16.66
3.25
1.00
3.02
2.00
1.00

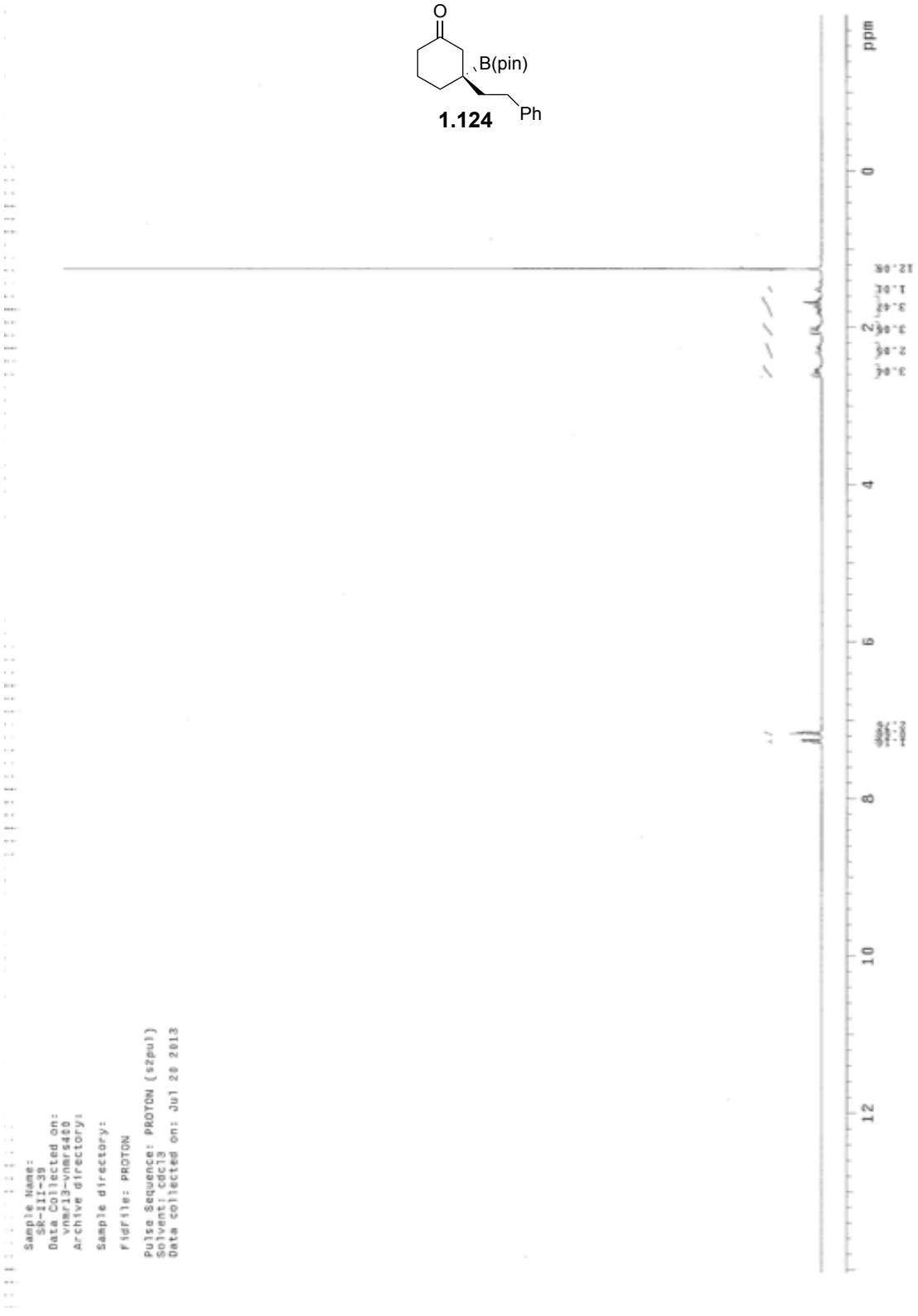
O
B(pin)
Ph
1.124
Sample Name:
SR-III-39
Data Collected on:
vnmr13-vnmrs400
Archive directory:
Sample directory:
FidFile: PROTON
Pulse Sequence: PROTON (s2pul)
Solvent: cdcl3
Data collected on: Jul 28 2013
ppm
0
2
4
6
8
10
12

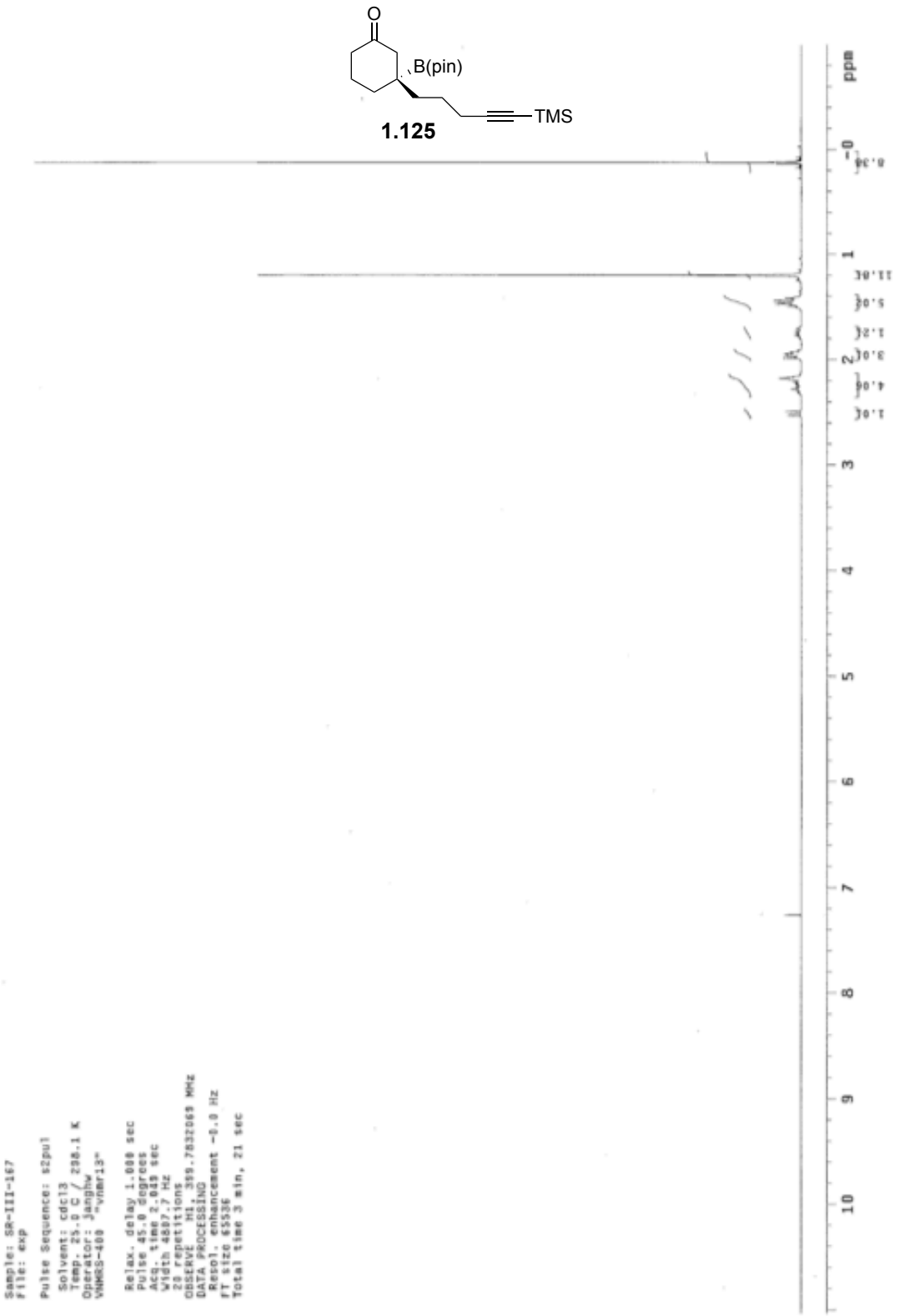
O
B(pin)
TMS
1.125
Sample: SR-III-167
File: exp
Pulse Sequence: s2pul
Solvent: cdcl3
Temp. 25.0 C / 298.1 K
Operator: janghw
VNMRS-400 "vnmr13"
Relax. delay 1.000 sec
Pulse 45.0 degrees
Acq. time 2.048 sec
Width 4887.7 Hz
20 repetitions
observe H1 399.7832069 MHz
DATA PROCESSING
Resol. enhancement -0.0 Hz
FT size 65536
Total time 3 min, 21 sec
ppm

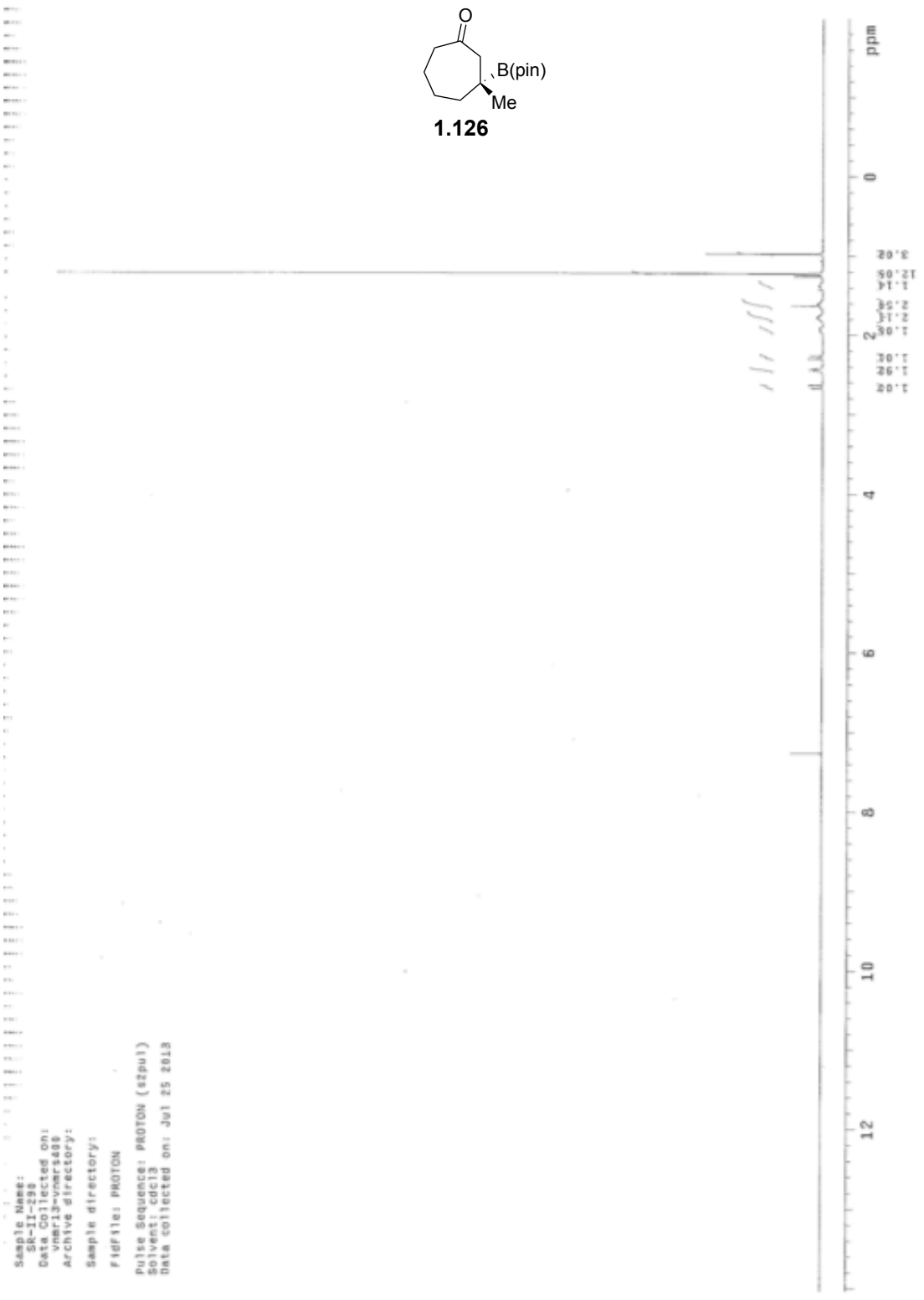
O
B(pin)
Me
1.126
Sample Name:
SR-II-298
Data Collected on:
vnmrj3-vnmrs400
Archive directory:
Sample directory:
FidFile: PROTON
Pulse Sequence: PROTON (s2pul)
Solvent: cdcl3
Data collected on: Jul 25 2018
ppm
0
2
4
6
8
10
12
3.02
12.05
1.14
2.14
2.04
1.00
1.92
1.00

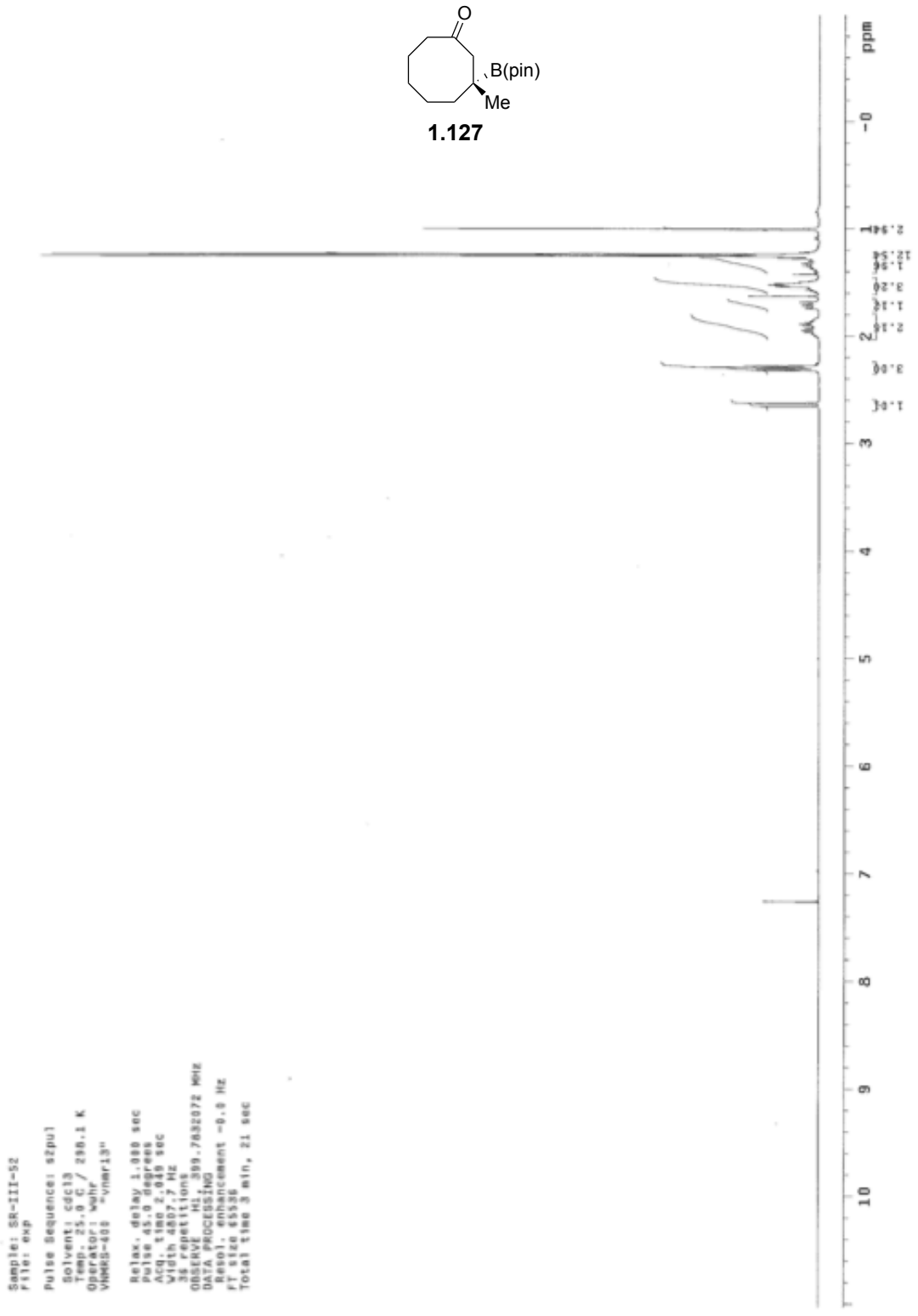
O
B(pin)
Me
1.127
ppm
Sample: SR-III-52
File: exp
Pulse Sequence: s2pul
Solvent: cdcl3
Temp: 25.0 C / 298.1 K
Operator: wohr
VNMRS-400 "vnmr13"
Relax. delay 1.000 sec
Pulse 45.0 degrees
Acq. time 2.049 sec
Width 4807.7 Hz
36 repetitions
OBSERVE H1, 399.7832072 MHz
DATA PROCESSING
Resol. enhancement -0.8 Hz
FT size 65536
Total time 3 min, 21 sec

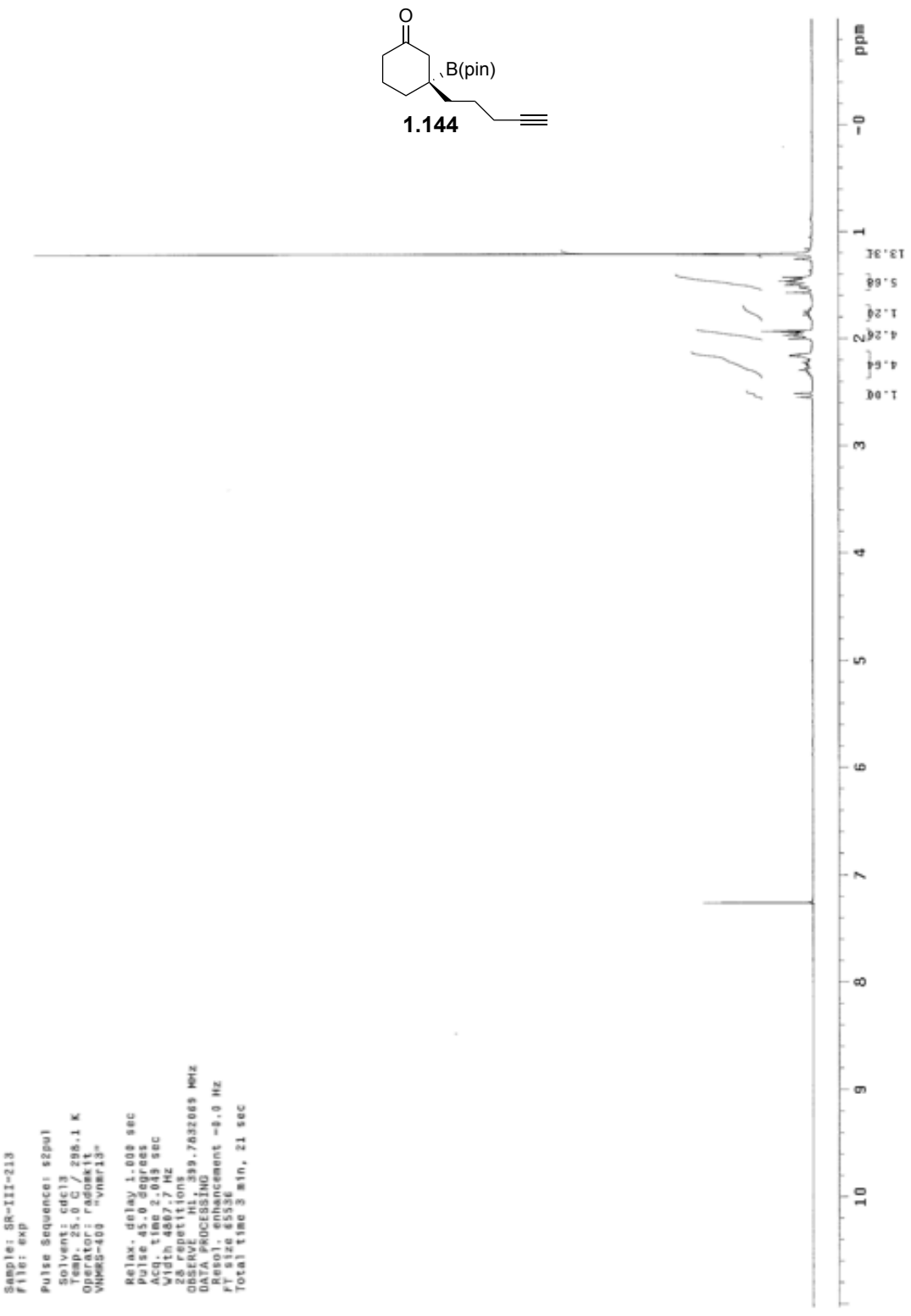
O
B(pin)
1.144
Sample: SR-III-213
File: exp
Pulse Sequence: s2pul
Solvent: cdcl3
Temp. 25.0 C / 298.1 K
Operator: radomkit
VNMRS-400 "vnmr13"
Relax. delay 1.000 sec
Pulse 45.0 degrees
Acq. time 2.049 sec
Width 4807.7 Hz
28 repetitions
OBSERVE H1, 399.7832069 MHz
DATA PROCESSING
Resol. enhancement -0.0 Hz
FT size 65536
Total time 3 min, 21 sec
ppm
13.36
5.66
1.26
4.26
4.64
1.06

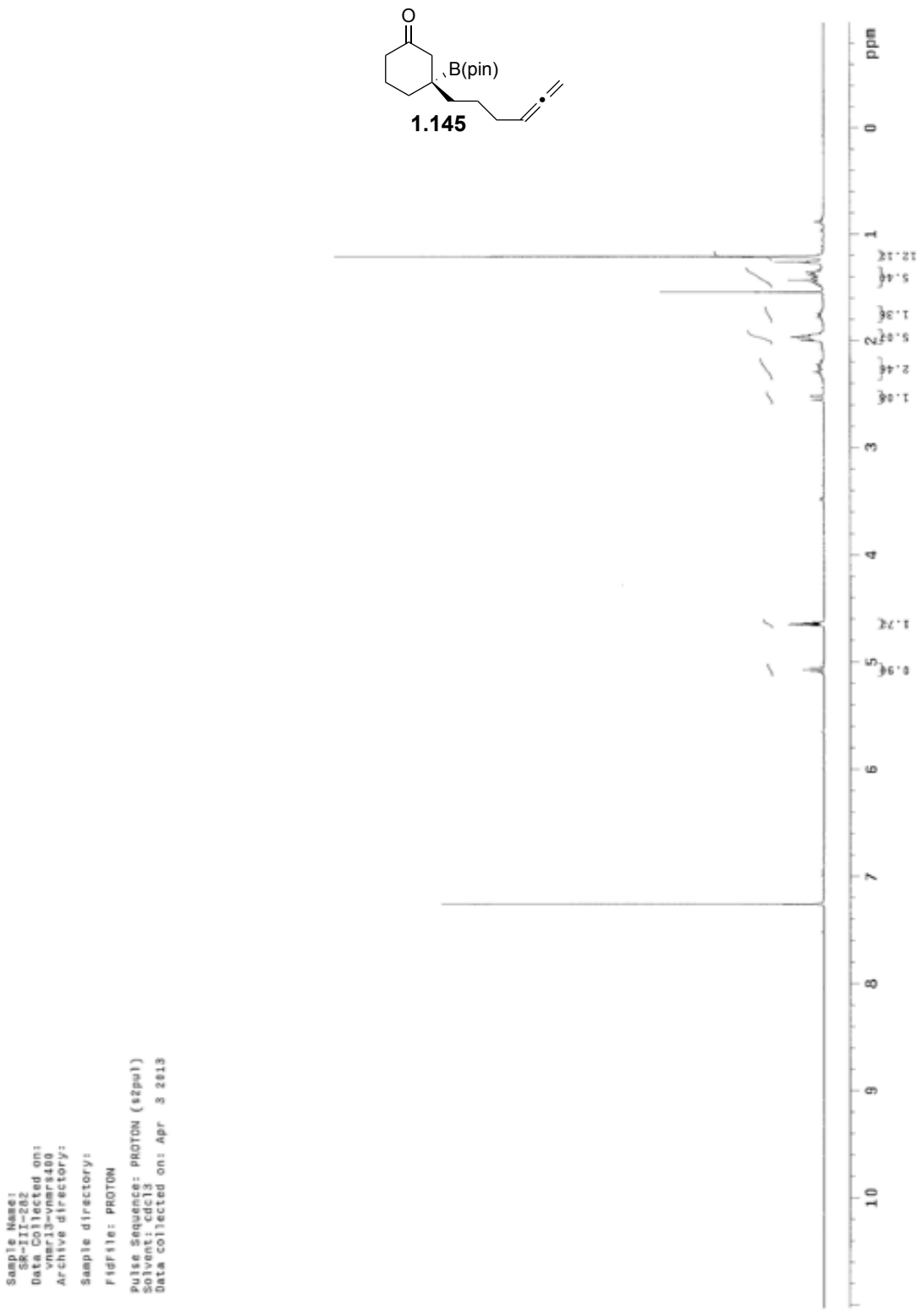
O
B(pin)
1.145
ppm
0
1
2
3
4
5
6
7
8
9
10
12.12
5.44
1.38
5.07
2.44
1.08
1.74
0.96
Sample Name:
SR-II-282
Data Collected on:
vnmr13-vnmrs400
Archive directory:
Sample directory:
FidFile: PROTON
Pulse Sequence: PROTON (s2pul)
Solvent: cdcl3
Data collected on: Apr 3 2013

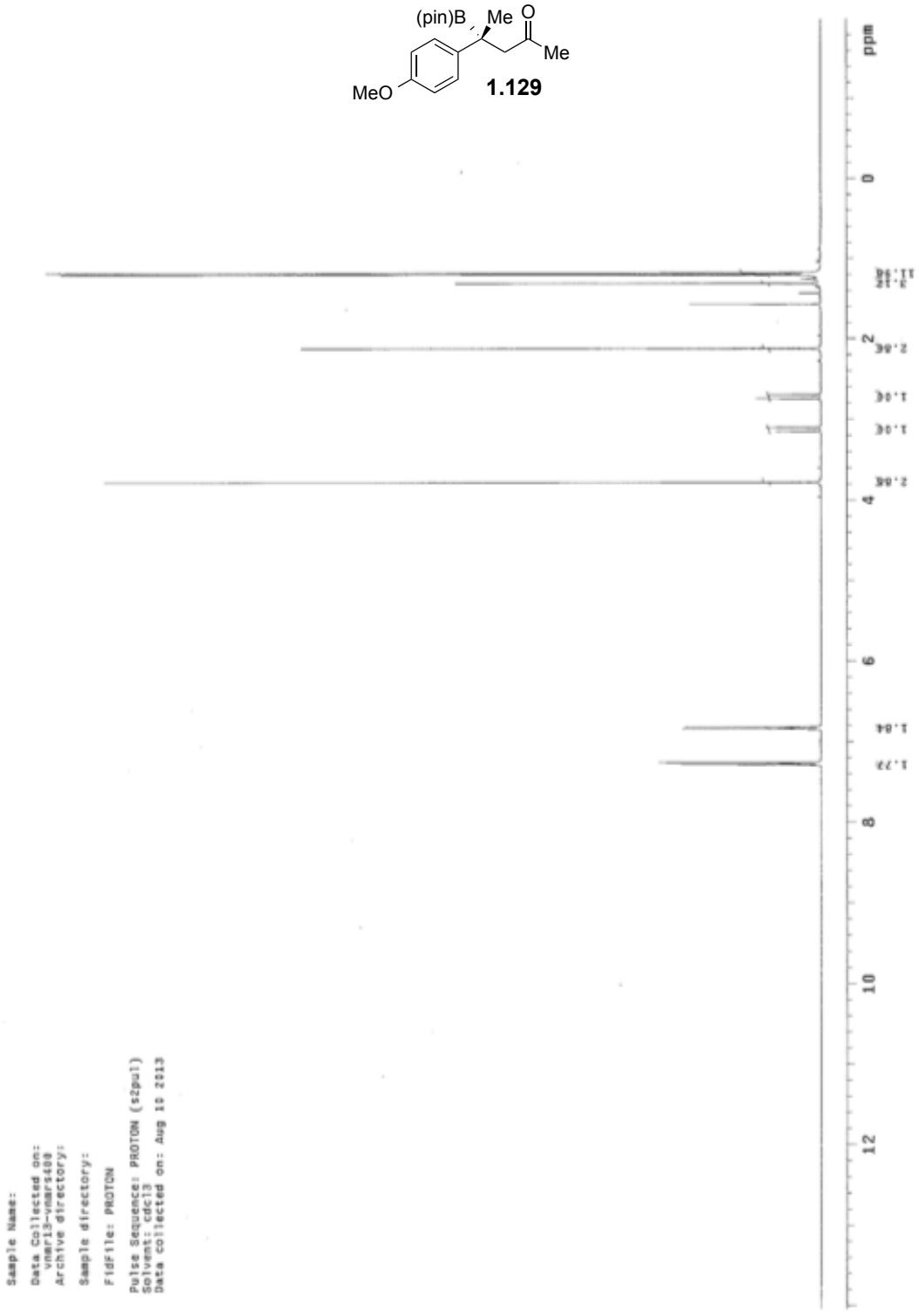
(pin)B
Me
O
Me
MeO
1.129
ppm
0
2
4
6
8
10
12
Sample Name:
Data Collected on:
vnmr13-vnmrs400
Archive directory:
Sample directory:
FidFile: PROTON
Pulse Sequence: PROTON (s2pul)
Solvent: cdcl3
Data collected on: Aug 10 2013

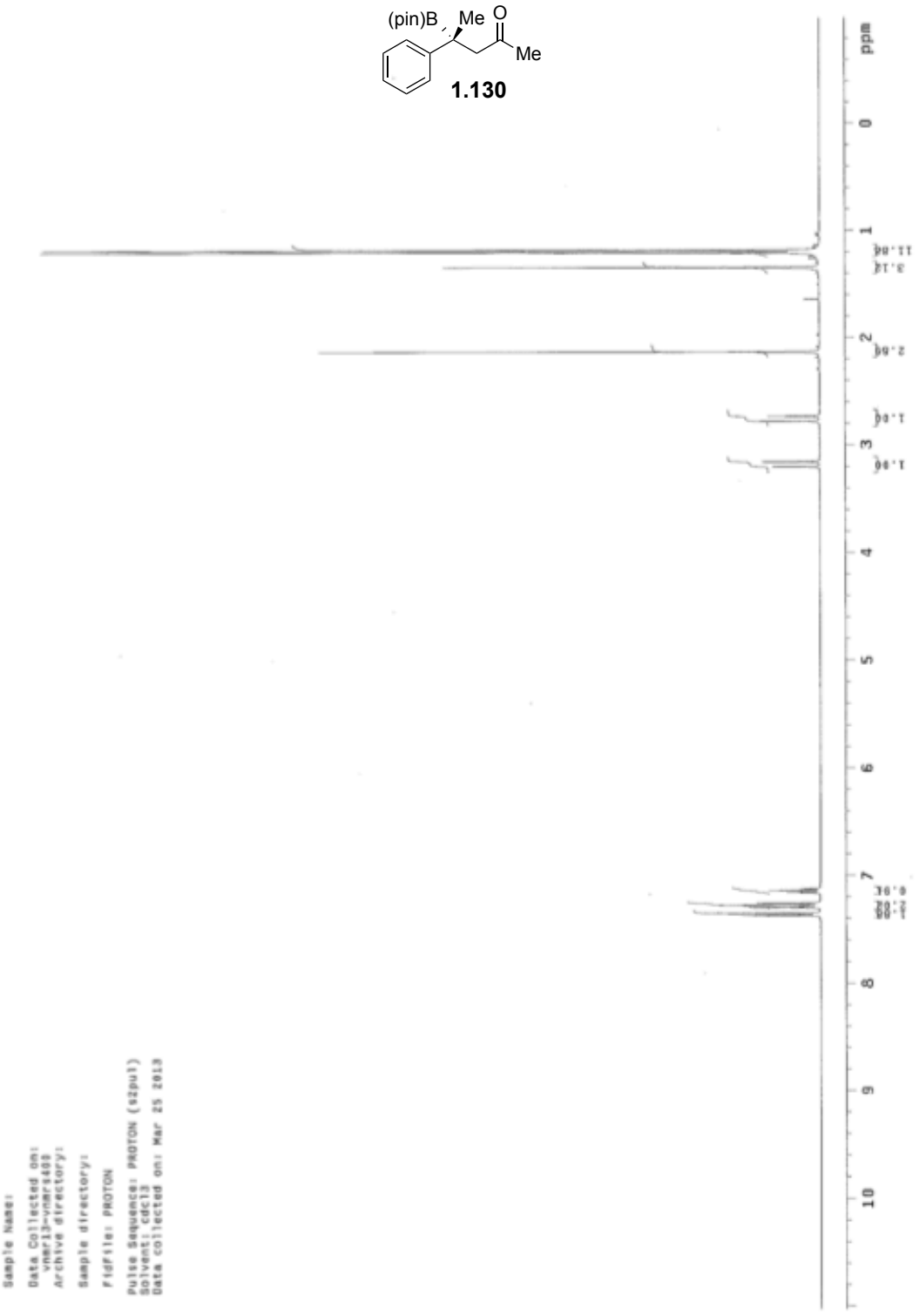
(pin)B
Me
O
Me
1.130
ppm
0
1
2
3
4
5
6
7
8
9
10
11.84
3.14
2.04
1.01
1.96
0.96
2.02
2.00
Sample Name:
Data Collected on:
vnmr13-vnmr1400
Archive directory:
Sample directory:
FidFile: PROTON
Pulse Sequence: PROTON (s2pul)
Solvent: cdcl3
Data collected on: Mar 25 2013

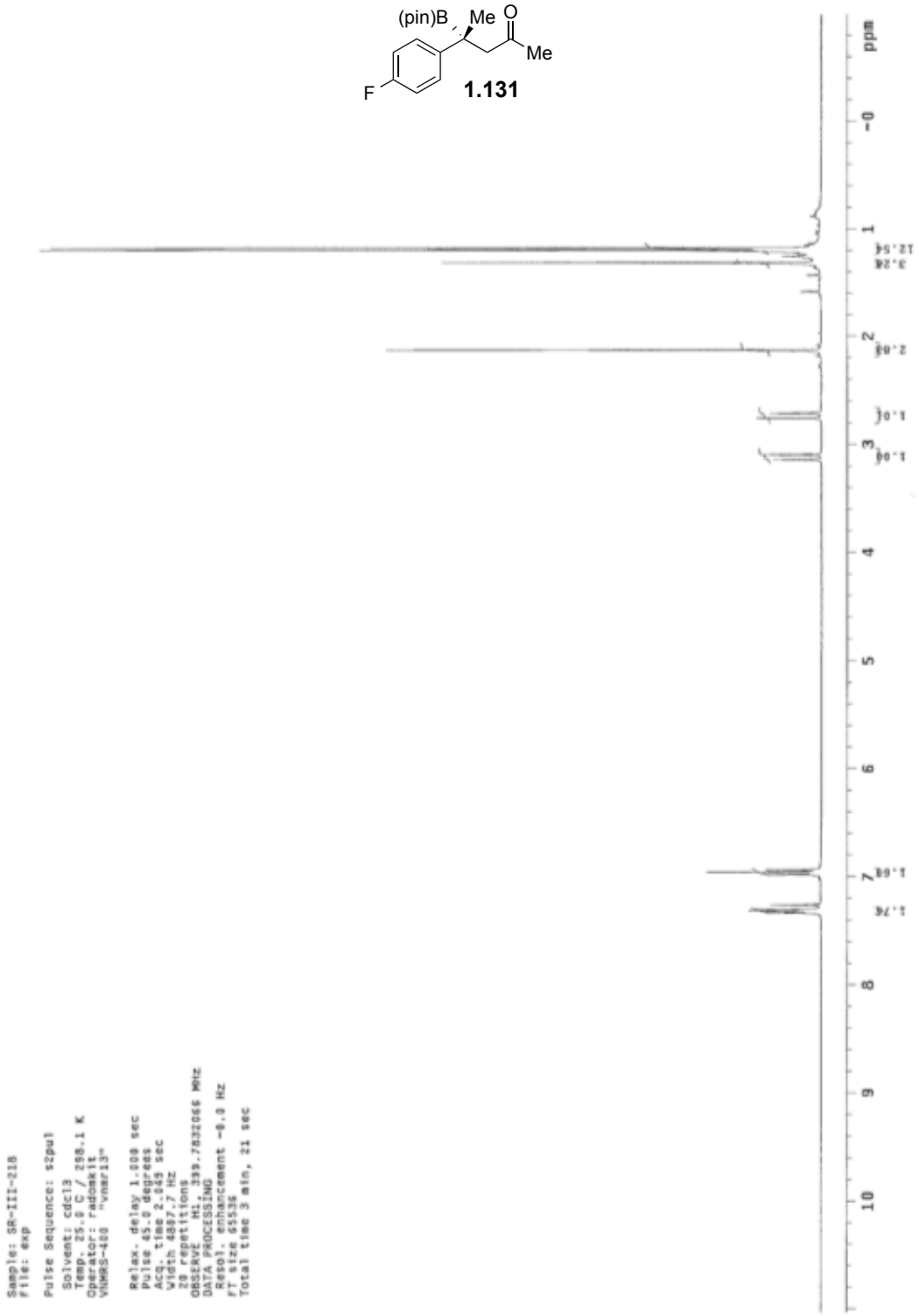
(pin)B
Me
O
Me
F
1.131
ppm
Sample: SR-III-218
File: exp
Pulse Sequence: s2pul
Solvent: cdcl3
Temp. 25.0 C / 298.1 K
Operator: radomkit
VNMRS-400 "vnmr13"
Relax. delay 1.000 sec
Pulse 45.0 degrees
Acq. time 2.043 sec
Width 4807.7 Hz
20 repetitions
OBSERVE H1, 399.7832066 MHz
DATA PROCESSING
Resol. enhancement -0.0 Hz
FT size 65536
Total time 3 min, 21 sec

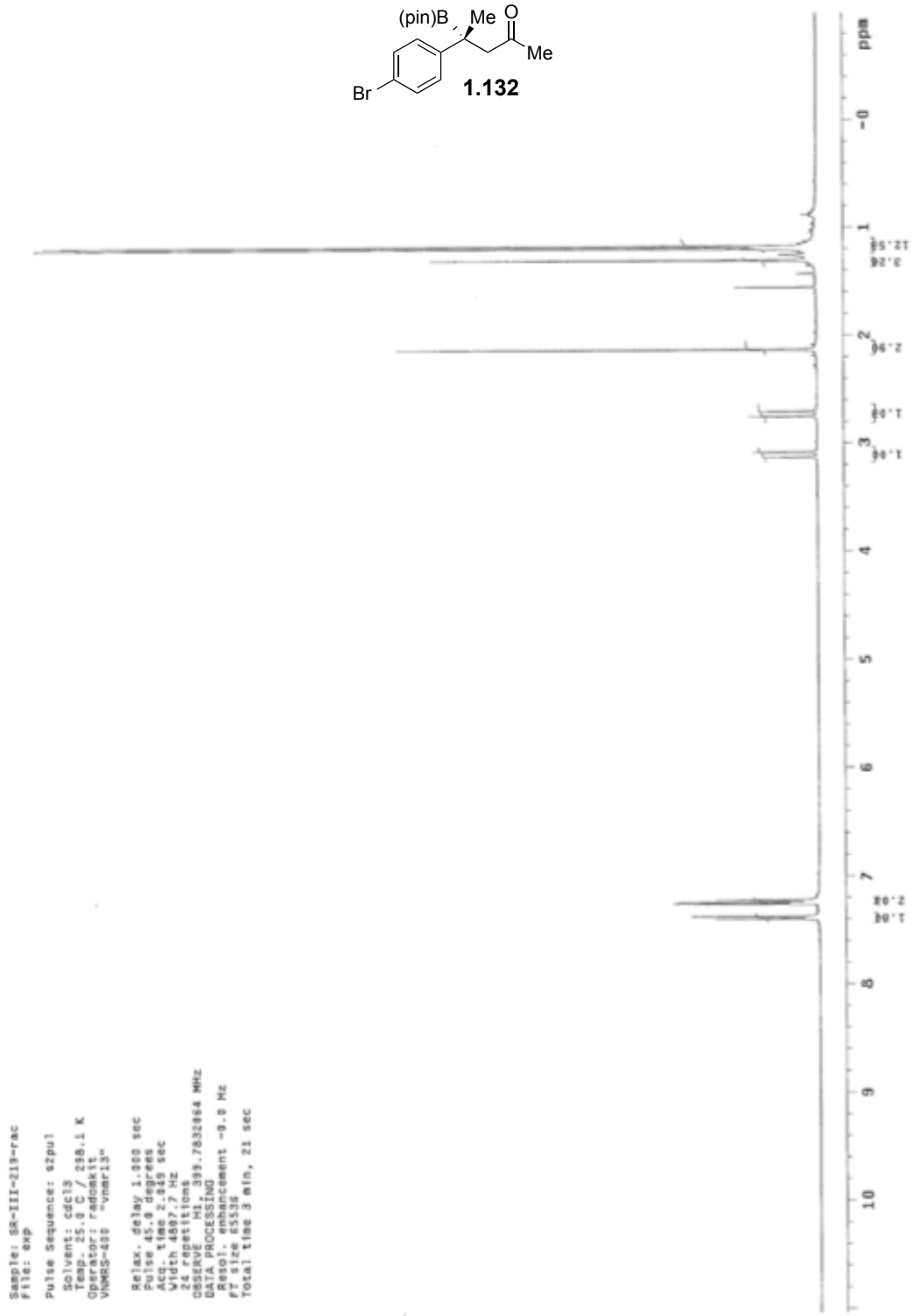
(pin)B
Me
O
Me
Br
1.132
ppm
Sample: SR-III-219-rac
File: exp
Pulse Sequence: s2pul
Solvent: cdcl3
Temp. 25.0 C / 298.1 K
Operator: radomkit
VNMRS-400 "vmar13"
Relax. delay 1.000 sec
Pulse 45.0 degrees
Acq. time 2.049 sec
Width 4807.7 Hz
24 repetitions
OBSERVE H1, 399.7832064 MHz
DATA PROCESSING
Resol: enhancement -0.8 Hz
FT size 65536
Total time 3 min, 21 sec

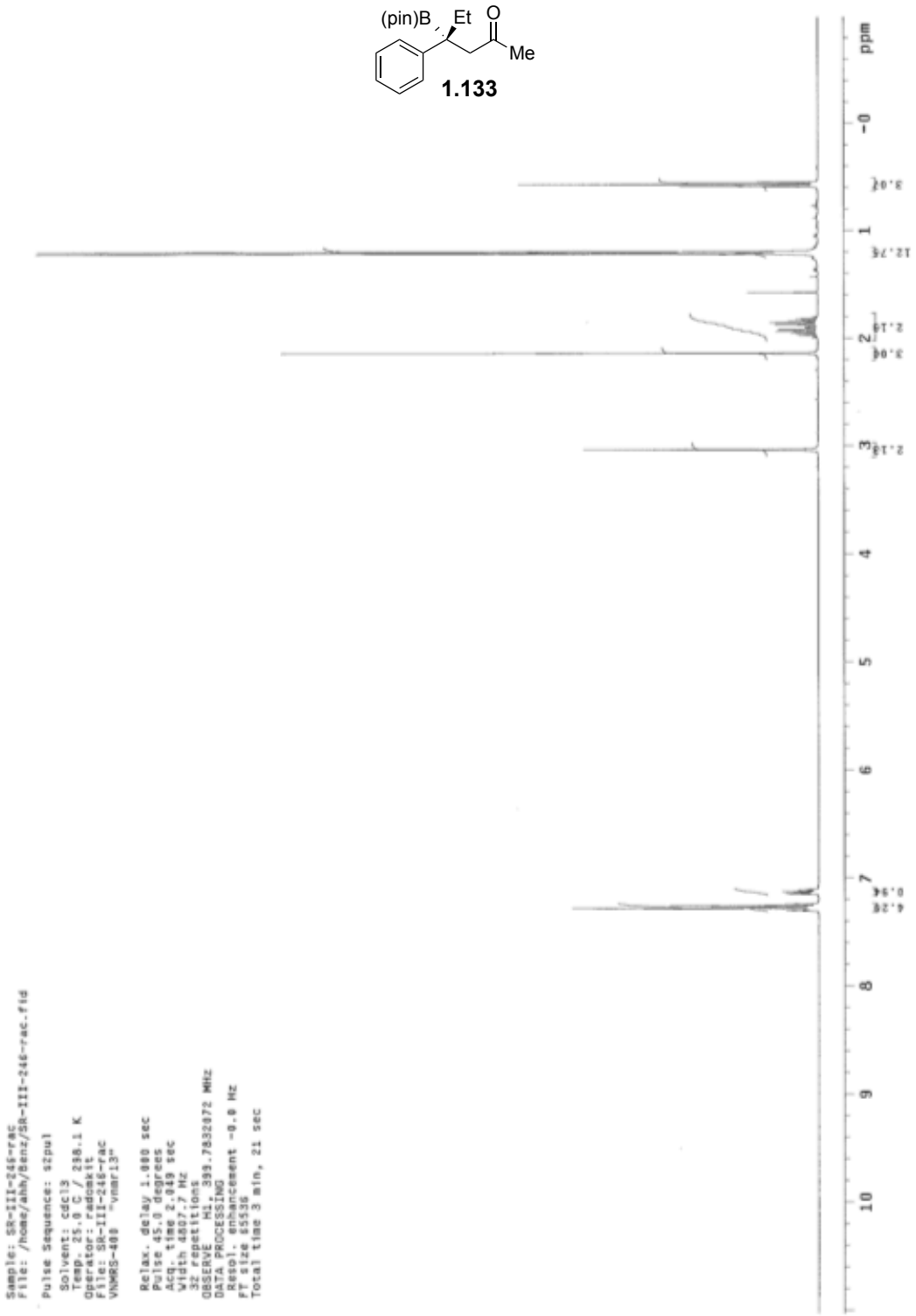
(pin)B
Et
O
Me
1.133
Sample: SR-III-246-rac
File: /home/ahk/denz/SR-III-246-rac.fid
Pulse Sequence: s2pul
Solvent: cdcl3
Temp. 25.0 C / 298.1 K
Operator: readmkit
File: SR-III-246-rac
VNMRS-400 "vmar13"
Relax. delay 1.000 sec
Pulse 45.0 degrees
Acq. time 2.049 sec
Width 18027.7 Hz
32 repetitions
OBSERVE H1, 399.7832872 MHz
DATA PROCESSING
Resol. enhancement -0.9 Hz
FT size 65536
Total time 3 min, 21 sec
ppm
3.07
12.76
2.18
3.04
2.13
6.28
0.94

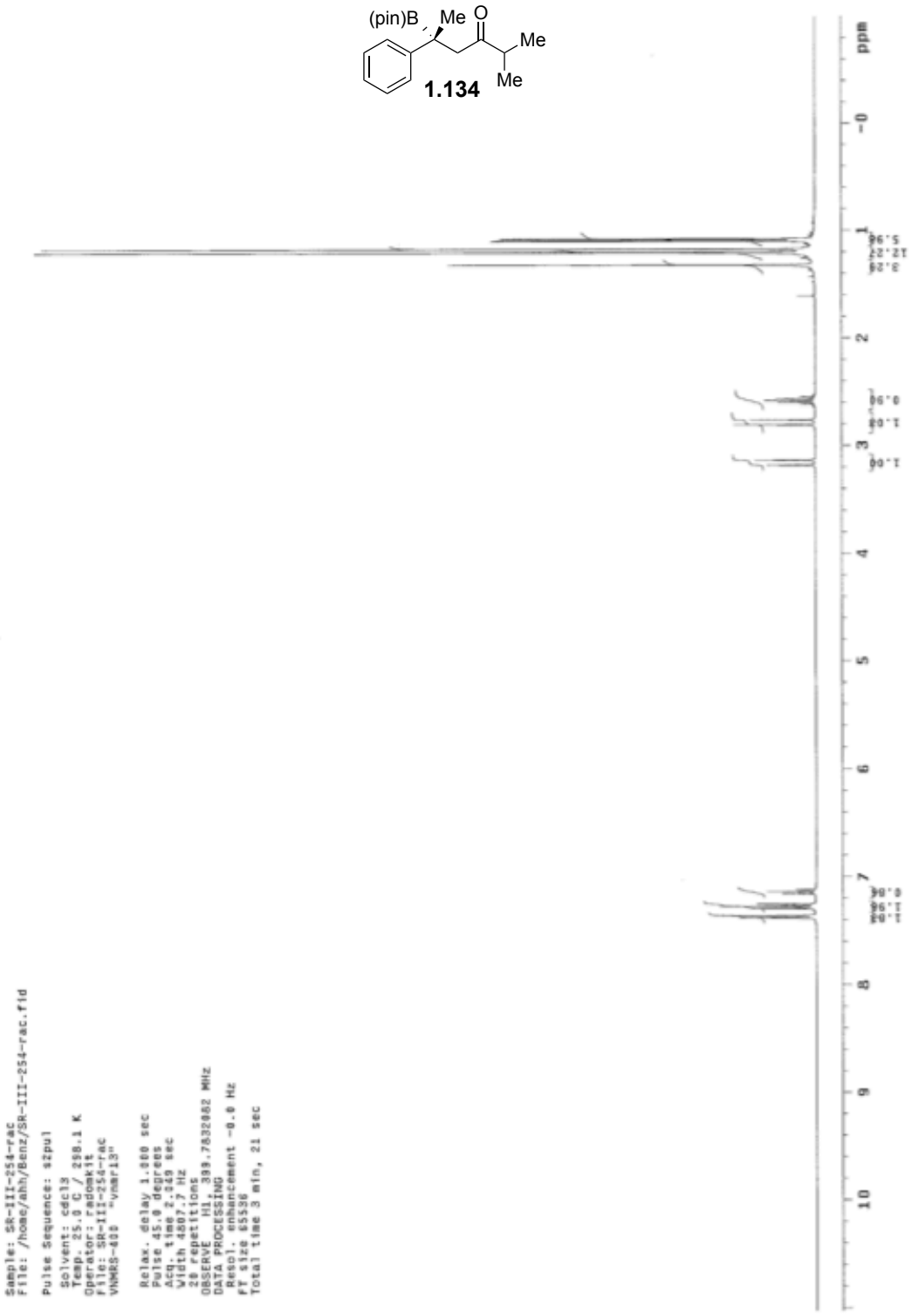
(pin)B
Me
O
Me
Me
1.134
Sample: SR-III-254-rac
File: /home/ahh/Benz/SR-III-254-rac.fid
Pulse Sequence: s2pul
Solvent: cdcl3
Temp. 25.0 C / 298.1 K
Operator: radomkit
File: SR-III-254-rac
VNMRS-400 "vmar13"
Relax. delay 1.000 sec
Pulse 45.0 degrees
Acq. time 2.049 sec
Width 4807.7 Hz
28 repetitions
OBSERVE H1 399.7832682 MHz
DATA PROCESSING
Resol. enhancement -0.0 Hz
FT size 65536
Total time 3 min, 21 sec
ppm

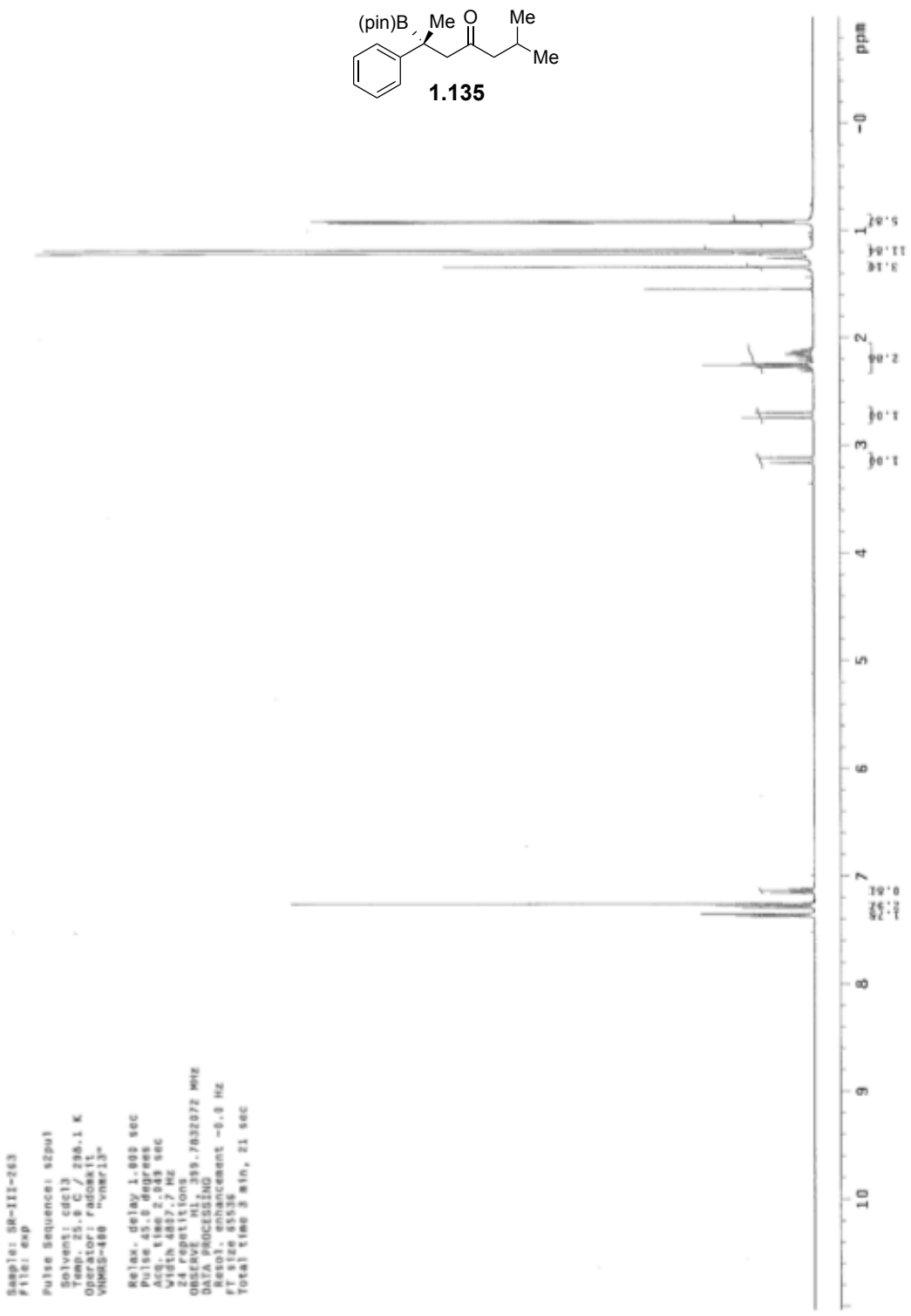
(pin)B
Me
O
Me
Me
1.135
ppm
Sample: SR-III-263
File: exp
Pulse Sequence: s2pul
Solvent: cdcl3
Temp. 25.0 C / 298.1 K
Operator: radoskit
VNMRS-400 "vnmr13"
Relax. delay 1.000 sec
Pulse 45.0 degrees
Acq. time 2.049 sec
Width 4807.7 Hz
24 repetitions
OBSERVE H1, 399.7832072 MHz
DATA PROCESSING
Resol. enhancement -0.0 Hz
FT size 65536
Total time 3 min, 21 sec

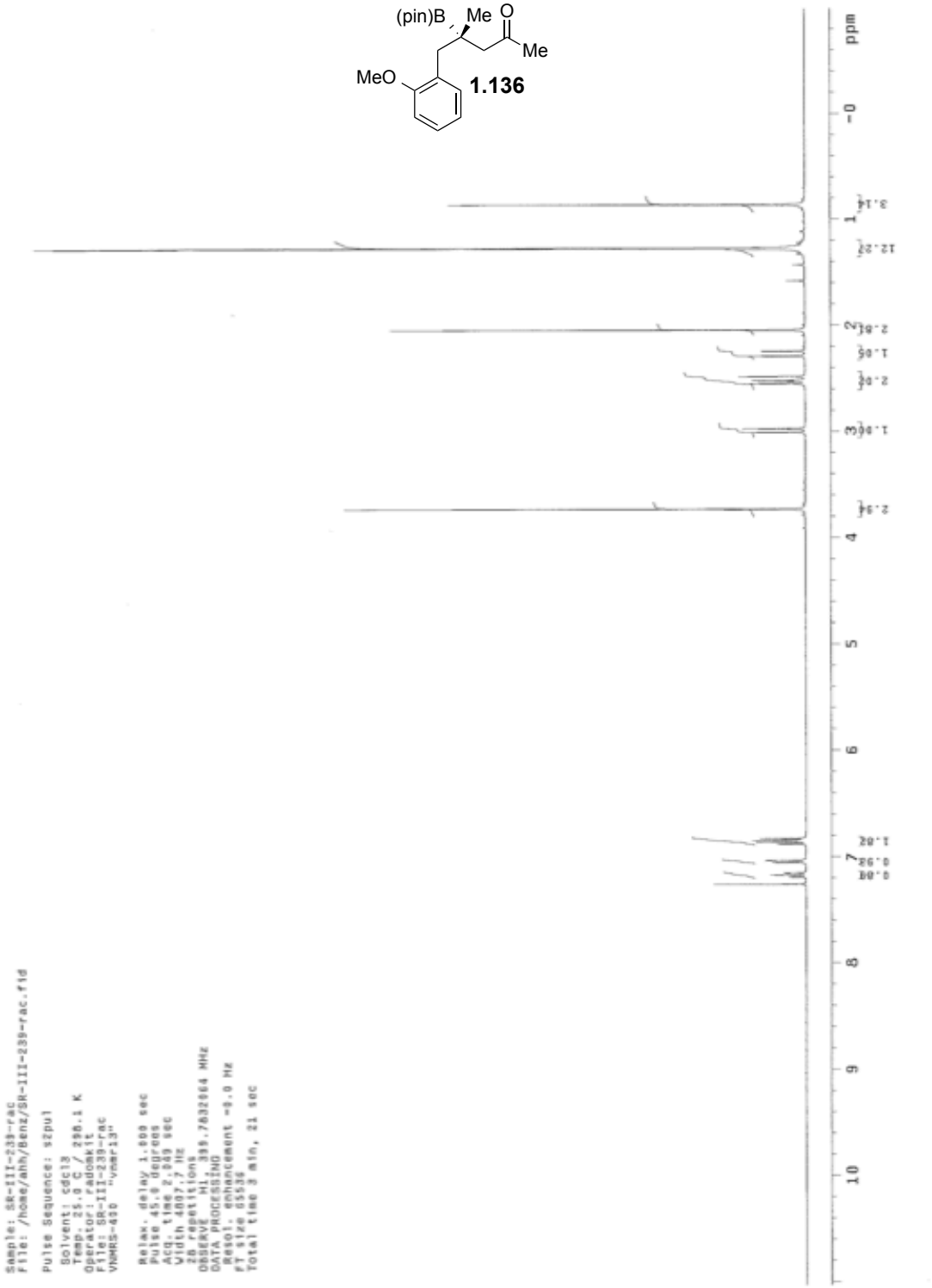
(pin)B
Me
O
Me
MeO
1.136
ppm
Sample: SR-III-239-rac
File: /home/anh/Benz/SR-III-239-rac.fid
Pulse Sequence: s2pul
Solvent: cdcl3
Temp.: 25.9 C / 298.1 K
Operator: radomkit
File: SR-III-239-rac
VNMRS-400 "vnmr13"
Relax. delay 1.000 sec
Pulse 45.0 degrees
Acq. time 2.049 sec
Width 4807.7 Hz
20 repetitions
OBSERVE H1, 399.7832864 MHz
DATA PROCESSING
Resol. enhancement -0.0 Hz
FT size 65536
Total time 3 min, 21 sec

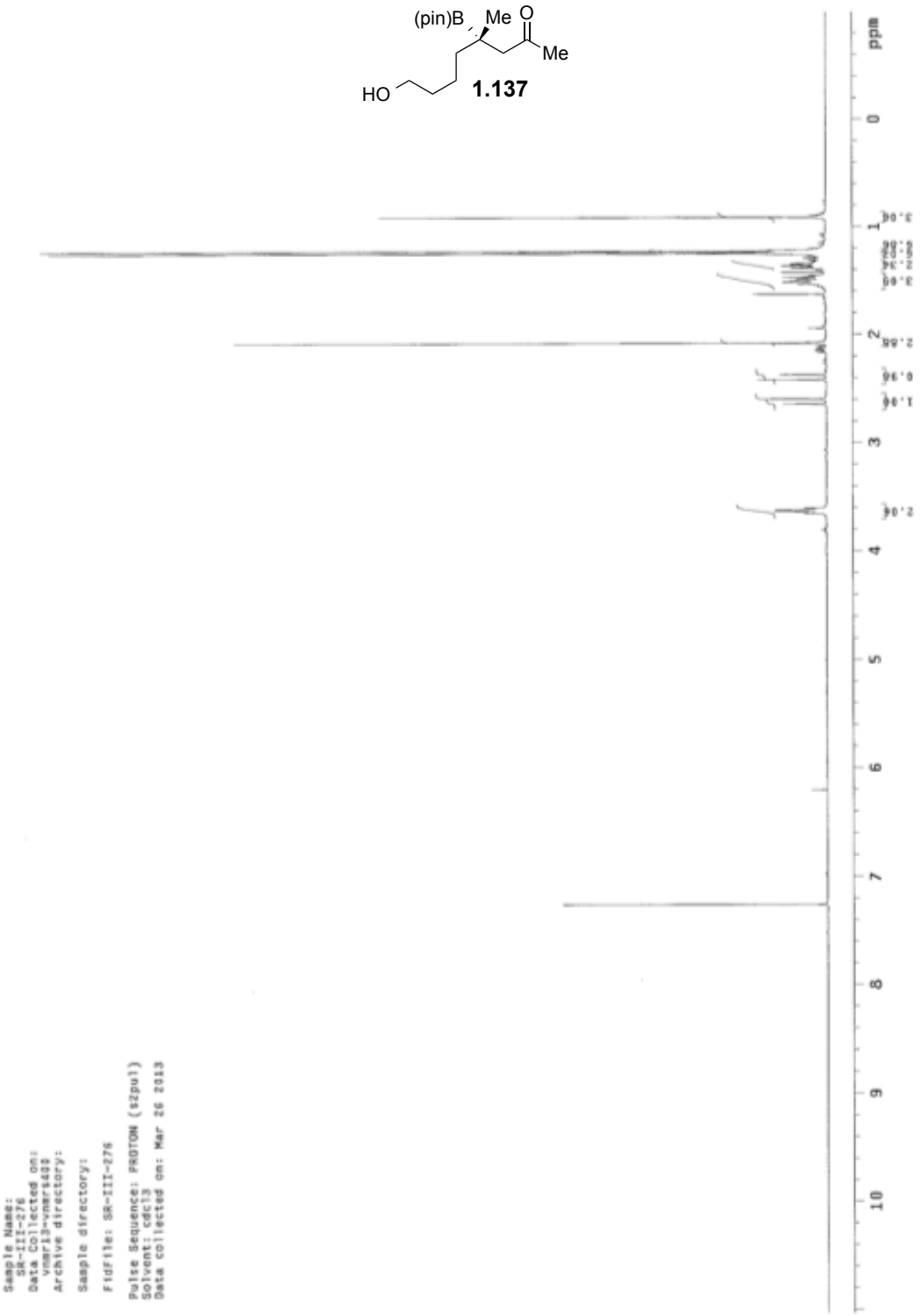
(pin)B
Me
O
Me
HO
1.137
ppm
Sample Name:
SR-III-276
Data Collected on:
vnmr13-vnmr640
Archive directory:
Sample directory:
FidFile: SR-III-276
Pulse Sequence: PROTON (s2pul)
Solvent: cdcl3
Data collected on: Mar 26 2013

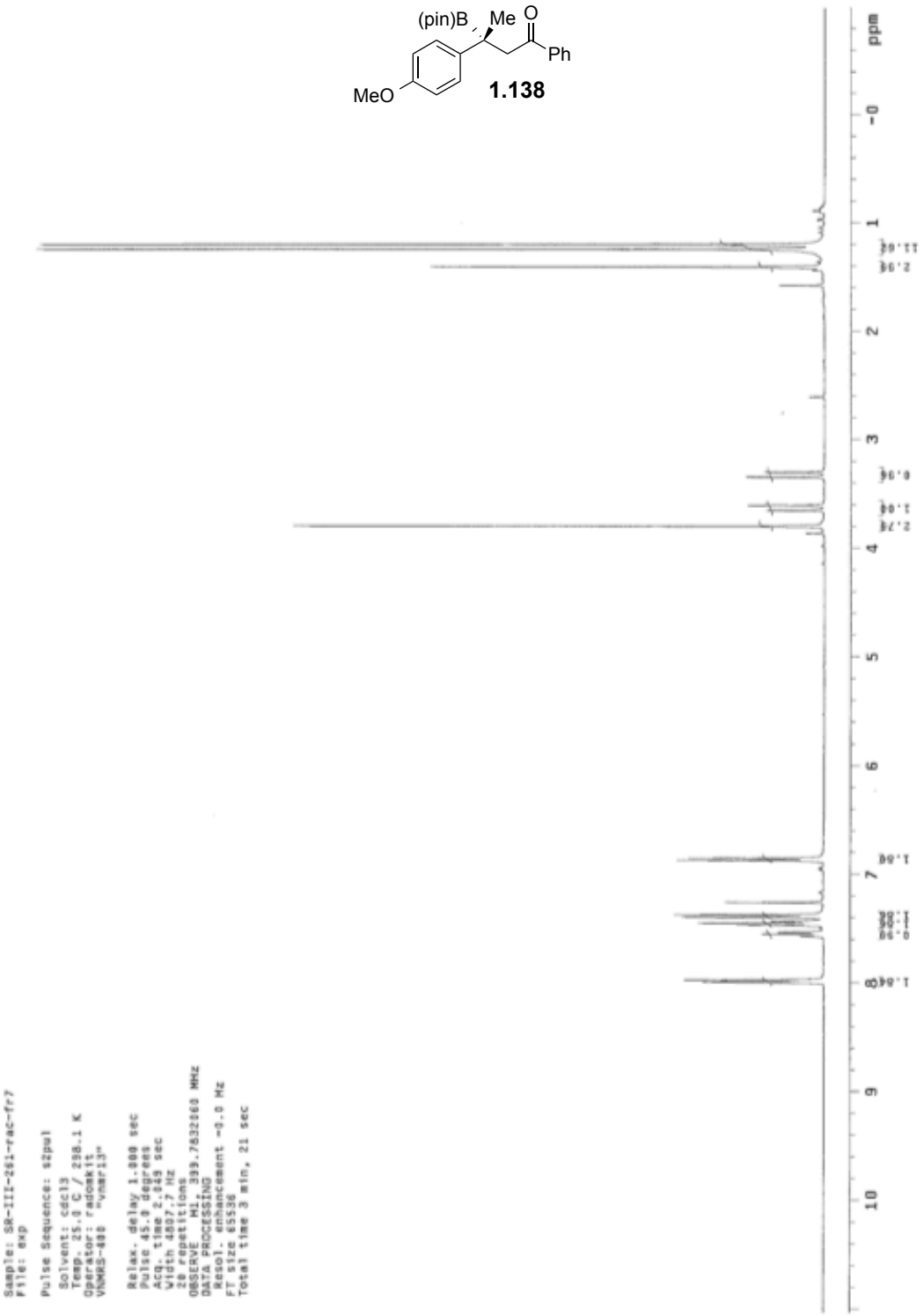
(pin)B
Me
O
Ph
MeO
1.138
ppm
Sample: SR-III-261-rac-fr7
File: exp
Pulse Sequence: s2pul
Solvent: cdcl3
Temp: 25.0 C / 298.1 K
Operator: raquel
VNMRS-400 "vnmrs13"
Relax. delay 1.000 sec
Pulse 45.0 degrees
Acq. time 2.049 sec
Width 4807.7 Hz
28 repetitions
OBSERVE H1, 399.7832060 MHz
DATA PROCESSING
Resol- enhancement -0.0 Hz
FT size 65536
Total time 3 min, 21 sec

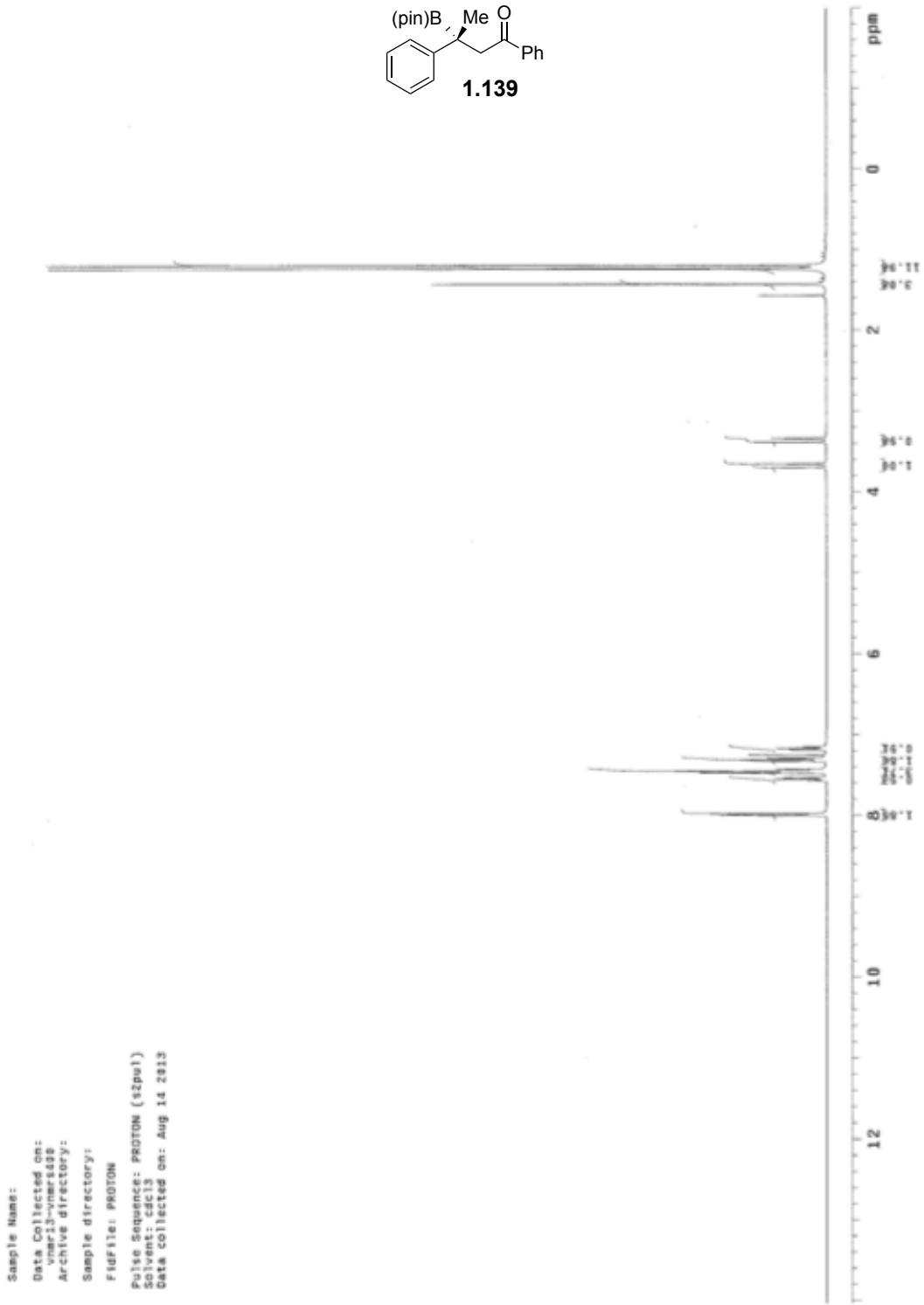
(pin)B
Me
O
Ph
1.139
ppm
0
2
4
6
8
10
12
Sample Name:
Data Collected on:
vnmr13-vnmrs430
Archive directory:
Sample directory:
FidFile: PROTON
Pulse Sequence: PROTON (s2pul)
Solvent: cdcl3
Data collected on: Aug 14 2013

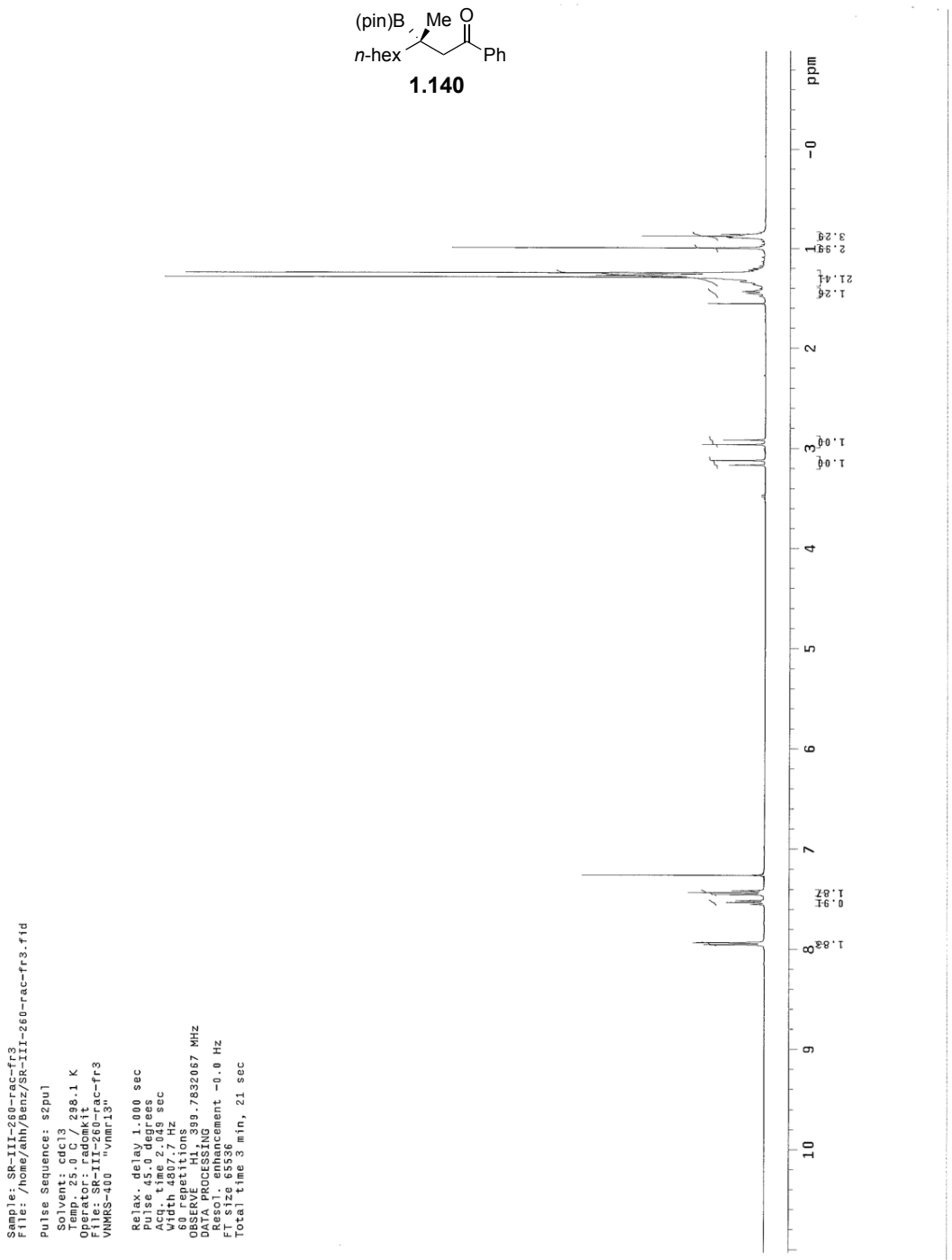
(pin)B
Me
O
n-hex
Ph
1.140
Sample: SR-III-260-rac-fr3
File: /home/ahh/Benz/SR-III-260-rac-fr3.fid
Pulse Sequence: s2pul
Solvent: cdcl3
Temp. 25.0 C / 298.1 K
Operator: radomkit
File: SR-III-260-rac-fr3
VNMRS-400 "vnmr13"
Relax. delay 1.000 sec
Pulse 45.0 degrees
Acq. time 2.049 sec
Width 4807.7 Hz
60 repetitions
OBSERVE H1, 399.7832067 MHz
DATA PROCESSING
Resol. enhancement -0.0 Hz
FT size 65536
Total time 3 min, 21 sec
ppm
1.84
1.87
0.91
1.00
1.00
1.24
21.41
2.99
3.24

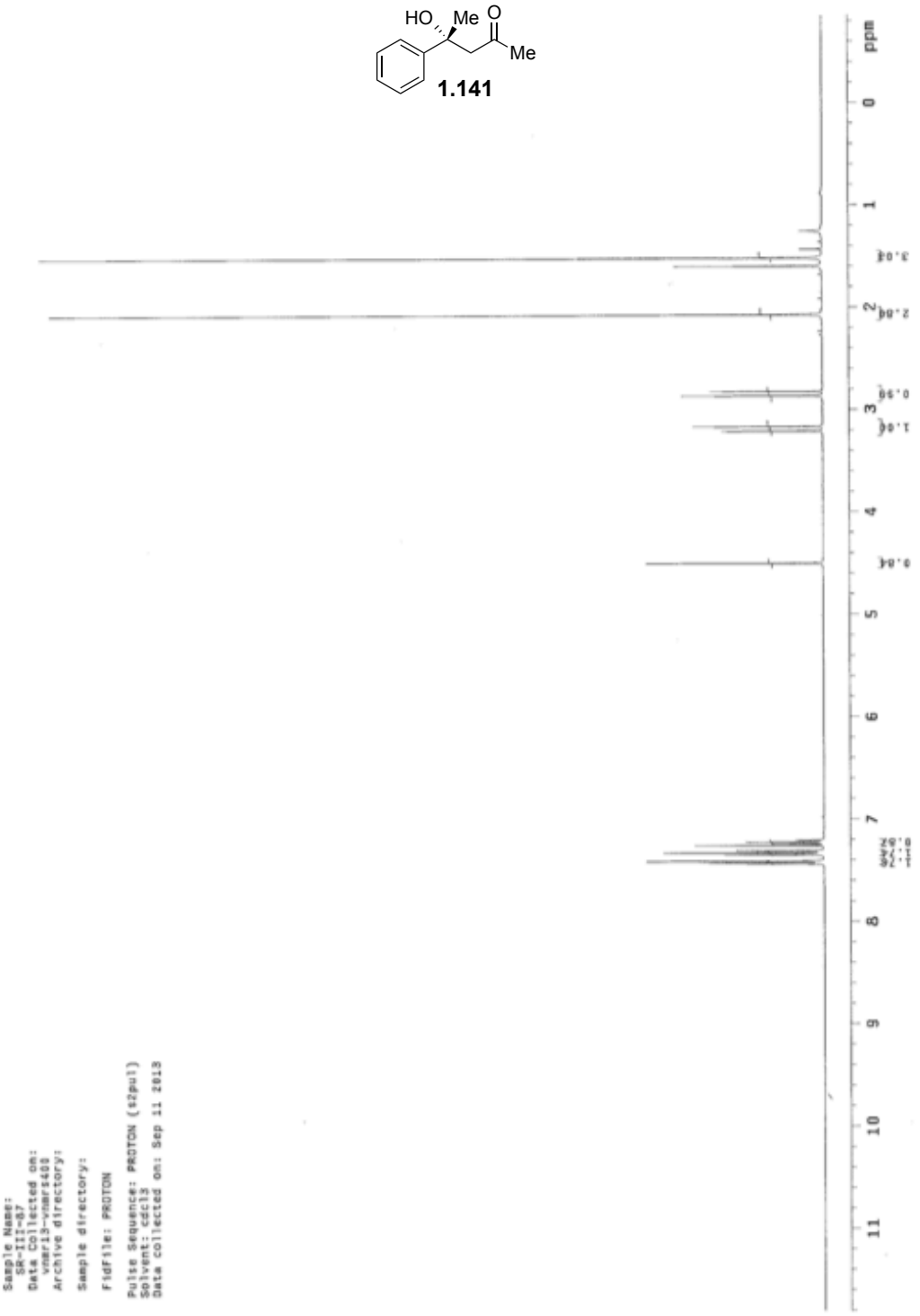
HO
Me
O
Me
1.141
ppm
Sample Name:
SR-III-87
Data Collected on:
vnmr13-vnmrs400
Archive directory:
Sample directory:
FidFile: PROTON
Pulse Sequence: PROTON (s2pul)
Solvent: cdcl3
Data collected on: Sep 11 2018

HO
Me
O
OH

1.142

Sample Name:
Bleach-12-7-2012-fr4-6
Archive directory:
Sample directory:
FidFile: SR-III-209-fr4-6
Pulse Sequence: Proton (s2pul)
Solvent: cdcl3
Data collected on: Dec 8 2012
0
1
2
3
4
5
6
7
8
9
10

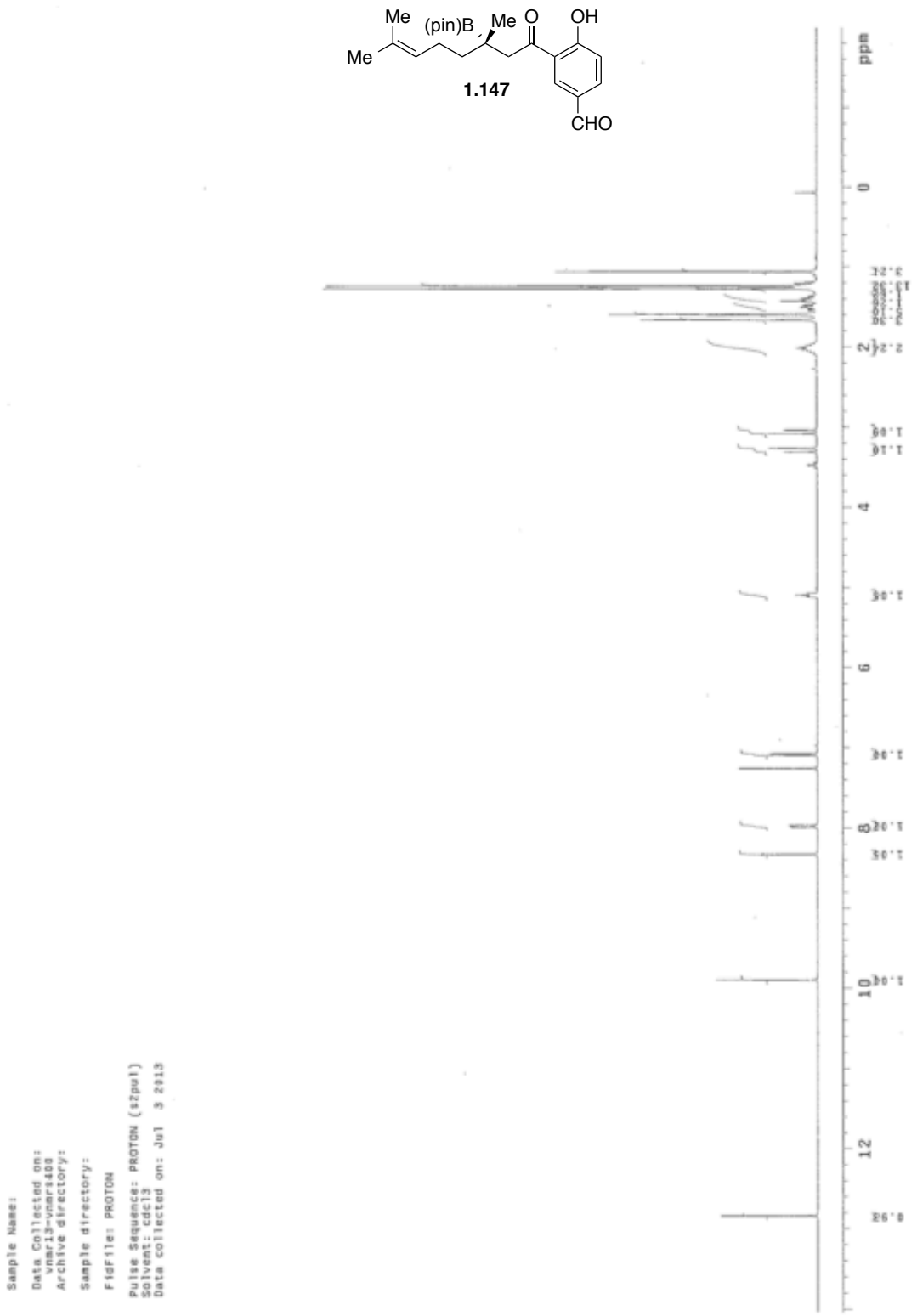
Me
(pin)B
Me
O
OH
Me
CHO
1.147
ppm
0
2
4
6
8
10
12
Sample Name:
Data Collected on:
vnmr13-vmrs400
Archive directory:
Sample directory:
FidFile: PROTON
Pulse Sequence: PROTON (s2pul)
Solvent: cdcl3
Data collected on: Jul 3 2013

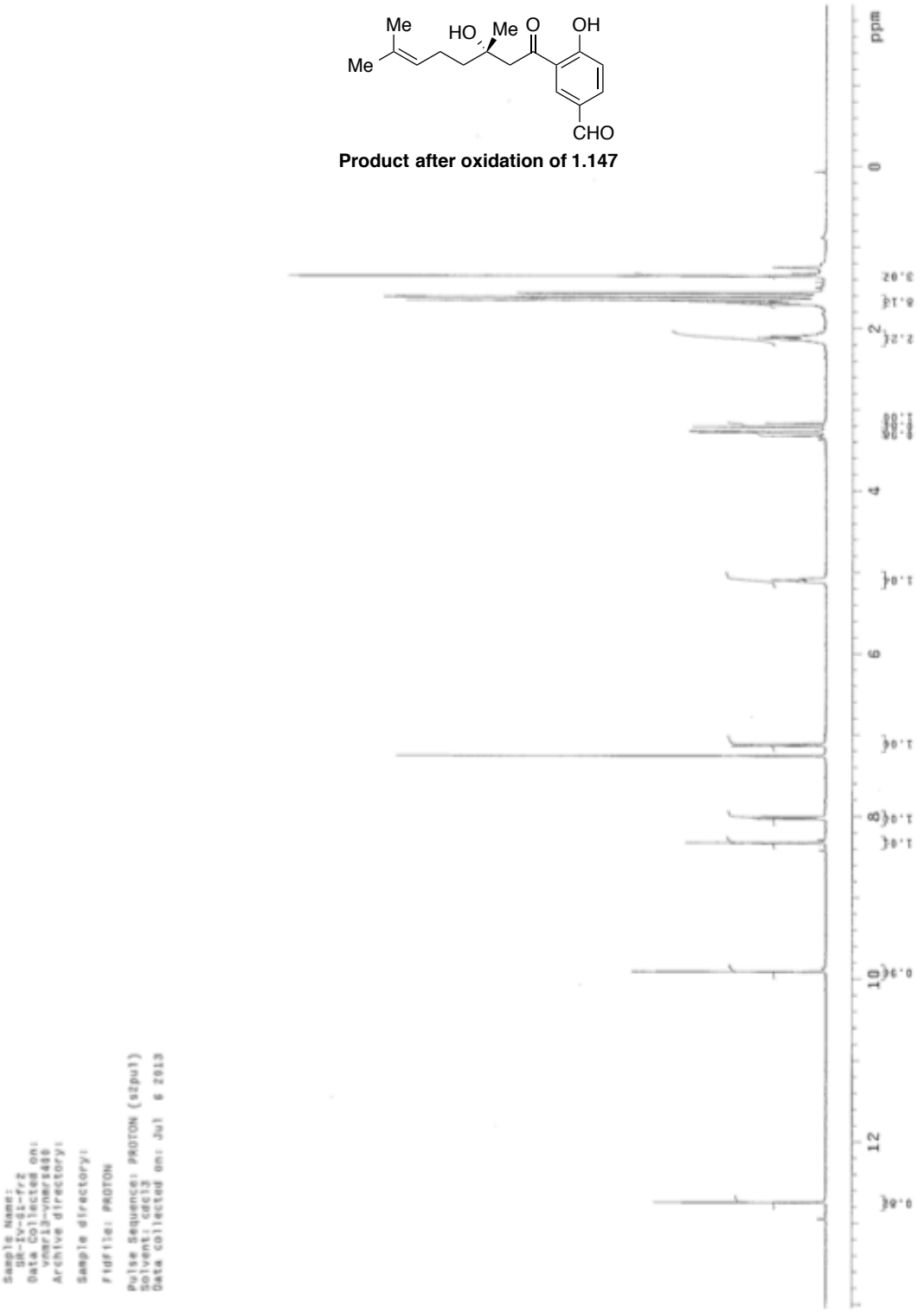
Me
HO
Me
O
OH
Me
CHO
Product after oxidation of 1.147
ppm
0
2
4
6
8
10
12
3.02
6.14
2.22
1.04
1.04
1.04
1.04
0.94
0.86
Sample Name:
SR-EV-01-fr2
Data Collected on:
vnmrj3-vnmrs400
Archive directory:
Sample directory:
Fidfile: PROTON
Pulse Sequence: PROTON (s2pul)
Solvent: cdcl3
Data collected on: Jul 6 2013

Chapter 2

Enantioselectivity Fluctuations in Phosphine–Cu-Catalyzed Enantioselective Boron-Allyl Addition to Aryl-Substituted Olefins

2.1. Introduction

There are many examples of catalytic additions of achiral organometallic nucleophiles to unsaturated organic molecules (e.g., alkenyl sites). Product enantiomeric purity is thus determined in the C–C bond forming step.[73] There are also examples where a metal-substituted stereogenic carbon center reacts with an electrophile[74] and either the chiral catalyst causes one of the rapidly interconverting stereoisomers to react (enantioselectivity by diastereoselective equilibration)[75] or an isomer is transformed faster (kinetic resolution or dynamic enantioselective synthesis)[76]; whichever the case, manipulating the stereochemical identity of a metal-substituted stereogenic carbon center is key. A distinct category of transformations proceeds through enantioselective formation of metal-substituted stereogenic carbon center that then reacts *in situ* with an electrophile. Product enantiomeric purity is now determined when the organometallic

(73) Ogasawara, M.; Hayashi, T. in *Catalytic Asymmetric Synthesis* (Ojima. I. Ed.), Wiley–VCH, 2000, 651.

(74) Malinakova, H. C. *Chem. Eur. J.* **2004**, *10*, 2636–2646.

(75) Beak, P.; Anderson, D. R.; Curtis, M. D.; Laumer, J. M.; Pippel, D. J.; Weisenburger, G. A. *Acc. Chem. Res.* **2000**, *33*, 715–727.

(76) (a) Cherney, A. H.; Kadunce, N. T.; Reisman, S. E. *Chem. Rev.* **2015**, *115*, 9587–9652. (b) Jiang, X.; Kulbitski, K.; Nisnevich, G.; Gandelman, M. *Chem. Sci.* **2016**, *7*, 2762–2767. (c) Kainz, Q. M.; Matier, C. D.; Bartoszewicz, A.; Zultanski, S. L.; Peters, J. C.; Fu, G. C. *Science* **2016**, *351*, 681–684.

species is generated (vs when the C–C bond is formed) and kinetic stereoselectivity must be retained. In this chapter, the studies regarding what factors may cause the variations in enantioselectivity observed in the products despite the formation of organocopper intermediates being stereochemistry determining will be discussed.

2.2. Background

In 2009, our laboratories reported an enantioselective proto-boration of β-substituted aryl olefins.[77] As illustrated in Scheme 2.1a, the reaction was shown to be site- and diastereoselective (>98% homobenzylic C–B and >98:2 dr). A stereochemistry-determining step is likely to be at the Cu–B addition step. Later in 2015, Liao and co-workers reported the use of a chiral Cu–B(pin) complex and an achiral palladium-based co-catalyst in reactions of aryl-olefins and allyl-*tert*-butyl carbonates (Scheme 2.1b).[78] A very interesting observation but has not been discussed is that enantioselectivity of product **2.7** is dependent on electrophile identity despite the earlier step being stereochemistry-determining. When allylic carbonate **2.5** is used, **2.7** is formed in 95.5:4.5 er; however, with an allylic electrophile is **2.6**, the er value of **2.7** is obtained in 98.5:1.5 er.

(77) Lee, Y.; Hoveyda, A. H. *J. Am. Chem. Soc.* **2009**, *131*, 3160–3161.
(78) Jia, T.; Cao, P.; Wang, B.; Lou, Y.; Yin, X.; Wang, M.; Liao, J. *J. Am. Chem. Soc.* **2015**, *137*, 13760–13763.

Scheme 2.1. Intermediates with a Cu-substituted stereogenic carbon generated through copper–boryl additions

a) Proto-boration reaction by NHC–Cu catalysis

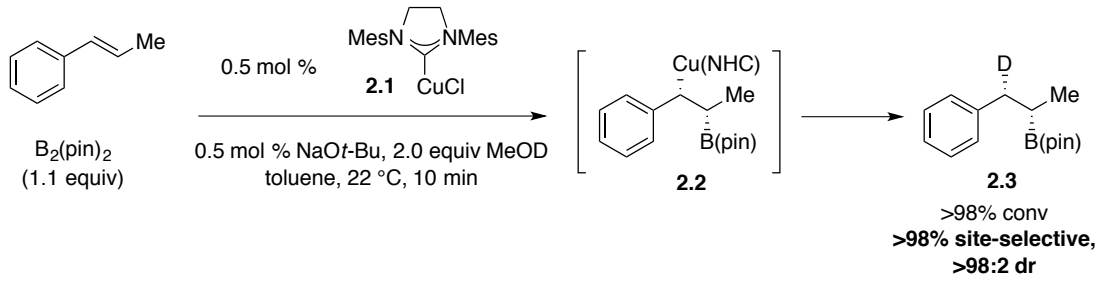

b) Allyl-boration reaction by Cu/Pd catalysis

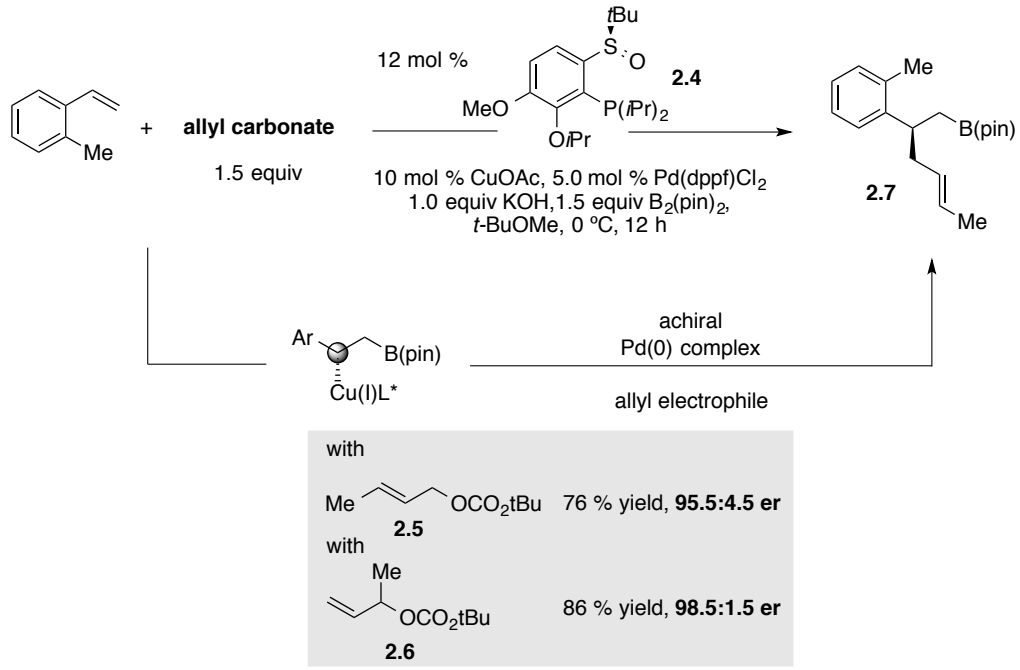

Similar observations on enantioselectivity variation with different electrophiles were also found in hydroamination reactions. As shown in Scheme 2.2a, Buchwald and co-workers published an enantioselective phosphine–Cu–H addition to styrenes followed by amination reaction in the presence of an *O*-benzoylhydroxylamine.[79] With **2.10**, the product is generated with >99:1 er, while **2.11** leads to 95:5 er. In another example, Miura and co-workers reported hydroamination of an alkenyl–B(dan) (dan, 1,8-

(79) Zhu, S.; Niljianskul, N.; Buchwald, S. L. *J. Am. Chem. Soc.* **2013**, *135*, 15746–15749.

diaminonaphthyl) compound with the same phosphine–Cu–H complex reported by Buchwald.[80] Again *O*-benzoylhydroxylamine structure has an impact on stereoselectivity (97:3 vs 88:12 er, Scheme 2.2b). We decided to investigate the above scenario while developing enantioselective multicomponent boron–allyl additions to aryl-olefins promoted by a chiral Cu complex without the need for a Pd-based co-catalyst (Section 3.3).

Scheme 2.2. Intermediates with a Cu-substituted stereogenic carbon generated through copper–hydride additions

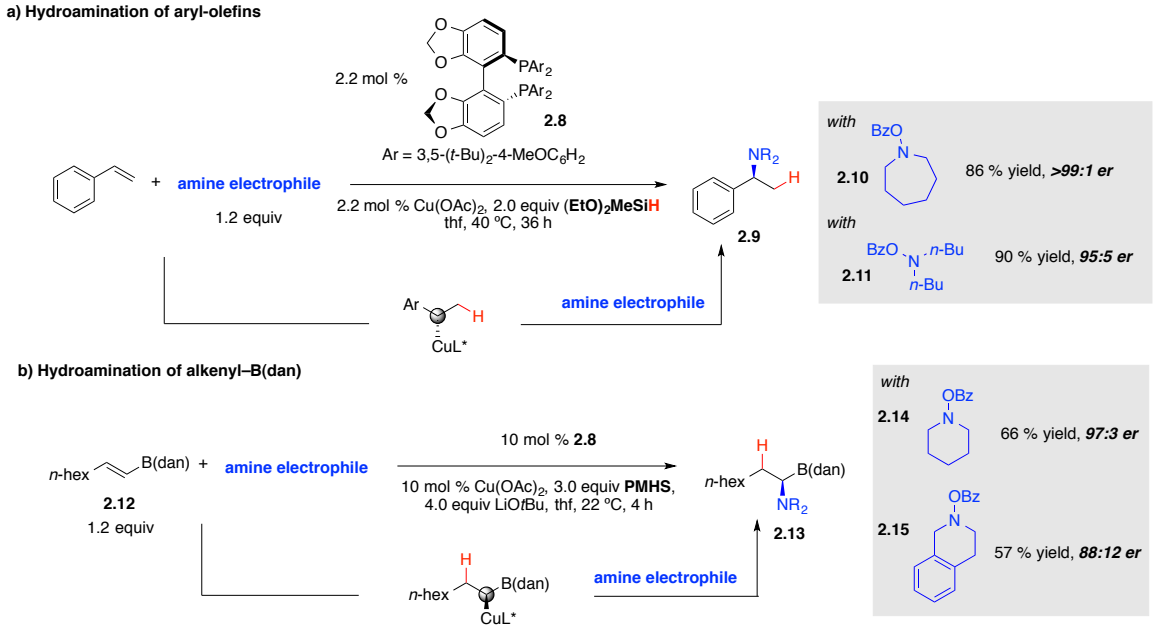

2.3. Phosphine–Cu-Catalyzed Enantioselective Boron-Allyl Addition to Aryl-Substituted Olefins

2.3.1. Identification of an effective enantioselective Cu-based catalyst

A mixture of styrene, allyl *t*-butylcarbonate (**2.16**) and $B_2(pin)_2$ in the absence of a ligand did not afford **2.18a** (Table 2.1, entry 1), which is consistent with the previously disclosed where a Pd-based co-catalyst is needed to promote electrophile activation.[3] In

(80) Nishikawa, D.; Hirano, K.; Miura, M. *J. Am. Chem. Soc.* **2015**, *137*, 15620–15623.

contrast, with allylphosphate (**2.17**), under otherwise the same conditions (entry 2), there was 32% conversion to **2a** [9% allyl–B(pin)]. With the NHC–Cu complex derived from **im-1**, there was minimal conversion with allylcarbonate **2.16** (entry 3), but with allylphosphate **2.17**, **2.18a** was isolated in 78% yield (entry 4). The catalyst derived from the more sizeable imidazolinium salt **im-2** was much less effective (entry 5). Reactions with several chiral NHC–Cu catalysts were examined and found to be minimally enantioselective and at times inefficient due to allyl–B(pin) being formed predominantly, which is generally the reason for discrepancy between conversion and yield values (entries 6–14, Table 2.1).

Table 2.1. Examination of different types of NHC–Cu complexes[a]

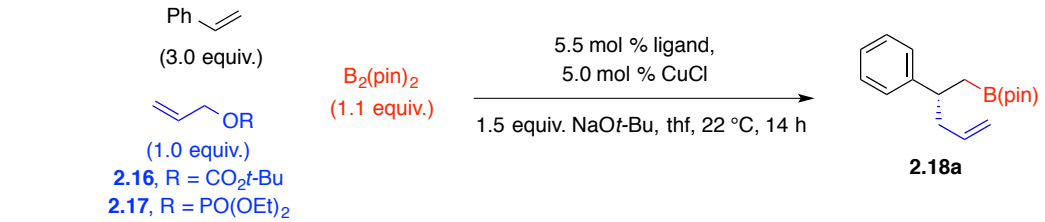

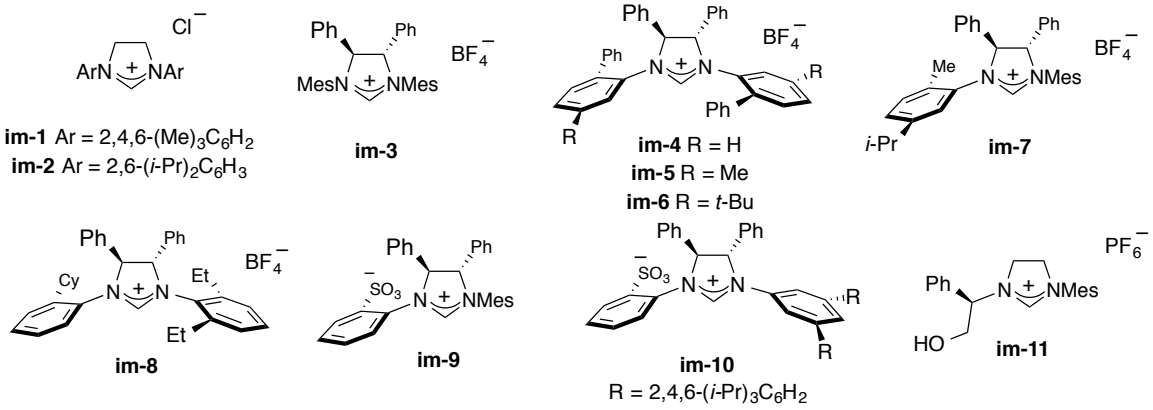

entry	allyl reagent	ligand	conv (%)[b]	yield (%)[c]	er[d]
1	**2.16**	none	<2	nd	na
2	**2.17**	none	41	nd	na
3	**2.16**	**im-1**	5	na	na
4	**2.17**	**im-1**	88	78	na
5	**2.17**	**im-2**	8	nd	na
6	**2.17**	**im-3**	94	41	56:44
7	**2.17**	**im-4**	80	71	61:39
8	**2.17**	**im-5**	84	78	60:40
9	**2.17**	**im-6**	35	25	17:83
10	**2.17**	**im-7**	40	25	58:42
11	**2.17**	**im-8**	>98	78	56:44
12	**2.17**	**im-9**	44	<2[e]	na
13	**2.17**	**im-10**	>98	33	60:40
14	**2.17**	**im-11**	>98	<2[e]	na

[a] Reactions were performed under N_2 atmosphere. [b] Conversions of the limiting reagent (**2.16**, **2.17**) were determined by analysis of 400 MHz ^{1}H NMR spectra of unpurified mixtures. [c] Yield of isolated and purified product. [d] Determined by HPLC analysis. [e] Only allyl–B(pin) detected. Mes = 2,4,6-$(Me)_3C_6H_2$.

We then turned to examining the possibility for a chiral phosphine being efficient and enantioselective (Table 2.2). Although we initially found that Ph_3P–Cu complex produced **2.18a** efficiently (76% conv, 69% yield), various chiral phosphine–Cu species were ineffective including the phosphine-sulfoxide (**2.4**, entry 5, Table 2.2) utilized in the

dual-catalytic (Cu/Pd) protocol. Only a family of bis-phosphines derived from camphor (**2.24a–c**)[81] delivered the desired product in appreciable yield and enantioselectivity. The complexes derived from **2.24a** and **2.24b** delivered **2.18a** in ≥51% yield and ≥92:8 er (entries 8–9). With **2.24c**, the enantioselectivity was reversed (62% yield, 20:80 er, entry 10).

(81) Kadyrov, R.; Iladinov, I. Z.; Almena, J.; Monsees, A.; Riermeier, T. H. *Tetrahedron Lett.* **2005**, *46*, 7397–7400.

Table 2.2. Examination of Different Types of Cu Complexes[a]

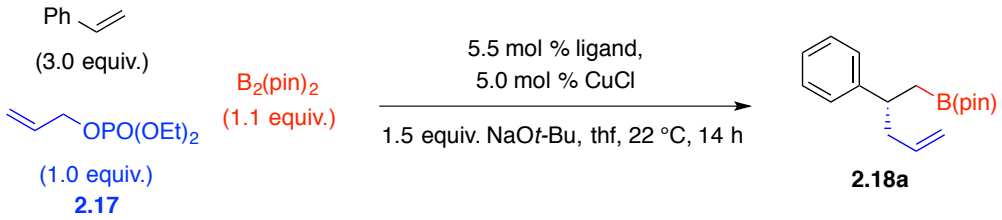

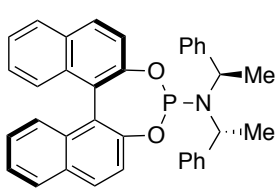

2.19

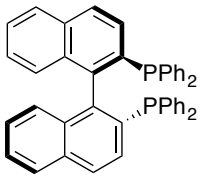

2.20

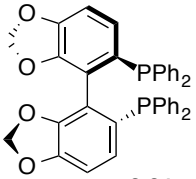

2.21

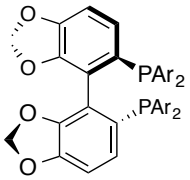

2.8
Ar = 3,5-(*t*-Bu)$_2$-4-OMeC$_6$H$_2$

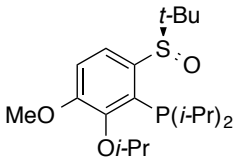

2.4

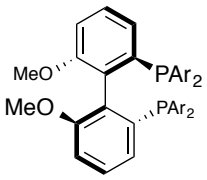

2.22
Ar = 3,5-(*t*-Bu)$_2$C$_6$H$_3$

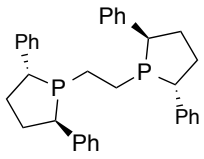

2.23

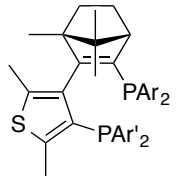

2.24a Ar = Ph, Ar' = Ph
2.24b Ar = 3,5-(Me)$_2$C$_6$H$_3$, Ar' = Ph
2.24c Ar = Ph, Ar' = 3,5-(Me)$_2$C$_6$H$_3$

entry	ligand	conv (%)	yield (%)	er
1	**2.19**	96	26	65:35
2	**2.20**	39	11	55:45
3	**2.21**	30	<5	na
4	**2.8**	66	<2[b]	na
5	**2.4**	15	6	9:91
6	**2.22**	86	11	51:49
7	**2.23**	>98	22	55:45
8	**2.24a**	>98	67	95:5
9	**2.24b**	94	51	92:8
10	**2.24c**	>98	62	20:80

[a] See Table 2.1. [b] Only allyl–B(pin) detected

2.3.2. Scope of the bis-phosphine–Cu catalyzed boron–allyl addition to aryl-olefins

Next, we investigated the scope of the reaction with different steric and electronic factors of the olefins (Scheme 2.3). *ortho*-Substituted products **2.18b-d** as well as those

containing a *meta*-methyl or *meta*-allyloxy group (**2.18e**–**f**) were formed with similar efficiency and enantioselectivity as **2.18a** (93:7–97:3 er). In contrast, reaction with *meta*-carboxylic ester styrene afforded **2.18g** in somewhat lower enantioselectivity (82:18 er). Formation of *para*-MIDA boronate **2.18h** (MIDA, *N*-methyliminodiacetic acid),[82] *para*-tolyl **2.18i** and *para*-trimethylsilylphenyl **2.18j** were again highly enantioselective (95:5–96:4 er). The reaction leading to *para*-methoxyphenyl-substituted **2.18k** was inefficient [28% yield; slow Cu–B(pin) addition] yet highly enantioselective (97:3 er); on the other hand, *para*-carboxylic ester containing **2.18l** was generated in 14% yield (reduced organocopper nucleophilicity) and 51:49 er. Transformations affording heterocyclic **2.18m**–**o** proceed smoothly affording the corresponding products in 58–64% yield and 90:10–98:2 er (<5% conv with unprotected indole). Reactions with aliphatic olefins were inefficient (<10% conv) probably because these more electron-rich substrates react much less efficiently with Cu–B(pin) and thus allyl–B(pin) is generated from reaction of Cu–B(pin) with an allylic phosphate.

(82) Li, J.; Ballmer, S. G.; Gillis, E. P.; Fujii, S.; Schmidt, M. J.; Palazzolo A. M. E.; Lehmann, J. W.; Morehouse, G. F.; Burke, M. D. *Science* **2015**, *347*, 1221–1226.

Scheme 2.3. Products of bis-phosphine–Cu-catalyzed multicomponent reactions (3:1 alkene:allyl phosphate)[a]

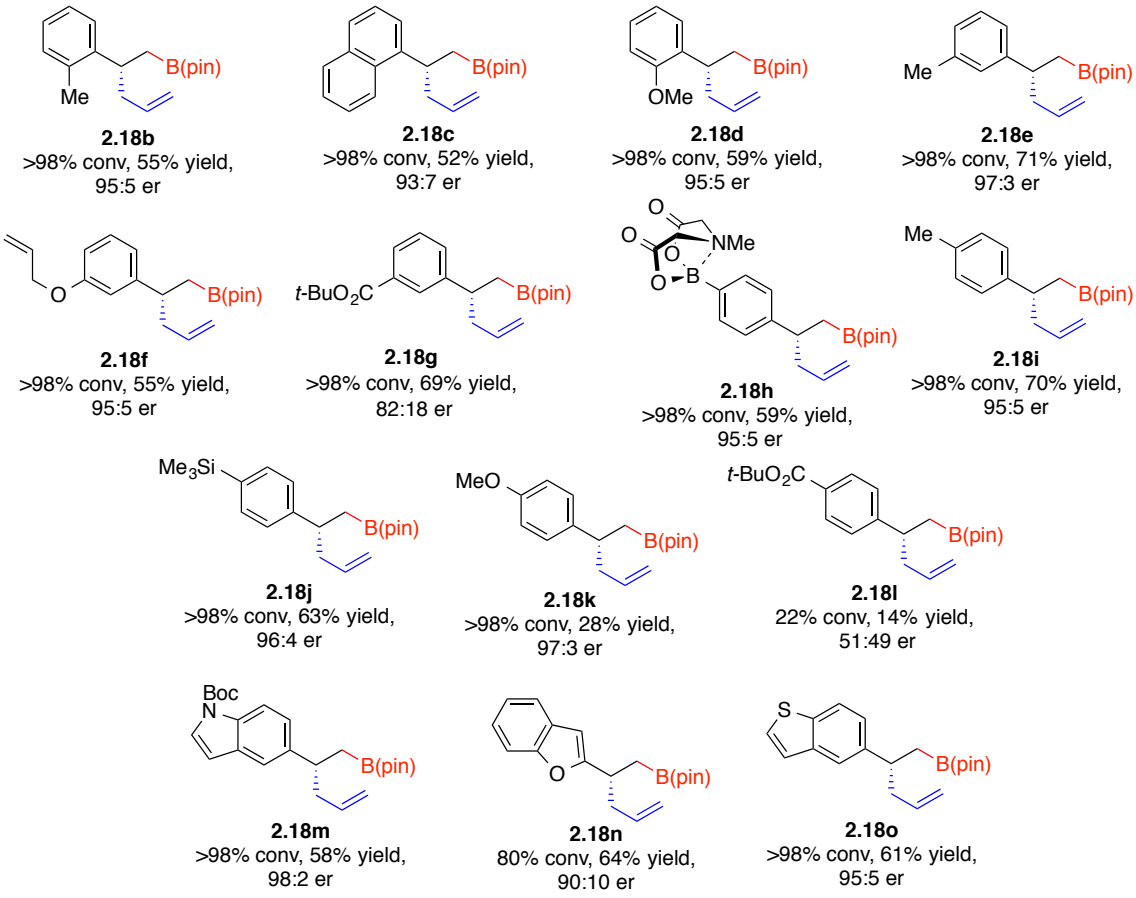

[a] See Table 2.2 for reaction conditions with ligand **2.24a**.

The lower er values for carboxylic ester **2.18g** and **2.18l** compared to a high er of **2.18k** could be due to a difference in the kinetic enantioselectivity in the copper–B(pin) addition step. Alternatively, it might be that a slower forming but more nucleophilic organocopper intermediate (affording **2.18k**) can react rapidly with allylphosphate so that high enantioselectivity may be preserved. If lower nucleophilicity of the electron-deficient alkenes, such as those with the *meta*-ester phenyl moiety in **2.18g**, reduces the rate of allylic substitution such that there is diminution in organocopper enantiopurity prior to C–C bond formation, then increasing allylphosphate concentration should cause allylic substitution to occur faster and kinetic enantioselectivity should be better

preserved. Indeed, whereas **2.18g** was formed in 69% yield and 82:18 er with a 3:1 aryl olefin:**2.17** ratio, reversing the ratio led to increase in enantioselectivity (95:5 er, 62% yield, Scheme 2.4). The same applies to *para*-bromophenyl-substituted **2.18p** (90:10 vs 84:16 er), *para*-B(pin)phenyl-substituted **2.18q** (92:8 vs 82:18 er), *meta*-B(pin)phenyl-substituted **2.18r** (96.5:3.5 vs 83:17 er) and 2-naphthyl-substituted **2.18s** (96:4 vs 89:11 er). However, the same strategy did not result in any er enhancement for *para*-esterphenyl-substituted **2.18l**. Because product enantiomeric purity can be improved by adjustment of substrate concentration, we concluded that the differences in kinetic selectivity in the initial Cu–B(pin) addition step is not the main cause for er fluctuation.

Scheme 2.4. Products of bis-phosphine–Cu-catalyzed multicomponent reactions (effect of higher allyl phosphate concentration)[a]

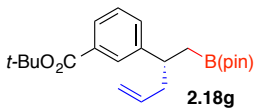

2.18g

3:1 alkene:allylphosphate: >98% conv, 69% yield, 82:18 er
1:3 alkene:allylphosphate: **83% conv, 62% yield, 95:5 er**

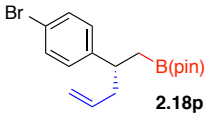

2.18p

3:1 alkene:allylphosphate: 75% conv, 57% yield, 84:16 er
1:3 alkene:allylphosphate: **84% conv, 62% yield, 90:10 er**

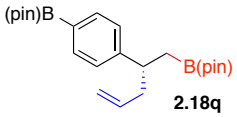

2.18q

3:1 alkene:allylphosphate: >98% conv, 48% yield, 82:18 er
1:3 alkene:allylphosphate: **66% conv, 56% yield, 92:8 er**

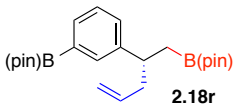

2.18r

3:1 alkene:allylphosphate: >98% conv, 44% yield, 83:17 er
1:3 alkene:allylphosphate: **71% conv, 52% yield, 96.5:3.5 er**

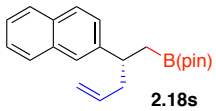

2.18s

3:1 alkene:allylphosphate: >98% conv, 65% yield, 89:11 er
1:3 alkene:allylphosphate: **80% conv, 50% yield, 96:4 er**

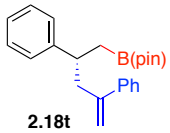

2.18t

3:1 alkene:allylic phosphate: >98% conv, 60% yield, 90:10 er
1:3 alkene:allylic phosphate: **>98% conv, 51% yield, 96:4 er**

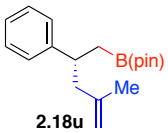

2.18u

3:1 alkene:allylic phosphate: 45% conv, 29% yield, 90:10 er
1:6 alkene:allylic phosphate: **>98% conv, 84% yield, 95:5 er**

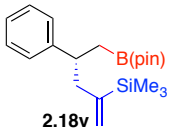

2.18v

3:1 alkene:allylic phosphate: >98% conv, 63% yield, 95:5 er
1:3 alkene:allylic phosphate: 88% conv, 73% yield, 96:4 er

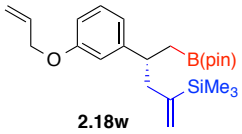

2.18w

3:1 alkene:allylic phosphate: >98% conv, 71% yield, 95:5 er
1:3 alkene:allylic phosphate: 77% conv, 55% yield, 96:4 er

[a] See Table 2.2 for reaction conditions with ligand **2.24a**, except **2.18t** and **2.18u**, ligand **2.24b** was used.

With a larger allylic phosphate, C–C bond formation might be slower, engendering lowering of er and thus higher allylic phosphate concentration could allow for better retention of kinetic stereoselectivity. This led us to find that **2.18t** and **2.18u** (Scheme 2.4), can be formed in higher enantioselectivity with 1:3 ratio of aryl olefin:allylic phosphate (96:4 vs 90:10 er and 95:5 vs 90:10 er, respectively). However, at this point we did not see much improvement for reactions to generate alkenylsilanes **2.18v** and **2.18w**.

Reactions with allylphenyl carbonate (**2.25**) were efficient but more enantioselective than when allylphosphate was employed. *ortho*- and *para*-Fluorophenyl-containing **2.18x** and **2.18y** and *ortho*-, and *para*-trifluoromethylphenyl-substituted **2.18z** and **2.18aa** were isolated in 50–68% yield and 96:4–98:2 er (vs 81:19–92:8 er with **2.17**). These findings expand the scope of the approach but were initially puzzling because allylphenyl carbonate is less electrophilic than allylphosphate as evidenced in lower conversion to the product in the absence of any ligand (e.g., ~40% vs ~10% conv to **2.18a** after 14 h). If slower C–C bond formation means loss of enantioselectivity, why would reactions with allylphenyl carbonate give higher er (vs allylphosphate)?

Scheme 2.5. Products of bis-phosphine–Cu-catalyzed multicomponent reactions (effect of electrophile identity)[a]

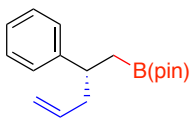

2.18a
LG = $OPO(OEt)_2$ (2.17):
>98% conv, 67% yield, 95:5 er
LG = OCO_2Ph (2.25):
87% conv, 44% yield, 97:3 er

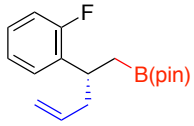

2.18x
LG = $OPO(OEt)_2$ (2.17):
>98% conv, 54% yield, 89:11 er
LG = OCO_2Ph (2.25):
79% conv, 64% yield, 96:4 er

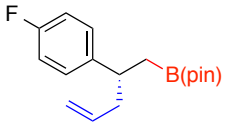

2.18y
LG = $OPO(OEt)_2$ (2.17):
>98% conv, 66% yield, 92:8 er
LG = OCO_2Ph (2.25):):
>98% conv, 65% yield, 98:2 er

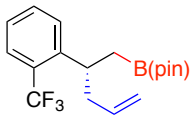

2.18z
LG = $OPO(OEt)_2$ (2.17):
86% conv, 65% yield, 88:12 er
LG = OCO_2Ph (2.25):
68% conv, 50% yield, 96:4 er

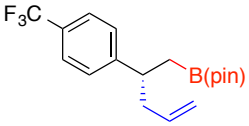

2.18aa
LG = $OPO(OEt)_2$ (2.17):
83% conv, 53% yield, 74:26 er
LG = OCO_2Ph (2.25):
>98% conv, 68% yield, 96:4 er

[a] See Table 2.2 for reaction conditions with ligand **2.24a**; except **2.18z** and **2.18aa**, 1:3 alkene:allyl electrophile was used

2.3.3. Comparison of Cu versus Cu/Pd system

As results in Scheme 2.6 indicate, under either set of conditions, products derived from strongly electron withdrawing *para* substituent were formed in low enantioselectivity (**2.18l**), indicating that this type of substituent is problematic with the two-catalyst method as well. While with a Pd-based co-catalyst,[78] *para*-bromophenyl containing product **2.18p** was formed in higher enantioselectivity (2:98 vs 90:10 er), reaction with allylphosphate and the bisphosphine ligand (**2.24a**) was more efficient (62% vs 43% yield). In some cases, one of approaches is superior. The single-catalyst conditions afforded *para*-methoxyphenyl-substituted product **2.18k** in better yield (28% vs <5%) and in 97:3 er. MIDA boronates are insoluble in *tert*-butylmethyl ether, the optimal solvent for the two-catalyst strategy resulting in no conversion to **2.18h**, while our procedure affords **2.18h** in 59% yield and 95:5 er. As underscored by less efficient processes leading to **2.18r** (24% vs 52% yield), the presence of the Pd complex may be

incompatible with an aryl-boron substituent present. The transformation with the 2-methyl-substituted allylic electrophiles was more efficient and enantioselective with the single-catalyst conditions (i.e., **2.18u** in 84% yield, 95:5 er vs 19 % yield, 11:89 er). With the allylic electrophile derived from 2-butene-1-ol, the Cu/Pd combination afforded **2.18ab** in 76% yield, >98% *E* selectivity and 4.5:95.5 er; with the corresponding secondary allylic phosphate and the single-catalyst method, the process was fully S_N2'-selective (>98%), affording **2.18ab** in 50% yield, 50:50 *E*:*Z*, 92:8 er (for either alkene isomer).

Scheme 2.6. Comparison of two-catalyst (chiral Cu and achiral Pd complexes) and single catalyst (chiral Cu complex) approaches

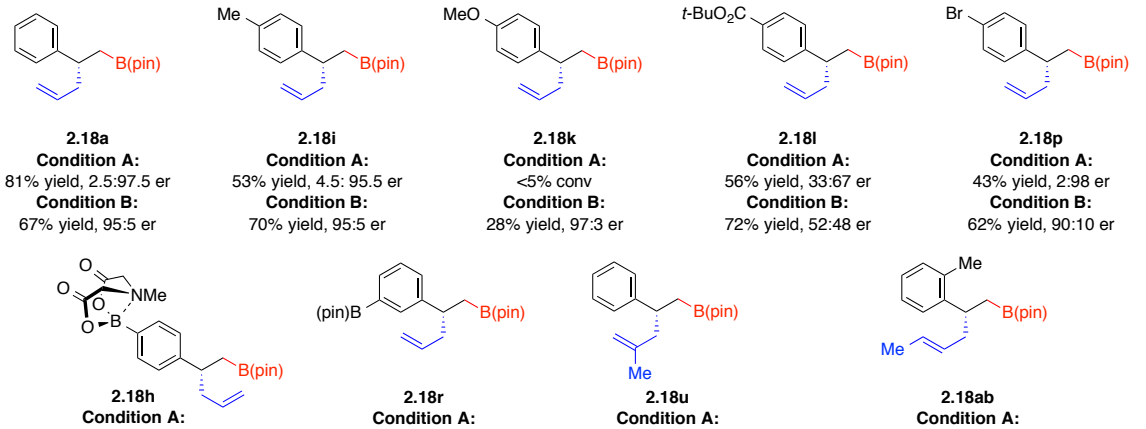

2.18a
Condition A:
81% yield, 2.5:97.5 er
Condition B:
67% yield, 95:5 er

2.18i
Condition A:
53% yield, 4.5: 95.5 er
Condition B:
70% yield, 95:5 er

2.18k
Condition A:
<5% conv
Condition B:
28% yield, 97:3 er

2.18l
Condition A:
56% yield, 33:67 er
Condition B:
72% yield, 52:48 er

2.18p
Condition A:
43% yield, 2:98 er
Condition B:
62% yield, 90:10 er

2.18h
Condition A:
<2% conv
Condition B:
59% yield, 95:5 er

2.18r
Condition A:
24% yield, 2:98 er
Condition B:
52% yield, 96.5:3.5 er

2.18u
Condition A:
19% yield, 11:89 er
Condition B:
84% yield, 95:5 er

2.18ab
Condition A:
76% yield, >98% *E*, >98% S_N2, 4.5:95.5 er
Condition B:
50% yield, 50% *E*, >98% S_N2', 92:8 er (*E* & *Z*)

The Conditions:
A (previous work, ref 78): alkene/allyl *t*-butylcarbonate (**2.16**): 1:1.5,
12 mol % **2.4**, 10 mol % CuOAc, 5.0 mol % Pd(dppf)Cl_2, 1.5 equiv $B_2(pin)_2$, 1.0 equiv KOH, *t*-BuOMe, 0 °C, 12 h
B (this work): alkene/allylic phosphate: 3:1 for **2.18a,i,k,h,u,ab**; 1:3 otherwise
5.5 mol % **2.24a** (for **2.18u** & **2.18ab**, **2.24b** used) , 5.0 mol % CuCl, 1.1 equiv $B_2(pin)_2$, 1.5 equiv NaO*t*-Bu, thf, 22 °C, 14 h

2.3.4. Application in the synthesis of natural product

The distinguishing attributes of the method are underscored in a formal enantioselective synthesis of heliespirones A and C (Scheme 2.7).[83] Reaction with alkene **2.26**, ligand **2.24b** and one gram of commercially available **2.17** afforded **2.27** in 64% yield and 97:3

(83) (a) Huang, C.; Liu, B. *Chem. Commun.* **2010**, *46*, 5280–5282. (b) Bai, W.-J.; Green, J. C.; Pettus, T. R. R. *J. Org. Chem.* **2012**, *77*, 379–387.

er; excess **2.26** can be recovered in 91% yield as part of purification by silica gel chromatography. With the two-catalyst protocol, **2.27** was isolated in similar yield (62%) but lower enantioselectivity (9:91 er). Cross-metathesis with 1.0 mol % **2.28** and 2-methyl-2-butene gave **2.29**, which was converted to **2.30** (92% after two steps).[84] Enantioselective epoxidation of **2.30** with **2.31**,[85] concomitant C–B oxidation, and acid-catalyzed hydrolysis generated triol **2.33** in 46% yield and 89:11 dr. Triol **2.33** was previously employed to access heliespirones A and C.[83a]

Scheme 2.7. Application to enantioselective synthesis of heliespirones A and C

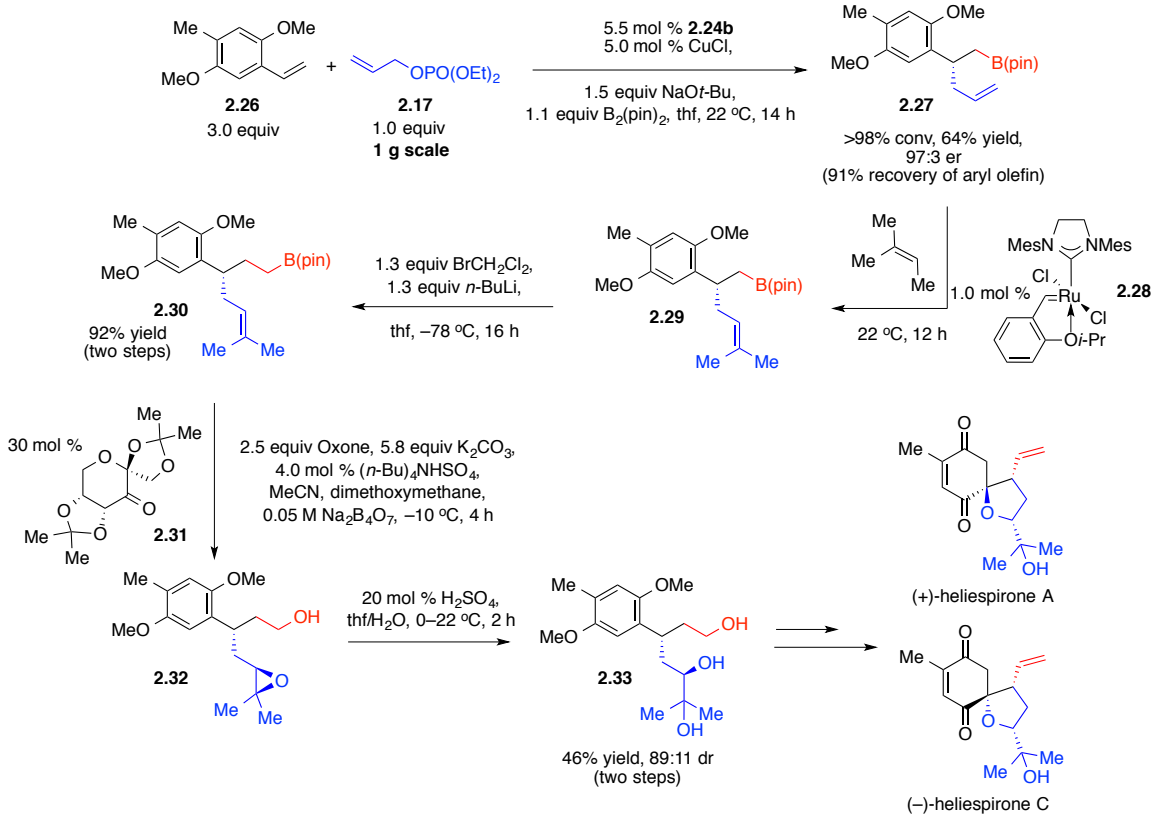

2.4. Mechanistic Investigation on Enantioselectivity Variations

2.4.1. Enantioselectivity loss by epimerization

(84) Sadhu, K. M.; Matteson, D. S. *Organometallics* **1985**, *4*, 1687–1689.

(85) Wang, Z.-X.; Tu, Y.; Frohn, M.; Zhang, J.-R.; Shi, Y. *J. Am. Chem. Soc.* **1997**, *119*, 11224–11235.

To probe the origins of enantioselectivity fluctuations, we first investigated the diastereoselectivity of reactions of *E*- and *Z*-β-deuterio-alkenes (2.34-*E* and 2.34-*Z*). As shown in Scheme 2.8, in the case of *para*-*tert*-butyl ester substituted styrene, regardless of the deuterated olefin isomer used, **2.35** was generated with minimal stereoselectivity (60:40–35:65 dr); the same was observed with the Cu/Pd system. Therefore, in this case there is facile epimerization at the copper-substituted stereogenic center.

Scheme 2.8. Probing enantioselectivity loss by epimerization

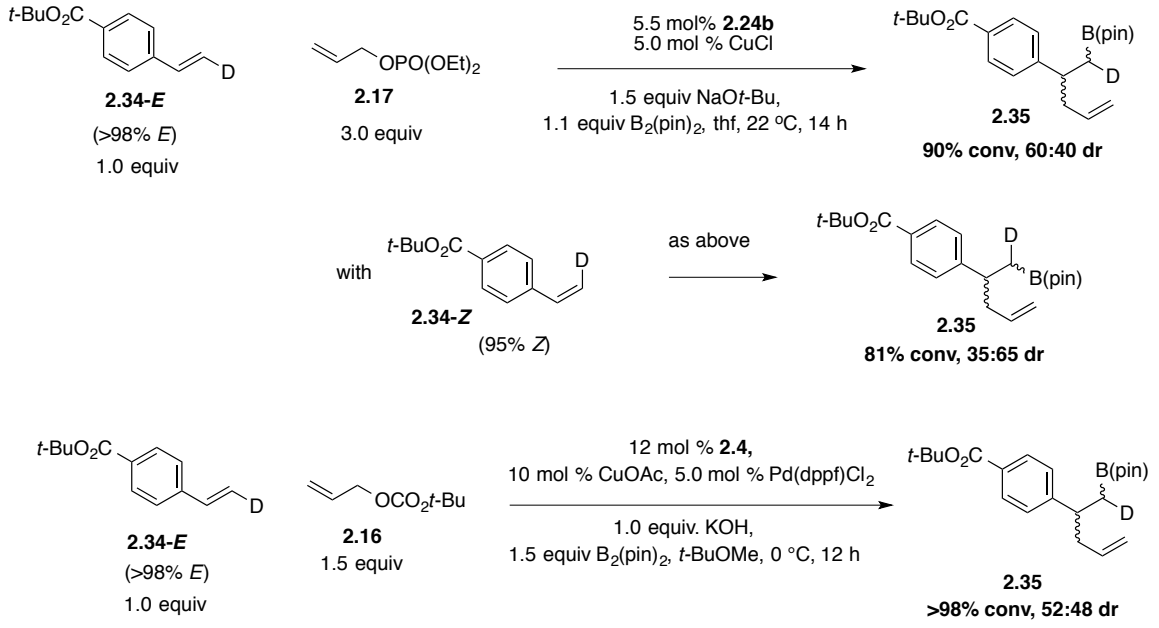

To probe whether epimerization at the Cu-substituted carbon center might occur by homolytic or heterolytic Cu–C bond rupture/re-formation, we investigated reactions with cyclopropenyl **2.36** (Table 2.3). With NHC–Cu complexes such as that derived imidazolinium salt **im-2**, only trisubstituted alkenyl–B(pin) compound **2.37** was generated (entry 1). With PPh3 (entry 2), sulfoxide-phosphine **2.4** (entry 3) or bisphosphine **2.24b**, with or without a Pd complex (entries 4–5), cyclopropyl containing **2.38** was formed exclusively.

Table 2.3. Examination the possibility of homolytic vs heterolytic Cu–C cleavage[a]

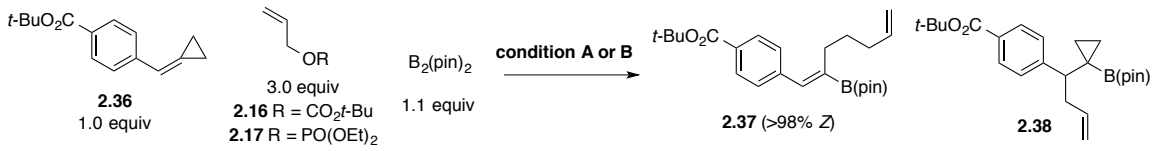

entry	ligand	condition	co-catalyst	conv (%); yield (%)	2.37:2.38	er of 2.38
1	**im-2**	**B**	none	87; 28	>98:2	NA
2	PPh_3	**B**	none	76; 19	<2:>98	NA
3	**2.4**	**A**	$Pd(dppf)Cl_2$	85; 71	<2:>98	58:42
4	**2.24b**	**B**	none	66; 35	<2:>98	46:54
5	**2.24b**	**B**	$Pd(dppf)Cl_2$	18; 8	<2:>98	50:50

[a] See Scheme 2.6 for conditions A and B.

Although, NHC ligands can stabilize odd-electron intermediates[86] but when diene **2.39** was used with an NHC- or a bisphosphine-based complex (Scheme 2.9), none of the cyclopentenyl product **2.41** was observed. This signified that ionic pathways are involved with *para-tert*-butyl ester styrene and NHC– or phosphine–Cu complexes and cyclopropyl rupture in the NHC–Cu system is due to the stronger electron donating ability of the carbene ligands resulting in higher electron density at the benzylic carbon. Based on the above findings, it appears that a strongly electron withdrawing aryl unit can stabilize accumulation of electron density at the benzylic site, facilitating heterolytic cleavage/re-formation of the Cu–C bond.

Scheme 2.9. Examination the possibility of homolytic vs heterolytic Cu–C cleavage

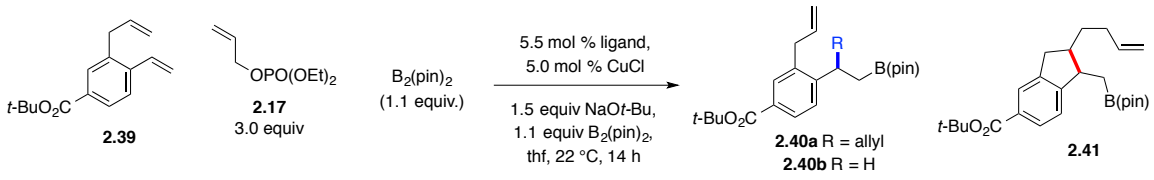

2.4.2. Fluctuation in enantioselectivity due to Cu–H elimination

(86) Styra, S.; Melaimi, M.; Moore, C. E.; Rheingold, A. L.; Augenstein, T.; Breher, F.; Bertrand, G. *Chem. Eur. J.* **2015**, *21*, 8441–8446.

Results were different with other deuterium-labeled alkenes (Scheme 2.10): *anti*- and *syn*-**2.18g-*d***, **2.18aa-*d*** and **2.18t-*d*** were formed with >98% diastereospecificity (ds); the outcomes were the same under the two-catalyst conditions. These data showed that there is hardly or no epimerization at the Cu-substituted stereogenic center in these cases. Thus, there must be other mechanisms responsible for changes in er values.

Scheme 2.10. Probing the isomerization at the Cu-substituted carbon stereogenic center by isotopic labeling[a]

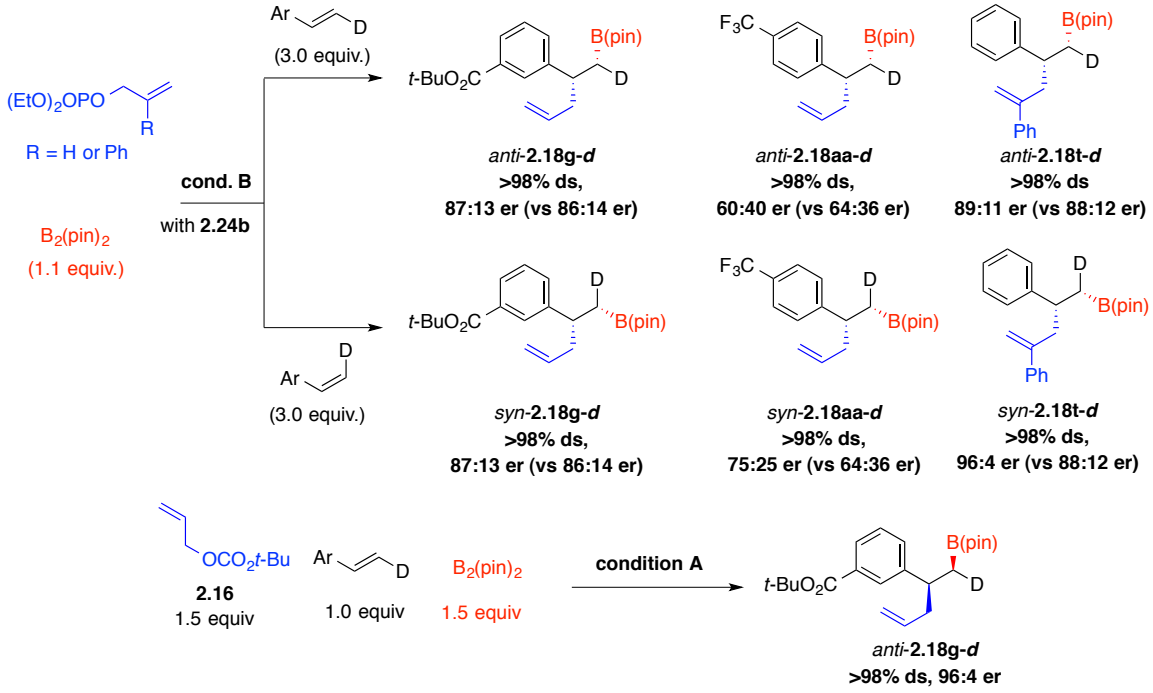

[a] See Scheme 2.6 for conditions A and B. The er values in parenthesis correspond to reactions with non-labeled substrates.

Two pathways may account for the er variability (other than epimerization): Cu–B(pin) and Cu–H elimination/re-addition from the opposite face of the alkene. The Cu–boryl elimination/re-addition possibility was ruled out because computational studies (DFT) performed by Dr. Sebastian Torker revealed that this would be energetically unfavorable; energy barrier for Cu–B elimination is ~30 kcal/mol (Scheme 2.11).

Scheme 2.11. Selected energy barriers obtained through DFT studies with model system

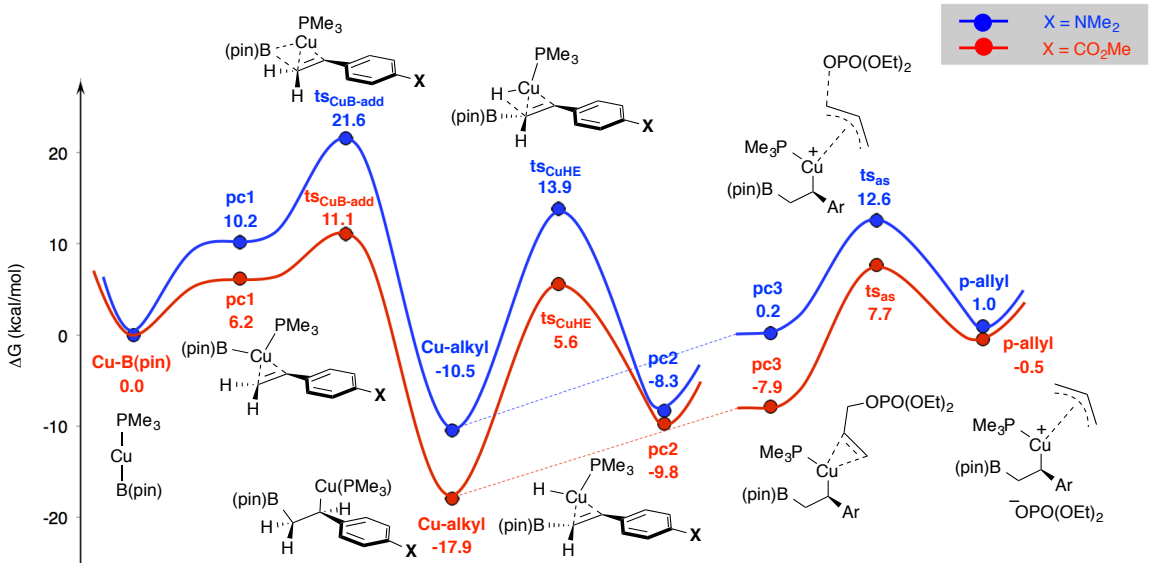

Concerning the Cu–H elimination/re-addition possibility, alkenyl–B(pin) byproducts could be detected (~10% during synthesis of **2.18a** with allylphenyl carbonate **2.25**). Moreover, *syn*-**2.18aa-*d*** and *syn*-**2.18t-*d*** were obtained with higher enantioselectivity compared to reactions with the non-labeled aryl olefins (75:25 vs 64:36 er and 96:4 vs 88:12 er, respectively, Scheme 2.10). This is probably because, as illustrated in Scheme 2.12, Cu–D elimination to afford *syn*-**2aa-*d*** and *syn*-**2t-*d*** is slower. Cu–H elimination can have a significant impact on enantioselectivity when *p*-CF_3 styrene is used due to much less nucleophilic organocopper to react with allyl electrophile or when the allylating agent is hindered (slower C–C bond formation).

Scheme 2.12. Influence of aryl olefin D-labeling on variations in er

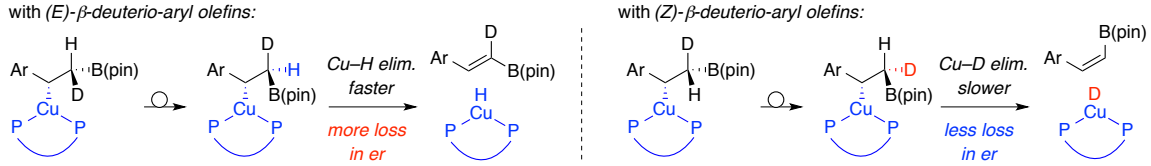

However, it does not appear to be the re-addition of Cu–H species causing the lower er because Cu–H adds to alkenyl–B(pin) with the opposite site selectivity (Scheme

2.13).[87] It is more likely that loss in enantioselectivity comes from the major alkylcopper diastereomer undergoes Cu–H elimination faster.

Scheme 2.13. Probing the possibility of Cu–H re-addition

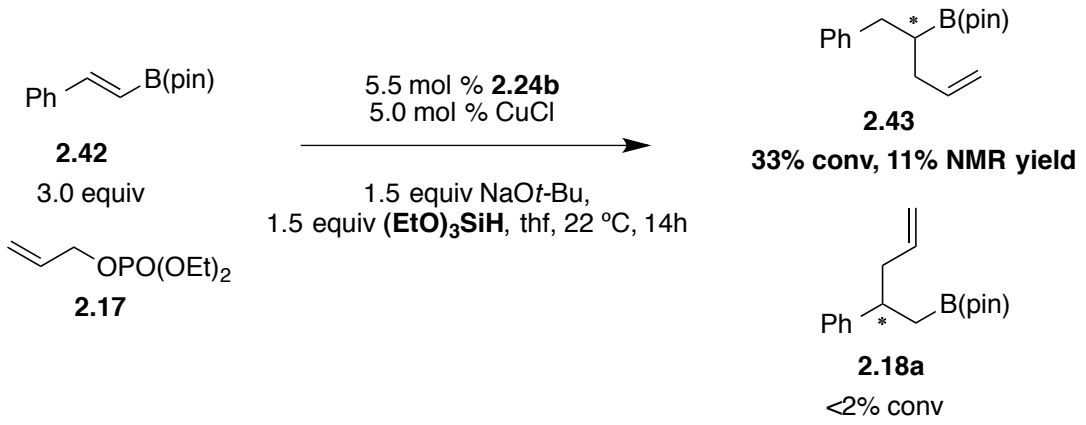

2.4.3. Competitive pathways via achiral Cu complexes

In addition to epimerization and Cu–H elimination, the presence of a Cu complex without a chiral phosphine on it could lead to formation of racemic product, which will lower the er values. As data in Scheme 2.14a indicate, reaction of **2.42** and **2.17-d$_2$** generates the product with lower S_N2' selectivity in the absence of a ligand (85% S_N2'). When bis-phosphine **2.24b** is present, 91% S_N2' is observed (with un-optimal 3:1 alkene:allylphosphate). In contrast, with **2.24b** or PPh_3 present and optimal 1:3 alkene:allylphosphate, the product is formed in >98% S_N2'. This suggests that in an un-optimal condition, there may be a reaction involving an achiral Cu complex. Furthermore, with larger amounts of the chiral ligand (**2.24b**), high enantioselectivity can be obtained even with an un-optimal alkene:allylphosphate ratio (3:1). As shown in Scheme 2.14b, with 20 mol % **2.24b**, compound **2.18g** was formed in 95:5 er, similar to the result with excess allylphosphate (optimal result; see Scheme 2.4).

(87) Laitar, D. S.; Tsui, E. Y.; Sadighi, J. P. *Organometallics* **2006**, *25*, 2405–2408.

Scheme 2.14. Impact of bis-phosphine ligand

a) Influence of bis-phosphine ligand on S_N2' selectivity

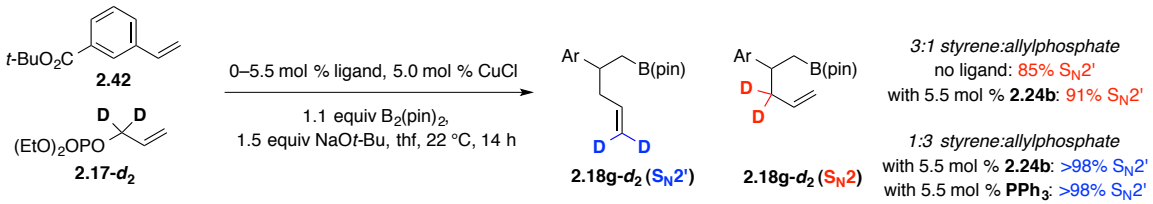

b) Influence of ligand loading on er

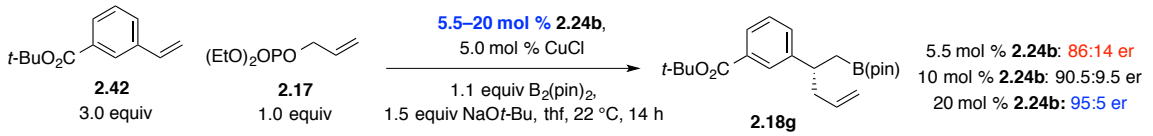

The most enantioselective pathway might begin with formation of alkylcopper ***S*-iii** from addition of **ii** to olefin, eventually affording product **vi** in high S_N2' and enantioselectivity (Scheme 2.15). However, ***S*-iii** could undergo diastereoselective Cu–H elimination more facile compared ***R*-iii** leading to lower er, especially with an electron-deficient aryl olefins (less nucleophilic alkylcopper) or at lower concentration and/or bulkier allylic electrophiles.

Metal alkoxide bridging to Cu centers can prevent phosphine chelation (**vii**).[88] With a more electrophilic olefin such as *m*-ester or *p*-CF_3 styrene, additions can be facile with less reactive achiral Cu–B(pin) (**ix** via **viii**); as a result, lower S_N2' and er value were observed at higher concentration of olefin. Thus increasing the amount of the chiral bis-phosphine ligand results in higher enantioselectivity (cf. Scheme 2.14b).

With a more reactive allylic phosphate, the achiral Cu–B(pin) **viii** is partially removed by conversion to allyl–B(pin). Thus at higher concentration of allylic phosphate there is some increase in er value.

(88) (a) Lemmen, T. H.; Goeden, G. V.; Huffman, J. C.; Geerts, R. L.; Caulton, K. G. *Inorg. Chem.* **1990**, *29*, 3680–3685. (b) Dubinina, G. G.; Furutachi, H.; Vicic, D. A. *J. Am. Chem. Soc.* **2008**, *130*, 8600–8601.

In the case of allylphenyl carbonate (**2.25**), although it is less reactive and should result in lower enantioselectivity of the product. However, we found that in the reaction with allylphenyl carbonate in the absence of phosphine ligand, there is significant amount of alkenyl–B(pin) formed. This implies that **2.25** does not react efficiently with **ix** to generate ***rac*-vi**. Cu–H elimination to form **xiii** serves as a corrective mechanism here.

Scheme 2.15. Rationale for variations in enantioselectivity and S_N2':S_N2 selectivity

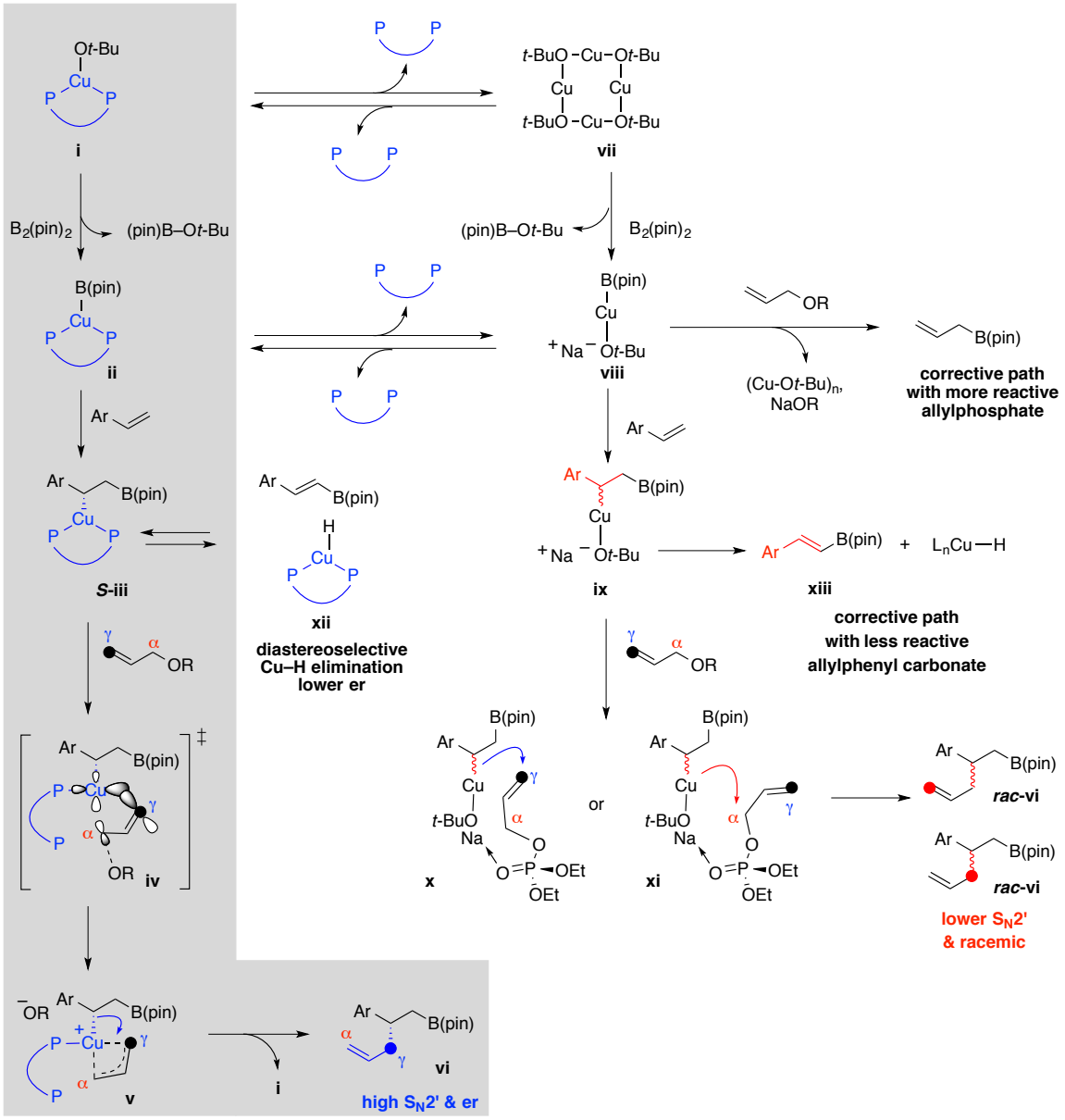

2.4.4. Relevance to other catalytic processes

The principles outlined above are applicable to catalytic hydroaminations. In the instances shown in Scheme 2.16, increasing the amount of the hydroxylamine improves enantioselectivity (93:7 to 96:4 er for **2.45** and 88:12 to 96:4 er for **2.46**); this is despite the initially high selectivities and the narrow window for improvement in the former case (corresponding to $DDG^{‡}$ = 0.35 and 0.70 kcal/mol, respectively). Excess bis-phosphine does not alter enantioselectivity of the reaction with the more electron rich dihydronaphthalene[79] (93:7 er for **2.45** with 2.2 or 8.8 mol % **2.8**), but the case of a more electrophilic alkenylboronate,[80] higher er is obtained when **2.8** is used in larger amounts (97:3 and 88:12 er for **2.46** with 40 and 10 mol % **2.8**, respectively).

Scheme 2.16. Relevance to other catalytic systems

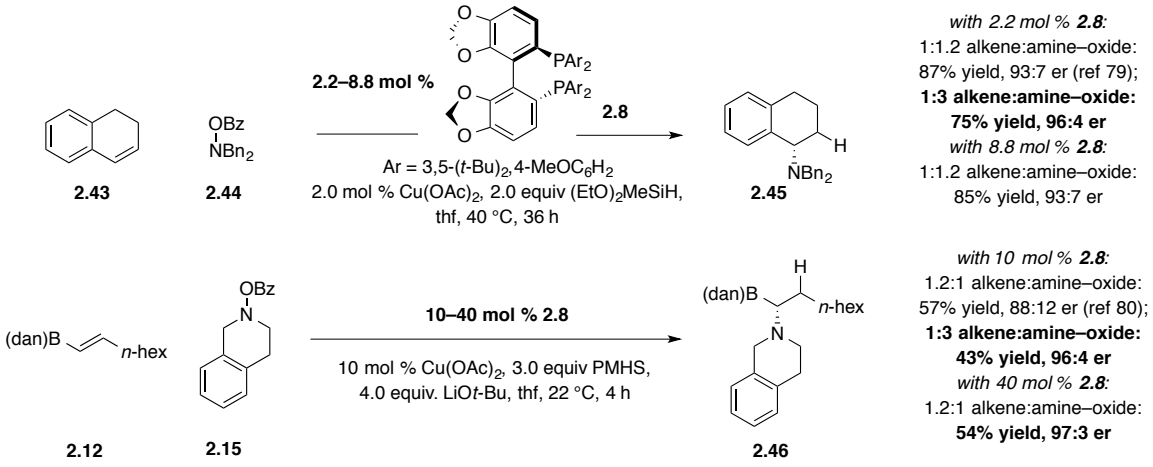

2.5. Conclusions

We illustrate that catalytic allyl–boron additions can be performed without a co-catalyst at ambient temperature efficiently and with high enantioselectivity. Rationally designed strategies, not applicable to processes where a C–C bond generating event is stereochemistry determining (vs C–metal bond formation), may be adopted for

maximizing enantioselectivity. We show how the stereochemical integrity of organocopper intermediates depends on their steric and/or electronic attributes and in what ways enantioselectivity of the processes may vary according to the concentration of the alkene substrate and/or the allylic electrophile. The principles underscored by this investigation are expected to aid future endeavors regarding the development of enantioselective transformations catalyzed by organocopper entities.

2.6. Experimental Section

General. Infrared (IR) spectra were recorded on a Bruker FT-IR Alpha (ATR mode) spectrophotometer, ν_{max} in cm^{-1}. Bands are characterized as broad (br), strong (s), medium (m), and weak (w). ^{1}H NMR spectra were recorded on Varian Unity INOVA 400 (400 MHz), 500 (500 MHz), or 600 (600 MHz) spectrometers. Chemical shifts are reported in ppm from tetramethylsilane with the solvent resonance as the internal standard ($CDCl_3$: δ 7.26 ppm). Data are reported as follows: chemical shift, integration, multiplicity (s = singlet, d = doublet, t = triplet, q = quartet, pent = pentet, m = multiplet, br = broad, app = apparent), and coupling constants (Hz). ^{13}C NMR spectra were recorded on Varian Unity INOVA 400 (100 MHz), 500 (125 MHz), or 600 (150 MHz) spectrometers with complete proton decoupling. Chemical shifts are reported in ppm from tetramethylsilane with the solvent resonance as the internal standard ($CDCl_3$: δ 77.16 ppm). High-resolution mass spectrometry was performed on a JEOL AccuTOF DART (positive mode) at the Mass Spectrometry Facility, Boston College. Enantiomeric ratios were determined by HPLC analysis (high-performance liquid chromatography) with a Shimadzu chromatograph [Chiral Technologies Chiralcel AZ-H (4.6 x 250 mm), Chiral Technologies Chiralcel OC-H (4.6 x 250 mm), Chiral Technologies Chiralcel OD-

H (4.6 x 250 mm), Chiral Technologies Chiralcel OJ-H (4.6 x 250 mm), Chiral Technologies Chiralcel OZ-H (4.6 x 250 mm), or Chiral Technologies Chiralpak AD-H (4.6 x 250 mm)] in comparison with authentic racemic materials. Specific rotations were measured on a Rudolph Research Analytical Autopol IV Polarimeter. Melting points were measured on a Thomas Hoover capillary melting point apparatus and are uncorrected. X-ray structures were obtained, as described in the cif file, with a Microfocus sealed Cu tube from Incote. It is well established that that aforementioned detector allows for the determination of absolute configuration of molecules that do not have a heavy atom.

Unless otherwise noted, reactions were carried out with distilled and degassed solvents under an atmosphere of dry N_2 in oven- (135 ºC) or flame-dried glassware with standard dry box or vacuum-line techniques. Hexanes was purified under a positive pressure of dry argon by a modified Innovative Technologies purification system through a copper oxide and alumina column. Tetrahydrofuran (thf; Aldrich Chemical Co.) was purified by distillation from sodium benzophenone ketyl immediately prior to use. All work-up and purification procedures were carried out with reagent grade solvents (purchased from Fisher Scientific) under air.

■ **Reagents:**

Allyl phenyl carbonate (2.25): purchased from Aldrich and used as received.

Allyl *tert*-butyl carbonate (2.16): prepared according to a previously reported procedure.[89]

(89) Zhang, P.; Brozek, L. A.; Morken, J. P. *J. Am. Chem. Soc.* **2010**, *132*, 10686–10688.

Bis(pinacolato)diboron [$B_2(pin)_2$]: purchased from Frontier Scientific, Inc., recrystallized from pentane and dried under vacuum prior to use.

***n*-Butyllithium (1.6 M in hexanes):** purchased from Aldrich and used as received.

Chlorotrimethylsilane: purchased from Acros and used as received.

Copper(I) chloride: purchased from Strem and used as received.

Deuterium oxide (D_2O): purchased from Cambridge Isotope Laboratories and used as received.

Diethyl allyl phosphate (2.17): purchased from Aldrich and used as received.

Diisobutylaluminum hydride (dibal-H): purchased neat from Aldrich and used as received.

Di-*tert*-butyl-dicarbonate (Boc_2O): purchased from Advanced ChemTech and used as received.

Hoveyda-Grubbs catalyst 2nd generation (2.28): purchased from Aldrich and used as received.

Hydrogen peroxide (30 wt % in H_2O): purchased from Aldrich and used as received.

Imidazolinium salt im-1 and im-2: purchased from Aldrich and used as received.

Imidazolinium salt im-3–im-7: prepared according to a previously reported procedure.[90]

Imidazolinium salt im-9 and im-10: prepared according to a previously reported procedure.[91]

Imidazolinium salt im-11: prepared according to a previously reported procedure.[92]

---

(90) Lee, K-s.; Hoveyda, A. H. *J. Org. Chem.* **2009**, *74*, 4455–4462.

(91) (a) Brown, M. K.; May, T. L.; Baxter, C. A.; Hoveyda, A. H. *Angew. Chem., Int. Ed.* **2007**, *46*, 1097–1100. (b) May, T. L.; Brown, M. K.; Hoveyda, A. H. *Angew. Chem., Int. Ed.* **2008**, *47*, 7468–7472.

2-Isopropoxy-4,4,5,5-tetramethyl-1,3,2-dioxaborolane [*i*-PrOB(pin)]: purchased from Aldrich and used as received.

Oxone®, monopersulfate compound: purchased from Aldrich and used as received.

Phosphine 2.4: prepared according to a previously reported procedure.[93]

Phosphine ligands (2.8, 2.19–2.24a–c): purchased from Strem and used as received.

Pyridinium dichromate (PDC): purchased from Aldrich and used as received.

Sodium *tert*-butoxide: purchased from Strem and used as received.

Sodium hydroxide (2 M): prepared from NaOH purchased from Fisher (used as received) and deionized water.

Sulfuric acid: purchased from Fisher and used as received.

Tetrabutylammonium fluoride (tbaf, 1.0 M in thf): purchased from Oakwood and used as received.

Preparation of aryl or heteroaryl olefins: unless otherwise noted, olefins were purchased from Acros, Aldrich, Alfa Aesar, Combi-Blocks, Matrix Scientific, or TCI, and distilled over CaH_2 under reduced pressure prior to use.

The following olefins were synthesized from the corresponding aldehydes by Wittig olefination.[94]

1,4-Dimethoxy-2-methyl-5-vinylbenzene (2.26): Melting point: 41–42°C. IR (neat): 2995 (w), 2935 (w), 2830 (w), 1623 (w), 1501 (s), 1464 (m), 1416 (m), 1399 (m), 1207

---

(92) Clavier, H.; Coutable, L.; Toupet, L.; Guillemin, J.-C.; Mauduit, M. *J. Organomet. Chem.* **2005**, *690*, 5237–5254.

(93) Jia, T.; Cao, P.; Wang, B.; Lou, Y.; Yin, X.; Wang, M.; Liao, J. *J. Am. Chem. Soc.* **2015**, *137*, 13760–13763.

(94) Cho, S. J.; Jensen, N. H.; Kurome, T.; Kadari, S.; Manzano, M. L.; Malberg, J. E.; Caldarone, B.; Roth, B. L.; Kozikowski, A. P. *J. Med. Chem.* **2009**, *52*, 1885–1902.

(s), 1182 (m), 1042 (s), 996 (m), 902 (m) cm^{-1}; ^1H NMR (400 MHz, $CDCl_3$): δ 7.02 (1H, dd, *J* = 18.0, 11.2 Hz), 6.95 (1H, s), 6.70 (1H, s), 5.68 (1H, dd, *J* = 17.8, 1.4 Hz), 5.22 (1H, dd, *J* = 11.2, 1.2 Hz), 3.82 (3H, s), 3.80 (3H, s), 2.23 (3H, s); ^{13}C NMR (100 MHz, $CDCl_3$): δ 152.0, 150.8, 131.7, 127.5, 124.5, 114.7, 113.3, 108.2, 56.4, 55.9, 16.4; HRMS (DART): Calcd for $C_{11}H_{15}O_2$ $[M+H]^+$: 179.1072, Found: 179.1069.

1-(Allyloxy)-3-vinylbenzene (substrate for 2.18f and 2.18w): The spectroscopic data match those reported previously.[95] ^1H NMR (400 MHz, $CDCl_3$): δ 7.24 (1H, t, *J* = 8.0 Hz), 7.03–6.96 (2H, m), 6.83 (1H, ddd, *J* = 8.2, 2.6, 0.9 Hz), 6.68 (1H, dd, *J* = 17.6, 10.8 Hz), 6.07 (1H, ddt, *J* = 17.3, 10.6, 5.3 Hz), 5.73 (1H, dd, *J* = 17.6, 0.9 Hz), 5.43 (1H, dq, *J* = 17.3, 1.6 Hz), 5.29 (1H, dq, *J* = 10.5, 1.4 Hz), 5.25 (1H, dd, *J* = 10.9, 0.9 Hz), 4.56 (2H, dt, *J* = 5.3, 1.5 Hz).

***tert*-Butyl 5-vinyl-1*H*-indole-1-carboxylate (substrate for 2.18m)**: The spectroscopic data match those reported previously.[96] ^1H NMR (400 MHz, $CDCl_3$): δ 8.08 (1H, d, *J*= 8.0 Hz), 7.58–7.57 (2H, m), 7.41 (1H, dd, *J* = 8.4, 1.2 Hz), 6.81 (1H, dd, *J* = 17.6, 10.8 Hz), 6.55–6.54 (1H, m), 5.75 (1H, dd, *J* = 17.2, 1.2 Hz), 5.21 (1H, dd, *J* = 10.4, 0.8 Hz), 1.68 (9H, s).

2-Vinylbenzofuran (substrate for 2.18n): The spectroscopic data match those reported previously.[97] ^1H NMR (400 MHz, $CDCl_3$): δ 7.52 (1H, ddd, *J* = 7.6, 1.4, 0.7 Hz), 7.45 (1H, dq, *J* =8.2, 0.9 Hz), 7.30–7.24 (2H, m), 6.64 (1H, dd, *J* = 17.5, 11.2 Hz), 6.60 (1H, s), 5.96 (1H, ddd, *J* = 17.4, 1.3, 0.6 Hz), 5.41 (1H, dd, *J* = 11.2, 1.2 Hz).

---

(95) Paul, C. E.; Rajagopalan, A.; Lavandera, I.; Gotor-Fernández, V.; Kroutil, W.; Gotor V. *Chem. Commun*. **2012**, *48*, 3303–3305.

(96) Molander, G. A.; Brown, A. R. *J. Org. Chem.* **2006**, *71*, 9681–9686.

(97) (a) Brewer, J. D.; Elix, J. A. *Aust. J. Chem.* **1975**, *28*, 1059–1081, (b) Aitken, R. A.; Burns, G. *J. Chem. Soc., Perkin Trans. 1* **1994**, 2455–2460.

The following olefins were synthesized from the corresponding aryl bromides by a two-step lithium halogen exchange/addition to TMSCl or *i*-PrOB(pin). To a flame-dried round bottom flask equipped with a stir bar was added 4-bromostyrene (0.71 mL, 5.5 mmol) and thf (30 mL) under N_2. The resulting solution was allowed to cool to –78 ºC (dry ice/acetone) and *n*-butyllithium (1.6 M in hexanes, 3.8 mL, 6.0 mmol) was added dropwise into the solution through syringe. The resulting light yellow solution was allowed to stir for 1 h at –78 ºC and then TMSCl (0.84 mL, 6.6 mmol) was added dropwise by syringe. The mixture was allowed to slowly warm up to 22 ºC. After 16 h, the reaction was quenched by the addition of H_2O (10 mL) and a saturated solution of aqueous NH_4Cl (10 mL). The layers were separated and the aqueous layer was washed with Et_2O (3 x 20 mL). The combined organic layers were dried over $MgSO_4$ and concentrated under reduced pressure. The resulting yellow oil was purified by silica gel chromatography (100% hexanes) to afford **trimethyl(4-vinylphenyl)silane** (substrate for **2.18j**) as colorless oil (876 mg, 5.0 mmol, 91%): IR (neat): 3063 (w), 3008 (w), 2956 (m), 1629 (w), 1389 (m), 1248 (m), 1105 (m), 989 (m), 906 (m), 826 (s), 761 (m), 730 (m), 692 (m), 642 (m) cm^{-1}; ^1H NMR ($CDCl_3$, 400 MHz): δ 7.51 (2H, d, J = 7.6 Hz), 7.43 (2H, d, J = 8.0 Hz), 6.74 (1H, dd, J = 17.6, 10.9, Hz), 5.80 (1H, d, J = 17.6 Hz), 5.27 (1H, d, J = 10.9 Hz), 0.29 (9H, s); ^{13}C NMR ($CDCl_3$, 100 MHz): δ 140.3, 138.1, 137.0, 133.7, 125.7, 114.2, –1.0; HRMS (DART): Calcd for $C_{11}H_{17}Si$ $[M+H]^+$: 177.1100, Found: 177.1101.

4,4,5,5-Tetramethyl-2-(4-vinylphenyl)-1,3,2-dioxaborolane (substrate for 2.18q): Following the above procedure except *i*-PrOB(pin) was used instead of TMSCl, the product was obtained as colorless oil [purified by silica gel chromatography

(hexanes:Et_2O = 25:1)] (1.0 g, 4.5 mmol, 82%). IR (neat): 2978 (m), 2930 (w), 1629 (m), 1552 (w), 1397 (m), 1356 (s), 1322 (s), 1269 (m), 1213 (w), 1142 (s), 1088 (s), 1018 (m), 990 (m), 962 (m), 830 (m), 758 (w), 682 (m) cm^{-1}; ^1H NMR ($CDCl_3$, 400 MHz): δ 7.82 (2H, d, *J* = 8.0 Hz), 7.44 (2H, d, *J* = 8.0 Hz), 6.76 (1H, dd, *J* = 17.6, 10.8 Hz), 5.84 (1H, dd, *J* = 17.6, 1.2 Hz), 5.32 (1H, dd, *J* = 10.8, 0.8 Hz), 1.38 (12H, s); ^{13}C NMR ($CDCl_3$, 100 MHz): δ 140.3, 137.0, 135.1, 125.6, 114.9, 83.8, 25.0, 24.9; HRMS (DART): Calcd for $C_{14}H_{20}BO_2$ $[M+H]^+$: 231.1556; Found: 231.1563.

4,4,5,5-Tetramethyl-2-(3-vinylphenyl)-1,3,2-dioxaborolane (substrate for 2.18r): Following the above except 3-bromostyrene and *i*-PrOB(pin) were used instead of 4-bromostyrene and TMSCl, respectively, the product was obtained as colorless oil [purified by silica gel chromatography (hexanes:Et_2O = 25:1)] (1.1 g, 4.7 mmol, 85%). IR (neat): 2978 (w), 2929 (m), 1380 (m), 1353 (s), 1319 (s), 1141 (s), 1079 (s), 990 (m), 963 (m), 908 (m), 831 (m), 710 (w), 699 (s), 681 (m) cm^{-1}; ^1H NMR ($CDCl_3$, 400 MHz): δ 7.87 (1H, s), 7.73 (1H, d, *J* = 7.3 Hz), 7.53 (1H, dt, *J* = 7.8, 1.6 Hz), 7.35 (1H, t, *J* = 7.5 Hz), 6.75 (1H, dd, 17.6, 10.9 Hz), 5.81 (1H, dd, *J* = 17.6, 0.9 Hz), 5.26 (1H, dd, *J* = 10.9, 0.9 Hz), 1.37 (12H, s); ^{13}C NMR ($CDCl_3$, 100 MHz): δ 137.0, 136.9, 134.3, 132.9, 129.0, 128.0, 114.0, 83.9, 25.0, 24.9; HRMS (DART): Calcd for $C_{14}H_{20}BO_2$ $[M+H]^+$: 231.1556, Found: 231.1567.

***tert*-Butyl 3-vinylbenzoate (substrate for 2.18g)**: Prepared according to the reported procedure.[98] IR (neat): 2978 (w), 2932 (w), 1711 (s), 1367 (m), 1294 (s), 1271 (m), 1256 (m), 1158 (s), 1113 (m), 1086 (m), 909 (m), 763 (s) cm^{-1}; ^1H NMR (400 MHz, $CDCl_3$): δ

(98) Miller, W. H.; Seefeld, M. A.; Newlander, K. A.; Uzinskas, I. N.; Burgess, W. J.; Heerding, D. A.; Yuan, C. C. K.; Head, M. S.; Payne, D. J.; Rittenhouse, S. F.; Moore, T. D.; Pearson, S. C.; Berry, V.; DeWolf, Jr. W. E.; Keller, P. M.; Polizzi, B. J.; Qiu, X.; Janson, C. A.; Huffman, W. F. *J. Med. Chem.* **2000**, *45*, 3246–3256.

8.03 (1H, dd, *J* = 2.2, 1.0 Hz), 7.88 (1H, dt, *J* = 7.6, 1.2 Hz), 7.57–7.55 (1H, m), 7.37 (1H, t, *J* = 7.8 Hz), 6.75 (1H, dd, *J* = 17.6, 10.8 Hz), 5.82 (1H, dd, *J* = 17.6, 0.4 Hz), 5.31 (1H, dd, *J* = 11.0, 0.6 Hz), 1.61 (9H, s); ^{13}C NMR (100 MHz, $CDCl_3$): δ 165.8, 137.8, 136.2, 132.4, 130.1, 128.8, 128.5, 127.3, 115.0, 81.2, 28.3, ; HRMS (DART): Calcd for $C_{13}H_{17}O_2$ $[M+H]^+$: 205.1229, Found: 205.1235.

***tert*-Butyl 4-vinylbenzoate (substrate for 2.18l)**: Prepared according to the reported procedure.[98] The spectroscopic data match those reported previously.[99] ^{1}H NMR (400 MHz, $CDCl_3$): δ 7.94 (2H, d, *J*= 8.0 Hz), 7.44 (2H, d, *J* = 8.0 Hz), 6.75 (1H, dd, *J* = 17.6, 10.8 Hz), 5.84 (1H, dd, *J* = 17.6, 1.2 Hz), 5.36 (1H, dd, *J* = 11.0, 0.2 Hz), 1.60 (9H, s).

Preparation of allylic phosphates (substrates for 2.18t, 2.18v–w): Allylic alcohols were synthesized from the corresponding alkenyl bromides (purchased from Aldrich and used as received) by a two-step lithium halogen exchange/addition to formaldehyde sequence.[100] Subsequently, allylic alcohols were converted to the corresponding allylic phosphates based on an established method.[101]

Diethyl (2-phenylallyl) phosphate (substrates for 2.18t): IR (neat): 2983 (w), 2908 (w), 1444 (w), 1262 (m), 1165 (w), 1016 (s), 975 (s), 778 (m), 707 (m) cm^{-1}; ^{1}H NMR (400 MHz, $CDCl_3$): δ 7.43–7.46 (2H, m), 7.28–7.37 (3H, m), 5.57 (1H, s), 5.44 (1H, s), 4.93 (2H, d, *J* = 7.2 Hz), 4.11–4.03 (4H, m), 1.31–1.28 (6H, m); ^{13}C NMR (100 MHz, $CDCl_3$): δ 142.9 (d, *J* = 7.5 Hz), 137.7, 128.6, 128.2, 126.2, 115.4, 68.7 (d, *J* = 5.3 Hz), 63.9 (d, *J*

(99) Mäsing, F.; Mardyukov, A.; Doerenkamp, C.; Eckert, H.; Malkus, U.; Nüsse, H.; Klingauf, J.; Studer, A. *Angew. Chem. Int. Ed.* **2015**, *54*, 12612–12617.

(100) Amat, M.; Arioli, F.; Pérez, M.; Molins, E.; Bosch, J. *Org. Lett.* **2013**, *15*, 2470–2473.

(101) Kacprzynski, M. A.; May, T. L.; Kazane, S. A.; Hoveyda, A. H. *Angew. Chem., Int. Ed.* **2007**, *46*, 4554–4558.

= 5.3 Hz), 16.2 (d, *J* = 6.8 Hz); HRMS (DART): Calcd for $C_{13}H_{20}O_4P_1$ $[M+H]^+$: 271.1099, Found: 271.1087.

Diethyl (2-(trimethylsilyl)allyl) phosphate (substrate for 2.18v–w): IR (neat): 2982 (w), 2957 (w), 2908 (m), 1394 (w), 1250 (m), 1167 (w), 1024 (s), 976 (m), 840 (s) cm^{-1}; ^1H NMR (400 MHz, $CDCl_3$): δ 5.85 (1H, s), 5.45 (1H, s), 4.65 (2H, d, *J* = 6.0 Hz), 4.15–4.08 (4H, m), 1.33 (6H, t, *J* = 7.0 Hz), 0.13 (9H, s); ^{13}C NMR (100 MHz, $CDCl_3$): δ 146.8 (d, *J* = 7.6 Hz), 125.1, 70.7 (d, *J* = 6.0 Hz), 63.9 (d, *J* = 6.1 Hz), 16.3 (d, *J* = 6.9 Hz), –1.5; HRMS (DART): Calcd for $C_{10}H_{24}O_4P_1Si_1$ $[M+H]^+$: 267.1182, Found: 267.1177.

Preparation of an allylic phosphate for 2.18u: 2-Methyl-2-propen-1-ol (purchased from Aldrich and used as received) was converted to the corresponding allylic phosphate based on a previously disclosed method.[101]

Diethyl (2-methylallyl) phosphate (substrate for 2.18u): IR (neat): 2983 (w), 2911 (w), 1447 (w), 1264 (m), 1166 (w), 1008 (s), 973 (s) cm^{-1}; ^1H NMR (400 MHz, $CDCl_3$): δ 4.94 (1H, s), 4.83 (1H, s), 4.32 (2H, d, *J* = 7.2 Hz), 4.05–3.98 (4H, m), 1.67 (3H, s), 1.26–1.21 (6H, m); ^{13}C NMR (100 MHz, $CDCl_3$): δ 140.0 (d, *J* = 6.8 Hz), 113.0, 70.5 (d, *J* = 6.1 Hz), 63.7 (d, *J* = 6.1 Hz), 18.9, 16.0 (d, *J* = 6.8 Hz); HRMS (DART): Calcd for $C_8H_{18}O_4P_1$ $[M+H]^+$: 209.0943, Found: 209.0944.

Preparation of allyl-1,1-*d*$_2$-diethyl phosphate (2.17-*d*$_2$): Allylic alcohol was synthesized from the reported procedure.[102] Subsequently, allylic alcohol was converted to the corresponding allylic phosphates based on an established method.[101] IR (neat): 2984 (w), 2934 (w), 1265 (m), 1017(s), 976 (s), 801 (m) cm^{-1}; ^1H NMR (400 MHz,

(102) Schuetz, R. D.; Millard, F. W. *J. Org. Chem.* **1959**, *24*, 297–300.

CDCl3): δ 5.91 (1H, dd, *J* = 17.2, 10.4 Hz), 5.33 (1H, dt, *J* = 17.2, 1.5 Hz), 5.21 (1H, dt, *J* = 10.0, 1.4 Hz), 4.12–4.04 (4H, m), 1.32–1.28 (6H, m); ^{13}C NMR (100 MHz, CDCl3): δ 135.6 (d, *J* = 6.8 Hz), 118.3, 63.8 (d, *J* = 6.1 Hz), 16.2 (d, *J* = 6.8 Hz); HRMS (DART): Calcd for $C_7H_{14}D_2O_4P_1$ [M+H]+: 197.0912, Found: 197.0920.

■ **Representative Procedure for the Catalytic Enantioselective Boron-Allyl Addition to Aryl Alkenes**

In a N_2-filled glove box, an oven-dried 1 dram vial equipped with a stir bar was charged with bisphosphine **2.24a** (3.4 mg, 0.0055 mmol), NaO*t*-Bu (14 mg, 0.15 mmol), and CuCl (0.50 mg, 0.0050 mmol), and thf (1.0 mL). The mixture was allowed to stir for 1 h under N_2 at 22 °C; during this time the solution turned light-yellow. Bis(pinacolato)diboron (28 mg, 0.11 mmol) was added to the mixture, causing the solution to turn dark brown immediately. Styrene (31 mg, 0.30 mmol), allylphosphate (**2.17**) (19 mg, 0.10 mmol), and thf (0.50 mL) were added. The vial was sealed with a cap and electrical tape before removal from the glove box. The resulting mixture was allowed to stir at 22 °C for 14 h. The mixture was then passed through a short plug of silica gel (4 x 1 cm) and eluted with Et_2O. The organic layer was concentrated under reduced pressure, affording yellow oil, which was purified by silica gel chromatography (100% hexanes→hexanes:Et_2O = 10:1) to afford **2.18a** as colorless oil (18 mg, 0.067 mmol, 67% yield). **(*R*)-4,4,5,5-Tetramethyl-2-(2-phenylpent-4-en-1-yl)-1,3,2-dioxaborolane (2.18a)**. IR (neat): 3027 (w), 2977 (m), 2925 (w), 1452 (m), 1367 (s), 1319 (s), 1270 (w), 12134(w), 1164 (m), 1143 (s), 968 (m), 911 (m), 847 (m), 756 (m), 699 (s) cm^{-1}; ^{1}H NMR ($CDCl_3$, 400 MHz): δ 7.25–7.09 (5H, m), 5.68 (1H, ddt, *J* =17.2, 10.0, 7.2 Hz), 4.96–4.88 (2H, m), 2.96–2.88 (1H, m), 2.40–2.27 (2H, m), 1.23 (1H, dd, *J* =15.4, 6.6

Hz), 1.14–1.08 (1H, m), 1.10 (6H, s), 1.09 (6H, s); ^{13}C NMR ($CDCl_3$, 100 MHz): δ 146.9, 137.3, 128.2, 127.6, 126.0, 116.1, 83.1, 43.9, 41.5, 24.83, 24.78; HRMS (DART): Calcd for $C_{17}H_{26}B_1O_2$ $[M+H]^+$: 273.2026, Found: 273.2015. Specific rotation: $[\alpha]_D^{20}$ +6.7 (*c* 0.30, $CHCl_3$) for an enantiomerically enriched sample of 95:5 er. Enantiomeric purity was determined by HPLC analysis in comparison with authentic racemic material (95:5 er shown; Chiralcel OD–H column, 100% hexanes, 0.3 mL/min, 220 nm).

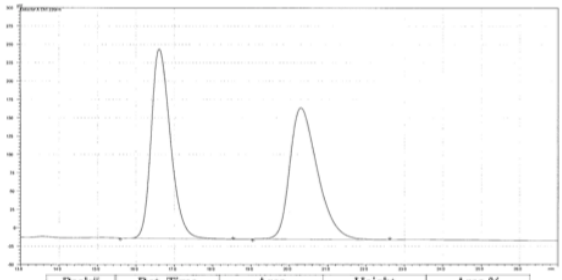

Peak#	Ret. Time	Area	Height	Area %
1	16.604	8995664	258220	50.067
2	20.296	8971612	179187	49.933
Total		17967275	437407	100.000

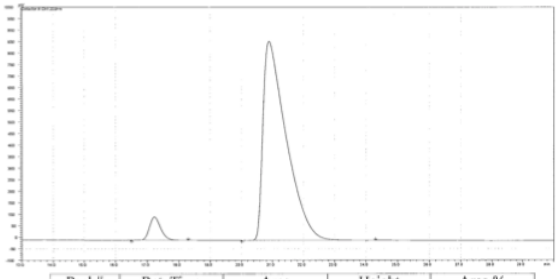

Peak#	Ret. Time	Area	Height	Area %
1	17.223	2468299	100781	5.239
2	20.890	44643911	865166	94.761
Total		47112211	965948	100.000

Peak #	Time (min)	Area (%)	Peak #	Time (min)	Area (%)
1	16.604	50.067	1	17.223	5.239
2	20.296	49.933	2	20.890	94.761

(*R*)-4,4,5,5-Tetramethyl-2-(2-(*o*-tolyl)pent-4-en-1-yl)-1,3,2-dioxaborolane (2.18b): IR (neat): 2977 (w), 2928 (w), 1365 (s), 1317 (s), 1144 (s), 968 (m), 911 (m), 846 (m), 758 (m), 726 (m) cm^{-1}; ^{1}H NMR ($CDCl_3$, 400 MHz): δ 7.20 (1H, d, *J* = 8.0 Hz), 7.14 (1H, t, *J* = 7.2 Hz), 7.09–7.01 (2H, m), 5.74–5.63 (1H, m), 4.99–4.91 (2H, m), 3.23 (1H, app pent, *J* = 7.3 Hz), 2.38–2.24 (2H, m), 2.36 (3H, s), 1.23 (1H, dd, *J* = 14.6, 7.8 Hz), 1.12 (1H, dd, *J* = 16.0, 8.0 Hz), 1.05 (s, 6H), 1.03 (6H, s); ^{13}C NMR ($CDCl_3$, 100 MHz): δ 145.1, 137.3, 135.7, 130.0, 126.1, 125.6, 116.1, 83.0, 43.6, 36.0, 24.7, 20.0; HRMS (DART): Calcd for $C_{18}H_{28}B_1O_2$ $[M+H]^+$: 287.2182, Found: 287.2177; Specific Rotation: $[a]_D^{20}$ +8.8 (*c* 1.32, $CHCl_3$) for an enantiomerically enriched sample of 95:5 er. Enantiomeric

purity was determined by HPLC analysis in comparison with authentic racemic material (95:5 er shown; Chiralcel OD–H column, 100% hexanes, 0.3 mL/min, 220 nm).

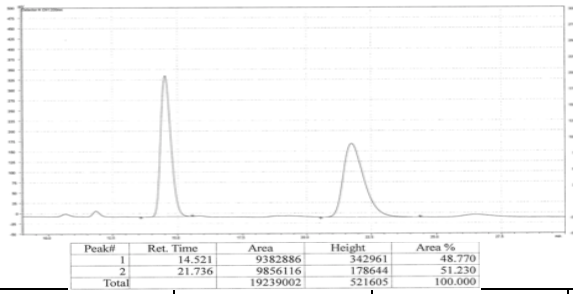

Peak#	Ret. Time	Area	Height	Area %
1	14.521	9382886	342961	48.770
2	21.736	9856116	178644	51.230
Total		19239002	521605	100.000

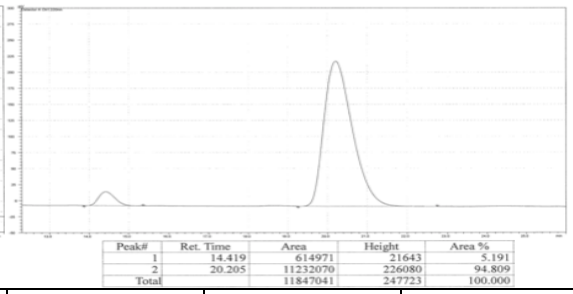

Peak#	Ret. Time	Area	Height	Area %
1	14.419	614971	21643	5.191
2	20.205	11232070	226080	94.809
Total		11847041	247723	100.000

Peak #	Time (min)	Area (%)	Peak #	Time (min)	Area (%)
1	14.521	48.770	1	14.419	5.191
2	21.736	51.230	2	20.205	94.809

(*R*)-4,4,5,5-Tetramethyl-2-(2-(naphthalen-1-yl)pent-4-enyl)-1,3,2-dioxaborolane (2.18c): IR (neat): 2976 (w), 2975 (w), 1367 (s), 1312 (s), 1251 (w), 1142 (s), 967 (m), 846 (m), 792 (s) cm^{-1}; ^1H NMR ($CDCl_3$, 400 MHz): δ 8.22 (1H, d, J = 8.1 Hz), 7.83 (1H, dd, J = 7.9, 1.6 Hz), 7.68 (1H, dd, J = 6.9, 2.5 Hz), 7.56–7.37 (4H, m), 5.75 (1H, ddt, J =17.2, 10.1, 7.0 Hz), 5.06–4.91 (2H, m), 3.90 (1H, app pent, J = 7.3 Hz), 2.66–2.53 (1H, m), 2.50–2.38 (1H, m), 1.47–1.35 (1H, m), 1.35–1.23 (1H, m), 1.04 (6H, s), 0.96 (6H, s); ^{13}C NMR ($CDCl_3$, 100 MHz): δ 143.2, 137.2, 134.0, 131.8, 128.8, 126.4, 125.6, 125.6, 125.3, 123.9, 123.4, 116.4, 83.1, 43.3, 35.0, 24.7; HRMS (DART): Calcd for $C_{21}H_{28}B_1O_2$ $[M+H]^+$: 323.2182, Found: 323.2185; Specific Rotation: $[a]_D^{20}$ +5.6 (*c* 1.08, $CHCl_3$) for an enantiomerically enriched sample of 93:7 er. Enantiomeric purity was determined by HPLC analysis in comparison with authentic racemic material (93:7 er shown; Chiralcel OJ–H column, 100% hexanes, 0.3 mL/min, 220 nm).

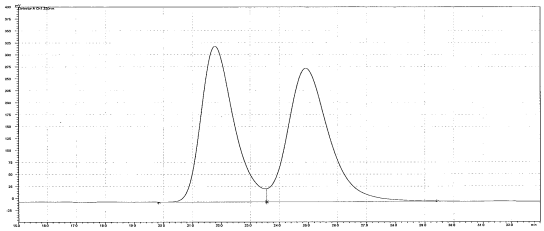

Peak#	Ret. Time	Area	Height	Area %
1	21.777	25778878	325680	48.483
2	24.906	27392466	279410	51.517
Total		53171343	605090	100.000

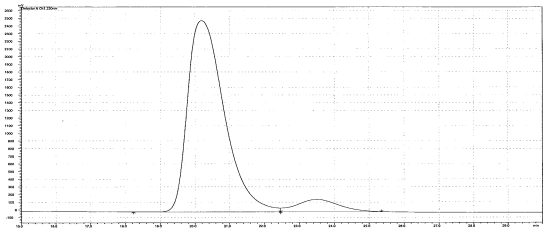

Peak#	Ret. Time	Area	Height	Area %
1	20.183	183585831	2496092	93.067
2	23.495	13676947	162887	6.933
Total		197262778	2658979	100.000

Peak #	Time (min)	Area (%)	Peak #	Time (min)	Area (%)
1	21.777	48.483	1	20.183	93.067
2	24.906	51.517	2	23.495	6.933

(*R*)-2-(2-(2-Methoxyphenyl)pent-4-enyl)-4,4,5,5-tetramethyl-1,3,2-dioxaborolane

(2.18d): IR (neat): 2976 (w), 2929 (w), 2836 (w), 1599 (w), 1585 (w), 1491 (m), 1464 (w), 1438 (w), 1368 (s), 1318 (s), 1215 (s), 1143 (s), 1101 (s), 1031 (m), 968 (m), 909 (m), 885 (w), 749 (s) cm^{-1}; ^{1}H NMR ($CDCl_3$, 400 MHz): δ 7.17–7.10 (2H, m), 6.88 (1H, t, J = 7.4 Hz), 6.81 (1H, d, J = 8.4 Hz), 5.75–5.65 (1H, m), 4.96–4.88 (2H, m), 3.81 (3H, s), 3.42 (1H, app pent, J = 7.5 Hz), 2.44–2.26 (2H, m), 1.26–1.19 (1H, m), 1.16–1.08 (1H, m), 1.11 (6H, s), 1.08 (6H, s); ^{13}C NMR ($CDCl_3$, 100 MHz): δ 157.2, 137.8, 135.1, 127.8, 126.7, 120.4, 115.7, 110.6, 82.9, 55.5, 42.3, 33.9, 24.80, 24.77; HRMS (DART): Calcd for $C_{18}H_{28}B_1O_3$ $[M+H]^+$: 303.2132, Found: 303.2128; Specific Rotation: $[a]_D^{20}$ +13.9 (*c* 1.61, $CHCl_3$) for an enantiomerically enriched sample of 95:5 er. Enantiomeric purity was determined by HPLC analysis in comparison with authentic racemic material (95:5 er shown; Chiralcel OZ–H column, 100% hexanes, 0.3 mL/min, 220 nm).

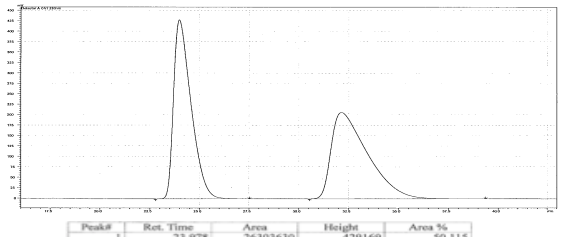

Peak#	Ret. Time	Area	Height	Area %
1	23.978	26303630	429169	50.115
2	32.136	26182411	207068	49.885
Total		52486041	636237	100.000

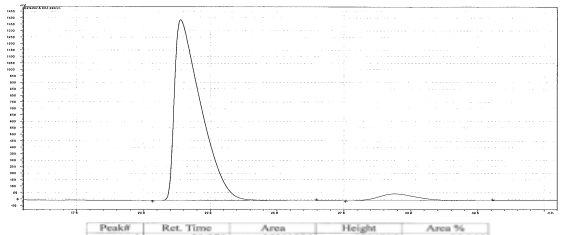

Peak#	Ret. Time	Area	Height	Area %
1	21.378	95311996	1394885	95.065
2	29.394	4947535	51312	4.935
Total		100259531	1446197	100.000

Peak #	Time (min)	Area (%)	Peak #	Time (min)	Area (%)
1	23.978	50.115	1	21.378	95.065

2	32.136	49.885	2	29.394	4.935

(*R*)-4,4,5,5-Tetramethyl-2-(2-(*m*-tolyl)pent-4-en-1-yl)-1,3,2-dioxaborolane (2.18e): IR (neat): 2977 (w), 2922 (w), 1366 (s), 1319 (s), 1144 (s), 968 (m), 847 (m), 704 (m) cm^{-1}; ^1H NMR ($CDCl_3$, 400 MHz): δ 7.15 (1H, dd, *J* = 9.0, 6.2 Hz), 7.00 (1H, s), 6.97–6.93 (2H, m), 5.72–5.62 (1H, m), 4.98–4.89 (2H, m), 2.89 (1H, app pent, *J* = 7.6 Hz), 2.40–2.26 (5H, m), 1.25–1.18 (1H, m), 1.11–1.03 (13H, m); ^{13}C NMR ($CDCl_3$, 100 MHz): δ 146.9, 137.5, 137.46, 128.4, 128.1, 126.7, 124.5, 116.0, 83.1, 43.7, 41.4, 24.82, 24.79, 21.6; HRMS (DART): Calcd for $C_{18}H_{28}B_1O_2$ $[M+H]^+$: 287.2182, Found: 287.2188; Specific Rotation: $[a]_D^{20}$ +16.9 (*c* 0.98, $CHCl_3$) for an enantiomerically enriched sample of 97:3 er. Enantiomeric purity was determined by HPLC analysis in comparison with authentic racemic material (97:3 er shown; Chiralcel OD–H column, 100% hexanes, 0.3 mL/min, 220 nm).

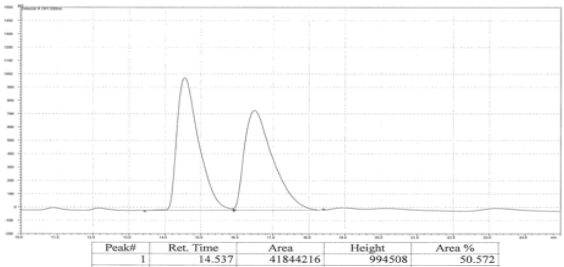

Peak#	Ret. Time	Area	Height	Area %
1	14.537	41844216	994508	50.572
2	16.483	40897888	747456	49.428
Total		82742104	1741964	100.000

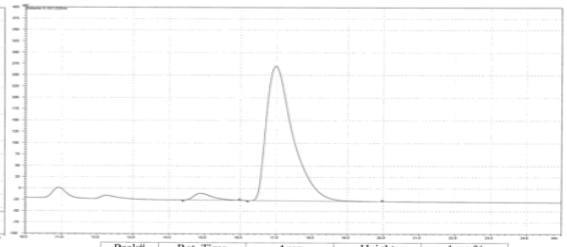

Peak#	Ret. Time	Area	Height	Area %
1	14.887	520079	14680	3.297
2	16.975	15256111	297016	96.703
Total		15776189	311696	100.000

Peak #	Time (min)	Area (%)	Peak #	Time (min)	Area (%)
1	14.537	50.572	1	14.887	3.297
2	16.483	49.428	2	16.975	96.703

(*R*)-2-(2-(3-(Allyloxy)phenyl)pent-4-enyl)-4,4,5,5-tetramethyl-1,3,2-dioxaborolane (2.18f): IR (neat): 3076 (w), 2977 (w), 2925 (w), 1600 (m), 1583 (m), 1422 (s), 1366 (s), 1265 (m), 1142 (s), 1034 (w), 913 (m), 846 (m), 776 (m), 699 (m) cm^{-1}; ^1H NMR ($CDCl_3$, 400 MHz): δ 7.16 (1H, t, *J* = 7.9 Hz), 6.84–6.76 (2H, m), 6.71 (1H, ddd, *J* = 8.2, 2.6, 0.9 Hz), 6.06 (1H, ddt *J* = 17.3, 10.6, 5.3 Hz), 5.67 (1H, dddd, *J* = 16.9, 10.1, 7.5, 6.6

Hz), 5.40 (1H, dd, *J* = 17.3, 1.6 Hz), 5.27 (1H, dd, *J* = 10.5, 1.5 Hz), 5.00–4.87 (2H, m), 4.52 (2H, dt, *J* = 5.3, 1.5 Hz), 3.04–2.82 (1H, m), 2.43–2.26 (2H, m), 1.29–1.16 (2H, m), 1.12 (6H, s), 1.11 (6H, s); ^{13}C NMR ($CDCl_3$, 100 MHz): δ 158.6 148.7, 137.3, 133.7, 129.1, 120.2, 117.6, 116.2, 114.2, 112.2, 83.1, 68.8, 43.7, 41.5, 24.85, 24.82; HRMS (DART): Calcd for $C_{20}H_{30}B_1O_3$ $[M+H]^+$: 329.2288, Found: 329.2295; Specific Rotation: $[a]_D^{20}$ +6.4 (*c* 1.17, $CHCl_3$) for an enantiomerically enriched sample of 95:5 er. Enantiomeric purity was determined by HPLC analysis in comparison with authentic racemic material (95:5 er shown; Chiralcel OD–H column, 100% hexanes, 0.3 mL/min, 220 nm).

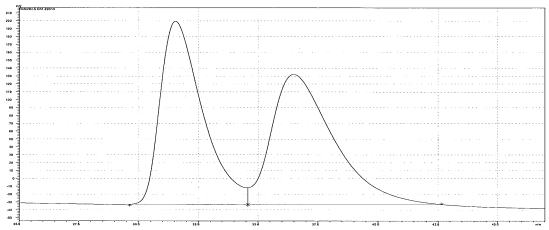

Peak#	Ret. Time	Area	Height	Area %
1	31.532	28645850	232498	49.049
2	36.476	29756939	165229	50.951
Total		58402788	397727	100.000

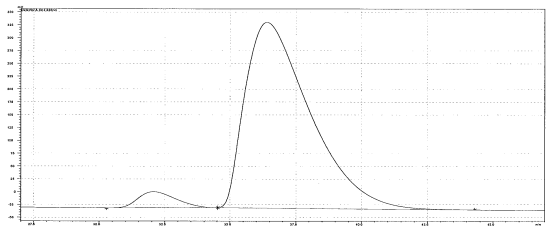

Peak#	Ret. Time	Area	Height	Area %
1	32.064	3105696	31399	4.765
2	36.398	62073723	362214	95.235
Total		65179419	393613	100.000

Peak #	Time (min)	Area (%)	Peak #	Time (min)	Area (%)
1	31.532	49.049	1	32.064	4.765
2	36.476	50.951	2	36.398	95.235

***tert*-Butyl (*R*)-3-(1-(4,4,5,5-tetramethyl-1,3,2-dioxaborolan-2-yl)pent-4-en-2-yl)benzoate (2.18g):** Following the representative procedure except for 1:3 alkene:phosphate used. IR (neat): 2977 (w), 2929 (w), 1713 (s), 1440 (w), 1390 (w), 1367 (s), 1320 (m), 1294 (s), 1161 (s), 1144 (s), 1110 (m) cm^{-1}; ^{1}H NMR (400 MHz, $CDCl_3$): δ 7.83 (1H, dd, *J* = 1.6, 1.2 Hz), 7.78 (1H, ddd, *J* = 7.7, 2.3, 1.1 Hz), 7.37 (1H, dd, *J* = 7.6, 1.6 Hz), 7.30 (1H, t, *J* = 7.4 Hz), 5.66 (1H, ddt, *J* = 17.2, 10.0, 7.2 Hz), 4.98–4.91 (2H, m), 3.04–2.96 (1H, m), 2.44–2.32 (2H, m), 1.59 (9H, s), 1.25 (1H, dd, *J* = 15.8, 7.0 Hz), 1.20–1.06 (13H, m); ^{13}C NMR (100 MHz, $CDCl_3$): δ 166.2, 147.1, 137.0, 131.9, 131.6,

128.8, 128.1, 127.2, 116.5, 83.2, 80.9, 43.4, 41.4, 28.4, 24.9, 24.8; HRMS (DART): Calcd for $C_{22}H_{34}B_1O_4$ $[M+H]^+$: 373.2550, Found: 373.2565; Specific Rotation: $[\alpha]_D^{20}$ +4.9 (*c* 1.05, $CHCl_3$) for an enantiomerically enriched sample of 94:6 er. Enantiomeric purity was determined by HPLC analysis in comparison with authentic racemic material (94:6 er shown; Chiralcel OZ–H column, 100% hexanes, 0.3 mL/min, 220 nm).

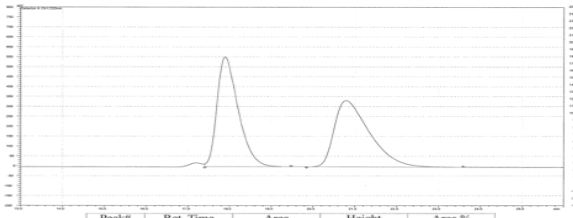

Peak#	Ret. Time	Area	Height	Area %
1	17.885	19631455	553324	50.079
2	20.783	19569298	334519	49.921
Total		39200753	887842	100.000

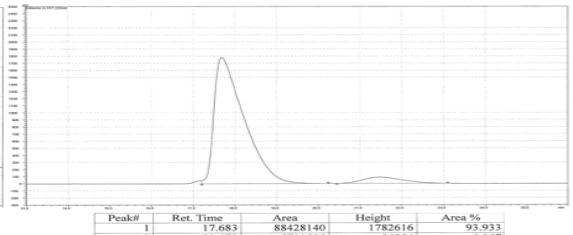

Peak#	Ret. Time	Area	Height	Area %
1	17.683	88428140	1782616	93.933
2	21.473	5711585	86854	6.067
Total		94139725	1869470	100.000

Peak #	Time (min)	Area (%)	Peak #	Time (min)	Area (%)
1	17.885	50.079	1	17.683	93.933
2	20.783	49.921	2	21.473	6.067

***tert*-Butyl (*R*)-3-(1-(4,4,5,5-tetramethyl-1,3,2-dioxaborolan-2-yl)pent-4-en-2-yl-5,5-d_2)benzoate [2.18g-d_2 (S_N2')]:** Following the representative procedure except **2.17-d_2** and **2.24b** was used. IR (neat): 2977 (w), 2929 (w), 1713 (s), 1367 (s), 1320 (m), 1295 (s), 1162 (s), 1145 (s), 1111 (m), 968 (m), 848 (m) cm^{-1}; ^1H NMR (400 MHz, $CDCl_3$): δ 7.83 (1H, t, *J* = 1.6 Hz), 7.78 (1H, dt, *J* = 7.6, 1.6 Hz), 7.37 (1H, dt, *J* = 7.2, 1.6 Hz), 7.30 (1H, t, *J* = 7.8 Hz), 5.65 (1H, t, *J* = 7.0 Hz, 3.04–2.96 (1H, m), 2.44–2.32 (2H, m), 1.59 (9H, s), 1.25 (1H, dd, *J* = 15.2, 6.0 Hz) 1.11 (6H, s), 1.10 (6H, s), 1.12–1.06 (1H, m); ^{13}C NMR (100 MHz, $CDCl_3$): δ 166.2, 147.1, 136.8, 131.9, 131.6, 128.8, 128.1, 127.2, 83.2, 80.9, 43.3, 41.4, 28.4, 24.9, 24.8; HRMS (DART): Calcd for $C_{22}H_{35}D_2B_1N_1O_4$ $[M+NH_4]^+$: 392.2941, Found: 392.2954.

(*R*)-6-Methyl-2-(4-(1-(4,4,5,5-tetramethyl-1,3,2-dioxaborolan-2-yl)pent-4-en-2-yl)phenyl)-1,3,6,2-dioxazaborocane-4,8-dione (2.18h): IR (neat): 2977 (w), 2927 (w),

1765 (s), 1457 (w), 1370 (m), 1334 (m), 1293 (m), 1235 (m), 1145 (m), 1040 (m), 993 (m) cm^{-1}; ^1H NMR (400 MHz, $CDCl_3$): δ 7.40 (2H, d, *J* = 7.6 Hz), 7.23 (2H, d, *J* = 8.0 Hz), 5.69–5.59 (1H, m), 4.96–4.88 (2H, m), 3.93 (2H, d, *J* = 16.4 Hz), 3.75 (2H, d, *J* = 16.0 Hz), 2.95 (1H, app pent, *J* = 7.5 Hz), 2.51 (3H, s), 2.38–2.32 (2H, m), 1.23 (1H, dd, *J* = 15.2, 7.2 Hz), 1.12–1.06 (13H, m); ^{13}C NMR (100 MHz, $CDCl_3$): δ 167.5, 149.0, 137.1, 132.2, 127.7, 116.3, 83.1, 61.8, 47.5, 43.6, 41.4, 24.9, 24.8; HRMS (DART): Calcd for $C_{22}H_{35}B_2N_2O_6$ $[M+NH_4]^+$: 445.2681, Found: 445.2689. Specific Rotation: $[\alpha]_D^{20}$ +6.4 (*c* 0.87, $CHCl_3$) for an enantiomerically enriched sample of 95:5 er. Enantiomeric purity was determined by HPLC analysis of the product from oxidation/acetylation in comparison with authentic racemic material (95:5 er shown; Chiralcel OC–H column, 98% hexanes, 2% *i*-PrOH, 0.3 mL/min, 220 nm).

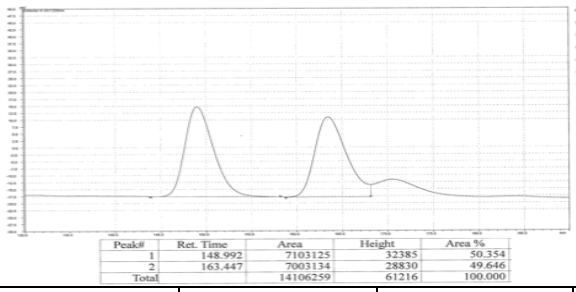

Peak#	Ret. Time	Area	Height	Area %
1	148.992	7103125	32385	50.354
2	163.447	7003134	28830	49.646
Total		14106259	61216	100.000

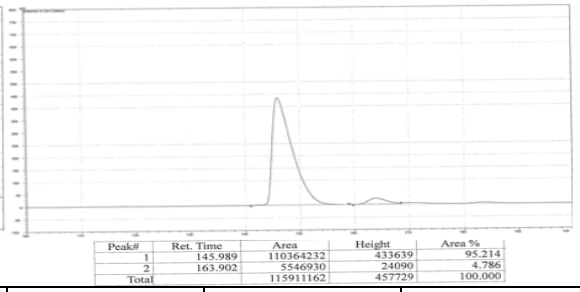

Peak#	Ret. Time	Area	Height	Area %
1	145.989	110364232	433639	95.214
2	163.902	5546930	24090	4.786
Total		115911162	457729	100.000

Peak #	Time (min)	Area (%)	Peak #	Time (min)	Area (%)
1	148.992	50.354	1	145.989	95.214
2	163.447	49.646	2	163.902	4.786

(*R*)-4,4,5,5-Tetramethyl-2-(2-(*p*-tolyl)pent-4-en-1-yl)-1,3,2-dioxaborolane (2.18i): IR (neat): 2977 (m), 2924 (m), 1514 (w), 1368 (s), 1322 (s), 1145 (s), 968 (m), 911 (m), 846 (m), 813 (m) cm^{-1}; ^1H NMR ($CDCl_3$, 600 MHz): δ 7.09 (2H, d, *J* = 5.2 Hz), 7.06 (2H, d, *J* = 5.6 Hz), 5.71–5.64 (1H, m), 4.97–4.90 (2H, m), 2.91 (1H, app pent, *J* = 5.0 Hz), 2.39–2.30 (5H, m), 1.21 (1H, dd, *J* = 9.8, 4.2 Hz), 1.12–1.06 (13H, m); ^{13}C NMR ($CDCl_3$, 150 MHz): δ 143.9, 137.5, 135.3, 128.9, 127.4, 116.0, 83.1, 43.8, 41.0, 24.84,

24.81, 21.1; HRMS (DART): Calcd for $C_{18}H_{28}B_1O_2$ $[M+H]^+$: 287.2182, Found: 287.2184; Specific Rotation: $[a]_D^{20}$ +8.6 (*c* 1.00, $CHCl_3$) for an enantiomerically enriched sample of 95:5 er. Enantiomeric purity was determined by HPLC analysis in comparison with authentic racemic material (95:5 er shown; Chiralcel OD–H column, 100% hexanes, 0.3 mL/min, 220 nm).

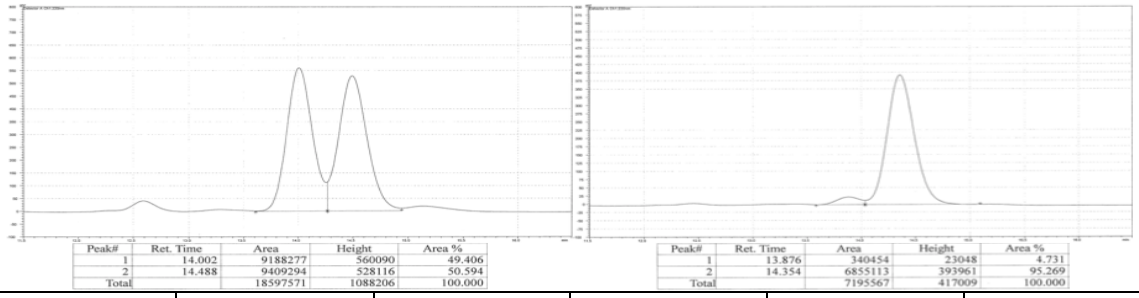

Peak#	Ret. Time	Area	Height	Area %
1	14.002	9188277	560090	49.406
2	14.488	9409294	528116	50.594
Total		18597571	1088206	100.000

Peak#	Ret. Time	Area	Height	Area %
1	13.876	340454	23048	4.731
2	14.354	6855113	393961	95.269
Total		7195567	417009	100.000

Peak #	Time (min)	Area (%)	Peak #	Time (min)	Area (%)
1	14.002	49.406	1	13.876	4.731
2	14.488	50.594	2	14.354	95.269

(*R*)-Trimethyl(4-(1-(4,4,5,5-tetramethyl-1,3,2-dioxaborolan-2-yl)pent-4-en-2-yl)phenyl)silane (2.18j): IR (neat): 3068 (w), 2977 (m), 2955 (m), 2926 (w), 1640 (w), 1599 (w), 1365 (s), 1322 (s), 1164 (m), 1144 (s), 1110 (m), 997 (m), 968 (m), 911 (m), 837 (s), 757 (m), 725 (m) cm^{-1}; ^1H NMR ($CDCl_3$, 400 MHz): δ 7.41 (2H, d, *J* = 8.1 Hz), 7.23–7.17 (2H, m), 5.70 (1H, dddd, *J* = 16.8, 10.1, 7.6, 6.5 Hz), 4.98 (1H, ddt, *J* = 17.2, 2.5, 1.4 Hz), 4.93 (1H, ddt, *J* = 10.1, 2.1, 1.0 Hz), 2.99–2.88 (1H, m), 2.46–2.26 (2H, m), 1.29–1.20 (2H, m), 1.09 (6H, s), 1.08 (6H, s), 0.23 (9H, s); ^{13}C NMR ($CDCl_3$, 100 MHz): δ147.6, 137.5, 137.3, 133.2, 127.0, 116.1, 83.0, 43.5, 41.4, 24.8, 24.7, –0.8, –0.9; HRMS (DART): Calcd for $C_{20}H_{34}BO_2Si$ $[M+H]^+$: 345.2421, Found: 345.2431; Specific Rotation: $[a]_D^{20}$ +8.2 (*c* 0.85, $CHCl_3$) for an enantiomerically enriched sample of 96:4 er. Enantiomeric purity was determined by HPLC analysis of the alcohol product after

oxidation in comparison with authentic racemic material (96:4 er shown; Chiralcel AZ–H column, 99% hexanes, 1% *i*-PrOH, 0.3 mL/min, 220 nm).

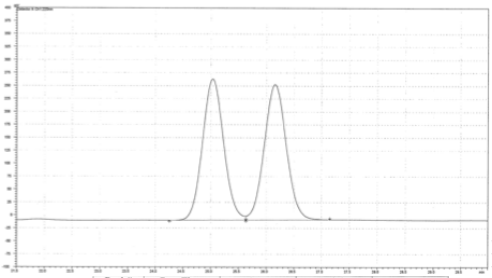

Peak#	Ret. Time	Area	Height	Area %
1	25.030	7233091	272759	49.887
2	26.150	7266002	261783	50.113
Total		14499093	534542	100.000

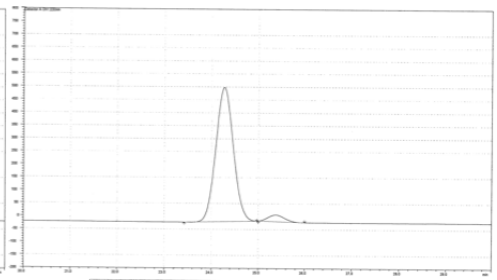

Peak#	Ret. Time	Area	Height	Area %
1	24.263	13449364	517639	95.727
2	25.372	600312	25247	4.273
Total		14049676	542886	100.000

Peak #	Time (min)	Area (%)	Peak #	Time (min)	Area (%)
1	25.030	49.887	1	24.263	95.727
2	26.150	50.113	2	25.372	4.273

(*R*)-2-(2-(4-Methoxyphenyl)pent-4-enyl)-4,4,5,5-tetramethyl-1,3,2-dioxaborolane (2.18k): IR (neat): 2976 (w), 2926 (w), 2834 (w), 1610 (w), 1511 (s), 1366 (s), 1319 (m), 1244 (s), 1214 (w), 1177 (m), 1165 (s), 1143 (w), 1104 (m), 1037 (m), 967 (m), 910 (w), 885 (w), 846 (m), 828 (m), 806 (w) cm^{-1}; ^{1}H NMR ($CDCl_3$, 400 MHz): δ 7.12 (2H, dd, *J* = 6.4, 2.0 Hz), 6.80 (2H, dd, *J* = 6.4, 2.0 Hz), 5.67 (1H, ddt, *J* = 17.2, 9.6, 7.2 Hz), 4.97–4.90 (2H, m) 3.77 (3H, s), 2.94–2.86 (1H, m), 2.38–2.26 (2H, m), 1.25–1.18 (1H, m), 1.11–1.04 (13H, m). ^{13}C NMR ($CDCl_3$, 100 MHz): δ 157.9, 139.1, 137.4, 128.4, 116.0, 113.6, 83.1, 55.4, 44.1, 40.7, 24.9, 24.8; HRMS (DART): Calcd for $C_{18}H_{28}BO_3$ $[M+H]^+$: 303.2132, Found: 303.2126; Specific Rotation: $[a]_D^{20}$ +9.8 (*c* 0.76, $CHCl_3$) for an enantiomerically enriched sample of 97:3 er. Enantiomeric purity was determined by HPLC analysis in comparison with authentic racemic material (97:3 er shown; Chiralcel OD–H column, 100% hexanes, 0.3 mL/min, 220 nm).

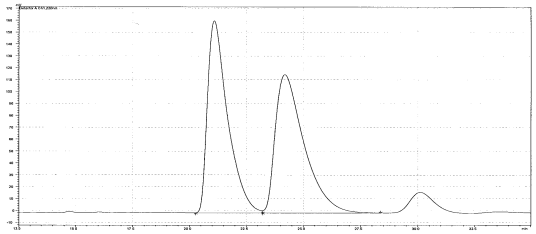

Peak#	Ret. Time	Area	Height	Area %
1	21.084	10063076	161641	49.788
2	24.175	10148737	116341	50.212
Total		20211813	277981	100.000

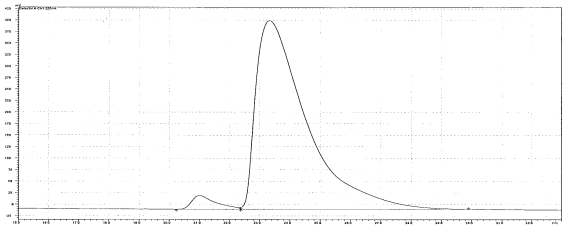

Peak#	Ret. Time	Area	Height	Area %
1	20.993	1662337	30072	3.369
2	23.315	47674508	409729	96.631
Total		49336845	439801	100.000

Peak #	Time (min)	Area (%)	Peak #	Time (min)	Area (%)
1	21.084	49.788	1	20.993	3.369
2	24.175	50.212	2	23.315	96.631

***tert*-Butyl (*R*)-4-(1-(4,4,5,5-tetramethyl-1,3,2-dioxaborolan-2-yl)pent-4-en-2-yl)benzoate (2.18l):** IR (neat): 2978 (m), 2930 (w), 1712 (s), 1609 (w), 1367 (s), 1312 (m), 1290 (s), 1166 (s), 1145 (s), 1116 (s), 848 (m) cm^{-1}; ^1H NMR (400 MHz, $CDCl_3$): δ 7.88 (2H, d, J = 8.0 Hz), 7.24 (2H, d, J = 8.0 Hz), 5.68–5.58 (1H, m), 4.96–4.90 (2H, m), 3.00 (1H, app pent, J = 7.5 Hz), 2.35 (2H, t, J = 7.2 Hz), 1.58 (9H, s), 1.27–1.21 (1H, m), 1.14–1.08, (1H, m) 1.12 (6H, s), 1.11 (6H, s); ^{13}C NMR (100 MHz, $CDCl_3$): δ 166.1, 152.0, 136.8, 129.9, 129.5, 127.4, 116.5, 83.2, 80.8, 43.5, 41.5, 28.4, 24.9, 24.8; HRMS (DART): Calcd for $C_{22}H_{34}B_1O_4$ $[M+H]^+$: 373.2550, Found: 373.2534; Specific Rotation: $[\alpha]_D^{20}$ –3.0 (*c* 1.00, $CHCl_3$) for an enantiomerically enriched sample of 67:33 er. Enantiomeric purity was determined by HPLC analysis in comparison with authentic racemic material (52:48 er shown; Chiralcel OD–H column, 100% hexanes, 0.3 mL/min, 220 nm).

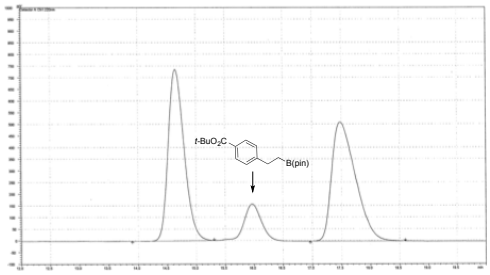

Peak#	Ret. Time	Area	Height	Area %
1	14.638	14061810	735507	49.374
2	17.479	14418511	510741	50.626
Total		28480320	1246248	100.000

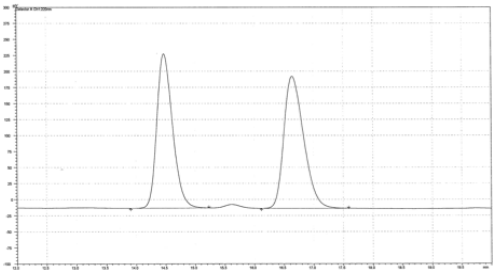

Peak#	Ret. Time	Area	Height	Area %
1	14.474	4480291	240810	48.271
2	16.639	4801309	206218	51.729
Total		9281600	447028	100.000

Peak #	Time (min)	Area (%)	Peak #	Time (min)	Area (%)
1	14.638	49.374	1	14.474	48.271
2	17.479	50.626	2	16.639	51.729

***tert*-Butyl (*R*)-5-(1-(4,4,5,5-tetramethyl-1,3,2-dioxaborolan-2-yl)pent-4-en-2-yl)-1*H*-indole-1-carboxylate (2.18m)**: Following the representative procedure except for 6:1 alkene:phosphate used. IR (neat): 2977 (m), 2927 (w), 1731 (s), 1469 (m), 1441 (w), 1352 (s), 1318 (s), 1253 (m), 1162 (s), 1141 (s), 1081 (m), 1022 (m), 968 (w), 846 (w), 766 (m), 725 (m) cm^{-1}; ^{1}H NMR (400 MHz, $CDCl_3$): δ 8.00 (1H, d, *J* = 8 Hz), 7.54 (1H, d, *J* = 3.6 Hz), 7.38 (1H, d, *J* = 1.6 Hz), 7.17 (1H, dd, *J* = 8.8, 2.0 Hz), 6.50 (1H, d, *J* = 3.6 Hz), 5.68 (1H, ddt, *J* = 17, 10.4, 6.4 Hz), 4.98–4.88 (2H, m), 3.04 (1H, app pent, *J* = 7.0 Hz), 2.46–2.34 (2H, m), 1.66 (9H, s), 1.30–1.25 (1H, m), 1.19–1.13 (1H, m), 1.09 (6H, s), 1.08 (6H, s); ^{13}C NMR (100 MHz, $CDCl_3$): δ 150.1, 141.4, 137.5, 133.8, 130.7, 125.9, 124.1, 119.5, 116.0, 114.8, 107.5, 83.5, 83.1, 44.2, 41.4, 28.4, 24.9, 24.8; HRMS (DART): Calcd for $C_{24}H_{35}B_1N_1O_4$ $[M+H]^+$: 412.2659, Found: 412.2653; Specific Rotation: $[a]_D^{20}$ +17.1 (*c* 0.43, $CHCl_3$) for an enantiomerically enriched sample of 98:2 er. Enantiomeric purity was determined by HPLC analysis in comparison with authentic racemic material (98:2 er shown; Chiralcel AD–H column, 100% hexanes, 0.3 mL/min, 220 nm).

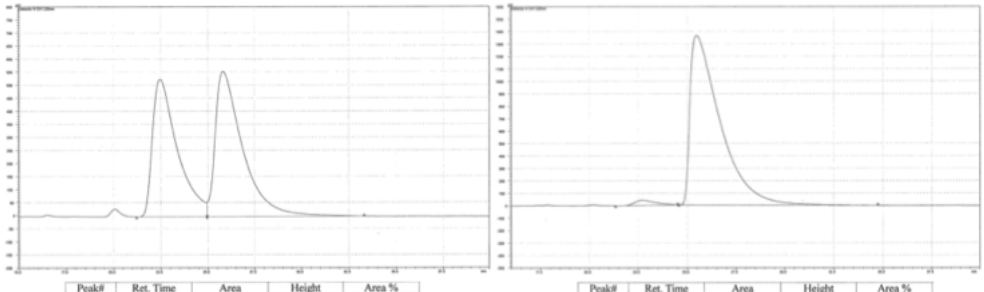

Peak#	Ret. Time	Area	Height	Area %
1	22.469	48390167	527379	46.056
2	25.810	56677153	556188	53.944
Total		105067320	1083567	100.000

Peak#	Ret. Time	Area	Height	Area %
1	22.708	2977277	40960	1.990
2	25.481	146670197	1361804	98.010
Total		149647473	1402765	100.000

Peak #	Time (min)	Area (%)	Peak #	Time (min)	Area (%)
1	22.469	46.056	1	22.708	1.990
2	25.810	53.944	2	25.481	98.010

(*R*)-2-(2-(Benzofuran-2-yl)pent-4-enyl)-4,4,5,5-tetramethyl-1,3,2-dioxaborolane (2.18n) : IR (neat): 2977 (w), 2928 (w), 1584 (w), 1455 (m), 1370 (s), 1321 (s), 1253(w), 1142 (s), 1006 (m), 912 (m), 846 (m), 796 (m), 749 (s), 738 (s), 671 (w) cm^{-1}; ^{1}H NMR ($CDCl_3$, 400 MHz): δ 7.49–7.44 (1H, m), 7.42–7.38 (1H, m), 7.22–7.13 (2H, m), 6.38 (1H, s), 5.76 (1H, ddt, *J* = 17.2, 10.1, 7.1 Hz), 5.08–4.96 (2H, m), 3.26–3.16 (1H, m), 2.63–2.53 (1H, m), 2.49–2.38 (1H, m), 1.23 (2H, d, *J* = 7.7 Hz), 1.20 (6H, s), 1.18 (6H, s); ^{13}C NMR ($CDCl_3$, 100 MHz): δ 163.3, 154.7, 136.3, 129.0, 123.1, 122.4, 120.4, 117.0, 110.9, 101.4, 83.3, 40.3, 35.0, 24.94, 24.88; HRMS (DART): Calcd for $C_{19}H_{26}BO_3$ $[M+H]^+$: 313.1975, Found: 313.1987; Specific Rotation: $[\alpha]_D^{20}$ +17.2 (*c* 1.67, $CHCl_3$) for an enantiomerically enriched sample of 90:10 er. Enantiomeric purity was determined by HPLC analysis in comparison with authentic racemic material (90:10 er shown; Chiralcel OZ–H column, 100% hexanes, 0.3 mL/min, 220 nm).

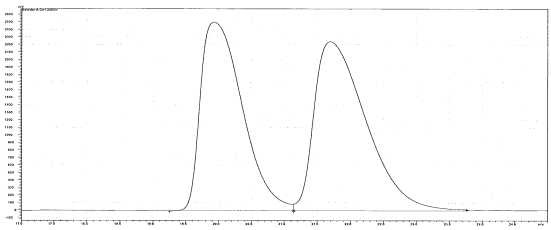

Peak#	Ret. Time	Area	Height	Area %
1	19.923	111510728	2504369	47.625
2	21.690	122634341	2245527	52.375
Total		234145069	4749896	100.000

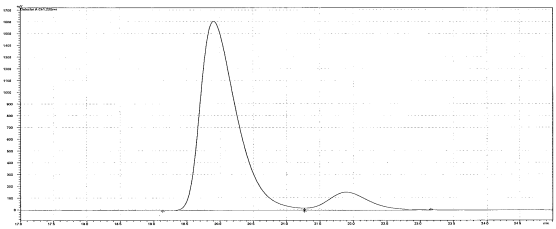

Peak#	Ret. Time	Area	Height	Area %
1	19.900	61004630	1610521	90.179
2	21.888	6644064	153966	9.821
Total		67648694	1764486	100.000

Peak #	Time (min)	Area (%)	Peak #	Time (min)	Area (%)
1	19.923	47.625	1	19.900	90.179
2	21.690	52.375	2	21.888	9.821

(*R*)-2-(2-(Benzo[b]thiophen-5-yl)pent-4-en-1-yl)-4,4,5,5-tetramethyl-1,3,2-dioxaborolane (2.18o): Following the representative procedure except for 1:3 alkene:phosphate used. IR (neat): 3073 (w), 2976 (w), 2924 (w), 1365 (s), 1319 (s),

11142 (s), 846 (m), 820 (m), 699 (s) cm^{-1}; ^1H NMR ($CDCl_3$, 400 MHz): δ 7.76 (1H, d, *J* = 8.4 Hz), 7.65 (1H, s), 7.38 (1H, dd, *J* = 5.4, 0.6 Hz), 7.27 (1H, d, *J* = 5.2 Hz), 7.22 (1H, d, *J* = 8.4 Hz), 5.74–5.64 (1H, m), 4.97 (1H, d, *J* = 17.2 Hz), 4.92 (1H, dd *J* = 10.4, 0.8 Hz), 3.08 (1H, app pent, *J* = 7.5 Hz), 2.48–2.36 (2H, m), 1.30 (1H, dd, *J* = 15.8, 7.0 Hz), 1.17 (1H, dd, *J* = 15.4, 9.0 Hz), 1.07 (12H, s); ^{13}C NMR ($CDCl_3$, 100 MHz): δ 152.3, 140.0, 139.2, 136.4, 124.0, 123.4, 122.9, 122.3, 119.8, 116.9, 83.4, 43.8, 37.6, 24.9, 24.8; HRMS (DART): Calcd for $C_{19}H_{26}B_1O_2S_1$ $[M+H]^+$: 329.1747, Found: 329.1744; Specific Rotation: $[a]_D^{20}$ +18.0 (*c* 1.23, $CHCl_3$) for an enantiomerically enriched sample of 95:5 er. Enantiomeric purity was determined by HPLC analysis in comparison with authentic racemic material (95:5 er shown; Chiralcel OZ–H column, 100% hexanes, 0.3 mL/min, 220 nm).

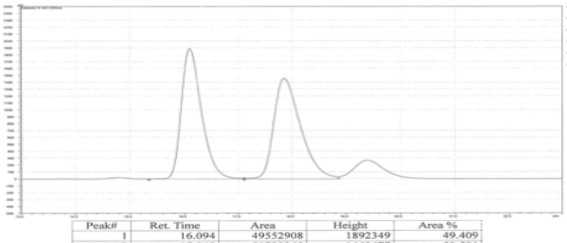

Peak#	Ret. Time	Area	Height	Area %
1	16.094	49552908	1892349	49.409
2	17.848	50738265	1463677	50.591
Total		100291173	3356026	100.000

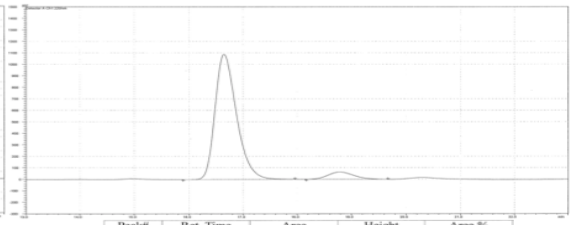

Peak#	Ret. Time	Area	Height	Area %
1	16.643	30009118	1088972	94.738
2	18.783	1666797	56629	5.262
Total		31675915	1145601	100.000

Peak #	Time (min)	Area (%)	Peak #	Time (min)	Area (%)
1	16.094	49.409	1	16.643	94.738
2	17.848	50.591	2	18.783	5.262

(*R*)-2-(2-(4-Bromophenyl)pent-4-en-1-yl)-4,4,5,5-tetramethyl-1,3,2-dioxaborolane (2.18p): Following the representative procedure except for 1:3 alkene:phosphate used. IR (neat): 2977 (w), 2926 (w), 1488 (w), 1368 (s), 1320 (s), 1143 (s), 1073 (m), 1010 (m), 968 (m), 913 (m), 846 (m), 820 (m) cm^{-1}; ^1H NMR (400 MHz, $CDCl_3$): δ 7.37 (2H, d, *J* = 6.4, Hz), 7.07 (2H, d, *J* = 7.6 Hz), 5.63 (1H, ddt, 17.2, 10.0, 7.2 Hz), 4.97–4.91 (2H, m), 2.94–2.87 (1H, m), 2.32 (2H, t, *J* = 7.0 Hz), 1.21 (1H, dd, *J* = 15.4, 6.6 Hz), 1.12 (6H, s),

1.10 (6H, s), 1.09–1.03 (1H, m); ^{13}C NMR (100 MHz, $CDCl_3$): δ 145.9, 136.8, 131.2, 129.4, 119.6, 116.5, 83.2, 43.6, 41.0, 24.9, 24.8; HRMS (DART): Calcd for $C_{17}H_{25}B_1Br_1O_2$ $[M+H]^+$: 351.1131, Found: 351.1141; Specific Rotation: $[\alpha]_D^{20}$ +4.1 (*c* 0.85, $CHCl_3$) for an enantiomerically enriched sample of 90:10 er. Enantiomeric purity was determined by HPLC analysis in comparison with authentic racemic material (90:10 er shown; Chiralcel OZ–H column, 100% hexanes, 0.3 mL/min, 220 nm).

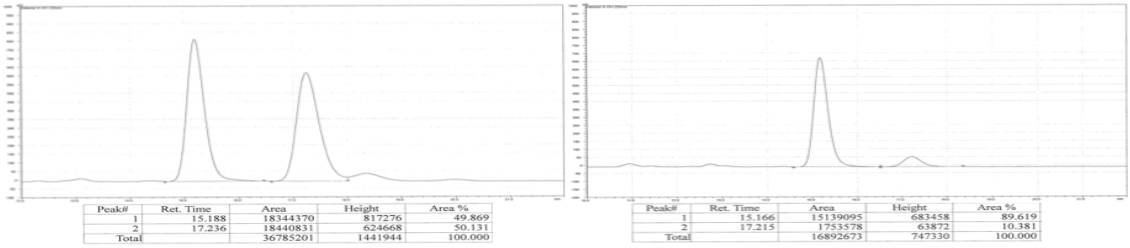

Peak#	Ret. Time	Area	Height	Area %
1	15.188	18344370	817276	49.869
2	17.236	18440831	624668	50.131
Total		36785201	1441944	100.000

Peak#	Ret. Time	Area	Height	Area %
1	15.166	15139095	683458	89.619
2	17.215	1753578	63872	10.381
Total		16892673	747330	100.000

Peak #	Time (min)	Area (%)	Peak #	Time (min)	Area (%)
1	15.188	49.869	1	15.166	89.619
2	17.236	50.131	2	17.215	10.381

(*R*)-4,4,5,5-Tetramethyl-2-(4-(1-(4,4,5,5-tetramethyl-1,3,2-dioxaborolan-2-yl)pent-4-en-2-yl)phenyl)-1,3,2-dioxaborolane (2.18q): Following the representative procedure except for 1:3 alkene:phosphate used. IR (neat): 2977 (m), 2925 (m), 2041 (w), 2034 (w), 2024 (w), 1611 (m), 1399 (m), 1360 (s), 1319 (m), 1271 (w), 1144 (m), 1090 (s), 964 (w), 860 (w), 830 (w), 660 (m)cm^{-1}; ^{1}H NMR ($CDCl_3$, 400 MHz): δ 7.70 (2H, d, *J*= 8.0 Hz), 7.21 (2H, d, *J* = 8.0 Hz), 5.73–5.57 (1H, m), 4.97–4.88 (2H, m), 3.01–2.90 (1H, m), 2.43–2.28 (2H, m), 1.33 (12H, s), 1.28–1.16 (2H, m), 1.12 (6H, s), 1.11 (6H, s); ^{13}C NMR ($CDCl_3$, 100 MHz): δ 150.4, 137.2, 134.8, 127.0, 116.2, 83.6, 83.1, 43.5, 41.6, 25.0, 24.8; HRMS (DART): Calcd for $C_{23}H_{40}B_2N_1O_4$ $[M+NH_4]^+$: 416.3143, Found: 416.3158; Specific Rotation: $[a]_D^{20}$ +9.1 (*c* 1.02, $CHCl_3$) for an enantiomerically enriched sample of 92:8 er. Enantiomeric purity was determined by HPLC analysis in comparison

with authentic racemic material (92:8 er shown; Chiralcel AZ–H column, 99% hexanes, 1% *i*-PrOH, 0.3 mL/min, 220 nm).

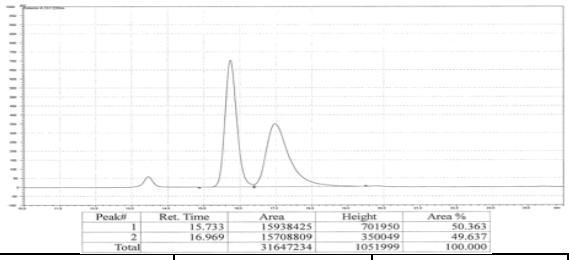

Peak#	Ret. Time	Area	Height	Area %
1	15.733	15938425	701950	50.363
2	16.969	15708809	350049	49.637
Total		31647234	1051999	100.000

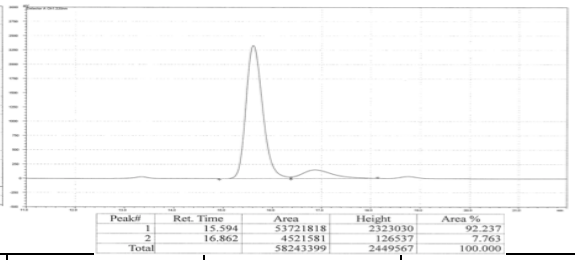

Peak#	Ret. Time	Area	Height	Area %
1	15.594	53721818	2323030	92.237
2	16.862	4521581	126537	7.763
Total		58243399	2449567	100.000

Peak #	Time (min)	Area (%)	Peak #	Time (min)	Area (%)
1	15.733	50.363	1	15.594	92.237
2	16.969	49.637	2	16.862	7.763

(*R*)-4,4,5,5-Tetramethyl-2-(3-(1-(4,4,5,5-tetramethyl-1,3,2-dioxaborolan-2-yl)pent-4-en-2-yl)phenyl)-1,3,2-dioxaborolane (2.18r): Following the representative procedure except for 1:3 alkene:phosphate used. IR (neat): 2977 (m), 2926 (w), 2035 (w), 1611 (w), 1457 (w), 1399 (m), 1360 (s), 1320 (m), 1271 (w), 1214 (w), 1144 (s), 1090 (m), 964 (w), 860 (w), 829 (w), 659 (w) cm^{-1}; ^1H NMR ($CDCl_3$, 400 MHz): δ 7.66 (1H, s), 7.60 (1H, d, J = 7.1 Hz), 7.34–7.23 (2H, m), 5.68 (1H, ddt, J = 17.1, 10.1, 7.0 Hz), 4.97 (1H, dd, J = 17.2, 1.9 Hz), 4.94–4.89 (1H, m), 3.03–2.91 (1H, m), 2.49–2.29 (2H, m), 1.34 (6H, s), 1.33 (6H, s), 1.27–1.17 (2H, m), 1.10 (12H, s);^{13}C NMR ($CDCl_3$, 100 MHz): δ 146.2, 137.5, 134.2, 132.5, 130.3, 127.6, 116.0, 83.7, 83.0, 43.3, 41.4, 25.0, 24.9, 24.8; HRMS (DART): Calcd for $C_{23}H_{37}B_2O_4$ $[M+H]^+$: 399.2878, Found: 399.2887; Specific rotation: $[a]_D^{20}$ +5.8 (*c* 0.43, $CHCl_3$) for an enantiomerically enriched sample of 96.5:3.5 er. Enantiomeric purity was determined by HPLC analysis in comparison with authentic racemic material (96.5:3.5 er shown; Chiralcel OD–H column, 98% hexanes, 2% *i*-PrOH, 0.3 mL/min, 220 nm).

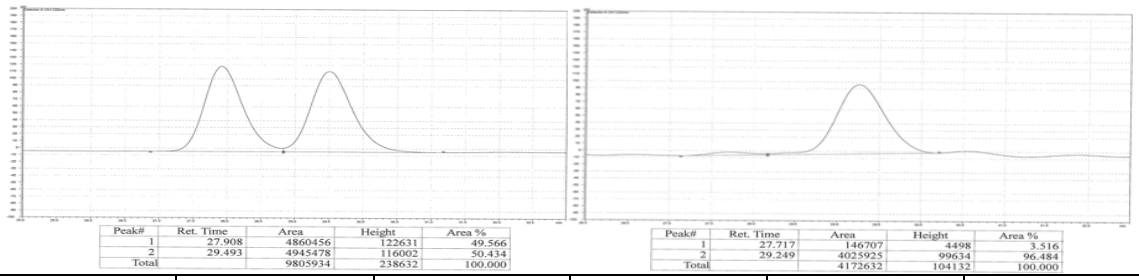

Peak#	Ret. Time	Area	Height	Area %
1	27.908	4860456	122631	49.566
2	29.493	4945478	116002	50.434
Total		9805934	238632	100.000

Peak#	Ret. Time	Area	Height	Area %
1	27.717	146707	4498	3.516
2	29.249	4025925	99634	96.484
Total		4172632	104132	100.000

Peak #	Time (min)	Area (%)	Peak #	Time (min)	Area (%)
1	27.908	49.566	1	27.717	3.516
2	29.493	50.434	2	29.249	96.484

(*R*)-4,4,5,5-Tetramethyl-2-(2-(naphthalen-2-yl)pent-4-en-1-yl)-1,3,2-dioxaborolane (2.18s): Following the representative procedure except for 1:3 alkene:phosphate used. IR (neat): 2976 (w), 2923 (s), 2853 (m), 1639 (w), 1362 (s), 1315 (s), 1143 (s), 968 (m), 911 (m), 847 (s), 814 (s), 744 (s), 476 (s) cm^{-1}; ^{1}H NMR ($CDCl_3$, 400 MHz): δ 7.81–7.73 (3H, m), 7.65–7.62 (1H, m), 7.46–7.35 (3H, m), 5.76–5.64 (1H, m), 5.01–4.89 (2H, m), 3.19–3.08 (1H, m), 2.55–2.37 (2H, m), 1.28–1.17(2H, m), 1.06 (6H, s), 1.07 (6H, s); ^{13}C NMR ($CDCl_3$, 100 MHz): δ 144.5, 137.2, 133.6, 132.3, 127.82, 127.78, 127.74, 127.68, 126.3, 125.81, 125.79, 125.1, 116.3, 83.1, 43.6, 41.6, 24.85, 24.77; HRMS (DART): Calcd for $C_{21}H_{28}B_1O_2$ $[M+H]^+$: 323.2182, Found: 323.2194; Specific Rotation: $[a]_D^{20}$ +16.4 (*c* 0.72, $CHCl_3$) for an enantiomerically enriched sample of 96:4 er. Enantiomeric purity was determined by HPLC analysis in comparison with authentic racemic material (96:4 er shown; Chiralcel OZ–H column, 100% hexanes, 0.3 mL/min, 254 nm).

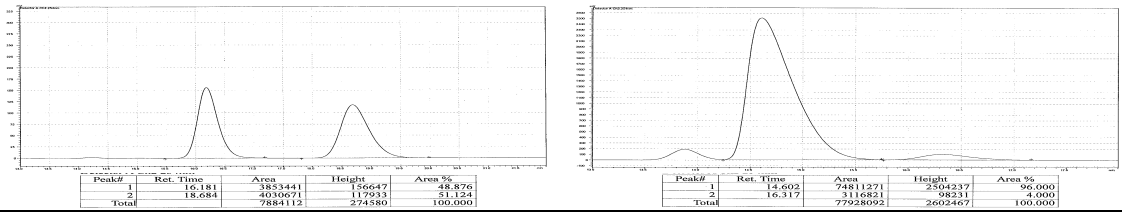

Peak#	Ret. Time	Area	Height	Area %
1	16.181	3853441	156647	48.876
2	18.684	4030671	117933	51.124
Total		7884112	274580	100.000

Peak#	Ret. Time	Area	Height	Area %
1	14.602	7481271	2504237	96.000
2	16.317	3116821	98231	4.000
Total		77928092	2602467	100.000

Peak #	Time (min)	Area (%)	Peak #	Time (min)	Area (%)
1	16.181	48.876	1	14.602	96.000
2	18.684	51.124	2	16.317	4.000

(*R*)-2-(2,4-Diphenylpent-4-en-1-yl)-4,4,5,5-tetramethyl-1,3,2-dioxaborolane (2.18t): Following the representative procedure except for 1:3 alkene:phosphate used. IR (neat): 3027 (w), 2977 (w), 2929 (w), 1494 (m), 1452 (w), 1369 (s), 1320 (s), 1145 (s), 699 (s) cm^{-1}; ^{1}H NMR (400 MHz, $CDCl_3$): δ 7.39–7.36 (2H, m), 7.33–7.19 (5H, m), 7.14–7.09 (3H, m), 5.15 (1H, d, *J* = 2.0 Hz), 4.83 (1H, d, *J* = 1.2 Hz), 2.96 (1H, app pent, *J* = 7.7 Hz), 2.87 (1H, dd, *J* = 13.8, 7.0 Hz), 2.73 (1H, dd, *J* = 13.6, 8.0 Hz), 1.26 (1H, dd, *J* = 15.6, 6.8 Hz), 1.13 (1H, dd, *J* = 15.6, 9.2 Hz), 1.07 (6H, s), 1.05 (6H, s); ^{13}C NMR (100 MHz, $CDCl_3$): δ 146.9, 146.8, 141.2, 128.4, 128.1, 127.6, 127.4, 126.6, 125.9, 114.5, 83.1, 45.7, 39.9, 24.8, 24.7; HRMS (DART): Calcd for $C_{23}H_{30}B_1O_2$ $[M+H]^+$: 349.2339, Found: 349.2347; Specific Rotation: $[\alpha]_{20}^{D}$ –11.9 (c 0.50, $CHCl_3$) for an enantiomerically enriched sample of 88:12 er. Enantiomeric purity was determined by HPLC analysis of the alcohol product after oxidation in comparison with authentic racemic material (96:4 er shown; Chiralcel OD–H column, 99% hexanes, 1% *i*-PrOH, 0.3 mL/min, 220 nm).

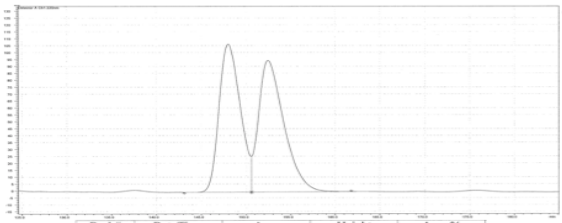

Peak#	Ret. Time	Area	Height	Area %
1	148.008	17684600	107007	48.370
2	152.465	18876400	95038	51.630
Total		36561001	202046	100.000

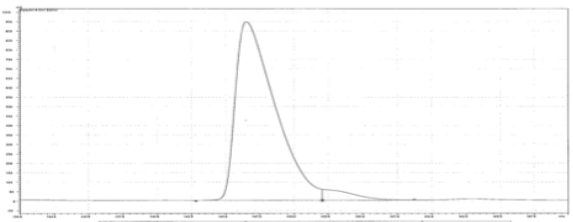

Peak#	Ret. Time	Area	Height	Area %
1	146.542	190523901	945369	95.605
2	152.058	8759003	57348	4.395
Total		199282904	1002718	100.000

Peak #	Time (min)	Area (%)	Peak #	Time (min)	Area (%)
1	148.008	48.370	1	146.542	95.605
2	152.465	51.630	2	152.058	4.395

(*R*)-4,4,5,5-Tetramethyl-2-(4-methyl-2-phenylpent-4-en-1-yl)-1,3,2-dioxaborolane (2.18u): Following the representative procedure except for 1:6 alkene:phosphate used. IR (neat): 3028 (w), 2978 (m), 2929 (m), 1453 (w), 1369 (s), 1320 (m), 1145 (s), 968 (w), 888 (w), 699 (m) cm^{-1}; ^{1}H NMR (400 MHz, $CDCl_3$): δ 7.24–7.18 (4H, m), 7.13–7.10

(1H, m), 4.64 (1H, s), 4.56 (1H, s), 3.03 (1H, app pent, J = 7.7 Hz), 2.29 (2H, d, J = 7.6 Hz), 1.65 (3H, s), 1.24–1.16 (1H, m), 1.09–1.03 (13H, m); ^{13}C NMR (100 MHz, $CDCl_3$): δ 147.2, 144.3, 128.1, 127.5, 125.9, 112.4, 83.0, 48.3, 39.8, 24.83, 24.75, 22.5; HRMS (DART): Calcd for $C_{18}H_{28}B_1O_2$ $[M+H]^+$: 287.2182, Found: 287.2189; Specific Rotation: $[\alpha]_D^{20}$ +5.7 (*c* 0.33, $CHCl_3$) for an enantiomerically enriched sample of 90:10 er. Enantiomeric purity was determined by HPLC analysis of the alcohol product after oxidation in comparison with authentic racemic material (95:5 er shown; Chiralpak AD–H column, 99% hexanes, 1% *i*-PrOH, 0.3 mL/min, 220 nm).

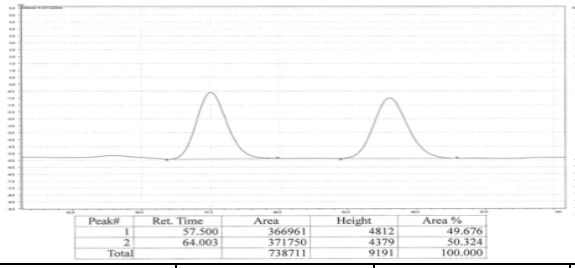

Peak#	Ret. Time	Area	Height	Area %
1	57.500	366961	4812	49.676
2	64.003	371750	4379	50.324
Total		738711	9191	100.000

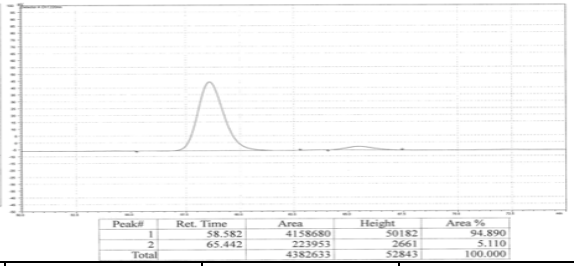

Peak#	Ret. Time	Area	Height	Area %
1	58.582	4158680	50182	94.890
2	65.442	223953	2661	5.110
Total		4382633	52843	100.000

Peak #	Time (min)	Area (%)	Peak #	Time (min)	Area (%)
1	57.500	49.676	1	58.582	94.890
2	64.003	50.324	2	65.442	5.110

(*R*)-Trimethyl(4-phenyl-5-(4,4,5,5-tetramethyl-1,3,2-dioxaborolan-2-yl)pent-1-en-2-yl)silane (2.18v): IR (neat): 2978 (w), 2955 (w), 1368 (s), 1319 (m), 1247 (m), 1145 (s), 968 (w), 836 (s), 757 (m), 699 (m) cm^{-1}; ^{1}H NMR (400 MHz, $CDCl_3$): δ 7.25–7.18 (4H, m), 7.15–7.10 (1H, m), 5.45–5.44 (1H, m), 5.31 (1H, d, J = 3.2 Hz), 3.06–2.98 (1H, m), 2.49–2.35 (1H, m), 1.26–1.20 (1H, m), 1.09–1.01 (13H, m), 0.07 (9H, m); ^{13}C NMR (100 MHz, $CDCl_3$): δ 150.3, 147.4, 128.1, 127.7, 126.5, 125.8, 83.0, 45.9, 40.7, 24.9, 24.8, –1.2; HRMS (DART): Calcd for $C_{20}H_{34}B_1O_2Si_1$ $[M+H]^+$: 345.2421, Found: 345.2424. Specific Rotation: $[\alpha]_D^{20}$ +7.9 (*c* 0.33, $CHCl_3$) for an enantiomerically enriched sample of 95:5 er. Enantiomeric purity was determined by HPLC analysis in comparison with

authentic racemic material (96:4 er shown; Chiralcel OD–H column, 100% hexanes, 0.3 mL/min, 220 nm).

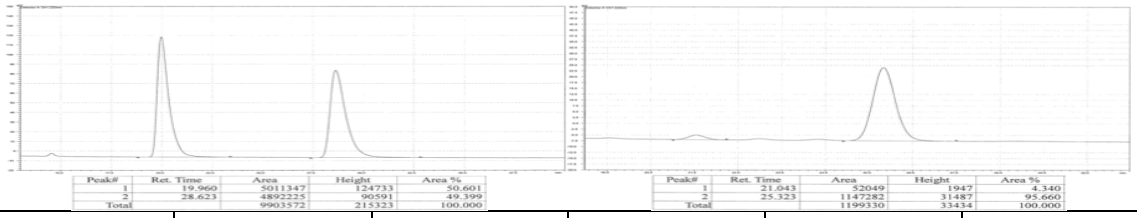

Peak #	Time (min)	Area (%)	Peak #	Time (min)	Area (%)
1	19.960	50.601	1	21.043	4.340
2	28.623	49.399	2	25.323	95.660

(*R*)-(4-(3-(Allyloxy)phenyl)-5-(4,4,5,5-tetramethyl-1,3,2-dioxaborolan-2-yl)pent-1-en-2-yl)trimethylsilane (2.18w): IR (neat): 2977 (w), 2954 (w), 1600 (w), 1584 (w), 1366 (m), 1317 (m), 1247 (m), 1144 (s), 924 (m), 836 (s) cm^{-1}; ^{1}H NMR (500 MHz, $CDCl_3$): δ 7.14 (1H, t, *J* = 6.2 Hz), 6.80–6.77 (2H, m), 6.69 (1H, dd, *J* = 6.4, 2.0 Hz), 6.10–6.02 (1H, m), 5.45–5.38 (2H, m), 5.32–5.26 (2H, m), 4.52–4.51 (2H, m), 2.99 (1H, app pent, *J* = 6.1 Hz), 2.45 (1H, dd, *J* = 11.2, 6.0 Hz), 2.38 (1H, dd, *J* = 11.2, 6.0 Hz), 1.21 (1H, dd, *J* = 14.0, 3.6 Hz), 1.11 (6H, s), 1.09 (6H, s), 1.02 (1H, dd, *J* = 12.2, 7.0 Hz), 0.07 (9H, s); ^{13}C NMR (125 MHz, $CDCl_3$): δ 158.5, 150.3, 149.3, 133.8, 129.0, 126.5, 120.4, 117.5, 114.3, 112.1, 83.0, 68.8, 45.7, 40.7, 24.9, 24.8, –1.2; HRMS (DART): Calcd for $C_{23}H_{38}B_1O_3Si_1$ $[M+H]^+$: 401.2683, Found: 401.2695; Specific Rotation: $[\alpha]_D^{20}$ +4.7 (*c* 0.88, $CHCl_3$) for an enantiomerically enriched sample of 95:5 er. Enantiomeric purity was determined by HPLC analysis in comparison with authentic racemic material (96:4 er shown; Chiralcel OD–H column, 100% hexanes, 0.3 mL/min, 220 nm).

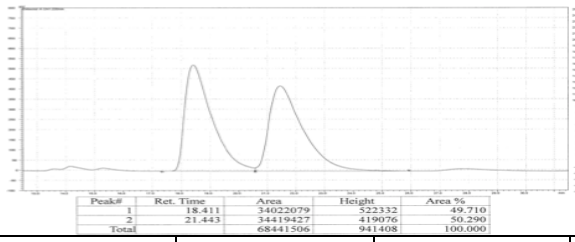

Peak#	Ret. Time	Area	Height	Area %
1	18.411	34022079	522332	49.710
2	21.443	34419427	419076	50.290
Total		68441506	941408	100.000

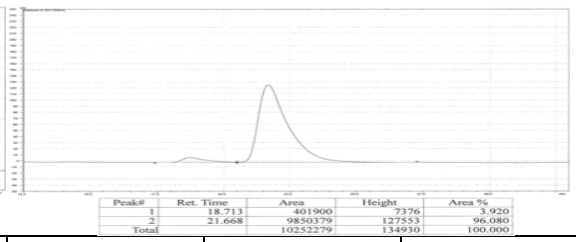

Peak#	Ret. Time	Area	Height	Area %
1	18.713	401900	7376	3.920
2	21.668	9850379	127553	96.080
Total		10252279	134930	100.000

Peak #	Time (min)	Area (%)	Peak #	Time (min)	Area (%)
1	18.411	49.710	1	18.713	3.920
2	21.443	50.290	2	21.668	96.080

(*R*)-2-(2-(2-Fluorophenyl)pent-4-en-1-yl)-4,4,5,5-tetramethyl-1,3,2-dioxaborolane (2.18x): Following the representative procedure except **2.25** was used. IR (neat): 2978 (w), 2931 (w), 1765 (s), 1490 (m), 1401 (s), 1369 (s), 1223 (m), 1144 (s), 968 (m), 913 (m), 846 (m), 754 (s) cm^{-1}; ^{1}H NMR (400 MHz, $CDCl_3$): δ 7.21 (1H, td, *J* = 7.6, 1.6 Hz), 7.13–7.10 (1H, m), 7.09–7.02 (1H, m), 6.98–6.94 (1H, m), 5.68 (1H, ddt, *J* = 16.8, 10.4, 6.8 Hz), 4.97–4.90 (2H, m), 3.35–3.27 (1H, m), 2.43–2.32 (2H, m), 1.28–1.22 (1H, m), 1.19–1.08 (1H, m), 1.11 (6H, s), 1.08 (6H, s); ^{13}C NMR (100 MHz, $CDCl_3$): δ 160.9 (d, *J* = 243.7 Hz), 136.9, 133.5 (d, *J* = 14.4 Hz), 128.8 (d, *J* = 5.3 Hz), 127.3 (d, *J* = 8.4 Hz), 123.9 (d, *J* = 3.8 Hz), 116.4, 115.3 (d, *J* = 22.8 Hz), 83.1, 42.5, 34.3, 24.8, 24.7; HRMS (DART): Calcd for $C_{17}H_{25}B_1F_1O_2$ $[M+H]^+$: 291.1932, Found: 291.1937; Specific Rotation: $[\alpha]_D^{20}$ +14.2 (*c* 0.87, $CHCl_3$) for an enantiomerically enriched sample of 96:4 er. Enantiomeric purity was determined by HPLC analysis in comparison with authentic racemic material (96:4 er shown; Chiralcel OD–H column, 100% hexanes, 0.3 mL/min, 220 nm).

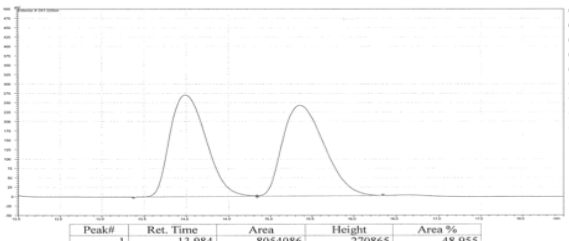

Peak#	Ret. Time	Area	Height	Area %
1	13.984	8054086	270865	48.955
2	15.351	8397818	241482	51.045
Total		16451904	512347	100.000

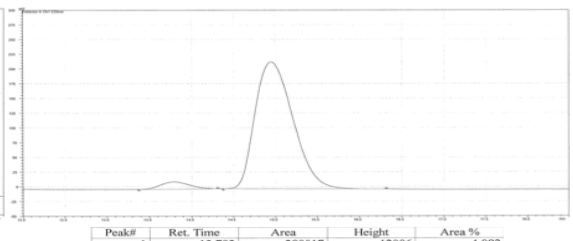

Peak#	Ret. Time	Area	Height	Area %
1	13.782	289017	12096	4.082
2	14.947	6790935	215149	95.918
Total		7079952	227246	100.000

Peak #	Time (min)	Area (%)	Peak #	Time (min)	Area (%)
1	13.984	48.955	1	13.782	4.082
2	15.351	51.045	2	14.947	95.918

***(R)*-2-(2-(4-Fluorophenyl)pent-4-en-1-yl)-4,4,5,5-tetramethyl-1,3,2-dioxaborolane (2.18y):** Following the representative procedure except **2.25** was used. IR (neat): 2978 (w), 2925 (w), 2855 (w), 1604 (w), 1509 (s), 1369 (s), 1322 (m), 1223 (m), 1144 (s), 968 (w), 912 (w), 832 (m) cm^{-1}; ^{1}H NMR (400 MHz, $CDCl_3$): δ 7.17–7.13 (2H, m), 6.98–6.91 (2H, m), 5.65 (1H, ddt, *J* = 17.2, 10.0, 7.2 Hz), 4.96–4.91 (2H, m), 2.97–2.89 (1H, m), 2.36–2.27 (2H, m), 1.26–1.16 (1H, m), 1.09–1.04 (13H, m); ^{13}C NMR (100 MHz, $CDCl_3$): δ 161.4 (d, *J* = 241.3 Hz), 142.5 (d, *J* = 3.0 Hz), 137.0, 128.9 (d, *J* = 7.6 Hz), 116.4, 114.9 (d, *J* = 20.5 Hz), 83.2, 44.0, 40.8, 24.8, 24.7; HRMS (DART): Calcd for $C_{17}H_{25}B_1F_1O_2$ $[M+H]^+$: 291.1932, Found: 291.1939; Specific Rotation: $[\alpha]_D^{20}$ +14.9 (*c* 1.20, $CHCl_3$) for an enantiomerically enriched sample of 92:8 er. Enantiomeric purity was determined by HPLC analysis in comparison with authentic racemic material (98:2 er shown; Chiralcel OZ–H column, 100% hexanes, 0.3 mL/min, 220 nm).

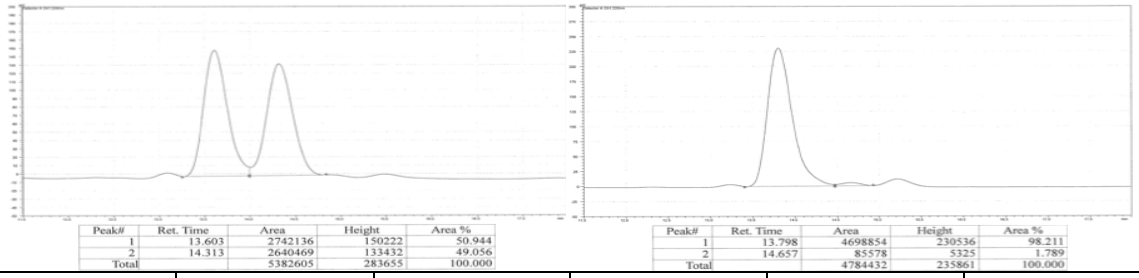

Peak#	Ret. Time	Area	Height	Area %
1	13.603	2742136	150222	50.944
2	14.313	2640469	133432	49.056
Total		5382605	283655	100.000

Peak#	Ret. Time	Area	Height	Area %
1	13.798	4698854	230536	98.211
2	14.657	85578	5325	1.789
Total		4784432	235861	100.000

Peak #	Time (min)	Area (%)	Peak #	Time (min)	Area (%)
1	13.603	50.944	1	13.798	98.211
2	14.313	49.056	2	14.657	1.789

(*R*)-4,4,5,5-Tetramethyl-2-(2-(2-(trifluoromethyl)phenyl)pent-4-en-1-yl)-1,3,2-dioxaborolane (2.18z): Following the representative procedure except **2.25** was used. IR (neat): 2979 (w), 2928 (w), 1363 (m), 1312 (s), 1145 (s), 1124 (s), 1036 (m), 768 (m) cm^{-}

[1]; ^{1}H NMR (400 MHz, $CDCl_3$): δ 7.58 (1H, d, *J* = 8.0 Hz), 7.50–7.43 (2H, m), 7.26–7.22 (1H, m), 5.70 (1H, ddt, *J* = 18.0, 10.0, 7.2 Hz), 4.99–4.92 (2H, m), 3.42 (1H, app pent, *J* = 7.4 Hz), 2.45–2.25 (2H, m), 1.26 (1H, dd, *J* = 15.4, 7.0 Hz), 1.14 (1H, dd, *J* = 15.6, 8.4 Hz), 1.08 (6H, s), 1.05 (6H, s); ^{13}C NMR (100 MHz, $CDCl_3$): δ 146.5, 136.7, 131.8, 128.2 (q, *J* = 29.0 Hz), 128.18, 125.7, 125.6, 124.7 (q, *J* = 272.5 Hz), 116.6, 83.1, 43.9, 36.0, 24.7, 18.6 (br, C–B); HRMS (DART): Calcd for $C_{18}H_{25}B_1F_3O_2$ $[M+H]^+$: 341.1900, Found: 341.1903; Specific Rotation: $[\alpha]_D^{20}$ +11.9 (*c* 1.20, $CHCl_3$) for an enantiomerically enriched sample of 88:12 er. Enantiomeric purity was determined by HPLC analysis in comparison with authentic racemic material (96:4 er shown; Chiralcel OZ–H column, 100% hexanes, 0.3 mL/min, 220 nm).

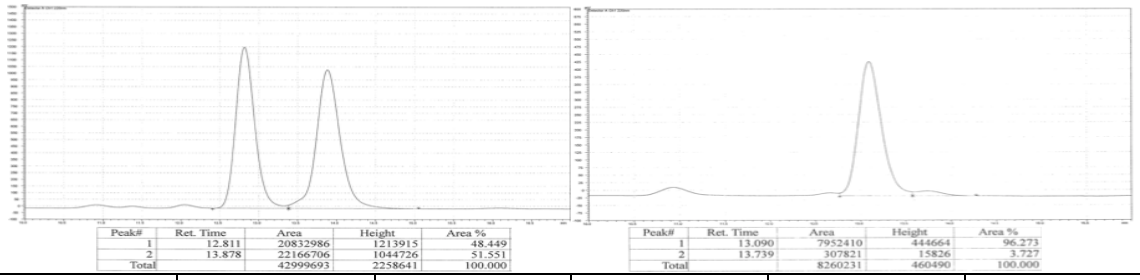

Peak#	Ret. Time	Area	Height	Area %
1	12.811	20832986	1213915	48.449
2	13.878	22166706	1044726	51.551
Total		42999693	2258641	100.000

Peak#	Ret. Time	Area	Height	Area %
1	13.090	7952410	444664	96.273
2	13.739	307821	15826	3.727
Total		8260231	460490	100.000

Peak #	Time (min)	Area (%)	Peak #	Time (min)	Area (%)
1	12.811	48.449	1	13.090	96.273
2	13.878	51.551	2	13.739	3.727

(*R*)-4,4,5,5-Tetramethyl-2-(2-(4-(trifluoromethyl)phenyl)pent-4-en-1-yl)-1,3,2-dioxaborolane (2.18aa): Following the representative procedure except **2.25** was used. The spectroscopic data match those reported previously.[93] ^{1}H NMR (400 MHz, $CDCl_3$): δ 7.58 (1H, d, *J* = 8.0 Hz), 7.50–7.43 (2H, m), 7.26–7.22 (1H, m), 5.70 (1H, ddt, *J* = 18.0, 10.0, 7.2 Hz), 4.99–4.92 (2H, m), 3.42 (1H, app pent, *J* = 7.4 Hz), 2.45–2.25 (2H, m), 1.26 (1H, dd, *J* = 15.4, 7.0 Hz), 1.14 (1H, dd, *J* = 15.6, 8.4 Hz), 1.08 (6H, s), 1.05 (6H, s). Specific Rotation: $[\alpha]_D^{20}$ +6.1 (*c* 0.45, $CHCl_3$) for an enantiomerically enriched sample of

96:4 er. Enantiomeric purity was determined by HPLC analysis of the alcohol product after oxidation in comparison with authentic racemic material (96:4 er shown; Chiralcel OZ–H column, 99% hexanes, 0.3 mL/min, 220 nm).

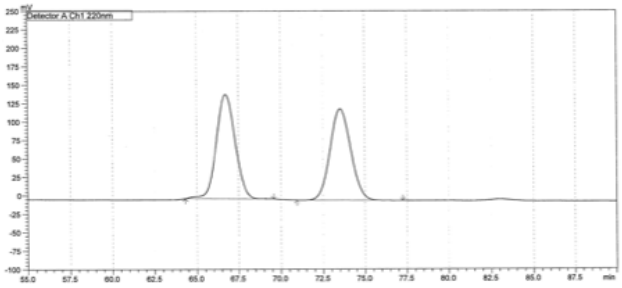

Peak#	Ret. Time	Area	Height	Area%
1	66.741	11143770	141643	50.949
2	73.532	10728683	124323	49.051
Total		21872454	265966	100.000

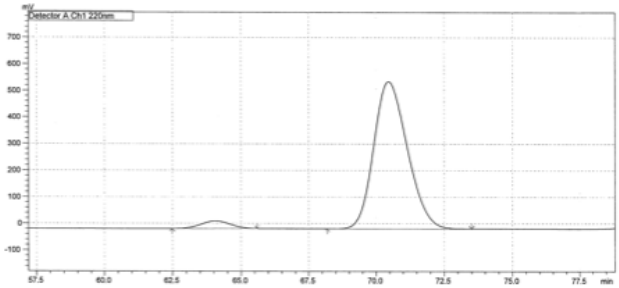

Peak#	Ret. Time	Area	Height	Area%
1	64.054	2108669	28141	4.220
2	70.462	47865409	554084	95.780
Total		49974079	582225	100.000

Peak #	Time (min)	Area (%)	Peak #	Time (min)	Area (%)
1	66.741	50.949	1	64.054	4.220
2	73.532	49.051	2	70.462	95.780

(*R*)-4,4,5,5-Tetramethyl-2-(2-(*o*-tolyl)hex-4-en-1-yl)-1,3,2-dioxaborolane (2.18ab): Following the representative procedure except **2.24b** was used. The spectroscopic data match those reported previously.[93] ^{1}H NMR (400 MHz, $CDCl_3$): δ 7.26–7.01 (8H, m, *E/Z*), 5.46–5.28 (4H, m, *E/Z*), 3.24–3.13 (2H, m, *E/Z*), 2.36 (3H, s, *E*) 2.35 (3H, s, *Z*), 2.32–2.13 (4H, m, *E/Z*), 1.59 (3H, d, J = 5.6 Hz, *E*), 1.54 (3H, d, J = 6 Hz, *Z*), 1.23–1.10 (4H, m, *E/Z*), 1.053 (6H, s, *E*), 1.045 (6H, s, *E*), 1.03 (6H, s, *Z*), 1.02 (6H, s, *Z*) Specific Rotation: $[\alpha]_D^{20}$ +6.1 (*c* 0.45, $CHCl_3$) for an enantiomerically enriched sample of 92:8 er. Enantiomeric purity was determined by HPLC analysis of the alcohol product after oxidation in comparison with authentic racemic material prepared according to the procedure reported previously obtaining ***rac*-*E*-2ab**.[93] (92:8 er shown for *E* and *Z*; Chiralcel OJ–H column, 98% hexanes, 0.3 mL/min, 220 nm).

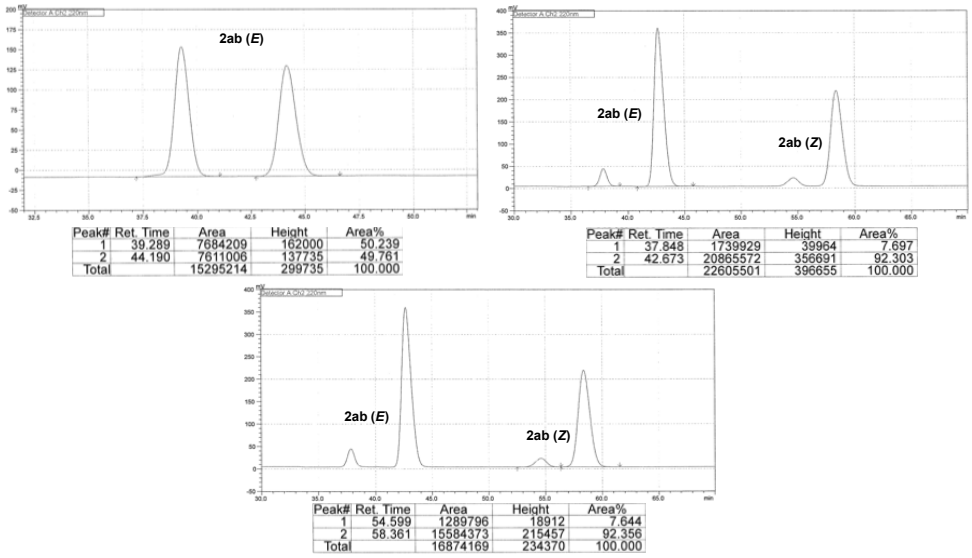

Peak #	Time (min)	Area (%)	Peak #	Time (min)	Area (%)
1 (*rac*)	39.389	50.239	1 (*E*)	37.848	7.697
2 (*rac*)	44.190	49.761	2 (*E*)	42.673	92.303
			1 (*Z*)	54.599	7.644
			2 (*Z*)	58.361	92.356

■ **Formal Synthesis of (+)-Heliespirone A and (–)-Heliespirone C**

(*R*)-2-(2-(2,5-Dimethoxy-4-methylphenyl)pent-4-en-1-yl)-4,4,5,5-tetramethyl-1,3,2-dioxaborolane (2.27): In a N_2-filled glove box, a flame-dried 100 mL round-bottom flask equipped with a stir bar was charged with bisphosphine **2.24b** (188 mg, 0.28 mmol), NaO*t*-Bu (742 mg, 7.7 mmol), and CuCl (26 mg, 0.26 mmol). The flask was sealed with a septum and electrical tape before removal from the glove box. Tetrahydrofuran (20 mL) was added and the resulting yellow solution was allowed to stir for 1 h under N_2 at 22 °C. A solution of $B_2(pin)_2$ (1.4 g, 5.7 mmol) in thf (15 mL) was added to the mixture at 0 °C, causing the solution to turn dark brown immediately. After 15 min, a solution of **2.26** (2.75 g, 15.5 mmol) in thf (5 mL) and allylphosphate (**2.17**) [0.92 mL (1.0 g), 5.15 mmol] was added by syringe. The resulting mixture was allowed to stir at 22 °C for 18 h. Then,

the mixture was passed through a short plug of silica gel (4x4 cm) and eluted with Et_2O. The organic layer was concentrated under reduced pressure, affording yellow oil, which was purified by silica gel chromatography (100% hexanes→hexanes:Et_2O = 10:1) to afford **2.27** as colorless oil (1.1 g, 3.3 mmol, 64% yield) and recovered **2.26** (1.68 g, 9.4 mmol, 91%). IR (neat): 2976 (w), 2931 (w), 2830 (w), 1506 (m), 1465 (m), 1398 (m), 1369 (m), 1316 (m), 1207 (s), 1143 (s), 1046 (s), 968 (m), 846 (m), 802 (m) cm^{-1}; ^1H NMR (400 MHz, $CDCl_3$): δ 6.68 (1H, s), 6.64 (1H, s), 5.71 (1H, ddt, *J* = 17.2, 9.8, 7.4 Hz), 4.98–4.89 (2H, m), 3.78 (3H, s), 3.76 (3H, s), 3.36 (1H, app pent, *J* = 7.5 Hz), 2.43–2.25 (2H, m), 2.18 (3H, s), 1.22 (1H, dd, *J* = 15.6, 7.6 Hz), 1.15–1.10 (1H, m), 1.13 (6H, s), 1.10 (6H, s); ^{13}C NMR (100 MHz, $CDCl_3$): δ 151.7, 151.0, 137.8, 133.2, 124.2, 115.7, 114.4, 110.9, 82.9, 56.5, 56.2, 42.3, 34.2, 24.84, 24.81, 16.2; HRMS (DART): Calcd for $C_{20}H_{32}B_1O_4$ $[M+H]^+$: 347.2394, Found: 347.2377; Specific Rotation: $[\alpha]_D^{20}$ +36.6 (*c* 0.56, $CHCl_3$) for an enantiomerically enriched sample of 97:3 er. Enantiomeric purity was determined by HPLC analysis of the alcohol product after oxidation in comparison with authentic racemic material (97:3 er shown; Chiralpak AD–H column, 99% hexanes, 1% *i*-PrOH, 0.3 mL/min, 220 nm).

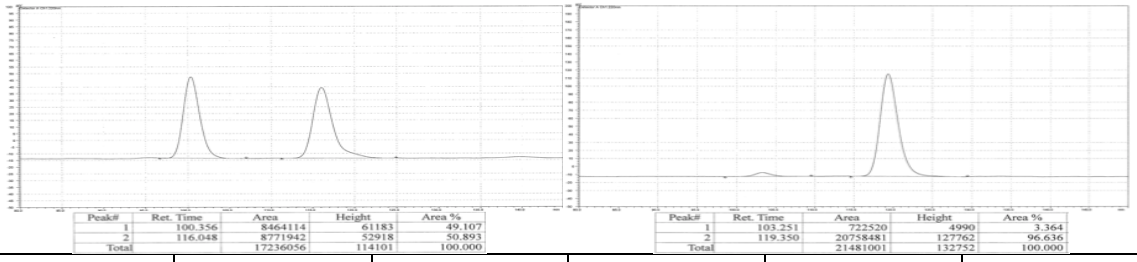

Peak#	Ret. Time	Area	Height	Area %
1	100.356	8464114	61183	49.107
2	116.048	8771942	52918	50.893
Total		17236056	114101	100.000

Peak#	Ret. Time	Area	Height	Area %
1	103.251	722520	4990	3.364
2	119.350	20758481	127762	96.636
Total		21481001	132752	100.000

Peak #	Time (min)	Area (%)	Peak #	Time (min)	Area (%)
1	100.356	49.107	1	103.251	3.364
2	116.048	50.893	2	119.350	96.636

(*R*)-2-(3-(2,5-Dimethoxy-4-methylphenyl)-6-methylhept-5-en-1-yl)-4,4,5,5-tetramethyl-1,3,2-dioxaborolane (2.30): Compound **2.27** was converted to **2.30** by a two step sequence olefin cross metathesis/homologation based on the reported procedures except Hoveyda-Grubbs catalyst 2nd generation was used in the cross metathesis.[103] IR (neat): 2977 (w), 2931 (w), 2854 (w), 1504 (m), 1466 (m), 1398 (m), 1372 (m), 1317 (m), 1208 (s), 1145 (m), 1049 (m), 968 (w) cm^{-1}; ^{1}H NMR (400 MHz, $CDCl_3$): δ 6.65 (1H, s), 6.62 (1H, s), 5.09–5.06 (1H, m), 3.77 (3H, s), 3.73 (3H, s), 3.02 (1H, app pent, J = 7.2 Hz), 2.35–2.19 (2H, m), 1.81 (3H, s), 1.80–1.70 (1H, m), 1.68–1.56 (4H, m), 1.54 (3H, s), 1.21 (12H, s), 0.74–0.60 (2H, m); ^{13}C NMR (100 MHz, $CDCl_3$): δ 151.9, 151.7, 132.1, 131.7, 124.2, 123.6, 114.5, 110.7, 82.9, 56.6, 56.2, 40.5, 33.8, 29.3, 25.9, 25.0, 24.9, 17.9, 16.2; HRMS (DART): Calcd for $C_{23}H_{38}B_1O_4$ $[M+H]^+$: 389.2863, Found: 389.2862; Specific Rotation: $[\alpha]_D^{20}$ +18.0 (*c* 0.50, $CHCl_3$).

(3*R*,5*R*)-3-(2,5-Dimethoxy-4-methylphenyl)-6-methylheptane-1,5,6-triol (2.33): Compound **2.30** was converted to **2.33** by a two step sequence enantioselective epoxidation/hydrolysis based on the reported procedures except the oxidation was performed with 2.5 equiv of oxone.[104] The spectroscopic data match those reported previously.[105] ^{1}H NMR (400 MHz, $CDCl_3$): δ 6.72 (1H, s), 6.66 (1H, s), 3.80 (3H, s), 3.79 (3H, s), 3.58–3.53 (2H, m), 3.46–3.35 (2H, m), 2.20 (3H, s), 2.12–2.01 (1H, m), 1.88–1.84 (1H, m), 1.74–1.59 (2H, m), 1.21 (3H, s), 1.15 (3H, s); HRMS (DART): Calcd

(103) For cross-metathesis, see: Chatterjee, A. K.; Sanders, D. P.; Grubbs, R. H. *Org. Lett.* ***2002***, *4*, 1939–1942. For homologation, see: Kliman, L. T.; Mlynarski, S. N.; Morken, J. P. *J. Am. Chem. Soc.* ***2009***, *131*, 13210–13211.

(104) Wang, Z.-X.; Tu, Y.; Frohn, M.; Zhang, J.-R.; Shi, Y. *J. Am. Chem. Soc.* **1997**, *119*, 11224–11235.

(105) Huang, C.; Liu, B. *Chem. Commun.* **2010**, *46*, 5280–5282.

for $C_{17}H_{28}O_5$ $[M]^+$: 312.1937, Found: 312.1939. Specific Rotation: $[\alpha]_D^{20}$ +23.4 (*c* 0.23, $CHCl_3$). Literature precedence: $[\alpha]_D^{13}$ +29.2 (*c* 0.10, CH_2Cl_2).[105]

■ Study of the Possibility of Epimerization through Isotopic Labeling

Scheme S1. Synthesis of *E* and *Z* Deuterium-Labeled Aryl Olefins

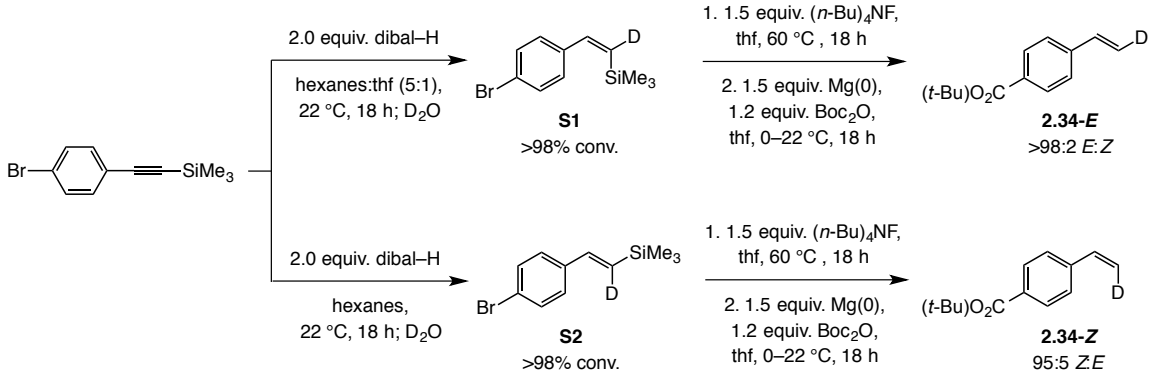

(*Z*)-(2-(4-Bromophenyl)vinyl-1-*d*)trimethylsilane (S1): To a flame-dried round bottom flask equipped with a stir bar was added hexanes (20 mL) under N_2, after which dibal–H (8.6 mL, 48 mmol, USE WITH CAUTION, PYROPHORIC) was added by a gas-tight syringe. The resulting mixture was allowed to cool to 0 °C, and a solution of trimethyl(4-bromophenylethynyl)silane (6.1 g, 24 mmol) in thf (4 mL) was added drop-wise by syringe. The mixture was allowed to stir for an additional 5 min at 0 °C and then warmed to 22 °C and allowed to stir for 23 h. The reaction was then quenched upon drop-wise addition of D_2O (1.2 mL, 72 mmol) at 0 °C and allowed to stir for 1 h at 22 °C. The mixture was transferred to a separatory funnel and Rochelle's salt (50 mL) and a saturated solution of aqueous ammonium chloride (40 mL) were added. The layers were separated, and the aqueous layer was washed with Et_2O (3 x 20 mL). The combined organic layers were dried over Na_2SO_4 and concentrated in vacuo. The resulting yellow oil was purified by silica gel chromatography (100% pentane) and Kugelrohr distillation to afford **S1**.

(*E*)-(2-(4-Bromophenyl)vinyl-1-*d*)trimethylsilane (S2): This compound was prepared similarly to **S1**, except 100% hexanes (24 mL) was used for silica gel chromatography.

tert*-Butyl-(*E*)-4-(vinyl-2-*d*)benzoate (2.34-*E*):** To a solution of **S1** in thf (15 mL) was added tbaf (1.0 M in thf, 8.25 mL, 8.25 mmol) at 22 °C under N_2. The mixture was allowed to stir at 60 °C for 18 hours after which it was transferred to a separatory funnel; water (25 mL) was added and the layers separated. The aqueous layer was washed with Et_2O (3x20 mL). The combined organic layers were dried over $MgSO_4$ and concentrated under reduced pressure. The resulting yellow oil was purified by Kugelrohr distillation to afford **(*E*)-1-Bromo-4-(vinyl-2-*d*)benzene** which was converted to **2.34-*E following the previously reported procedure.[98] The resulting colorless oil was purified by silica gel chromatography and Kugelrohr distillation to afford **2.34-*E*** as colorless liquid (200 mg, >98% D, >98% *E)*. IR (neat): 2979 (w), 1709 (s), 1608 (w), 1393 (m), 1291 (s), 1162 (s), 1112 (s), 1066 (s), 1067 (m), 865 (s), 771 (s), 702 (m) cm^{-1}; ^1H NMR ($CDCl_3$, 400 MHz): δ 7.97–7.94 (2H, m), 7.43 (2H, d, J = 8.4 Hz), 6.74 (1H, d, J = 17.6 Hz), 5.82 (1H, d, J = 17.6 Hz), 1.60 (9H, s); ^{13}C NMR ($CDCl_3$, 100 MHz): δ 165.6, 141.5, 136.1, 131.3, 129.8, 127.2, 126.0, 121.4, 115.9 (t, J = 24.3 Hz), 81.0, 28.3; HRMS (DART): Calcd for $C_{13}H_{16}DO_2$ $[M+H]^+$: 206.1291; Found: 206.1300.

***tert*-Butyl-(*Z*)-4-(vinyl-2-*d*)benzoate (2.34-*Z*):** To a solution of **S2** in thf (15 mL) was added (nBu)$_4$NF (1.0 M in thf, 8.25 mL, 8.25 mmol) at 22 °C under N_2. The mixture was allowed to stir at 60 °C for 18 h after which it was transferred to a separatory funnel, water (25 mL) was added and the layers separated. The aqueous layer was washed with Et_2O (3x20 mL). The combined organic layers were dried over $MgSO_4$ and concentrated under reduced pressure. The resulting yellow oil was purified by Kugelrohr distillation to

afford **(Z)-1-Bromo-4-(vinyl-2-*d*)benzene** which was converted to **2.34-*Z*** following the previously reported procedure.[98] The product was purified by silica gel chromatography and Kugelrohr distillation to afford **2.34-*Z*** as colorless liquid (199.4 mg, >98%D, 95:5 *Z*:*E)*. IR (neat): 2977 (w), 1707 (s), 1607 (w), 1367 (m), 1287 (s), 1161 (s), 1104 (s), 1016 (m), 848 (s), 774 (s), 706 (s), 438 (w) cm^{-1}; ^1H NMR ($CDCl_3$, 400 MHz): δ 7.94 (2H, d, *J*= 8.4 Hz), 7.43 (2H, d, *J* = 8.4 Hz), 6.75–6.79 (1H, m), 5.35 (1H, *J* = 10.4 Hz), 1.60 (9H, s); ^{13}C NMR ($CDCl_3$, 100 MHz): δ 165.7, 141.5, 136.2, 131.3, 129.8, 126.1, 116.0 (t, *J* = 23.5 Hz), 81.0, 28.3 HRMS (DART): Calcd for $C_{13}H_{16}DO_2$ $[M+H]^+$: 206.1291; Found: 206.1293

***tert*-Butyl-4-((1*S*,2*R*)-1-(4,4,5,5-tetramethyl-1,3,2-dioxaborolan-2-yl)pent-4-en-2-yl-1-*d*)benzoate (2.35 *from* 2.34-*E*):** Following the representative procedure except **2.24b** and 1:3 alkene:phosphate used, **2.35** was obtained as colorless oil (60:40 dr, determined from ^1H NMR of the product after oxidation). IR (neat): 2977 (w), 2929 (w), 1711 (s), 1609 (w), 1391 (m), 1364 (s), 1312 (s), 1288 (s), 1255 (m), 1164 (s), 1143 (s), 1112 (s), 850 (m) cm^{-1}; ^1H NMR ($CDCl_3$, 400 MHz): δ 7.88 (2H, d, *J* = 8.0 Hz), 7.24 (2H, d, *J* = 8.0 Hz), 5.63 (1H, ddt, *J* = 17.2, 10.4, 6.8 Hz), 4.96–4.90 (2H, m), 2.99 (1H, app q, *J* = 7.2 Hz), 2.35 (2H, t, *J* = 7.0 Hz), 1.58 (9H, s), 1.22 (1H, br s), 1.12 (6H, s), 1.11 (2.46H, s, minor), 1.10 (3.54H, s, major); ^{13}C NMR ($CDCl_3$, 150 MHz): δ 166.1, 151.95 (minor), 151.93 (major), 136.8, 129.8, 129.5, 127.4, 116.5, 83.2, 80.8, 43.51 (major), 43.48 (minor), 41.4, 28.4, 24.9, 24.80 (minor), 24.79 (major); HRMS (DART): Calcd for $C_{22}H_{33}D_1B_1O_4$ $[M+H]^+$: 374.2613; Found: 374.2620.

***tert*-Butyl-4-((1*R*,2*R*)-1-(4,4,5,5-tetramethyl-1,3,2-dioxaborolan-2-yl)pent-4-en-2-yl-1-*d*)benzoate (2.35 *from* 2.34-*Z*):** Following the representative procedure except **2.24b**

and 1:3 alkene:phosphate used, **2.35** was obtained as colorless oil (35:65 dr, determined from ^{1}H NMR of the product after oxidation). IR (neat): 2977 (w), 2929 (w), 1711 (s), 1609 (w), 1391 (m), 1364 (s), 1312 (s), 1288 (s), 1255 (m), 1164 (s), 1143 (s), 1112 (s), 850 (s) cm^{-1}; ^{1}H NMR ($CDCl_3$, 400 MHz): δ 7.88 (2H, d, *J* = 8.0 Hz), 7.24 (2H, d, *J* = 8.0 Hz), 5.63 (1H, ddt, *J* = 17.2, 10.4, 6.8 Hz), 4.96–4.90 (2H, m), 2.99 (1H, app q, *J* = 7.5 Hz), 2.35 (2H, t, *J* = 7.0 Hz), 1.58 (9H, s), 1.22 (1H, br s), 1.12 (6H, s), 1.11 (3.76H, s, major), 1.10 (2.24H, s, minor); ^{13}C NMR ($CDCl_3$, 150 MHz): δ 166.1, 151.95 (major), 151.93 (minor), 136.8, 129.8, 129.5, 127.4, 116.5, 83.2, 80.8, 43.51 (minor), 43.48 (major), 41.4, 28.4, 24.9, 24.80 (major), 24.79 (minor); HRMS (DART): Calcd for $C_{22}H_{33}D_1B_1O_4$ $[M+H]^+$: 374.2613; Found: 374.2620.

tert*-Butyl-(*E*)-3-(vinyl-2-*d*)benzoate (substrate for synthesis of *anti*-2.18g-*d*):** Following the procedure for preparation of **2.34-*E except trimethyl(3-bromophenylethynyl)silane was used. The product was obtained as >98:2 *E*:*Z*. IR (neat): 2977 (w), 1710 (s), 1367 (m), 1297 (s), 1254 (m), 1157 (s), 1079 (m), 1036 (m), 999 (m), 883 (m), 785 (w), 753 (s), 408 (w) cm^{-1}; ^{1}H NMR (400 MHz, $CDCl_3$): δ 8.02 (1H, s), 7.87 (1H, dt, *J* = 7.6, 1.2 Hz), 7.56–7.55 (1H, m), 7.35 (1H, t, *J* = 7.2 Hz), 6.75 (1H, d, *J* = 17.6 Hz), 5.80 (1H, d, *J* = 17.6 Hz), 1.60 (9H, s); ^{13}C NMR (100 MHz, $CDCl_3$): δ 165.7, 137.7, 136.1, 132.4, 130.1, 128.8, 128.5, 127.3, 114.7 (t, *J* = 24.3 Hz), 81.1, 28.3; HRMS (DART): Calcd for $C_{13}H_{16}D_1O_2$ $[M+H]^+$: 206.1291, Found: 206.1297.

tert*-Butyl-(*Z*)-3-(vinyl-2-*d*)benzoate (substrate for synthesis of *syn*-2.18g-*d*):** Following the procedure for preparation of **2.34-*Z except trimethyl(3-bromophenylethynyl)silane was used. The product was obtained as 90:10 *Z*:*E*. IR (neat): 2977 (w), 1711 (s), 1367 (m), 1291 (s), 1277 (s), 1156 (s), 1109 (m), 1082 (m), 848 (m),

818 (m), 755 (m), 697 (m), 406 (w) cm^{-1}; ^1H NMR (400 MHz, $CDCl_3$): δ 8.03 (1H, t, *J* = 2 Hz), 7.88 (1H, dt, *J* = 7.6, 1.6 Hz), 7.57–7.55 (1H, m), 7.37 (1H, t, *J* = 7.6 Hz), 6.74 (1H, dt, *J* = 10.8, 2.4 Hz), 5.29 (1H, d, *J* = 10.8 Hz), 1.61 (9H, s); ^{13}C NMR (100 MHz, $CDCl_3$): δ 165.7, 137.7, 136.1, 132.4, 130.1, 128.7, 128.5, 127.3, 114.6 (t, *J* = 23.5 Hz), 81.1, 28.2; HRMS (DART): Calcd for $C_{13}H_{16}D_1O_2$ $[M+H]^+$: 206.1291, Found: 206.1302.

***tert*-Butyl-3-((1*S*,2*R*)-1-(4,4,5,5-tetramethyl-1,3,2-dioxaborolan-2-yl)pent-4-en-2-yl-1-*d*)benzoate (*anti*-2.18g-*d*):** IR (neat): 2977 (m), 2927 (w), 1713 (s), 1479 (w), 1366 (s), 1316 (s), 1295 (s), 1161 (s), 1145 (s), 1111 (m), 755 (m), 697 (w) cm^{-1}; ^1H NMR (400 MHz, $CDCl_3$): δ 7.83 (1H, t, *J* = 1.8 Hz), 7.78 (1H, dt, *J* = 8.0, 1.2 Hz), 7.37 (1H, dt, *J* = 7.6, 1.2 Hz), 7.30 (1H, t, *J* = 7.6 Hz), 5.66 (1H, ddt, *J* = 17.0, 10.0, 7.2 Hz), 4.99–4.90 (2H, m), 2.99 (1H, q, *J* = 7.2 Hz), 2.44–2.32 (2H, m), 1.59 (9H, s), 1.22 (1H, d, *J* = 7.6 Hz), 1.11 (6H, s), 1.10 (6H, s); ^{13}C NMR (100 MHz, $CDCl_3$): δ 166.2, 147.1, 137.0, 131.9, 131.6, 128.8, 128.1, 127.2, 116.4, 83.2, 80.9, 43.4, 41.3, 28.4, 24.9, 24.8; HRMS (DART): Calcd for $C_{22}H_{33}D_1B_1O_4$ $[M+H]^+$: 374.2613, Found: 374.2614. Enantiomeric purity was determined by HPLC analysis in comparison with authentic racemic material (87:13 er shown; Chiralcel OZ–H column, 100% hexanes, 0.3 mL/min, 220 nm).

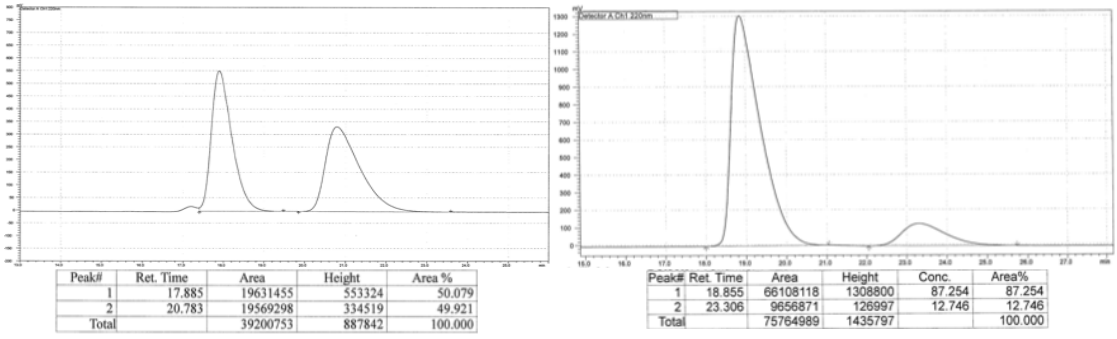

Peak#	Ret. Time	Area	Height	Area %
1	17.885	19631455	553324	50.079
2	20.783	19569298	334519	49.921
Total		39200753	887842	100.000

Peak#	Ret. Time	Area	Height	Conc.	Area%
1	18.855	66108118	1308800	87.254	87.254
2	23.306	9656871	126997	12.746	12.746
Total		75764989	1435797		100.000

Peak #	Time (min)	Area (%)	Peak #	Time (min)	Area (%)
1	17.885	50.079	1	18.855	87.254

2	20.783	49.921	2	23.306	12.746

***tert*-Butyl-3-((1*R*,2*R*)-1-(4,4,5,5-tetramethyl-1,3,2-dioxaborolan-2-yl)pent-4-en-2-yl-1-*d*)benzoate (*syn*-2.18g-*d*):** IR (neat): 2977 (m), 2927 (w), 1713 (s), 1479 (w), 1366 (s), 1316 (s), 1295 (s), 1161 (s), 1145 (s), 1111 (m), 755 (m), 697 (w) cm^{-1}; ^1H NMR (400 MHz, $CDCl_3$): δ 7.83 (1H, t, *J* = 1.6 Hz), 7.78 (1H, dt, *J* = 7.6, 1.2 Hz), 7.37 (1H, dt, *J* = 8, 1.6 Hz), 7.30 (1H, t, *J* = 7.6 Hz), 5.66 (1H, ddt, *J* = 17.0, 10.0, 7.2 Hz), 4.99–4.91 (2H, m), 2.99 (1H, q, *J* = 7.2 Hz), 2.44–2.32 (2H, m), 1.59 (9H, s), 1.11 (6H, s), 1.10 (6H, s), 1.07 (1H, d, *J* = 9.2 Hz); ^{13}C NMR (100 MHz, $CDCl_3$): δ 166.2, 147.1, 137.0, 131.9, 131.6, 128.8, 128.1, 127.2, 116.5, 83.2, 80.9, 43.4, 41.3, 28.4, 24.9, 24.8; HRMS (DART): Calcd for $C_{22}H_{33}D_1B_1O_4$ $[M+H]^+$: 374.2613, Found: 374.2614. Enantiomeric purity was determined by HPLC analysis in comparison with authentic racemic material (87:13 er shown; Chiralcel OZ–H column, 100% hexanes, 0.3 mL/min, 220 nm).

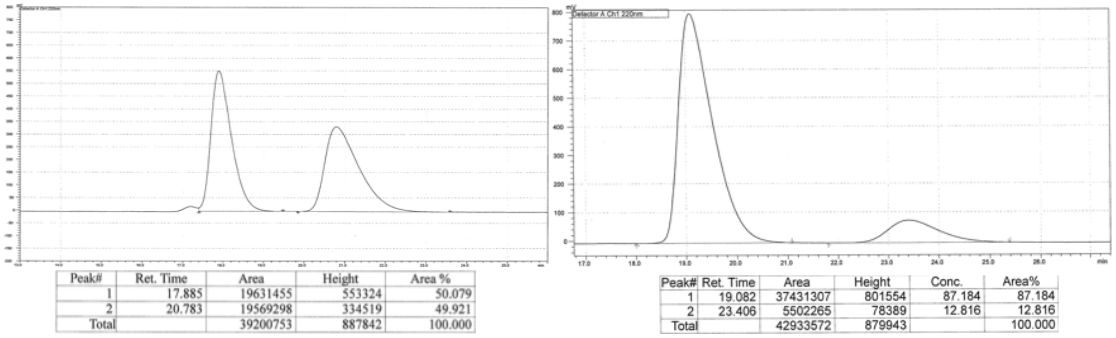

Peak#	Ret. Time	Area	Height	Area %
1	17.885	19631455	553324	50.079
2	20.783	19569298	334519	49.921
Total		39200753	887842	100.000

Peak#	Ret. Time	Area	Height	Conc.	Area%
1	19.082	37431307	801554	87.184	87.184
2	23.406	5502265	78389	12.816	12.816
Total		42933572	879943		100.000

Peak #	Time (min)	Area (%)	Peak #	Time (min)	Area (%)
1	17.885	50.079	1	19.082	87.184
2	20.783	49.921	2	23.406	12.816

Scheme S2. Synthesis of *E* and *Z* Deuterium-Labeled Aryl Olefins

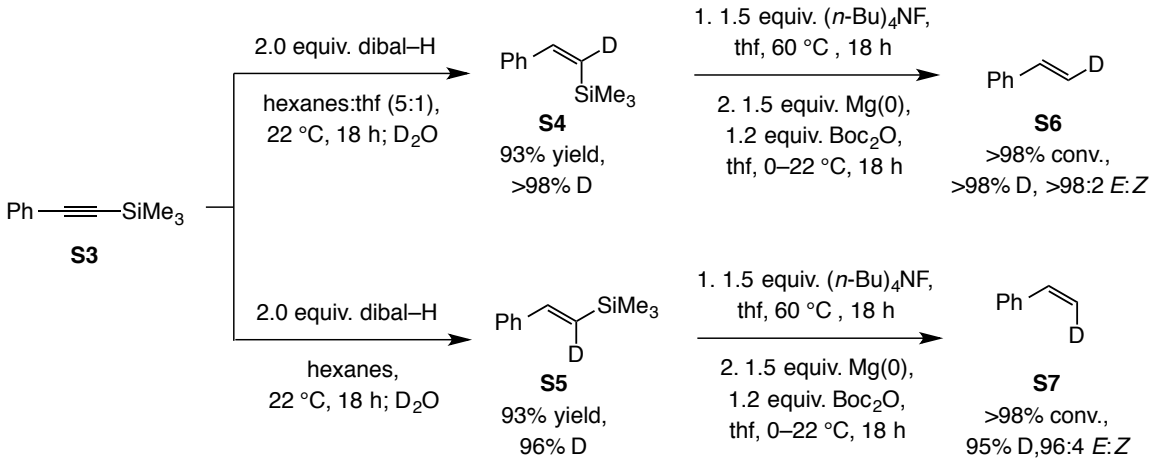

(*Z*)-Trimethyl(2-phenylvinyl-1-*d*)silane (S4): To a flame-dried round bottom flask equipped with a stir bar was added hexanes (20 mL) and thf (4 mL) under N_2 after which dibal–H (8.6 mL, 48 mmol, USE CAUTION, PYROPHORIC) was added through a gas tight syringe. The mixture was allowed to cool to 0 °C (ice/water bath) and trimethyl(phenylethynyl)silane (4.8 mL, 24 mmol) was added by syringe drop-wise. The mixture was allowed to stir for an additional 5 min at 0 °C and then warm to 55 °C and stir for 23 h. The reaction was quenched upon drop-wise addition of D_2O (0.8 mL, 48 mmol) at 0 °C and stir for additional 1 h at 22 °C. The mixture was transferred to a separatory funnel, Rochelle's salt (30 ml) and saturated aqueous solution of ammonium chloride (30 ml) were added to separate layers. The aqueous layer was washed with Et_2O (3 x 20 mL). The combined organic layers were dried over Na_2SO_4 and concentrated. The resulting yellow oil was purified by silica gel chromatography (100% pentane) and Kugelrohr distillation to afford **S4** as clear colorless liquid (4.0 g, 93%, >98% D). IR (neat): 2954 (w), 2897 (w), 1590 (w), 1569 (w), 1491 (w), 1247 (m), 1073 (w), 833 (s), 755 (s), 695 (s), 619 (m), 486 (m), 458 (w) cm^{-1}; ^1H NMR ($CDCl_3$, 400 MHz): 7.40–7.21

(6H, m), 0.06 (9H, s); ^{13}C NMR ($CDCl_3$, 100 MHz): δ 146.6, 128.4, 128.3, 128.0, 127.9, 127.5, 0.3; HRMS (DART): Calcd for $C_{11}H_{15}DSi$ $[M+H]^+$: 177.1084; Found: 177.1097.

(*E*)-Trimethyl(2-phenylvinyl-1-*d*)silane (S5): Prepared similarly to **S4**, 100% hexanes was used for silica gel chromatography to afford **S5** (4.0 g, 93%, 96% D) as a colorless liquid. IR (neat): 3025 (w), 2954 (w), 1594 (w), 1570 (w), 1494 (w), 1297 (s), 1082 (m), 922 (w), 834 (s), 754 (s), 692 (s), 485 (w) cm^{-1}; ^{1}H NMR ($CDCl_3$, 400 MHz): 7.47–7.41 (2H, m), 7.36–7.13 (3H, m), 6.89–6.85 (1H, m), 0.16 (9H, s); ^{13}C NMR ($CDCl_3$, 100 MHz): δ 143.7, 128.7, 128.4, 128.1, 127.9, 126.5, 125.6, –1.1, –1.6; HRMS (DART): Calcd for $C_{11}H_{15}DSi$ $[M+H]^+$: 177.1084; Found: 177.1092.

***trans*-Styrene-(β)-*d* (S6):** To a solution of (*Z*)-trimethyl(2-phenylvinyl-1-*d*)silane (2.5 g, 14 mmol) in thf (15 mL) was added (*n*-Bu)$_4$NF (21 mL of 1M in thf) at 22 °C under N_2. The mixture was allowed to stir at 60 °C for 3 h, after which it was transferred to a separatory funnel. Water (25 mL) was added and the layers separated. The aqueous layer was washed with Et_2O (3 x 20 mL). The combined organic layers were dried over $MgSO_4$ and concentrated under house vacuum. The resulting yellow oil was purified by Kugelrohr distillation to afford the product (>98% *E*, >98% D) as colorless liquid. The spectroscopic data match those reported previously.[106] ^{1}H NMR ($CDCl_3$, 400 MHz): δ 7.45–7.23 (5H, m), 6.73 (1H, dt, *J* = 17.6, 1.6 Hz) 5.74 (1H, d, *J* = 17.6 Hz)

***cis*-Styrene-(β)-*d* (S7):** This compound was prepared similarly to *trans*-Styrene-(β)-d, starting from (*E*)-trimethyl(2-phenylvinyl-1-*d*)silane (2.5 g, 14 mmol) and TBAF (56 mL of 1 M in thf) for 18 hours. The product was obtained as colorless liquid (96% *Z*, 95% D). The spectroscopic data match those reported previously.[34] ^{1}H NMR ($CDCl_3$, 400 MHz): δ

(106) Kapeller, D.; Barth, R.; Mereiter, K.; Hammerschmidt, F. *J. Am. Chem. Soc.* **2007**, *129*, 914–923.

7.45–7.22 (5H, m), 6.72 (1H, dt, *J* = 10.9, 2.6 Hz), 5.23 (1H, d, *J* = 10.9 Hz)

2-((1*R*,2*R*)-2,4-Diphenylpent-4-en-1-yl-1-*d*)-4,4,5,5-tetramethyl-1,3,2-dioxaborolane (*anti*-2.18t-*d*): IR (neat): 2923 (m), 2854 (w), 1453 (w), 1351 (m), 1314 (m), 1214 (w), 1143 (s), 969 (m), 896 (w), 777 (m), 734 (m), 698 (s), 547 (w) cm^{-1}; ^{1}H NMR ($CDCl_3$, 600 MHz): δ 7.40–7.36 (2H, m), 7.33–7.29 (2H, m), 7.28–7.19 (3H, m), 7.15–7.09 (3H, m), 5.15 (1H, d, *J* = 1.8 Hz), 4.83 (1H, *J* = 1.2 Hz), 2.95 (1H, q, *J* = 6.6 Hz), 2.87 (1H, dd, *J* = 13.2, 6 Hz), 2.73 (1H, dd, *J* = 12.6 7.8 Hz), 1.23 (1H, d, *J* = 6), 1.07 (6H, s), 1.05 (6H, s); ^{13}C NMR ($CDCl_3$, 150 MHz): δ 146.9, 146.8, 141.2, 128.4, 128.1, 127.6, 127.4, 126.6, 125.9, 114.5, 83.0, 45.7, 39.9, 24.9, 24.7; HRMS (DART): Calcd for $C_{22}H_{27}DBO_2$ $[M+H]^+$: 336.2245; Found: 336.2241. Enantiomeric purity was determined by HPLC analysis of the alcohol product after oxidation in comparison with authentic racemic material (89:11 er shown; Chiralcel OZ–H column, 99% hexanes, 1% *i*-PrOH, 0.3 mL/min, 220 nm).

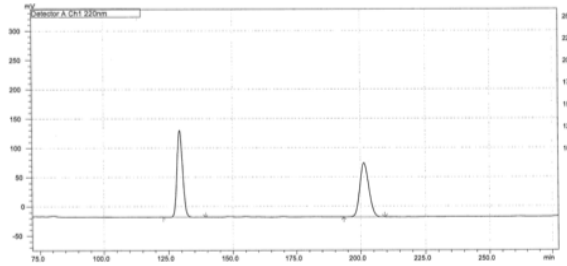

Peak#	Ret. Time	Area	Height	Conc.	Area%
1	129.355	22288828	147877	49.803	49.803
2	201.412	22465067	92552	50.197	50.197
Total		44753895	240429		100.000

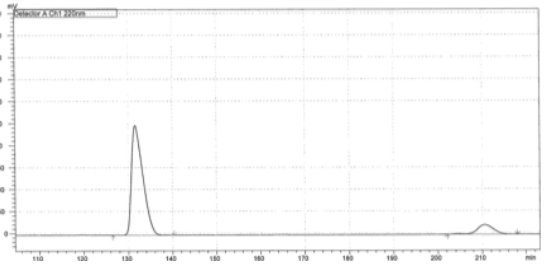

Peak#	Ret. Time	Area	Height	Conc.
1	131.578	221968013	1247086	88.668
2	210.567	28367150	110170	11.332
Total		250335164	1357256	

Peak #	Time (min)	Area (%)	Peak #	Time (min)	Area (%)
1	129.355	49.803	1	131.578	88.668
2	201.412	50.197	2	210.567	11.332

2-((1*S*,2*R*)-2,4-Diphenylpent-4-en-1-yl-1-*d*)-4,4,5,5-tetramethyl-1,3,2-dioxaborolane (*syn*-2.18t-*d*): IR (neat): 2977 (w), 2924 (m), 2854 (w), 1194 (w), 1389 (s), 1316 (s), 1142 (s), 1110 (w), 970 (m), 895 (m), 859 (m), 777 (m), 697 (s), 521 (w) cm^{-1}; ^{1}H NMR

($CDCl_3$, 600 MHz): δ 7.42–7.35 (2H, m), 7.34–7.29 (2H, m), 7.28–7.19 (3H, m), 7.14–7.09 (3H, m), 5.15 (1H, d, *J* =1.2 Hz), 4.83 (1H, s), 2.96 (1H, q, *J* = 8.4 Hz), 2.87 (1H, dd, J = 13.8, 6 Hz), 2.73 (1H, dd, *J* = 13.2, 7.8 Hz), 1.11 (1H, d, *J* = 9 Hz), 1.08 (6H, s), 1.05 (6H, s); ^{13}C NMR ($CDCl_3$, 150 MHz): δ 146.9, 146.8, 141.2, 128.4, 128.1, 127.6, 127.4, 126.7, 125.9, 114.5, 83.1, 45.6, 39.9, 24.9, 24.7; HRMS (DART): Calcd for $C_{22}H_{27}BO_2$ $[M+H]^+$: 336.2245; Found: 336.2245. Enantiomeric purity was determined by HPLC analysis of the alcohol product after oxidation in comparison with authentic racemic material (96:4 er shown; Chiralcel OZ–H column, 99% hexanes, 1% *i*-PrOH, 0.3 mL/min, 220 nm).

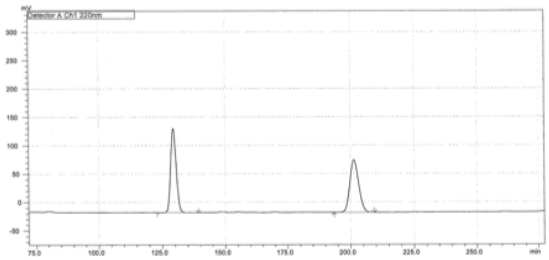

Peak#	Ret. Time	Area	Height	Conc.	Area%
1	129.355	22288828	147877	49.803	49.803
2	201.412	22465067	92552	50.197	50.197
Total		44753895	240429		100.000

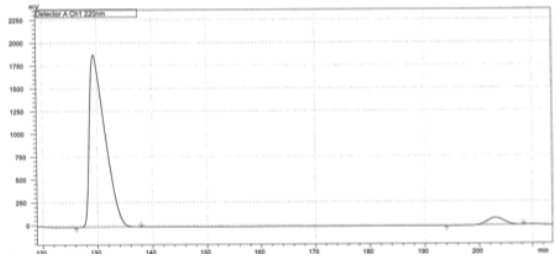

Peak#	Ret. Time	Area	Height	Conc.	Area%
1	129.403	370626114	1885975	95.564	95.564
2	202.960	17203506	78726	4.436	4.436
Total		387829619	1964701		100.000

Peak #	Time (min)	Area (%)	Peak #	Time (min)	Area (%)
1	129.355	49.803	1	129.403	95.564
2	201.412	50.197	2	202.960	4.436

(*E*)-1-(Trifluoromethyl)-4-(vinyl-2-*d*)benzene (substrate for synthesis of *anti*-2.18aa-*d*): Following the procedure for preparation of **S6** except 1-[(Trimethylsilyl)ethynyl]-4-(trifluoromethyl)benzene was used. The product was obtained in 91:9 *E*:*Z* selectivity. The spectroscopic data match those reported previously.[107] ^1H NMR (400 MHz, $CDCl_3$): δ 7.58 (2H, d, *J* = 8.4 Hz), 7.50 (2H, d, *J* = 8.4 Hz), 6.75 (1H, d, *J* = 17.6 Hz), 5.83 (1H, d, *J* = 17.6 Hz).

(107) Gao, F.; Hoveyda, A. H. *J. Am. Chem. Soc.* **2010**, *132*, 10961–10963.

(*Z*)-1-(Trifluoromethyl)-4-(vinyl-2-*d*)benzene (substrate for synthesis of *syn*-2.18aa-*d*): Following the procedure for preparation of **S7** except 1-[(Trimethylsilyl)ethynyl]-4-(trifluoromethyl)benzene was use. The product was obtained as a 90:10 ratio of *Z*:*E* isomers. IR (neat): 2954 (m), 2925 (m), 2854 (m), 1325 (s), 1168 (m), 1129 (m), 1068 (m) cm^{-1}; ^{1}H NMR (400 MHz, $CDCl_3$): δ 7.57 (2H, d, *J* = 8.4 Hz), 7.48 (2H, d, *J* = 8.4 Hz), 6.72 (1H, dt, *J* = 11.2, 2.6 Hz), 5.36 (1H, d, *J* = 11.2 Hz); ^{13}C NMR (100 MHz, $CDCl_3$): δ 141.1, 135.7, 129.8 (q, *J* = 32.4 Hz), 126.5, 125.6, 124.3 (q, *J* = 270.2 Hz), 116.3 (t, *J* = 23.6 Hz); HRMS (EI): Calcd for $C_9H_7D_1F_3$ $[M]^+$: 173.0563, Found: 173.0560.

4,4,5,5-Tetramethyl-2-((1S,2R)-2-(4-(trifluoromethyl)phenyl)pent-4-en-1-yl-1-*d*)-1,3,2-dioxaborolane (*anti*-2.18aa-*d*): IR (neat): 2979 (w), 2926 (w), 1359 (m), 1322 (s), 1162 (m), 1143 (m), 1120 (s), 1069 (m), 836 (m) cm^{-1}; ^{1}H NMR (400 MHz, $CDCl_3$): δ 7.51 (2H, d, *J* = 8.0 Hz), 7.31 (2H, d, *J* = 8.4 Hz), 5.64 (1H, ddt, *J* = 17.0, 10.2, 7.0 Hz), 4.98–4.92 (2H, m), 3.00 (1H, q, *J* = 7.1 Hz), 2.36 (2H, t, *J* = 7.2 Hz), 1.22 (1H, d, *J* = 1.2 Hz), 1.10 (6H, s), 1.08 (6H, s); ^{13}C NMR (100 MHz, $CDCl_3$): δ 151.1, 136.5, 128.3 (q, *J* = 32.1 Hz), 127.9, 125.1 (q, *J* = 3.8 Hz), 124.5 (q, *J* = 270.4 Hz), 116.7, 83.3, 43.5, 41.4, 24.8, 24.7; HRMS (DART): Calcd for $C_{18}H_{24}D_1B_1F_3O_2$ $[M+H]^+$: 342.1963, Found: 342.1961. Enantiomeric purity was determined by HPLC analysis in comparison with authentic racemic material (60:40 er shown; Chiralcel OZ–H column, 100% hexanes, 0.3 mL/min, 220 nm).

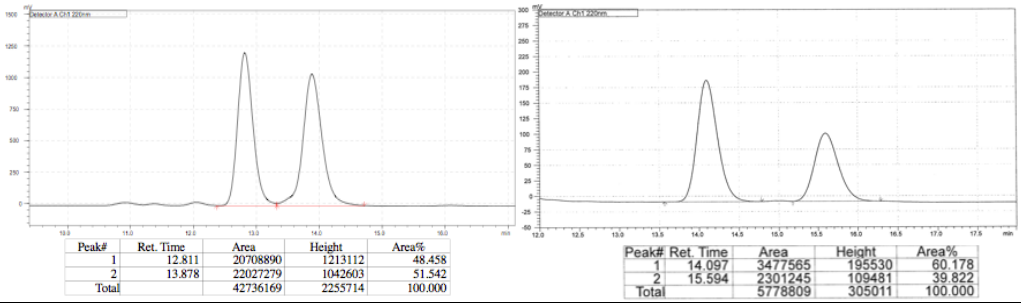

Peak#	Ret. Time	Area	Height	Area%
1	12.811	20708890	1213112	48.458
2	13.878	22027279	1042603	51.542
Total		42736169	2255714	100.000

Peak#	Ret. Time	Area	Height	Area%
1	14.097	3477565	195530	60.178
2	15.594	2301245	109481	39.822
Total		5778809	305011	100.000

Peak #	Time (min)	Area (%)	Peak #	Time (min)	Area (%)
1	12.811	48.458	1	14.097	60.178
2	13.878	51.542	2	15.594	39.822

4,4,5,5-Tetramethyl-2-((1R,2R)-2-(4-(trifluoromethyl)phenyl)pent-4-en-1-yl-1-d)-1,3,2-dioxaborolane (*syn*-2.18aa-*d*): IR (neat): 2979 (w), 2926 (w), 1359 (m), 1322 (s), 1162 (m), 1143 (m), 1120 (s), 1069 (m), 836 (m) cm^{-1}; ^{1}H NMR (400 MHz, $CDCl_3$): δ 7.51 (2H, d, J = 8.4 Hz), 7.31 (2H, d, J = 8.4 Hz), 5.64 (1H, ddt, J = 17.2, 10.4, 6.8 Hz), 4.98–4.91 (2H, m), 3.00 (1H, q, J = 7.9 Hz), 2.36 (2H, t, J = 7.2 Hz), 1.10 (6H, s), 1.09 (6H, s), 1.10–1.09 (1H, m); ^{13}C NMR (100 MHz, $CDCl_3$): δ 151.1, 136.5, 128.3 (q, J = 32.1 Hz), 127.9, 125.1 (q, J = 3.8 Hz), 124.5 (q, J = 270.2 Hz), 116.7, 83.3, 43.5, 41.4, 24.8, 24.7; HRMS (DART): Calcd for $C_{18}H_{24}D_1B_1F_3O_2$ $[M+H]^+$: 342.1963, Found: 342.1961. Enantiomeric purity was determined by HPLC analysis in comparison with authentic racemic material (74:26 er shown; Chiralcel OZ–H column, 100% hexanes, 0.3 mL/min, 220 nm).

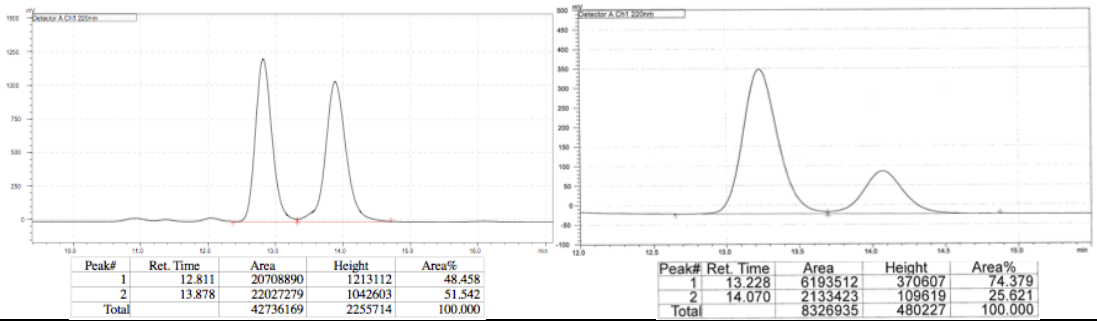

Peak#	Ret. Time	Area	Height	Area%
1	12.811	20708890	1213112	48.458
2	13.878	22027279	1042603	51.542
Total		42736169	2255714	100.000

Peak#	Ret. Time	Area	Height	Area%
1	13.228	6193512	370607	74.379
2	14.070	2133423	109619	25.621
Total		8326935	480227	100.000

Peak #	Time (min)	Area (%)	Peak #	Time (min)	Area (%)
1	12.811	48.458	1	13.228	74.379

2	13.878	51.542	2	14.070	25.621

■ Study of the Possibility of Homolytic versus Heterolytic Cu–C Bond Cleavage

Scheme S3. Synthesis of Cyclopropane **2.36**

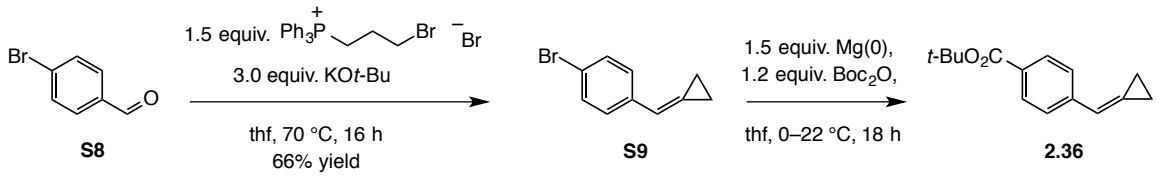

1-Bromo-4-(cyclopropylidenemethyl)benzene (S9): Prepared from aldehyde **S8** (purchased from Aldrich and used as received) by formerly reported procedure.[108] The spectroscopic data match those reported previously.[109] ^{1}H NMR (400 MHz, $CDCl_3$): δ 7.46–7.42 (2H, m), 7.40–7.38 (2H, m), 6.70–6.68 (1H, m), 1.42–1.38 (2H, m), 1.20–1.16 (2H, m).

***tert*-Butyl-4-(cyclopropylidenemethyl)benzoate (2.36):** Prepared from **S9** according to the reported procedure.[98] IR (neat): 2977 (w), 1706 (s), 1606 (m), 1367 (m), 1307 (s), 1292 (s), 1254 (m), 1161 (s), 1107 (s), 1015 (m), 863 (m), 849 (m), 757 (m) cm^{-1}; ^{1}H NMR (400 MHz, $CDCl_3$): δ 7.96 (2H, d, J = 8.4 Hz), 7.55 (2H, d, J = 8.4 Hz), 6.79–6.78 (1H, m), 1.61 (9H, s), 1.48–1.42 (2H, m), 1.22–1.18 (2H, m); ^{13}C NMR (100 MHz, $CDCl_3$): δ 165.8, 142.3, 130.1, 129.7, 127.6, 126.3, 117.9, 80.8, 28.3, 4.5, 0.8; HRMS (DART): Calcd for $C_{15}H_{19}O_2$ $[M+H]^+$: 231.1391, Found: 231.1385.

***tert*-Butyl-(*S*)-4-(1-(1-(4,4,5,5-tetramethyl-1,3,2-dioxaborolan-2-yl)cyclopropyl)but-3-en-1-yl)benzoate (2.38):** IR (neat): 2976 (w), 2932 (m), 1710 (s), 1640 (w), 1440 (m), 1409 (m), 1290 (s), 1164 (s), 1140 (s), 1113 (s), 851 (s), 708 (m), 685 (m), 420 (w) cm^{-1};

(108) Evans, P. A.; Inglesby, P. A.; Kilbride, K. *Org. Lett.* **2013**, *15*, 1798–1801.
(109) Katritzky, A. R.; Du, W.; Levell, J. R.; Li, J. *J. Org. Chem.* **1998**, *63*, 6710–6711.

^{1}H NMR (400 MHz, $CDCl_3$): δ 7.88 (2H, d, *J* = 8), 7.38 (2H, d, *J* =8), 5.69 (1H, ddt, *J* = 17.2, 9.6, 7.2), 5.00–4.95 (1H, m), 4.89–4.85 (1H, m), 2.75–2.71 (2H, m), 1.20 (1H, t, *J* =7.8), 1.58 (9H, s), 1.20 (12H, s), 0.74 (1H, ddd, *J* = 9.2, 5.6, 3.2), 0.66 (1H, ddd, *J* = 8, 4.8, 2.8), 0.41 (1H, ddd, *J* =8.4, 5.2, 3.2), 0.35 (1H, ddd, *J* = 8.4, 5.2, 3.2); ^{13}C NMR (100 MHz, $CDCl_3$): δ 166.1, 150.3, 138.1, 129.8, 129.2, 128.5, 115.5, 83.1, 80.7, 53.4, 38.8, 28.4, 25.0, 24.5, 14.1, 10.2; HRMS (DART): Calcd for $C_{24}H_{36}BO_4$ $[M+H]^+$: 399.2707, Found: 399.2723. Enantiomeric purity was determined by HPLC analysis of the alcohol product after oxidation in comparison with authentic racemic material (54:46 er shown; Chiralcel OZ–H column, 99% hexanes, 1% *i*-PrOH, 0.3 mL/min, 220 nm).

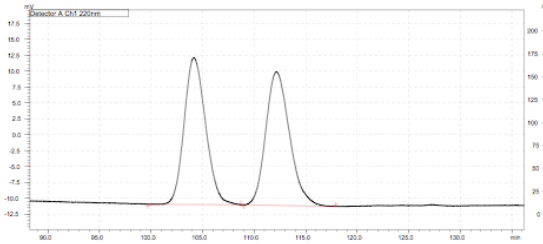

Peak#	Ret. Time	Area	Height	Area%
1	104.145	3349312	23097	49.894
2	112.153	3363590	21013	50.106
Total		6712902	44110	100.000

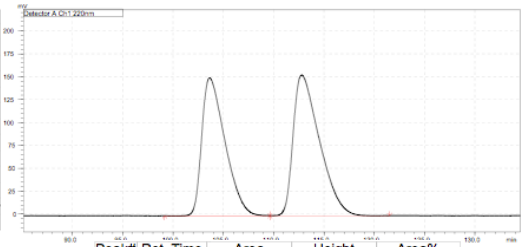

Peak#	Ret. Time	Area	Height	Area%
1	103.637	24149247	150345	46.394
2	112.787	27903537	153742	53.606
Total		52052783	304087	100.000

Peak #	Time (min)	Area (%)	Peak #	Time (min)	Area (%)
1	104.145	49.894	1	103.637	46.394
2	112.153	50.106	2	112.787	53.606

Scheme S4. Synthesis of Diene **2.39**

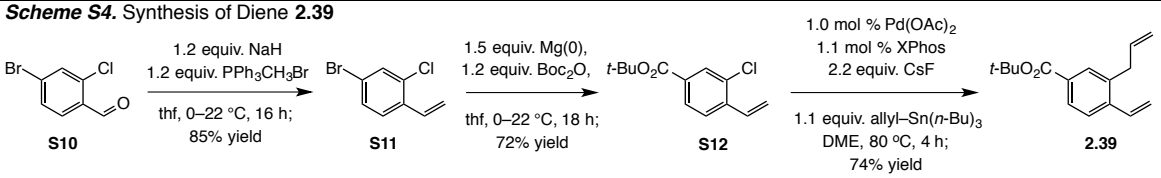

4-Bromo-2-chloro-1-vinylbenzene (S11): Prepared from aldehyde **S10** (purchased from Combi-Blocks and used as received) following the previously reported procedure.[22] IR (neat): 3089 (w), 3060 (w), 1579 (m), 1467 (s), 1371 (m), 1085 (m), 1049 (m), 985 (m), 917 (s), 867 (m), 812 (s) cm^{-1}; ^{1}H NMR (400 MHz, $CDCl_3$): δ 7.53 (1H, s), 7.42 (1H, d, *J* = 8.4 Hz), 7.36 (1H, dd, *J* = 8.4, 1.6 Hz), 7.02 (1H, dd, *J* = 17.4, 11.0 Hz), 5.74 (1H, d, *J* = 17.2 Hz), 5.41 (1H, d, *J* = 10.8 Hz); ^{13}C NMR (100 MHz, $CDCl_3$): δ 134.9, 133.9,

132.4, 132.3, 130.2, 127.7, 121.7, 117.3; HRMS (DART): Calcd for $C_8H_7Br_1Cl_1$ $[M+H]^+$: 216.9420, Found: 216.9427.

***tert*-Butyl-3-chloro-4-vinylbenzoate (S12):** Prepared from **S11** according to the reported procedure.[98] IR (neat): 2978 (w), 2933 (w), 1716 (s), 1392 (m), 1368 (m), 1298 (s), 1258 (m), 1168 (s), 1118 (s), 773 (m), 849 cm^{-1}; ^1H NMR (400 MHz, $CDCl_3$): δ 7.95 (1H, d, *J* = 1.6 Hz), 7.83 (1H, dd, *J* = 8.5, 2.1 Hz), 7.59 (1H, d, *J* = 8.0 Hz), 7.11 (1H, dd, *J* = 17.6, 10.8 Hz), 5.82 (1H, dd, *J* = 17.4, 0.6 Hz), 5.48 (1H, dd, *J* = 11.0, 1.0 Hz), 1.59 (9H, s); ^{13}C NMR (100 MHz, $CDCl_3$): δ 164.5, 139.5, 133.1, 132.7, 132.5, 130.8, 127.8, 126.3, 118.6, 81.7, 28.3; HRMS (DART): Calcd for $C_{13}H_{16}Cl_1O_2$ $[M+H]^+$: 239.0839,

***tert*-Butyl-3-allyl-4-vinylbenzoate (2.39):** Prepared from **S12** according to the reported procedure.[110] . IR (neat): 2977 (w), 2931 (w), 1709 (s), 1367 (m), 1293 (s), 1253 (s), 1163 (s), 1118 (s), 989 (m), 914 (s), 849 (s) cm^{-1}; ^1H NMR (400 MHz, $CDCl_3$): δ 7.82 (1H, dd, *J* = 7.8, 1.4 Hz), 7.78 (1H, d, *J* = 1.6 Hz), 7.53 (1H, d, *J* = 8.4 Hz), 6.97 (1H, dd, *J* = 17.2, 11.2 Hz), 6.01–5.91 (1H, m), 5.73 (1H, dd, *J* = 17.4, 1.4 Hz), 5.39 (1H, dd, *J* = 11.2, 1.2 Hz), 5.10–5.06 (1H, m), 5.00–4.94 (1H, m), 3.48 (2H, dt, J = 6.4, 1.6 Hz), 1.59 (9H, s); ^{13}C NMR (100 MHz, $CDCl_3$): δ 165.8, 140.9, 137.1, 136.4, 134.1, 131.4, 131.0, 127.8, 125.7, 117.5, 116.4, 81.0, 37.5, 28.3; HRMS (DART): Calcd for $C_{16}H_{21}O_2$ $[M+H]^+$: 244.1463, Found: 244.1471.

***tert*-Butyl-(*R*)-3-allyl-4-(1-(4,4,5,5-tetramethyl-1,3,2-dioxaborolan-2-yl)pent-4-en-2-yl)benzoate (2.40a):** IR (neat): 2977 (w), 2930 (w), 1711 (s), 1367 (s), 1298 (s), 1253 (m), 1166 (s), 1143 (s), 1121 (m), 912 (m), 849 (m) cm^{-1}; ^1H NMR (400 MHz, $CDCl_3$): δ 7.78 (1H, dd, *J* = 8.0, 2.0 Hz), 7.75 (1H, d, *J* = 2.0 Hz), 7.27 (1H, d, *J* = 7.6 Hz), 6.00

(110) Naber, J. R.; Buchwald, S. L. *Adv. Synth. Catal.* **2008**, *350*, 957–961.

(1H, ddt, J = 17.0, 10.2, 6.2 Hz), 5.70–5.60 (1H, m), 5.09–5.02 (2H, m),), 4.99–4.91 (2H, m), 3.59–3.45 (2H, m), 3.32–3.24 (1H, m), 2.36–2.23 (2H, m), 1.58 (9H, s), 1.26–1.21 (1H, m), 1.08 (6H, s), 1.05 (6H, s), 1.12–1.05 (1H, m); ^{13}C NMR (100 MHz, $CDCl_3$): δ 166.2, 150.3, 137.6, 137.3, 136.8, 130.6, 129.5, 127.6, 126.4, 116.6, 116.1, 83.2, 80.7, 43.5, 37.4, 35.6, 28.4, 24.8, 24.77; HRMS (DART): Calcd for $C_{25}H_{38}B_1O_4$ $[M+H]^+$: 413.2863, Found: 413.2858.

■ **Relevance to Catalytic Processes that Involve Cu–H Additions**

(*S*)-*N*,*N*-Dibutyl-1,2,3,4-tetrahydronaphthalen-1-amine (2.45): Following the previously reported procedure except 1:3 alkene:hydroxylamine was used. The spectroscopic data are consistent with those reported formerly.[111] ^{1}H NMR (400 MHz, $CDCl_3$): δ 8.07 (1H, dt, J = 7.8, 1.2 Hz), 7.53 (4H, d, J = 7.3 Hz), 7.38 (4H, dd, J = 8.2, 6.9 Hz), 7.32–7.22 (3H, m), 7.17 (1H, tt, J = 7.3, 1.1 Hz), 7.09 (1H, d, J = 7.9 Hz), 4.00 (1H, dd, J = 10.2, 5.7 Hz), 3.87 (2H, d, J = 13.6 Hz), 3.54 (2H, d, J = 13.6 Hz), 2.91–2.66 (2H, m), 2.32–2.14 (1H, m), 2.06 (1H, dtt, J = 13.7, 5.6, 3.1 Hz), 1.85 (1H, tdd, J = 12.5, 10.1, 2.8 Hz), 1.76–1.58 (1H, m); Specific Rotation: $[\alpha]_D^{20}$ –62.0 (*c* 1.00, $CHCl_3$) for an enantiomerically enriched sample of 97:3 er. Enantiomeric purity was determined by HPLC analysis in comparison with authentic racemic material (97:3 er shown; Chiralcel OJ–H column, 97% hexanes, 3% *i*-PrOH, 0.8 mL/min, 220 nm).

(111) Zhu, S.; Niljianskul, N.; Buchwald, S. L. *J. Am. Chem. Soc.* **2013**, *135*, 15746–15749.

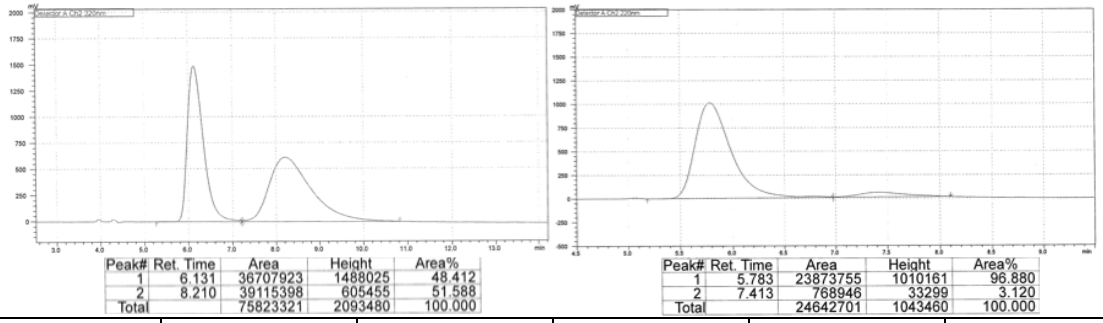

Peak#	Ret. Time	Area	Height	Area%
1	6.131	36707923	1488025	48.412
2	8.210	39115398	605455	51.588
Total		75823321	2093480	100.000

Peak#	Ret. Time	Area	Height	Area%
1	5.783	23873755	1010161	96.880
2	7.413	768946	33299	3.120
Total		24642701	1043460	100.000

Peak #	Time (min)	Area (%)	Peak #	Time (min)	Area (%)
1	6.131	48.412	1	5.783	96.880
2	8.210	51.588	2	7.413	3.120

***(R)*-2-(1-(3,4-Dihydroisoquinolin-2(1H)-yl)octyl)-2,3-dihydro-1H-naphtho[1,8-de][1,3,2]diazaborinine (2.46):** Following the previously reported procedure except 40 mol % of **2.8** was used. The spectroscopic data match those reported previously.[112] ^{1}H NMR (400 MHz, $CDCl_3$): δ 7.10–7.01 (7H, m), 6.88 (1H, d, *J* = 6.8 Hz), 6.00 (2H, dd, 6.8, 1.6 Hz), 5.66 (2H, bs), 3.81 (1H, d, *J* = 14.8 Hz), 3.55 (1H, d, *J* = 14.8 Hz), 2.86–2.79 (1H, m), 2.73–2.55 (3H, m), 1.78 (1H, dd, *J* = 9.2, 4.4 Hz), 1.71–1.64 (1H, m), 1.59–1.50 (1H, m), 1.46–1.37 (1H, m), 1.33–1.24 (9H, m), 0.89 (3H, t, *J* = 6.8 Hz); Enantiomeric purity was determined by HPLC analysis in comparison with authentic racemic material (97:3 er shown; Chiralcel OD–H column, 95% hexanes, 5% *i*-PrOH, 0.5 mL/min, 330 nm).

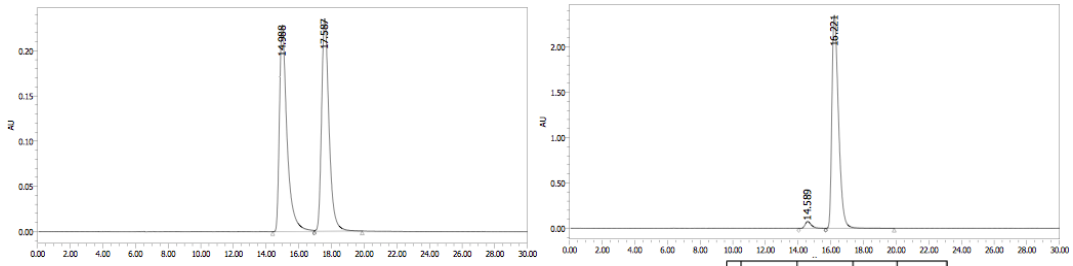

	保持時間 (分)	面積 (μV秒)	%面積	高さ (μV)
1	14.988	7375266	49.72	228425
2	17.587	7458781	50.28	235465

	保持時間 (分)	面積 (μV秒)	%面積	高さ (μV)
1	14.589	2038125	2.99	75250
2	16.221	66191474	97.01	2351533

Peak #	Time (min)	Area (%)	Peak #	Time (min)	Area (%)

(112) Nishikawa, D.; Hirano, K.; Miura, M. *J. Am. Chem. Soc.* **2015**, *137*, 15620–15623.

1	14.988	49.72	1	14.589	2.99
2	17.587	50.28	2	16.221	97.01

■ Determination of Absolute Stereochemistry

In addition to comparison of specific rotation of **2.33** to the reported values suggesting a (*R*) configuration of the products, we synthesized (***R*)-S14** and obtained the X-ray crystal structure to ascertain the absolute stereochemical identity of the products.

Scheme S5

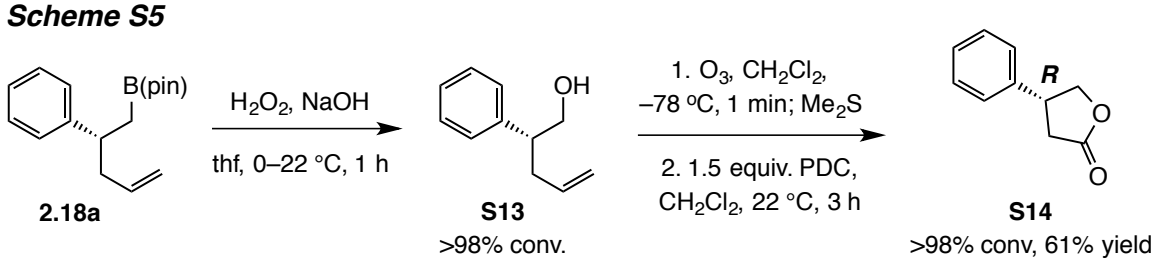

Compound (***R*)-S14** was synthesized from enantiomerically enriched **2.18a** (95:5 er), as illustrated in Scheme S5. **(*R*)-4-Phenyldihydrofuran-2(3*H*)-one [(*R*)-S14]**: The spectroscopic data match those reported previously.[113] ^{1}H NMR (400 MHz, $CDCl_3$): δ 7.40–7.22 (5H, m), 4.67 (1H, dd, *J* = 8.8, 8.0 Hz), 4.28 (1H, dd, *J* = 9.0, 8.2 Hz), 3.79 (1H, app pent, *J* = 8.5 Hz), 2.93 (1H, dd, *J* = 17.6 and 8.8 Hz), 2.68 (1H, dd, *J* = 17.6, 8.8 Hz); Specific Rotation: $[\alpha]_D^{20}$ –40.8 (*c* 0.50, $CHCl_3$). The absolute configuration of **(*R*)-S14** was established by X-ray analysis, which was assigned to be (*R*). Compound **2.18a** is thus assigned to possess the (*R*) configuration. The absolute stereochemistry for other enantiomerically enriched products has been assigned by inference.

(113) Malkov, A. V.; Friscourt, F.; Bell, M.; Swarbrick, M. E.; Kočovský, P. *J. Org. Chem.* **2008**, *73*, 3996–4003.

■ **Data for X-ray Crystallography of (*R*)-S14**

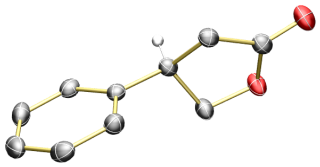

Table 1. **Crystal data and structure refinement for $C_{10}H_{10}O_2$**

Identification code	C10H10O2
Empirical formula	C10 H10 O2
Formula weight	162.18
Temperature	100(2) K
Wavelength	1.54178 Å
Crystal system	Monoclinic
Space group	$P2_1$
Unit cell dimensions	a = 6.1692(7) Å
	b = 7.7518(8) Å
	c = 8.6969(9) Å
Volume	415.33(8) $Å^3$
Z	2
Density (calculated)	1.297 Mg/m^3
Absorption coefficient	0.729 mm^{-1}
F(000)	172
Crystal size	0.600 x 0.070 x 0.050 mm^3
Theta range for data collection	5.092 to 66.613°.
Index ranges	-7<=h<=7, -8<=k<=9, -10<=l<=10
Reflections collected	4434
Independent reflections	1435 [R(int) = 0.0455]
Completeness to theta = 67.679°	98.2 %
Absorption correction	Semi-empirical from equivalents
Max. and min. transmission	0.7528 and 0.5867
Refinement method	Full-matrix least-squares on F^2
Data / restraints / parameters	1435 / 1 / 109
Goodness-of-fit on F^2	1.091

Final R indices [I>2sigma(I)]	R1 = 0.0341, wR2 = 0.0848
R indices (all data)	R1 = 0.0346, wR2 = 0.0858
Absolute structure parameter	-0.05(11)
Extinction coefficient	na
Largest diff. peak and hole	0.145 and -0.213 e. $Å^{-3}$

Table 2. **Atomic coordinates ($x10^4$) and equivalent isotropic displacement parameters ($Å^2 x 10^3$) for $C_{10}H_{10}O_2$. U(eq) is defined as one third of the trace of the orthogonalized U^{ij} tensor**

	x	y	z	U(eq)
O(1)	4872(2)	3283(2)	344(2)	29(1)
O(2)	8163(2)	4179(2)	-234(2)	34(1)
C(1)	6684(3)	4254(3)	609(2)	25(1)
C(2)	6464(3)	5329(3)	2029(2)	23(1)
C(3)	4017(3)	5331(3)	2238(2)	22(1)
C(4)	3365(3)	3581(3)	1546(2)	26(1)
C(5)	3258(3)	5568(2)	3851(2)	21(1)
C(6)	4294(3)	4761(3)	5124(2)	26(1)
C(7)	3475(4)	4930(3)	6572(2)	31(1)
C(8)	1594(4)	5872(3)	6774(2)	32(1)
C(9)	571(3)	6695(3)	5510(3)	31(1)
C(10)	1411(3)	6549(3)	4071(2)	24(1)

Table 3. **Bond lengths [Å] and angles [°] for $C_{10}H_{10}O_2$**

O(1)-C(1)	1.357(3)

O(1)-C(4)	1.453(2)
O(2)-C(1)	1.202(3)
C(1)-C(2)	1.502(3)
C(2)-C(3)	1.530(3)
C(2)-H(2A)	0.9900
C(2)-H(2B)	0.9900
C(3)-C(5)	1.513(3)
C(3)-C(4)	1.530(3)
C(3)-H(3)	1.0000
C(4)-H(4A)	0.9900
C(4)-H(4B)	0.9900
C(5)-C(10)	1.392(3)
C(5)-C(6)	1.396(3)
C(6)-C(7)	1.388(3)
C(6)-H(6)	0.9500
C(7)-C(8)	1.390(3)
C(7)-H(7)	0.9500
C(8)-C(9)	1.393(3)
C(8)-H(8)	0.9500
C(9)-C(10)	1.384(3)
C(9)-H(9)	0.9500
C(10)-H(10)	0.9500
C(1)-O(1)-C(4)	110.01(15)
O(2)-C(1)-O(1)	120.97(19)
O(2)-C(1)-C(2)	129.3(2)
O(1)-C(1)-C(2)	109.77(17)
C(1)-C(2)-C(3)	103.33(16)
C(1)-C(2)-H(2A)	111.1
C(3)-C(2)-H(2A)	111.1
C(1)-C(2)-H(2B)	111.1
C(3)-C(2)-H(2B)	111.1
H(2A)-C(2)-H(2B)	109.1
C(5)-C(3)-C(4)	112.65(16)

C(5)-C(3)-C(2)	117.74(15)
C(4)-C(3)-C(2)	101.13(16)
C(5)-C(3)-H(3)	108.3
C(4)-C(3)-H(3)	108.3
C(2)-C(3)-H(3)	108.3
O(1)-C(4)-C(3)	105.02(16)
O(1)-C(4)-H(4A)	110.7
C(3)-C(4)-H(4A)	110.7
O(1)-C(4)-H(4B)	110.7
C(3)-C(4)-H(4B)	110.7
H(4A)-C(4)-H(4B)	108.8
C(10)-C(5)-C(6)	118.66(18)
C(10)-C(5)-C(3)	119.28(17)
C(6)-C(5)-C(3)	121.98(18)
C(7)-C(6)-C(5)	120.31(19)
C(7)-C(6)-H(6)	119.8
C(5)-C(6)-H(6)	119.8
C(6)-C(7)-C(8)	120.6(2)
C(6)-C(7)-H(7)	119.7
C(8)-C(7)-H(7)	119.7
C(7)-C(8)-C(9)	119.20(18)
C(7)-C(8)-H(8)	120.4
C(9)-C(8)-H(8)	120.4
C(10)-C(9)-C(8)	120.0(2)
C(10)-C(9)-H(9)	120.0
C(8)-C(9)-H(9)	120.0
C(9)-C(10)-C(5)	121.13(19)
C(9)-C(10)-H(10)	119.4
C(5)-C(10)-H(10)	119.4

Symmetry transformations used to generate equivalent atoms:

Table 4. **Anisotropic displacement parameters ($Å^2x10^3$) for $C_{10}H_{10}O_2$. The**

anisotropic

displacement factor exponent takes the form: $-2\pi^2[h^2 a^{*2}U^{11} + ... + 2 h k a^* b^* U^{12}]$

	U^{11}	U^{22}	U^{33}	U^{23}	U^{13}	U^{12}
O(1)	25(1)	38(1)	24(1)	-7(1)	4(1)	-6(1)
O(2)	28(1)	46(1)	30(1)	-1(1)	8(1)	0(1)
C(1)	24(1)	28(1)	23(1)	3(1)	0(1)	1(1)
C(2)	20(1)	24(1)	25(1)	2(1)	0(1)	-1(1)
C(3)	21(1)	24(1)	22(1)	3(1)	0(1)	1(1)
C(4)	23(1)	34(1)	23(1)	-4(1)	3(1)	-3(1)
C(5)	21(1)	18(1)	24(1)	-2(1)	1(1)	-3(1)
C(6)	29(1)	23(1)	26(1)	1(1)	2(1)	2(1)
C(7)	42(1)	24(1)	25(1)	0(1)	-2(1)	-5(1)
C(8)	40(1)	31(1)	27(1)	-9(1)	9(1)	-10(1)
C(9)	25(1)	31(1)	37(1)	-11(1)	6(1)	0(1)
C(10)	21(1)	21(1)	30(1)	-2(1)	-2(1)	-2(1)

Table 5. **Hydrogen coordinates ($x10^4$) and isotropic displacement parameters ($Å^2 x10^3$) for $C_{10}H_{10}O_2$**

	x	y	z	U(eq)
H(2A)	7011	6515	1879	28
H(2B)	7263	4805	2930	28
H(3)	3343	6256	1569	27
H(4A)	3494	2663	2336	31

H(4B)	1850	3610	1109	31
H(6)	5564	4094	4998	31
H(7)	4208	4395	7435	37
H(8)	1014	5954	7761	39
H(9)	-704	7357	5636	37
H(10)	715	7129	3218	29

Table 6. **Torsion angles [°] for $C_{10}H_{10}O_2$**

C(4)-O(1)-C(1)-O(2)	178.59(19)
C(4)-O(1)-C(1)-C(2)	-1.5(2)
O(2)-C(1)-C(2)-C(3)	161.0(2)
O(1)-C(1)-C(2)-C(3)	-18.9(2)
C(1)-C(2)-C(3)-C(5)	153.11(17)
C(1)-C(2)-C(3)-C(4)	29.95(18)
C(1)-O(1)-C(4)-C(3)	21.5(2)
C(5)-C(3)-C(4)-O(1)	-158.08(16)
C(2)-C(3)-C(4)-O(1)	-31.48(18)
C(4)-C(3)-C(5)-C(10)	-100.7(2)
C(2)-C(3)-C(5)-C(10)	142.14(19)
C(4)-C(3)-C(5)-C(6)	76.0(2)
C(2)-C(3)-C(5)-C(6)	-41.1(3)
C(10)-C(5)-C(6)-C(7)	0.5(3)
C(3)-C(5)-C(6)-C(7)	-176.25(19)
C(5)-C(6)-C(7)-C(8)	1.3(3)
C(6)-C(7)-C(8)-C(9)	-2.0(3)
C(7)-C(8)-C(9)-C(10)	0.9(3)
C(8)-C(9)-C(10)-C(5)	0.9(3)
C(6)-C(5)-C(10)-C(9)	-1.6(3)
C(3)-C(5)-C(10)-C(9)	175.24(19)

Symmetry transformations used to generate equivalent atoms:

■ NMR Spectra

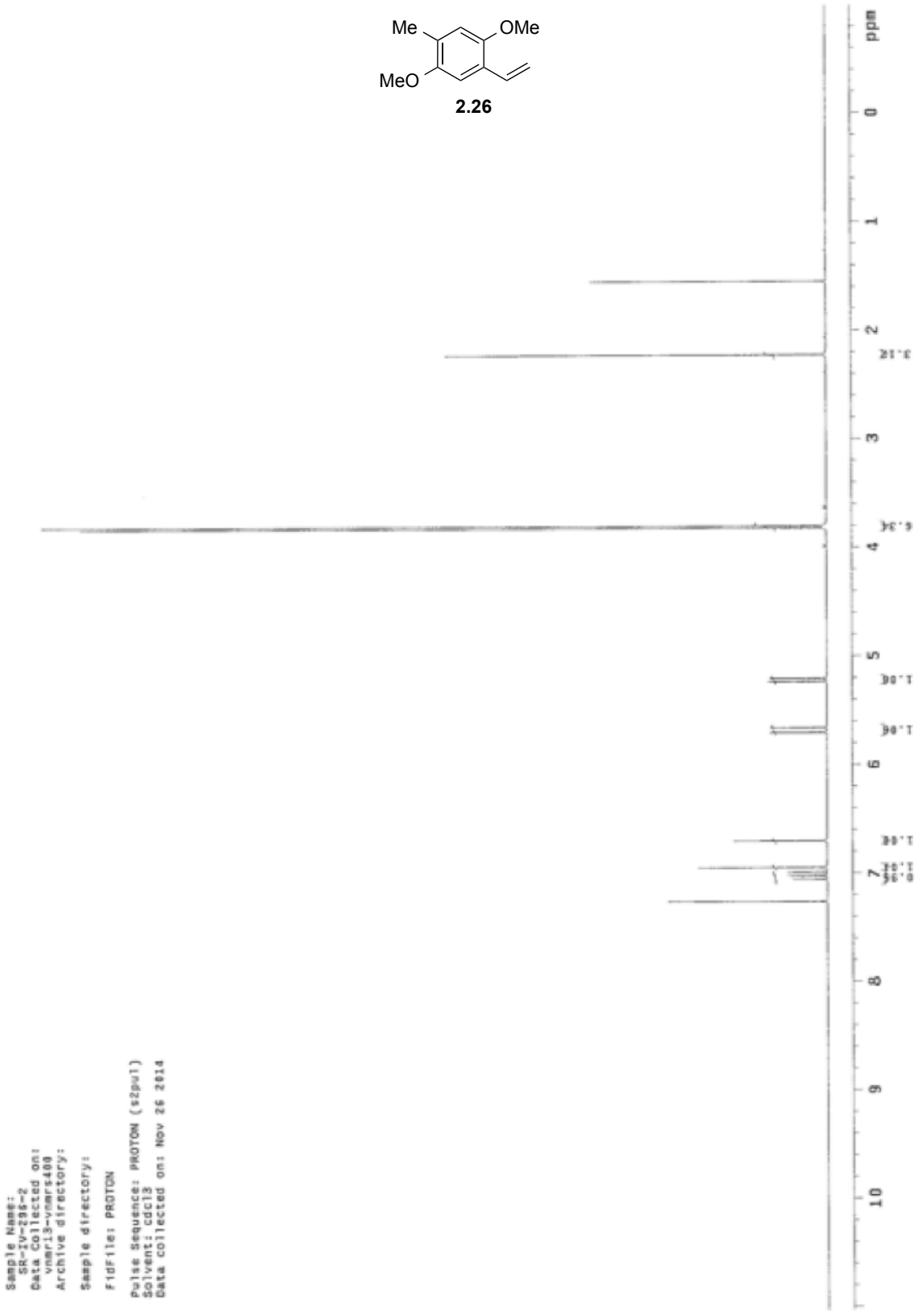
Me
OMe
MeO
2.26
Sample Name:
SR-IV-296-2
Data Collected on:
vnmri3-vnmrs400
Archive directory:
Sample directory:
FidFile: PROTON
Pulse Sequence: PROTON (s2pul)
Solvent: cdcl3
Data collected on: Nov 26 2014
ppm
3.12
6.34
1.00
1.06
1.00
1.00
2.04

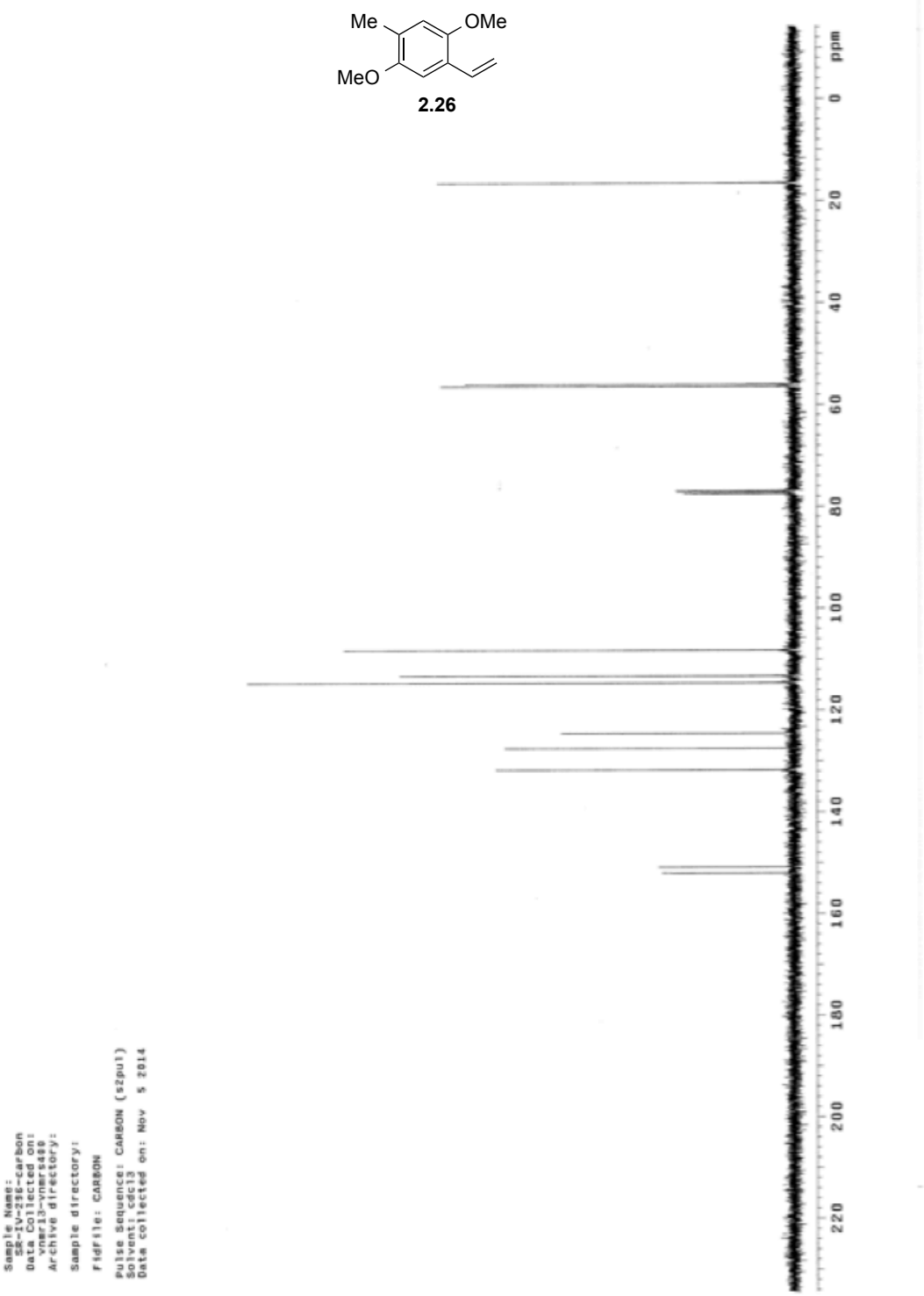
Me
OMe
MeO
2.26
ppm
0
20
40
60
80
100
120
140
160
180
200
220
Sample Name:
SR-IV-256-Carbon
Data Collected on:
vnmr13-vnmrs400
Archive directory:
Sample directory:
FidFile: CARBON
Pulse Sequence: CARBON (s2pul)
Solvent: cdcl3
Data collected on: Nov 5 2014

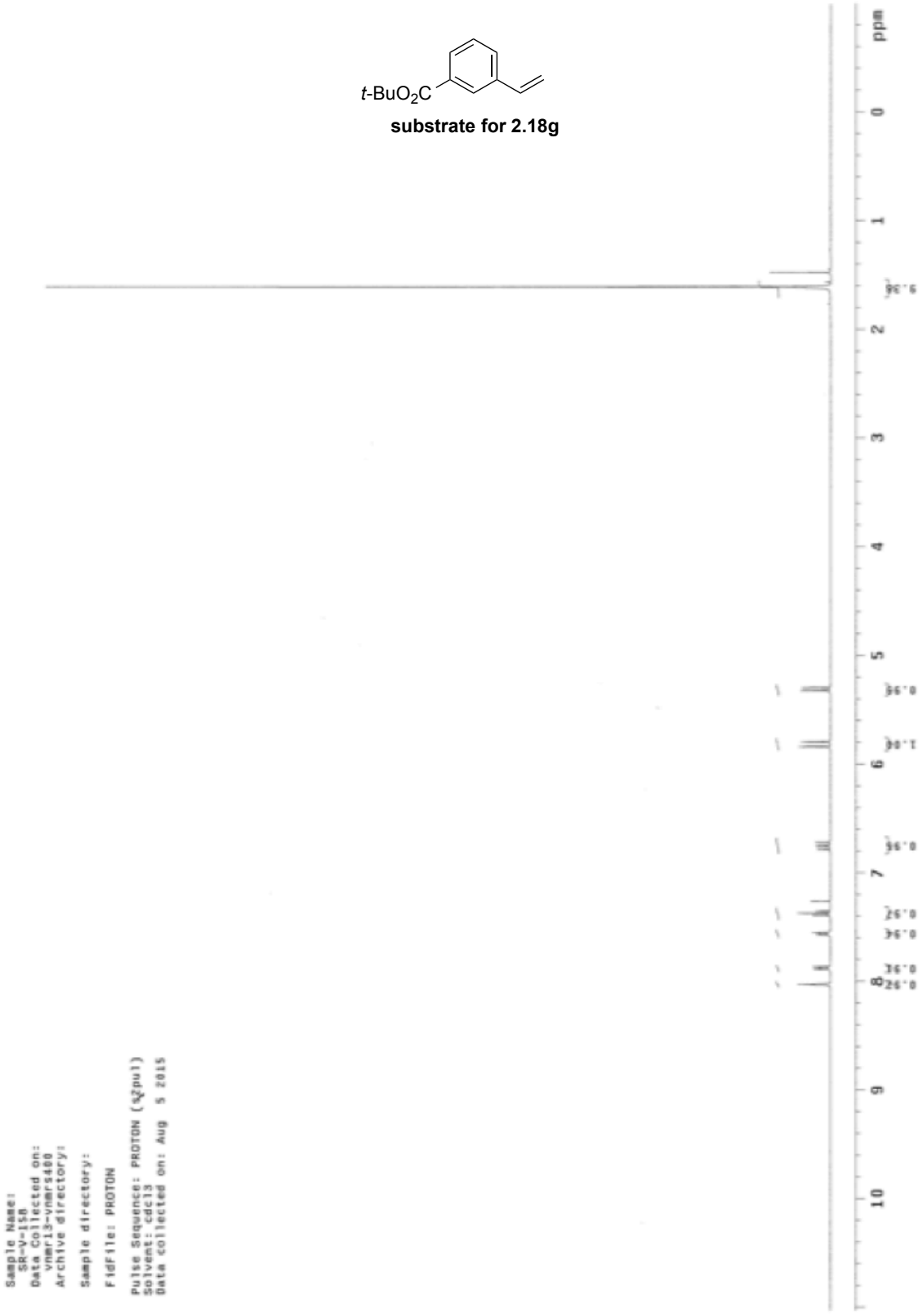
t-BuO2C
substrate for 2.18g
Sample Name:
SR-V-158
Data Collected on:
vnmr13-vnmrs400
Archive directory:
Sample directory:
FidFile: PROTON
Pulse Sequence: PROTON (%Zpul)
Solvent: cdcl3
Data collected on: Aug 5 2015
ppm
0
1
2
3
4
5
6
7
8
9
10
1.00
0.96
1.04
0.96
0.97
0.96
0.96
0.96

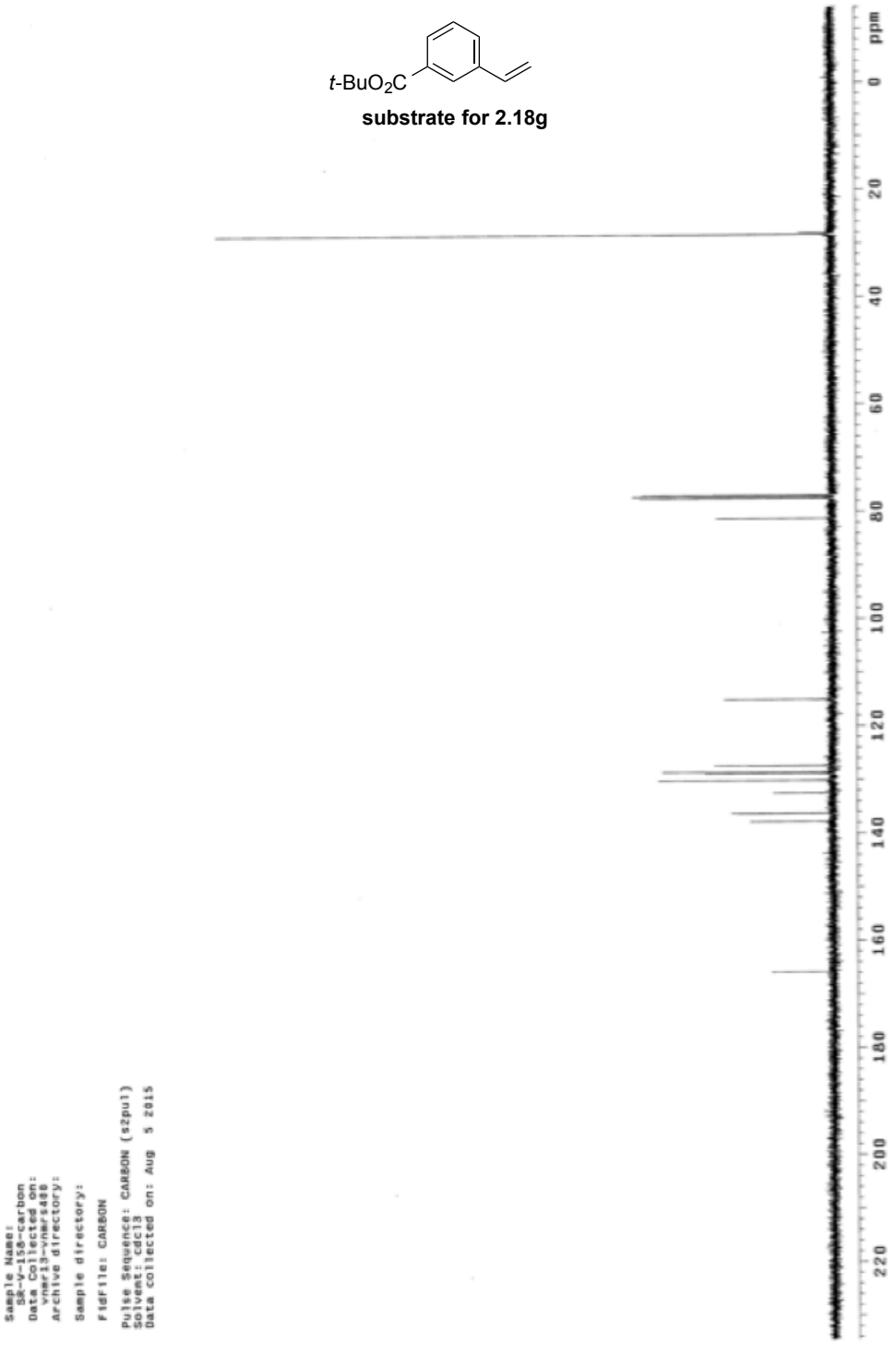
t-BuO2C
substrate for 2.18g
Sample Name:
SB-V-158-carbon
Data Collected on:
vnmr13-vnmrs400
Archive directory:
Sample directory:
FidFile: CARBON
Pulse Sequence: CARBON (s2pul)
Solvent: cdcl3
Data collected on: Aug 5 2015
ppm
0
20
40
60
80
100
120
140
160
180
200
220

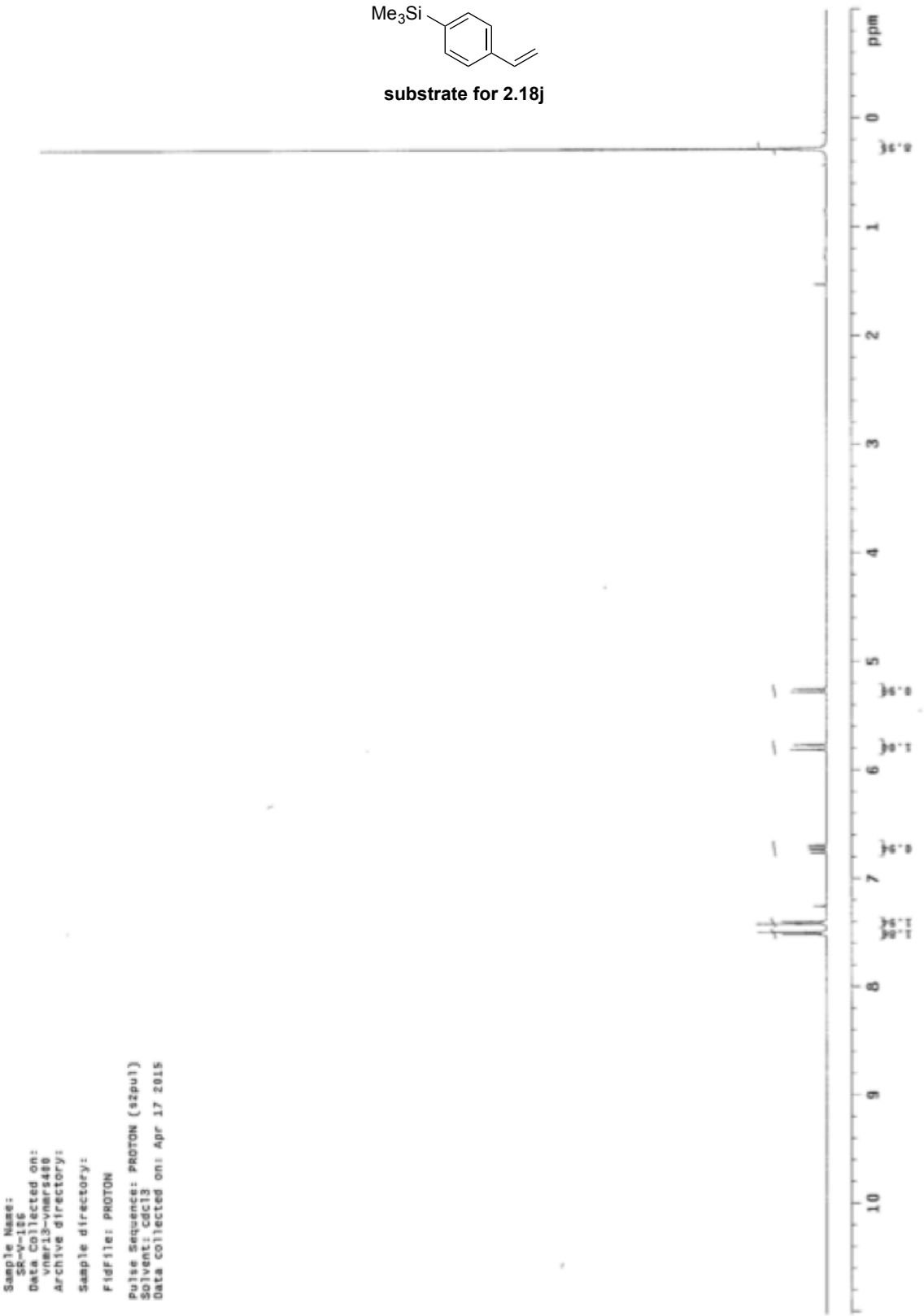
Me3Si
substrate for 2.18j
Sample Name:
SR-V-186
Data Collected on:
vnmr13-vmar4480
Archive directory:
Sample directory:
FidFile: PROTON
Pulse Sequence: PROTON (s2pul)
Solvent: cdcl3
Data collected on: Apr 17 2015
ppm
0
1
2
3
4
5
6
7
8
9
10

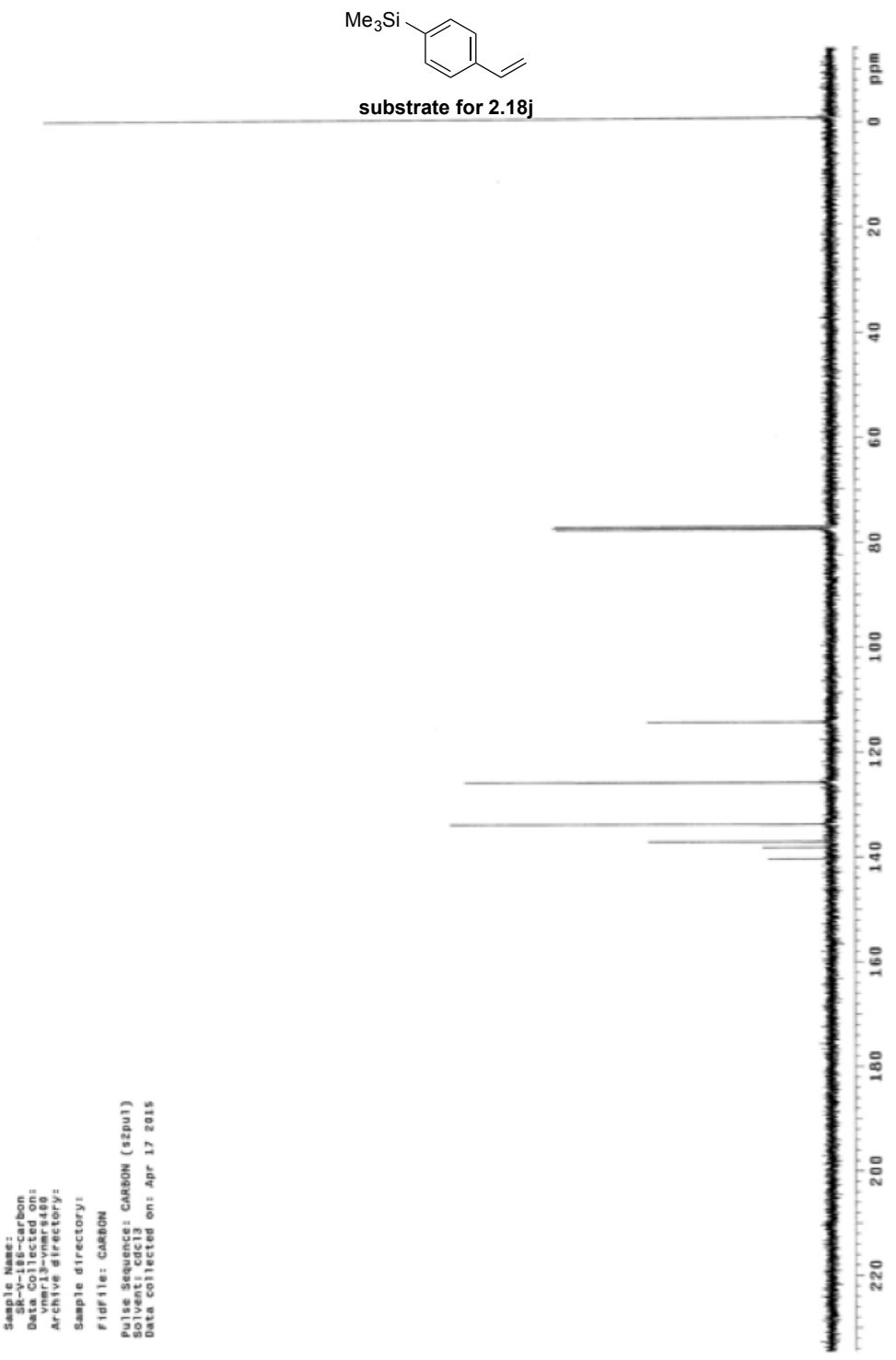
Me3Si
substrate for 2.18j
Sample Name:
SR-Y-186-carbon
Data Collected on:
vnmri3-vnmrs460
Archive directory:
Sample directory:
Fidfile: CARBON
Pulse Sequence: CARBON (s2pul)
Solvent: cdcl3
Data collected on: Apr 17 2015
ppm
0
20
40
60
80
100
120
140
160
180
200
220

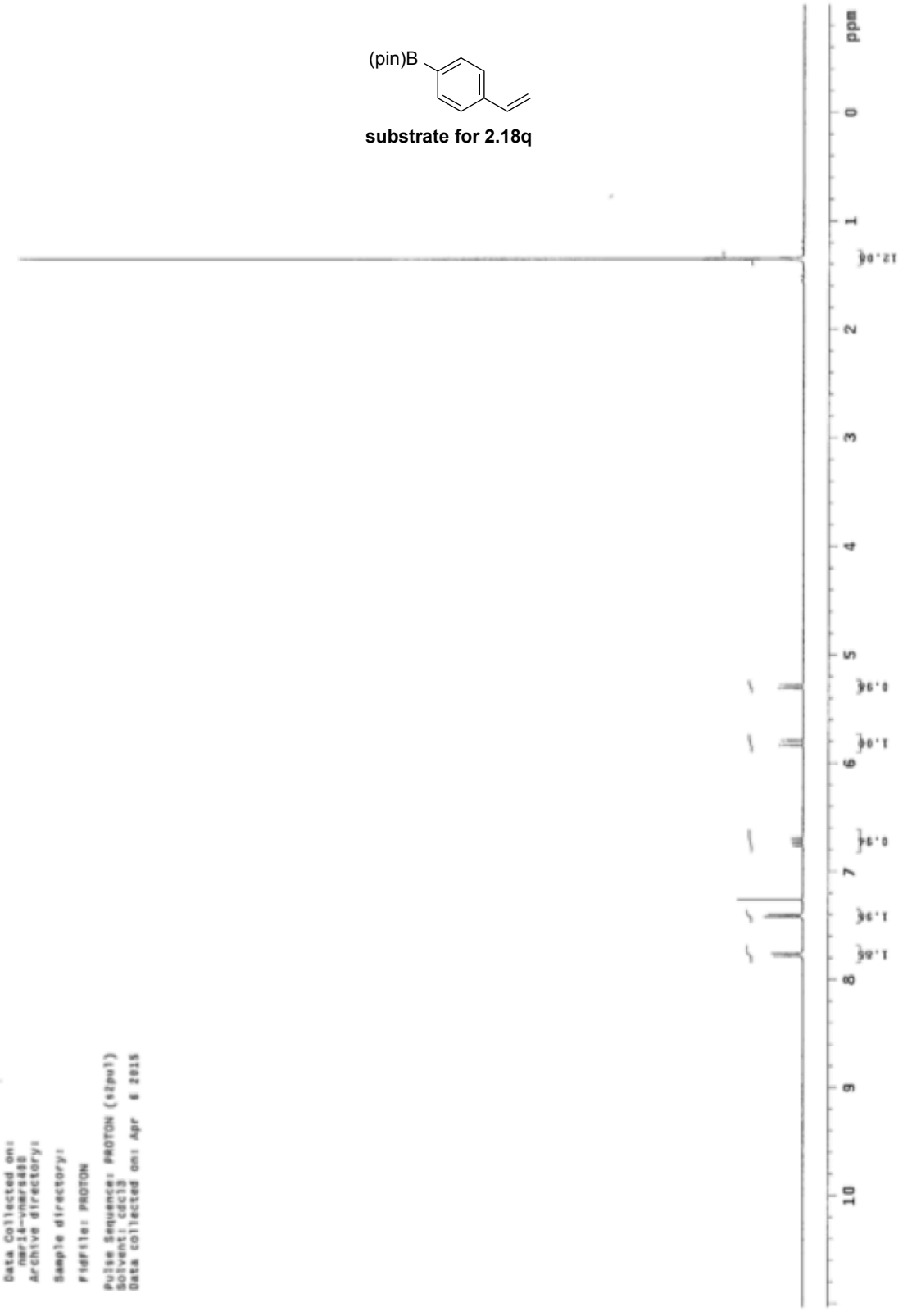
(pin)B
substrate for 2.18q
Data Collected on:
mar14-vmar4480
Archive directory:
Sample directory:
FidFile: PROTON
Pulse Sequence: PROTON (s2pul)
Solvent: cdcl3
Data collected on: Apr 6 2015
ppm
12.04
0.94
1.04
0.94
1.96
1.86

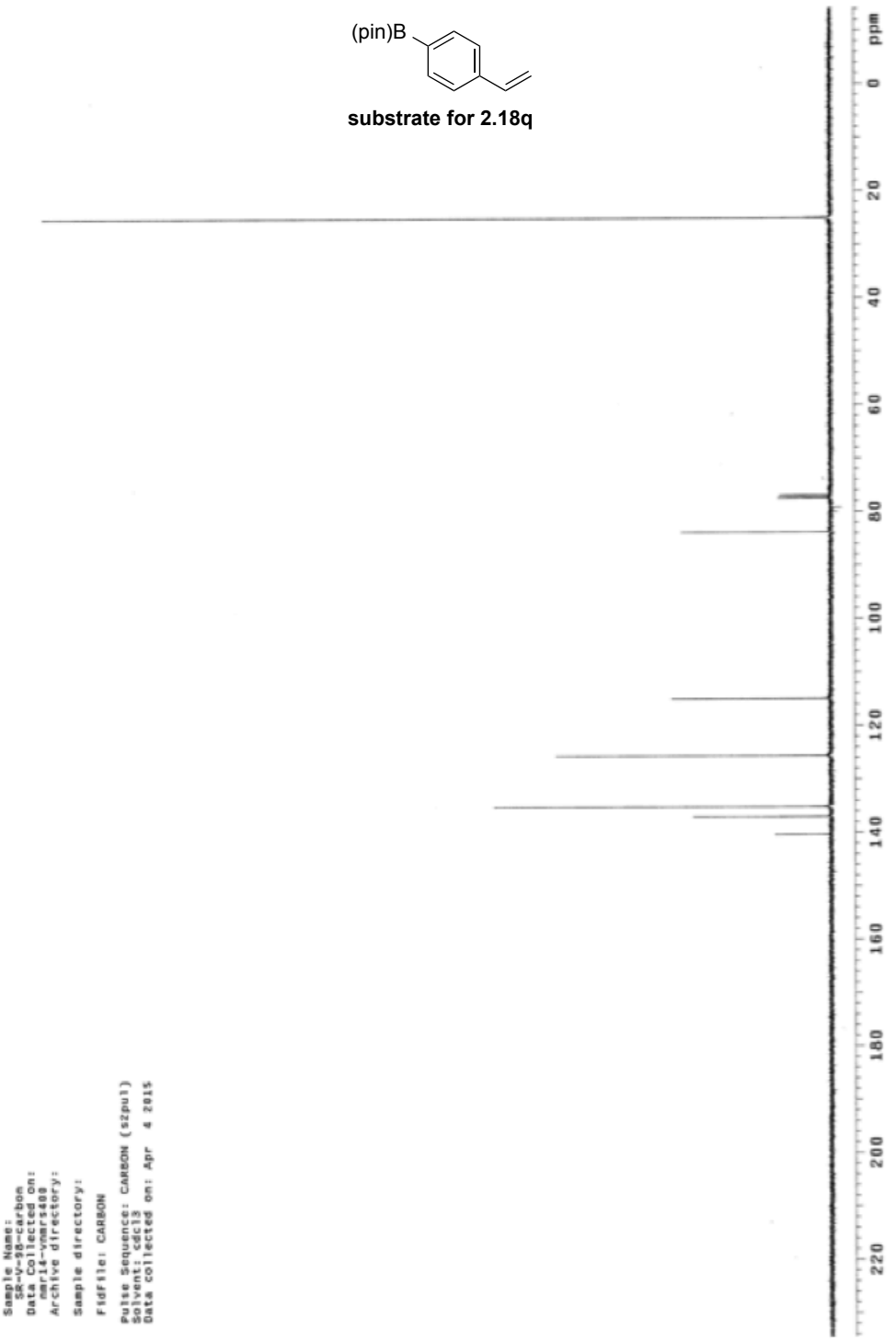
(pin)B
substrate for 2.18q
Sample Name:
SR-V-98-carbon
Data Collected on:
nmr14-vnmrs400
Archive directory:
Sample directory:
FidFile: CARBON
Pulse Sequence: CARBON (s2pul)
Solvent: cdcl3
Data collected on: Apr 4 2015
ppm
0
20
40
60
80
100
120
140
160
180
200
220

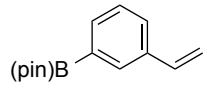

substrate for 2.18r

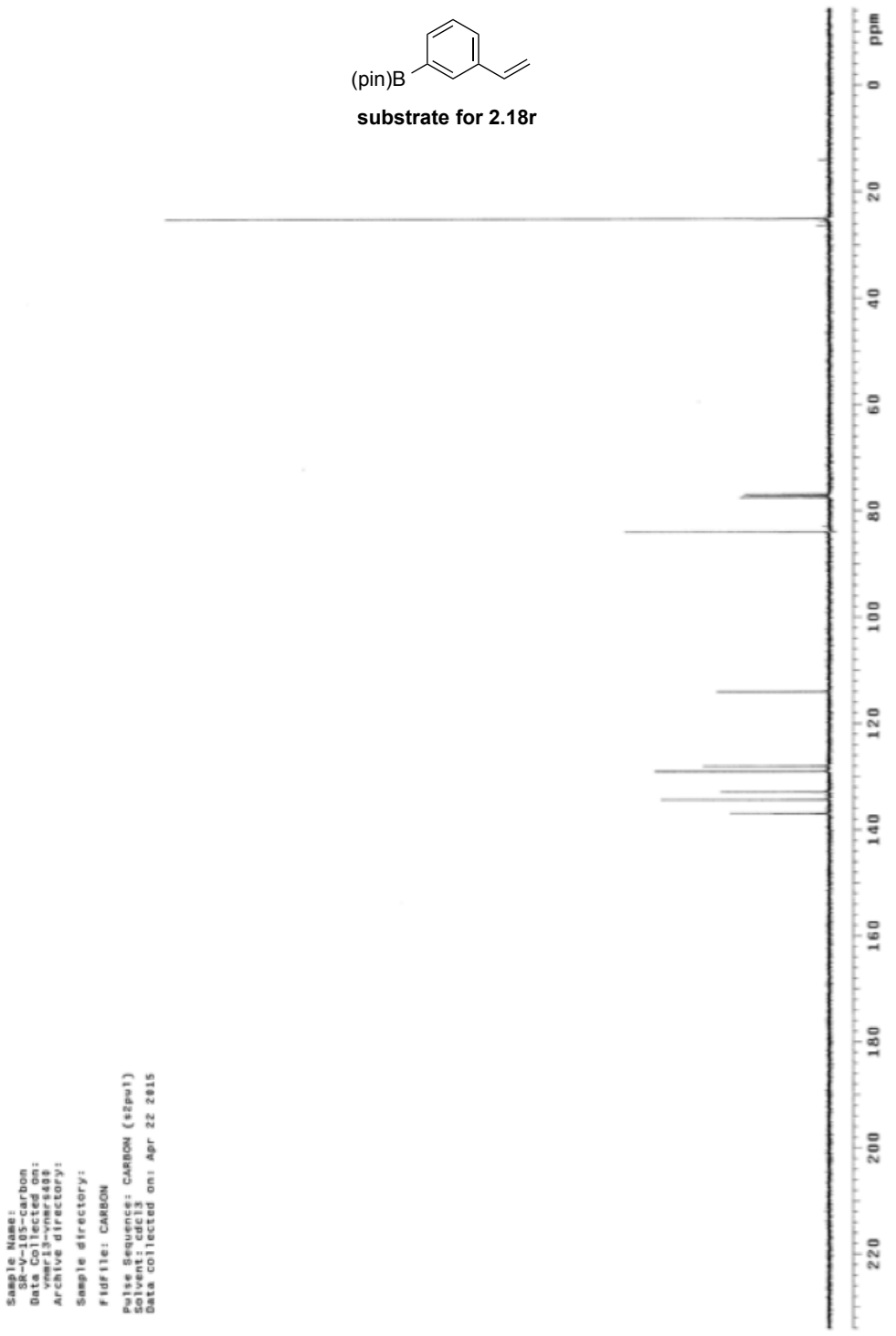
(pin)B
substrate for 2.18r
Sample Name:
SR-V-105-carbon
Data Collected on:
vnmr13-vnmr400
Archive directory:
Sample directory:
Fidfile: CARBON
Pulse Sequence: CARBON (s2pul)
Solvent: cdcl3
Data collected on: Apr 22 2015
220
200
180
160
140
120
100
80
60
40
20
0
ppm

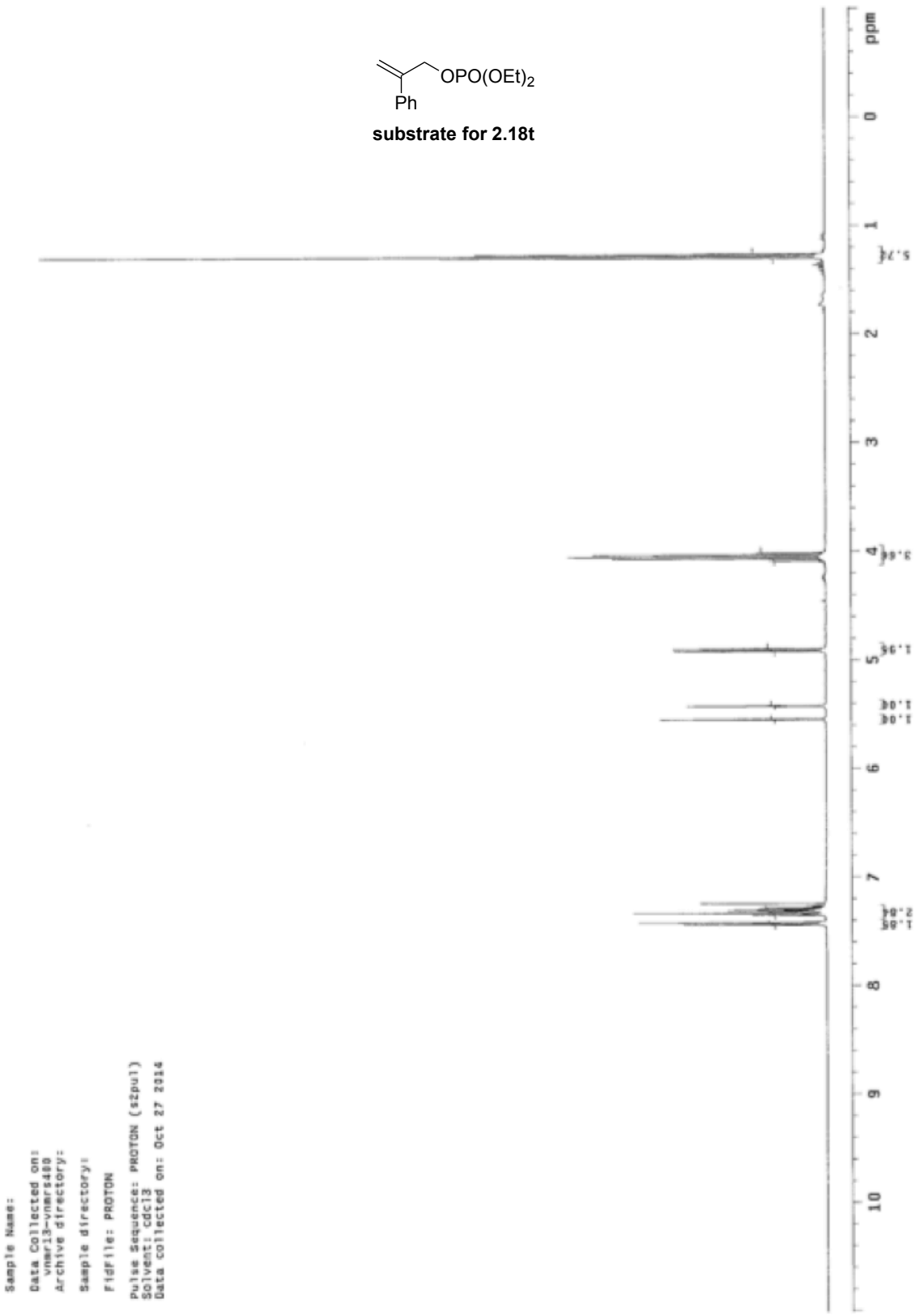
OPO(OEt)2
Ph
substrate for 2.18t
Sample Name:
Data Collected on:
vnmr13-vnmrs400
Archive directory:
Sample directory:
Fidfile: PROTON
Pulse Sequence: PROTON (s2pul)
Solvent: cdcl3
Data collected on: Oct 27 2014
ppm
0
1
2
3
4
5
6
7
8
9
10

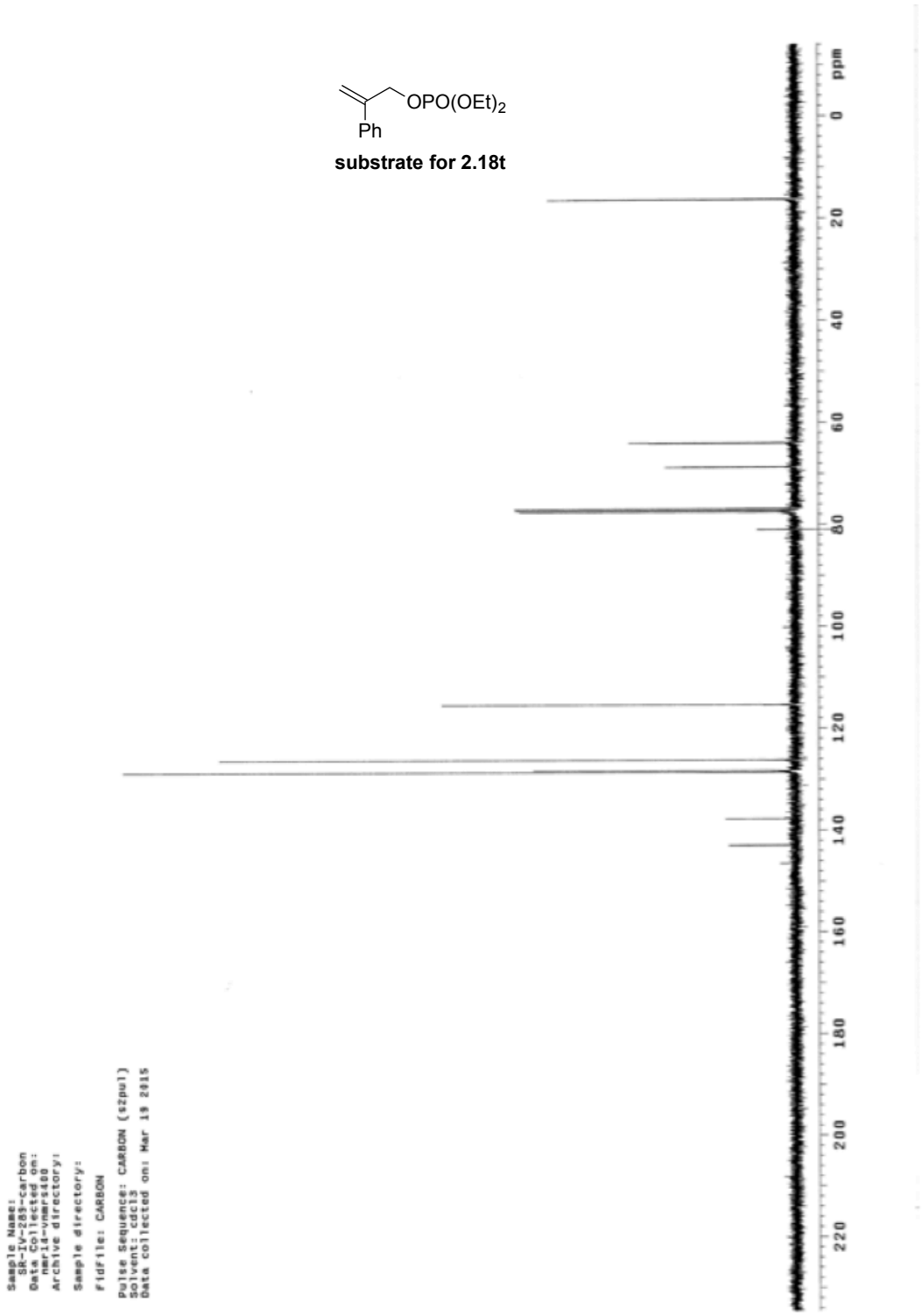
OPO(OEt)2
Ph
substrate for 2.18t
Sample Name:
SR-IV-289-carbon
Data Collected on:
nmr14-vnmrs400
Archive directory:
Sample directory:
FidFile: CARBON
Pulse Sequence: CARBON (s2pul)
Solvent: cdcl3
Data collected on: Mar 19 2015
ppm
0
20
40
60
80
100
120
140
160
180
200
220

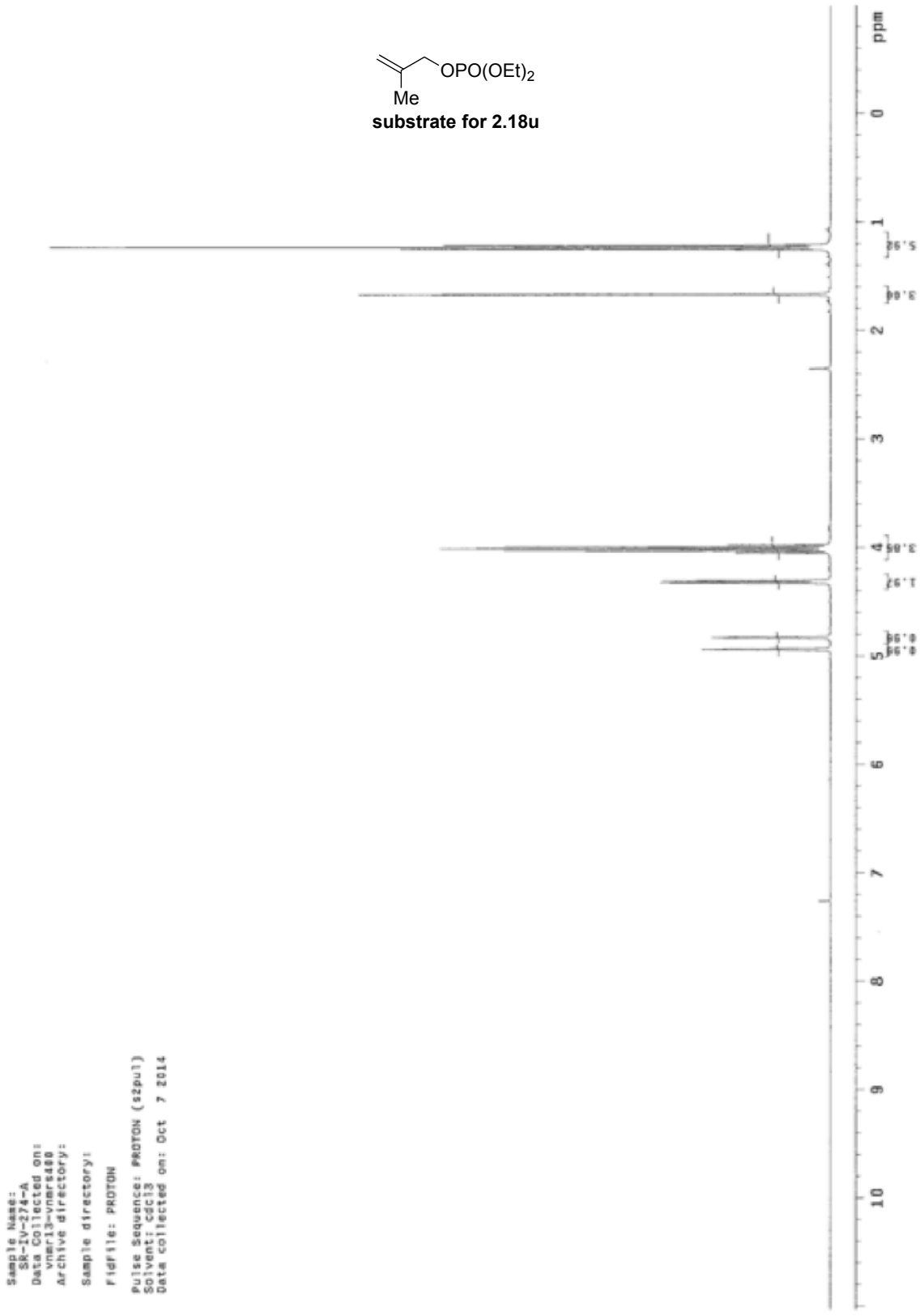
OPO(OEt)2
Me
substrate for 2.18u
Sample Name:
SR-IV-274-A
Data Collected on:
vnmr13-vnmrs400
Archive directory:
Sample directory:
FidFile: PROTON
Pulse Sequence: PROTON (s2pul)
Solvent: cdcl3
Data collected on: Oct 7 2014
ppm
5.92
3.04
3.05
1.97
0.98
0.96

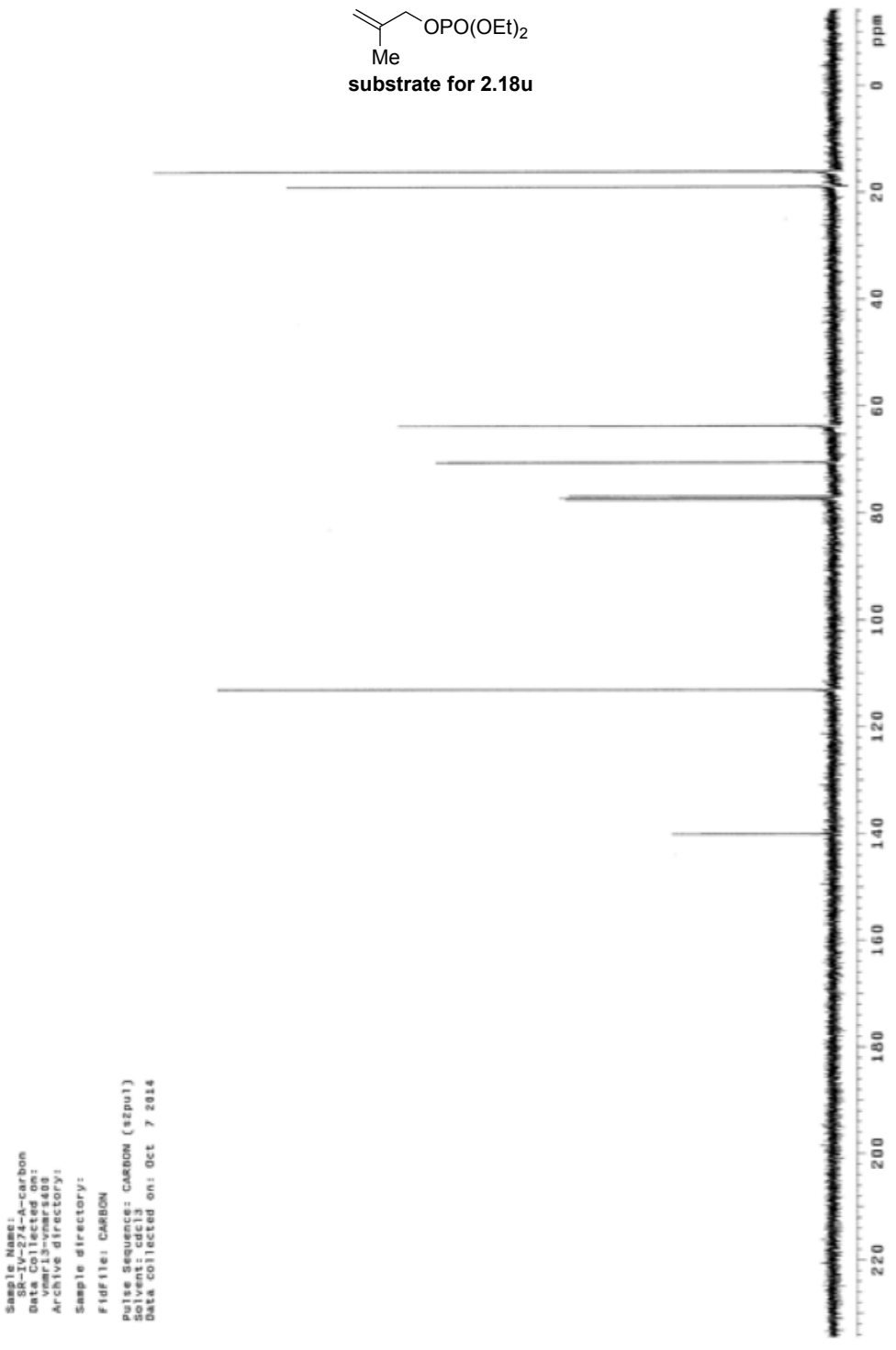
OPO(OEt)2
Me
substrate for 2.18u
Sample Name:
SR-IV-274-A-carbon
Data Collected on:
vnmr13-vnmrs600
Archive directory:
Sample directory:
FidFile: CARBON
Pulse Sequence: CARBON (s2pul)
Solvent: cdcl3
Data collected on: Oct 7 2014
ppm
0
20
40
60
80
100
120
140
160
180
200
220

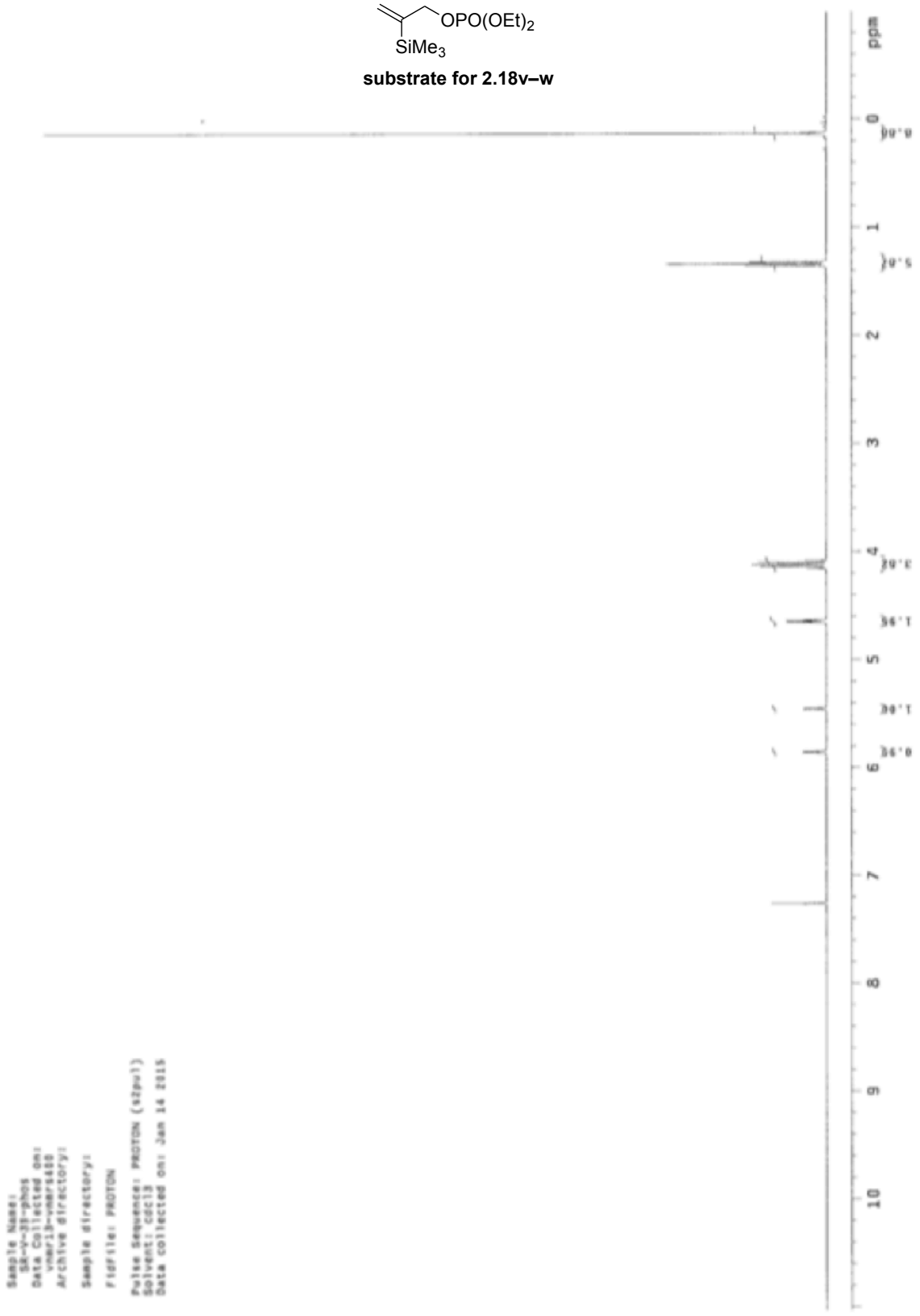
OPO(OEt)2
SiMe3
substrate for 2.18v–w
Sample Name:
SR-v-38-phos
Data Collected on:
vnmrj3-vnmr5400
Archive directory:
Sample directory:
Fidfile: PROTON
Pulse Sequence: PROTON (s2pul)
Solvent: cdcl3
Data collected on: Jan 14 2015
ppm

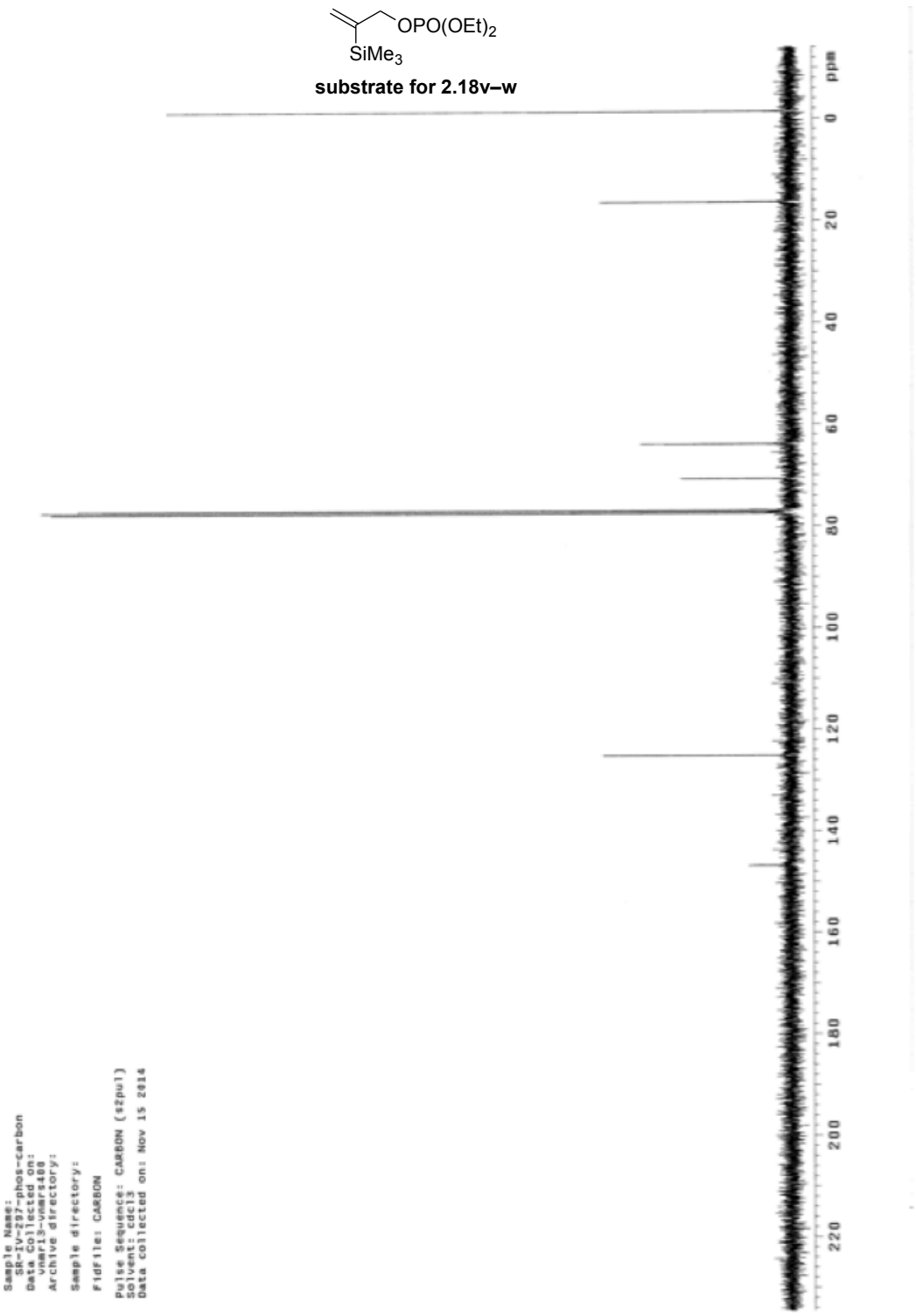
OPO(OEt)2
SiMe3
substrate for 2.18v–w
Sample Name:
SR-IV-287-phos-carbon
Data Collected on:
vnmr13-vnmrs400
Archive directory:
Sample directory:
FidFile: CARBON
Pulse Sequence: CARBON (s2pul)
Solvent: cdcl3
Data collected on: Nov 15 2014
ppm
0
20
40
60
80
100
120
140
160
180
200
220

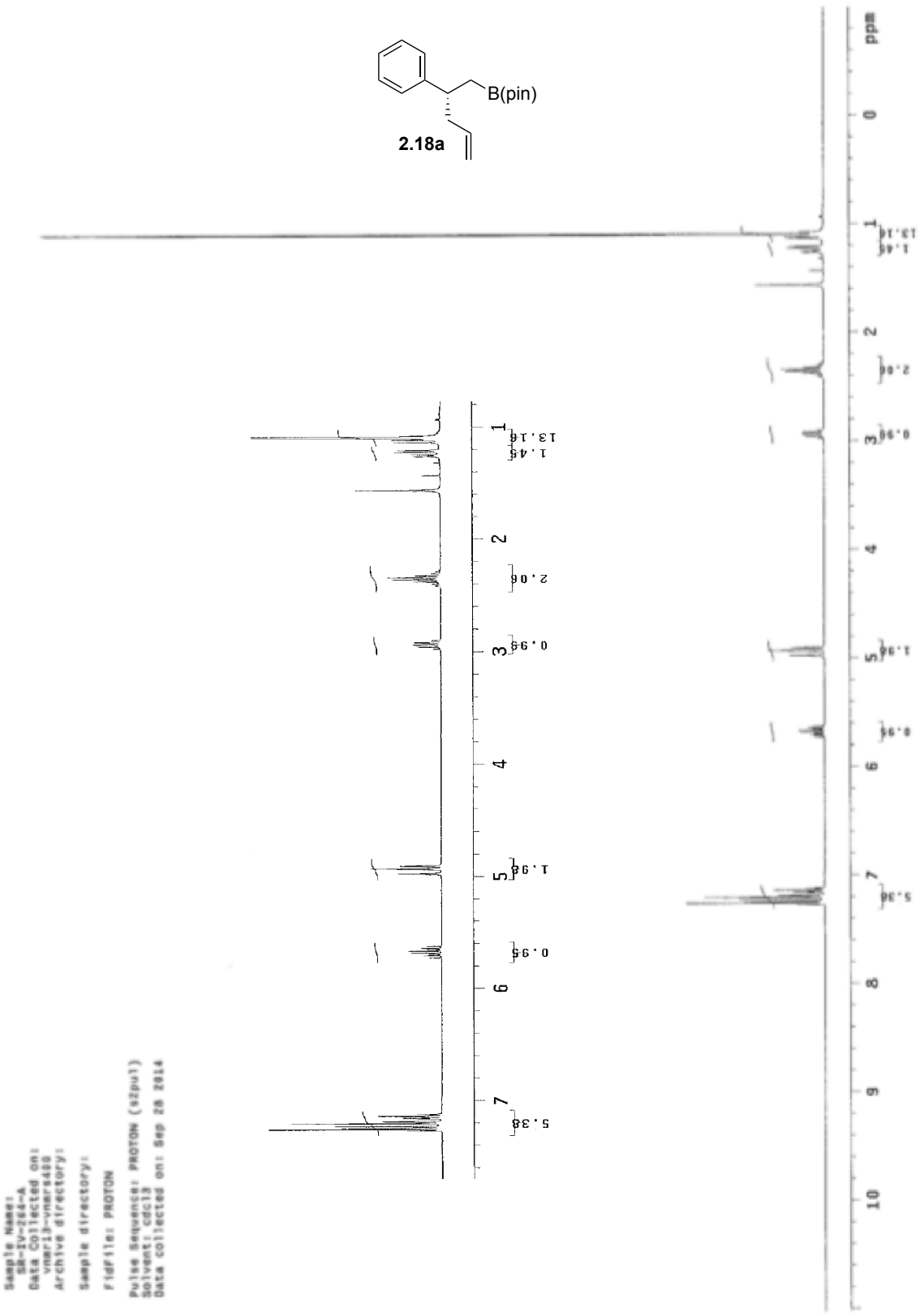
B(pin)
2.18a
Sample Name:
SR-IV-264-A
Data Collected on:
vnmrj-vnmrs400
Archive directory:
Sample directory:
FidFile: PROTON
Pulse Sequence: PROTON (s2pul)
Solvent: cdcl3
Data collected on: Sep 28 2014
ppm

B(pin)
2.18a
Sample Name:
SR-IV-264-A-carbon
Data Collected on:
vnmr13-vnmrs400
Archive directory:
Sample directory:
FidFile: CARBON
Pulse Sequence: CARBON (s2pul)
Solvent: cdcl3
Data collected on: Sep 28 2014
220
200
180
160
140
120
100
80
60
40
20
0
ppm

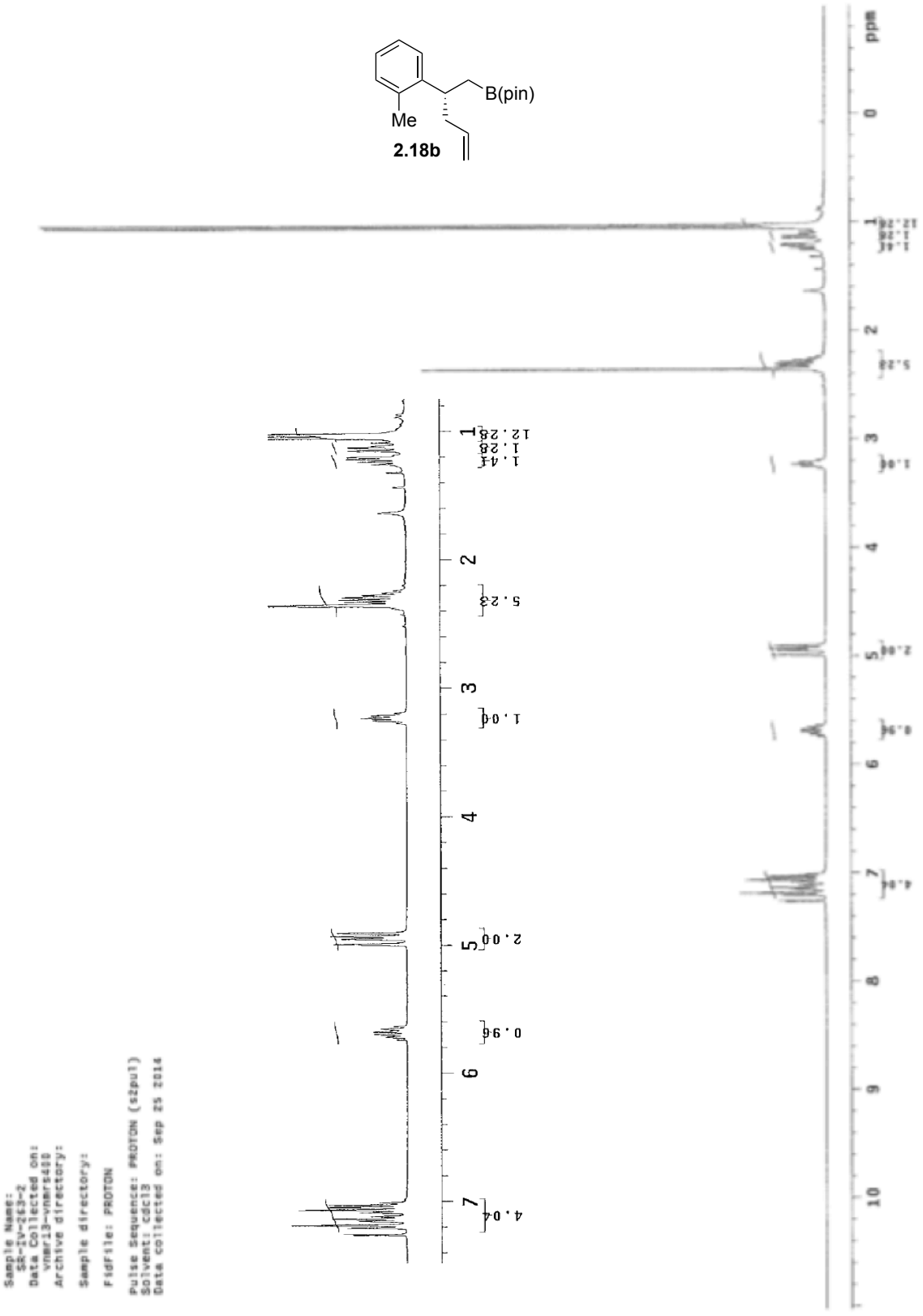
B(pin)
Me
2.18b
Sample Name:
SS-IV-263-2
Data Collected on:
vnmr13-vnmrs60
Archive directory:
Sample directory:
FidFile: PROTON
Pulse Sequence: PROTON (s2pul)
Solvent: cdcl3
Data collected on: Sep 25 2014
ppm

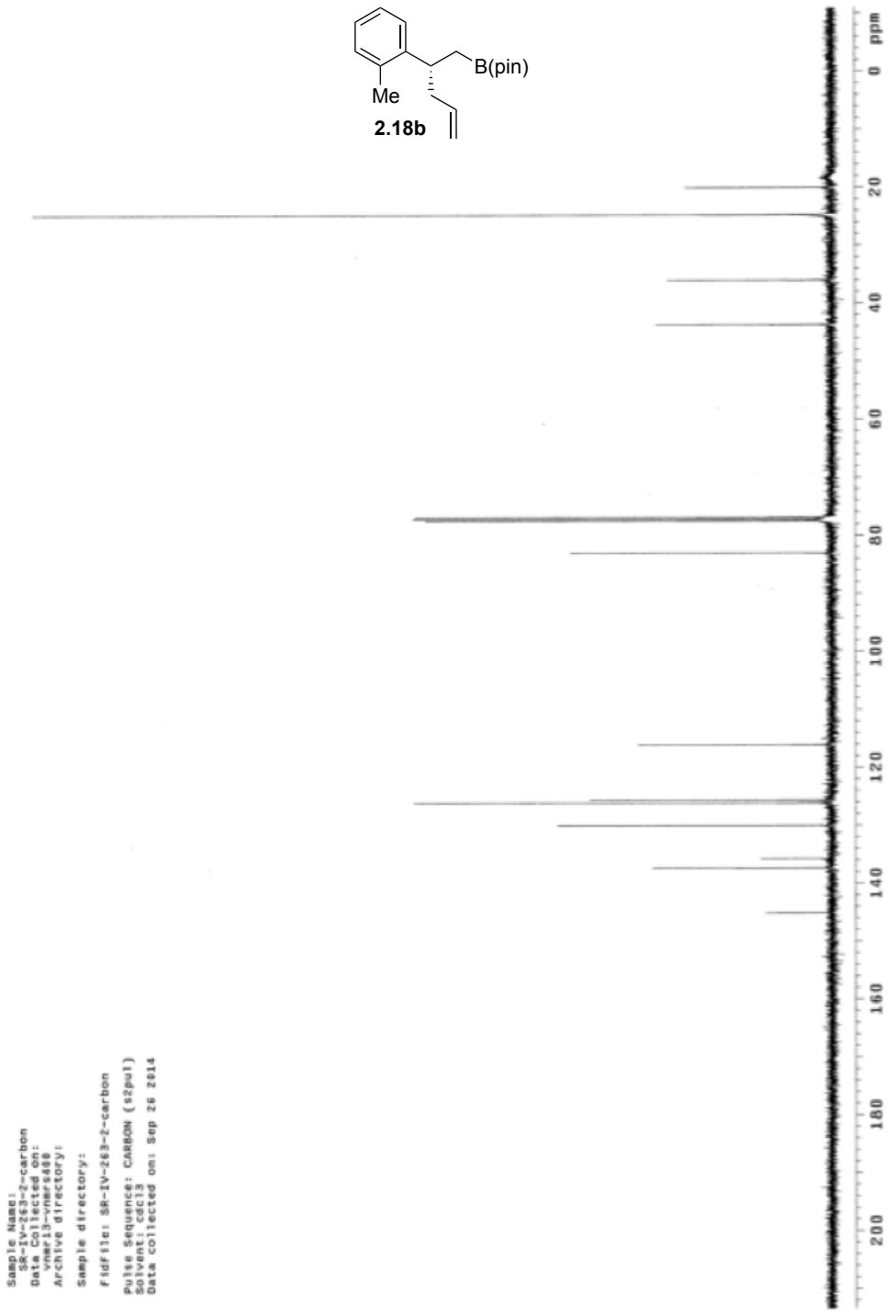
B(pin)
Me
2.18b
ppm
0
20
40
60
80
100
120
140
160
180
200
Sample Name:
SR-IV-263-2-carbon
Data Collected on:
vnmrj3-vnmrs400
Archive directory:
Sample directory:
FidFile: SR-IV-263-2-carbon
Pulse Sequence: CARBON (s2pul)
Solvent: cdcl3
Data collected on: Sep 26 2014

B(pin)
2.18c
Sample Name:
JL-II-252PD
Data Collected on:
vnmr13-vnmrs400
Archive directory:
Sample directory:
FidFile: PROTON
Pulse Sequence: PROTON (s2pul)
Solvent: cdcl3
Data collected on: Nov 4 2014
1.07 1.03 1.01 4.19
1.00 2.11
1.09
1.12 1.12
1.47 6.67 1.24 6.65
ppm

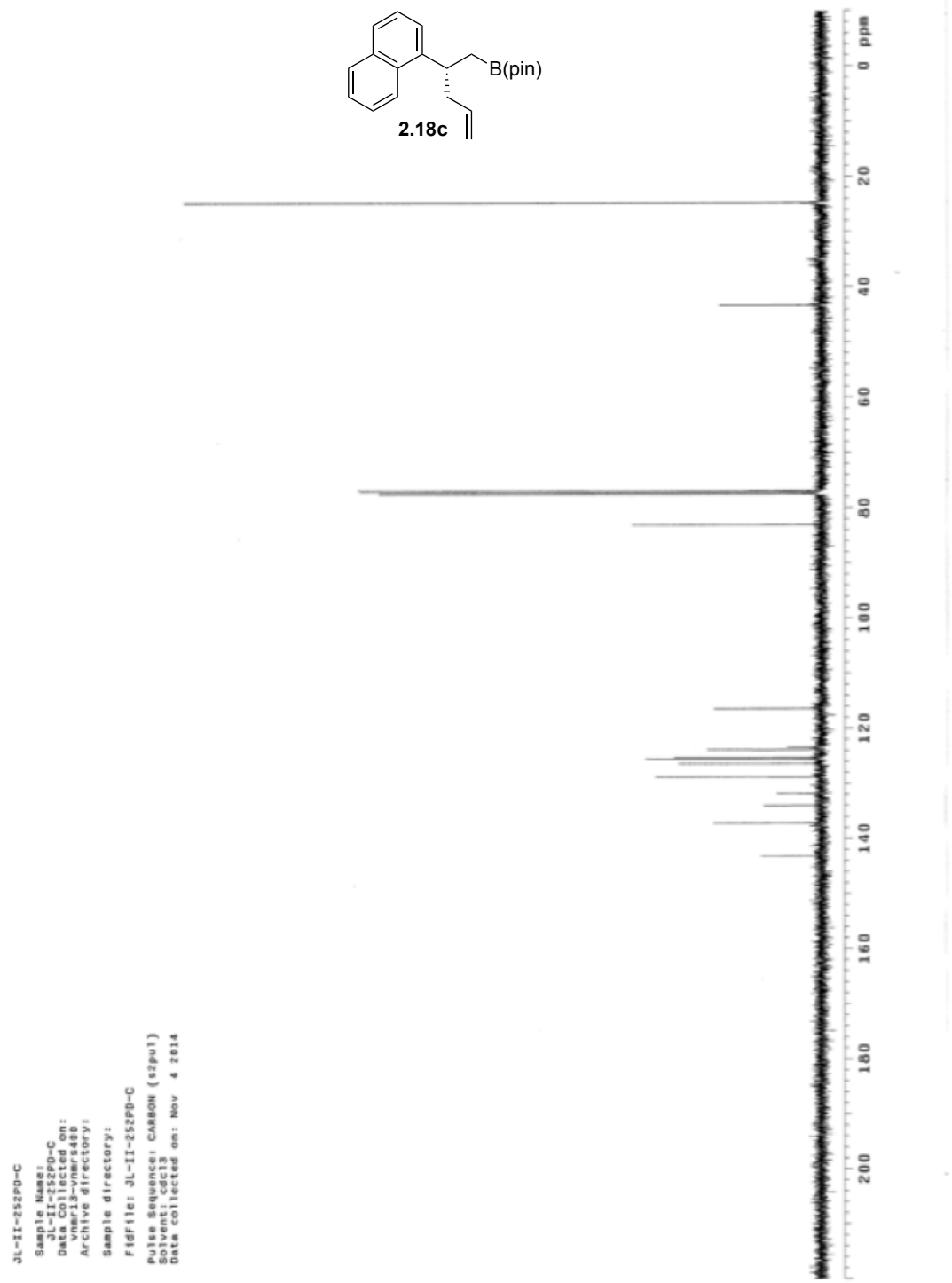
JL-II-252PD-C
Sample Name:
JL-II-252PD-C
Data Collected on:
vnmr13-vnmrs400
Archive directory:
Sample directory:
FidFile: JL-II-252PD-C
Pulse Sequence: CARBON (s2pul)
Solvent: cdcl3
Data collected on: Nov 4 2014
B(pin)
2.18c
0 ppm
20
40
60
80
100
120
140
160
180
200

B(pin)
OMe
2.18d
Sample Name:
SR-IV-251-B
Data Collected on:
vnmrj3-vnmrs400
Archive directory:
Sample directory:
FidFile: PROTON
Pulse Sequence: PROTON (s2pul)
Solvent: cdcl3
Data collected on: Aug 23 2014
ppm

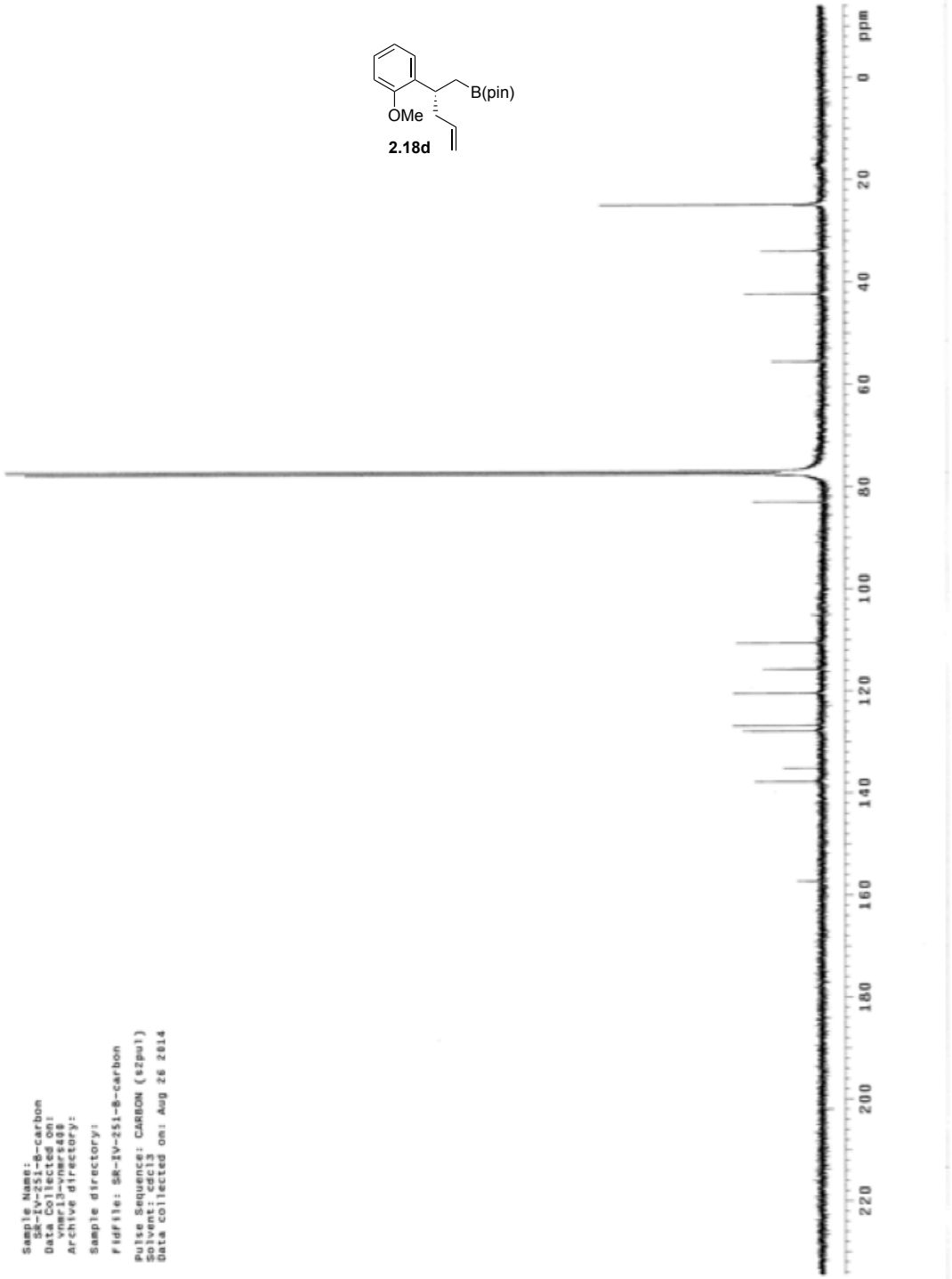
B(pin)
OMe
2.18d
Sample Name:
SR-IV-251-B-carbon
Data Collected on:
vnmrj3-vnmrs400
Archive directory:
Sample directory:
FidFile: SR-IV-251-B-carbon
Pulse Sequence: CARBON (s2pul)
Solvent: cdcl3
Data collected on: Aug 26 2014
220
200
180
160
140
120
100
80
60
40
20
0
ppm

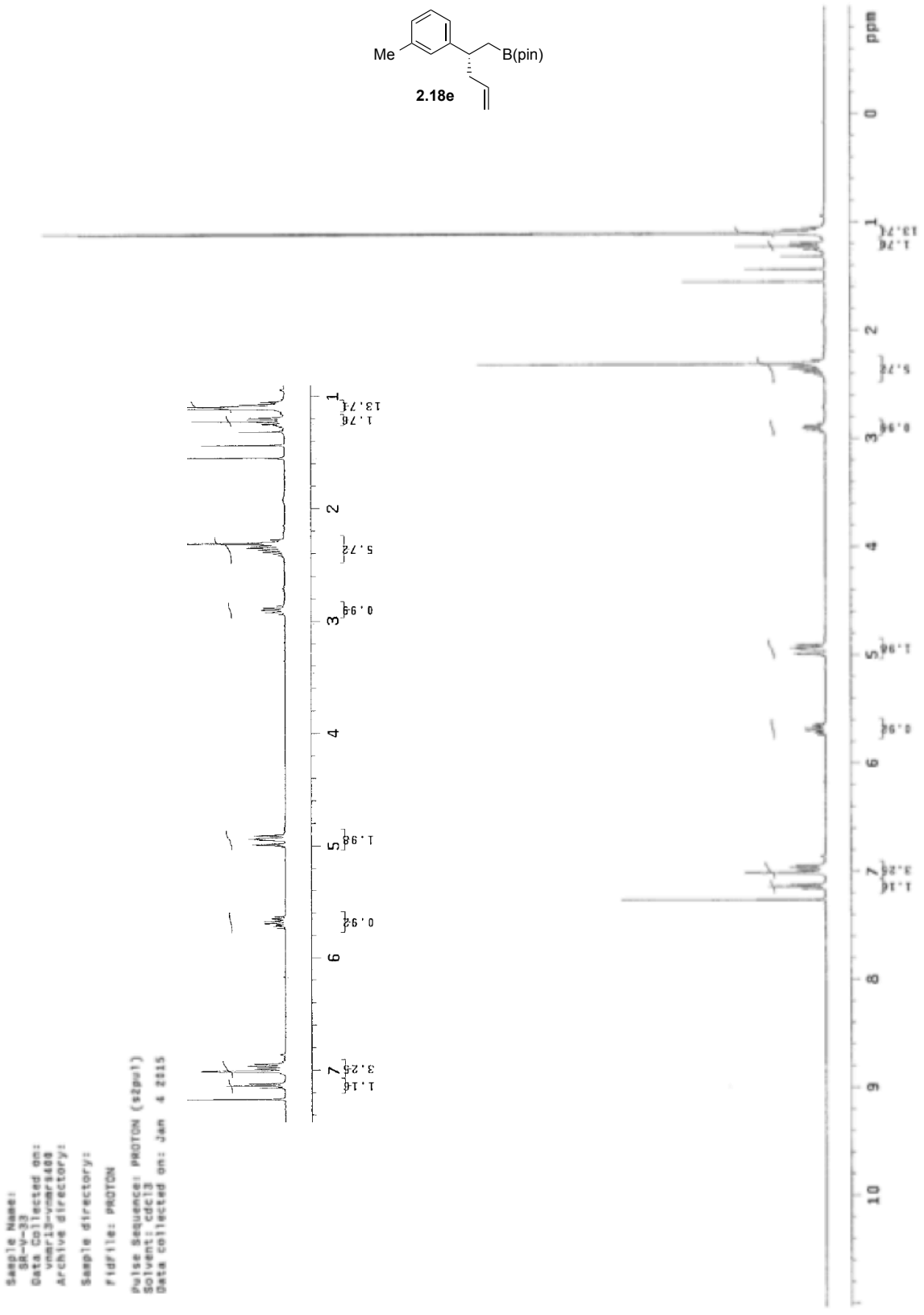
Me
B(pin)
2.18e
Sample Name:
SR-y-33
Data Collected on:
vnmrl3-vnmr400
Archive directory:
Sample directory:
Fidfile: PROTON
Pulse Sequence: PROTON (s2pul)
Solvent: cdcl3
Data collected on: Jan 4 2015
ppm

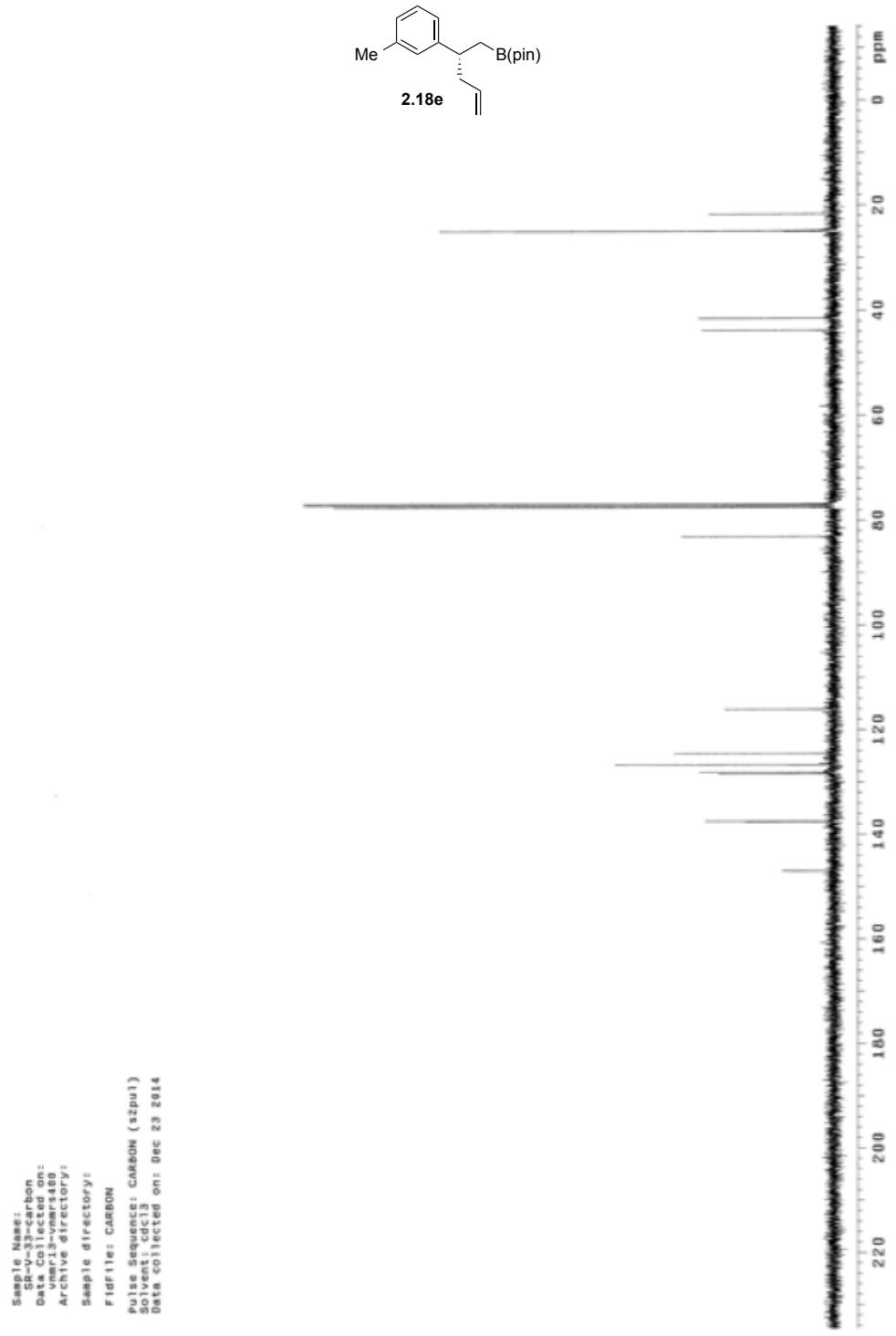
Me
B(pin)
2.18e
ppm
0
20
40
60
80
100
120
140
160
180
200
220
Sample Name:
SR-V-33-carbon
Data Collected on:
vnmr13-vmars400
Archive directory:
Sample directory:
FidFile: CARBON
Pulse Sequence: CARBON (s2pul)
Solvent: cdcl3
Data collected on: Dec 23 2014

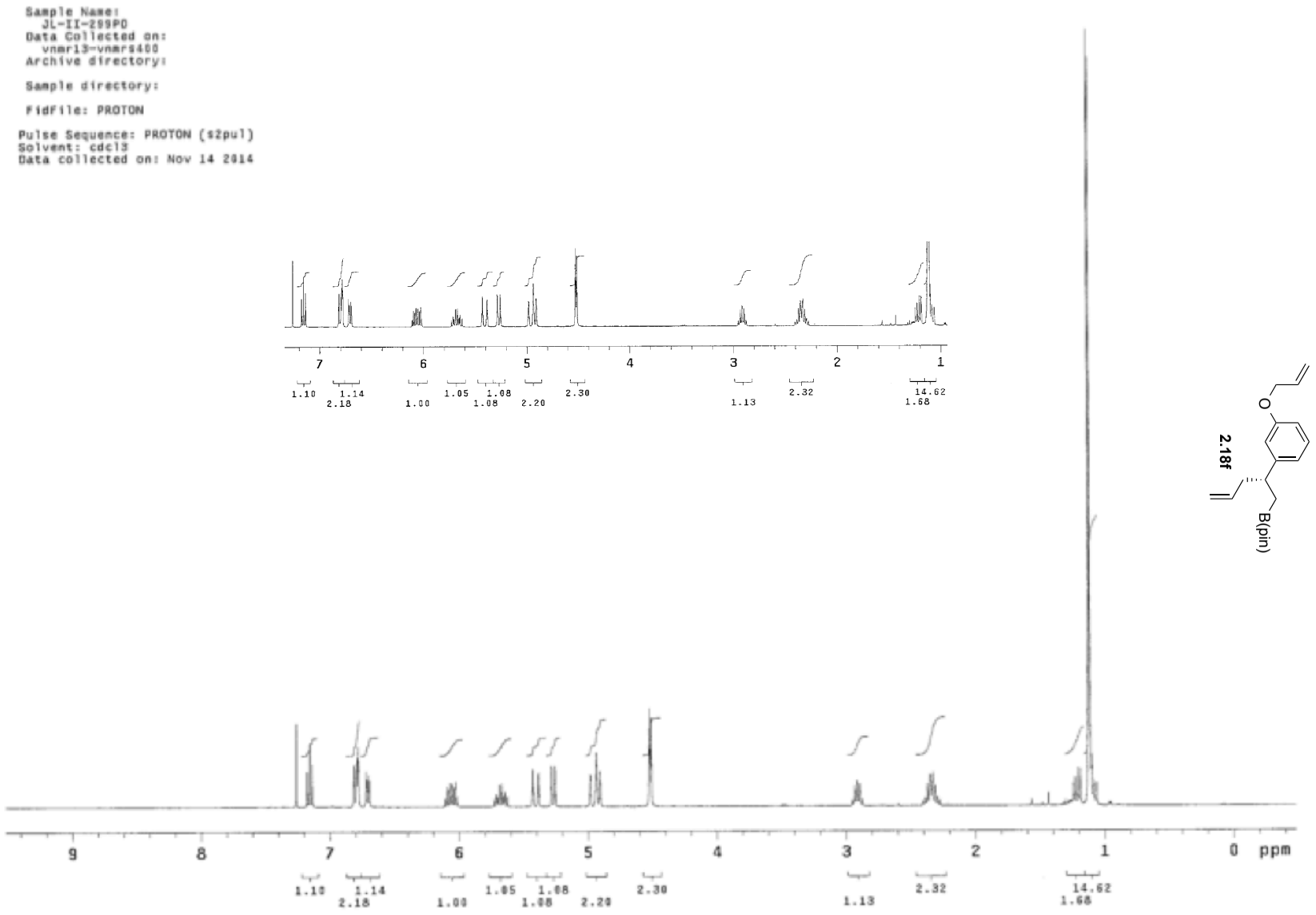
Sample Name:
JL-II-299PD
Data Collected on:
vnmr13-vnmrs400
Archive directory:
Sample directory:
FidFile: PROTON
Pulse Sequence: PROTON (s2pul)
Solvent: cdcl3
Data collected on: Nov 14 2014
2.18f
B(pin)
ppm

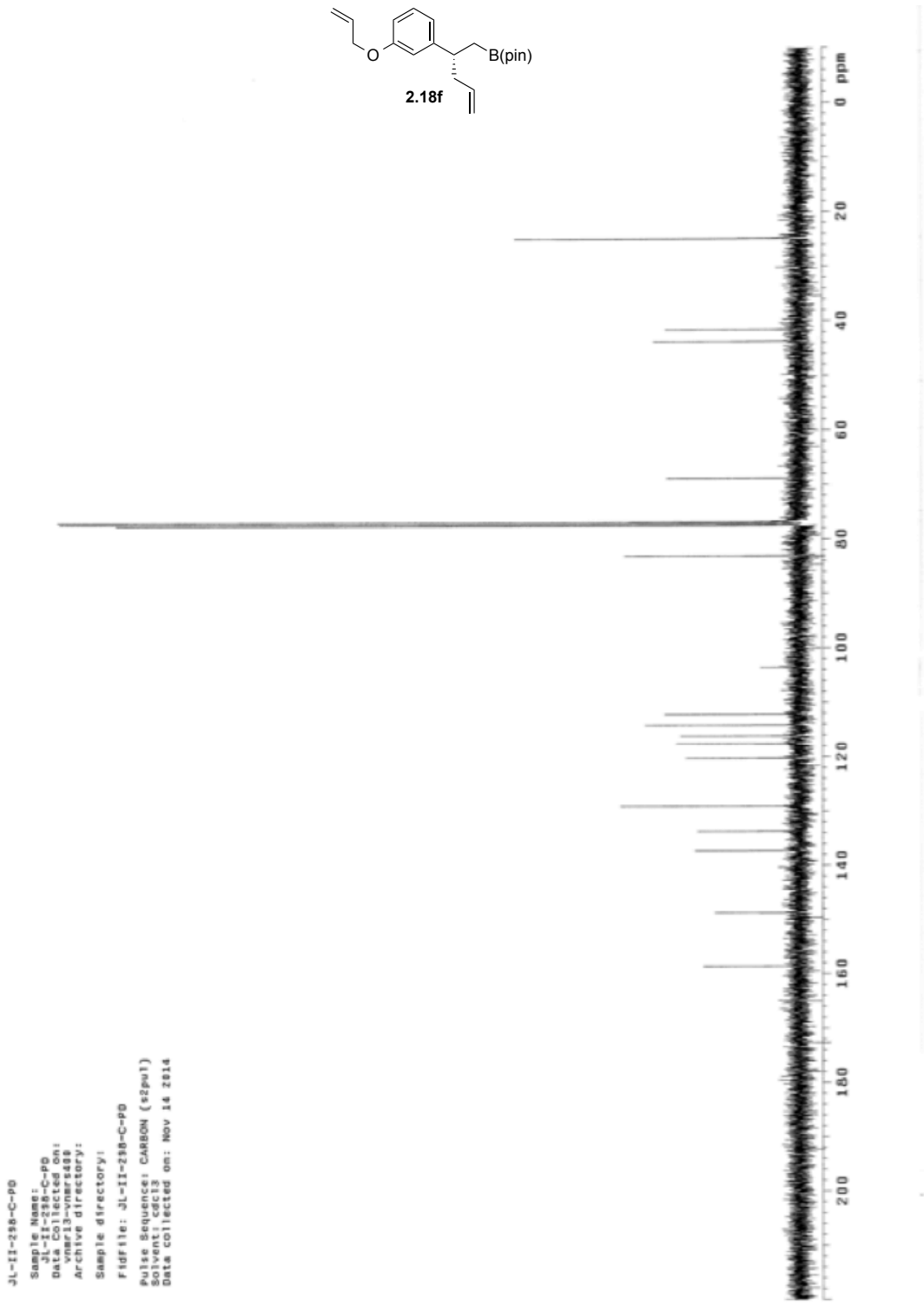
O
B(pin)
2.18f
JL-II-298-C-PD
Sample Name:
JL-II-298-C-PD
Data Collected on:
vnmr13-vnmrsys
Archive directory:
Sample directory:
FidFile: JL-II-298-C-PD
Pulse Sequence: CARBON (s2pul)
Solvent: cdcl3
Data collected on: Nov 14 2014
0 ppm
20
40
60
80
100
120
140
160
180
200

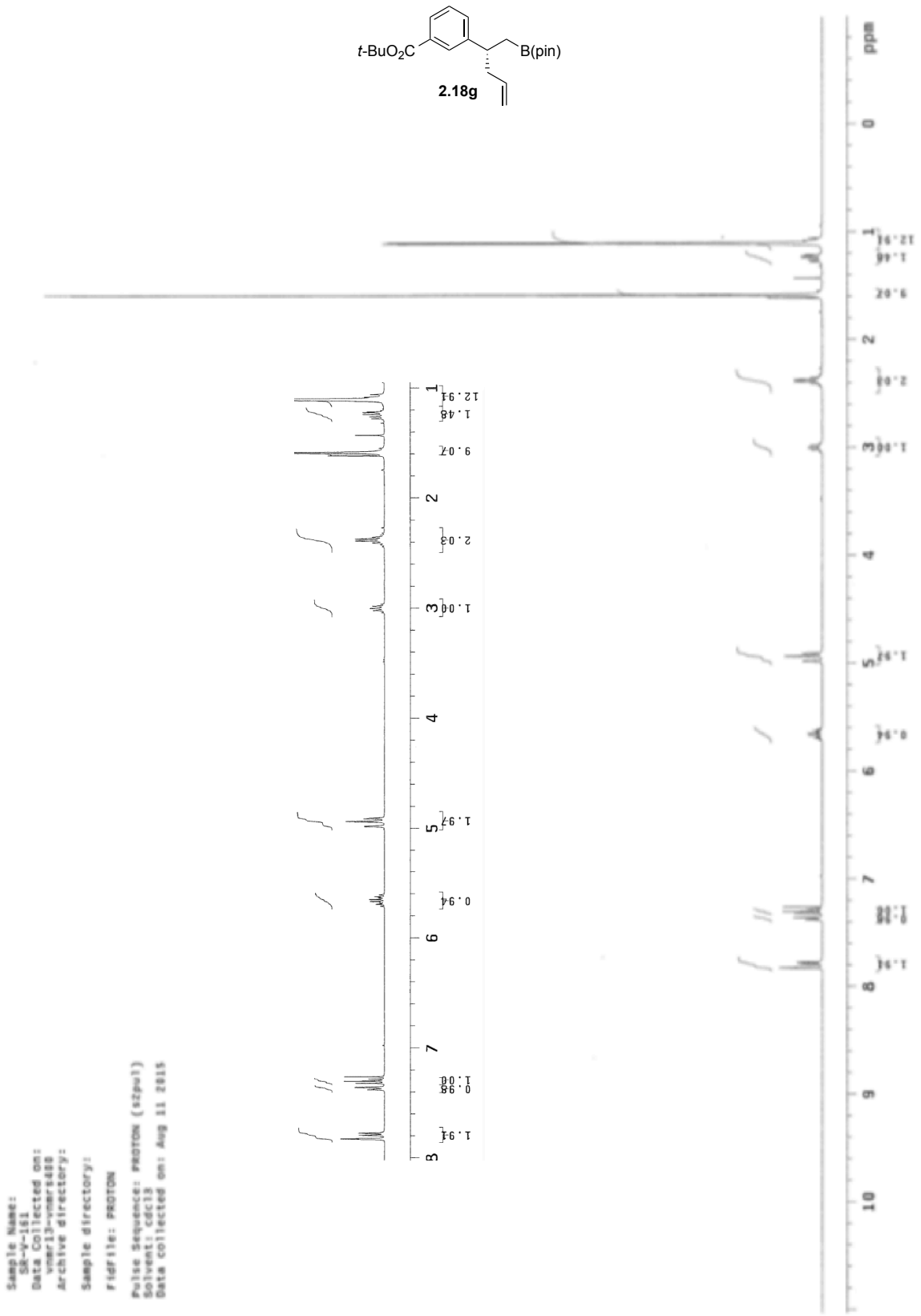
t-BuO2C
B(pin)
2.18g
Sample Name:
SR-V-161
Data Collected on:
vnmr13-vnmrs400
Archive directory:
Sample directory:
Fidfile: PROTON
Pulse Sequence: PROTON (s2pul)
Solvent: cdcl3
Data collected on: Aug 11 2015
ppm

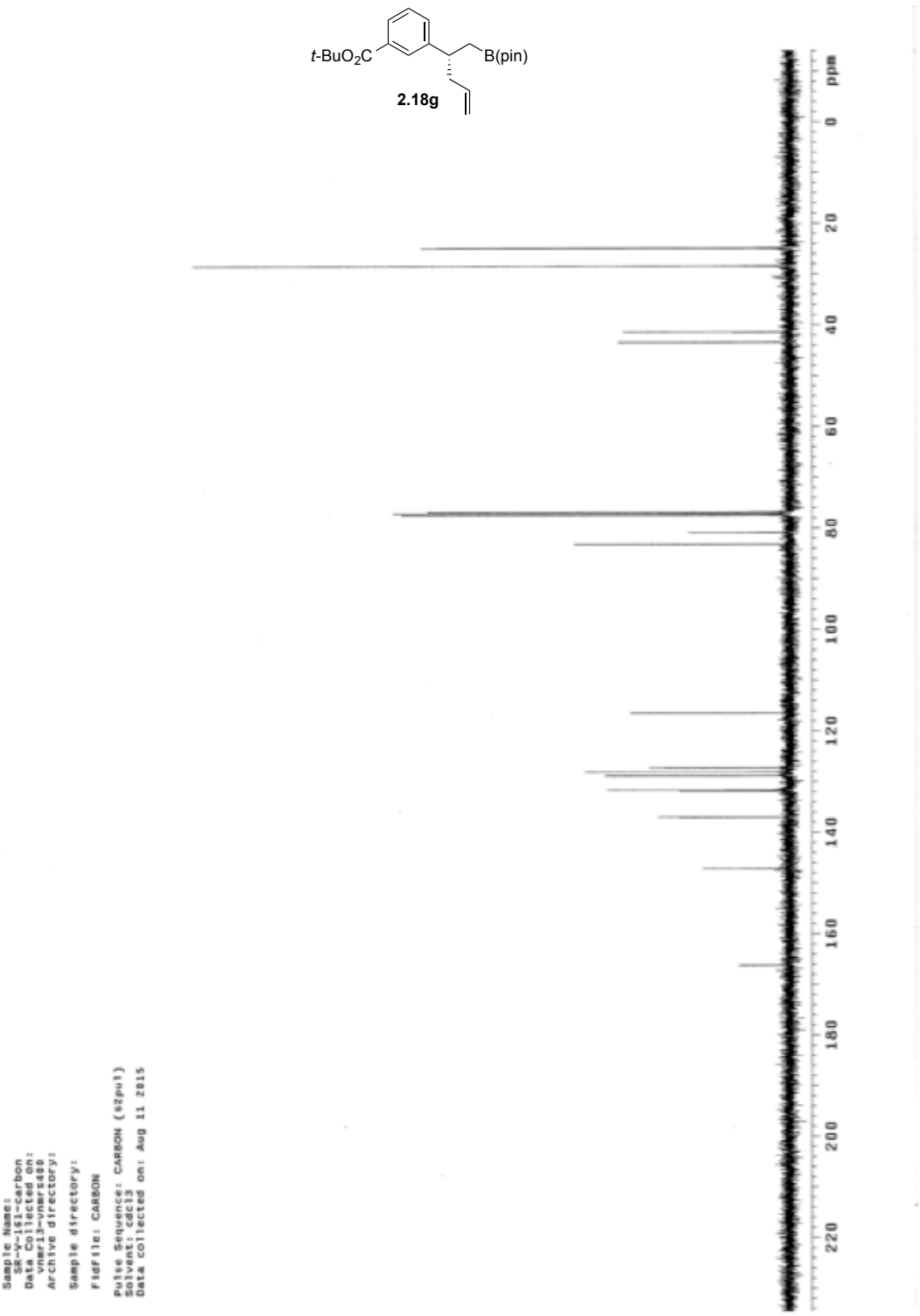
t-BuO2C
B(pin)
2.18g
Sample Name:
SR-V-161-carbon
Data Collected On:
vnmr13-vnmrs480
Archive directory:
Sample directory:
FidFile: CARBON
Pulse Sequence: CARBON (s2pul)
Solvent: cdcl3
Data collected on: Aug 11 2015
ppm
0
20
40
60
80
100
120
140
160
180
200
220

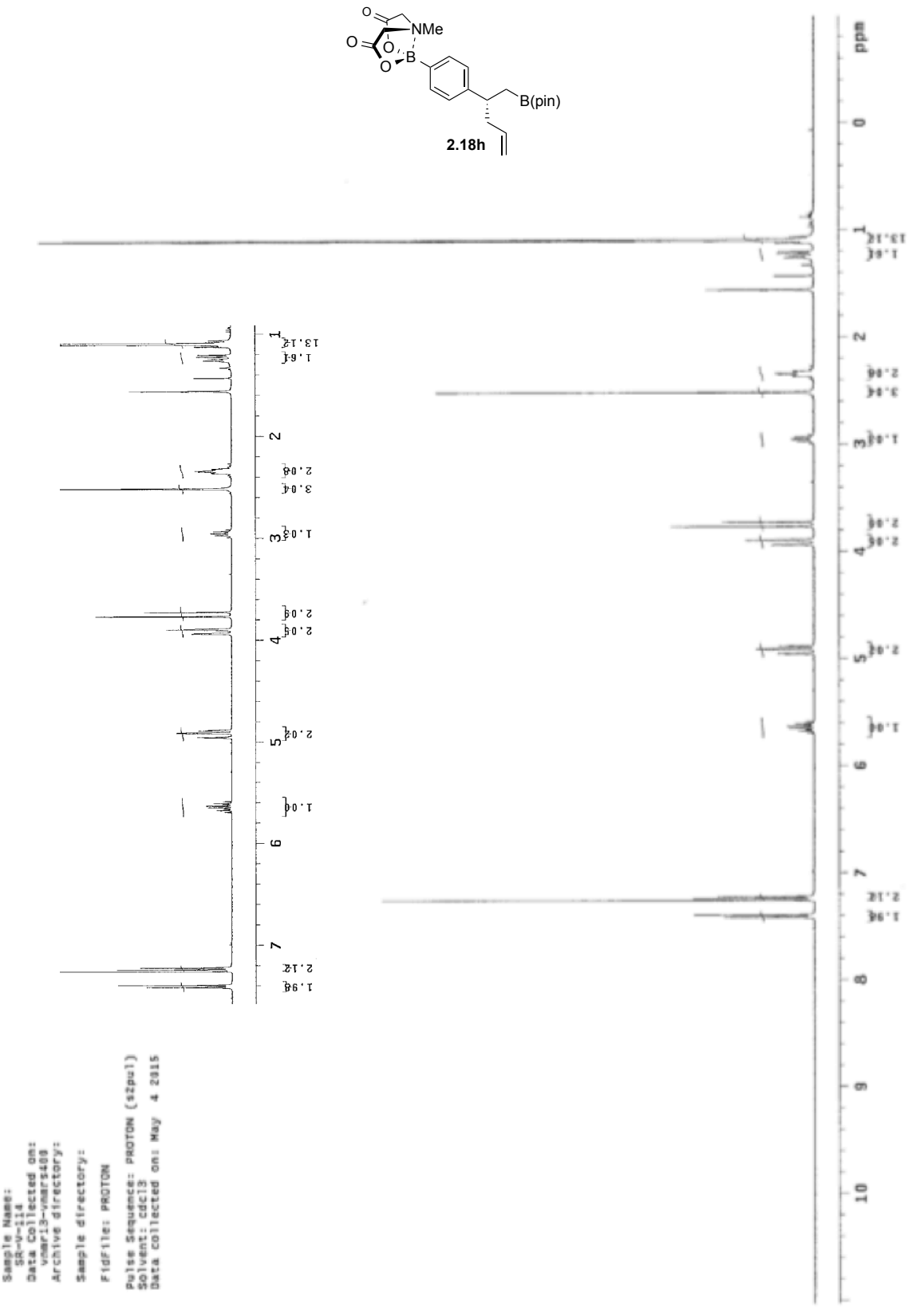
O
NMe
O
O
O
B
B(pin)
2.18h
Sample Name:
SR-v-114
Data Collected on:
vnmr13-vnmrs400
Archive directory:
Sample directory:
FidFile: PROTON
Pulse Sequence: PROTON (s2pul)
Solvent: cdcl3
Data collected on: May 4 2015
ppm

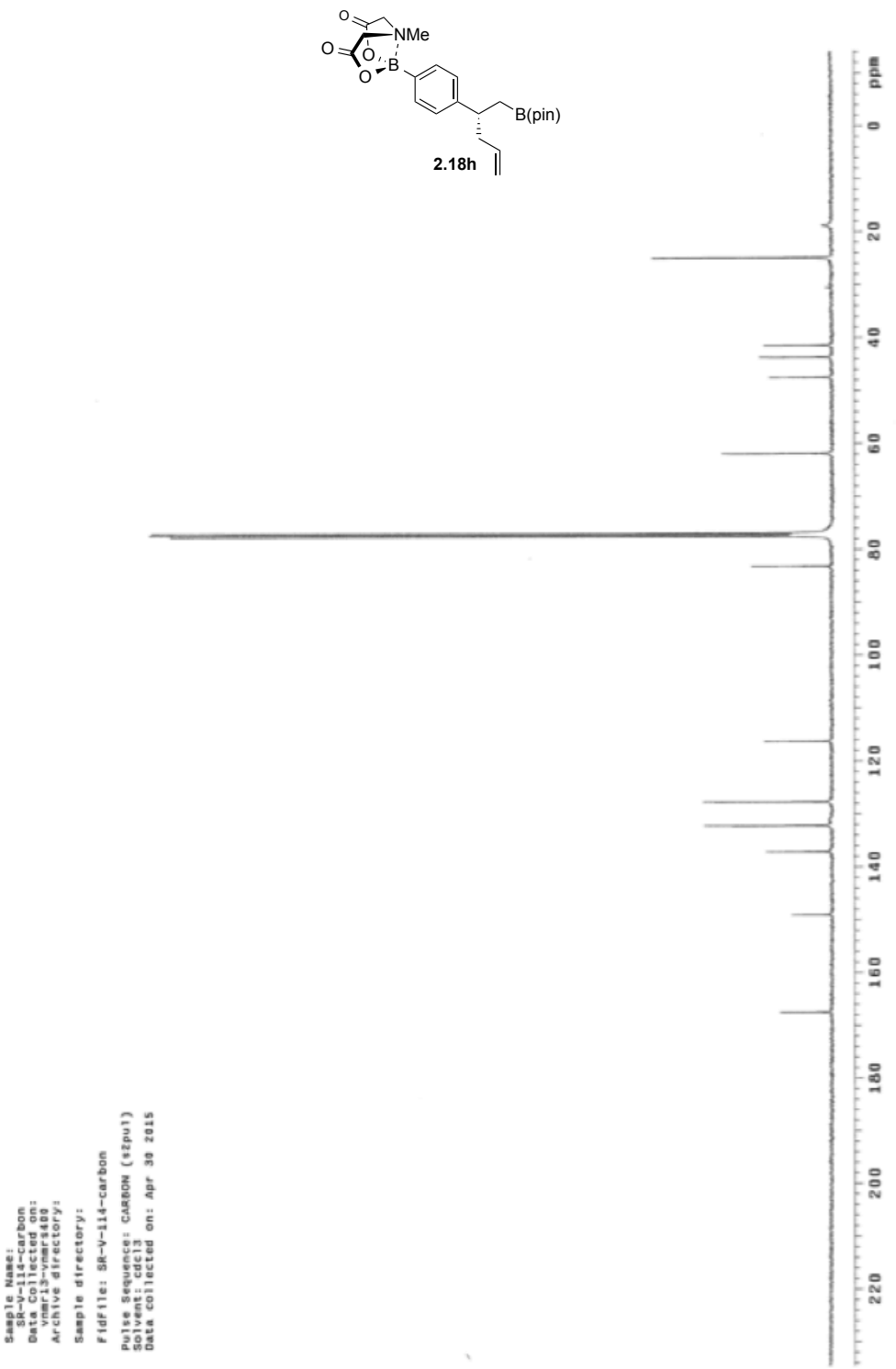
O
NMe
O
O
O
B
B(pin)
2.18h
Sample Name:
SR-V-114-carbon
Data Collected on:
vnmr13-vnmrs400
Archive directory:
Sample directory:
FidFile: SR-V-114-carbon
Pulse Sequence: CARBON (s2pul)
Solvent: cdcl3
Data collected on: Apr 30 2015
220
200
180
160
140
120
100
80
60
40
20
0
ppm

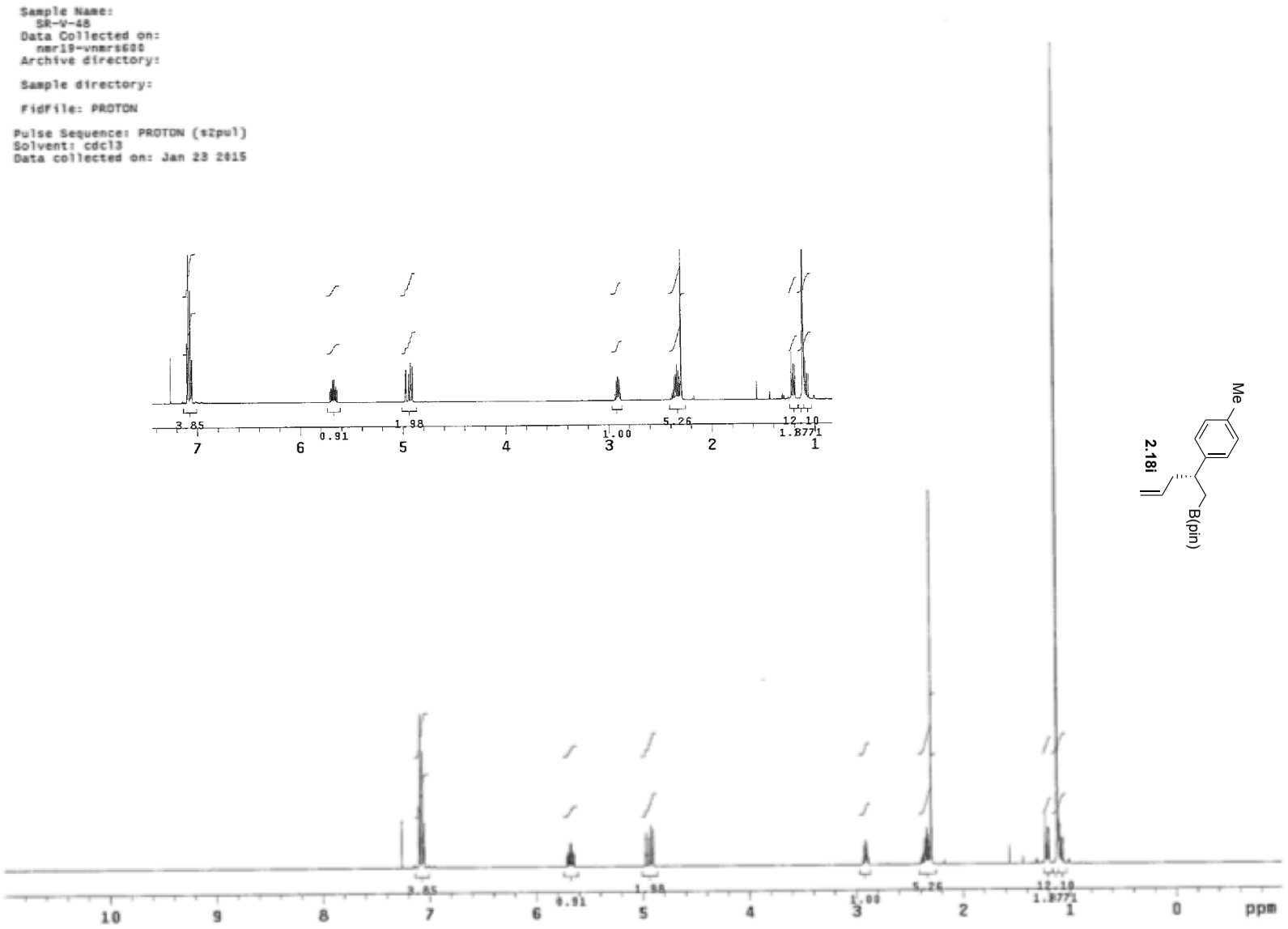
Sample Name:
SR-V-48
Data Collected on:
nmr19-vnmrs600
Archive directory:
Sample directory:
Fidfile: PROTON
Pulse Sequence: PROTON (s2pul)
Solvent: cdcl3
Data collected on: Jan 23 2015
3.85
0.91
1.98
1.00
5.26
12.10
1.8771
Me
2.18i
B(pin)
ppm

Me
B(pin)
2.18i
ppm
0
20
40
60
80
100
120
140
160
180
200
220
Sample Name:
SR-V-48-carbon
Data Collected on:
nmr19-vnmrs600
Archive directory:
Sample directory:
FidFile: CARBON
Pulse Sequence: CARBON (s2pul)
Solvent: cdcl3
Data collected on: Jan 23 2015

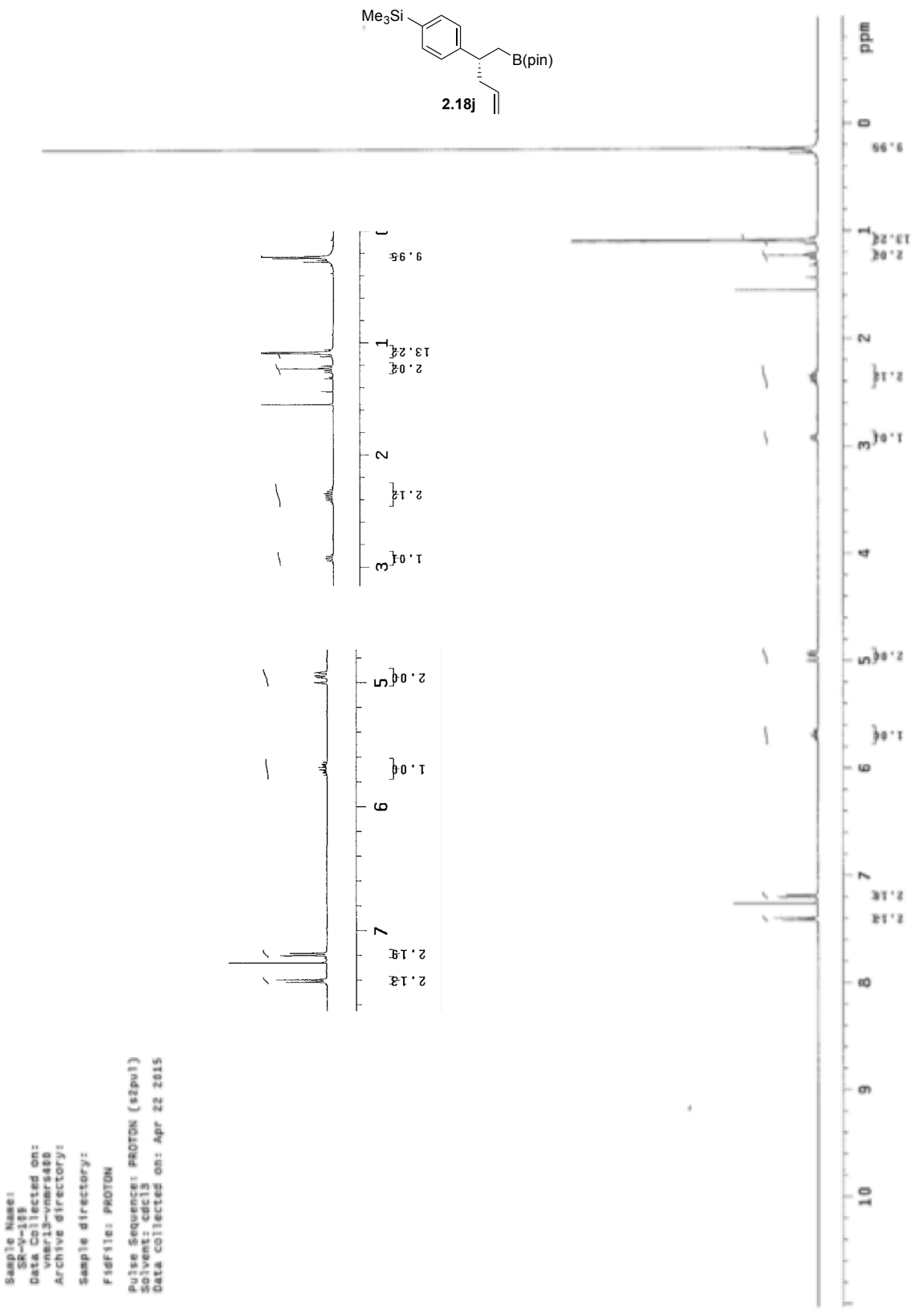
Me3Si
B(pin)
2.18j
Sample Name:
SR-V-169
Data Collected on:
vnmr13-vnmrs400
Archive directory:
Sample directory:
FidFile: PROTON
Pulse Sequence: PROTON (s2pul)
Solvent: cdcl3
Data collected on: Apr 22 2015
ppm

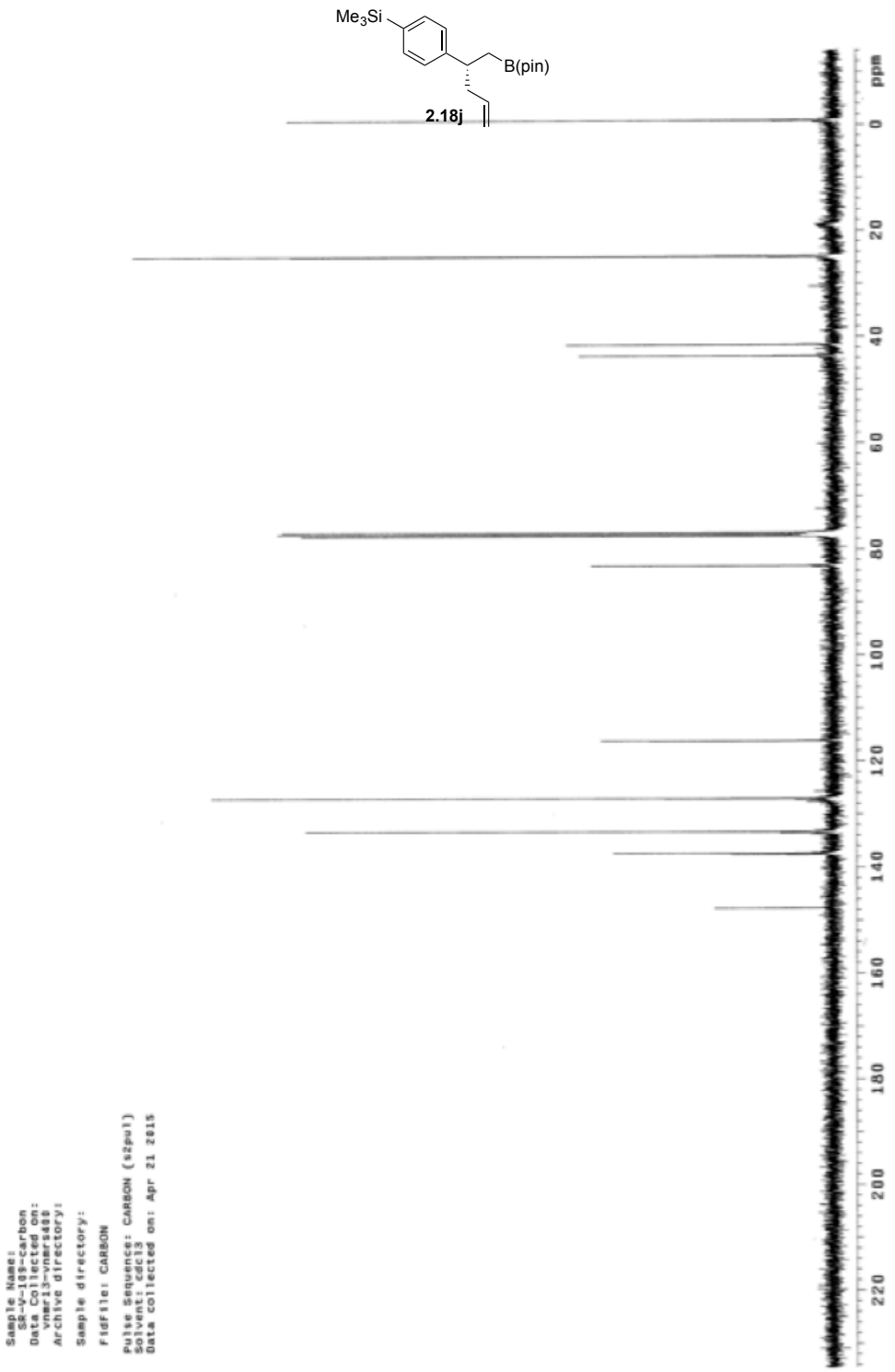
Me3Si
B(pin)
2.18j
ppm
0
20
40
60
80
100
120
140
160
180
200
220
Sample Name:
SR-V-109-carbon
Data Collected on:
vnmr13-vnmrs400
Archive directory:
Sample directory:
FidFile: CARBON
Pulse Sequence: CARBON (s2pul)
Solvent: cdcl3
Data collected on: Apr 21 2015

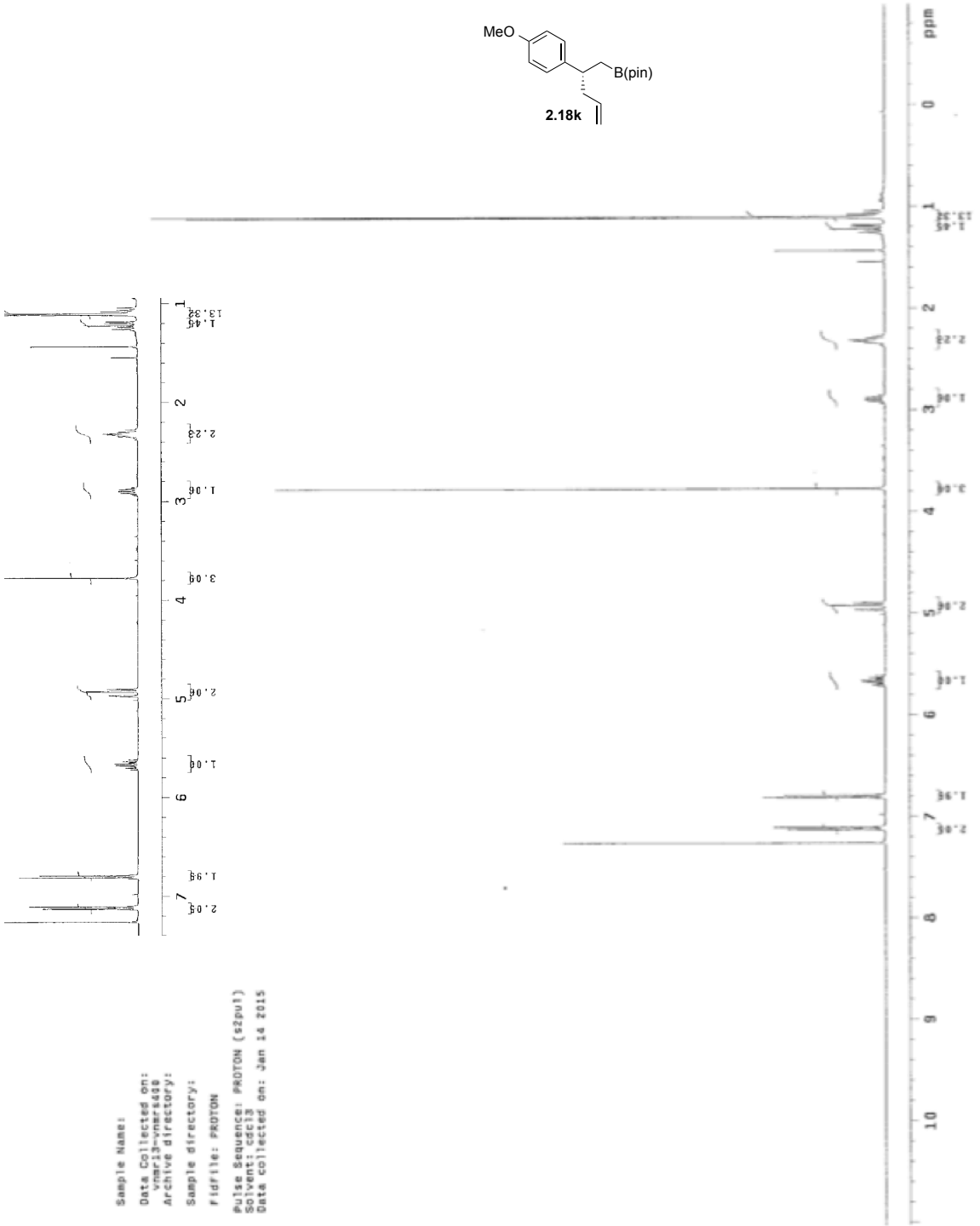
MeO
B(pin)
2.18k
ppm
Sample Name:
Data Collected on:
vnmrj3-vnmrs400
Archive directory:
Sample directory:
Fidfile: PROTON
Pulse Sequence: PROTON (s2pul)
Solvent: cdcl3
Data collected on: Jan 14 2015

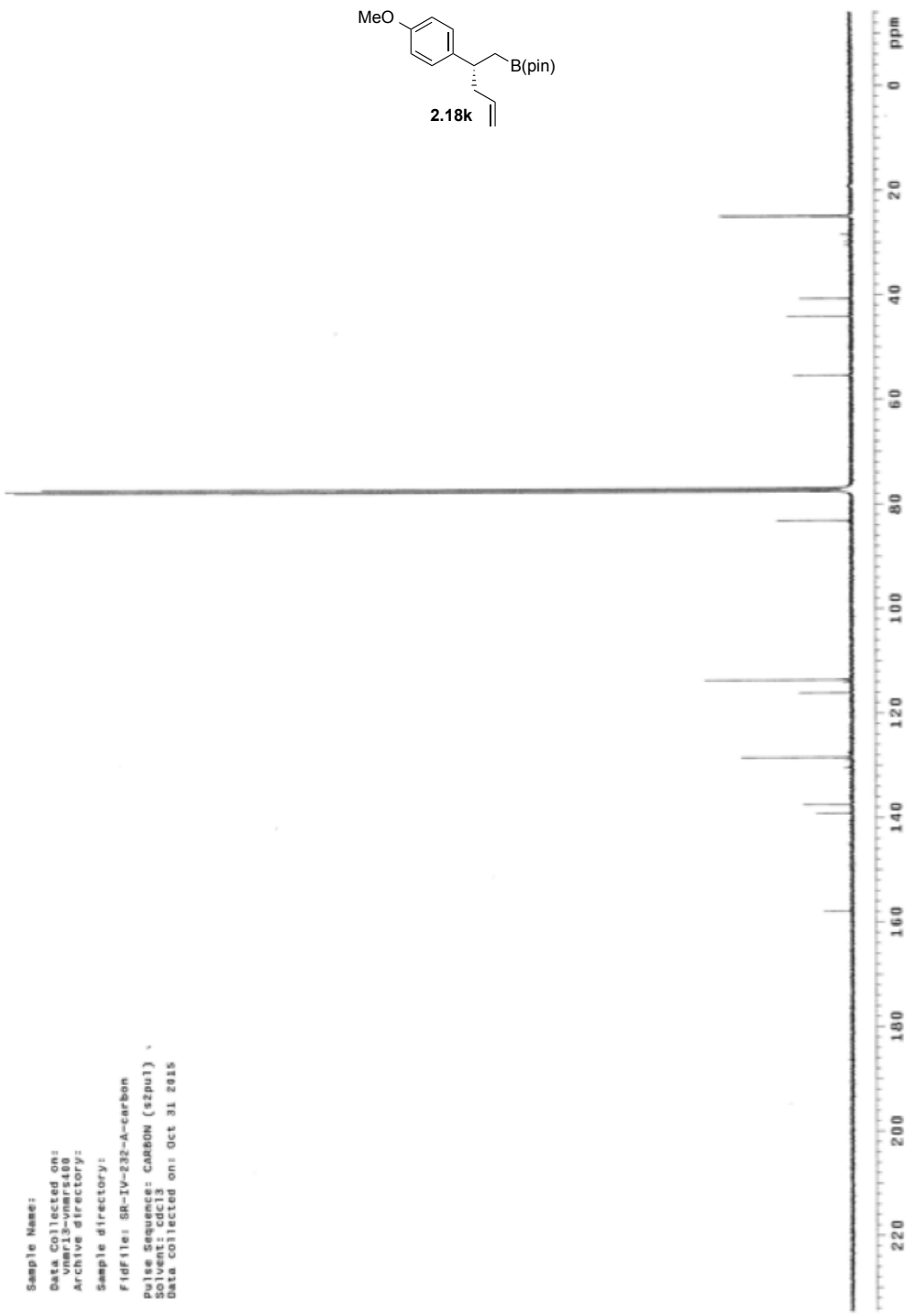
MeO
B(pin)
2.18k
Sample Name:
Data Collected on:
vnmr13-vnmrs400
Archive directory:
Sample directory:
FidFile: SR-IV-232-A-carbon
Pulse Sequence: CARBON (s2pul)
Solvent: cdcl3
Data collected on: Oct 31 2015
ppm
0
20
40
60
80
100
120
140
160
180
200
220

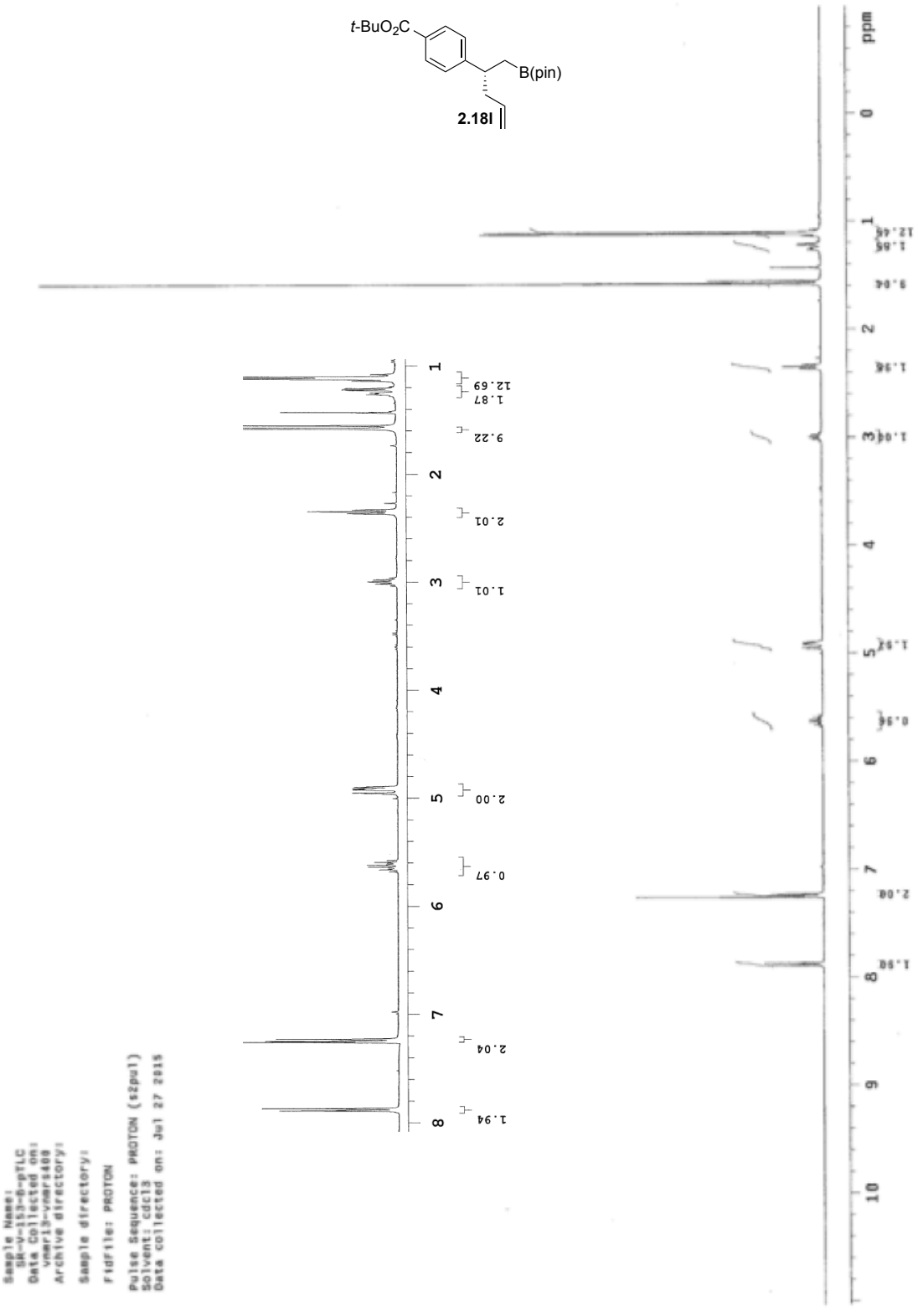
t-BuO2C
B(pin)
2.18l
Sample Name:
SR-V-153-B-pTLC
Data Collected on:
vnmr13-vnmrs400
Archive directory:
Sample directory:
FidFile: PROTON
Pulse Sequence: PROTON (s2pul)
Solvent: cdcl3
Data collected on: Jul 27 2015
ppm
12.65
1.85
9.04
1.96
1.00
1.92
0.94
2.08
1.98
1.87
12.69
9.22
2.01
1.01
2.00
0.97
2.04
1.94

t-BuO2C
B(pin)
2.18l
Sample Name:
SR-V-153-B-carbon
Data Collected on:
vnmr13-vnmrs400
Archive directory:
Sample directory:
FidFile: SR-V-153-carbon
Pulse Sequence: CARBON (s2pul)
Solvent: cdcl3
Data collected on: Jul 27 2015
ppm
0
20
40
60
80
100
120
140
160
180
200
220

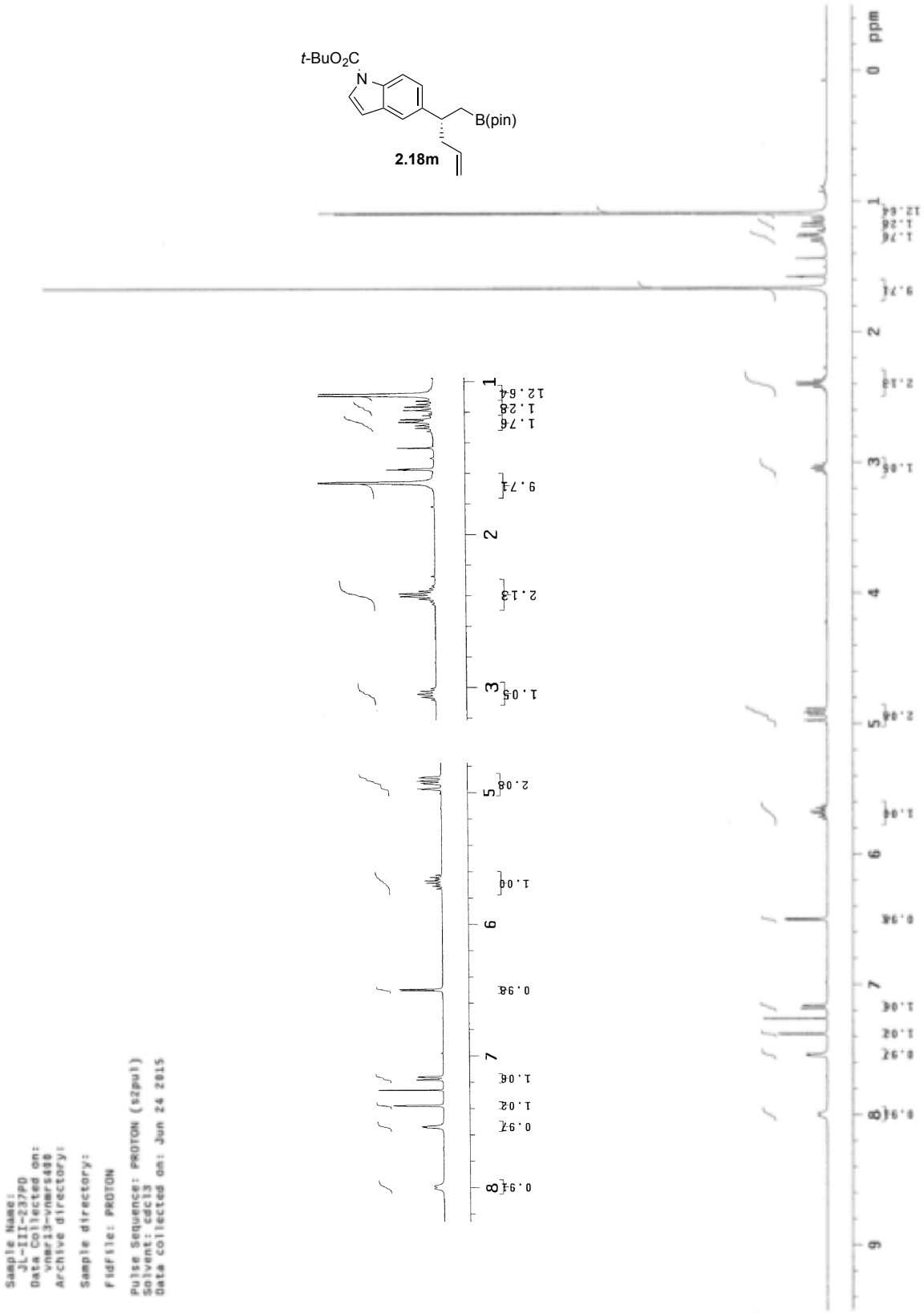
t-BuO2C
N
B(pin)
2.18m
Sample Name:
JL-III-237PD
Data Collected on:
vnmrj3-vnmrs400
Archive directory:
Sample directory:
Fidfile: PROTON
Pulse Sequence: PROTON (s2pul)
Solvent: cdcl3
Data collected on: Jun 24 2015
ppm

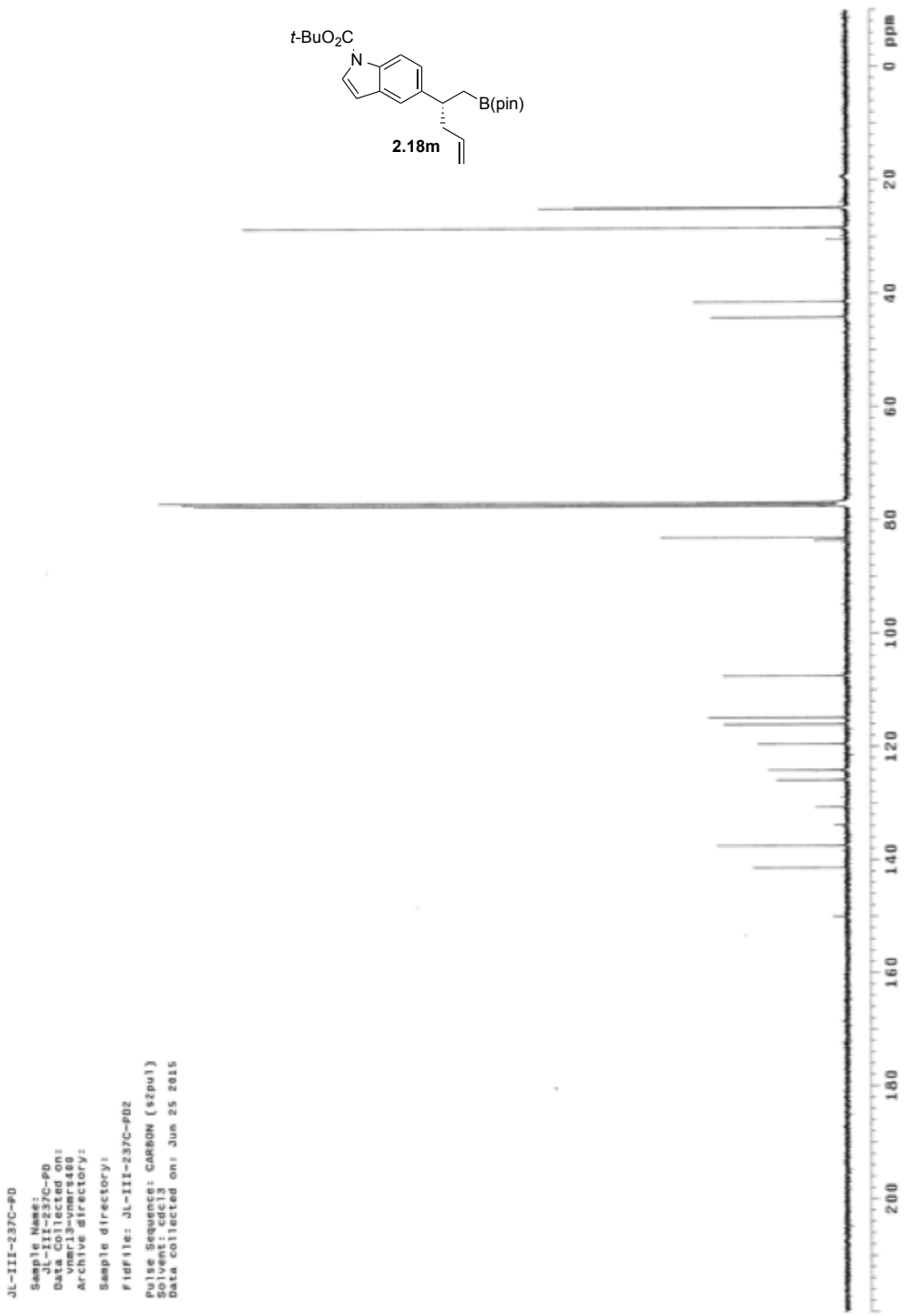
t-BuO2C
N
B(pin)
2.18m
JL-III-237C-PD
Sample Name:
JL-III-237C-PD
Data Collected on:
vnmrj3-vnmrs400
Archive directory:
Sample directory:
FidFile: JL-III-237C-PD2
Pulse Sequence: CARBON (s2pul)
Solvent: cdcl3
Data collected on: Jun 25 2015
200
180
160
140
120
100
80
60
40
20
0 ppm

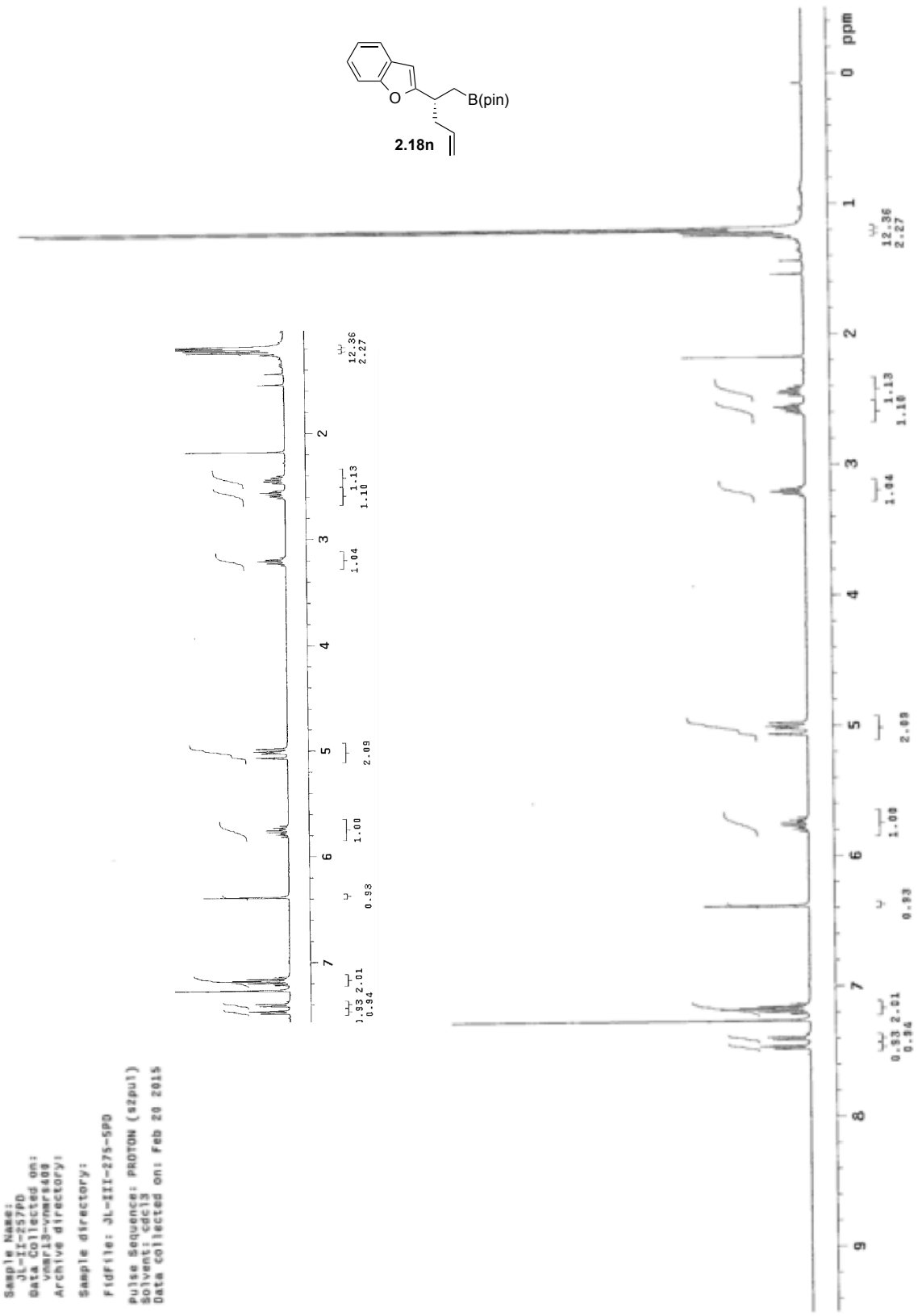
B(pin)
O
2.18n
Sample Name:
JL-II-257PD
Data Collected on:
vnmrj3-vnmrs400
Archive directory:
Sample directory:
Fidfile: JL-III-275-5PD
Pulse Sequence: PROTON (s2pul)
Solvent: cdcl3
Data collected on: Feb 20 2015
ppm

JL-III-127PD-C
Sample Name:
JL-III-127PD-C
Data Collected on:
vnmrj3-vnmrs400
Archive directory:
Sample directory:
FidFile: JL-III-127PD-C
Pulse Sequence: CARBON (s2pul)
Solvent: cdcl3
Data collected on: Mar 20 2015
O
B(pin)
2.18n
200
180
160
140
120
100
80
60
40
20
0 ppm

S
B(pin)

2.18o

Sample Name:
SR-V-139
Data Collected on:
nmr14-ynmrs400
Archive directory:
Sample directory:
FidFile: PROTON
Pulse Sequence: PROTON (s2pul)
Solvent: cdcl3
Data collected on: Jun 26 2015
ppm

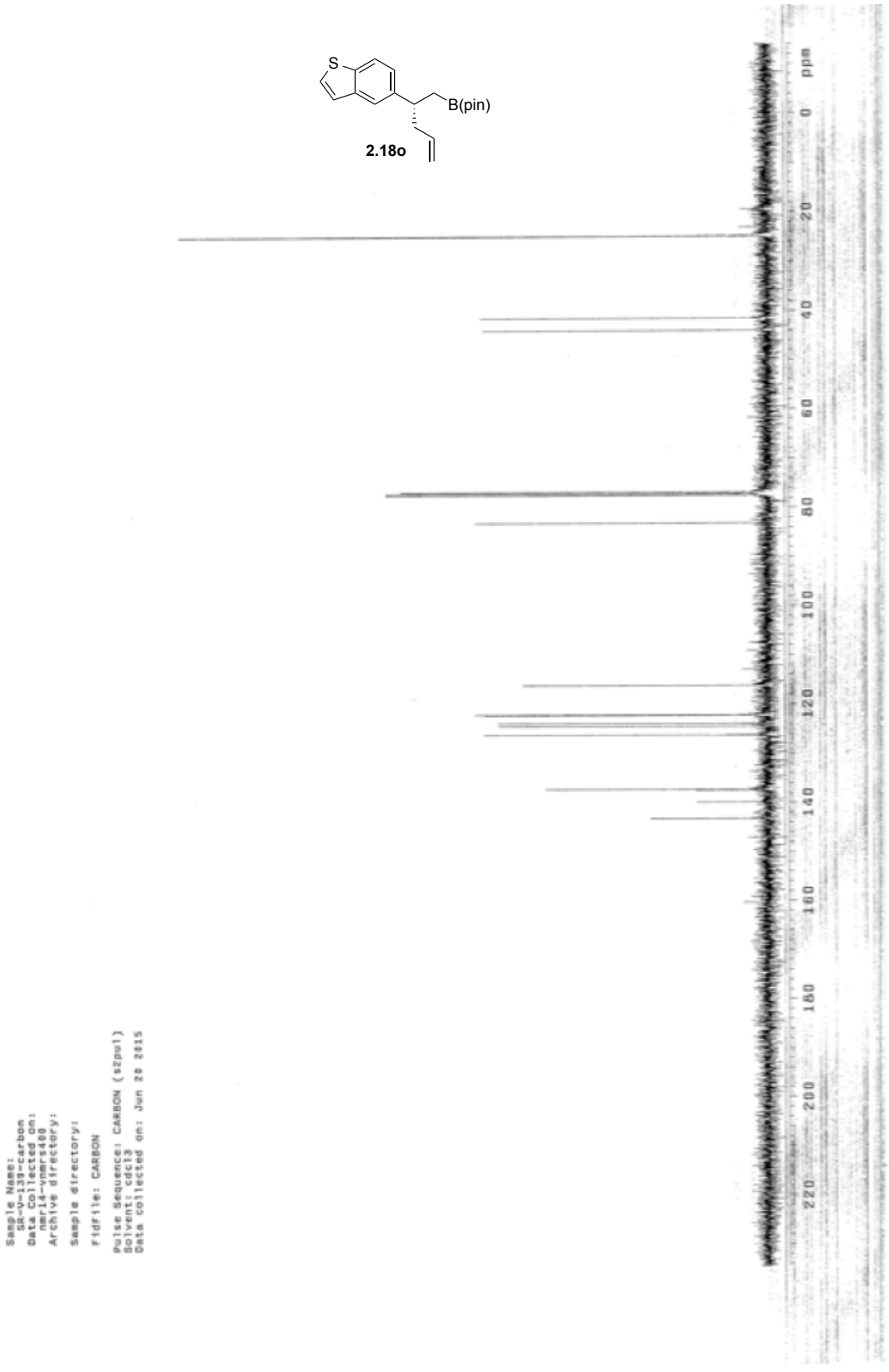
S
B(pin)
2.18o
Sample Name:
SR-V-139-carbon
Data Collected on:
nmr14-vnmrs400
Archive directory:
Sample directory:
Fidfile: CARBON
Pulse Sequence: CARBON (s2pul)
Solvent: cdcl3
Data collected on: Jun 28 2015
ppm

Br
B(pin)
2.18p
Sample Name:
SK-IV-263-3
Data Collected on:
vnmrj3-vnmrs400
Archive directory:
Sample directory:
FidFile: PROTON
Pulse Sequence: PROTON (s2pul)
Solvent: cdcl3
Data collected on: Sep 26 2014
ppm

Br
B(pin)
2.18p
Sample Name:
SR-IV-263-3-carbon
Data Collected on:
vnmr13-vnmrs400
Archive directory:
Sample directory:
FidFile: SR-IV-263-3-carbon
Pulse Sequence: CARBON (s2pul)
Solvent: cdcl3
Data collected on: Sep 26 2014
200
180
160
140
120
100
80
60
40
20
0
ppm

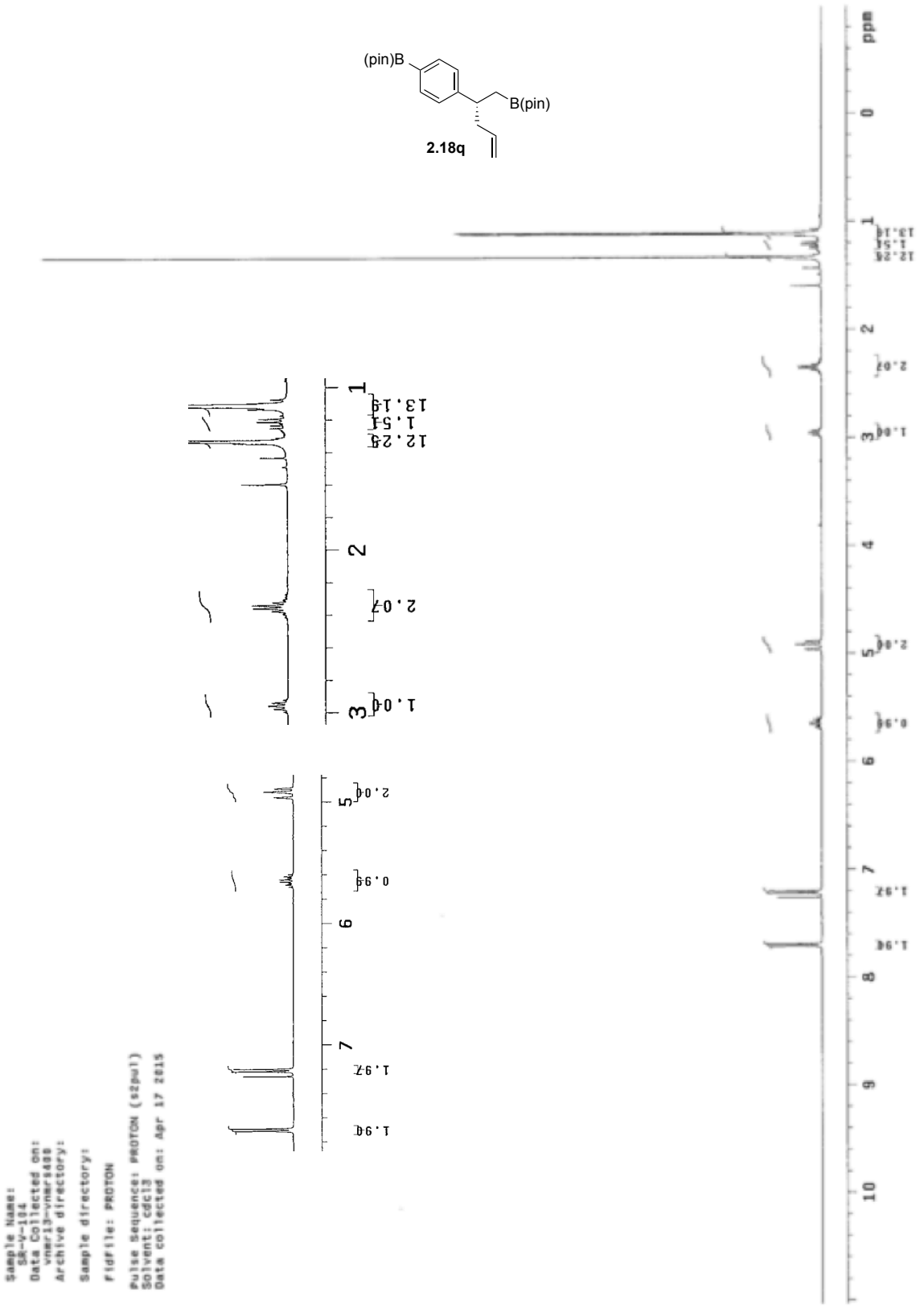
(pin)B
B(pin)
2.18q
Sample Name:
SR-V-104
Data Collected on:
vnmrj3-vnmrs488
Archive directory:
Sample directory:
FidFile: PROTON
Pulse Sequence: PROTON (s2pul)
Solvent: cdcl3
Data collected on: Apr 17 2015
ppm

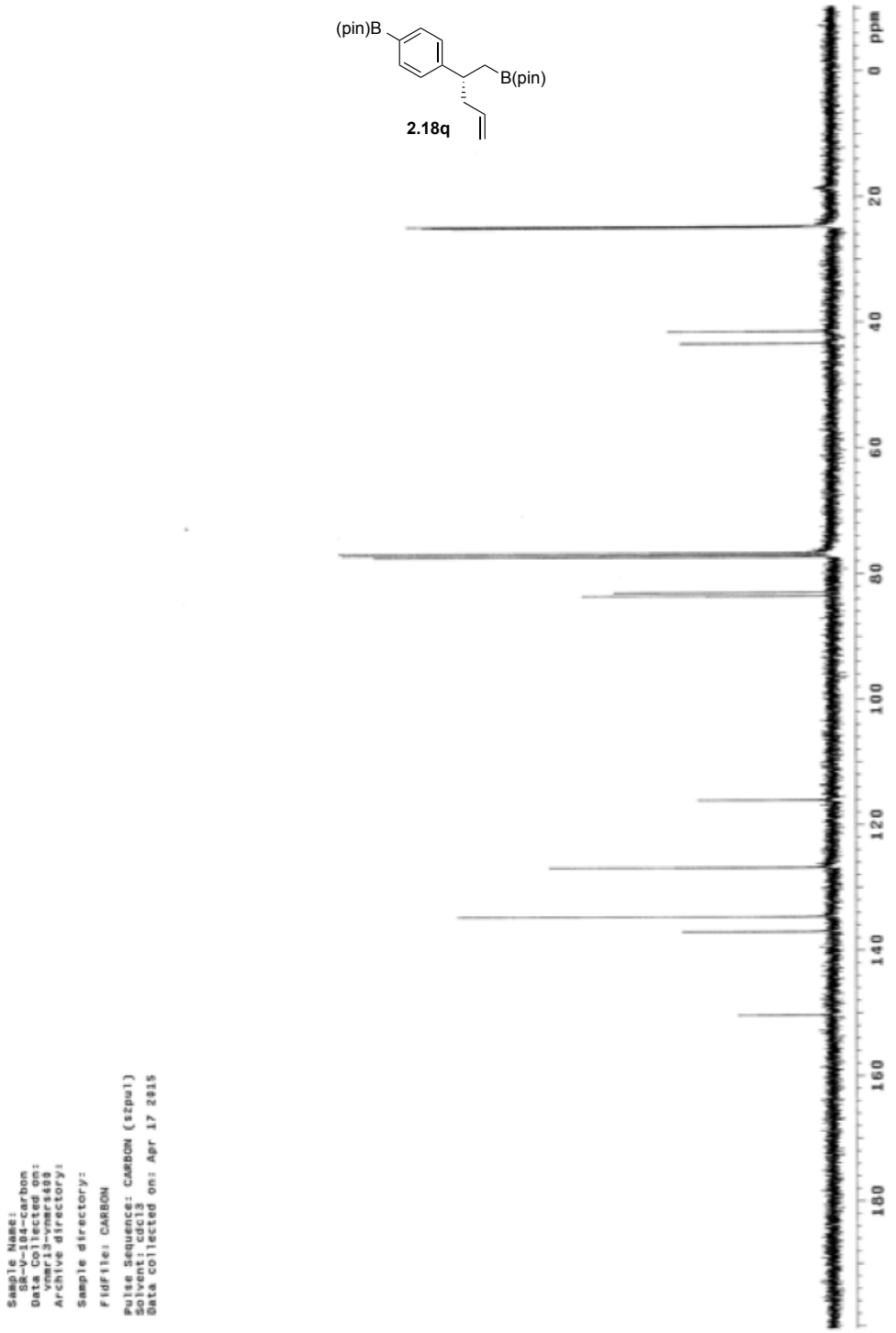
(pin)B
B(pin)
2.18q
Sample Name:
SR-V-104-carbon
Data Collected on:
vnmrj3-vnmrs400
Archive directory:
Sample directory:
FidFile: CARBON
Pulse Sequence: CARBON (s2pul)
Solvent: cdcl3
Data collected on: Apr 17 2015
ppm
0
20
40
60
80
100
120
140
160
180

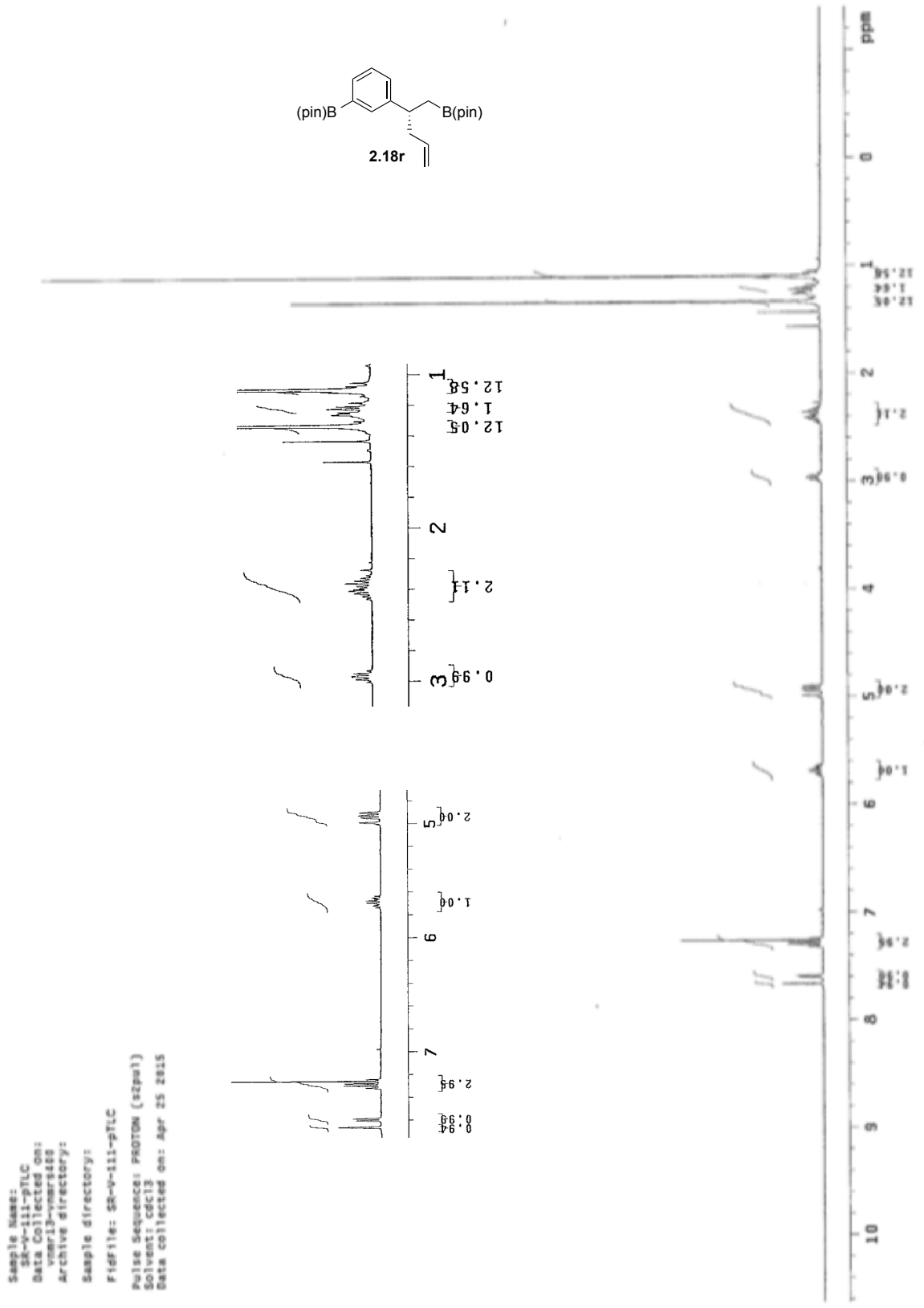
(pin)B
B(pin)
2.18r
Sample Name:
SR-V-111-pTLC
Data Collected on:
vnmr13-vnmr5400
Archive directory:
Sample directory:
FidFile: SR-V-111-pTLC
Pulse Sequence: PROTON (s2pul)
Solvent: cdcl3
Data collected on: Apr 25 2015
ppm

(pin)B
B(pin)
2.18r

Sample Name:
SR-V-111-carbon
Data Collected on:
vnmr13-vnmrs400
Archive directory:
Sample directory:
FidFile: CARBON
Pulse Sequence: CARBON (s2pul)
Solvent: cdcl3
Data collected on: Apr 25 2015
220
200
180
160
140
120
100
80
60
40
20
0
ppm

Sample Name:
JL-III-195PD-1
Data Collected on:
vnmrj3-vnmrs400
Archive directory:
Sample directory:
FidFile: PROTON
Pulse Sequence: PROTON (s2pul)
Solvent: cdcl3
Data collected on: May 21 2015
B(pin)
2.18s
ppm

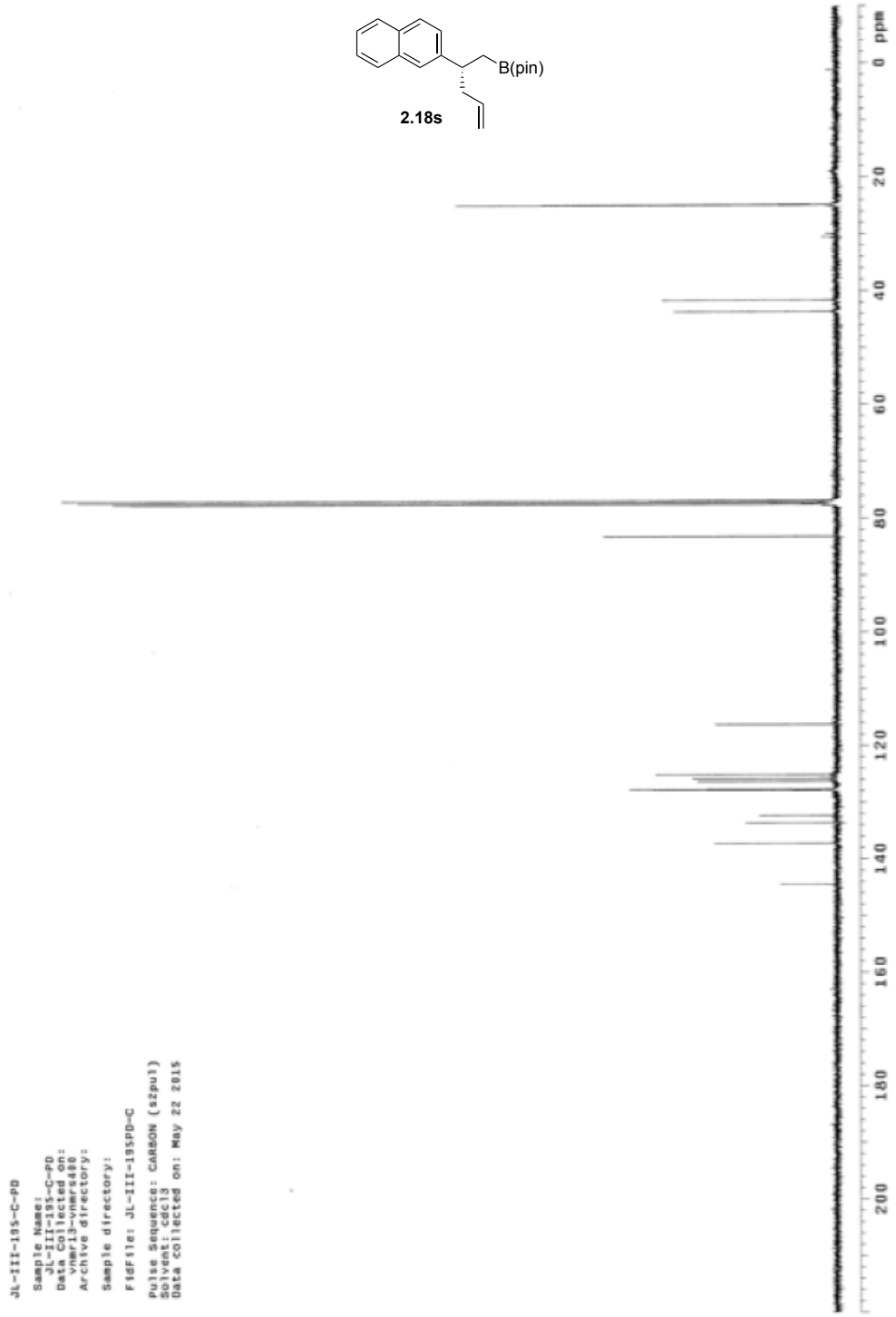
B(pin)
2.18s
JL-III-195-C-PD
Sample Name:
JL-III-195-C-PD
Data Collected on:
vnmrj3-vnmrs400
Archive directory:
Sample directory:
FidFile: JL-III-195PD-C
Pulse Sequence: CARBON (s2pul)
Solvent: cdcl3
Data collected on: May 22 2015
0 ppm
20
40
60
80
100
120
140
160
180
200

B(pin)
Ph
2.18t
Sample Name:
SR-IV-292
Data Collected on:
vnmrj3-vmars400
Archive directory:
Sample directory:
Fidfile: PROTON
Pulse Sequence: PROTON (s2pul)
Solvent: cdcl3
Data collected on: Oct 28 2014
ppm

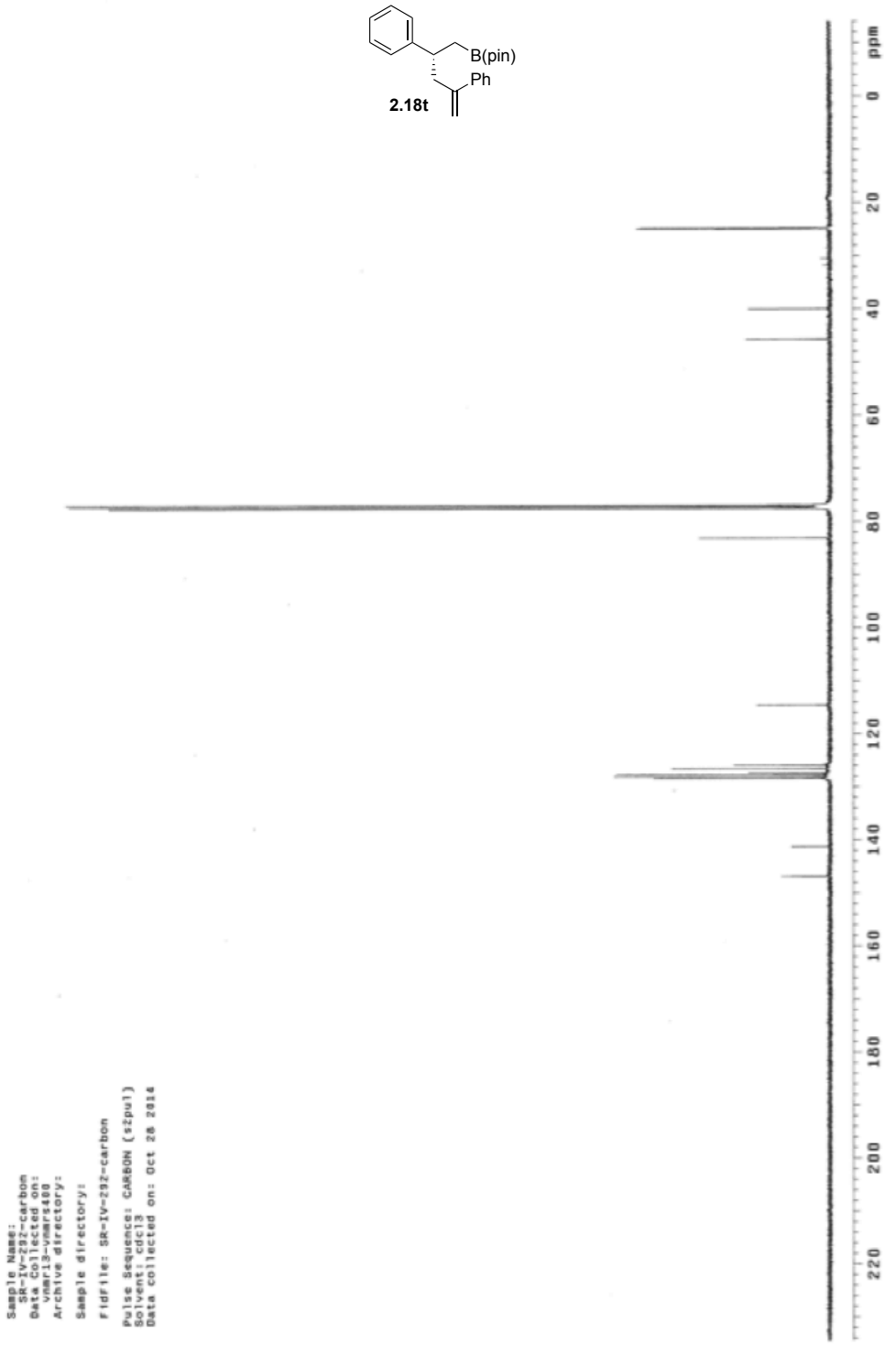
B(pin)
Ph
2.18t
Sample Name:
SR-IV-292-carbon
Data Collected on:
vnmr13-vmars400
Archive directory:
Sample directory:
FidFile: SR-IV-292-carbon
Pulse Sequence: CARBON (s2pul)
Solvent: cdcl3
Data collected on: Oct 28 2014
220
200
180
160
140
120
100
80
60
40
20
0
ppm

B(pin)
Me
2.18u

Sample Name:
Data Collected on:
vnmr13-vnmrs400
Archive directory:
Sample directory:
Fidfile: Ph-Me-product
Pulse Sequence: PROTON (s2pul)
Solvent: cdcl3
Data collected on: Jan 13 2015
ppm

B(pin)
Me
2.18u

Sample Name:
Data Collected on:
vnmr13-vnmrs400
Archive directory:
Sample directory:
FidFile: CARBON
Pulse Sequence: CARBON (s2pul)
Solvent: cdcl3
Data collected on: Jan 13 2015
ppm
0
20
40
60
80
100
120
140
160
180
200
220

B(pin)
SiMe3
2.18v
Sample Name:
SR-IV-302
Data Collected on:
vnmrj3-vnmrs400
Archive directory:
Sample directory:
FidFile: PROTON
Pulse Sequence: PROTON (s2pul)
Solvent: cdcl3
Data collected on: Jan 14 2015
ppm

B(pin)
SiMe3
2.18v
ppm
0
20
40
60
80
100
120
140
160
180
200
220
Sample Name:
SR-IV-302-carbon
Data Collected on:
vnmrj3-vnmrs400
Archive directory:
Sample directory:
Fidfile: CARBON
Pulse Sequence: CARBON (s2pul)
Solvent: cdcl3
Data collected on: Jan 14 2015

B(pin)
SiMe3
2.18w
Sample Name:
SA-V-46
Data Collected on:
maria-vnmrs500
Archive directory:
Sample directory:
Fidfile: PROTON
Pulse Sequence: PROTON (s2pul)
Solvent: cdcl3
Data collected on: Jan 18 2015
ppm

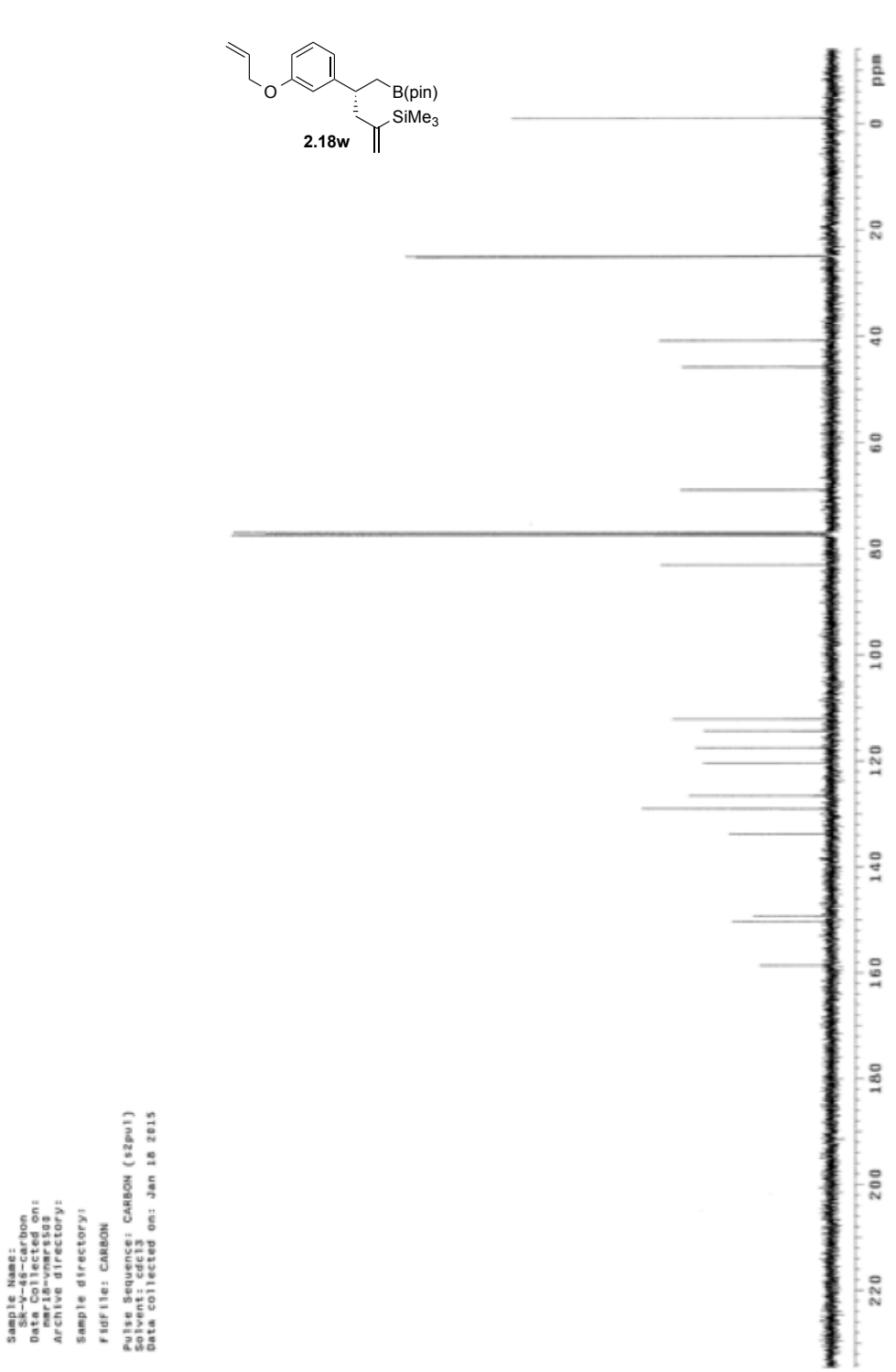
B(pin)
SiMe3
2.18w
ppm
0
20
40
60
80
100
120
140
160
180
200
220
Sample Name:
SK-V-46-carbon
Data Collected on:
mar18-vnmrs500
Archive directory:
Sample directory:
FidFile: CARBON
Pulse Sequence: CARBON (s2pul)
Solvent: cdcl3
Data collected on: Jan 18 2015

B(pin)
F
2.18x
Sample Name:
SR-IV-265-A
Data Collected on:
vnmrj3-vnmrs400
Archive directory:
Sample directory:
FidFile: PROTON
Pulse Sequence: PROTON (s2pul)
Solvent: cdcl3
Data collected on: Oct 1 2014
ppm

B(pin)
F
2.18x
ppm
0
20
40
60
80
100
120
140
160
180
200
220
Sample Name:
SR-IV-265-A-carbon
Data Collected on:
ynmr13-ynmrs400
Archive directory:
Sample directory:
fidfile: CARBON
Pulse Sequence: CARBON (s2pul)
Solvent: cdcl3
Data collected on: Oct 1 2014

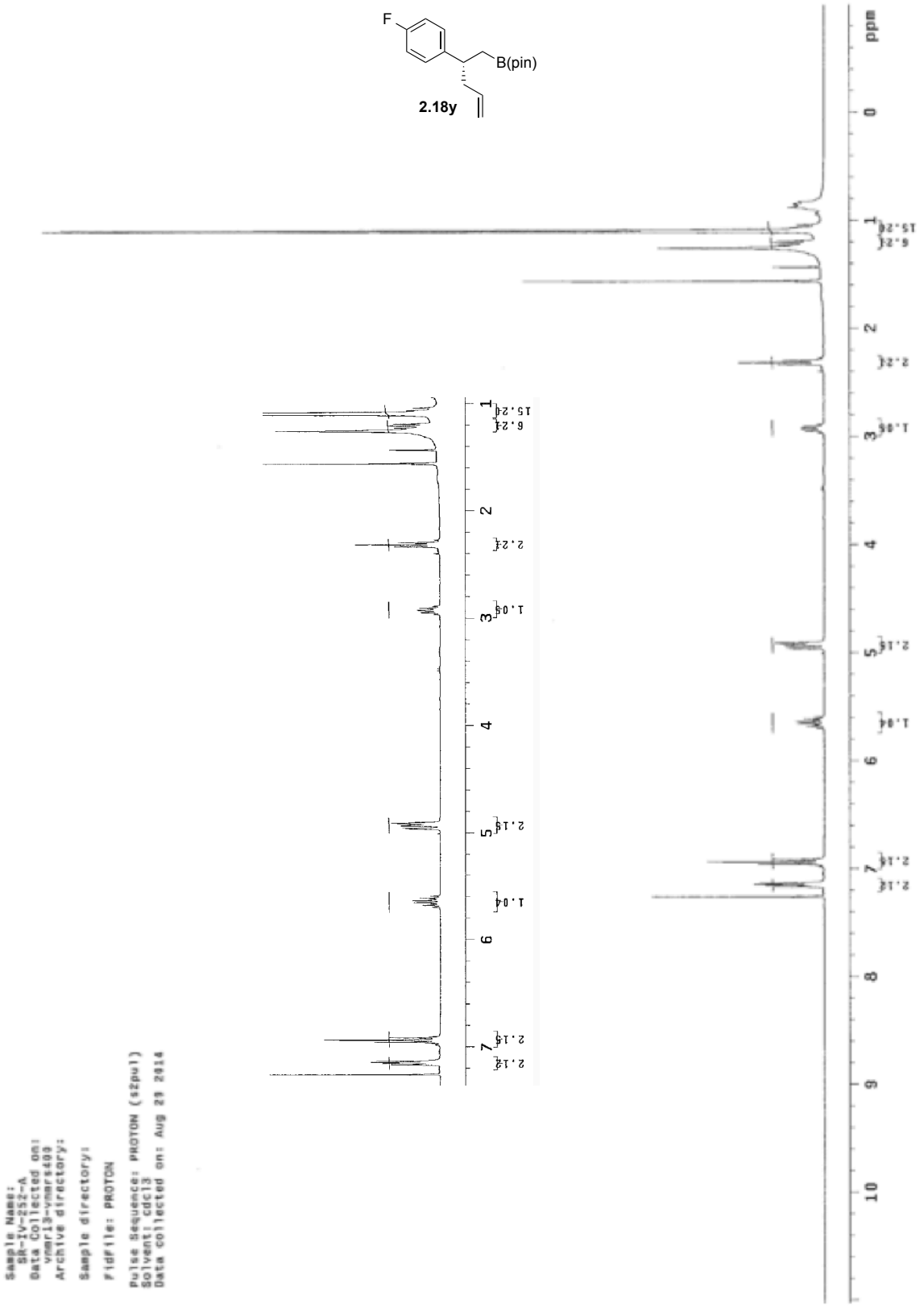
F
B(pin)
2.18y
ppm
Sample Name:
SR-IV-252-A
Data Collected on:
vnmr13-vnmrs499
Archive directory:
Sample directory:
FidFile: PROTON
Pulse Sequence: PROTON (s2pul)
Solvent: cdcl3
Data collected on: Aug 29 2014

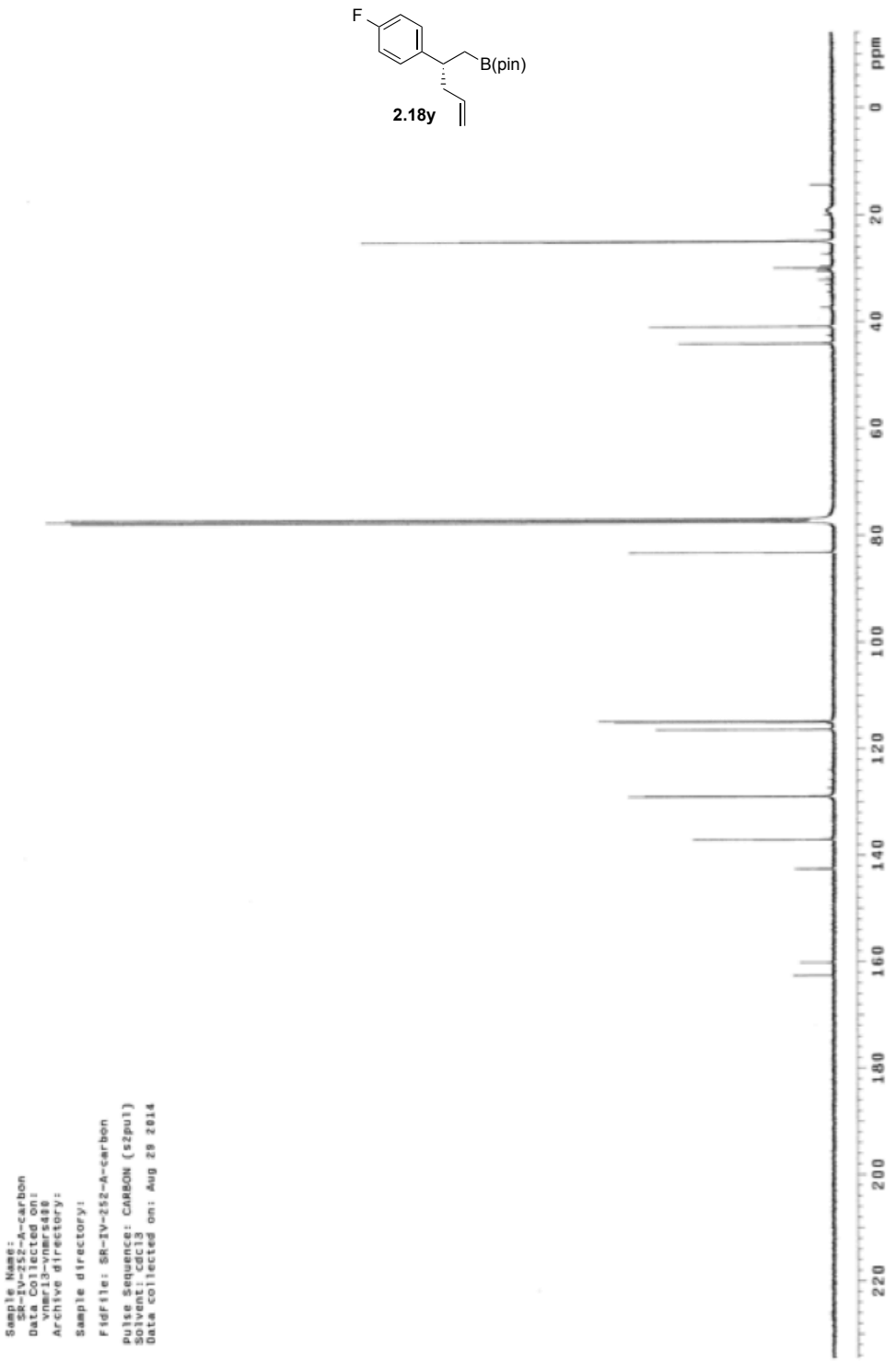
F
B(pin)
2.18y
ppm
0
20
40
60
80
100
120
140
160
180
200
220
Sample Name:
SR-IV-252-A-carbon
Data Collected on:
vnmr13-vnmrs400
Archive directory:
Sample directory:
FidFile: SR-IV-252-A-carbon
Pulse Sequence: CARBON (s2pul)
Solvent: CdCl3
Data collected on: Aug 29 2014

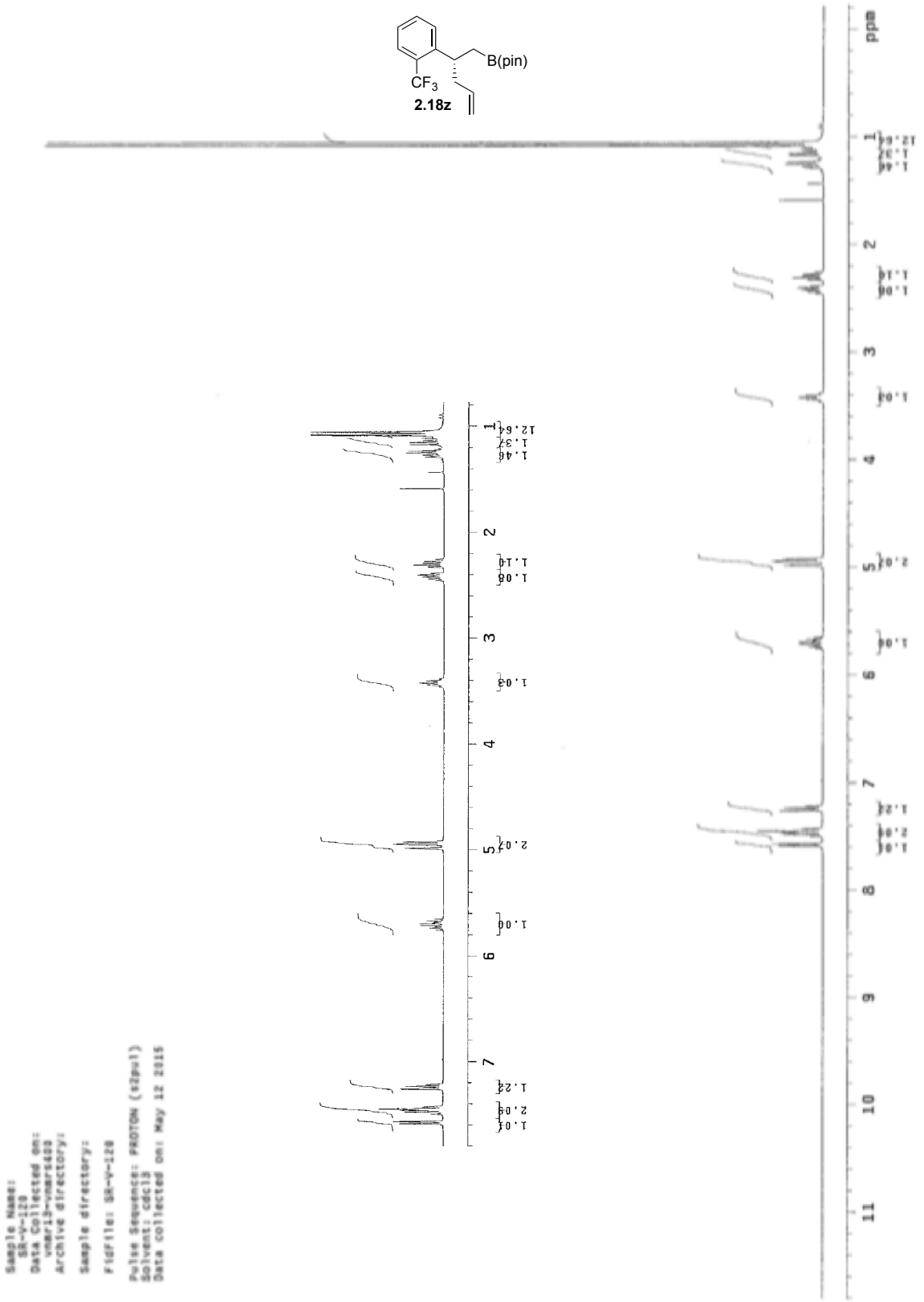
B(pin)
CF3
2.18z
Sample Name:
SR-v-128
Data Collected on:
vnmrj3-vmars449
Archive directory:
Sample directory:
Fidfile: SR-v-128
Pulse Sequence: PROTON (s2pul)
Solvent: cdcl3
Data collected on: May 12 2015
ppm

B(pin)
CF3
2.18z
Sample Name:
Data Collected on:
vnmr13-vnmrs480
Archive directory:
Sample directory:
FidFile: CARBON
Pulse Sequence: CARBON (s2pul)
Solvent: cdcl3
Data collected on: May 12 2015
ppm
0
20
40
60
80
100
120
140
160
180
200
220

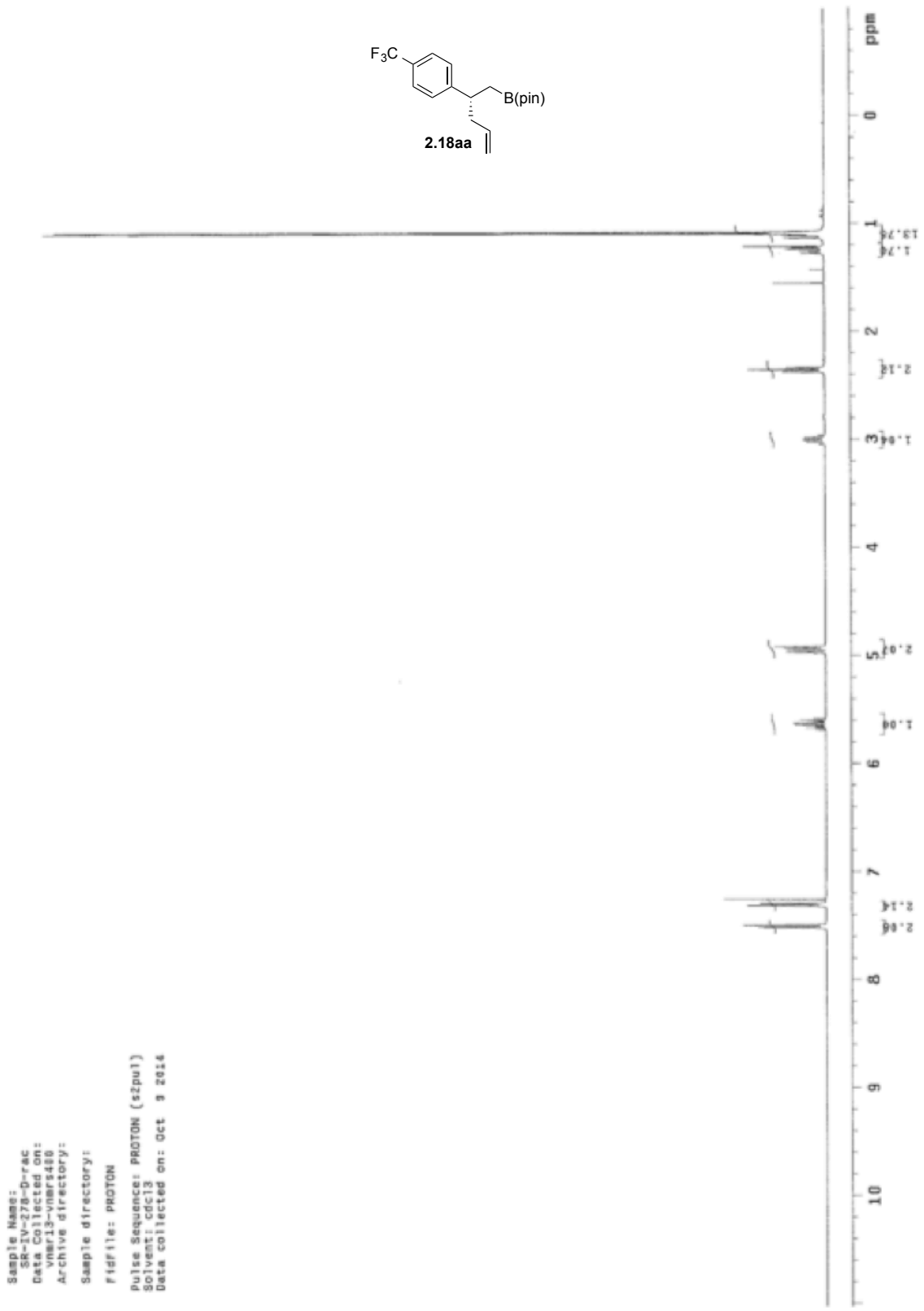
F3C
B(pin)
2.18aa
Sample Name:
SR-IV-278-D-rac
Data Collected on:
vnmr13-vnmrs400
Archive directory:
Sample directory:
FidFile: PROTON
Pulse Sequence: PROTON (s2pul)
Solvent: cdcl3
Data collected on: Oct 9 2014
ppm
13.74
1.74
2.12
1.96
2.02
1.04
2.14
2.06

JL-IV-169-2PD

Sample Name:
JL-IV-169-2PD
Data Collected on:
nmr13-vnmrs400
Archive directory:

Sample directory:

FidFile: JL-IV-169PD-2

Pulse Sequence: PROTON (s2pul)
Solvent: cdcl3
Data collected on: Jan 21 2016

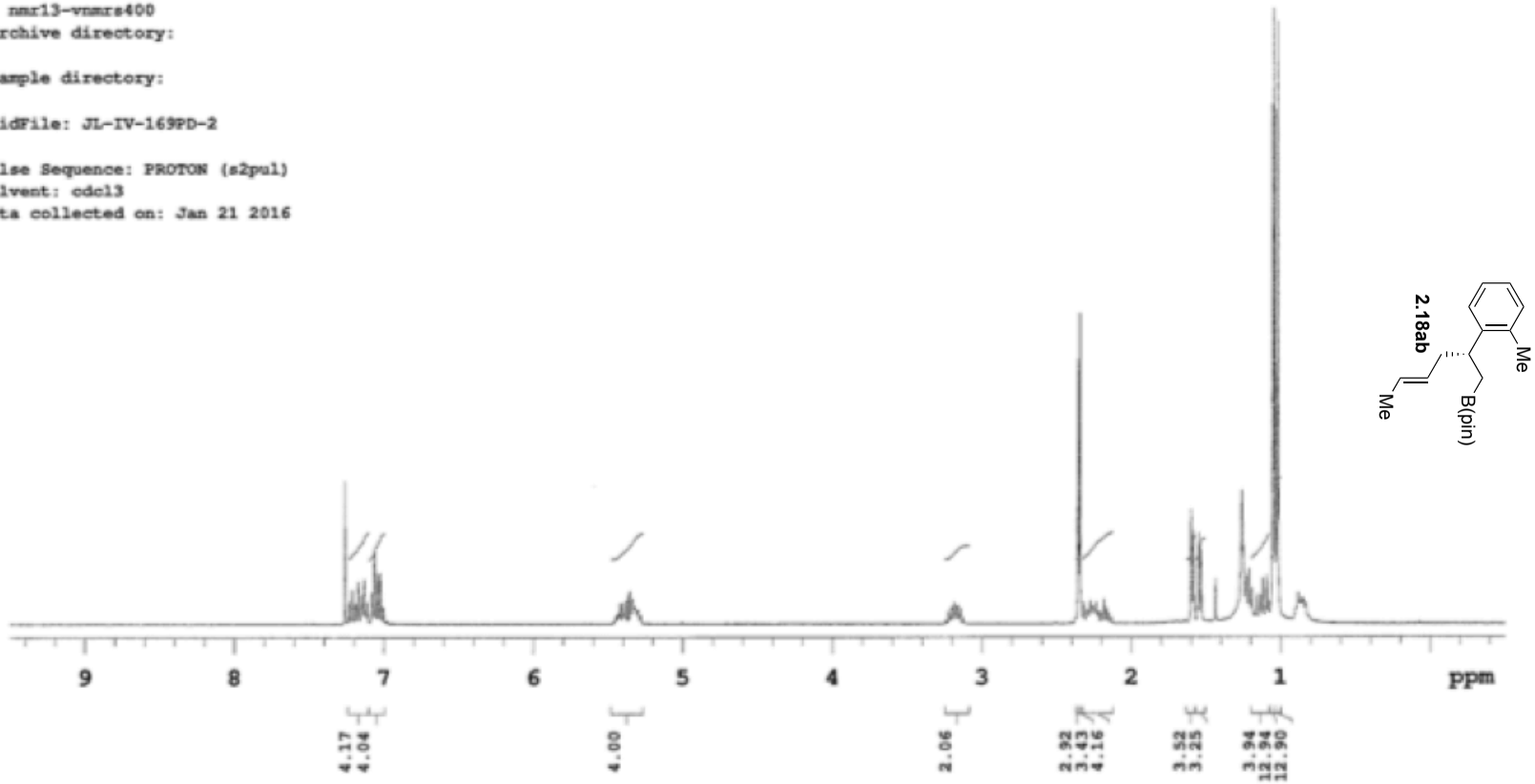

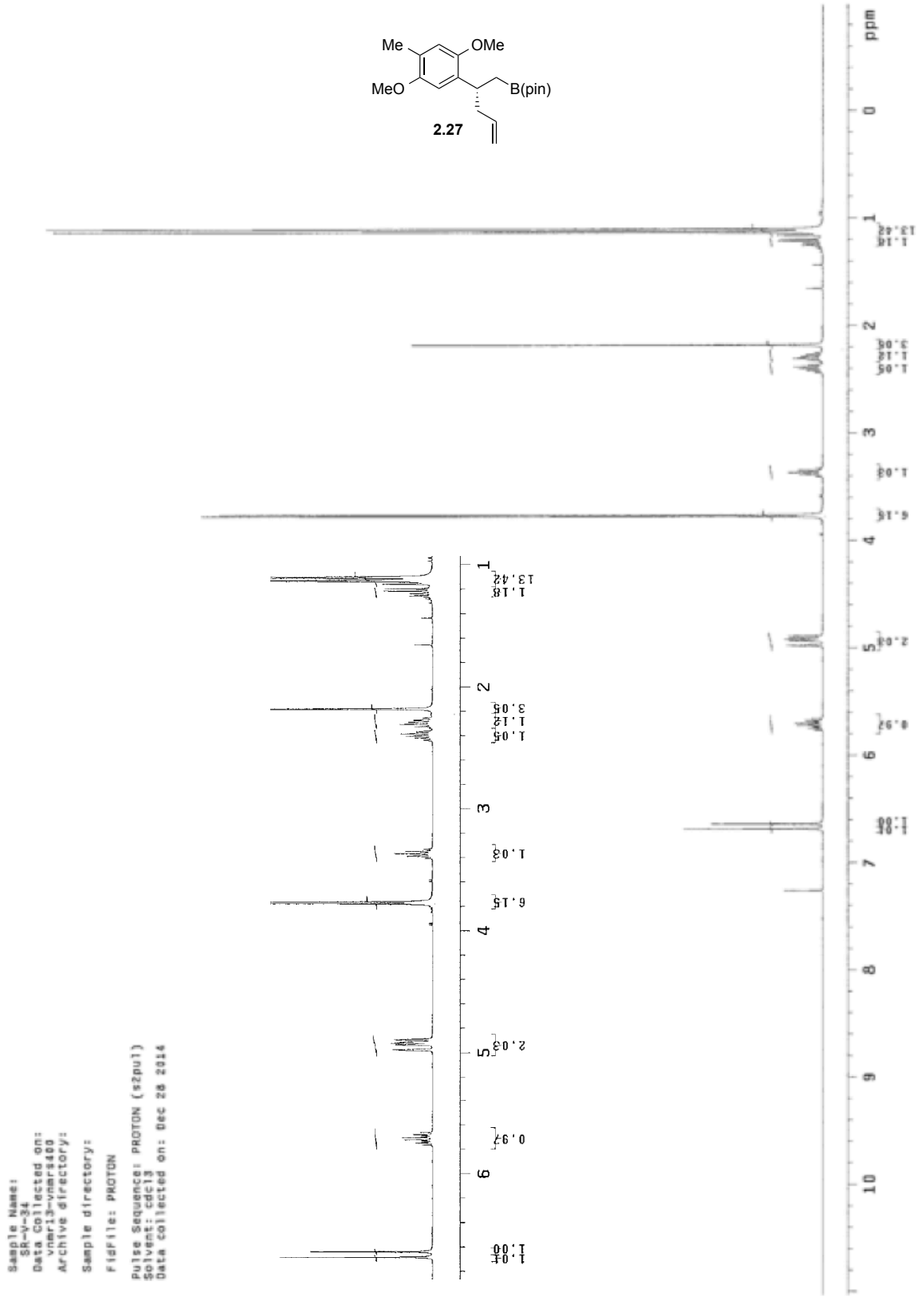
Me
OMe
MeO
B(pin)
2.27
Sample Name:
SR-V-34
Data Collected on:
vnmr13-vnmrs400
Archive directory:
Sample directory:
FidFile: PROTON
Pulse Sequence: PROTON (s2pul)
Solvent: cdcl3
Data collected on: Dec 28 2014
ppm

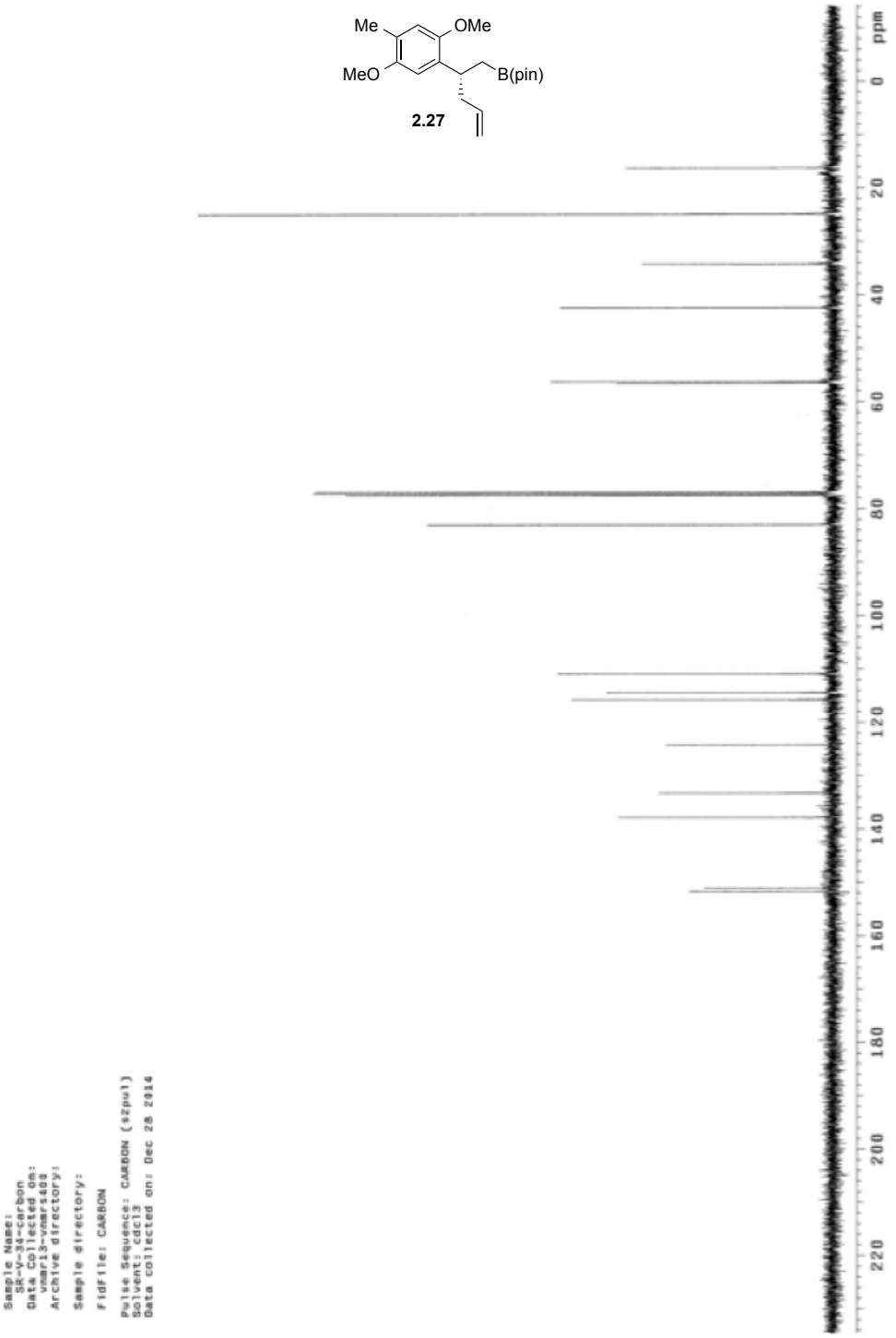
Me
OMe
MeO
B(pin)
2.27
ppm
0
20
40
60
80
100
120
140
160
180
200
220
Sample Name:
SR-V-34-carbon
Data Collected on:
vnmrj3-vmars400
Archive directory:
Sample directory:
Fidfile: CARBON
Pulse Sequence: CARBON (s2pul)
Solvent: cdcl3
Data collected on: Dec 28 2014

Me
OMe
MeO
B(pin)
2.30
Me
Me
Sample Name:
SR-V-36
Data collected on:
nmr18-vnmrs400
Archive directory:
Sample directory:
FidFile: SR-V-36
Pulse Sequence: PROTON (s2pul)
Solvent: cdcl3
Data collected on: Feb 18 2015
ppm

Me
OMe
MeO
B(pin)
2.30
Me
Me
ppm
0
20
40
60
80
100
120
140
160
180
200
220
Sample Name:
SR-V-36-carbon
Data Collected on:
mar14-vnmrs100
Archive directory:
Sample directory:
fidfile: CARBON
Pulse Sequence: CARBON (s2pul)
Solvent: cdcl3
Data collected on: Feb 18 2015

Me
OMe
MeO
OH
OH
2.33
Me
Me
OH
Sample Name:
SR-V-69-5
Data Collected on:
vnmrj3-vnmrs400
Archive directory:
Sample directory:
Fidfile: PROTON
Pulse Sequence: PROTON (s2pul)
Solvent: cdcl3
Data collected on: Mar 20 2015
ppm

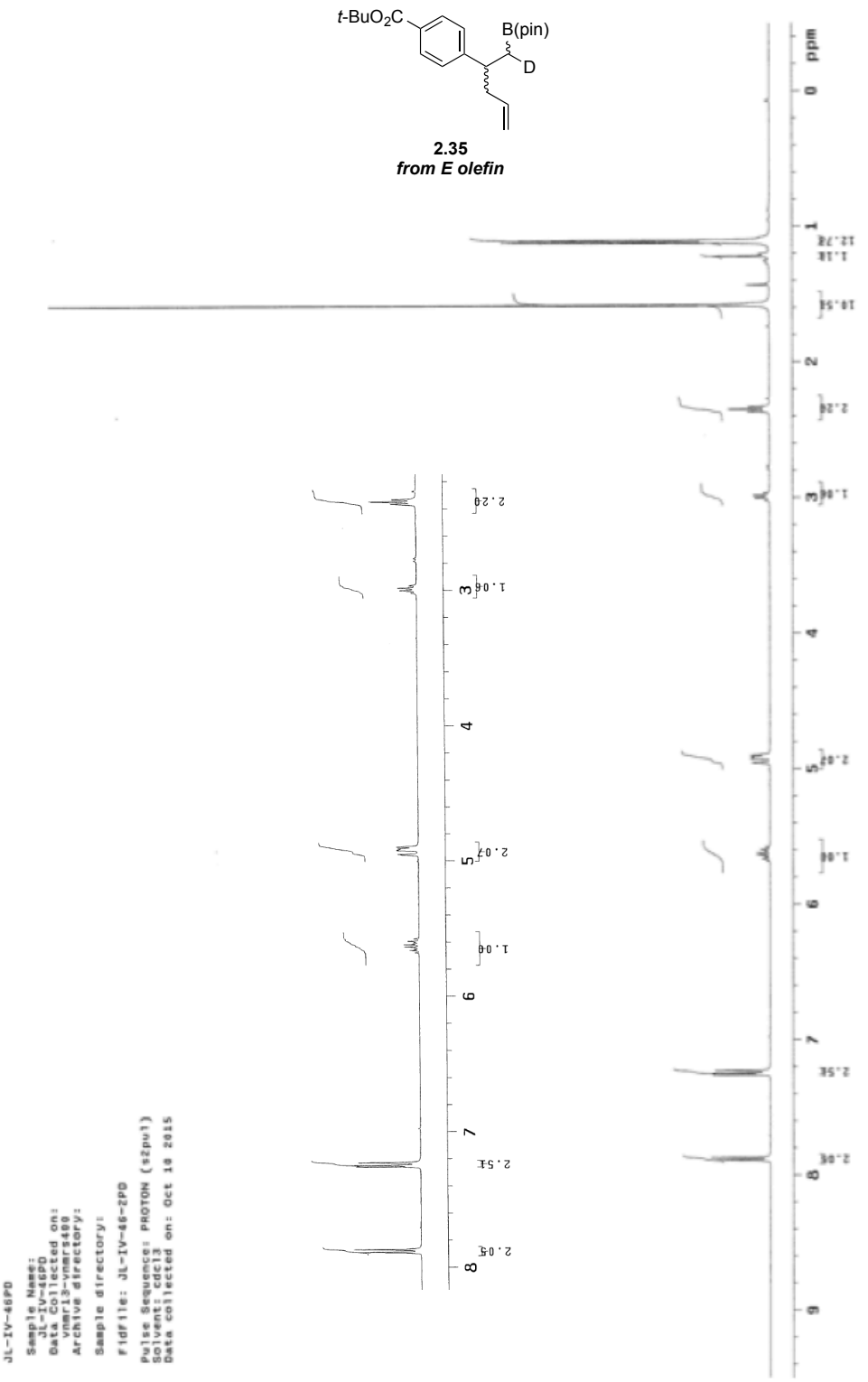
t-BuO2C
B(pin)
D
2.35
from E olefin
JL-IV-46PD
Sample Name:
JL-IV-46PD
Data Collected on:
vnmr13-vnmrs400
Archive directory:
Sample directory:
FidFile: JL-IV-46-2PD
Pulse Sequence: PROTON (s2pul)
Solvent: cdcl3
Data collected on: Oct 10 2015
ppm

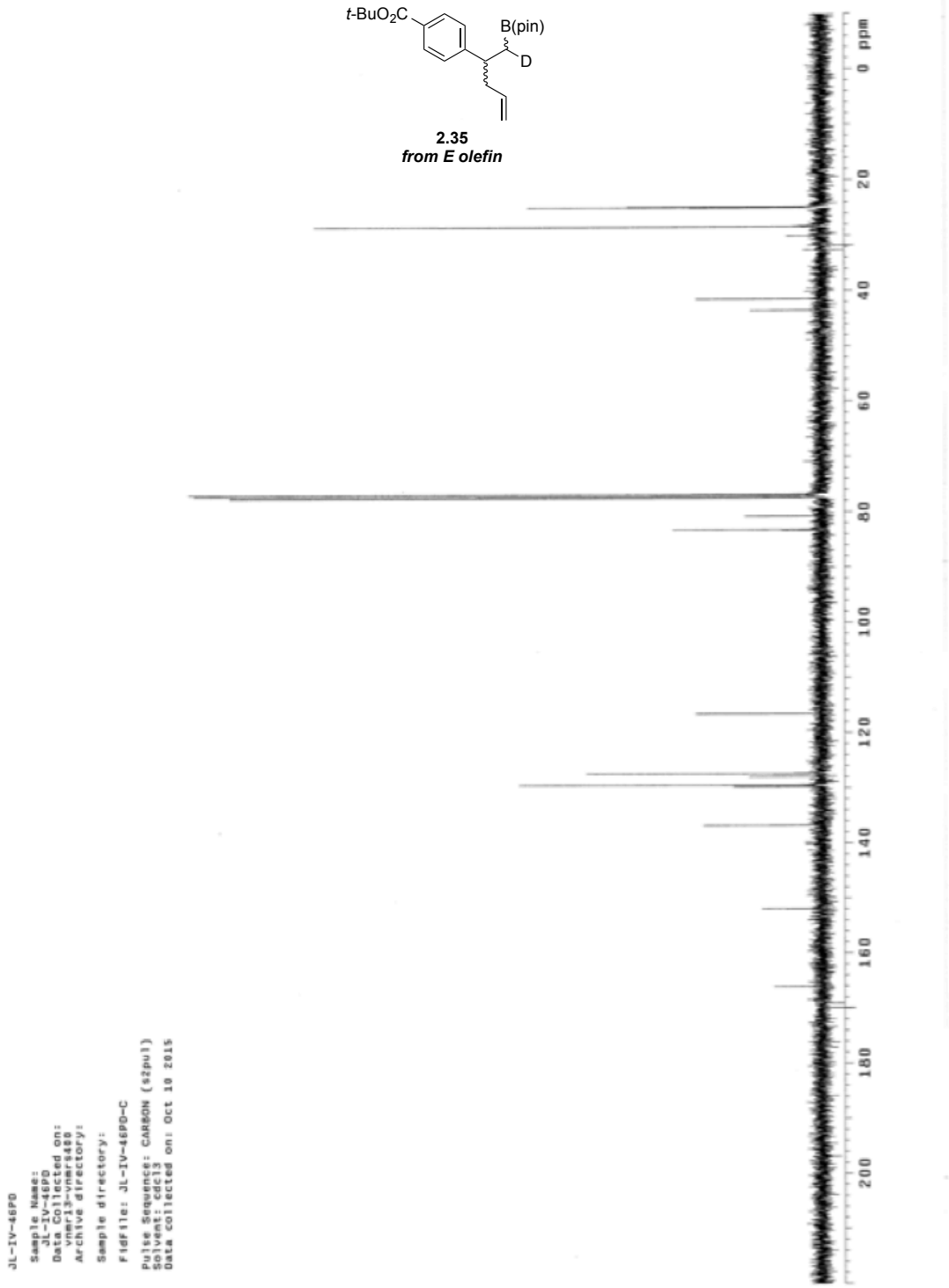
t-BuO2C
B(pin)
D
2.35
from E olefin
JL-IV-46PD
Sample Name:
JL-IV-46PD
Data Collected on:
vnmr13-vnmrs480
Archive directory:
Sample directory:
Fidfile: JL-IV-46PD-C
Pulse Sequence: CARBON (s2pul)
Solvent: cdcl3
Data collected on: Oct 10 2015
0 ppm
20
40
60
80
100
120
140
160
180
200

oxidation product of 2.35
from E olefin
60:40 d.r.

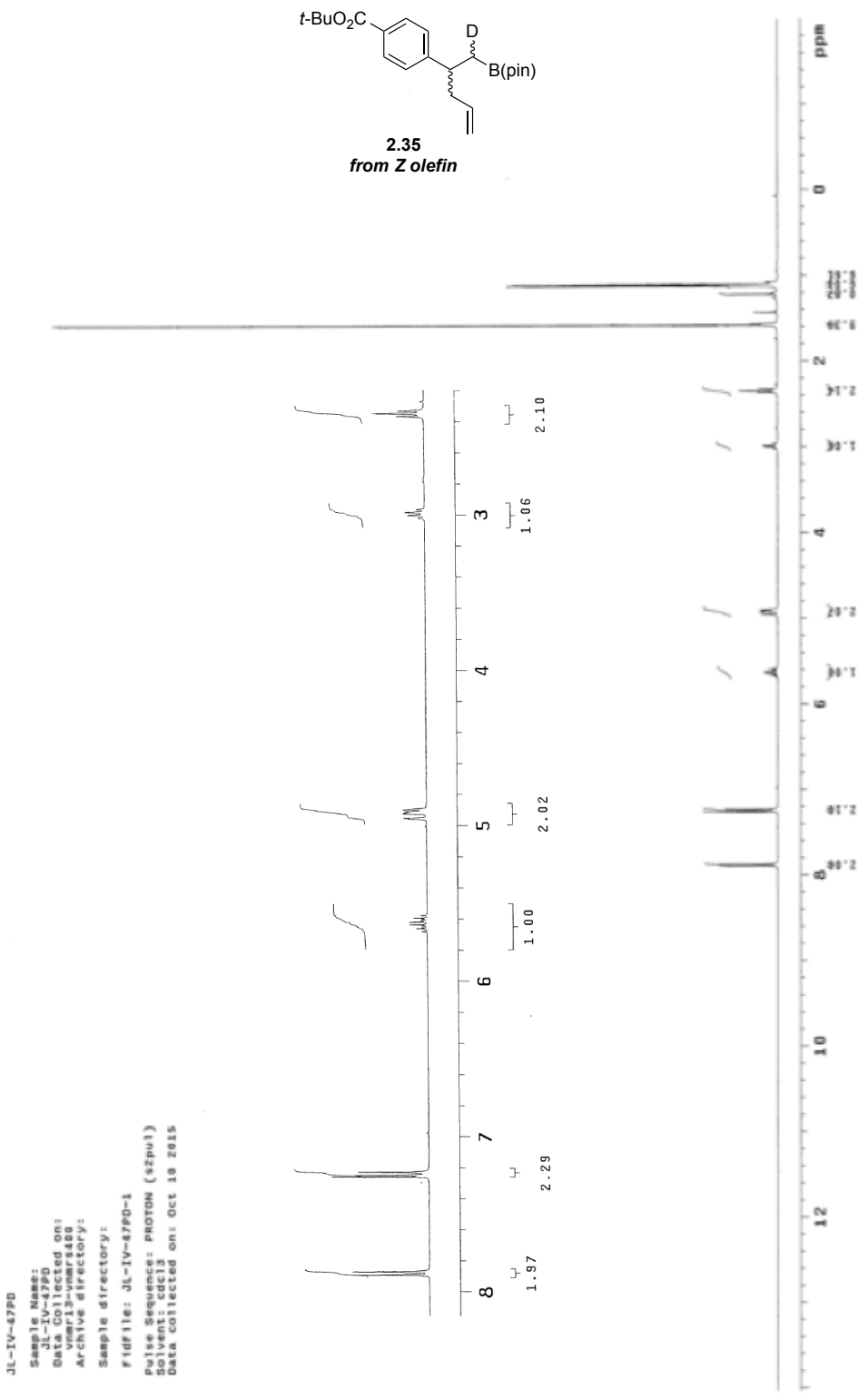
t-BuO2C
D
B(pin)
2.35
from Z olefin
JL-IV-47PD
Sample Name:
JL-IV-47PD
Data Collected on:
vnmr13-vmars480
Archive directory:
Sample directory:
FidFile: JL-IV-47PD-1
Pulse Sequence: PROTON (s2pul)
Solvent: cdcl3
Data collected on: Oct 10 2015
1.97
2.29
1.00
2.02
1.06
2.10
ppm

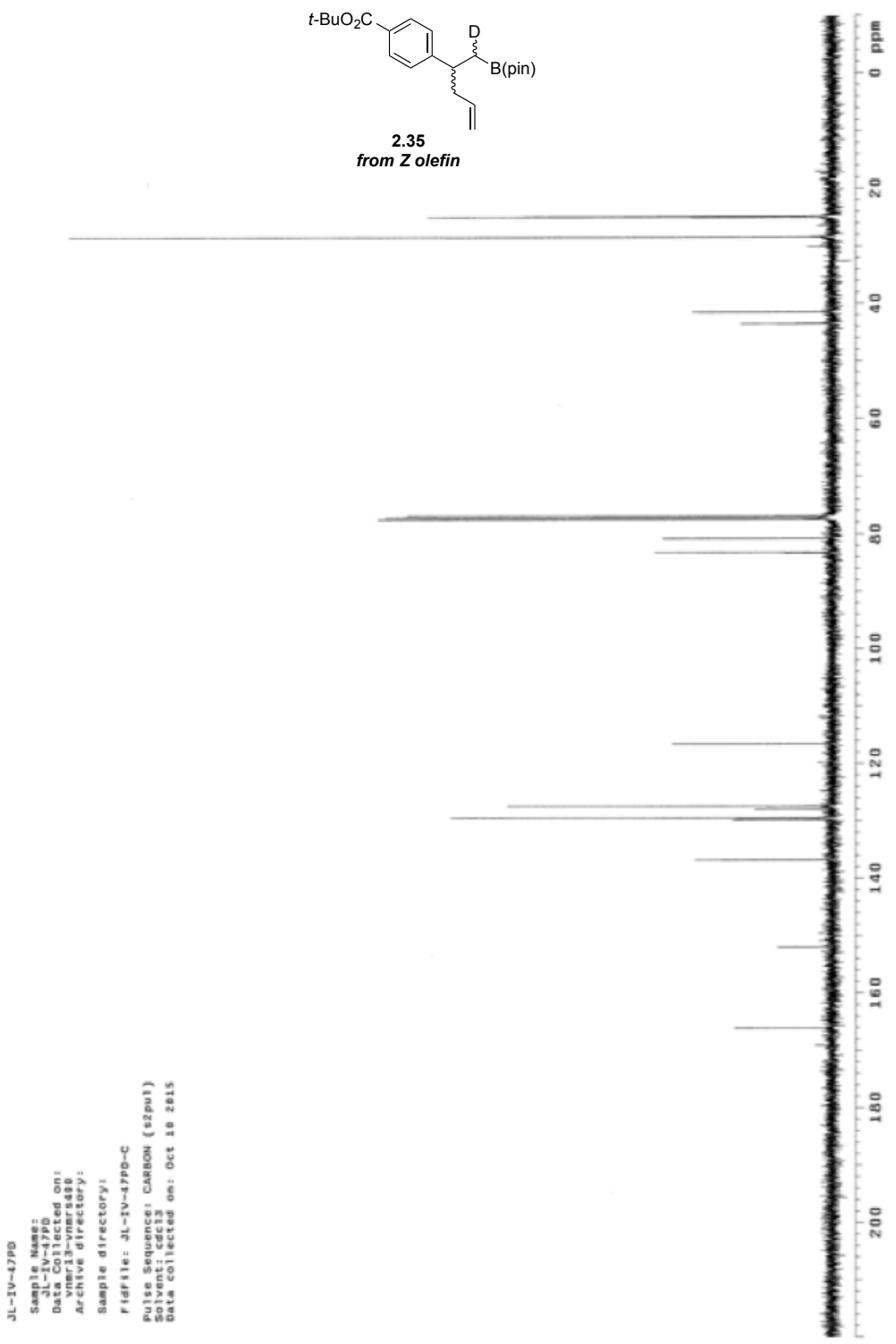
t-BuO2C
D
B(pin)
2.35
from Z olefin
JL-IV-47PD
Sample Name:
JL-IV-47PD
Data Collected on:
vnmr13-vnmrs400
Archive directory:
Sample directory:
FidFile: JL-IV-47PD-C
Pulse Sequence: CARBON (s2pul)
Solvent: cdcl3
Data collected on: Oct 10 2015
0 ppm
20
40
60
80
100
120
140
160
180
200

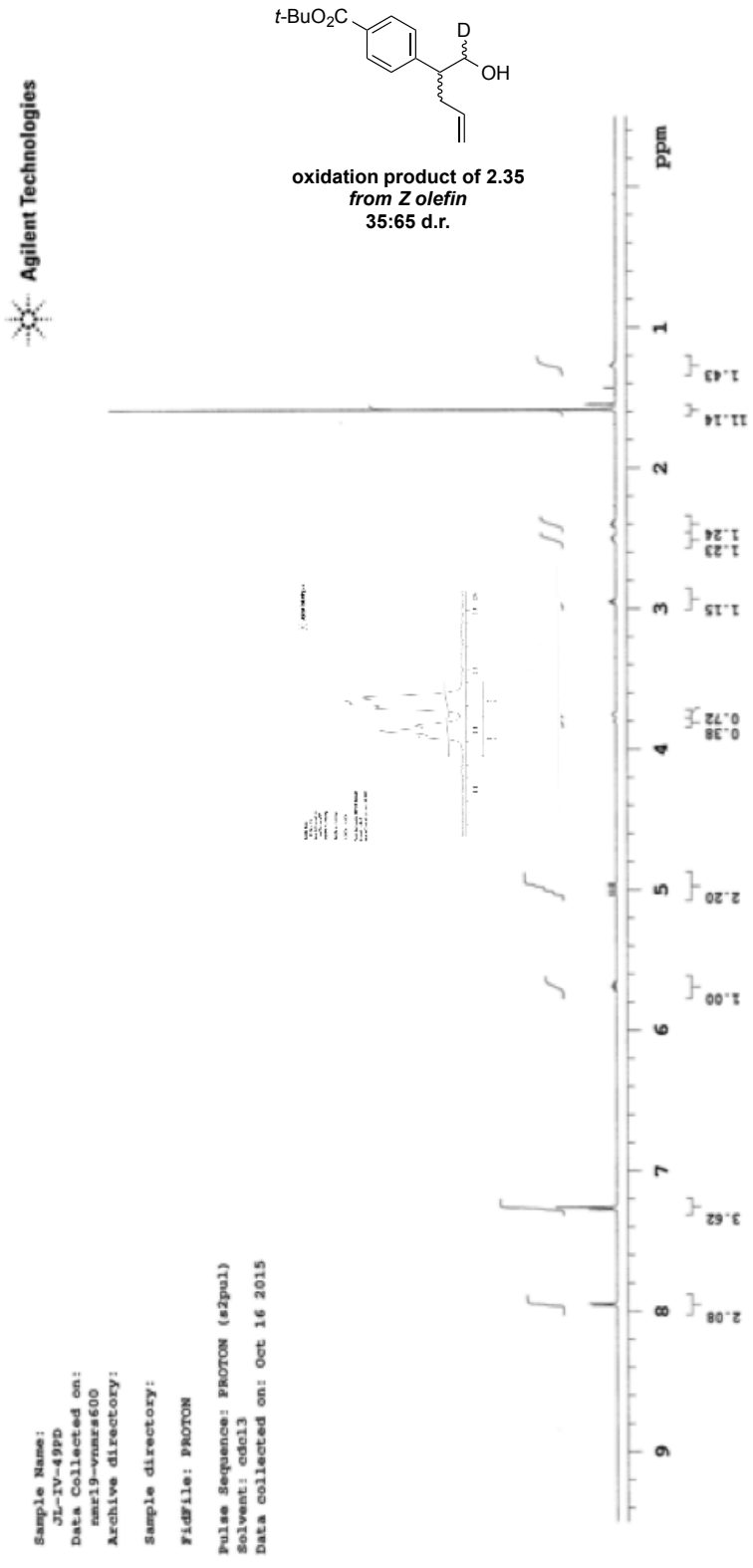
t-BuO2C
D
OH
oxidation product of 2.35
from Z olefin
35:65 d.r.
Agilent Technologies
Sample Name:
JL-IV-49PD
Data Collected on:
nmr19-vnmrs600
Archive directory:
Sample directory:
FidFile: PROTON
Pulse Sequence: PROTON (s2pul)
Solvent: cdcl3
Data collected on: Oct 16 2015
ppm
1.43
11.14
1.23
1.24
1.15
0.38
0.72
2.20
1.00
3.62
2.08

Br

S9

JL-IV-57PD
Sample Name:
JL-IV-57PD
Data Collected on:
vnmrj3-vnmrs400
Archive directory:
Sample directory:
FidFile: JL-IV-57PD
Pulse Sequence: PROTON (s2pul)
Solvent: cdcl3
Data collected on: Oct 30 2015
ppm
1
2
3
4
5
6
7
8
9
2.23
2.25
1.00
2.10
2.93

JL-IV-67CD
Sample Name:
JL-IV-67CD
Data Collected on:
vnmr13-vnmrs400
Archive directory:
Sample directory:
FidFile: JL-IV-67PD
Pulse Sequence: PROTON (s2pul)
Solvent: cdcl3
Data collected on: Nov 5 2015
t-BuO2C
2.36
ppm
1
2
3
4
5
6
7
8
9
9.36
2.88
2.32
1.00
2.14
1.92

JL-IV-67CD
Sample Name:
JL-IV-67CD
Data Collected on:
vnmr13-vnmr400
Archive directory:
Sample directory:
FidFile: JL-IV-67PD-C
Pulse Sequence: CARBON (s2pul)
Solvent: cdcl3
Data collected on: Nov 5 2015
220
200
180
160
140
120
100
80
60
40
20
ppm

t-BuO2C

2.36

t-BuO2C
B(pin)
2.38
JL-IV-72-2PD
Sample Name:
JL-IV-72-2PD
Data Collected on:
vnmr13-vnmrs400
Archive directory:
Sample directory:
FidFile: JL-IV-72-2PD
Pulse Sequence: PROTON (s2pul)
Solvent: cdcl3
Data collected on: Nov 6 2015
ppm

JL-IV-72PD-C
Sample Name:
JL-IV-72PD-C
Data Collected on:
nmr13-vnmrs400
Archive directory:
Sample directory:
FidFile: CARBON
Pulse Sequence: CARBON (s2pul)
Solvent: cdcl3
Data collected on: Nov 12 2015
t-BuO2C
B(pin)
2.38
ppm
220
200
180
160
140
120
100
80
60
40
20

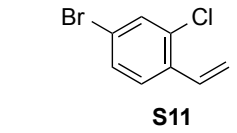

S11

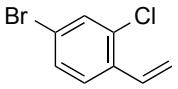

S11

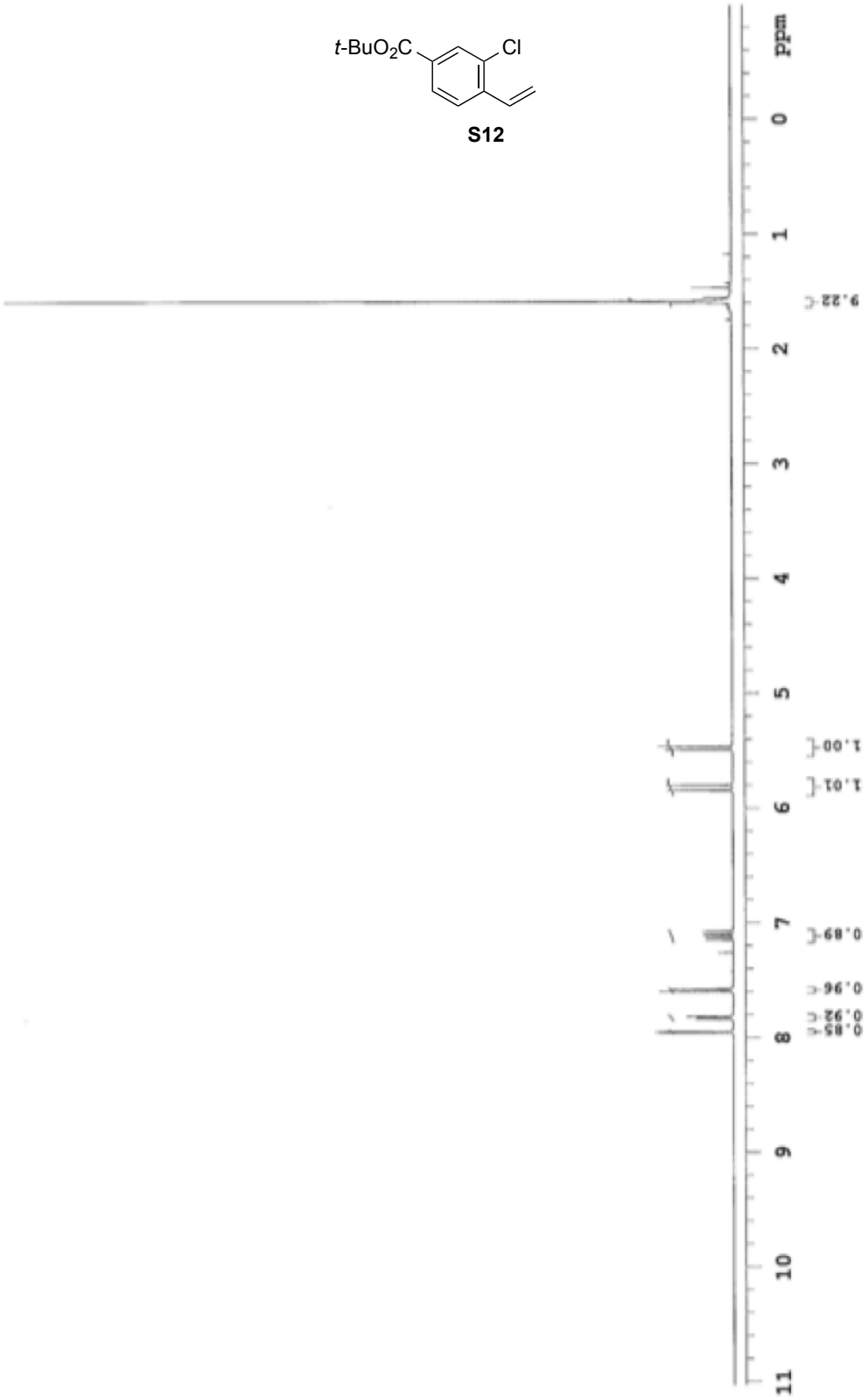
t-BuO2C
Cl
S12
ppm
0
1
2
3
4
5
6
7
8
9
10
11
9.22
1.00
1.01
0.89
0.96
0.92
0.85

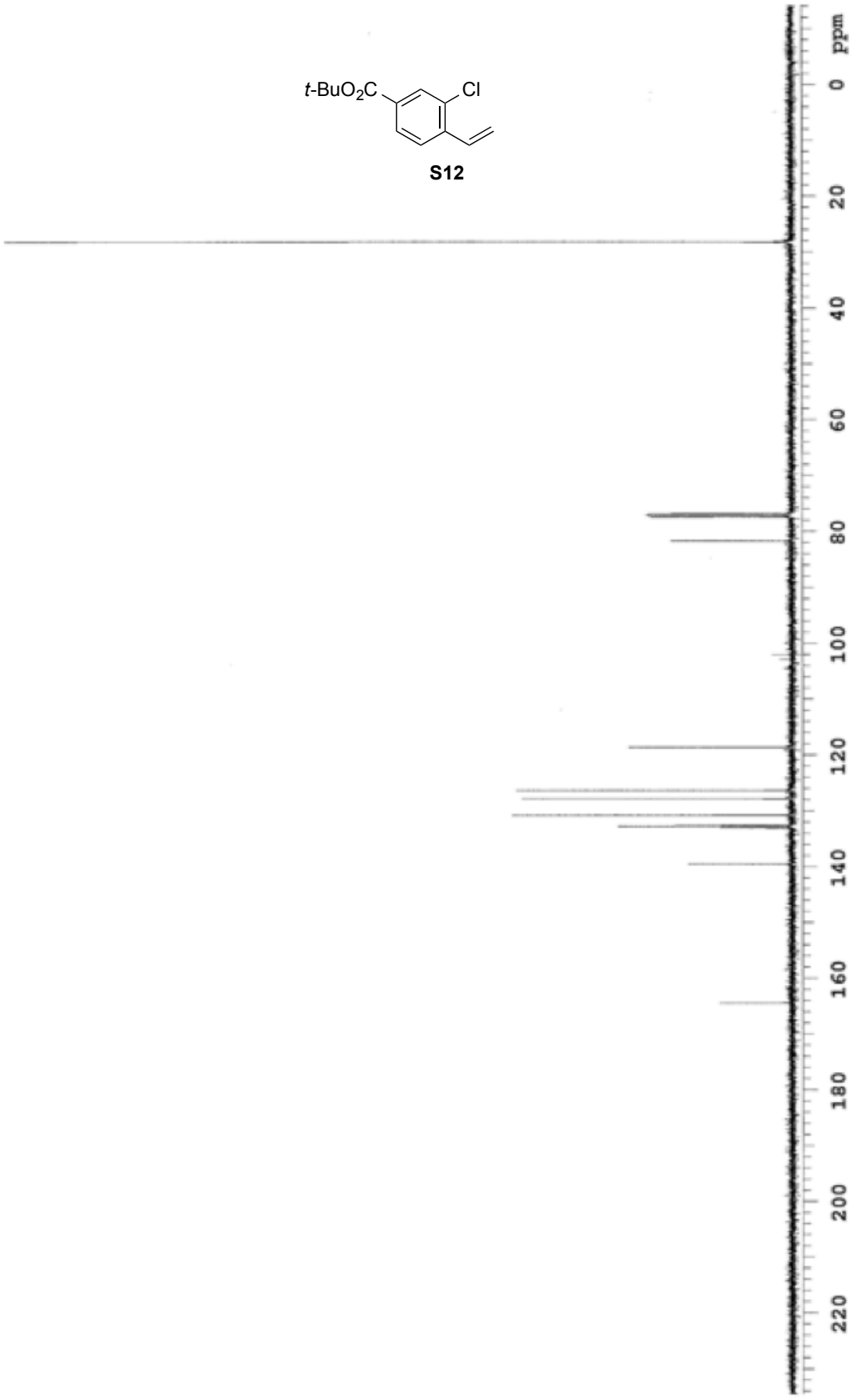

S12

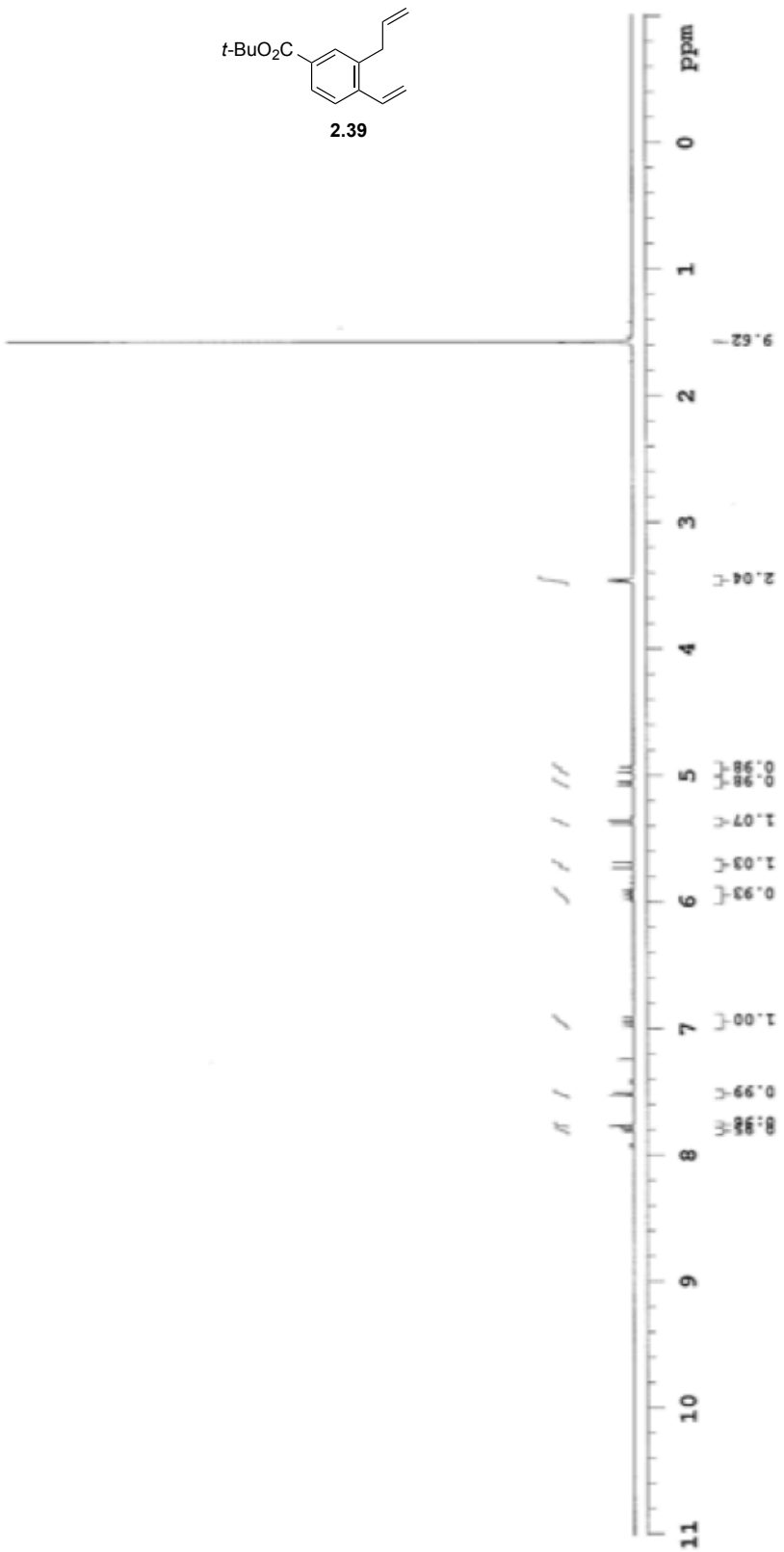
t-BuO2C
2.39
ppm
0
1
2
3
4
5
6
7
8
9
10
11
9.62
2.04
0.98
1.07
1.03
0.93
1.00
0.99
8.98

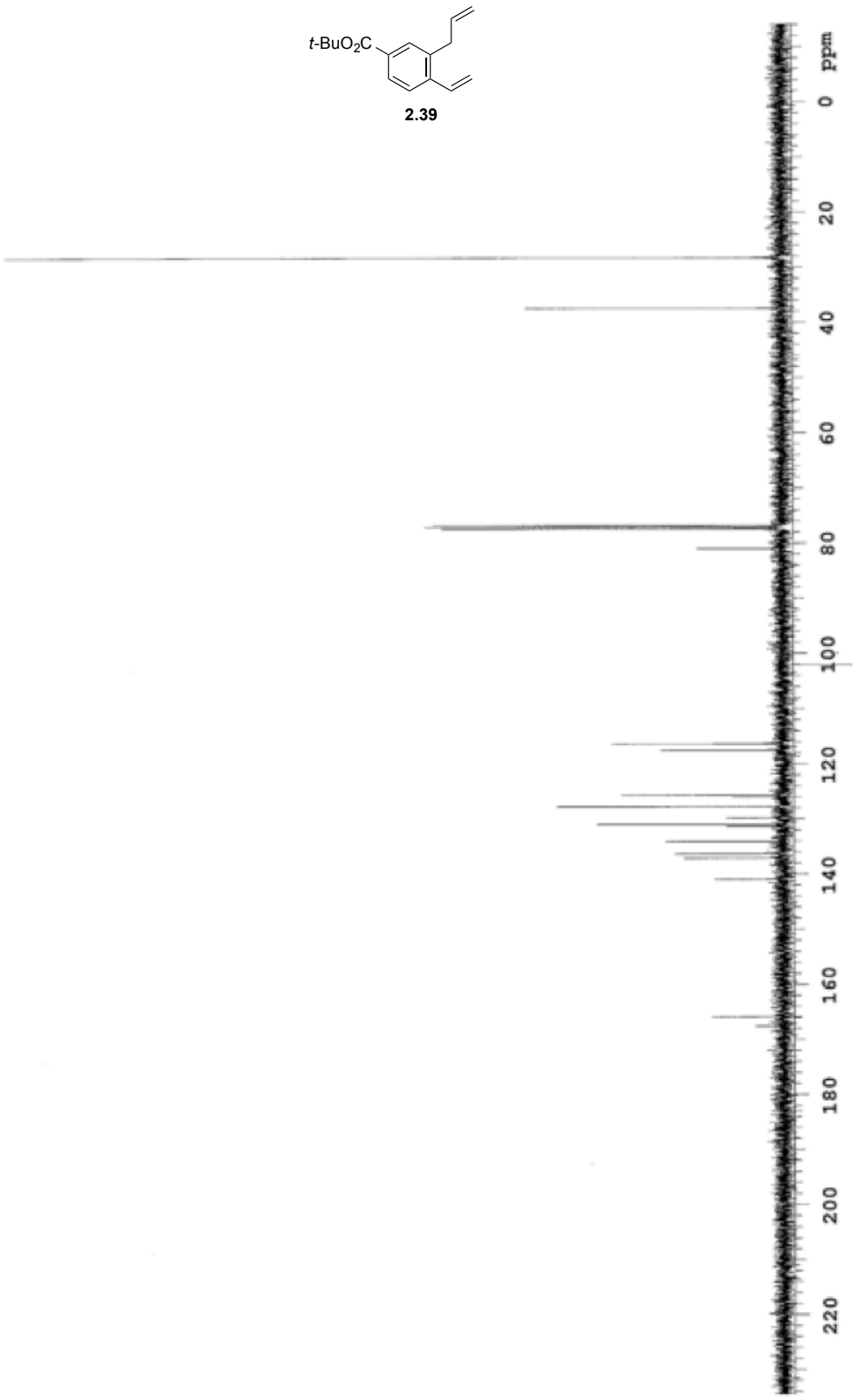
t-BuO2C
2.39
ppm
0
20
40
60
80
100
120
140
160
180
200
220

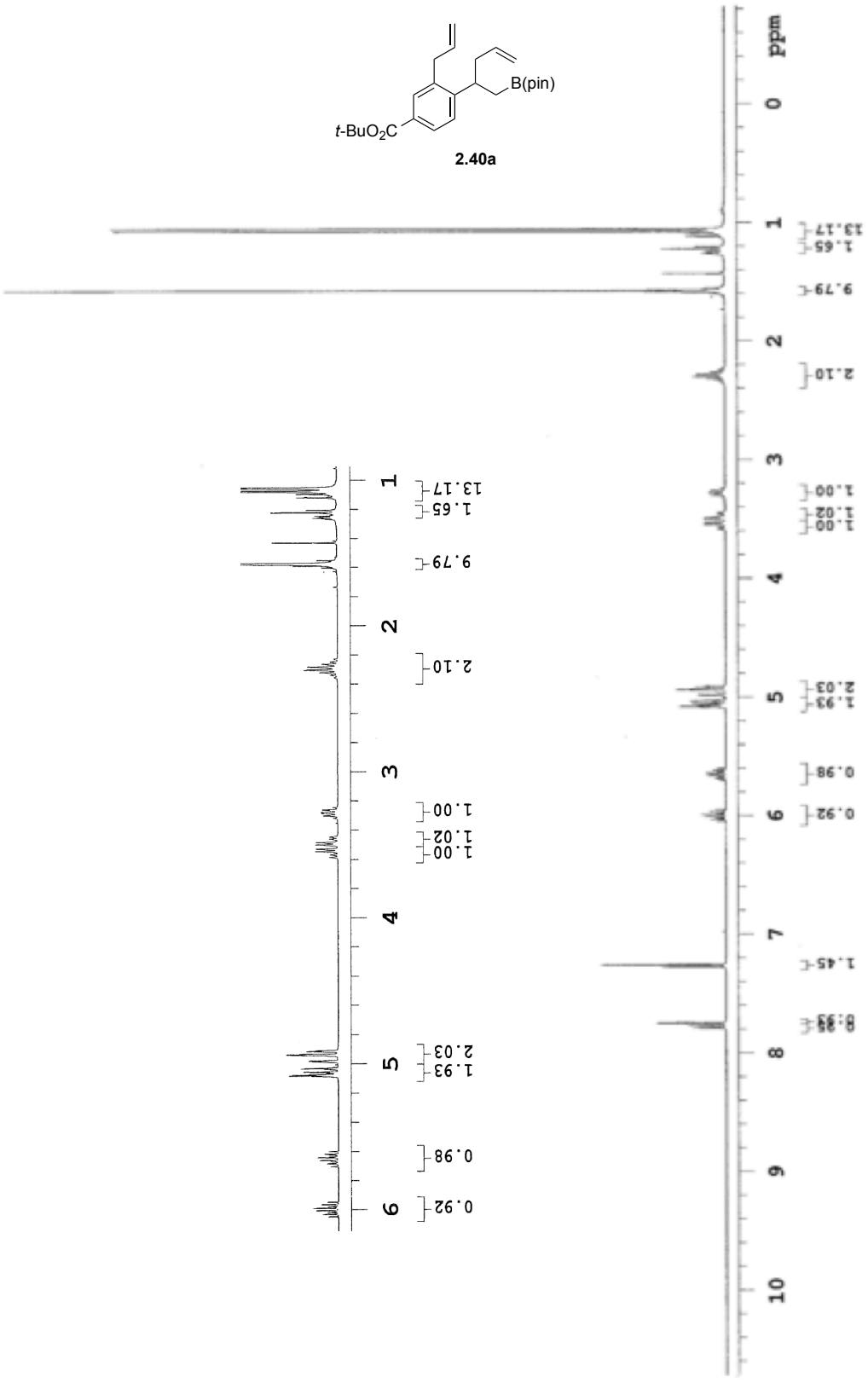
B(pin)
t-BuO2C
2.40a
ppm
13.17
1.65
9.79
2.10
1.00
1.02
1.00
2.03
1.93
0.98
0.92
1.45
8.03
8.01

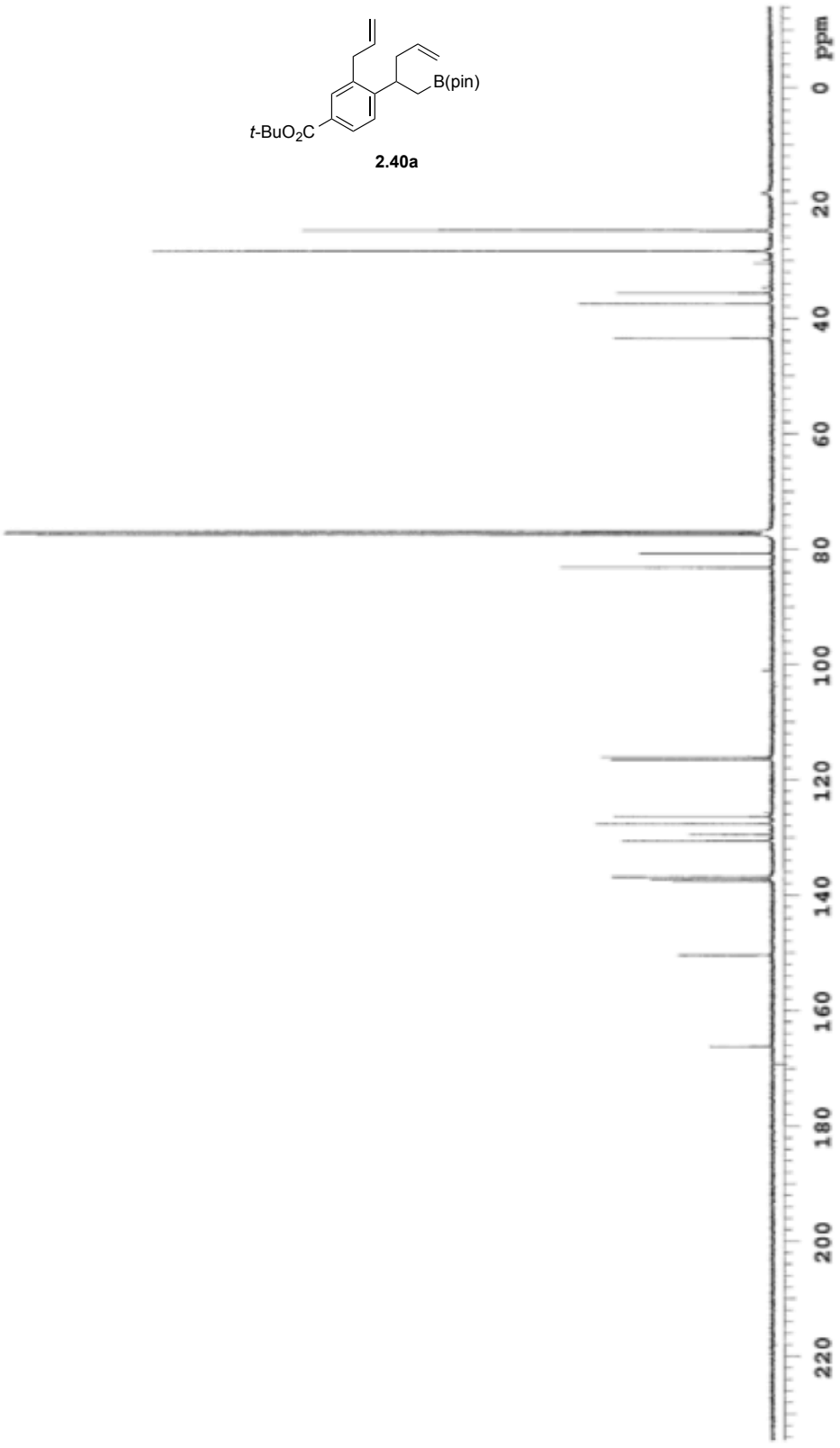
B(pin)
t-BuO2C
2.40a
0
20
40
60
80
100
120
140
160
180
200
220
ppm

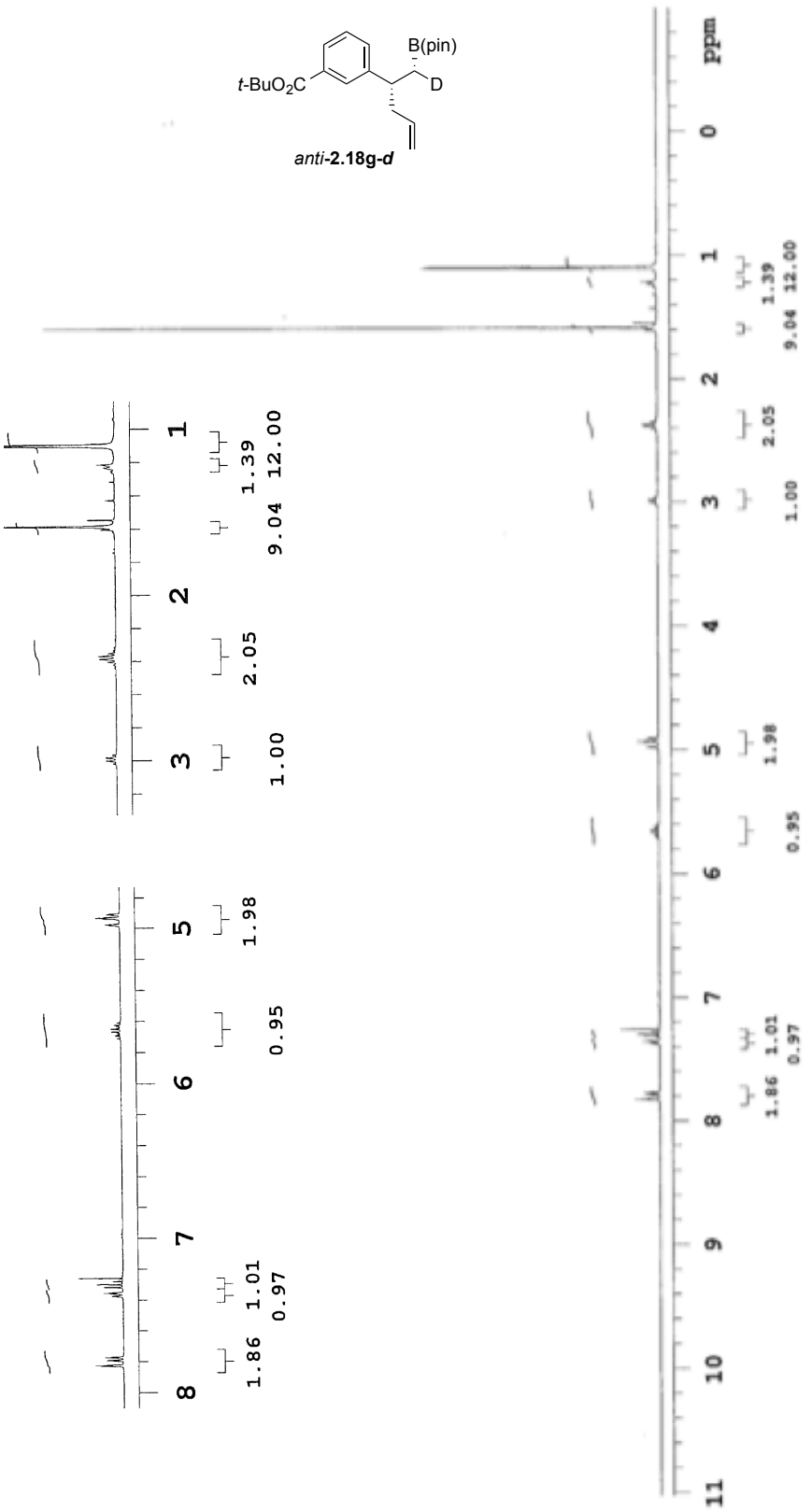
B(pin)
t-BuO2C
D
anti-2.18g-d
ppm
1.39
9.04
12.00
2.05
1.00
1.98
0.95
1.01
0.97
1.86

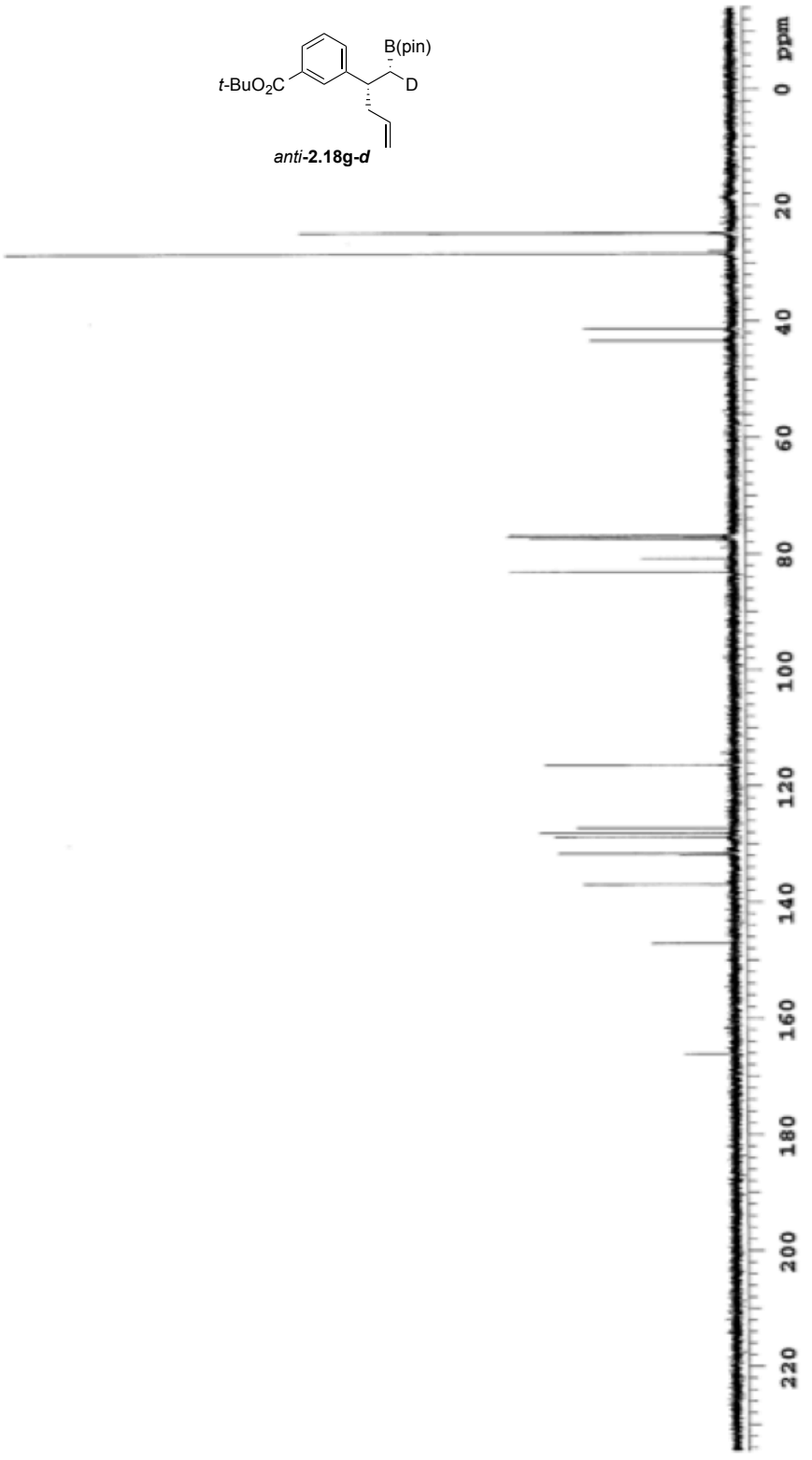
B(pin)
t-BuO2C
D
anti-2.18g-d
0 ppm
20
40
60
80
100
120
140
160
180
200
220

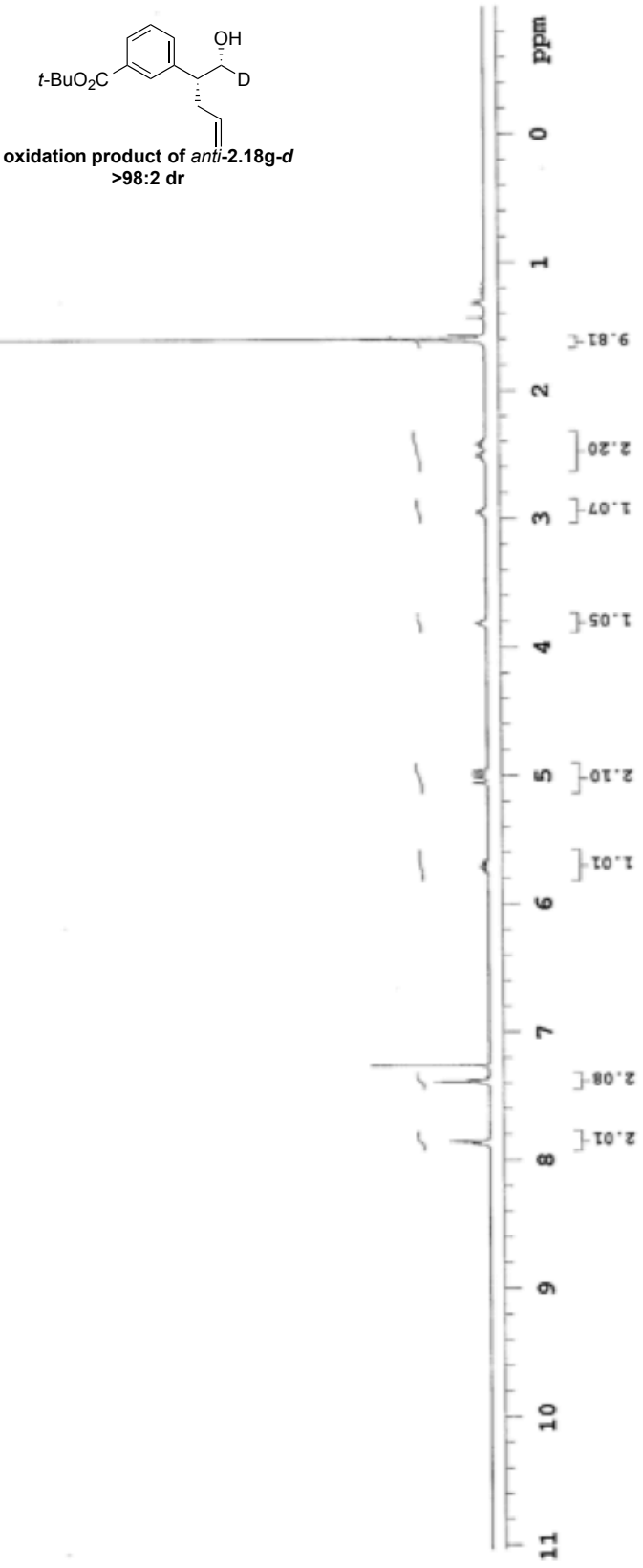
OH
t-BuO2C
D
oxidation product of anti-2.18g-d
>98:2 dr
ppm
0
1
2
3
4
5
6
7
8
9
10
11
9.81
2.20
1.07
1.05
2.10
1.01
2.08
2.01

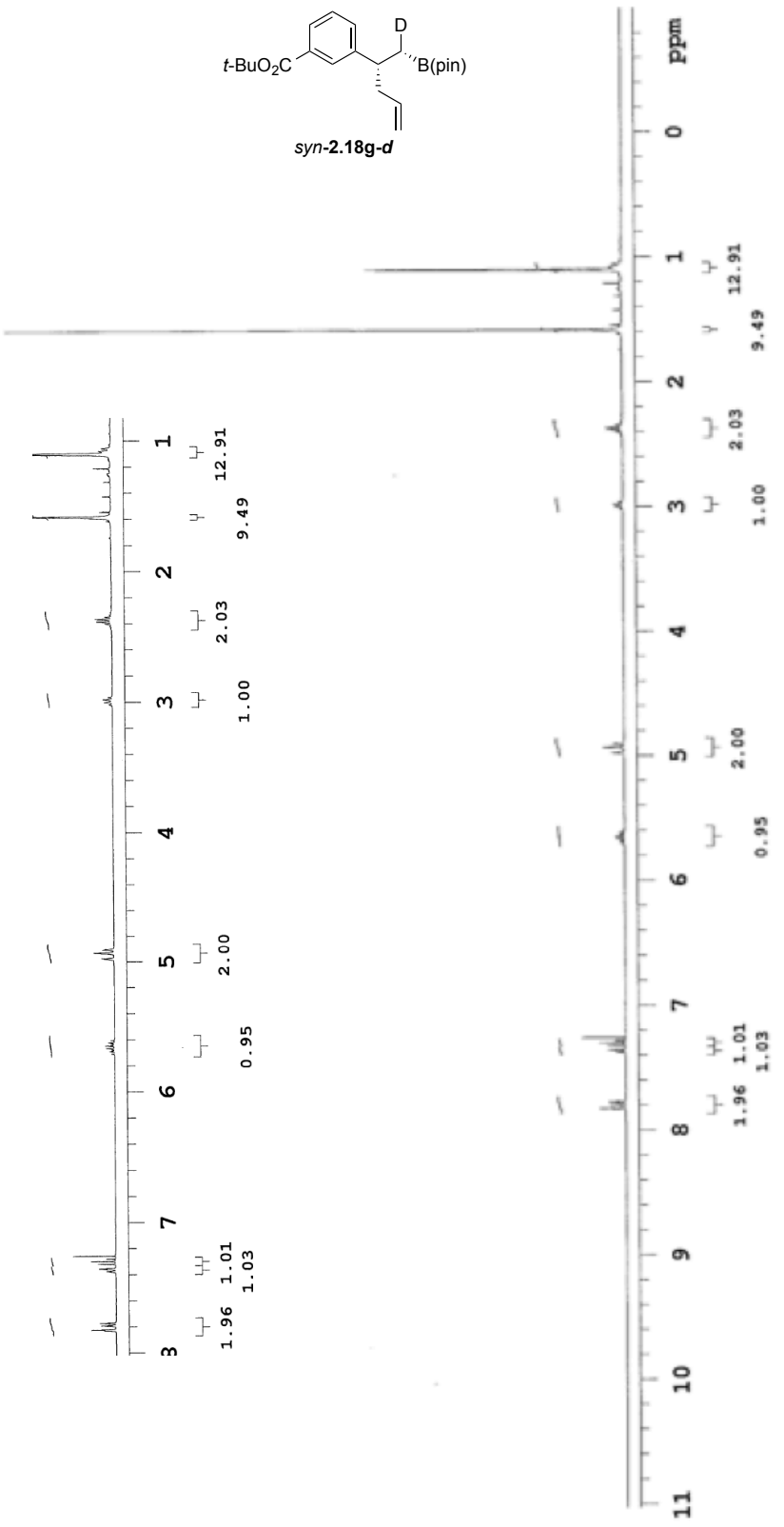
t-BuO2C
D
B(pin)
syn-2.18g-d
ppm

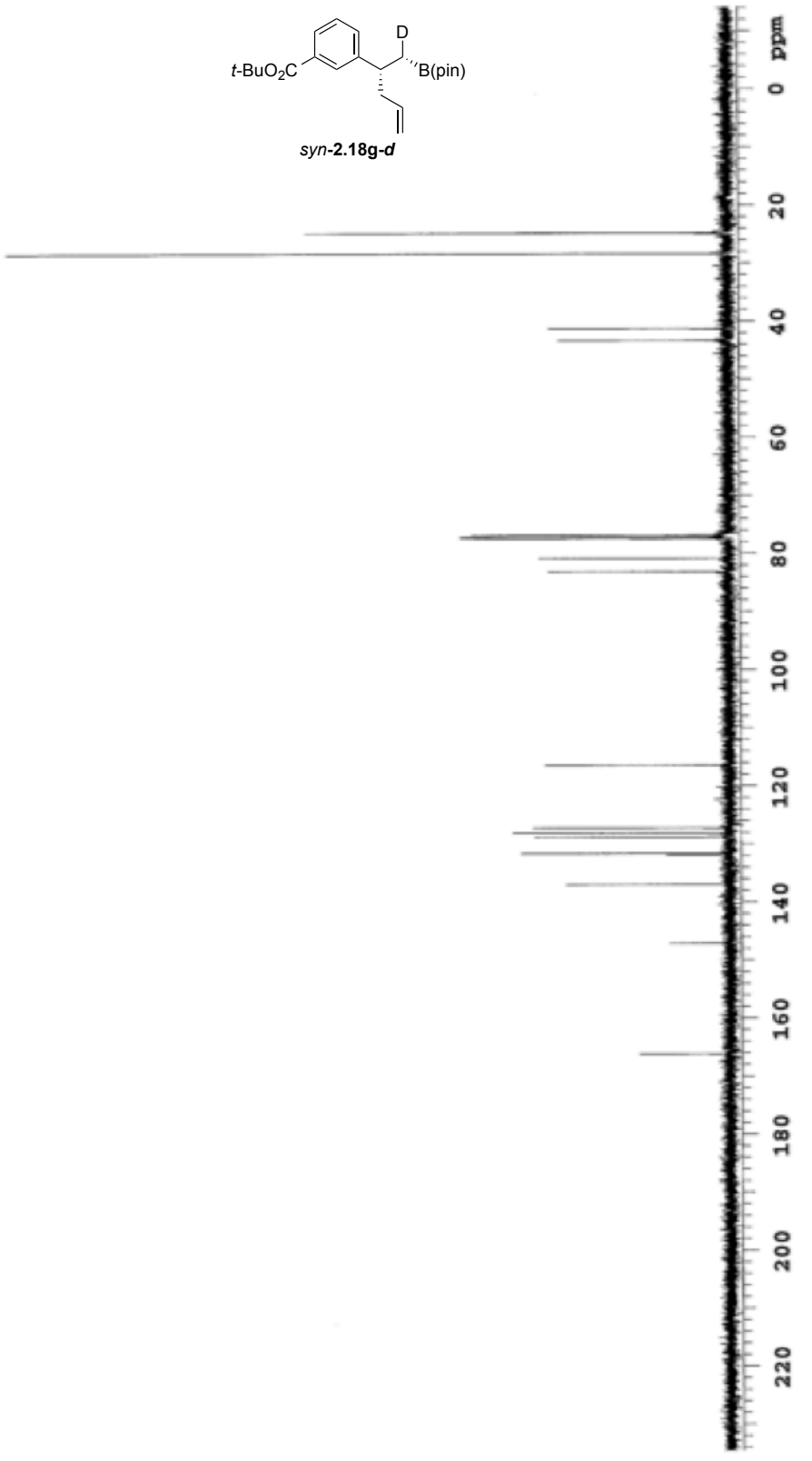
D
t-BuO2C
B(pin)
syn-2.18g-d
ppm
0
20
40
60
80
100
120
140
160
180
200
220

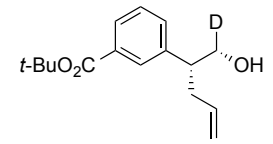

oxidation product of *syn*-2.18g-*d*
89:11 dr
(from 90:10 *Z*:*E* **S4**)

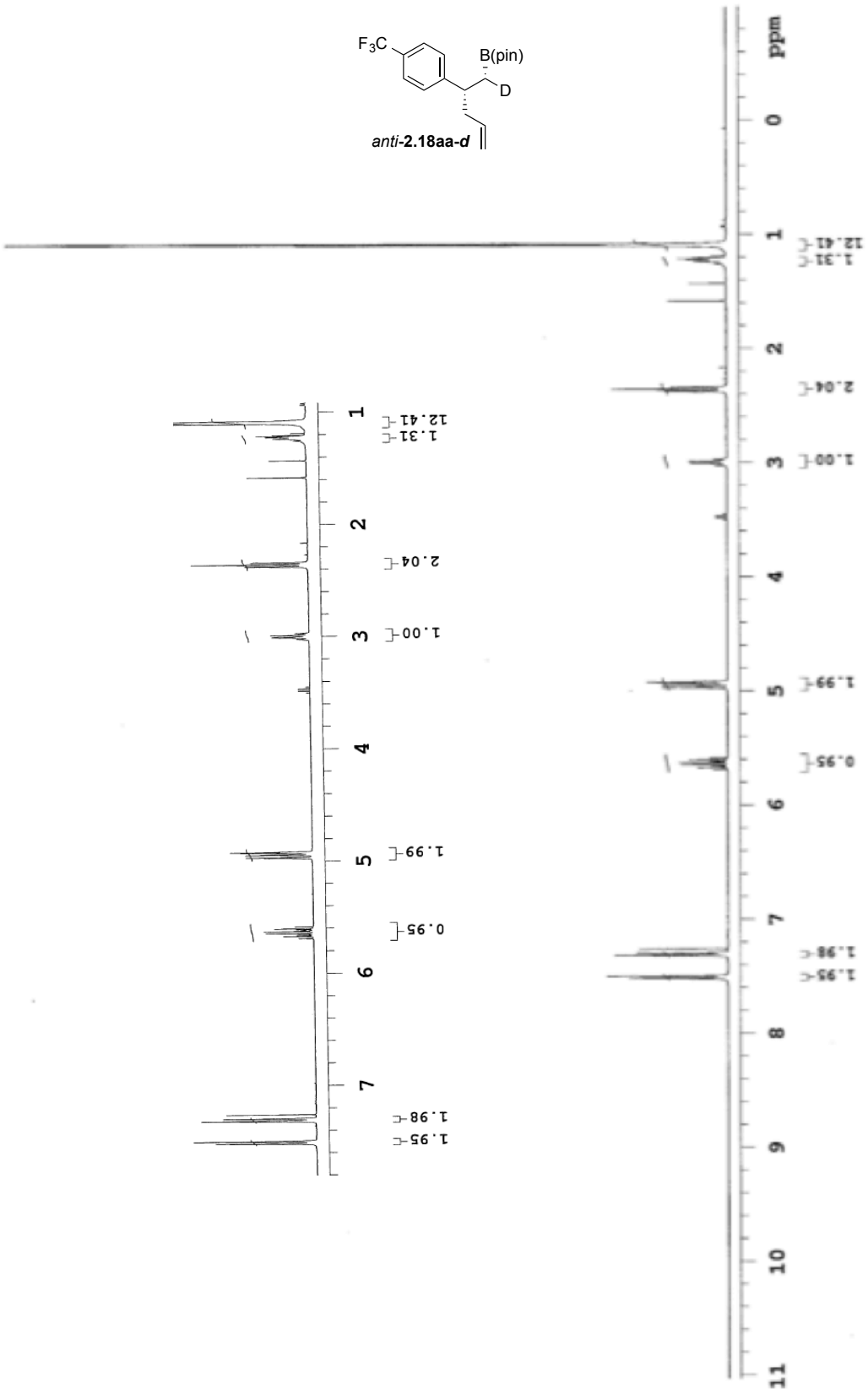
F3C
B(pin)
D
anti-2.18aa-d
ppm
12.41
1.31
2.04
1.00
1.99
0.95
1.98
1.95

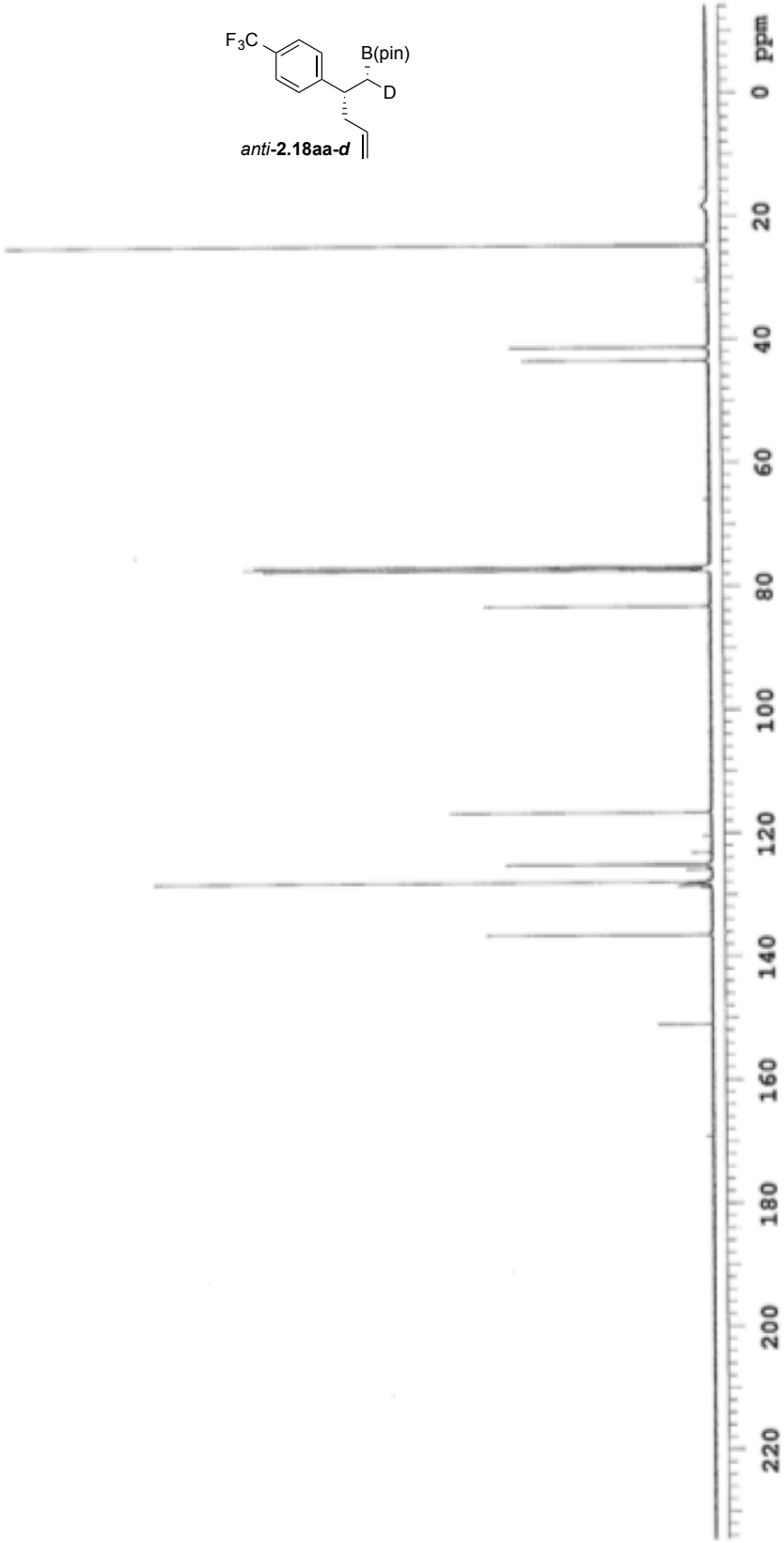
F3C
B(pin)
D
anti-2.18aa-d
0 ppm
20
40
60
80
100
120
140
160
180
200
220

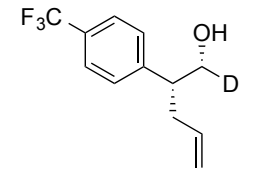

oxidation product of *anti*-2.18aa-*d*
92:8 dr
(from 91:9 *E*:*Z* alkene)

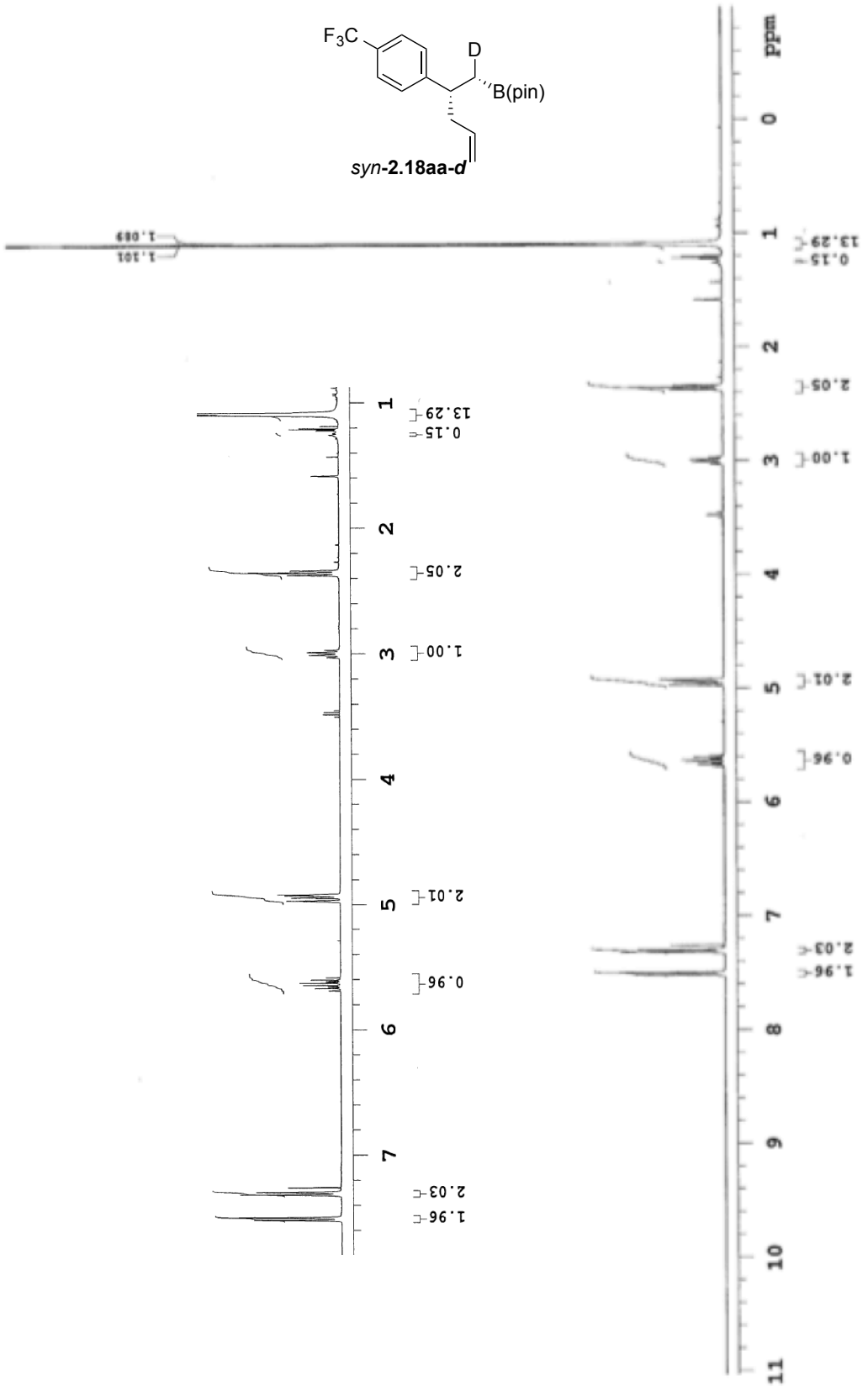
F3C
D
B(pin)
syn-2.18aa-d
ppm
13.29
0.15
2.05
1.00
2.01
0.96
2.03
1.96

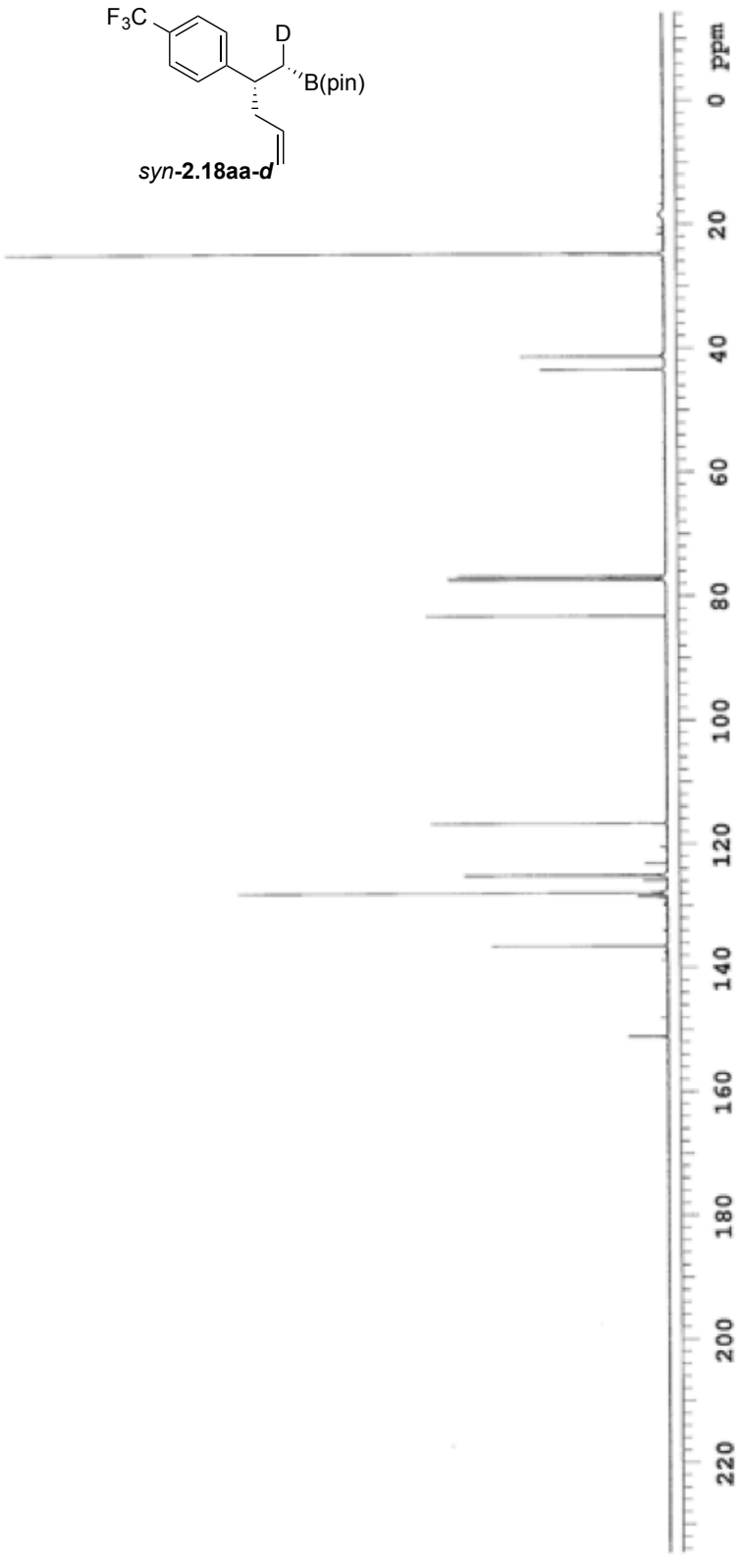
F3C
D
B(pin)
syn-2.18aa-d
ppm
0
20
40
60
80
100
120
140
160
180
200
220

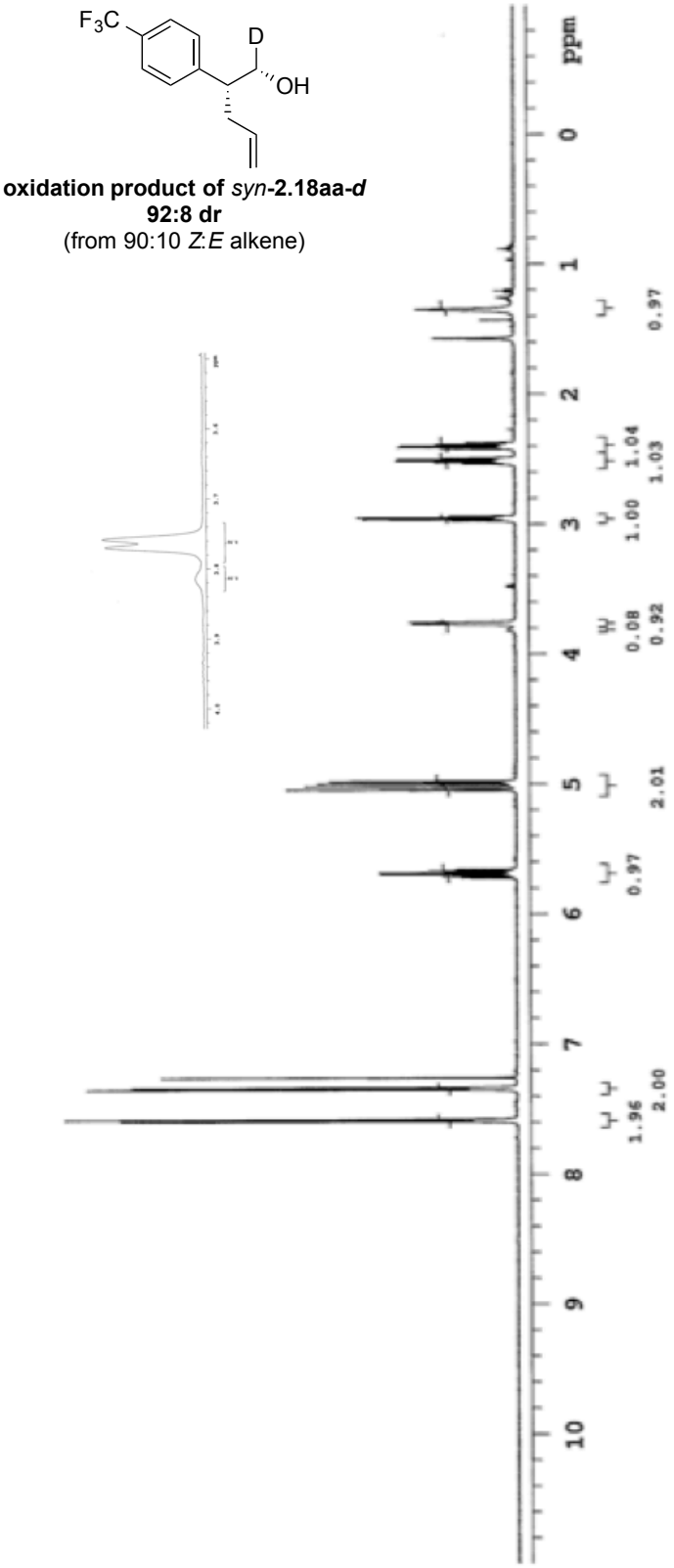

oxidation product of *syn*-2.18aa-*d*
92:8 dr
(from 90:10 *Z*:*E* alkene)

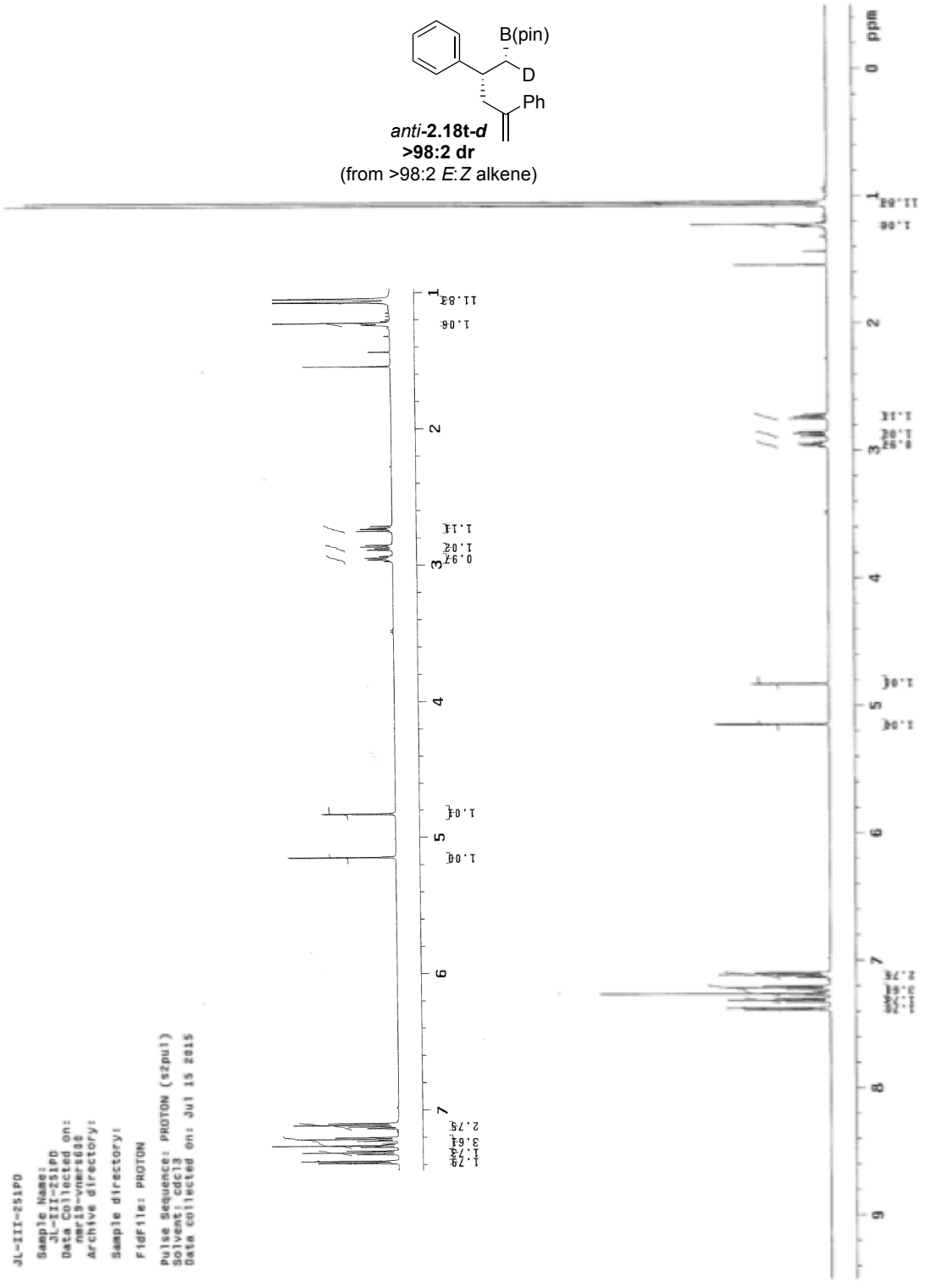
B(pin)
D
Ph
anti-2.18t-d
>98:2 dr
(from >98:2 E:Z alkene)
JL-III-251PD
Sample Name:
JL-III-251PD
Data Collected on:
mar19-vnmrs600
Archive directory:
Sample directory:
FidFile: PROTON
Pulse Sequence: PROTON (s2pul)
Solvent: cdcl3
Data collected on: Jul 15 2015
ppm

JL-III-106-C-PD
Sample Name:
JL-III-106-C-PD
Data Collected on:
vnmr13-vnmrs400
Archive directory:
Sample directory:
FidFile: JL-III-106-2-C-PD
Pulse Sequence: CARBON (s2pul)
Solvent: cdcl3
Data collected on: Feb 24 2015
B(pin)
D
Ph
anti-2.18t-d
>98:2 dr
(from >98:2 E:Z alkene)
ppm
220
200
180
160
140
120
100
80
60
40
20

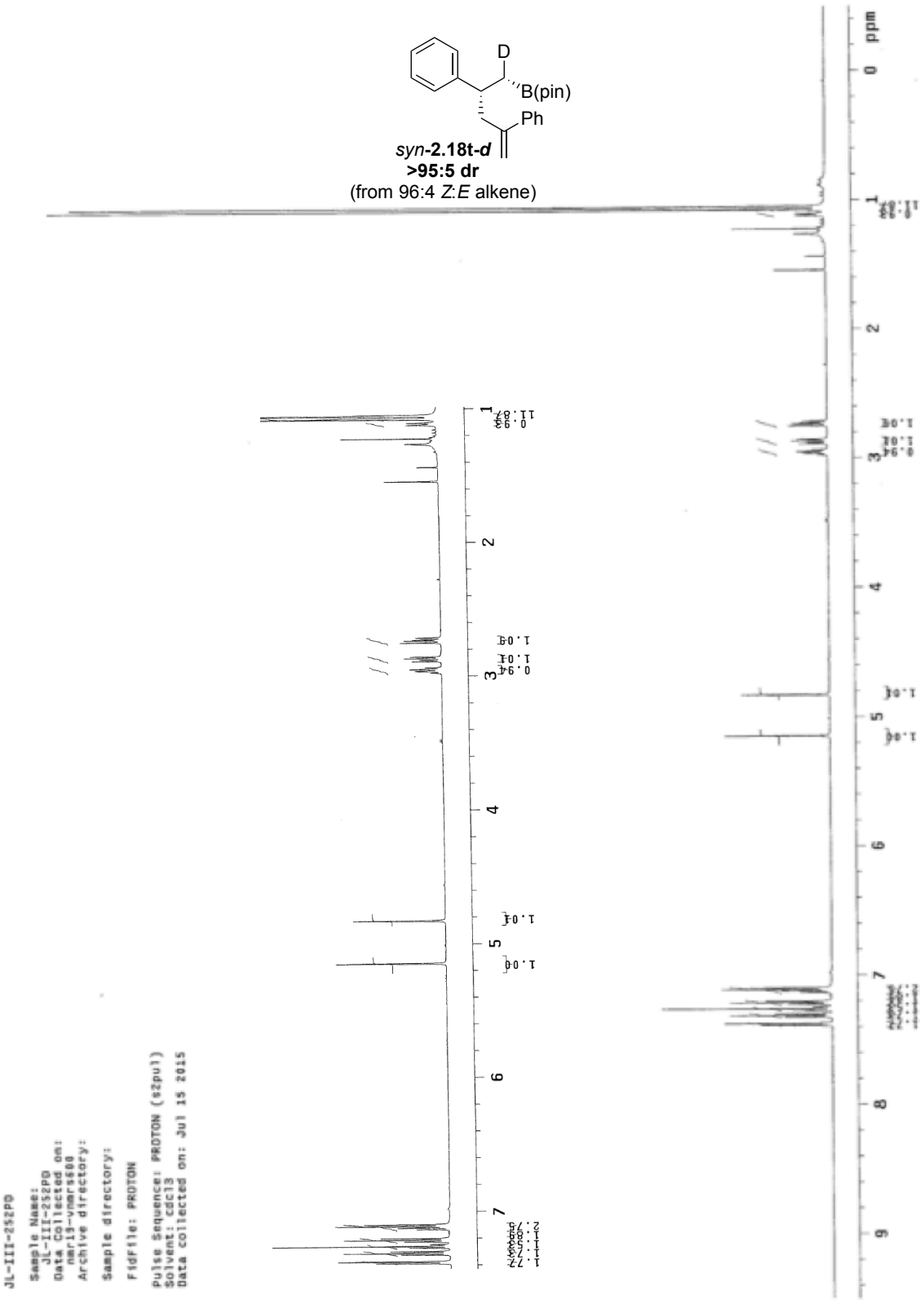
D
B(pin)
Ph
syn-2.18t-d
>95:5 dr
(from 96:4 Z:E alkene)
JL-III-252PD
Sample Name:
JL-III-252PD
Data Collected on:
nmr13-ynmr500
Archive directory:
Sample directory:
FidFile: PROTON
Pulse Sequence: PROTON (s2pul)
Solvent: cdcl3
Data collected on: Jul 15 2015
ppm

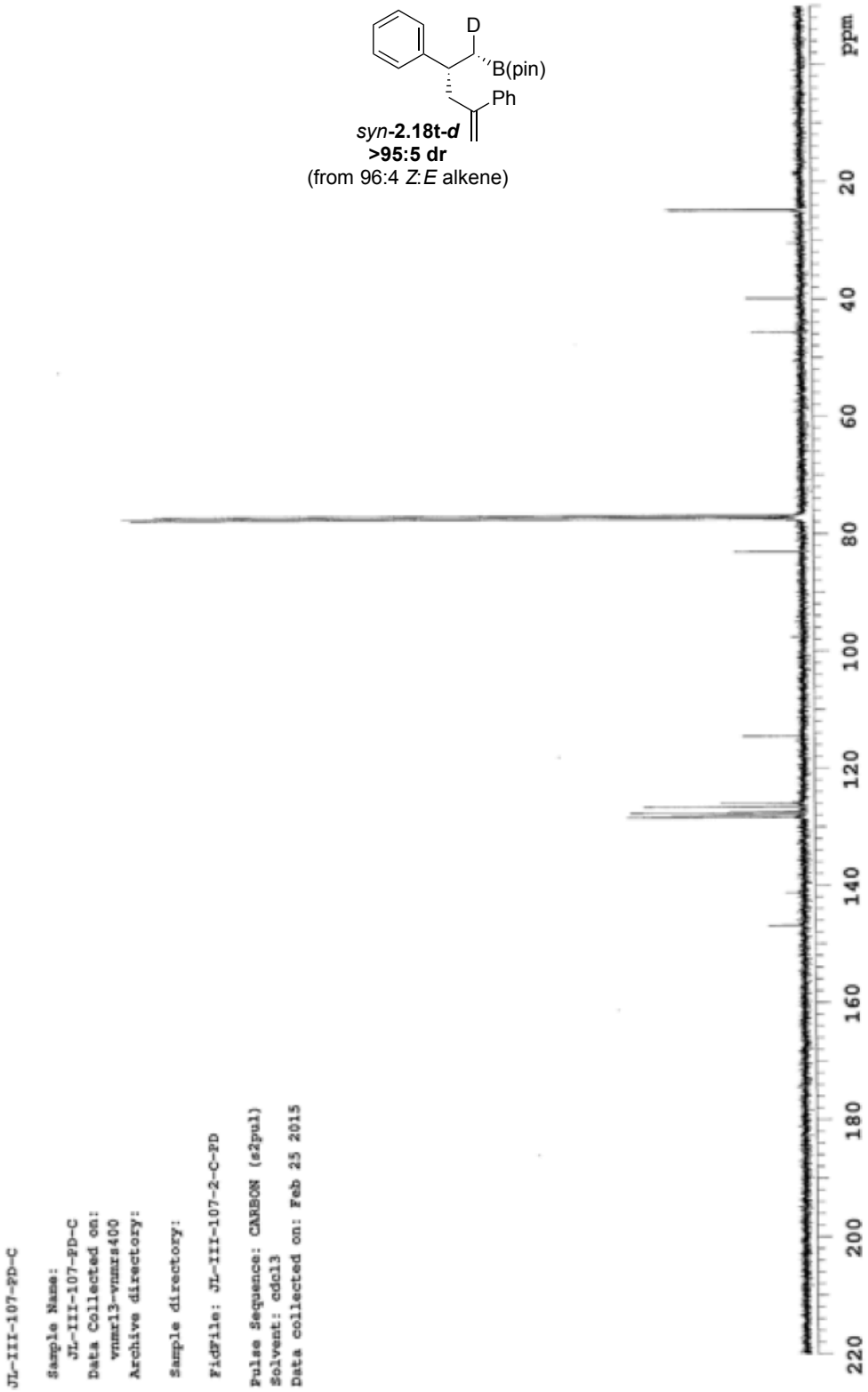

syn-**2.18t-*d***
>95:5 dr
(from 96:4 *Z*:*E* alkene)

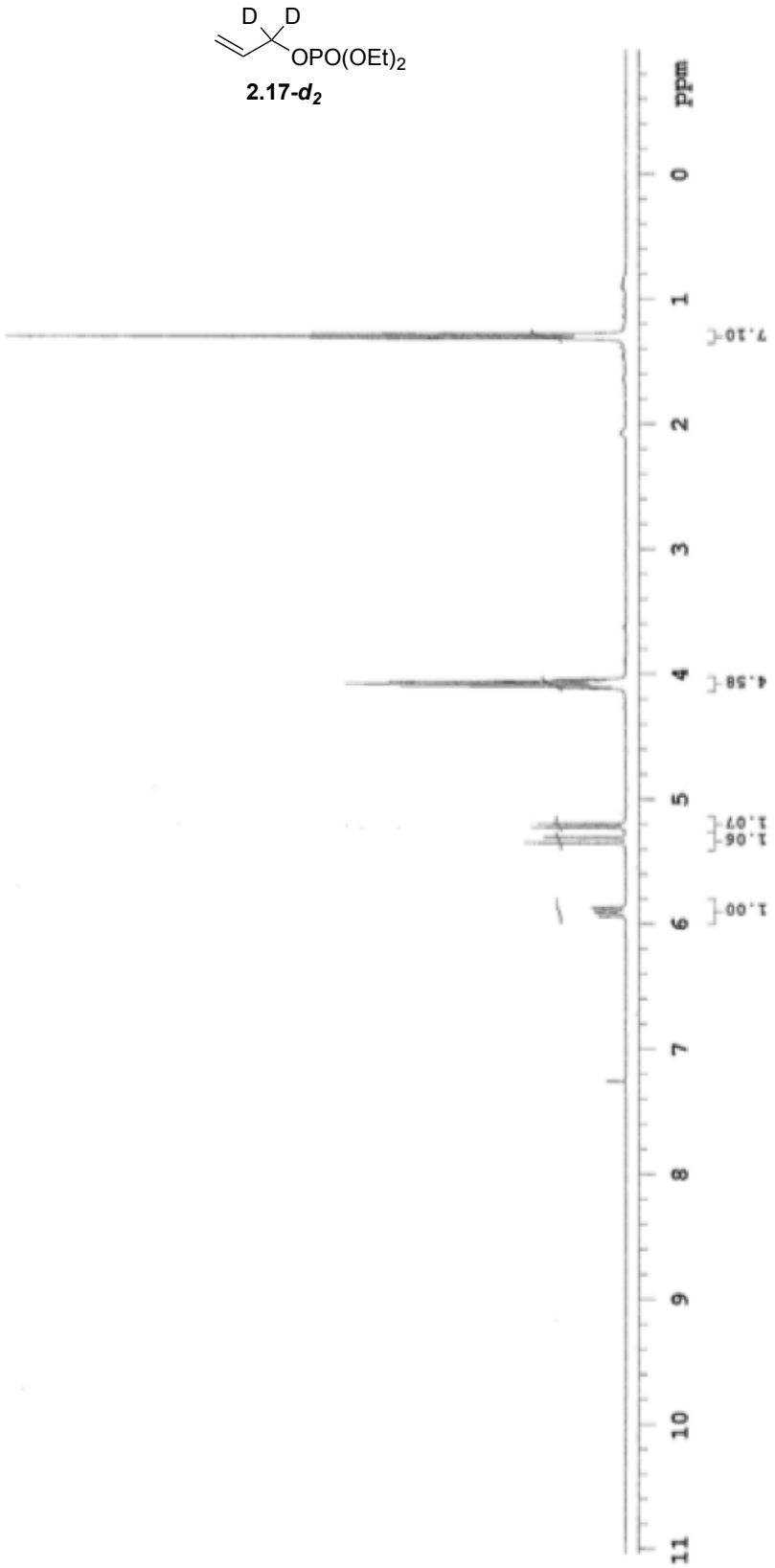
D
D
OPO(OEt)2
2.17-d2
ppm
0
1
2
3
4
5
6
7
8
9
10
11
7.10
4.58
1.07
1.06
1.00

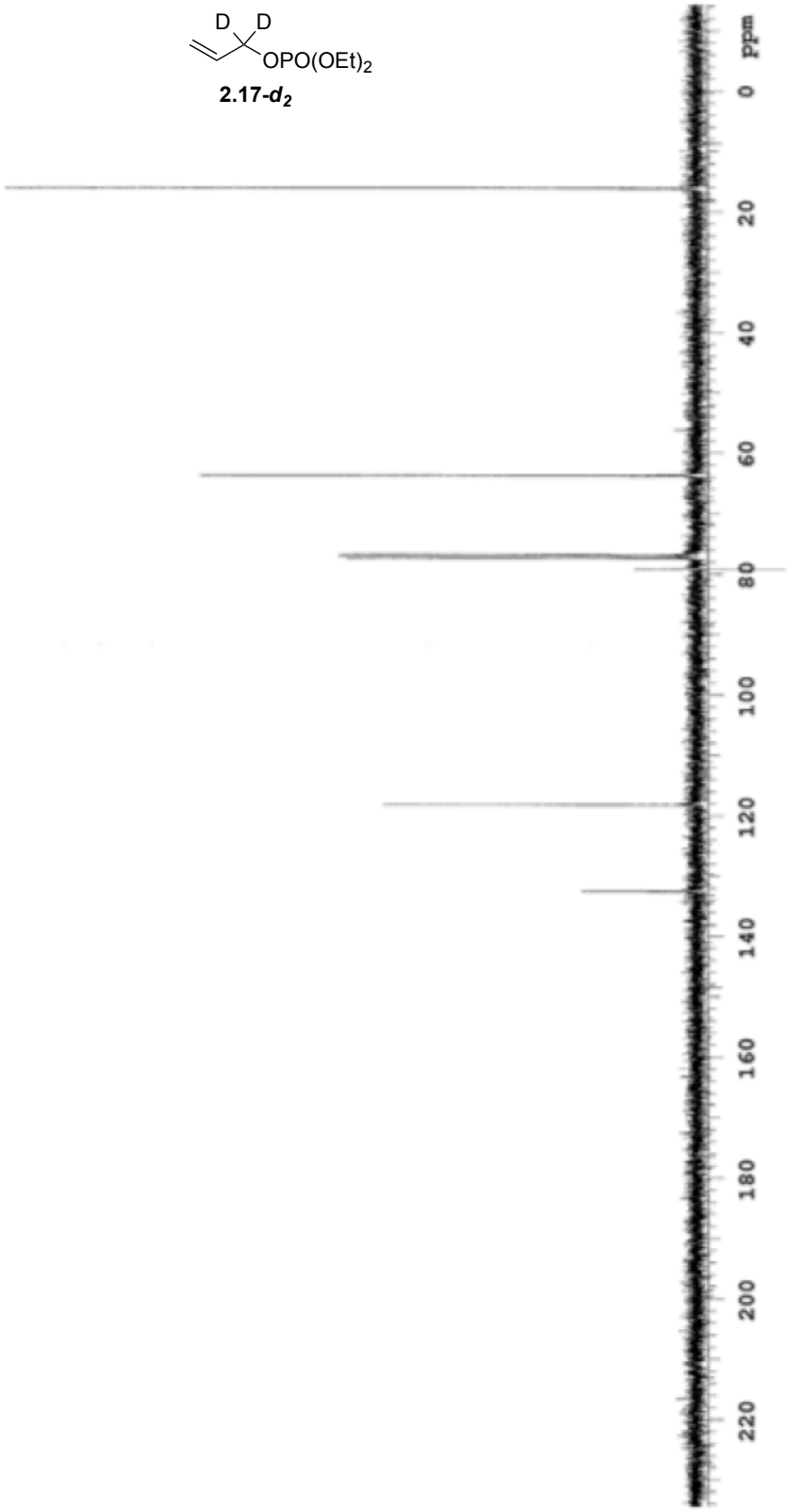
D D
OPO(OEt)2
2.17-d2
ppm
0
20
40
60
80
100
120
140
160
180
200
220

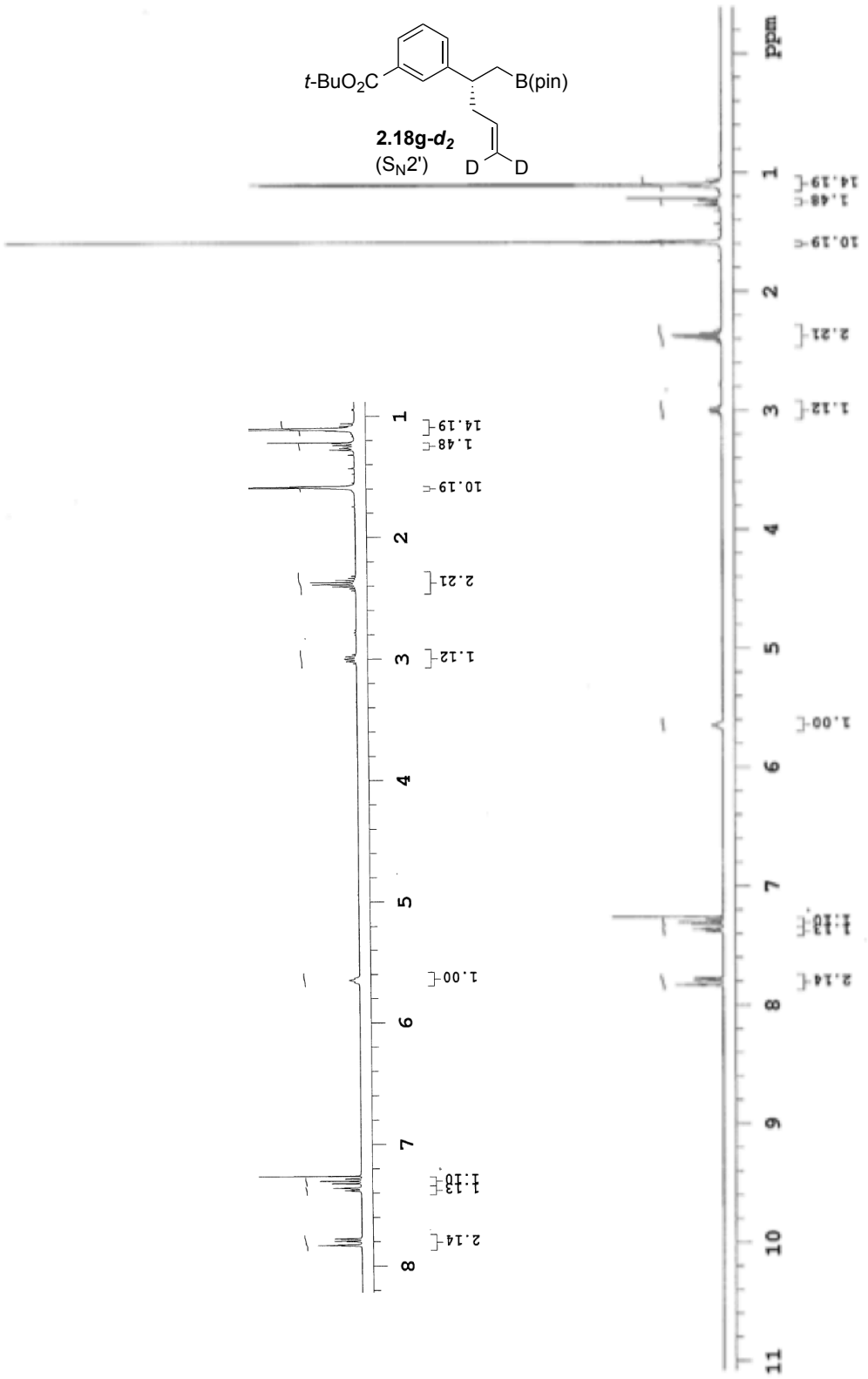
t-BuO2C
B(pin)
2.18g-d2
(SN2')
D
D
ppm
14.19
1.48
10.19
2.21
1.12
1.00
2.14

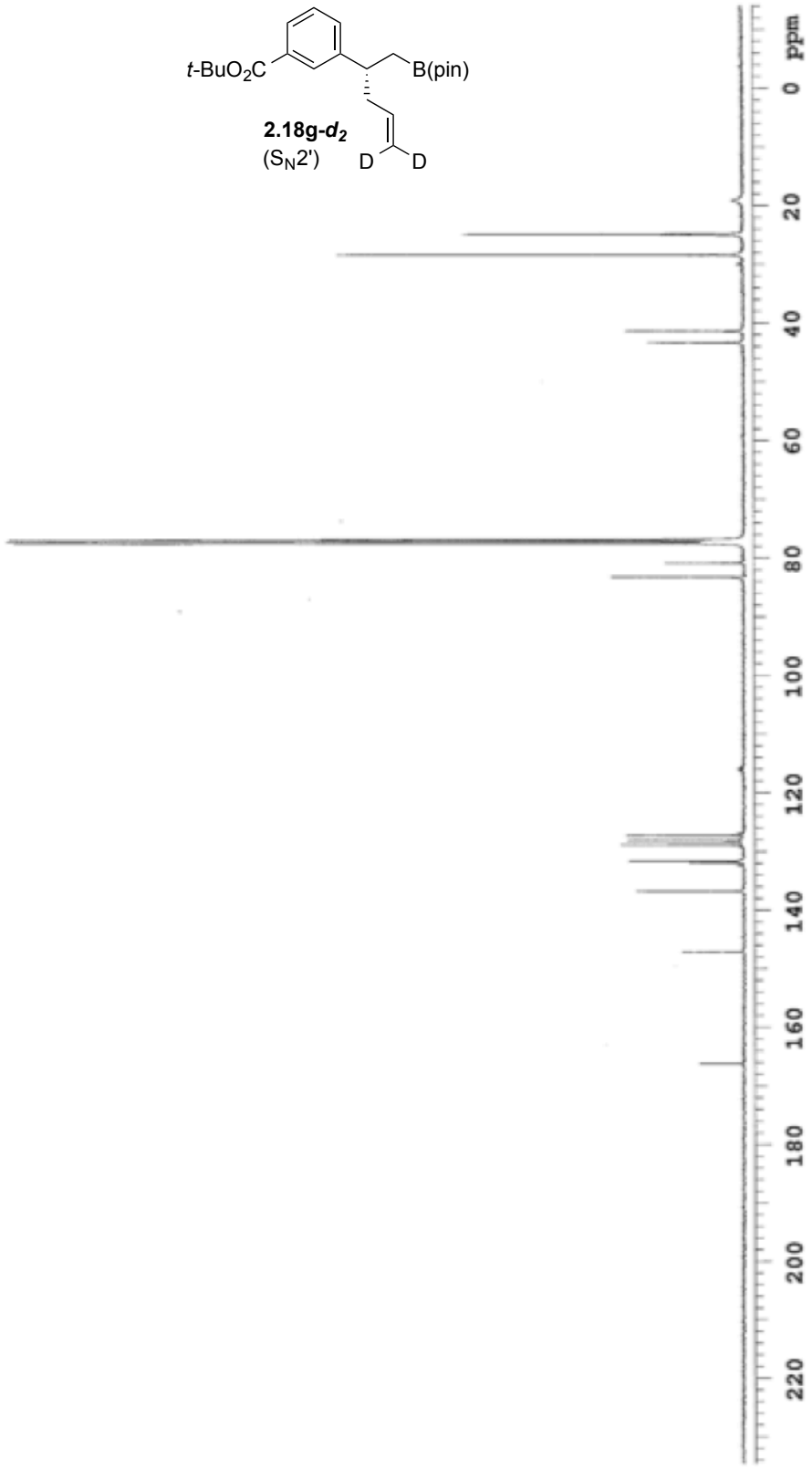
t-BuO2C
B(pin)
2.18g-d2
(SN2')
D
D
0 ppm
20
40
60
80
100
120
140
160
180
200
220

SR-VI-138-A
Sample Name SR-VI-138-A
Date collected 2016-12-19
Pulse sequence PROTON
Solvent cdcl3
Temperature 25
Spectrometer nmr13-vnmrs400
Study owner mengf
Operator mengf
NBn2
2.45
ppm

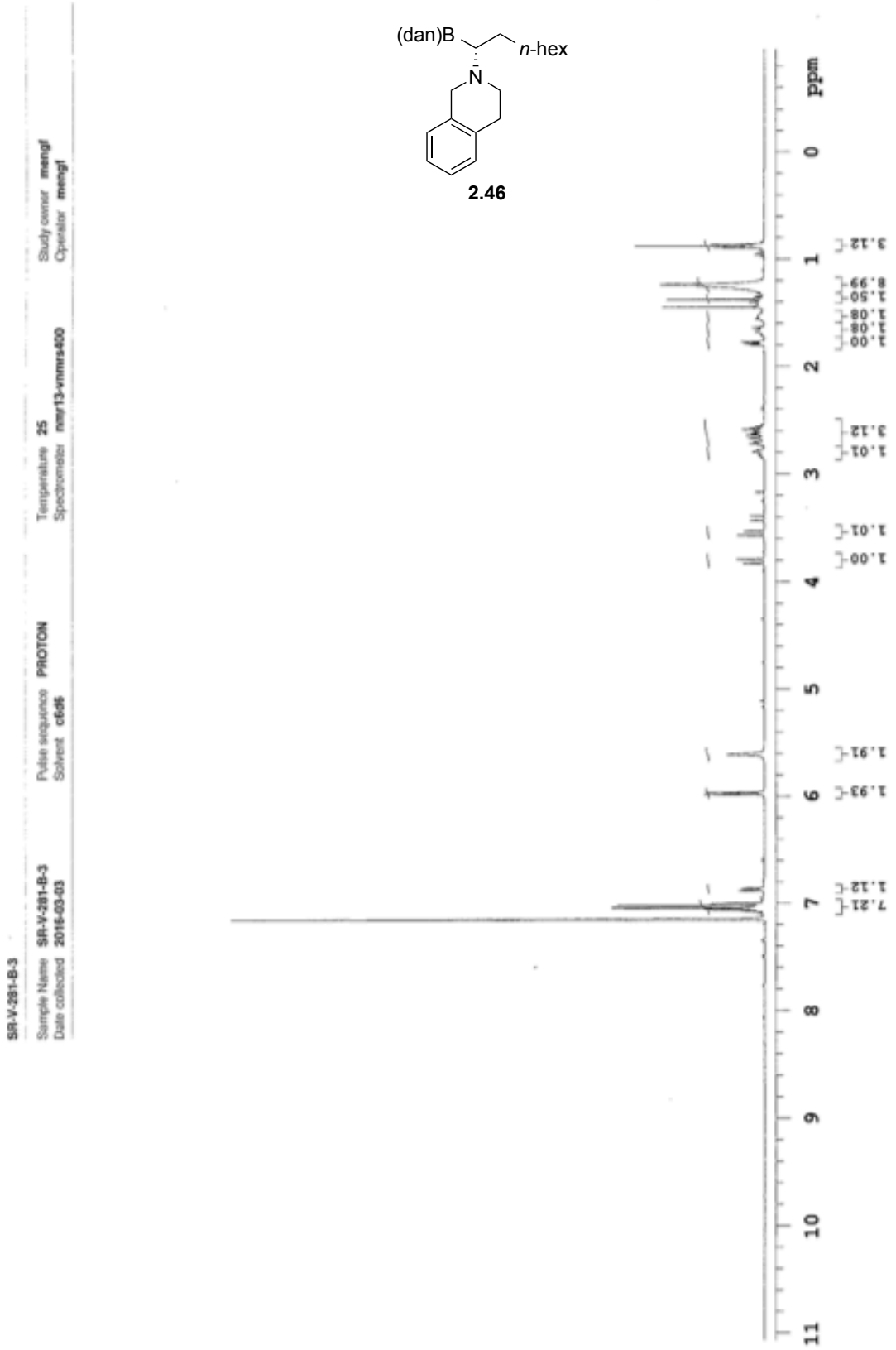
SR-V-261-B-3
Sample Name SR-V-261-B-3
Date collected 2015-03-03
Pulse sequence PROTON
Solvent c6d6
Temperature 25
Spectrometer nmr13-vnmrs400
Study owner mengf
Operator mengf
(dan)B
n-hex
N
2.46
ppm
7.21
1.12
1.91
1.93
1.01
1.00
1.01
3.12
2.01
2.00
2.08
2.08
1.50
8.99
3.12

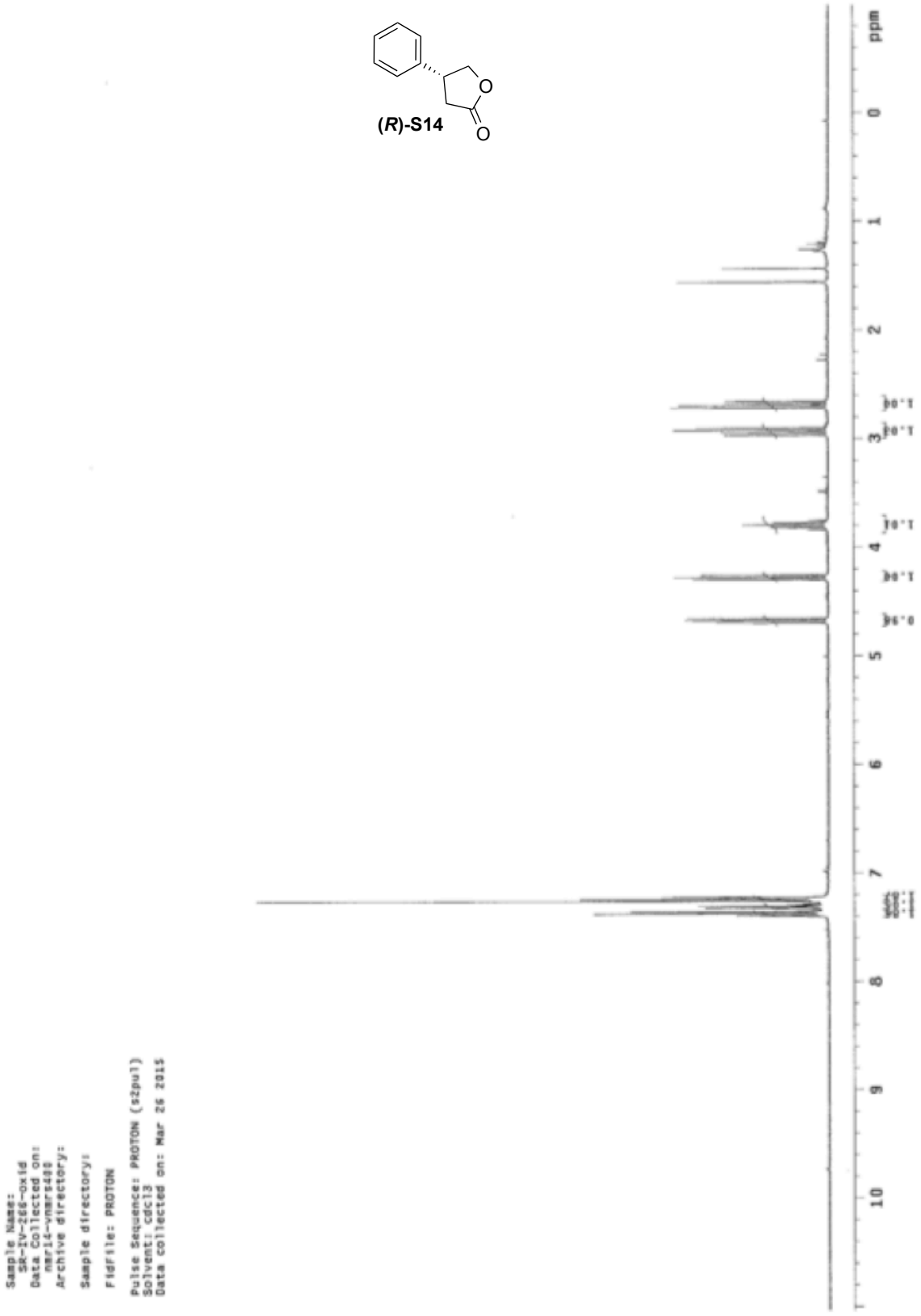
(R)-S14
O
O
ppm
0
1
2
3
4
5
6
7
8
9
10
1.00
1.00
1.00
0.96
Sample Name:
SR-IV-266-oxid
Data Collected on:
marl4-ynmrs408
Archive directory:
Sample directory:
Fidfile: PROTON
Pulse Sequence: PROTON (s2pul)
Solvent: cdcl3
Data collected on: Mar 26 2015

Chapter 3

Synthesis of Vicinal Diboronate Compounds through Practical Phosphine–Copper Catalyzed Three-Component Processes

3.1. Introduction

Organoboron compounds that contain one or more C–B(pin) (pin = pinacolato) bonds are of importance in chemical synthesis. Largely due to the pioneering investigations by the Morken group, it is widely appreciated that diboron additions of $B_2(pin)_2$ to alkenes may be catalyzed by Rh- or Pt-based complexes.[114] More recently it has been demonstrated that alkoxides[115] and carbohydrate-derived species[116] can promote such transformations.

Vicinal diboronates can be easily converted to the corresponding diols with complete retention of stereochemistry or more recent studies reveal that in the case of molecules containing a primary and a secondary C–B(pin) moiety, the former site can be site selectively induced to undergo cross-coupling reactions because of the activation by the latter.[117] Thus, development of a practical method to access vicinal diboronate

(114) For a representative report, see: (a) Kliman, L. T.; Mlynarski, S. N.; Morken, J. P. *J. Am. Chem. Soc.* **2009**, *131*, 13210–13211. (b) Coombs, J. R.; Haeffner, F.; Kliman, L. T.; Morken, J. P. *J. Am. Chem. Soc.* **2013**, *135*, 11222–11231. For processes promoted by Rh-based complexes, see: (c) Trudeau, S.; Morgan, J. B.; Shreshta, M.; Morken, J. P. *J. Org. Chem.* **2005**, *70*, 9538–9544. (d) Toribatake, K.; Nishiyama, H. *Angew. Chem., Int. Ed.* **2013**, *52*, 11011–11015.

(115) (a) Bonet, A.; Pubill-Ulldemolins, C.; Bo, C.; Gulyás, H.; Fernández, E. *Angew. Chem., Int. Ed.* **2011**, *50*, 7158–7161. (b) Blaisdell, T. P.; Caya, T. C.; Zhang, L.; Sanz-Marco, A.; Morken, J. P. *J. Am. Chem. Soc.* **2014**, *136*, 9264–9267.

(116) Fang, L.; Yan, L.; Haeffner, F.; Morken, J.P. *J. Am. Chem. Soc.* **2016**, *138*, 2508–2511.

(117) Mlynarski, S. N.; Schuster, C. H.; Morken, J. P. *Nature* **2014**, *505*, 386–390.

compounds with differentiable C–B bonds is compelling especially ones that allow selective functionalization of a secondary C–B bond over a primary one.

3.2. Background

3.2.1. Synthesis of vicinal diboronate compounds through transition-metal catalysis

In 2009, our laboratories reported an alternative procedure to access vicinal diboronate compounds through a sequential addition reaction of a NHC–Cu–B(pin) complex and a terminal alkyne (Scheme 3.1a).[118] In the first step, an alkenyl–B(pin) is generated from a site-selective proto-boryl addition of an alkyne. Then, the vicinal diboronate is obtained through a site- and enantioselective Cu–B(pin) addition to the in situ generated alkenyl–B(pin) followed by protonation (<2% germinal diboronate compound). The reactions provide access to a range of products including an alkyl- or aryl-substituent.

The Morken group showed that vicinal diboronate compounds can be obtained through the Pt-catalyzed enantioselective diboron addition to monosubstituted alkenes (Scheme 3.1b).[114b] Transformations are highly efficient with only 1.0 mol % of Pt-based complex, after 3 hours the diol products with an alkyl- or aryl-substituent (obtained after oxidation of diboronate compounds) are generated.

(118) (a) Lee, Y.; Jang, H.; Hoveyda, A. H. *J. Am. Chem. Soc.* **2009**, *131*, 18234–18235. For an application in synthesis of a biologically active molecules, see: (b) Meek, S. J.; O'Brien, R. V.; Llaveria, J.; Schrock, R. R.; Hoveyda, A. H. *Nature* **2011**, *471*, 461–466. For a related study, see: (c) Jung, H.-Y.; Yun, J. *Org. Lett.* **2012**, *14*, 2606–2609.

Scheme 3.1. Synthesis of vicinal diboronate compounds involving transition-metal complexes

a) NHC–Cu–B(pin) addition to alkynes

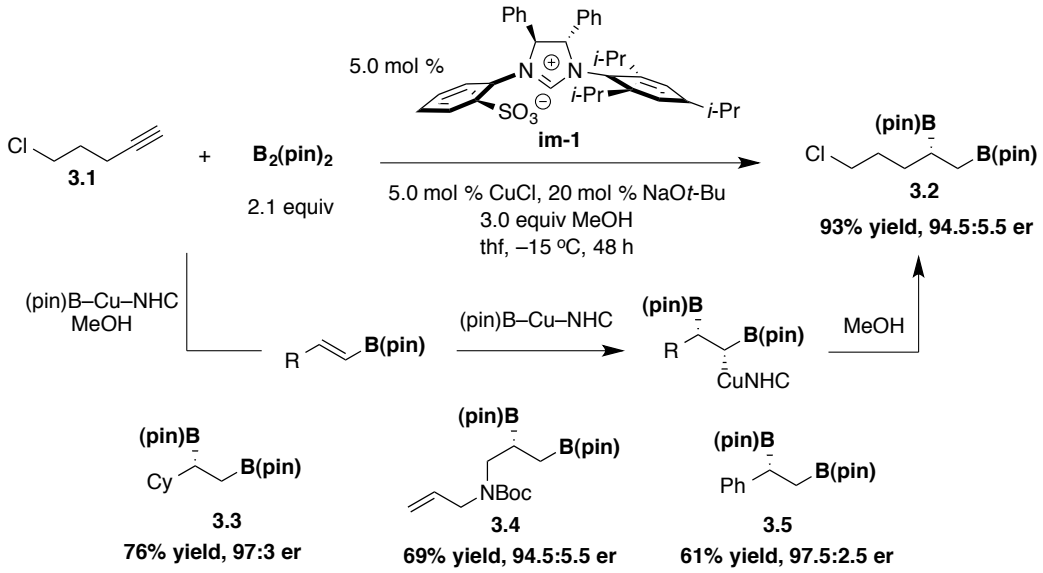

b) Phosphonite–Pt diboron addition to alkenes

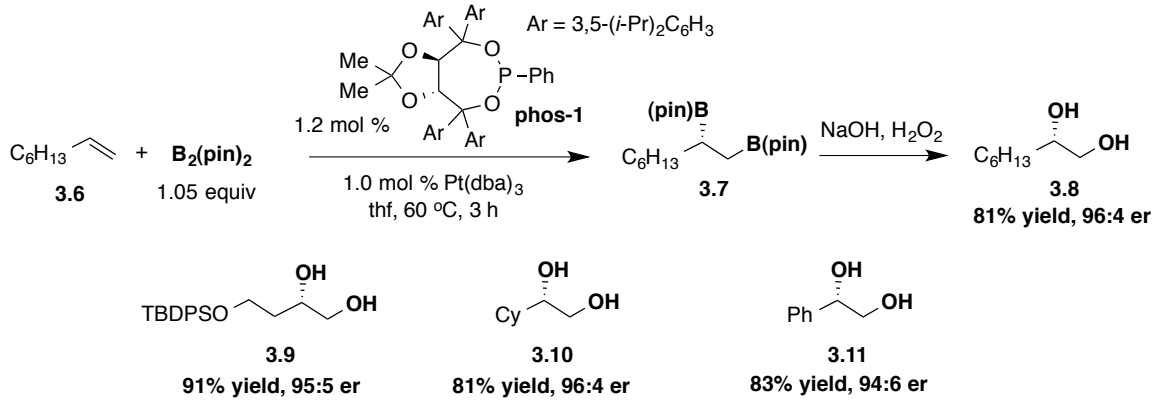

3.2.2. Synthesis of vicinal diboronate compounds through transition-metal free catalysis

In addition to reactions involving a transition-metal based catalyst to access vicinal diboronates, an alkoxide-catalyzed diboron addition to alkenes has been reported (Scheme 3.2a). Diboron addition of $B_2(pin)_2$ to alkenes occurs in the presence of 15 mol % Cs_2CO_3 and 5.0 equiv MeOH (A strategy related to Lewis-base catalyzed boryl conjugate additions discussed in Chapter 1). Alkyl- or aryl-substituted alkenes can be

used as substrates and proceed in the reaction to afford the diboron products with high selectivity (usually 99% diboronate vs monoboronate). It is worth to mention that compound **3.12** can be obtained from an internal alkene **3.13** in 69% yield with high syn selectivity (97%).[115a]

Recently, the Morken group reported a catalytic enantioselective diboron addition of alkenes with a carbohydrate-derived catalyst.[116] As shown in Scheme 3.2b, this time $B_2(neo)_2$ (neo = neopentylglycolato) is needed for high efficiency of the reaction [reaction with $B_2(pin)_2$ results in lower yield]. The corresponding diol products with an alkyl-substituent can be synthesized in good yield and high enantioselectivity; however, reaction with styrene is challenging affording the desired product in lower enantioselectivity (**3.11**, 61:39 er).

Scheme 3.2. Synthesis of vicinal diboronate compounds by transition-metal free catalysis

a) Methoxide-catalyzed diboron addition to alkenes

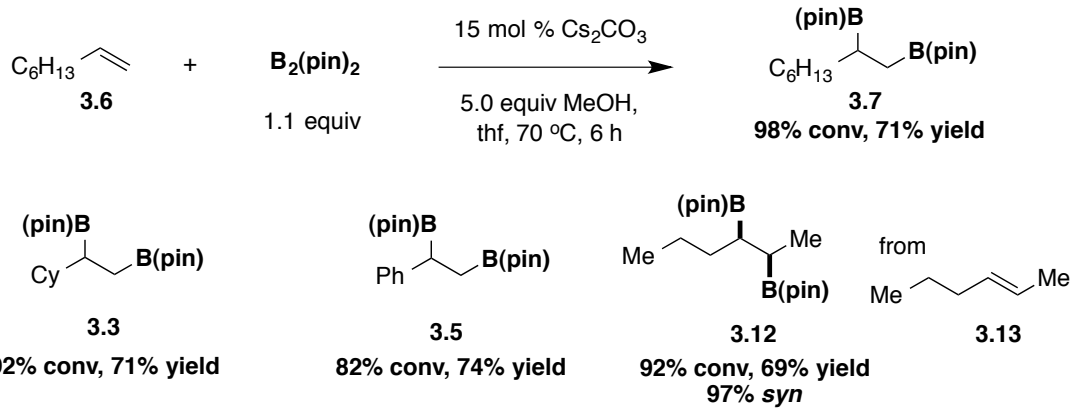

b) Carbohydrate-catalyzed enantioselective diboron addition to alkenes

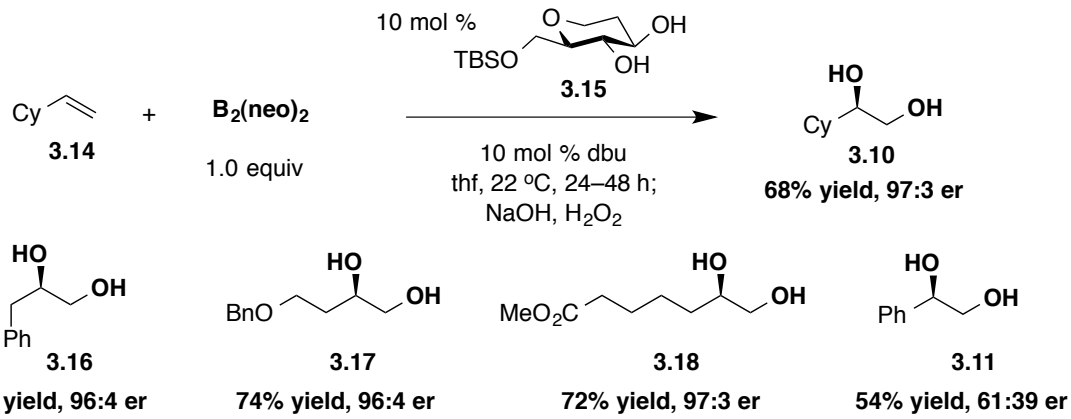

3.2.3. Synthesis of vicinal diboronate compounds from unsymmetrical diboron reagent

In 2010, the Suginome group introduced the use of an unsymmetrical diboron reagent [(dan)B–B(pin), (dan = naphthalene-1,8-diaminato)] in diboron addition reactions of alkynes.[119] As shown in Scheme 3.3a, in the presence of 3.0 mol % Ir-based complex, phenyl acetylene (**3.19**) proceeds to afford the diboron product **3.20** in 85% yield with

(119) (a) Iwadate, N.; Suginome, M. *J. Am. Chem. Soc.* **2010**, *132*, 2548–2549. For representative subsequent studies involving the use of (dan)B–B(pin), see: (b) Sake, R.; Hirano, K.; Miura, M. *J. Am. Chem. Soc.* **2015**, *137*, 6460–6463. (c) Guo, X.; Nelson, A. K.; Slebodnick, C.; Santos, W. L. *ACS Catal.* **2015**, *5*, 2172–2176.

high regioselectivity where the B(pin) unit is at the internal position. Substrates bearing heteroaryl- or alkyl-substituent are also suitable generating the products in 64–74% yield with 93–99% selectivity.

A report involving an alkoxide-promoted diboron addition of alkenes with (dan)B–B(pin) was subsequently reported in 2015.[120] In the presence of 30 mol % Cs_2CO_3 and MeOH as solvent, products are obtained in moderate yields with the B(pin) group is at the external position. In contrast to reactions with $B_2(pin)_2$ shown in Scheme 3.2a, reaction with styrene did not proceed to afford the diboron compounds.

(120) Miralles, N.; Cid, J.; Cuena, A. B.; Carbo, J. J.; Fernández, E. *Chem. Commun.* **2015**, *51*, 1693–1696.

Scheme 3.3. Synthesis of diboronate compounds with (dan)B–B(pin)

a) Ir-catalyzed diboron addition to alkynes

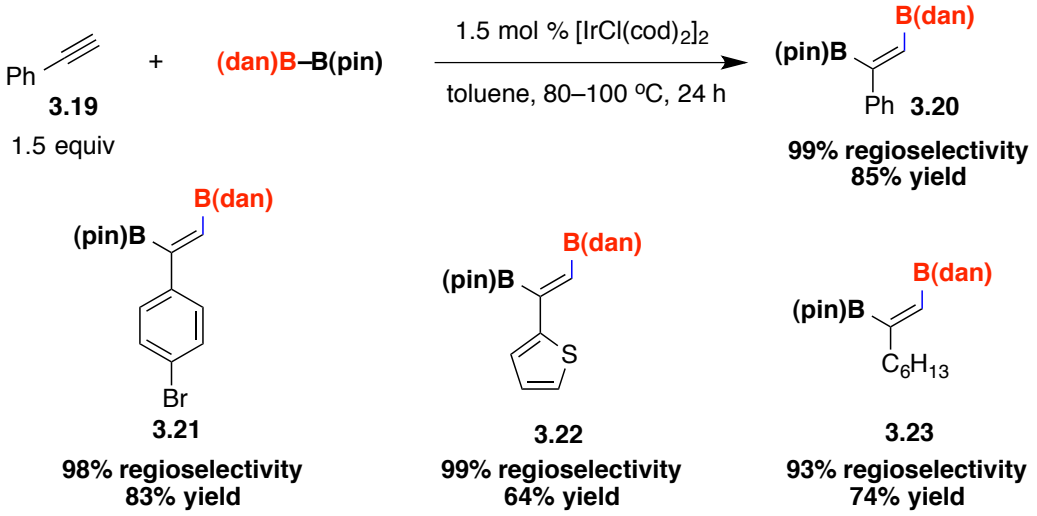

b) Alkoxide-catalyzed diboron addition to alkenes

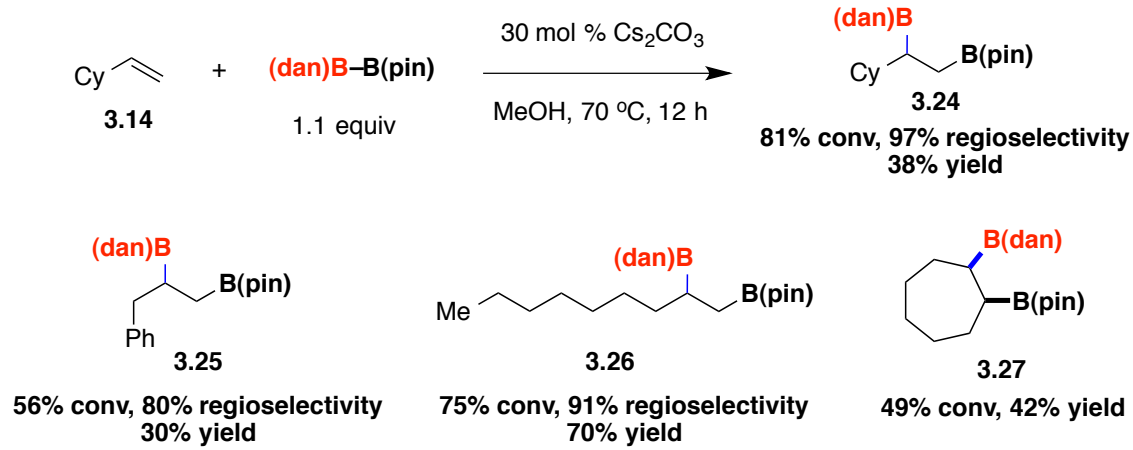

3.3. Synthesis of Vicinal Diboronate Compounds through Phosphine–Cu Catalyzed Boron–Allyl Addition to Alkenylboron Compounds

3.3.1. Reaction conditions optimization and ligand screen

As illustrated in Scheme 3.4, we envisioned the reaction of an alkenyl–B(pin) with $B_2(pin)_2$ and an allylic phosphate, in the presence of a Cu-based catalyst would

afford a product that contains a readily functionalizable alkene.[121,122] We viewed this as highly advantageous for synthesizing a number of otherwise difficult-to-access and desirable products.

The multicomponent strategy may have several distinct advantages, one of which would be the possibility of utilizing (dan)B–B(pin). We surmised that, as depicted in Scheme 3.4, the intermediate copper-alkoxide would favor interaction with the more Lewis acidic B(pin) unit, leading to the formation of the Cu–B(dan) complex (**v**), which would then generate a product with a terminal B(dan) and an internal B(pin) group (**viii**). As such, a sequence involving an alkenyl–B(dan) substrate and $B_2(pin)_2$ would furnish the alternative diboron isomer [i.e., primary C–B(pin) and secondary C–B(dan)]. Because differentiation of these two types of boronate groups is much more straightforward than that of two B(pin) groups, the resulting product would offer a distinct advantage regarding subsequent functionalization. This would be especially the case when selective reaction at the typically less reactive secondary C–B bond is desired.

(121) For related processes involing aryl olefins and promoted by a combination of a chiral bis-phosphine–Cu and an achiral bis-phosphine–Pd co-catalyst, see: a) Jia, T.; Cao, P.; Wang, B.; Lou, Y.; Yin, X.; Wang, M.; Liao, J. *J. Am. Chem. Soc.* **2015**, *137*, 13760–13763. For transformations that commence with an enantioselective Cu–H addition, see: b) Wang, Y.-M.; Buchwald, S. L. *J. Am. Chem. Soc.* **2016**, *138*, 5024–5027; c) Han, J. T.; Jang, W. J.; Kim, N.; Yun, J. *J. Am. Chem. Soc.* **2016**, *138*, 15146–15149.

(122) For hydroamination of alkenylboron compounds, see: a) Nishikawa, D.; Hirano, K.; Miura, M. *J. Am. Chem. Soc.* **2015**, *137*, 15620–15623. For aminoboration of alkenylboron compounds, see: b) Nishikawa, D.; Hirano, K.; Miura, M. *Org. Lett.* **2016**, *18*, 4856–4859.

Scheme 3.4. The key objectives of the study

With $B_2(pin)_2$ as the reagent

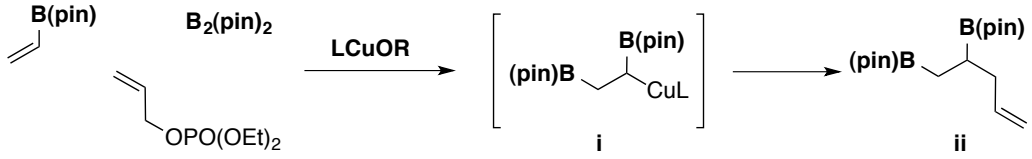

With (dan)B–B(pin) as the reagent

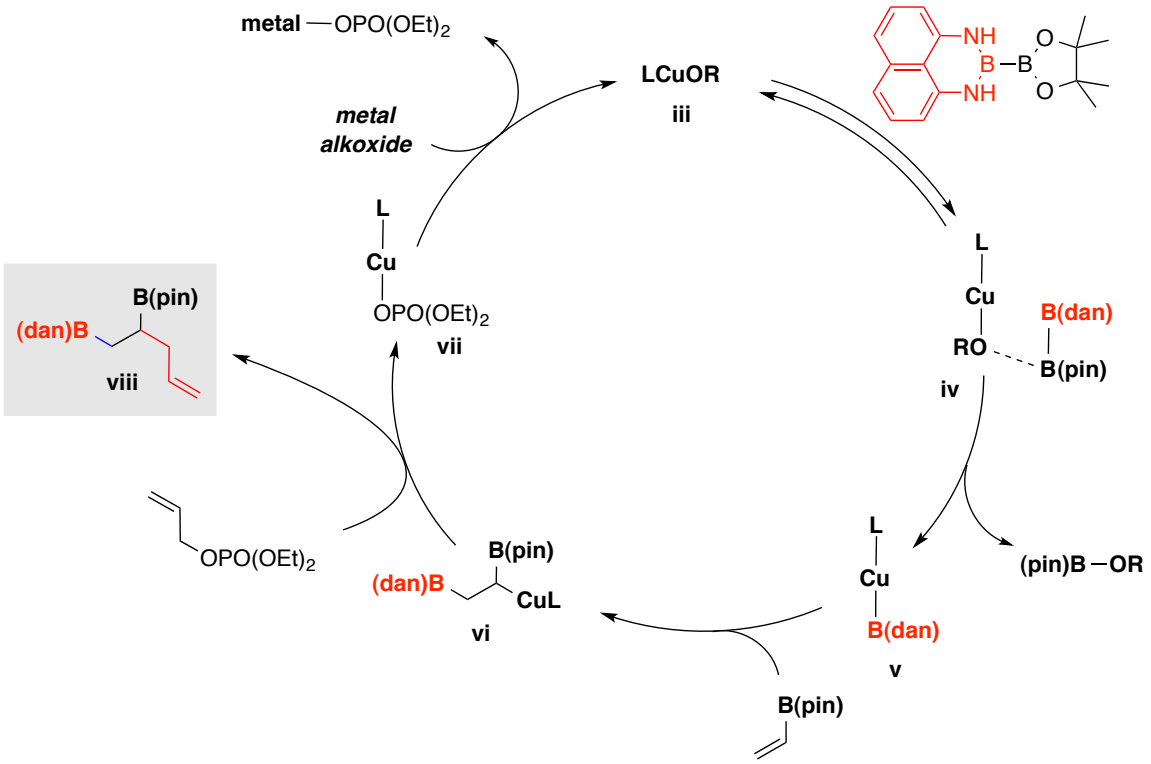

We began by investigating the possibility of a three-component process with vinyl–B(pin), allylphosphate and $B_2(pin)_2$ (Table 3.1). Reaction in the presence of 10 mol % Cu–PPh_3 and NaO*t*-Bu as a base, vicinal diboronate **3.28** was isolated in 81% yield (entry 1). However, in the absence of a ligand there was 90% conv of the limiting reagent [(vinyl–B(pin)] but **3.28** was obtained in only 13% yield indicating an important of the role of the ligand on Cu (entry 2). Evaluation of other metal alkoxides indicated that LiO*t*-Bu is the optimal generating the product in 92% yield after 2 hours (entries 3).

Table 3.1. Examination of different bases with PPh_3–Cu complex[a]

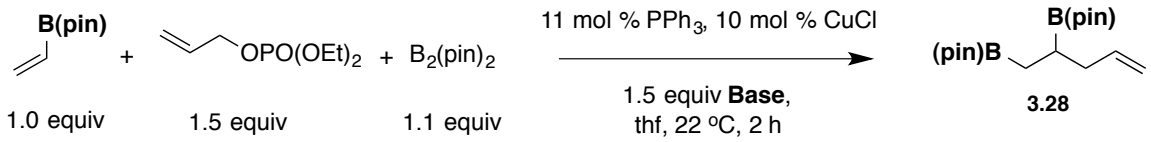

entry	base	conv (%)[b]	yield (%)[c]
1	NaO*t*-Bu	**>98**	**81**
2	NaO*t*-Bu (without PPh_3)	**90**	**13**
3	LiO*t*-Bu	**>98**	**92**
4	KO*t*-Bu	**>98**	**72**

[a] All reactions were performed under N_2 atm. [b] Determined by analysis of 400 MHz ^{1}H NMR spectra of unpurified mixtures. [c] Yields of purified products.

We then examined several mono- and bidentate phosphines (Scheme 3.5). It was found that use of PCy_3 is optimal affording the product in 92% yield after 1 hour. Reaction with NHC–Cu proved to be much less efficient (**im-1**, 17% yield). The diminished efficiency with the more Lewis basic ligand systems probably arises from a more nucleophilic Cu–B(pin) complex and thus a more competitive reaction with allylphosphate, leading to the generation of allyl–B(pin).[123] Thus, it appears that certain phosphine ligands (e.g., PPh_3 or PCy_3) offer sufficient catalyst activation to engender facile Cu–B(pin) addition to an alkenyl–B(pin) but not to an allylphosphate.

(123) a) Ito, H.; Ito, S.; Sasaki, Y.; Matsuura, K.; Sawamura, M. *J. Am. Chem. Soc.* **2007**, *129*, 14856–14857; b) Guzman-Martinez, A.; Hoveyda, A. H. *J. Am. Chem. Soc.* **2010**, *132*, 10634–10637.

Scheme 3.5. Examination of different Cu complexes

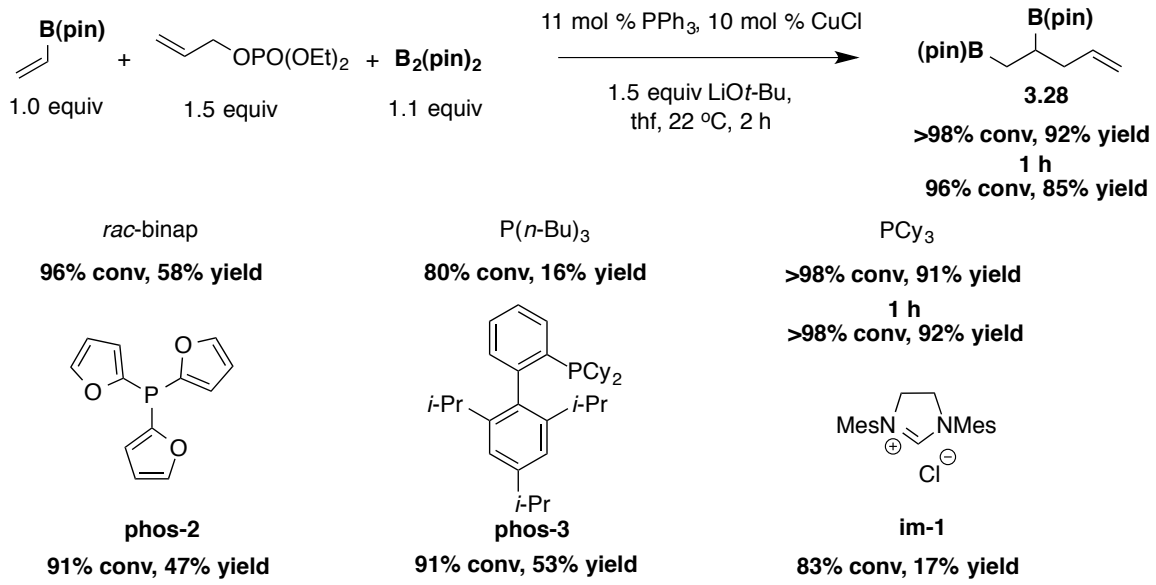

3.3.2. Scope of the three-component processes to access vicinal diboronate compounds

Reactions with a variety of 2-substituted allylic phosphates promoted by a catalyst derived from PCy_3 and CuCl are shown in Scheme 3.6. Reactions with electrophiles bearing an alkyl (**3.29**–**3.30**), aryl (**3.31**), heteroaryl (**3.32**), silyl (**3.33**) substituent proceed to afford products in 61–92% yield. It is noteworthy that products containing a functionalizable carboxylic ester (**3.34**) or an alkenyl chloride or bromide (**3.35–3.36**) can be obtained in 56–85% yield; interference by the carbon–halogen bond is minimal. The transformations are highly site-selective as the formation of the geminal diboronate isomer is not observed.

Scheme 3.6. Products with vicinal B(pin) units from reactions with various allylic phosphates

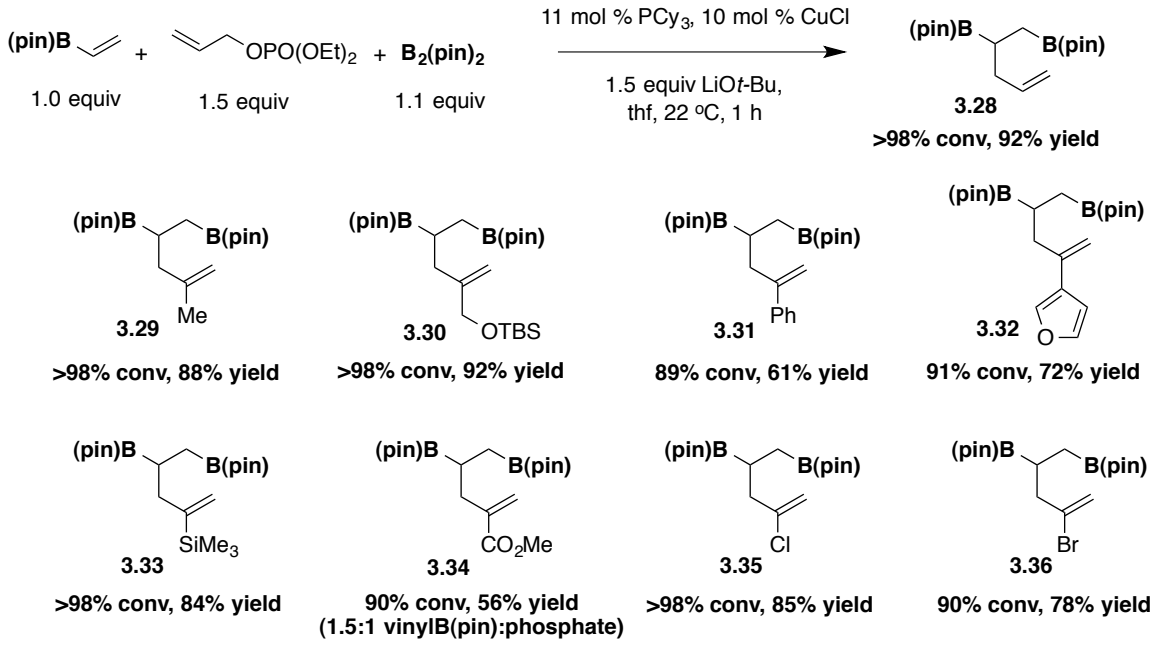

We then turned to exploring the possibility of site-selective generation of differentiated diboronate compounds through the use of (dan)B–B(pin). As illustrated in Scheme 3.7, the transformations afford products that contain a primary C–B(dan) and a secondary C–B(pin) moiety with complete selectivity (<2% of the alternative isomer detected by ^{1}H NMR of the unpurified mixture). Similar to the reactions with $B_2(pin)_2$ (Scheme 3.6), an assortment of allylic phosphates may be employed. It is interesting that transformation to produce **3.44** is not efficient generating the product in only 27% yield [vs 78% yield with $B_2(pin)_2$]. It might be because Cu–O*t*-Bu reacts with (dan)B–B(pin) less efficiently making side-reactions more competitive with Br-substituted allylic phosphate. We were also able to obtain the X-ray structures of vicinal diboronates **3.40** and **3.41** to ascertain the identity of the products.

Scheme 3.7. Products containing a secondary C–B(pin) and a primary C–B(dan)

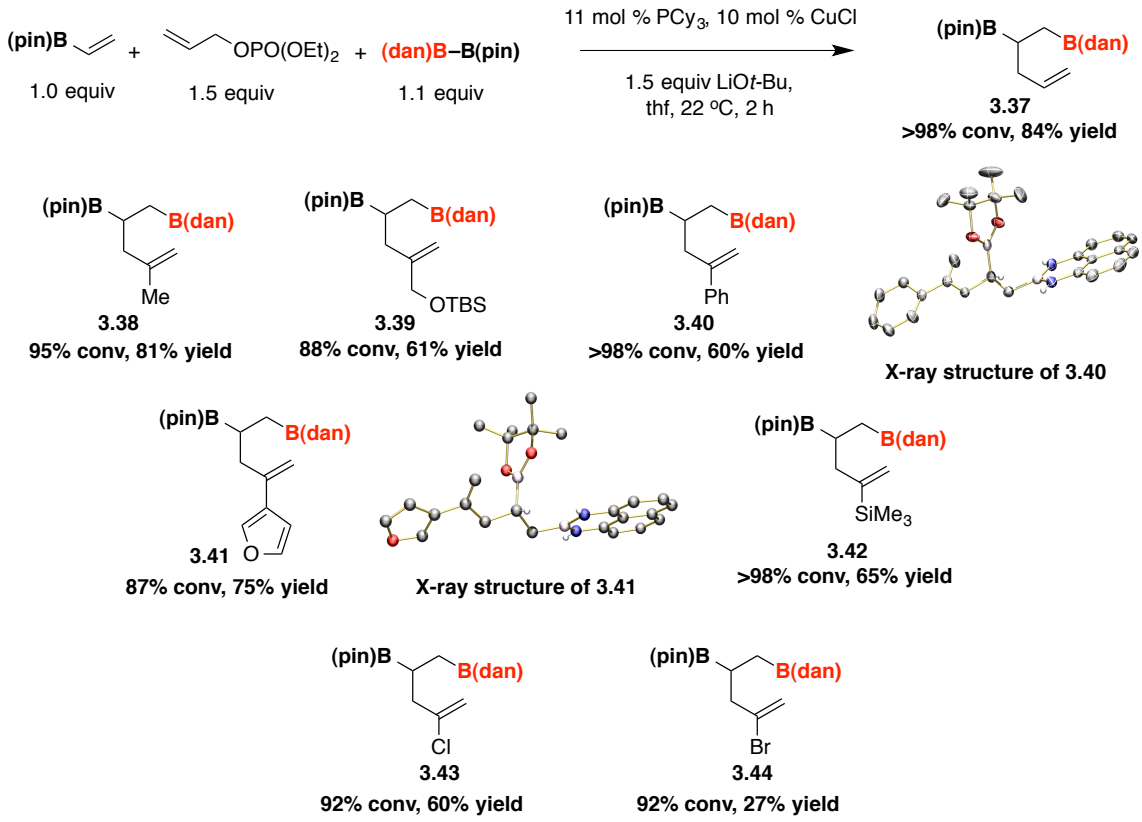

Another key advantage of the multicomponent approach is that it can allow access to vicinal diboronate products with a boron-substituted quaternary carbon center. These entities cannot be accessed efficiently through catalytic diboron additions to 1,1-disubstituted olefins or alkynes. The examples provided in Scheme 3.8 are illustrative (**3.46–3.52**). It is again noteworthy that products with an alkenyl halide group are tolerated (**3.51**–**3.52**). Furthermore, despite the increased steric hindrance of the substrate (**3.45**), reactions proceeded to completion within two hours under similar conditions as used for transformations involving vinyl–B(pin), except slightly excess of **3.45** is required for higher yields of the products.

Scheme 3.8. Products containing a tertiary C–B(pin) and a primary C–B(pin)

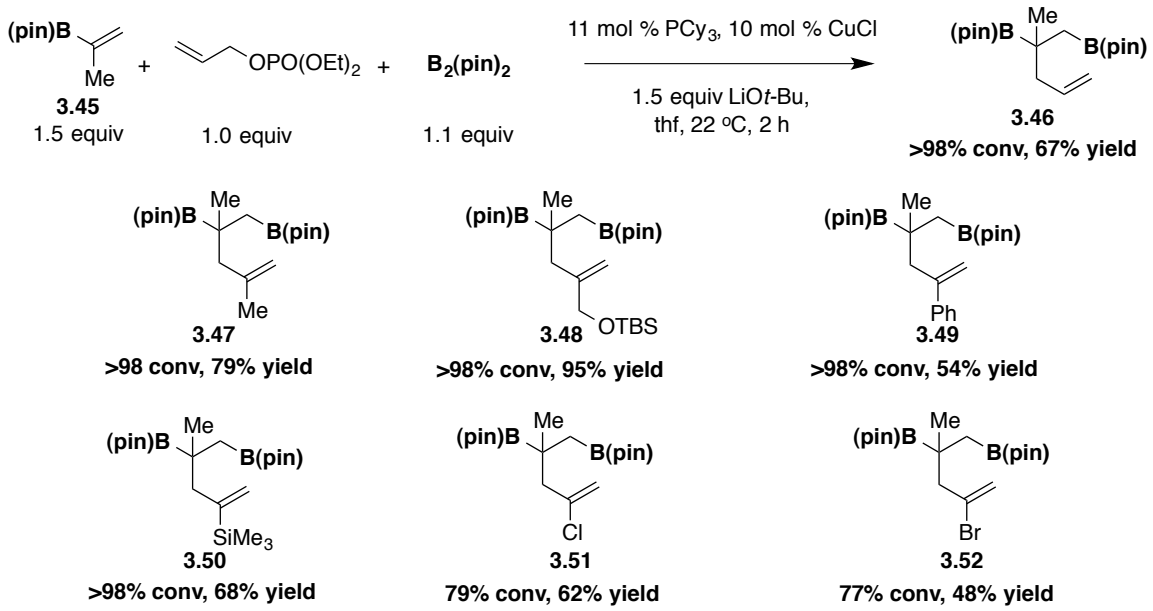

The catalytic transformations presented in Scheme 3.9 further underline the broad scope of the method. Differentiable vicinal organoboron products that contain a (pin)B-substituted carbon center can be prepared easily through the use of the appropriate alkenyl–B(pin) as the substrate and (dan)B–B(pin) as the reagent; thus compound **3.53** could be obtained in 68% yield after 4 hours at ambient temperature. Similarly noteworthy is the transformation with vinyl–B(dan), obtained easily from vinyl–B(pin) (single step), leading to the efficient formation (>98% conv, 1 h) of the diboronate product **3.55** in 88% yield, the identity of which was confirmed by X-ray crystallography (Scheme 3.9).

Scheme 3.9. Extended scope of the reaction

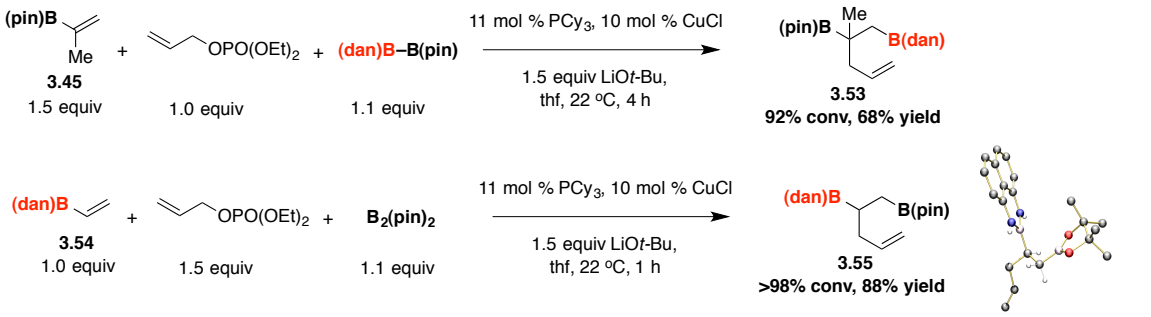

The multicomponent reactions are scalable and can be performed with reduced catalyst loading; two illustrative cases are shown in Scheme 3.10. These transformations were performed with 2.5 mol % of the PCy_3–Cu complex, although longer reaction time required (12 h). Diboron products **3.37** and **3.46** were obtained in 91% and 78% yield, respectively.

Scheme 3.10. Reactions performed on a larger scale with reduced catalyst loading

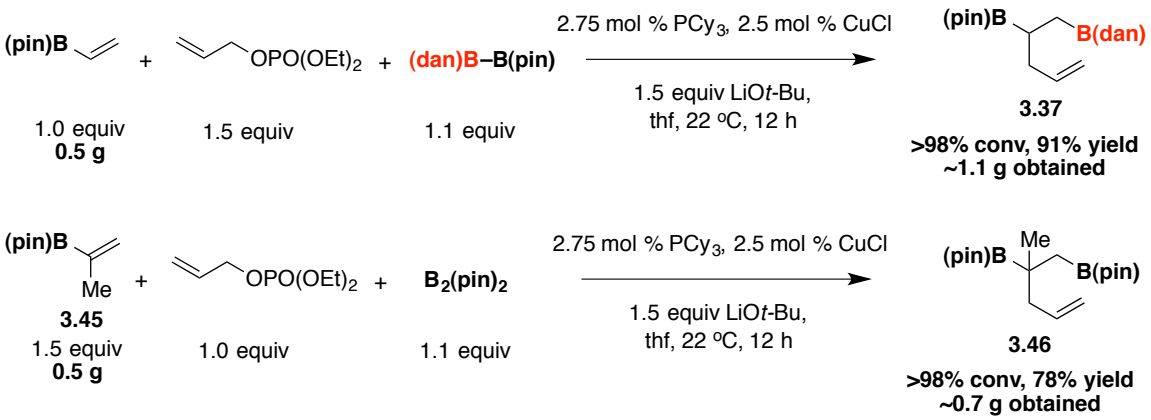

3.3.3. Functionalizations of the vicinal diboronate compounds

The C–B(pin) bond of the diboronate products can be site selectively oxidized to afford the corresponding alcohols containing C–B(dan) unit with high efficiency and selectivity (**3.56** and **3.57**, Scheme 3.11). The remaining C–B(dan) moiety can be

subsequently converted to a C–B(pin) and then used for C–C by a reported method,[124] leading to the formation of silyl ethers **3.59** and **3.61**. The state-of-the-art pertaining to direct conversion of a C–B(dan) to a C–C bond by means of catalytic cross-coupling is less advanced compared to those containing a C–B(pin). Thus, future developments in this key area will further enhance the utility of the present approach.

Scheme 3.11. Chemoselective functionalization

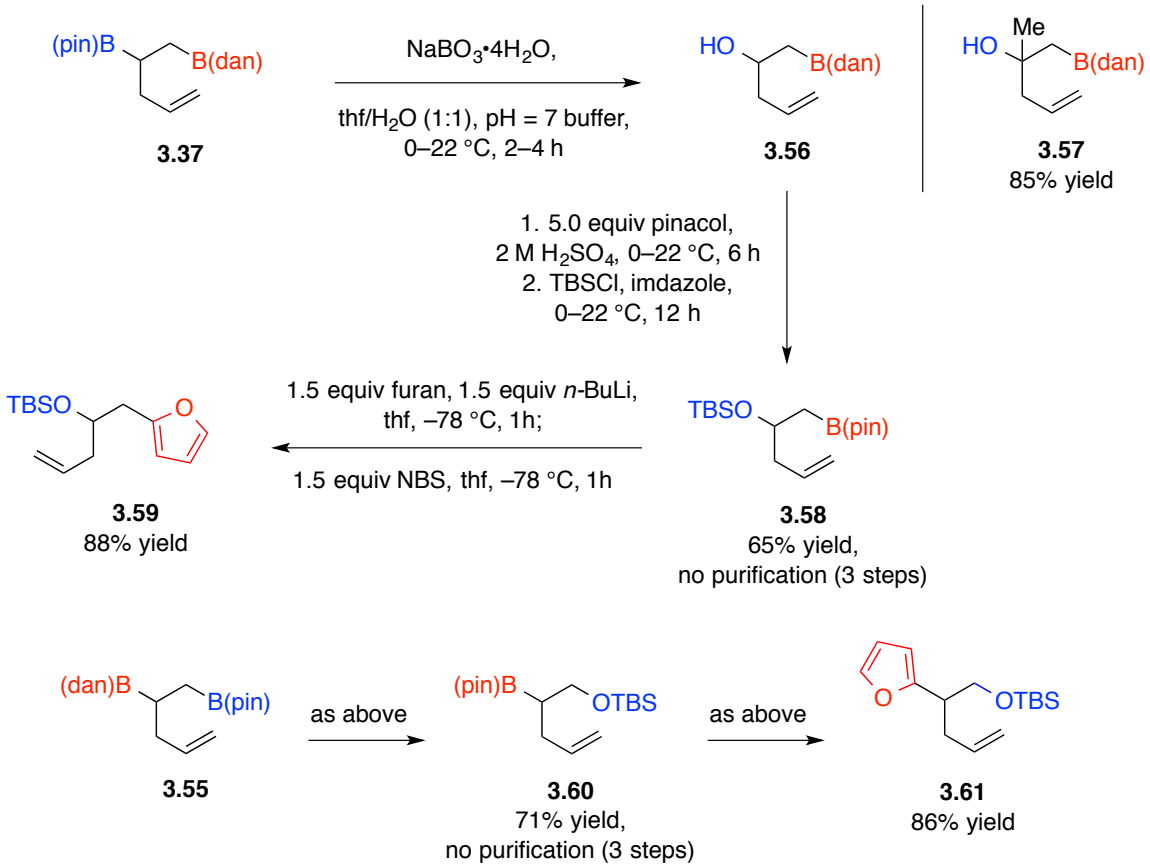

Another set of important functionalizations of products involves recently developed catalyst-controlled stereoselective cross-metathesis approaches for accessing

(124) Odachowski, M.; Bonet, A.; Essafi, S.; Conti-Ramsden, P.; Harvey, J. N.; Leonori, D.; Aggarwal, V. K. *J. Am. Chem. Soc.* **2016**, *138*, 9521–9532.

alkenyl halide compounds (Scheme 3.12).[125] With 5.0 mol % Mo-1, *Z*-alkenyl chlorides **3.62** and **3.64** were obtained in exceptionally high *Z* selectivity (>98:2 *Z*:*E*) and in 62% and 86% yield, respectively. Switching the cross partner to *Z*-1-bromo-2-fluoroethene, *Z*-alkenyl fluoride **3.63** and **3.65** can be synthesized with >98% *Z* selectivity, but with moderate F:Br ratios due to the unhindered nature of the olefin.

Scheme 3.12. Catalytic *Z*-selective cross-metathesis

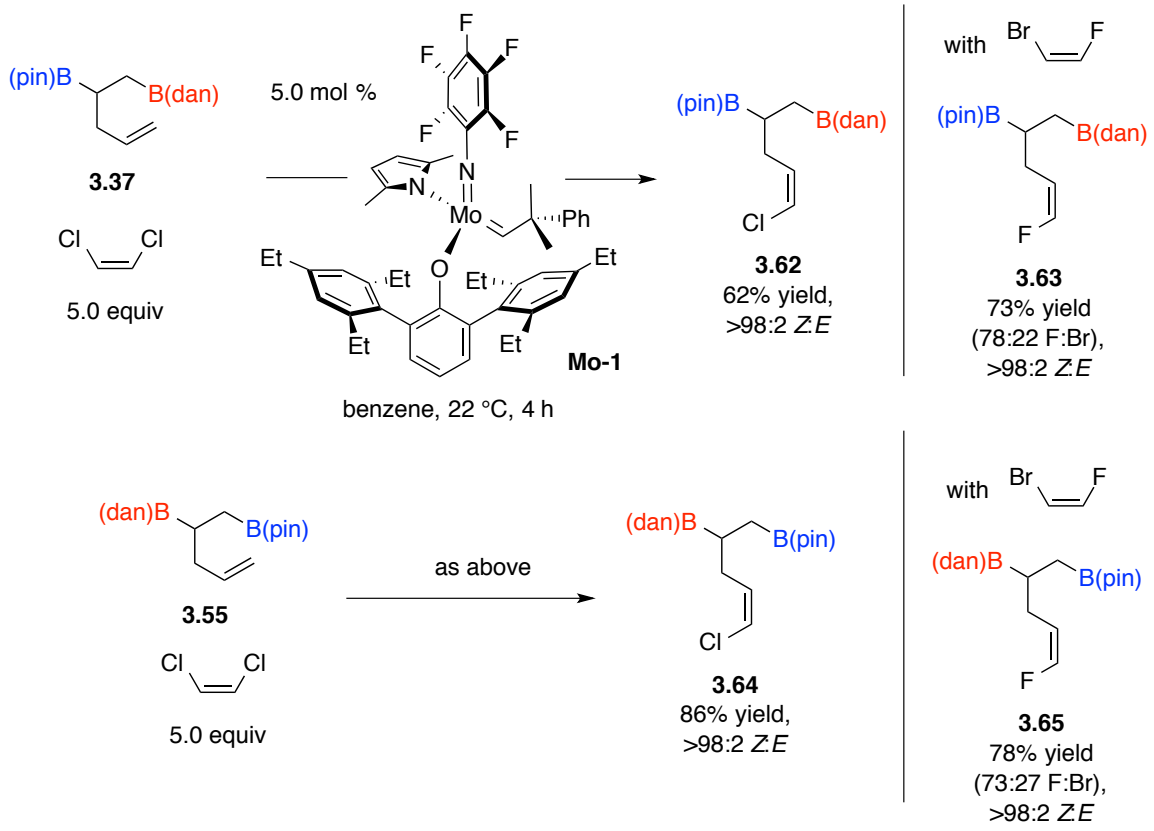

3.4. Conclusions

We have developed a practical and general catalytic multicomponent processes to access a variety of vicinal diboronate compounds. The transformations are promoted

(125) a) Koh, M. J.; Nguyen, T. T.; Zhang, H.; Schrock, R. R.; Hoveyda, A. H. *Nature* **2016**, *531*, 459–464. For the corresponding kinetically *E*-selective cross-metathesis reactions, see: b) Nguyen, T. T.; Koh, M. J.; Shen, X.; Romiti, F.; Schrock, R. R.; Hoveyda, A. H. *Science* **2016**, *352*, 569–575.

simply by a Cu complex derived from PCy_3 and CuCl and with commercially available diboron reagents [$B_2(pin)_2$ or (dan)B–B(pin)]. The ability for facile access to either regioisomeric products with a C–B(pin) and an adjacent C–B(dan) bond that can be site selectively modified is a particularly noteworthy feature of the new approach.

3.5. Experimental Section

General. Infrared (IR) spectra were recorded on a Bruker FT-IR Alpha (ATR mode) spectrophotometer, ν_{max} in cm^{-1}. Bands are characterized as broad (br), strong (s), medium (m), and weak (w). ^1H NMR spectra were recorded on Varian Unity INOVA 400 (400 MHz), 500 (500 MHz), or 600 (600 MHz) spectrometers. Chemical shifts are reported in ppm from tetramethylsilane with the solvent resonance as the internal standard ($CDCl_3$: δ 7.26 ppm). Data are reported as follows: chemical shift, integration, multiplicity (s = singlet, d = doublet, t = triplet, q = quartet, pent = pentet, m = multiplet, br = broad, app = apparent), and coupling constants (Hz). ^{13}C NMR spectra were recorded on Varian Unity INOVA 400 (100 MHz), 500 (125 MHz), or 600 (150 MHz) spectrometers with complete proton decoupling. Chemical shifts are reported in ppm from tetramethylsilane with the solvent resonance as the internal standard ($CDCl_3$: δ 77.16 ppm). High-resolution mass spectrometry was performed on a JEOL AccuTOF DART (positive mode) at the Mass Spectrometry Facility, Boston College. Melting points were measured on a Thomas Hoover capillary melting point apparatus and are uncorrected. X-ray structures were obtained, as described in the cif file, with a Microfocus sealed Cu tube from Incote. It is well established that that aforementioned detector allows for the determination of absolute configuration of molecules that do not have a heavy atom.

Unless otherwise noted, reactions were carried out with distilled and degassed solvents under an atmosphere of dry N_2 in oven- (135 ºC) or flame-dried glassware with standard dry box or vacuum-line techniques. Hexanes was purified under a positive pressure of dry argon by a modified Innovative Technologies purification system through a copper oxide and alumina column. Tetrahydrofuran (thf; Aldrich Chemical Co.) was purified by distillation from sodium benzophenone ketyl immediately prior to use. All work-up and purification procedures were carried out with reagent grade solvents (purchased from Fisher Scientific) under air.

■ **Reagents:**

Bis(pinacolato)diboron [$B_2(pin)_2$]: purchased from Frontier Scientific, Inc., recrystallized from pentane and dried under vacuum prior to use.

***n*-Butyllithium (1.6 M in hexanes):** purchased from Aldrich and used as received.

Copper(I) chloride: purchased from Strem and used as received.

Diethyl allyl phosphate: purchased from Aldrich and used as received.

Imidazolinium salt im-1: purchased from Aldrich and used as received.

Isopropenylboronic acid pinacol ester (3.45): purchased from Aldrich and used as received.

Lithium *tert*-butoxide: purchased from Strem and used as received.

Phosphine ligands: purchased from Strem and used as received.

Potassium *tert*-butoxide: purchased from Strem and used as received.

Sodium *tert*-butoxide: purchased from Strem and used as received.

2-(4,4,5,5-Tetramethyl-1,3,2-dioxaborolan-2-yl)-2,3-dihydro-1H-naphtho[1,8-

de][1,3,2]diazaborinine [(dan)B–B(pin)]: purchased from AKSci and used as received.

Vinylboronic acid pinacol ester [vinyl–B(pin)]: purchased from Combi-Blocks and distilled over CaH_2 prior to used.

Vinyl–B(dan) (3.54): prepared from vinyl–B(pin) according to a previously reported procedure.[126]

■ **Representative Procedure for the Catalytic Cu–B(pin) Addition to Vinyl–B(pin) Followed by Allylic Substitution Reaction (Scheme 3.6)**

In a N_2-filled glove box, an oven-dried 1 dram vial equipped with a stir bar was charged with PCy_3 (3.1 mg, 0.0055 mmol), Li*O*t-Bu (12 mg, 0.15 mmol), CuCl (0.50 mg, 0.0050 mmol), and thf (1.0 mL). The mixture was allowed to stir for 15 min at 22 °C; during this time the solution turned light-yellow. Bis(pinacolato)diboron (28 mg, 0.11 mmol) was added to the mixture, causing the solution to turn dark brown immediately. Vinyl–B(pin) (15.4 mg, 0.10 mmol), allylphosphate (29.1 mg, 0.15 mmol), and thf (0.50 mL) were added. The vial was sealed with a cap and electrical tape before removal from the glove box. The resulting mixture was allowed to stir at 22 °C for 1 h. The mixture was then passed through a short plug of silica gel (4 x 1 cm) and eluted with Et_2O. The organic layer was concentrated under reduced pressure, affording yellow oil, which was purified by silica gel chromatography (100% hexanes→hexanes:Et_2O = 10:1) to afford **3.28** as colorless oil (29.6 mg, 0.092 mmol, 92% yield). **2,2'-(Pent-4-ene-1,2-diyl)bis(4,4,5,5-tetramethyl-1,3,2-dioxaborolane) (3.28):** IR (neat): 2978 (m), 2927 (w),

(126) Iannazzo, L.; Vollhardt, K. P. C.; Malacria, M.; Aubert, C.; Gandon, V. *Eur. J. Org. Chem.* **2011**, 3238–3292.

1371 (s), 1314 (s), 1143 (s), 968 (w) cm–1; 1H NMR (400 MHz, CDCl3): δ 5.84–5.74 (1H, m), 5.00–4.90 (2H, m), 2.25–2.18 (1H, m), 2.11–2.04 (1H, m), 1.22 (12H, s), 1.21 (12H, s), 1.27–1.21 (1H, m), 0.90–0.78 (2H, m); 13C NMR (100 MHz, CDCl3): δ 138.8, 115.1, 83.0, 82.96, 38.0, 25.0, 24.99, 24.93, 24.91; HRMS (DART): Calcd for C17H33B2O4 [M+H]+: 323.2565, Found: 323.2575.

2,2'-(4-Methylpent-4-ene-1,2-diyl)bis(4,4,5,5-tetramethyl-1,3,2-dioxaborolane) (3.29): IR (neat): 2978 (m), 2928 (w), 1370 (s), 1314 (s), 1143 (s), 968 (w) cm^{-1}; ^{1}H NMR (400 MHz, $CDCl_3$): δ 4.68 (1H, d, *J* = 1.6 Hz), 4.66 (1H, d, *J* = 0.8 Hz), 2.20 (1H, dd, *J* = 14.0, 7.2 Hz), 2.00 (1H, dd, *J* = 14.2, 8.6 Hz), 1.58 (3H, s), 1.35–1.27 (1H, m), 1.22 (12H, s), 1.217 (12H, s), 0.85–0.74 (2H, m); ^{13}C NMR (100 MHz, $CDCl_3$): δ 135.2, 117.2, 83.3, 83.1, 44.6, 25.0, 24.97, 24.9; HRMS (DART): Calcd for $C_{18}H_{35}B_2O_4$ $[M+H]^+$: 337.2721, Found: 337.2722.

***tert*-Butyldimethyl((2-methylene-4,5-bis(4,4,5,5-tetramethyl-1,3,2-dioxaborolan-2-yl)pentyl)oxy)silane (3.30)**: IR (neat): 2977 (w), 2929 (w), 2856 (w), 1370 (s), 1313 (s), 1252 (m), 1142 (s), 1101 (m), 968 (m), 836 (s), 776 (m) cm^{-1}; ^{1}H NMR (400 MHz, $CDCl_3$): δ 5.05–5.04 (1H, m), 4.83–4.81 (1H, m), 4.05 (2H, s), 2.19 (1H, dd, *J* = 14.6, 7.4 Hz), 1.98 (1H, dd, *J* = 14.4, 8.4 Hz), 1.33–1.19 (1H, m), 1.22 (12H, s), 1.21 (12H, s), 0.90 (9H, s), 0.88–0.74 (2H, m), 0.05 (6H, s); ^{13}C NMR (100 MHz, $CDCl_3$): δ 148.0, 108.9, 83.0, 82.99, 65.7, 36.7, 26.1, 25.0, 24.97, 24.9, 18.6, –5.2; HRMS (DART): Calcd for $C_{24}H_{52}B_2N_1O_5Si_1$ $[M+NH_4]^+$: 484.3801, Found: 484.3795.

2,2'-(4-Phenylpent-4-ene-1,2-diyl)bis(4,4,5,5-tetramethyl-1,3,2-dioxaborolane) (3.31): IR (neat): 2977 (m), 2927 (w), 1370 (s), 1313 (s), 1142 (s), 968 (m) cm^{-1}; ^{1}H NMR (400 MHz, $CDCl_3$): δ 7.43–7.41 (2H, m), 7.30–7.22 (3H, m), 5.25 (1H, d, *J* = 2.0

Hz), 5.06 (1H, d, *J* = 1.2 Hz), 2.73 (1H, dd, *J* = 13.6, 7.6 Hz), 2.48 (1H, dd, *J* = 14.6, 7.8 Hz), 1.34–1.27 (1H, m), 1.22 (12H, s), 1.21 (12H, s), 0.88–0.79 (2H, m); ^{13}C NMR (100 MHz, $CDCl_3$): δ 148.4, 141.6, 128.2, 127.2, 126.5, 113.2, 83.0, 82.99, 39.0, 25.0, 24.99, 24.96, 24.92; HRMS (DART): Calcd for $C_{23}H_{40}B_2N_1O_4$ $[M+NH_4]^+$: 416.3143, Found: 416.3127.

2,2'-(4-(Furan-3-yl)pent-4-ene-1,2-diyl)bis(4,4,5,5-tetramethyl-1,3,2-dioxaborolane) (3.32): IR (neat): 2977 (m), 2928 (w), 1369 (s), 1312 (s), 1140 (s), 968 (m), 872 (m) cm^{-1}; ^{1}H NMR (400 MHz, $CDCl_3$): δ 7.54 (1H, s), 7.32 (1H, t, *J* = 1.6 Hz), 6.51 (1H, dd, *J* = 1.8, 1.0 Hz), 5.20 (1H, d, *J* = 1.2 Hz), 4.93 (1H, d, *J* = 1.6 Hz), 2.54 (1H, ddd, *J* = 14.1, 7.9, 0.9 Hz), 2.30 (1H, dd, *J* = 14.0, 7.6 Hz), 1.46–1.37 (1H, m), 1.23 (12H, s), 1.21 (12H, s), 0.90–0.81 (2H, m); ^{13}C NMR (100 MHz, $CDCl_3$): δ 142.9, 139.5, 139.3, 126.8, 110.9, 108.5, 83.1, 83.0, 38.7, 25.03, 25.01, 24.96, 24.94; HRMS (DART): Calcd for $C_{21}H_{35}B_2O_5$ $[M+H]^+$: 389.2671, Found: 389.2667.

(4,5-Bis(4,4,5,5-tetramethyl-1,3,2-dioxaborolan-2-yl)pent-1-en-2-yl)trimethylsilane (3.33): IR (neat): 2977 (m), 1370 (s), 1313 (s), 1247 (m), 1142 (s), 968 (m), 836 (s) cm^{-1}; ^{1}H NMR (400 MHz, $CDCl_3$): δ 5.57–5.56 (1H, m), 5.31–5.30 (1H, m), 2.38–2.32 (1H, m), 2.08 (1H, dd, *J* = 14.6, 8.2 Hz), 1.37–1.29 (1H, m), 1.22 (12H, s), 1.20 (12H, s), 0.86–0.73 (2H, m), 0.07 (9H, s); ^{13}C NMR (100 MHz, $CDCl_3$): δ 152.0, 124.4, 82.9, 82.87, 39.7, 25.0, 24.96, 24.9, –1.2; HRMS (DART): Calcd for $C_{20}H_{44}B_2N_1O_4Si_1$ $[M+NH_4]^+$: 412.3226, Found: 412.3222.

Methyl 2-methylene-4,5-bis(4,4,5,5-tetramethyl-1,3,2-dioxaborolan-2-yl)pentanoate (3.34): IR (neat): 2978 (m), 2928 (w), 1722 (m), 1629 (w), 1370 (s), 1315 (s), 1141 (s), 968 (m) cm^{-1}; ^{1}H NMR (400 MHz, $CDCl_3$): δ 6.14 (1H, d, *J* = 1.2 Hz), 5.53 (1H, dd, *J* =

2.8, 1.2 Hz), 3.72 (3H, s), 2.54 (1H, ddd, J = 14.6, 7.4, 0.8 Hz), 2.26 (1H, dd, J = 14.5, 7.7 Hz), 1.40–1.33 (1H, m), 1.22 (24H, s), 0.83 (2H, d, J = 7.6 Hz); ^{13}C NMR (100 MHz, $CDCl_3$): δ 168.0, 140.4, 125.5, 83.1, 83.06, 51.8, 35.4, 30.5, 25.0, 24.98, 24.9; HRMS (DART): Calcd for $C_{19}H_{35}B_2O_6$ $[M+H]^+$: 381.2620, Found: 381.2635.

2,2'-(4-Chloropent-4-ene-1,2-diyl)bis(4,4,5,5-tetramethyl-1,3,2-dioxaborolane) (3.35): IR (neat): 2979 (m), 2929 (w), 1633 (w), 1371 (s), 1317 (s), 1142 (s), 968 (w) cm^{-1}; ^{1}H NMR (400 MHz, $CDCl_3$): δ 5.13 (1H, d, J = 0.8 Hz), 5.10 (1H, d, J = 1.2 Hz), 2.52 (1H, ddd, J = 14.7, 6.5, 0.9 Hz), 2.35 (1H, ddd, J = 14.8, 8.8, 0.4 Hz), 1.53–1.42 (1H, m), 1.22 (24H, s), 0.90–0.79 (2H, m); ^{13}C NMR (100 MHz, $CDCl_3$): δ 143.0, 112.7, 83.3, 83.1, 42.4, 25.0, 24.97, 24.93, 24.92; HRMS (DART): Calcd for $C_{17}H_{32}B_2Cl_1O_4$ $[M+H]^+$: 357.2175, Found: 357.2179.

2,2'-(4-Bromopent-4-ene-1,2-diyl)bis(4,4,5,5-tetramethyl-1,3,2-dioxaborolane) (3.36): IR (neat): 2977 (m), 2928 (w), 1627 (w), 1369 (s), 1313 (s), 1139 (s), 967 (m), 882 (m), 856 (m), 844 (m) cm^{-1}; ^{1}H NMR (400 MHz, $CDCl_3$): δ 5.54 (1H, d, J = 1.2 Hz), 5.38 (1H, d, J = 1.2 Hz), 2.61 (1H, dd, J = 14.2, 5.8 Hz), 2.43 (1H, dd, J = 15.0, 9.0 Hz), 1.54–1.46 (1H, m), 1.23 (24H, s), 0.91–0.78 (2H, m); ^{13}C NMR (100 MHz, $CDCl_3$): δ 135.2, 117.2, 83.3, 83.1, 44.6, 25.0, 24.97, 24.9; HRMS (DART): Calcd for $C_{17}H_{32}B_2Br_1O_4$ $[M+H]^+$: 401.1670, Found: 401.1684.

■ **Representative Procedure for the Catalytic Cu–B(dan) Addition to Vinyl–B(pin) Followed by Allylic Substitution Reaction (Scheme 3.7)**

In a N_2-filled glove box, an oven-dried 1 dram vial equipped with a stir bar was charged with PCy_3 (3.1 mg, 0.0055 mmol), LiO*t*-Bu (12 mg, 0.15 mmol), CuCl (0.50 mg, 0.0050 mmol), and thf (1.0 mL). The mixture was allowed to stir for 15 min at 22 °C;

during this time the solution turned light-yellow. (dan)B–B(pin) (31.2 mg, 0.11 mmol) was added to the mixture, causing the solution to turn dark brown immediately. Vinyl–B(pin) (15.4 mg, 0.10 mmol), allylphosphate (29.1 mg, 0.15 mmol), and thf (0.50 mL) were added. The vial was sealed with a cap and electrical tape before removal from the glove box. The resulting mixture was allowed to stir at 22 °C for 2 h. The mixture was then passed through a short plug of celite and neutral alumina (4 x 1 cm) and eluted with Et_2O. The organic layer was concentrated under reduced pressure, affording brown oil, which was purified by neutralized silica gel chromatography (pre-treated with Et_3N, 100% hexanes→hexanes:Et_2O = 10:1) to afford **3.37** as off-white solid (30.4 mg, 0.084 mmol, 84% yield). **2-(2-(4,4,5,5-Tetramethyl-1,3,2-dioxaborolan-2-yl)pent-4-en-1-yl)-2,3-dihydro-1*H*-naphtho[1,8-*de*][1,3,2]diazaborinine (3.37):** Melting point: 104–105 ºC. IR (neat): 3399 (br), 2976 (w), 2899 (w), 1600 (s), 1510 (m), 1411 (m), 1373 (m), 1318 (m), 1139 (m), 820 (m), 763 (m) cm^{-1}; ^1H NMR (400 MHz, $CDCl_3$): δ 7.09 (2H, dd, *J* = 8.2, 7.4 Hz), 6.99 (2H, dd, *J* = 8.4, 0.8 Hz), 6.26 (2H, dd, *J* = 7.2, 0.8 Hz), 6.01 (2H, br s), 5.83 (1H, ddt, *J* = 17.2, 10.0, 6.8 Hz), 5.08–4.98 (2H, m), 2.34–2.27 (1H, m), 2.13 (1H, app pent, *J* = 7.0 Hz), 1.32–1.22 (1H, m), 1.27 (12H, s), 0.98 (2H, d, *J* = 8.0 Hz); ^{13}C NMR (100 MHz, $CDCl_3$): δ 141.5, 138.6, 136.5, 127.7, 119.7, 117.2, 115.4, 105.4, 83.5, 38.3, 25.01, 25.0; HRMS (DART): Calcd for $C_{21}H_{29}B_2N_2O_2$ $[M+H]^+$: 363.2415, Found: 363.2430.

2-(4-Methyl-2-(4,4,5,5-tetramethyl-1,3,2-dioxaborolan-2-yl)pent-4-en-1-yl)-2,3-dihydro-1*H*-naphtho[1,8-*de*][1,3,2]diazaborinine (3.38): IR (neat): 3395 (br), 2976 (w), 2919 (w), 1599 (s), 1510 (m), 1411 (s), 1372 (s), 1317 (m), 1139 (s), 820 (m), 763 (s) cm^{-1}; ^1H NMR (400 MHz, $CDCl_3$): δ 7.09 (2H, dd, *J* = 8.2, 7.4 Hz), 6.99 (2H, dd, *J* = 8.4,

0.8 Hz), 6.27 (2H, dd, *J* = 7.2, 0.8 Hz), 6.03 (2H, br s), 4.76 (1H, s), 4.73 (1H, s), 2.29 (1H, dd, *J* = 14.0, 8.0 Hz), 2.05 (1H, dd, *J* = 14.2, 8.2 Hz), 1.73 (3H, s), 1.43–1.35 (1H, m), 1.27 (12H, s), 1.01–0.88 (2H, m); ^{13}C NMR (100 MHz, $CDCl_3$): δ 145.6, 141.6, 136.5, 127.7, 119.7, 117.2, 111.0, 105.4, 83.5, 41.9, 25.0, 24.96, 22.4; HRMS (DART): Calcd for $C_{22}H_{31}B_2N_2O_2$ $[M+H]^+$: 377.2572, Found: 377.2574.

2-(4-(((*tert*-Butyldimethylsilyl)oxy)methyl)-2-(4,4,5,5-tetramethyl-1,3,2-dioxaborolan-2-yl)pent-4-en-1-yl)-2,3-dihydro-1*H*-naphtho[1,8-*de*][1,3,2]diazaborinine (3.39): IR (neat): 3398 (br), 2976 (w), 2955 (w), 2928 (w), 2891 (w), 2856 (w), 1601 (s), 1511 (m), 1411 (m), 1373 (m), 1320 (m), 1252 (m), 1141 (m), 1103 (m), 836 (m), 763 (m) cm^{-1}; ^{1}H NMR (400 MHz, $CDCl_3$): δ 7.08 (2H, dd, *J* = 8.0, 7.2 Hz), 6.98 (2H, dd, *J* = 8.6, 1.0 Hz), 6.26 (2H, dd, *J* = 7.6, 0.8 Hz), 6.03 (2H, br s), 5.09 (1H, d, *J* = 2.0 Hz), 4.87 (1H, d, *J* = 2.0 Hz), 4.08 (2H, s), 2.26 (1H, dd, *J* = 14.8, 8.0 Hz), 2.03 (1H, dd, *J* = 14.6, 7.8 Hz), 1.41–1.28 (1H, m), 1.25 (12H, s), 1.03–0.91 (2H, m), 0.92 (9H, s), 0.07 (6H, s); ^{13}C NMR (100 MHz, $CDCl_3$): δ 148.2, 141.5, 136.5, 127.7, 119.7, 117.2, 109.0, 105.4, 83.6, 65.8, 37.0, 26.1, 25.0, 24.97, 18.6, –5.19, –5.17; HRMS (DART): Calcd for $C_{28}H_{45}B_2N_2O_3Si_1$ $[M+H]^+$: 507.3386, Found: 507.3396.

2-(4-Phenyl-2-(4,4,5,5-tetramethyl-1,3,2-dioxaborolan-2-yl)pent-4-en-1-yl)-2,3-dihydro-1*H*-naphtho[1,8-*de*][1,3,2]diazaborinine (3.40): Melting point: 128–130 ºC. IR (neat): 3401 (br), 2976 (w), 2925 (w), 1627 (w), 1599 (s), 1411 (m), 1372 (m), 1318 (m), 1140 (m), 820 (m), 764 (m) cm^{-1}; ^{1}H NMR (400 MHz, $CDCl_3$): δ 7.42–7.40 (2H, m), 7.35–7.25 (3H, m), 7.07 (2H, dd, *J* = 8.4, 7.2 Hz), 6.97 (2H, dd, *J* = 8.2, 1.0 Hz), 6.22 (2H, dd, *J* = 7.2, 1.2 Hz), 5.91 (2H, br s), 5.28 (1H, d, *J* = 1.6 Hz), 5.11 (1H, d, *J* = 1.2 Hz), 2.81 (1H, dd, *J* = 14.5, 7.9 Hz), 2.48 (1H, dd, *J* = 14.1, 7.5 Hz), 1.37–1.31 (1H, m),

1.24 (12H, s), 1.02–0.89 (2H, m); ^{13}C NMR (100 MHz, $CDCl_3$): δ 148.6, 141.53, 141.5, 136.5, 128.4, 127.7, 127.5, 126.5, 119.7, 117.2, 113.4, 105.4, 83.5, 39.4, 25.0, 24.96; HRMS (DART): Calcd for $C_{27}H_{33}B_2N_2O_2$ $[M+H]^+$: 439.2728, Found: 439.2724.

2-(4-(Furan-3-yl)-2-(4,4,5,5-tetramethyl-1,3,2-dioxaborolan-2-yl)pent-4-en-1-yl)-2,3-dihydro-1*H*-naphtho[1,8-*de*][1,3,2]diazaborinine (3.41): Melting point: 139–140 ºC. IR (neat): 3396 (br), 2974 (w), 2926 (w), 1629 (w), 1600 (s), 1511 (m), 1411 (m), 1372 (m), 1317 (m), 1165 (m), 1139 (m), 765 (m) cm^{-1}; ^{1}H NMR (400 MHz, $CDCl_3$): δ 7.48 (1H, d, *J* = 1.2 Hz), 7.36 (1H, t, *J* = 1.6 Hz), 7.08 (2H, dd, *J* = 8.2, 8.4 Hz), 6.98 (2H, dd, *J* = 8.2, 1.0 Hz), 6.52 (1H, dd, *J* = 2.2, 1.0 Hz), 5.99 (2H, br s), 5.25 (1H, d, *J* = 1.2 Hz), 4.98 (1H, d, *J* = 1.2 Hz), 2.63 (1H, dd, *J* = 13.8, 7.8 Hz), 2.30 (1H, dd, *J* = 14.2, 7.4 Hz), 1.50–1.40 (1H, m), 1.24 (12H, s), 1.08–0.89 (2H, m); ^{13}C NMR (100 MHz, $CDCl_3$): δ 143.2, 141.5, 139.24, 139.2, 136.5, 127.7, 126.8, 119.7, 117.3, 111.0, 108.5, 105.4, 83.6, 39.0, 25.0, 24.9; HRMS (DART): Calcd for $C_{25}H_{31}B_2N_2O_3$ $[M+H]^+$: 429.2521, Found: 429.2507.

2-(2-(4,4,5,5-Tetramethyl-1,3,2-dioxaborolan-2-yl)-4-(trimethylsilyl)pent-4-en-1-yl)-2,3-dihydro-1*H*-naphtho[1,8-*de*][1,3,2]diazaborinine (3.42): IR (neat): 3386 (br), 2976 (w), 2897 (w), 1628 (w), 1601 (s), 1513 (m), 1411 (m), 1372 (s), 1317 (m), 1247 (m), 1141 (s), 836 (s), 820 (m), 763 (s) cm^{-1}; ^{1}H NMR (400 MHz, $CDCl_3$): δ 7.09 (2H, t, *J* = 7.8 Hz), 6.98 (2H, d, *J* = 8.4 Hz), 6.27 (2H, dd, *J* = 7.4, 1.0 Hz), 6.04 (2H, br s), 5.63 (1H, s), 5.37 (1H, s), 2.44 (1H, dd, *J* = 15.0, 8.6 Hz), 2.13 (1H, dd, *J* = 14.8, 7.6 Hz), 1.44–1.38 (1H, m), 1.25 (12H, s), 1.03–0.89 (2H, m), 0.10 (9H, s); ^{13}C NMR (100 MHz, $CDCl_3$): δ 152.1, 141.6, 136.5, 127.7, 124.3, 119.7, 117.2, 105.4, 83.4, 40.1, 25.0, 24.97, –1.2; HRMS (DART): Calcd for $C_{24}H_{37}B_2N_2O_2Si_1$ $[M+H]^+$: 435.2810, Found: 435.2826.

2-(4-Chloro-2-(4,4,5,5-tetramethyl-1,3,2-dioxaborolan-2-yl)pent-4-en-1-yl)-2,3-dihydro-1*H*-naphtho[1,8-*de*][1,3,2]diazaborinine (3.43): IR (neat): 3397 (br), 2977 (w), 2928 (w), 1630 (w), 1600 (s), 1511 (m), 1411 (m), 1372 (m), 1320 (m), 1139 (m), 820 (m), 764 (m) cm^{-1}; ^{1}H NMR (400 MHz, $CDCl_3$): δ 7.08 (2H, dd, *J* = 8.4, 7.2 Hz), 6.99 (2H, dd, *J* = 8.0, 0.8 Hz), 6.27 (2H, dd, *J* = 7.2, 1.2 Hz), 6.03 (2H, br s), 5.20 (1H, d, *J* = 0.8 Hz), 5.17 (1H, d, *J* = 1.2 Hz), 2.60 (1H, dd, *J* = 14.2, 7.0 Hz), 2.35 (1H, dd, *J* = 14.4, 8.0 Hz), 1.61–1.53 (1H, m), 1.27 (12H, s), 1.03–0.89 (2H, m); ^{13}C NMR (100 MHz, $CDCl_3$): δ 142.8, 141.5, 136.5, 127.7, 119.8, 117.3, 113.1, 105.5, 83.8, 42.9, 25.0; HRMS (DART): Calcd for $C_{21}H_{28}B_2Cl_1N_2O_2$ $[M+H]^+$: 397.2025, Found: 397.2043.

2-(4-Bromo-2-(4,4,5,5-tetramethyl-1,3,2-dioxaborolan-2-yl)pent-4-en-1-yl)-2,3-dihydro-1*H*-naphtho[1,8-*de*][1,3,2]diazaborinine (3.44): Melting point: 111–112 ºC. IR (neat): 3400 (br), 2976 (w), 2923 (w), 1628 (w), 1600 (s), 1512 (m), 1412 (m), 1373 (m), 1320 (m), 1140 (m), 820 (m), 764 (m) cm^{-1}; ^{1}H NMR (400 MHz, $CDCl_3$): δ 7.08 (2H, dd, *J* = 8.2, 7.4 Hz), 6.98 (2H, dd, *J* = 8.4, 0.8 Hz), 6.27 (2H, dd, *J* = 7.4, 1.0 Hz), 6.04 (2H, br s), 5.62 (1H, d, *J* = 1.2 Hz), 5.45 (1H, d, *J* = 1.6 Hz), 2.68 (1H, dd, *J* = 14.8, 6.8 Hz), 2.41 (1H, dd, *J* = 15.0, 8.2 Hz), 1.61–1.54 (1H, m), 1.27 (12H, s), 1.00 (1H, dd, *J* = 15.6, 4.8 Hz), 0.91 (1H, dd, *J* = 15.8, 10.6 Hz); ^{13}C NMR (100 MHz, $CDCl_3$): δ 141.5, 136.5, 135.0, 127.7, 119.8, 117.6, 117.3, 105.5, 102.0, 83.8, 45.0, 25.0; HRMS (DART): Calcd for $C_{21}H_{28}B_2Br_1N_2O_2$ $[M+H]^+$: 441.1520, Found: 441.1509.

2-(2-Methyl-2-(4,4,5,5-tetramethyl-1,3,2-dioxaborolan-2-yl)pent-4-en-1-yl)-2,3-dihydro-1*H*-naphtho[1,8-*de*][1,3,2]diazaborinine (3.53): IR (neat): 3399 (br), 2976 (w), 1627 (w), 1600 (s), 1509 (m), 1411 (m), 1372 (m), 1140 (m), 820 (m), 764 (m) cm^{-1}; ^{1}H NMR (400 MHz, $CDCl_3$): δ 7.08 (2H, dd, *J* = 8.2, 7.4 Hz), 6.98 (2H, dd, *J* = 8.2, 1.0 Hz),

6.25 (2H, dd, J = 7.2, 1.2 Hz), 6.17 (2H, br s), 5.85 (1H, ddt, J = 16.8, 10.0, 7.4 Hz), 5.07–5.00 (1H, m), 2.19–2.10 (2H, m), 1.32 (6H, s), 1.29 (6H, s), 1.08 (1H, d, J = 14.8 Hz), 1.02 (3H, s), 0.73 (1H, d, J = 14.4 Hz); ^{13}C NMR (100 MHz, $CDCl_3$): δ 141.7, 136.7, 136.5, 127.7, 119.8, 117.1, 116.7, 105.3, 83.7, 46.9, 25.2, 25.0; HRMS (DART): Calcd for $C_{22}H_{31}B_2N_2O_2$ $[M+H]^+$: 377.2572, Found: 377.2571.

2-(1-(4,4,5,5-Tetramethyl-1,3,2-dioxaborolan-2-yl)pent-4-en-2-yl)-2,3-dihydro-1*H*-naphtho[1,8-*de*][1,3,2]diazaborinine (3.55): Melting point: 70–71 ºC. IR (neat): 3380 (br), 2975 (w), 2902 (w), 1628 (w), 1598 (s), 1509 (m), 1410 (m), 1370 (m), 1312 (m), 1139 (s), 966 (m), 845 (m), 819 (m), 762 (s) cm^{-1}; ^{1}H NMR (400 MHz, $CDCl_3$): δ 7.08 (2H, t, J = 7.8 Hz), 6.98 (2H, d, J = 8.0 Hz), 6.27 (2H, dd, J = 7.2, 0.8 Hz), 5.98 (2H, br s), 5.84 (1H, ddt, J = 17.2, 10.0, 7.0 Hz), 5.08–4.99 (1H, m), 2.29 (1H, app pent, J = 6.9 Hz), 2.15 (1H, app pent, J = 7.2 Hz), 1.32–1.20 (1H, m), 1.26 (12H, s), 1.01–0.86 (2H, m); ^{13}C NMR (100 MHz, $CDCl_3$): δ 141.5, 138.7, 136.5, 127.7, 119.8, 117.3, 115.8, 105.5, 83.5, 38.7, 25.1, 25.0; HRMS (DART): Calcd for $C_{21}H_{29}B_2N_2O_2$ $[M+H]^+$: 363.2415, Found: 363.2430.

■ **Representative Procedure for the Catalytic Cu–B(pin) Addition to Isopropenyl–B(pin) (3.45) Followed by Allylic Substitution Reaction (Scheme 3.8)**

In a N_2-filled glove box, an oven-dried 1 dram vial equipped with a stir bar was charged with PCy_3 (3.1 mg, 0.0055 mmol), LiO*t*-Bu (12 mg, 0.15 mmol), CuCl (0.50 mg, 0.0050 mmol), and thf (1.0 mL). The mixture was allowed to stir for 15 min at 22 °C; during this time the solution turned light-yellow. Bis(pinacolato)diboron (28 mg, 0.11 mmol) was added to the mixture, causing the solution to turn dark brown immediately. Isopronenyl–B(pin) (**3.45**) (25.2 mg, 0.15 mmol), allylphosphate (19.4 mg, 0.10 mmol),

and thf (0.50 mL) were added. The vial was sealed with a cap and electrical tape before removal from the glove box. The resulting mixture was allowed to stir at 22 °C for 2 h. The mixture was then passed through a short plug of silica gel (4 x 1 cm) and eluted with Et_2O. The organic layer was concentrated under reduced pressure, affording yellow oil, which was purified by silica gel chromatography (100% hexanes→hexanes:Et_2O = 10:1) to afford **3.46** as colorless oil (22.5 mg, 0.067 mmol, 67% yield). **2,2'-(2-Methylpent-4-ene-1,2-diyl)bis(4,4,5,5-tetramethyl-1,3,2-dioxaborolane) (3.46):** IR (neat): 2977 (m), 2930 (w), 1360 (s), 1307 (s), 1139 (s), 969 (m), 845 (m) cm^{-1}; ^1H NMR (400 MHz, $CDCl_3$): δ 5.82 (1H, ddt, *J* = 17.0, 10.2, 7.4 Hz), 2.13 (1H, dd, *J* = 14.2, 7.2 Hz), 2.05 (1H, dd, *J* = 14.2, 7.0 Hz), 1.23 (12H, s), 1.21 (12H, s), 0.96 (3H, s), 0.94 (1H, d, *J* = 15.2 Hz), 0.70 (1H, d, *J* = 16.0 Hz); ^{13}C NMR (100 MHz, $CDCl_3$): δ 136.9, 116.2, 83.1, 82.9, 46.0, 25.1, 25.0, 24.9, 24.89, 24.0; HRMS (DART): Calcd for $C_{18}H_{35}B_2O_4$ $[M+H]^+$: 337.2721, Found: 337.2738.

2,2'-(2,4-Dimethylpent-4-ene-1,2-diyl)bis(4,4,5,5-tetramethyl-1,3,2-dioxaborolane) (3.47): IR (neat): 2977 (m), 2929 (w), 1461 (m), 1370 (s), 1359 (s), 1307 (s), 1213 (m), 1142 (s), 969 (m), 848 (m) cm^{-1}; ^1H NMR (400 MHz, $CDCl_3$): δ 4.74–4.72 (1H, m), 4.66 (1H, s), 2.18 (1H, d, *J* = 13.6 Hz), 2.06 (1H, d, *J* = 13.6 Hz), 1.72, (3H, s), 1.23 (12H, s), 1.22 (12H, s), 0.99 (3H, s), 0.96 (1H, d, *J* = 16.0 Hz), 0.73 (1H, d, *J* = 15.6 Hz); ^{13}C NMR (100 MHz, $CDCl_3$): δ 144.8, 112.8, 83.2, 82.9, 49.1, 25.1, 25.06, 24.9, 24.7, 24.3; HRMS (DART): Calcd for $C_{19}H_{37}B_2O_4$ $[M+H]^+$: 351.2878, Found: 351.2892.

***tert*-Butyldimethyl((4-methyl-2-methylene-4,5-bis(4,4,5,5-tetramethyl-1,3,2-dioxaborolan-2-yl)pentyl)oxy)silane (3.48)**: IR (neat): 2977 (m), 2929 (m), 2857 (m), 1462 (m), 1370 (s), 1360 (s), 1309 (s), 1253 (m), 1213 (m), 1142 (s), 1109 (s), 970 (m),

836 (s), 775 (s) cm^{-1}; ^{1}H NMR (400 MHz, $CDCl_3$): δ 5.14–5.12 (1H, m), 4.86 (1H, s), 4.03 (2H, s), 2.13 (1H, d, *J* = 14.0 Hz), 2.02 (1H, d, *J* = 14.4 Hz), 1.23 (12H, s), 1.22 (12H, s), 0.98 (3H, s), 0.94 (1H, d, *J* = 15.6 Hz), 0.90 (9H, s), 0.75 (1H, d, *J* = 15.6 Hz), 0.04 (6H, s); ^{13}C NMR (100 MHz, $CDCl_3$): δ 146.9, 110.6, 83.2, 82.9, 66.9, 43.7, 26.1, 25.1, 25.07, 25.0, 24.9, 24.4, 18.5, –5.2; HRMS (DART): Calcd for $C_{25}H_{54}B_2N_1O_5Si_1$ $[M+NH_4]^+$: 498.3967, Found: 498.3969.

2,2'-(2-Methyl-4-phenylpent-4-ene-1,2-diyl)bis(4,4,5,5-tetramethyl-1,3,2-dioxaborolane) (3.49): IR (neat): 2977 (m), 2928 (w), 1463 (w), 1369 (s), 1359 (s), 1310 (s), 1213 (m), 1143 (s), 970 (m), 700 (m) cm^{-1}; ^{1}H NMR (400 MHz, $CDCl_3$): δ 7.40–7.38 (2H, m), 7.28–7.18 (3H, m), 5.20 (1H, d, *J* = 2.0 Hz), 5.07 (1H, s), 2.72 (1H, d, *J* = 14.0 Hz), 2.57 (1H, d, *J* = 14.0 Hz), 1.21 (6H, s), 1.207 (6H, s), 1.14 (12H, s), 0.95 (1H, d, *J* = 15.6 Hz), 0.86 (3H, s), 0.72 (1H, d, *J* = 15.6 Hz); ^{13}C NMR (100 MHz, $CDCl_3$): δ 147.8, 143.9, 128.1, 127.0, 126.9, 116.1, 83.1, 82.9, 45.7, 25.1, 25.05, 24.94, 24.9; HRMS (DART): Calcd for $C_{24}H_{42}B_2N_1O_4$ $[M+NH_4]^+$: 430.3300, Found: 430.3287.

Trimethyl(4-methyl-4,5-bis(4,4,5,5-tetramethyl-1,3,2-dioxaborolan-2-yl)pent-1-en-2-yl)silane (3.50): IR (neat): 2977 (m), 1465 (w), 1378 (s), 1370 (s), 1359 (s), 1310 (s), 1248 (m), 1143 (s), 970 (m), 837 (s) cm^{-1}; ^{1}H NMR (400 MHz, $CDCl_3$): δ 5.67–5.65 (1H, m), 5.41–5.40 (1H, m), 2.32 (1H, dt, *J* = 15.6, 1.4 Hz), 2.12 (1H, dd, *J* = 15.6, 1.2 Hz), 1.23 (24H, s), 1.01 (3H, s), 0.99 (1H, d, *J* = 14.4 Hz), 0.74 (1H, d, *J* = 15.2 Hz), 0.06 (9H, s); ^{13}C NMR (100 MHz, $CDCl_3$): δ 150.8, 125.4, 83.1, 82.9, 45.5, 25.2, 25.1, 24.9, 24.0, –1.1; HRMS (DART): Calcd for $C_{121}H_{43}B_2O_4Si_1$ $[M+H]^+$: 409.3117, Found: 409.3119.

2,2'-(4-Chloro-2-methylpent-4-ene-1,2-diyl)bis(4,4,5,5-tetramethyl-1,3,2-dioxaborolane) (3.51): IR (neat): 2977 (m), 2929 (w), 1629 (w), 1461 (w), 1369 (s),

1311 (s), 1138 (s), 969 (m), 845 (m) cm^{-1}; ^{1}H NMR (400 MHz, $CDCl_3$): δ 5.17 (1H, d, *J* = 1.2 Hz), 5.11 (1H, d, *J* = 1.2 Hz), 2.54 (1H, d, *J* = 14.4 Hz), 2.45 (1H, d, *J* = 14.8 Hz), 1.24 (12H, s), 1.22 (12H, s), 1.05 (3H, s), 1.02 (1H, d, *J* = 15.6 Hz), 0.80 (1H, d, *J* = 16.0 Hz); ^{13}C NMR (100 MHz, $CDCl_3$): δ 141.5, 114.4, 83.4, 83.0, 49.4, 25.1, 25.03, 25.0, 24.9, 23.8; HRMS (DART): Calcd for $C_{18}H_{34}B_2Cl_1O_4$ $[M+H]^+$: 371.2332, Found: 371.2323.

2,2'-(4-Bromo-2-methylpent-4-ene-1,2-diyl)bis(4,4,5,5-tetramethyl-1,3,2-dioxaborolane) (3.52): IR (neat): 2977 (m), 2929 (w), 1623 (w), 1462 (m), 1369 (s), 1313 (s), 1140 (s), 969 (m), 845 (m) cm^{-1}; ^{1}H NMR (400 MHz, $CDCl_3$): δ 5.57 (1H, d, *J* = 1.2 Hz), 5.45 (1H, d, *J* = 1.6 Hz), 2.67 (1H, d, *J* = 14.8 Hz), 2.58 (1H, d, *J* = 14.8 Hz), 1.25 (12H, s), 1.23 (12H, s), 1.07 (3H, s), 1.04 (1H, d, *J* = 16.0 Hz), 0.83 (1H, d, *J* = 15.6 Hz); ^{13}C NMR (100 MHz, $CDCl_3$): δ 132.4, 119.0, 83.4, 83.0, 51.2, 25.1, 25.0, 24.97, 23.8; HRMS (DART): Calcd for $C_{18}H_{34}B_2Br_1O_4$ $[M+H]^+$: 415.1827, Found: 415.1843.

2-(2-Methyl-2-(4,4,5,5-tetramethyl-1,3,2-dioxaborolan-2-yl)pent-4-en-1-yl)-2,3-dihydro-1H-naphtho[1,8-de][1,3,2]diazaborinine (3.53): IR (neat): 3399 (br), 2976 (w), 1627 (w), 1600 (s), 1509 (m), 1411 (m), 1372 (m), 1140 (m), 820 (m), 764 (m) cm–1; 1H NMR (400 MHz, CDCl3): δ 7.08 (2H, dd, J = 8.2, 7.4 Hz), 6.98 (2H, dd, J = 8.2, 1.0 Hz), 6.25 (2H, dd, J = 7.2, 1.2 Hz), 6.17 (2H, br s), 5.85 (1H, ddt, J = 16.8, 10.0, 7.4 Hz), 5.07–5.00 (1H, m), 2.19–2.10 (2H, m), 1.32 (6H, s), 1.29 (6H, s), 1.08 (1H, d, J = 14.8 Hz), 1.02 (3H, s), 0.73 (1H, d, J = 14.4 Hz); 13C NMR (100 MHz, CDCl3): δ 141.7, 136.7, 136.5, 127.7, 119.8, 117.1, 116.7, 105.3, 83.7, 46.9, 25.2, 25.0; HRMS (DART): Calcd for C22H31B2N2O2 [M+H]+: 377.2572, Found: 377.2571.

2-(1-(4,4,5,5-Tetramethyl-1,3,2-dioxaborolan-2-yl)pent-4-en-2-yl)-2,3-dihydro-1H-naphtho[1,8-de][1,3,2]diazaborinine (3.55): Melting point: 70–71 ºC. IR (neat): 3380 (br), 2975 (w), 2902 (w), 1628 (w), 1598 (s), 1509 (m), 1410 (m), 1370 (m), 1312 (m), 1139 (s), 966 (m), 845 (m), 819 (m), 762 (s) cm–1; 1H NMR (400 MHz, CDCl3): δ 7.08 (2H, t, J = 7.8 Hz), 6.98 (2H, d, J = 8.0 Hz), 6.27 (2H, dd, J = 7.2, 0.8 Hz), 5.98 (2H, br s), 5.84 (1H, ddt, J = 17.2, 10.0, 7.0 Hz), 5.08–4.99 (1H, m), 2.29 (1H, app pent, J = 6.9 Hz), 2.15 (1H, app pent, J = 7.2 Hz), 1.32–1.20 (1H, m), 1.26 (12H, s), 1.01–0.86 (2H, m); 13C NMR (100 MHz, CDCl3): δ 141.5, 138.7, 136.5, 127.7, 119.8, 117.3, 115.8, 105.5, 83.5, 38.7, 25.1, 25.0; HRMS (DART): Calcd for C21H29B2N2O2 [M+H]+: 363.2415, Found: 363.2430.

■ **Data for X-ray Crystallography of 3.40**

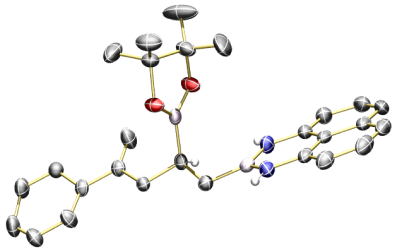

Table 1. Crystal data and structure refinement for $C_{27}H_{32}B_2N_2O_2$.

Identification code	C27H32B2N2O2	
Empirical formula	C27 H32 B2 N2 O2	
Formula weight	438.16	
Temperature	100(2) K	
Wavelength	1.54178 Å	
Crystal system	Monoclinic	
Space group	$P2_1/n$	
Unit cell dimensions	a = 11.7928(4) Å	a= 90º.
	b = 9.8354(4) Å	b= 95.934(3)º.
	c = 20.6121(8) Å	g = 90º.

Volume	2377.92(16) $Å^3$
Z	4
Density (calculated)	1.224 Mg/m^3
Absorption coefficient	0.586 mm^{-1}
F(000)	936
Crystal size	0.200 x 0.200 x 0.080 mm^3
Theta range for data collection	4.144 to 69.789º.
Index ranges	-14<=h<=13, -11<=k<=9, -24<=l<=24
Reflections collected	11807
Independent reflections	4197 [R(int) = 0.0410]
Completeness to theta = 66.500º	97.0 %
Absorption correction	Semi-empirical from equivalents
Max. and min. transmission	0.7533 and 0.6540
Refinement method	Full-matrix least-squares on F^2
Data / restraints / parameters	4197 / 0 / 324
Goodness-of-fit on F^2	1.036
Final R indices [I>2sigma(I)]	R1 = 0.0489, wR2 = 0.1220
R indices (all data)	R1 = 0.0724, wR2 = 0.1361
Extinction coefficient	n/a
Largest diff. peak and hole	0.247 and -0.222 e. $Å^{-3}$

Table 2. Atomic coordinates (x 10^4) and equivalent isotropic displacement parameters ($Å^2$x 10^3) for $C_{27}H_{32}B_2N_2O_2$. U(eq) is defined as one third of the trace of the orthogonalized U^{ij} tensor.

	x	y	z	U(eq)
O(1)	3349(1)	5792(2)	5712(1)	38(1)
O(2)	3952(1)	6823(2)	6673(1)	42(1)
N(1)	6786(1)	6903(2)	6488(1)	34(1)
N(2)	7137(1)	5288(2)	5663(1)	32(1)
B(1)	6521(2)	6431(2)	5838(1)	30(1)
B(2)	3961(2)	6847(2)	6011(1)	28(1)
C(1)	2750(2)	9637(3)	5920(1)	45(1)
C(2)	2890(2)	9456(2)	5294(1)	30(1)

C(3)	3844(2)	8597(2)	5078(1)	28(1)
C(4)	4623(2)	7894(2)	5624(1)	28(1)
C(5)	5605(2)	7140(2)	5333(1)	31(1)
C(6)	7666(2)	6371(2)	6922(1)	32(1)
C(7)	7965(2)	6926(2)	7531(1)	39(1)
C(8)	8870(2)	6368(3)	7939(1)	43(1)
C(9)	9453(2)	5258(2)	7757(1)	42(1)
C(10)	9162(2)	4641(2)	7139(1)	35(1)
C(11)	9725(2)	3477(2)	6932(1)	43(1)
C(12)	9441(2)	2955(2)	6323(1)	45(1)
C(13)	8590(2)	3552(2)	5887(1)	40(1)
C(14)	7999(2)	4668(2)	6075(1)	32(1)
C(15)	8268(2)	5229(2)	6711(1)	30(1)
C(16)	2104(2)	10109(2)	4775(1)	30(1)
C(17)	2199(2)	9898(2)	4118(1)	40(1)
C(18)	1470(2)	10514(2)	3633(1)	40(1)
C(19)	635(2)	11367(3)	3788(1)	47(1)
C(20)	655(8)	11816(12)	4419(4)	53(2)
C(21)	1355(7)	11184(11)	4901(2)	43(2)
C(20X)	348(11)	11257(16)	4447(5)	43(3)
C(21X)	1095(7)	10655(12)	4933(3)	32(2)
C(22)	2708(2)	5148(2)	6207(1)	37(1)
C(23)	3464(2)	5513(2)	6838(1)	44(1)
C(24)	1552(2)	5821(3)	6140(2)	65(1)
C(25)	2588(2)	3658(3)	6065(1)	57(1)
C(26)	4463(2)	4551(4)	6987(2)	86(1)
C(27)	2815(3)	5711(4)	7429(1)	90(1)

Table 3. Bond lengths [Å] and angles [º] for $C_{27}H_{32}B_2N_2O_2$.

O(1)-B(2)	1.373(3)
O(1)-C(22)	1.474(2)
O(2)-B(2)	1.365(2)
O(2)-C(23)	1.466(3)
N(1)-C(6)	1.400(2)
N(1)-B(1)	1.422(3)
N(1)-H(1N)	0.87(2)
N(2)-C(14)	1.396(2)
N(2)-B(1)	1.406(3)
N(2)-H(2N)	0.87(2)
B(1)-C(5)	1.582(3)
B(2)-C(4)	1.560(3)
C(1)-C(2)	1.331(3)
C(1)-H(1A)	0.9500
C(1)-H(1B)	0.9500
C(2)-C(16)	1.487(3)
C(2)-C(3)	1.510(3)
C(3)-C(4)	1.541(2)
C(3)-H(3A)	0.9900
C(3)-H(3B)	0.9900
C(4)-C(5)	1.548(2)
C(4)-H(4)	1.0000
C(5)-H(5A)	0.9900
C(5)-H(5B)	0.9900
C(6)-C(7)	1.379(3)
C(6)-C(15)	1.421(3)
C(7)-C(8)	1.402(3)
C(7)-H(7)	0.9500
C(8)-C(9)	1.364(3)
C(8)-H(8)	0.9500
C(9)-C(10)	1.421(3)
C(9)-H(9)	0.9500
C(10)-C(11)	1.411(3)

C(10)-C(15)	1.426(3)
C(11)-C(12)	1.365(3)
C(11)-H(11)	0.9500
C(12)-C(13)	1.405(3)
C(12)-H(12)	0.9500
C(13)-C(14)	1.377(3)
C(13)-H(13)	0.9500
C(14)-C(15)	1.427(3)
C(16)-C(21X)	1.375(7)
C(16)-C(17)	1.386(3)
C(16)-C(21)	1.418(5)
C(17)-C(18)	1.389(3)
C(17)-H(17)	0.9500
C(18)-C(19)	1.357(3)
C(18)-H(18)	0.9500
C(19)-C(20)	1.372(8)
C(19)-C(20X)	1.438(11)
C(19)-H(19)	0.9500
C(20)-C(21)	1.373(8)
C(20)-H(20)	0.9500
C(21)-H(21)	0.9500
C(20X)-C(21X)	1.395(12)
C(20X)-H(20X)	0.9500
C(21X)-H(21X)	0.9500
C(22)-C(25)	1.499(3)
C(22)-C(24)	1.509(3)
C(22)-C(23)	1.540(3)
C(23)-C(26)	1.518(4)
C(23)-C(27)	1.518(3)
C(24)-H(24A)	0.9800
C(24)-H(24B)	0.9800
C(24)-H(24C)	0.9800
C(25)-H(25A)	0.9800
C(25)-H(25B)	0.9800
C(25)-H(25C)	0.9800

C(26)-H(26A)	0.9800
C(26)-H(26B)	0.9800
C(26)-H(26C)	0.9800
C(27)-H(27A)	0.9800
C(27)-H(27B)	0.9800
C(27)-H(27C)	0.9800

B(2)-O(1)-C(22)	107.35(15)
B(2)-O(2)-C(23)	106.93(16)
C(6)-N(1)-B(1)	123.84(18)
C(6)-N(1)-H(1N)	113.8(16)
B(1)-N(1)-H(1N)	122.2(16)
C(14)-N(2)-B(1)	123.80(18)
C(14)-N(2)-H(2N)	117.4(16)
B(1)-N(2)-H(2N)	118.8(16)
N(2)-B(1)-N(1)	115.72(18)
N(2)-B(1)-C(5)	121.32(18)
N(1)-B(1)-C(5)	122.96(19)
O(2)-B(2)-O(1)	112.13(17)
O(2)-B(2)-C(4)	125.32(18)
O(1)-B(2)-C(4)	122.50(16)
C(2)-C(1)-H(1A)	120.0
C(2)-C(1)-H(1B)	120.0
H(1A)-C(1)-H(1B)	120.0
C(1)-C(2)-C(16)	120.56(18)
C(1)-C(2)-C(3)	122.15(18)
C(16)-C(2)-C(3)	117.29(15)
C(2)-C(3)-C(4)	116.20(15)
C(2)-C(3)-H(3A)	108.2
C(4)-C(3)-H(3A)	108.2
C(2)-C(3)-H(3B)	108.2
C(4)-C(3)-H(3B)	108.2
H(3A)-C(3)-H(3B)	107.4
C(3)-C(4)-C(5)	110.19(14)
C(3)-C(4)-B(2)	112.20(15)

C(5)-C(4)-B(2)	108.40(16)
C(3)-C(4)-H(4)	108.7
C(5)-C(4)-H(4)	108.7
B(2)-C(4)-H(4)	108.7
C(4)-C(5)-B(1)	116.36(15)
C(4)-C(5)-H(5A)	108.2
B(1)-C(5)-H(5A)	108.2
C(4)-C(5)-H(5B)	108.2
B(1)-C(5)-H(5B)	108.2
H(5A)-C(5)-H(5B)	107.4
C(7)-C(6)-N(1)	122.42(19)
C(7)-C(6)-C(15)	120.20(18)
N(1)-C(6)-C(15)	117.38(18)
C(6)-C(7)-C(8)	119.9(2)
C(6)-C(7)-H(7)	120.0
C(8)-C(7)-H(7)	120.0
C(9)-C(8)-C(7)	121.5(2)
C(9)-C(8)-H(8)	119.3
C(7)-C(8)-H(8)	119.3
C(8)-C(9)-C(10)	120.47(19)
C(8)-C(9)-H(9)	119.8
C(10)-C(9)-H(9)	119.8
C(11)-C(10)-C(9)	122.72(19)
C(11)-C(10)-C(15)	118.8(2)
C(9)-C(10)-C(15)	118.47(19)
C(12)-C(11)-C(10)	120.4(2)
C(12)-C(11)-H(11)	119.8
C(10)-C(11)-H(11)	119.8
C(11)-C(12)-C(13)	121.5(2)
C(11)-C(12)-H(12)	119.3
C(13)-C(12)-H(12)	119.3
C(14)-C(13)-C(12)	120.1(2)
C(14)-C(13)-H(13)	119.9
C(12)-C(13)-H(13)	119.9
C(13)-C(14)-N(2)	122.34(19)

C(13)-C(14)-C(15)	119.70(18)
N(2)-C(14)-C(15)	117.96(18)
C(6)-C(15)-C(10)	119.43(18)
C(6)-C(15)-C(14)	121.10(17)
C(10)-C(15)-C(14)	119.47(18)
C(21X)-C(16)-C(17)	116.7(3)
C(17)-C(16)-C(21)	113.9(3)
C(21X)-C(16)-C(2)	119.3(3)
C(17)-C(16)-C(2)	122.01(17)
C(21)-C(16)-C(2)	123.0(2)
C(16)-C(17)-C(18)	122.1(2)
C(16)-C(17)-H(17)	118.9
C(18)-C(17)-H(17)	118.9
C(19)-C(18)-C(17)	120.6(2)
C(19)-C(18)-H(18)	119.7
C(17)-C(18)-H(18)	119.7
C(18)-C(19)-C(20)	118.8(4)
C(18)-C(19)-C(20X)	115.1(5)
C(18)-C(19)-H(19)	120.6
C(20)-C(19)-H(19)	120.6
C(19)-C(20)-C(21)	119.4(6)
C(19)-C(20)-H(20)	120.3
C(21)-C(20)-H(20)	120.3
C(20)-C(21)-C(16)	123.0(4)
C(20)-C(21)-H(21)	118.5
C(16)-C(21)-H(21)	118.5
C(21X)-C(20X)-C(19)	121.1(8)
C(21X)-C(20X)-H(20X)	119.4
C(19)-C(20X)-H(20X)	119.4
C(16)-C(21X)-C(20X)	119.6(6)
C(16)-C(21X)-H(21X)	120.2
C(20X)-C(21X)-H(21X)	120.2
O(1)-C(22)-C(25)	109.28(17)
O(1)-C(22)-C(24)	105.79(17)
C(25)-C(22)-C(24)	110.2(2)

O(1)-C(22)-C(23)	100.97(16)
C(25)-C(22)-C(23)	115.30(19)
C(24)-C(22)-C(23)	114.4(2)
O(2)-C(23)-C(26)	106.24(19)
O(2)-C(23)-C(27)	108.5(2)
C(26)-C(23)-C(27)	111.2(2)
O(2)-C(23)-C(22)	102.45(15)
C(26)-C(23)-C(22)	113.3(2)
C(27)-C(23)-C(22)	114.3(2)
C(22)-C(24)-H(24A)	109.5
C(22)-C(24)-H(24B)	109.5
H(24A)-C(24)-H(24B)	109.5
C(22)-C(24)-H(24C)	109.5
H(24A)-C(24)-H(24C)	109.5
H(24B)-C(24)-H(24C)	109.5
C(22)-C(25)-H(25A)	109.5
C(22)-C(25)-H(25B)	109.5
H(25A)-C(25)-H(25B)	109.5
C(22)-C(25)-H(25C)	109.5
H(25A)-C(25)-H(25C)	109.5
H(25B)-C(25)-H(25C)	109.5
C(23)-C(26)-H(26A)	109.5
C(23)-C(26)-H(26B)	109.5
H(26A)-C(26)-H(26B)	109.5
C(23)-C(26)-H(26C)	109.5
H(26A)-C(26)-H(26C)	109.5
H(26B)-C(26)-H(26C)	109.5
C(23)-C(27)-H(27A)	109.5
C(23)-C(27)-H(27B)	109.5
H(27A)-C(27)-H(27B)	109.5
C(23)-C(27)-H(27C)	109.5
H(27A)-C(27)-H(27C)	109.5
H(27B)-C(27)-H(27C)	109.5

Symmetry transformations used to generate equivalent atoms:

Table 4. Anisotropic displacement parameters ($Å^2 x\ 10^3$) for $C_{27}H_{32}B_2N_2O_2$. The anisotropic displacement factor exponent takes the form: $-2p^2[\ h^2\ a^{*2}U^{11} + ...\ + 2\ h\ k\ a^*\ b^*\ U^{12}\ ]$

	U^{11}	U^{22}	U^{33}	U^{23}	U^{13}	U^{12}
O(1)	48(1)	40(1)	27(1)	3(1)	9(1)	-11(1)
O(2)	53(1)	49(1)	24(1)	3(1)	3(1)	-14(1)
N(1)	28(1)	36(1)	37(1)	1(1)	3(1)	7(1)
N(2)	31(1)	32(1)	31(1)	2(1)	2(1)	-1(1)
B(1)	25(1)	32(1)	34(1)	4(1)	5(1)	-5(1)
B(2)	22(1)	36(1)	27(1)	0(1)	-1(1)	4(1)
C(1)	48(1)	56(2)	31(1)	-2(1)	0(1)	20(1)
C(2)	30(1)	30(1)	28(1)	-4(1)	-1(1)	-2(1)
C(3)	27(1)	31(1)	25(1)	2(1)	0(1)	-2(1)
C(4)	27(1)	31(1)	25(1)	-2(1)	-1(1)	2(1)
C(5)	29(1)	34(1)	29(1)	1(1)	4(1)	-2(1)
C(6)	26(1)	37(1)	32(1)	9(1)	6(1)	0(1)
C(7)	35(1)	48(1)	35(1)	4(1)	6(1)	3(1)
C(8)	38(1)	62(2)	30(1)	7(1)	6(1)	-3(1)
C(9)	30(1)	61(2)	36(1)	23(1)	1(1)	1(1)
C(10)	25(1)	39(1)	43(1)	17(1)	8(1)	-2(1)
C(11)	29(1)	40(1)	61(1)	22(1)	8(1)	4(1)
C(12)	34(1)	32(1)	70(2)	10(1)	13(1)	5(1)
C(13)	35(1)	33(1)	51(1)	1(1)	9(1)	-2(1)
C(14)	24(1)	31(1)	40(1)	9(1)	5(1)	-4(1)
C(15)	24(1)	31(1)	35(1)	11(1)	8(1)	-2(1)
C(16)	29(1)	29(1)	30(1)	-4(1)	-3(1)	-2(1)
C(17)	46(1)	41(1)	32(1)	4(1)	4(1)	14(1)
C(18)	49(1)	39(1)	32(1)	5(1)	-3(1)	5(1)
C(19)	37(1)	58(2)	44(1)	2(1)	-9(1)	10(1)
C(20)	43(4)	53(5)	61(3)	-3(4)	-6(3)	20(3)
C(21)	47(3)	40(4)	39(2)	-11(2)	-3(2)	10(3)
C(20X)	34(4)	52(7)	43(4)	0(4)	-1(3)	12(4)
C(22)	38(1)	41(1)	32(1)	9(1)	9(1)	-4(1)

C(23)	56(1)	49(2)	28(1)	10(1)	3(1)	-13(1)
C(24)	33(1)	62(2)	99(2)	33(2)	11(1)	-2(1)
C(25)	78(2)	46(2)	50(1)	0(1)	21(1)	-16(1)
C(26)	62(2)	92(2)	99(2)	65(2)	-20(2)	-5(2)
C(27)	144(3)	91(2)	42(2)	-11(2)	45(2)	-58(2)

Table 5. Hydrogen coordinates (x 10^4) and isotropic displacement parameters (Å^{2}x 10^3) for $C_{27}H_{32}B_2N_2O_2$.

	x	y	z	U(eq)
H(1N)	6450(20)	7600(30)	6640(11)	45(7)
H(2N)	6986(19)	4950(20)	5276(12)	44(7)
H(1A)	2143	10188	6039	54
H(1B)	3256	9216	6248	54
H(3A)	4324	9181	4827	34
H(3B)	3504	7887	4778	34
H(4)	4958	8604	5934	34
H(5A)	6005	7800	5075	37
H(5B)	5267	6437	5028	37
H(7)	7557	7686	7672	47
H(8)	9082	6773	8353	52
H(9)	10057	4894	8046	51
H(11)	10304	3055	7217	52
H(12)	9828	2171	6191	54
H(13)	8423	3186	5461	47
H(17)	2782	9313	3996	47
H(18)	1557	10336	3187	48
H(19)	47	11647	3466	57
H(20)	190	12558	4522	64
H(21)	1337	11480	5339	51
H(20X)	-363	11600	4554	52
H(21X)	907	10623	5370	38

H(24A)	1643	6800	6219	97
H(24B)	1084	5430	6460	97
H(24C)	1178	5670	5699	97
H(25A)	2138	3528	5643	85
H(25B)	2201	3218	6408	85
H(25C)	3345	3254	6052	85
H(26A)	4864	4441	6598	129
H(26B)	4182	3665	7119	129
H(26C)	4987	4926	7343	129
H(27A)	3353	5922	7811	135
H(27B)	2400	4875	7511	135
H(27C)	2273	6462	7348	135

Table 6. Torsion angles [°] for $C_{27}H_{32}B_2N_2O_2$.

C(14)-N(2)-B(1)-N(1)	-3.0(3)
C(14)-N(2)-B(1)-C(5)	176.25(17)
C(6)-N(1)-B(1)-N(2)	5.5(3)
C(6)-N(1)-B(1)-C(5)	-173.80(17)
C(23)-O(2)-B(2)-O(1)	10.6(2)
C(23)-O(2)-B(2)-C(4)	-166.82(19)
C(22)-O(1)-B(2)-O(2)	10.8(2)
C(22)-O(1)-B(2)-C(4)	-171.68(17)
C(1)-C(2)-C(3)-C(4)	2.2(3)
C(16)-C(2)-C(3)-C(4)	-178.09(16)
C(2)-C(3)-C(4)-C(5)	-175.95(16)
C(2)-C(3)-C(4)-B(2)	63.2(2)
O(2)-B(2)-C(4)-C(3)	-126.9(2)
O(1)-B(2)-C(4)-C(3)	55.9(2)
O(2)-B(2)-C(4)-C(5)	111.2(2)
O(1)-B(2)-C(4)-C(5)	-66.0(2)
C(3)-C(4)-C(5)-B(1)	176.79(16)
B(2)-C(4)-C(5)-B(1)	-60.1(2)
N(2)-B(1)-C(5)-C(4)	152.57(18)
N(1)-B(1)-C(5)-C(4)	-28.2(3)

B(1)-N(1)-C(6)-C(7)	174.35(19)
B(1)-N(1)-C(6)-C(15)	-4.6(3)
N(1)-C(6)-C(7)-C(8)	-178.55(18)
C(15)-C(6)-C(7)-C(8)	0.4(3)
C(6)-C(7)-C(8)-C(9)	-1.6(3)
C(7)-C(8)-C(9)-C(10)	0.7(3)
C(8)-C(9)-C(10)-C(11)	-178.87(19)
C(8)-C(9)-C(10)-C(15)	1.4(3)
C(9)-C(10)-C(11)-C(12)	-177.49(19)
C(15)-C(10)-C(11)-C(12)	2.2(3)
C(10)-C(11)-C(12)-C(13)	0.0(3)
C(11)-C(12)-C(13)-C(14)	-1.8(3)
C(12)-C(13)-C(14)-N(2)	-179.24(18)
C(12)-C(13)-C(14)-C(15)	1.1(3)
B(1)-N(2)-C(14)-C(13)	-179.67(18)
B(1)-N(2)-C(14)-C(15)	0.0(3)
C(7)-C(6)-C(15)-C(10)	1.8(3)
N(1)-C(6)-C(15)-C(10)	-179.25(16)
C(7)-C(6)-C(15)-C(14)	-177.83(18)
N(1)-C(6)-C(15)-C(14)	1.1(3)
C(11)-C(10)-C(15)-C(6)	177.64(17)
C(9)-C(10)-C(15)-C(6)	-2.7(3)
C(11)-C(10)-C(15)-C(14)	-2.7(3)
C(9)-C(10)-C(15)-C(14)	176.96(17)
C(13)-C(14)-C(15)-C(6)	-179.30(17)
N(2)-C(14)-C(15)-C(6)	1.1(3)
C(13)-C(14)-C(15)-C(10)	1.1(3)
N(2)-C(14)-C(15)-C(10)	-178.54(16)
C(1)-C(2)-C(16)-C(21X)	-14.0(7)
C(3)-C(2)-C(16)-C(21X)	166.4(6)
C(1)-C(2)-C(16)-C(17)	-177.4(2)
C(3)-C(2)-C(16)-C(17)	2.9(3)
C(1)-C(2)-C(16)-C(21)	15.3(7)
C(3)-C(2)-C(16)-C(21)	-164.4(6)
C(21X)-C(16)-C(17)-C(18)	16.6(7)

C(21)-C(16)-C(17)-C(18)	-11.2(6)
C(2)-C(16)-C(17)-C(18)	-179.6(2)
C(16)-C(17)-C(18)-C(19)	0.7(4)
C(17)-C(18)-C(19)-C(20)	12.4(7)
C(17)-C(18)-C(19)-C(20X)	-18.0(8)
C(18)-C(19)-C(20)-C(21)	-13.9(9)
C(19)-C(20)-C(21)-C(16)	2.6(8)
C(17)-C(16)-C(21)-C(20)	9.6(8)
C(2)-C(16)-C(21)-C(20)	177.9(4)
C(18)-C(19)-C(20X)-C(21X)	19.2(12)
C(17)-C(16)-C(21X)-C(20X)	-15.0(8)
C(2)-C(16)-C(21X)-C(20X)	-179.3(5)
C(19)-C(20X)-C(21X)-C(16)	-2.6(11)
B(2)-O(1)-C(22)-C(25)	-147.90(19)
B(2)-O(1)-C(22)-C(24)	93.5(2)
B(2)-O(1)-C(22)-C(23)	-26.0(2)
B(2)-O(2)-C(23)-C(26)	92.9(2)
B(2)-O(2)-C(23)-C(27)	-147.5(2)
B(2)-O(2)-C(23)-C(22)	-26.2(2)
O(1)-C(22)-C(23)-O(2)	31.0(2)
C(25)-C(22)-C(23)-O(2)	148.64(18)
C(24)-C(22)-C(23)-O(2)	-82.1(2)
O(1)-C(22)-C(23)-C(26)	-83.0(2)
C(25)-C(22)-C(23)-C(26)	34.6(3)
C(24)-C(22)-C(23)-C(26)	163.9(2)
O(1)-C(22)-C(23)-C(27)	148.2(2)
C(25)-C(22)-C(23)-C(27)	-94.2(3)
C(24)-C(22)-C(23)-C(27)	35.1(3)

Symmetry transformations used to generate equivalent atoms:

Table 7. Hydrogen bonds for $C_{27}H_{32}B_2N_2O_2$ [Å and º].

D-H...A	d(D-H)	d(H...A)	d(D...A)	<(DHA)

N(2)-H(2N)...O(1)#1	0.87(2)	2.16(3)	3.026(2)	177(2)

Symmetry transformations used to generate equivalent atoms:
#1 -x+1,-y+1,-z+1

■ **Data for X-ray Crystallography of 3.41**

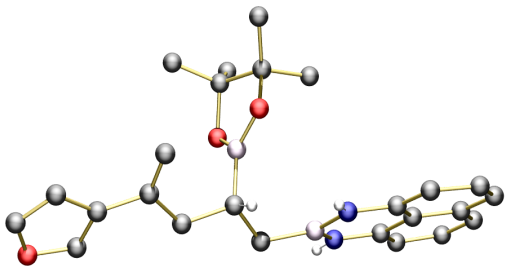

Table 1. Crystal data and structure refinement for $C_{25}H_{30}B_2N_2O_3$.

Identification code	C25H30B2N2O3	
Empirical formula	C25 H30 B2 N2 O3	
Formula weight	428.13	
Temperature	100(2) K	
Wavelength	1.54178 Å	
Crystal system	Monoclinic	
Space group	$P2_1/n$	
Unit cell dimensions	a = 11.4630(2) Å	a= 90º.
	b = 9.8897(2) Å	b= 98.190(2)º.
	c = 20.2832(4) Å	g = 90º.
Volume	2275.97(8) Å^3	
Z	4	
Density (calculated)	1.249 Mg/m^3	
Absorption coefficient	0.634 mm^{-1}	
F(000)	912	
Crystal size	0.180 x 0.120 x 0.110 mm^3	
Theta range for data collection	4.194 to 70.315∞.	
Index ranges	-13<=h<=13, -11<=k<=11, -24<=l<=18	
Reflections collected	9224	
Independent reflections	4102 [R(int) = 0.0431]	
Completeness to theta = 67.679º	97.1 %	
Absorption correction	Semi-empirical from equivalents	

Max. and min. transmission	0.7533 and 0.6406
Refinement method	Full-matrix least-squares on F^2
Data / restraints / parameters	4102 / 2 / 299
Goodness-of-fit on F^2	1.040
Final R indices [I>2sigma(I)]	R1 = 0.0463, wR2 = 0.1142
R indices (all data)	R1 = 0.0620, wR2 = 0.1228
Extinction coefficient	n/a
Largest diff. peak and hole	0.243 and -0.272 e. $Å^{-3}$

Table 2. Atomic coordinates (x 10^4) and equivalent isotropic displacement parameters ($Å^2$x 10^3) for $C_{25}H_{30}B_2N_2O_3$. U(eq) is defined as one third of the trace of the orthogonalized U^{ij} tensor.

	x	y	z	U(eq)
O(1)	8811(1)	-457(1)	6521(1)	32(1)
O(2)	6287(1)	2950(1)	3410(1)	26(1)
O(3)	6699(1)	4158(1)	4371(1)	24(1)
N(1)	3143(1)	2780(2)	3502(1)	23(1)
N(2)	2878(1)	4569(1)	4269(1)	22(1)
B(1)	3473(2)	3365(2)	4143(1)	21(1)
B(2)	6169(2)	3030(2)	4066(1)	21(1)
C(1)	7503(2)	212(2)	4259(1)	29(1)
C(2)	7284(1)	472(2)	4873(1)	23(1)
C(3)	6252(1)	1315(2)	5031(1)	22(1)
C(4)	5472(1)	1979(2)	4443(1)	20(1)
C(5)	4420(1)	2716(2)	4691(1)	21(1)
C(6)	1990(1)	5153(2)	3817(1)	21(1)
C(7)	1424(2)	6325(2)	3958(1)	25(1)
C(8)	544(2)	6888(2)	3483(1)	30(1)
C(9)	207(2)	6277(2)	2885(1)	29(1)
C(10)	746(1)	5052(2)	2723(1)	24(1)
C(11)	400(2)	4350(2)	2116(1)	29(1)
C(12)	958(2)	3176(2)	1983(1)	31(1)
C(13)	1887(2)	2642(2)	2434(1)	28(1)

C(14)	2241(1)	3286(2)	3029(1)	22(1)
C(15)	1664(1)	4493(2)	3193(1)	21(1)
C(16)	8043(1)	-71(2)	5458(1)	24(1)
C(17)	9014(2)	-1007(2)	5481(1)	38(1)
C(18)	9422(2)	-1190(2)	6124(1)	38(1)
C(19)	7973(2)	207(2)	6100(1)	27(1)
C(20)	6760(2)	4247(2)	3226(1)	26(1)
C(21)	5699(2)	5102(2)	2951(1)	44(1)
C(22)	7541(2)	3997(2)	2693(1)	42(1)
C(23)	7412(2)	4762(2)	3899(1)	23(1)
C(24)	7432(2)	6286(2)	3983(1)	37(1)
C(25)	8645(2)	4176(2)	4078(1)	34(1)

Table 3. Bond lengths [Å] and angles [°] for $C_{25}H_{30}B_2N_2O_3$.

O(1)-C(18)	1.350(2)
O(1)-C(19)	1.360(2)
O(2)-B(2)	1.359(2)
O(2)-C(20)	1.463(2)
O(3)-B(2)	1.374(2)
O(3)-C(23)	1.471(2)
N(1)-C(14)	1.398(2)
N(1)-B(1)	1.424(3)
N(1)-H(1N)	0.890(15)
N(2)-C(6)	1.395(2)
N(2)-B(1)	1.414(2)
N(2)-H(2N)	0.863(15)
B(1)-C(5)	1.575(2)
B(2)-C(4)	1.573(2)
C(1)-C(2)	1.330(3)
C(1)-H(1A)	0.9500
C(1)-H(1B)	0.9500
C(2)-C(16)	1.469(3)
C(2)-C(3)	1.517(2)
C(3)-C(4)	1.533(2)

C(3)-H(3A)	0.9900
C(3)-H(3B)	0.9900
C(4)-C(5)	1.553(2)
C(4)-H(4)	1.0000
C(5)-H(5A)	0.9900
C(5)-H(5B)	0.9900
C(6)-C(7)	1.379(2)
C(6)-C(15)	1.425(3)
C(7)-C(8)	1.406(3)
C(7)-H(7)	0.9500
C(8)-C(9)	1.362(3)
C(8)-H(8)	0.9500
C(9)-C(10)	1.420(3)
C(9)-H(9)	0.9500
C(10)-C(11)	1.418(3)
C(10)-C(15)	1.426(2)
C(11)-C(12)	1.371(3)
C(11)-H(11)	0.9500
C(12)-C(13)	1.404(3)
C(12)-H(12)	0.9500
C(13)-C(14)	1.375(3)
C(13)-H(13)	0.9500
C(14)-C(15)	1.427(2)
C(16)-C(19)	1.345(3)
C(16)-C(17)	1.443(2)
C(17)-C(18)	1.334(3)
C(17)-H(17)	0.9500
C(18)-H(18)	0.9500
C(19)-H(19)	0.9500
C(20)-C(22)	1.519(3)
C(20)-C(21)	1.520(3)
C(20)-C(23)	1.546(3)
C(21)-H(21A)	0.9800
C(21)-H(21B)	0.9800
C(21)-H(21C)	0.9800

C(22)-H(22A)	0.9800
C(22)-H(22B)	0.9800
C(22)-H(22C)	0.9800
C(23)-C(24)	1.517(2)
C(23)-C(25)	1.523(2)
C(24)-H(24A)	0.9800
C(24)-H(24B)	0.9800
C(24)-H(24C)	0.9800
C(25)-H(25A)	0.9800
C(25)-H(25B)	0.9800
C(25)-H(25C)	0.9800

C(18)-O(1)-C(19)	105.42(15)
B(2)-O(2)-C(20)	106.95(13)
B(2)-O(3)-C(23)	106.76(13)
C(14)-N(1)-B(1)	123.73(15)
C(14)-N(1)-H(1N)	113.6(14)
B(1)-N(1)-H(1N)	122.4(14)
C(6)-N(2)-B(1)	123.72(15)
C(6)-N(2)-H(2N)	115.4(14)
B(1)-N(2)-H(2N)	120.9(14)
N(2)-B(1)-N(1)	115.77(16)
N(2)-B(1)-C(5)	121.10(16)
N(1)-B(1)-C(5)	123.12(15)
O(2)-B(2)-O(3)	112.85(15)
O(2)-B(2)-C(4)	124.37(15)
O(3)-B(2)-C(4)	122.75(16)
C(2)-C(1)-H(1A)	120.0
C(2)-C(1)-H(1B)	120.0
H(1A)-C(1)-H(1B)	120.0
C(1)-C(2)-C(16)	121.04(16)
C(1)-C(2)-C(3)	124.08(16)
C(16)-C(2)-C(3)	114.88(15)
C(2)-C(3)-C(4)	117.20(15)
C(2)-C(3)-H(3A)	108.0

C(4)-C(3)-H(3A)	108.0
C(2)-C(3)-H(3B)	108.0
C(4)-C(3)-H(3B)	108.0
H(3A)-C(3)-H(3B)	107.2
C(3)-C(4)-C(5)	110.03(14)
C(3)-C(4)-B(2)	112.32(13)
C(5)-C(4)-B(2)	108.59(13)
C(3)-C(4)-H(4)	108.6
C(5)-C(4)-H(4)	108.6
B(2)-C(4)-H(4)	108.6
C(4)-C(5)-B(1)	116.76(14)
C(4)-C(5)-H(5A)	108.1
B(1)-C(5)-H(5A)	108.1
C(4)-C(5)-H(5B)	108.1
B(1)-C(5)-H(5B)	108.1
H(5A)-C(5)-H(5B)	107.3
C(7)-C(6)-N(2)	122.13(16)
C(7)-C(6)-C(15)	119.88(16)
N(2)-C(6)-C(15)	117.99(15)
C(6)-C(7)-C(8)	120.16(17)
C(6)-C(7)-H(7)	119.9
C(8)-C(7)-H(7)	119.9
C(9)-C(8)-C(7)	121.37(17)
C(9)-C(8)-H(8)	119.3
C(7)-C(8)-H(8)	119.3
C(8)-C(9)-C(10)	120.44(16)
C(8)-C(9)-H(9)	119.8
C(10)-C(9)-H(9)	119.8
C(11)-C(10)-C(9)	122.75(16)
C(11)-C(10)-C(15)	118.57(16)
C(9)-C(10)-C(15)	118.68(16)
C(12)-C(11)-C(10)	120.31(16)
C(12)-C(11)-H(11)	119.8
C(10)-C(11)-H(11)	119.8
C(11)-C(12)-C(13)	121.50(17)

C(11)-C(12)-H(12)	119.2
C(13)-C(12)-H(12)	119.2
C(14)-C(13)-C(12)	119.94(17)
C(14)-C(13)-H(13)	120.0
C(12)-C(13)-H(13)	120.0
C(13)-C(14)-N(1)	122.25(16)
C(13)-C(14)-C(15)	120.21(16)
N(1)-C(14)-C(15)	117.52(15)
C(6)-C(15)-C(10)	119.43(15)
C(6)-C(15)-C(14)	121.16(15)
C(10)-C(15)-C(14)	119.41(16)
C(19)-C(16)-C(17)	104.53(17)
C(19)-C(16)-C(2)	126.63(16)
C(17)-C(16)-C(2)	128.84(18)
C(18)-C(17)-C(16)	106.36(18)
C(18)-C(17)-H(17)	126.8
C(16)-C(17)-H(17)	126.8
C(17)-C(18)-O(1)	111.69(17)
C(17)-C(18)-H(18)	124.2
O(1)-C(18)-H(18)	124.2
C(16)-C(19)-O(1)	111.99(16)
C(16)-C(19)-H(19)	124.0
O(1)-C(19)-H(19)	124.0
O(2)-C(20)-C(22)	108.47(15)
O(2)-C(20)-C(21)	105.99(14)
C(22)-C(20)-C(21)	110.59(18)
O(2)-C(20)-C(23)	102.30(13)
C(22)-C(20)-C(23)	114.99(15)
C(21)-C(20)-C(23)	113.64(17)
C(20)-C(21)-H(21A)	109.5
C(20)-C(21)-H(21B)	109.5
H(21A)-C(21)-H(21B)	109.5
C(20)-C(21)-H(21C)	109.5
H(21A)-C(21)-H(21C)	109.5
H(21B)-C(21)-H(21C)	109.5

C(20)-C(22)-H(22A)	109.5
C(20)-C(22)-H(22B)	109.5
H(22A)-C(22)-H(22B)	109.5
C(20)-C(22)-H(22C)	109.5
H(22A)-C(22)-H(22C)	109.5
H(22B)-C(22)-H(22C)	109.5
O(3)-C(23)-C(24)	109.37(15)
O(3)-C(23)-C(25)	105.89(14)
C(24)-C(23)-C(25)	110.69(16)
O(3)-C(23)-C(20)	101.39(13)
C(24)-C(23)-C(20)	115.07(16)
C(25)-C(23)-C(20)	113.54(15)
C(23)-C(24)-H(24A)	109.5
C(23)-C(24)-H(24B)	109.5
H(24A)-C(24)-H(24B)	109.5
C(23)-C(24)-H(24C)	109.5
H(24A)-C(24)-H(24C)	109.5
H(24B)-C(24)-H(24C)	109.5
C(23)-C(25)-H(25A)	109.5
C(23)-C(25)-H(25B)	109.5
H(25A)-C(25)-H(25B)	109.5
C(23)-C(25)-H(25C)	109.5
H(25A)-C(25)-H(25C)	109.5
H(25B)-C(25)-H(25C)	109.5

Symmetry transformations used to generate equivalent atoms:

Table 4. Anisotropic displacement parameters ($Å^2$x 10^3) for $C_{25}H_{30}B_2N_2O_3$. The anisotropic displacement factor exponent takes the form: $-2p^2[h^2 a^{*2}U^{11} + ... + 2 h k a^* b^* U^{12}]$

	U^{11}	U^{22}	U^{33}	U^{23}	U^{13}	U^{12}
O(1)	31(1)	30(1)	31(1)	6(1)	-4(1)	2(1)
O(2)	29(1)	27(1)	21(1)	-1(1)	2(1)	-8(1)
O(3)	28(1)	26(1)	19(1)	0(1)	5(1)	-7(1)
N(1)	21(1)	24(1)	25(1)	0(1)	2(1)	4(1)
N(2)	21(1)	23(1)	19(1)	0(1)	-2(1)	0(1)
B(1)	18(1)	22(1)	24(1)	3(1)	4(1)	-4(1)
B(2)	16(1)	23(1)	22(1)	-1(1)	-2(1)	2(1)
C(1)	27(1)	29(1)	30(1)	0(1)	2(1)	2(1)
C(2)	21(1)	20(1)	29(1)	1(1)	1(1)	-3(1)
C(3)	20(1)	23(1)	23(1)	2(1)	1(1)	-2(1)
C(4)	19(1)	20(1)	20(1)	-2(1)	-1(1)	0(1)
C(5)	19(1)	23(1)	22(1)	1(1)	3(1)	-1(1)
C(6)	17(1)	21(1)	25(1)	7(1)	2(1)	-3(1)
C(7)	25(1)	20(1)	30(1)	2(1)	1(1)	-3(1)
C(8)	24(1)	20(1)	44(1)	7(1)	3(1)	1(1)
C(9)	21(1)	29(1)	35(1)	14(1)	0(1)	0(1)
C(10)	18(1)	29(1)	25(1)	11(1)	2(1)	-4(1)
C(11)	21(1)	42(1)	23(1)	11(1)	-2(1)	-3(1)
C(12)	29(1)	44(1)	19(1)	0(1)	2(1)	-7(1)
C(13)	26(1)	33(1)	24(1)	-2(1)	5(1)	0(1)
C(14)	18(1)	27(1)	21(1)	5(1)	4(1)	-2(1)
C(15)	18(1)	23(1)	22(1)	7(1)	3(1)	-4(1)
C(16)	20(1)	21(1)	31(1)	2(1)	3(1)	-1(1)
C(17)	33(1)	42(1)	39(1)	2(1)	6(1)	14(1)
C(18)	29(1)	42(1)	42(1)	8(1)	2(1)	14(1)
C(19)	25(1)	23(1)	31(1)	2(1)	-2(1)	2(1)
C(20)	29(1)	25(1)	22(1)	3(1)	2(1)	-6(1)
C(21)	37(1)	44(1)	46(1)	22(1)	-7(1)	-3(1)
C(22)	54(1)	46(1)	26(1)	-6(1)	14(1)	-18(1)

C(23)	26(1)	24(1)	21(1)	1(1)	5(1)	-5(1)
C(24)	48(1)	26(1)	39(1)	-2(1)	18(1)	-9(1)
C(25)	22(1)	40(1)	39(1)	10(1)	1(1)	-7(1)

Table 5. Hydrogen coordinates (x 10^4) and isotropic displacement parameters ($Å^2$x 10^3) for $C_{25}H_{30}B_2N_2O_3$.

	x	y	z	U(eq)
H(1N)	3456(18)	2014(17)	3379(10)	28
H(2N)	3036(18)	4980(20)	4646(8)	26
H(1A)	8160	-332	4193	35
H(1B)	7003	571	3886	35
H(3A)	6566	2038	5344	26
H(3B)	5746	730	5267	26
H(4)	5154	1257	4121	24
H(5A)	4741	3441	5002	26
H(5B)	4013	2062	4949	26
H(7)	1628	6754	4378	30
H(8)	178	7711	3582	36
H(9)	-393	6674	2573	34
H(11)	-220	4696	1801	35
H(12)	710	2713	1577	37
H(13)	2271	1836	2327	34
H(17)	9305	-1411	5112	45
H(18)	10064	-1767	6284	45
H(19)	7405	797	6243	32
H(21A)	5229	4620	2583	66
H(21B)	5969	5965	2789	66
H(21C)	5216	5272	3304	66
H(22A)	8138	3317	2852	62
H(22B)	7931	4842	2598	62
H(22C)	7059	3670	2287	62
H(24A)	6622	6630	3931	55

H(24B)	7850	6696	3644	55
H(24C)	7836	6519	4427	55
H(25A)	8962	4431	4535	52
H(25B)	9158	4531	3771	52
H(25C)	8608	3188	4041	52

Table 6. Torsion angles [°] for $C_{25}H_{30}B_2N_2O_3$.

C(6)-N(2)-B(1)-N(1)	2.2(2)
C(6)-N(2)-B(1)-C(5)	-176.55(14)
C(14)-N(1)-B(1)-N(2)	-3.9(2)
C(14)-N(1)-B(1)-C(5)	174.82(15)
C(20)-O(2)-B(2)-O(3)	-10.43(18)
C(20)-O(2)-B(2)-C(4)	167.82(15)
C(23)-O(3)-B(2)-O(2)	-10.59(18)
C(23)-O(3)-B(2)-C(4)	171.13(14)
C(1)-C(2)-C(3)-C(4)	-4.2(2)
C(16)-C(2)-C(3)-C(4)	176.43(14)
C(2)-C(3)-C(4)-C(5)	176.25(13)
C(2)-C(3)-C(4)-B(2)	-62.66(19)
O(2)-B(2)-C(4)-C(3)	121.06(17)
O(3)-B(2)-C(4)-C(3)	-60.9(2)
O(2)-B(2)-C(4)-C(5)	-117.02(17)
O(3)-B(2)-C(4)-C(5)	61.1(2)
C(3)-C(4)-C(5)-B(1)	-175.56(14)
B(2)-C(4)-C(5)-B(1)	61.14(18)
N(2)-B(1)-C(5)-C(4)	-146.63(15)
N(1)-B(1)-C(5)-C(4)	34.7(2)
B(1)-N(2)-C(6)-C(7)	179.63(15)
B(1)-N(2)-C(6)-C(15)	0.1(2)
N(2)-C(6)-C(7)-C(8)	179.08(15)
C(15)-C(6)-C(7)-C(8)	-1.4(2)
C(6)-C(7)-C(8)-C(9)	1.9(3)
C(7)-C(8)-C(9)-C(10)	-0.4(3)

C(8)-C(9)-C(10)-C(11)	177.80(17)
C(8)-C(9)-C(10)-C(15)	-1.5(2)
C(9)-C(10)-C(11)-C(12)	179.44(16)
C(15)-C(10)-C(11)-C(12)	-1.3(2)
C(10)-C(11)-C(12)-C(13)	-0.7(3)
C(11)-C(12)-C(13)-C(14)	1.2(3)
C(12)-C(13)-C(14)-N(1)	178.53(15)
C(12)-C(13)-C(14)-C(15)	0.3(3)
B(1)-N(1)-C(14)-C(13)	-175.20(16)
B(1)-N(1)-C(14)-C(15)	3.1(2)
C(7)-C(6)-C(15)-C(10)	-0.5(2)
N(2)-C(6)-C(15)-C(10)	179.03(14)
C(7)-C(6)-C(15)-C(14)	179.42(15)
N(2)-C(6)-C(15)-C(14)	-1.1(2)
C(11)-C(10)-C(15)-C(6)	-177.40(15)
C(9)-C(10)-C(15)-C(6)	1.9(2)
C(11)-C(10)-C(15)-C(14)	2.7(2)
C(9)-C(10)-C(15)-C(14)	-177.98(14)
C(13)-C(14)-C(15)-C(6)	177.88(16)
N(1)-C(14)-C(15)-C(6)	-0.5(2)
C(13)-C(14)-C(15)-C(10)	-2.2(2)
N(1)-C(14)-C(15)-C(10)	179.42(14)
C(1)-C(2)-C(16)-C(19)	174.13(18)
C(3)-C(2)-C(16)-C(19)	-6.5(2)
C(1)-C(2)-C(16)-C(17)	-6.0(3)
C(3)-C(2)-C(16)-C(17)	173.32(18)
C(19)-C(16)-C(17)-C(18)	-0.1(2)
C(2)-C(16)-C(17)-C(18)	-179.95(18)
C(16)-C(17)-C(18)-O(1)	-0.3(2)
C(19)-O(1)-C(18)-C(17)	0.6(2)
C(17)-C(16)-C(19)-O(1)	0.4(2)
C(2)-C(16)-C(19)-O(1)	-179.68(15)
C(18)-O(1)-C(19)-C(16)	-0.6(2)
B(2)-O(2)-C(20)-C(22)	147.47(15)
B(2)-O(2)-C(20)-C(21)	-93.75(17)

B(2)-O(2)-C(20)-C(23)	25.56(16)
B(2)-O(3)-C(23)-C(24)	147.31(16)
B(2)-O(3)-C(23)-C(25)	-93.38(16)
B(2)-O(3)-C(23)-C(20)	25.37(16)
O(2)-C(20)-C(23)-O(3)	-30.45(16)
C(22)-C(20)-C(23)-O(3)	-147.80(16)
C(21)-C(20)-C(23)-O(3)	83.32(17)
O(2)-C(20)-C(23)-C(24)	-148.35(15)
C(22)-C(20)-C(23)-C(24)	94.3(2)
C(21)-C(20)-C(23)-C(24)	-34.6(2)
O(2)-C(20)-C(23)-C(25)	82.65(17)
C(22)-C(20)-C(23)-C(25)	-34.7(2)
C(21)-C(20)-C(23)-C(25)	-163.58(16)

Symmetry transformations used to generate equivalent atoms:

Table 7. Hydrogen bonds for $C_{25}H_{30}B_2N_2O_3$ [Å and º].

D-H...A	d(D-H)	d(H...A)	d(D...A)	<(DHA)
N(2)-H(2N)...O(3)#1	0.863(15)	2.150(16)	3.0082(19)	173.5(19)

Symmetry transformations used to generate equivalent atoms:
#1 -x+1,-y+1,-z+1

■ **Data for X-ray Crystallography of 3.55**

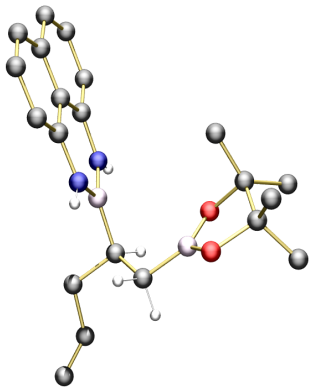

Table 1. Crystal data and structure refinement for $C_{21}H_{28}B_2N_2O_2$.

Identification code	C21H28B2N2O2	
Empirical formula	C21 H28 B2 N2 O2	
Formula weight	362.07	
Temperature	100(2) K	
Wavelength	1.54178 Å	
Crystal system	Triclinic	
Space group	P-1	
Unit cell dimensions	a = 9.9787(12) Å	α= 100.956(8)º.
	b = 10.6797(13) Å	β= 114.093(7)º.
	c = 11.8681(15) Å	γ= 100.609(8)º.
Volume	1084.2(2) $Å^3$	
Z	2	
Density (calculated)	1.109 Mg/m^3	
Absorption coefficient	0.543 mm^{-1}	
F(000)	388	
Crystal size	0.250 x 0.170 x 0.120 mm^3	
Theta range for data collection	4.271 to 66.697.	
Index ranges	-10<=h<=11, -12<=k<=12, -14<=l<=14	
Reflections collected	9561	
Independent reflections	3784 [R(int) = 0.0269]	
Completeness to theta = 66.697º	98.8 %	
Absorption correction	Semi-empirical from equivalents	
Max. and min. transmission	0.7528 and 0.6548	
Refinement method	Full-matrix least-squares on F^2	
Data / restraints / parameters	3784 / 339 / 339	
Goodness-of-fit on F^2	1.035	
Final R indices [I>2sigma(I)]	R1 = 0.0521, wR2 = 0.1394	
R indices (all data)	R1 = 0.0794, wR2 = 0.1586	
Extinction coefficient	n/a	
Largest diff. peak and hole	0.155 and -0.158 e. $Å^{-3}$	

Table 2. Atomic coordinates (x 10^4) and equivalent isotropic displacement parameters ($Å^2$x 10^3) for $C_{21}H_{28}B_2N_2O_2$. U(eq) is defined as one third of the trace of the orthogonalized U^{ij} tensor.

	x	y	z	U(eq)
O(1)	3515(2)	1845(1)	5296(1)	68(1)
N(1)	7339(2)	1370(2)	5886(2)	60(1)
N(2)	7489(2)	3651(2)	5950(2)	61(1)
B(1)	6735(3)	2284(2)	5258(2)	56(1)
B(2)	3587(2)	2765(2)	4654(2)	56(1)
C(1)	4721(8)	1701(8)	609(5)	163(3)
C(2)	4792(6)	1117(6)	1472(4)	102(2)
C(3)	5989(4)	1731(3)	2882(3)	61(1)
C(1X)	3370(40)	70(50)	90(30)	330(20)
C(2X)	3810(30)	130(30)	1250(20)	160(8)
C(3X)	5330(30)	1300(30)	2250(20)	145(8)
C(4)	5349(2)	1803(2)	3858(2)	62(1)
C(5)	8599(2)	1749(2)	7107(2)	63(1)
C(6)	9126(3)	830(3)	7711(2)	82(1)
C(7)	10415(3)	1256(3)	8918(3)	101(1)
C(8)	11169(3)	2566(4)	9520(3)	98(1)
C(9)	10672(3)	3551(3)	8943(2)	79(1)
C(10)	11408(3)	4933(3)	9528(3)	97(1)
C(11)	10857(3)	5842(3)	8968(3)	96(1)
C(12)	9538(3)	5440(2)	7776(2)	78(1)
C(13)	8795(2)	4102(2)	7151(2)	62(1)
C(14)	9346(2)	3131(2)	7724(2)	62(1)
C(15)	4243(2)	2675(2)	3673(2)	64(1)
O(2)	2962(3)	3729(3)	4934(3)	70(1)
C(16)	3122(4)	2406(4)	6314(5)	70(1)
C(17)	2251(4)	3333(3)	5724(4)	76(1)
C(18)	2264(6)	1316(5)	6612(5)	95(2)
C(19)	4657(4)	3174(5)	7521(3)	117(2)
C(20)	2329(6)	4555(3)	6625(5)	111(1)
C(21)	536(3)	2562(5)	4773(4)	108(1)
O(2X)	3610(20)	4020(20)	5420(20)	70(5)
C(16X)	3130(30)	2280(20)	6250(40)	86(5)

C(17X)	2930(30)	3640(20)	6220(20)	98(5)
C(18X)	1850(30)	1140(30)	6070(30)	73(7)
C(19X)	4640(30)	2320(40)	7410(30)	122(9)
C(20X)	3540(50)	4700(20)	7430(30)	127(8)
C(21X)	1170(30)	3520(30)	5430(30)	111(1)

Table 3. Bond lengths [Å] and angles [º] for $C_{21}H_{28}B_2N_2O_2$.

O(1)-B(2)	1.362(2)
O(1)-C(16)	1.473(5)
N(1)-C(5)	1.395(3)
N(1)-B(1)	1.412(3)
N(1)-H(1N)	0.86(2)
N(2)-C(13)	1.398(3)
N(2)-B(1)	1.417(3)
N(2)-H(2N)	0.83(2)
B(1)-C(4)	1.574(3)
B(2)-O(2)	1.355(3)
B(2)-C(15)	1.548(3)
C(1)-C(2)	1.281(6)
C(1)-H(1A)	0.9500
C(1)-H(1B)	0.9500
C(2)-C(3)	1.523(5)
C(2)-H(2)	0.9500
C(3)-C(4)	1.530(4)
C(3)-H(3A)	0.9900
C(3)-H(3B)	0.9900
C(4)-C(15)	1.547(3)
C(4)-H(4)	1.03(2)
C(5)-C(6)	1.379(3)
C(5)-C(14)	1.418(3)
C(6)-C(7)	1.395(3)
C(6)-H(6)	0.9500
C(7)-C(8)	1.352(4)
C(7)-H(7)	0.9500

C(8)-C(9)	1.417(4)
C(8)-H(8)	0.9500
C(9)-C(10)	1.412(4)
C(9)-C(14)	1.420(3)
C(10)-C(11)	1.354(4)
C(10)-H(10)	0.9500
C(11)-C(12)	1.400(3)
C(11)-H(11)	0.9500
C(12)-C(13)	1.379(3)
C(12)-H(12)	0.9500
C(13)-C(14)	1.418(3)
C(15)-H(15A)	0.9900
C(15)-H(15B)	0.9900
O(2)-C(17)	1.465(3)
C(16)-C(18)	1.500(4)
C(16)-C(17)	1.520(4)
C(16)-C(19)	1.539(4)
C(17)-C(20)	1.488(4)
C(17)-C(21)	1.559(4)
C(18)-H(18A)	0.9800
C(18)-H(18B)	0.9800
C(18)-H(18C)	0.9800
C(19)-H(19A)	0.9800
C(19)-H(19B)	0.9800
C(19)-H(19C)	0.9800
C(20)-H(20A)	0.9800
C(20)-H(20B)	0.9800
C(20)-H(20C)	0.9800
C(21)-H(21A)	0.9800
C(21)-H(21B)	0.9800
C(21)-H(21C)	0.9800

B(2)-O(1)-C(16)	107.19(19)
C(5)-N(1)-B(1)	123.82(19)
C(5)-N(1)-H(1N)	116.4(14)

B(1)-N(1)-H(1N)	119.8(14)
C(13)-N(2)-B(1)	123.44(18)
C(13)-N(2)-H(2N)	115.6(16)
B(1)-N(2)-H(2N)	120.5(15)
N(1)-B(1)-N(2)	115.8(2)
N(1)-B(1)-C(4)	121.72(19)
N(2)-B(1)-C(4)	122.44(19)
O(2)-B(2)-O(1)	112.2(2)
O(2)-B(2)-C(15)	124.2(2)
O(1)-B(2)-C(15)	123.54(18)
C(2)-C(1)-H(1A)	120.0
C(2)-C(1)-H(1B)	120.0
H(1A)-C(1)-H(1B)	120.0
C(1)-C(2)-C(3)	122.3(5)
C(1)-C(2)-H(2)	118.9
C(3)-C(2)-H(2)	118.9
C(2)-C(3)-C(4)	115.1(3)
C(2)-C(3)-H(3A)	108.5
C(4)-C(3)-H(3A)	108.5
C(2)-C(3)-H(3B)	108.5
C(4)-C(3)-H(3B)	108.5
H(3A)-C(3)-H(3B)	107.5
C(3)-C(4)-C(15)	112.61(19)
C(3)-C(4)-B(1)	108.52(19)
C(15)-C(4)-B(1)	112.89(17)
C(3)-C(4)-H(4)	101.5(12)
C(15)-C(4)-H(4)	109.4(12)
B(1)-C(4)-H(4)	111.3(11)
C(6)-C(5)-N(1)	122.3(2)
C(6)-C(5)-C(14)	120.1(2)
N(1)-C(5)-C(14)	117.64(18)
C(5)-C(6)-C(7)	120.2(3)
C(5)-C(6)-H(6)	119.9
C(7)-C(6)-H(6)	119.9
C(8)-C(7)-C(6)	121.1(3)

C(8)-C(7)-H(7)	119.5
C(6)-C(7)-H(7)	119.5
C(7)-C(8)-C(9)	121.0(3)
C(7)-C(8)-H(8)	119.5
C(9)-C(8)-H(8)	119.5
C(10)-C(9)-C(8)	123.4(3)
C(10)-C(9)-C(14)	118.1(2)
C(8)-C(9)-C(14)	118.5(2)
C(11)-C(10)-C(9)	121.5(3)
C(11)-C(10)-H(10)	119.2
C(9)-C(10)-H(10)	119.2
C(10)-C(11)-C(12)	120.8(3)
C(10)-C(11)-H(11)	119.6
C(12)-C(11)-H(11)	119.6
C(13)-C(12)-C(11)	119.9(2)
C(13)-C(12)-H(12)	120.1
C(11)-C(12)-H(12)	120.1
C(12)-C(13)-N(2)	122.0(2)
C(12)-C(13)-C(14)	120.2(2)
N(2)-C(13)-C(14)	117.76(18)
C(5)-C(14)-C(13)	121.42(19)
C(5)-C(14)-C(9)	119.2(2)
C(13)-C(14)-C(9)	119.4(2)
C(4)-C(15)-B(2)	113.40(16)
C(4)-C(15)-H(15A)	108.9
B(2)-C(15)-H(15A)	108.9
C(4)-C(15)-H(15B)	108.9
B(2)-C(15)-H(15B)	108.9
H(15A)-C(15)-H(15B)	107.7
B(2)-O(2)-C(17)	107.1(2)
O(1)-C(16)-C(18)	110.7(3)
O(1)-C(16)-C(17)	101.0(3)
C(18)-C(16)-C(17)	116.7(3)
O(1)-C(16)-C(19)	106.2(3)
C(18)-C(16)-C(19)	109.3(3)

C(17)-C(16)-C(19)	112.2(3)
O(2)-C(17)-C(20)	108.9(2)
O(2)-C(17)-C(16)	102.9(2)
C(20)-C(17)-C(16)	117.5(3)
O(2)-C(17)-C(21)	106.4(2)
C(20)-C(17)-C(21)	109.2(3)
C(16)-C(17)-C(21)	111.2(3)
C(16)-C(18)-H(18A)	109.5
C(16)-C(18)-H(18B)	109.5
H(18A)-C(18)-H(18B)	109.5
C(16)-C(18)-H(18C)	109.5
H(18A)-C(18)-H(18C)	109.5
H(18B)-C(18)-H(18C)	109.5
C(16)-C(19)-H(19A)	109.5
C(16)-C(19)-H(19B)	109.5
H(19A)-C(19)-H(19B)	109.5
C(16)-C(19)-H(19C)	109.5
H(19A)-C(19)-H(19C)	109.5
H(19B)-C(19)-H(19C)	109.5
C(17)-C(20)-H(20A)	109.5
C(17)-C(20)-H(20B)	109.5
H(20A)-C(20)-H(20B)	109.5
C(17)-C(20)-H(20C)	109.5
H(20A)-C(20)-H(20C)	109.5
H(20B)-C(20)-H(20C)	109.5
C(17)-C(21)-H(21A)	109.5
C(17)-C(21)-H(21B)	109.5
H(21A)-C(21)-H(21B)	109.5
C(17)-C(21)-H(21C)	109.5
H(21A)-C(21)-H(21C)	109.5
H(21B)-C(21)-H(21C)	109.5

Symmetry transformations used to generate equivalent atoms:

Table 4. Anisotropic displacement parameters (Å ^{2}x 10^{3}) for $C_{21}H_{28}B_2N_2O_2$. The

anisotropic displacement factor exponent takes the form: $-2p^2[h^2 a^{*2} U^{11} + ... + 2 h k a^* b^* U^{12}]$

	U^{11}	U^{22}	U^{33}	U^{23}	U^{13}	U^{12}
O(1)	81(1)	58(1)	81(1)	28(1)	48(1)	29(1)
N(1)	62(1)	55(1)	67(1)	22(1)	31(1)	19(1)
N(2)	67(1)	57(1)	69(1)	24(1)	35(1)	25(1)
B(1)	57(1)	58(1)	69(1)	24(1)	40(1)	22(1)
B(2)	48(1)	54(1)	68(1)	23(1)	25(1)	17(1)
C(1)	190(6)	250(7)	83(3)	51(4)	67(3)	125(5)
C(2)	111(3)	141(4)	49(2)	13(2)	33(2)	48(3)
C(3)	70(2)	67(2)	54(2)	17(1)	30(2)	32(1)
C(1X)	280(30)	490(50)	178(13)	66(15)	87(14)	80(30)
C(2X)	152(15)	209(19)	144(11)	20(11)	79(10)	112(13)
C(3X)	165(16)	206(18)	119(9)	54(9)	85(10)	126(13)
C(4)	63(1)	61(1)	71(1)	24(1)	35(1)	26(1)
C(5)	63(1)	73(1)	66(1)	29(1)	37(1)	26(1)
C(6)	88(2)	88(2)	84(2)	45(1)	40(1)	36(1)
C(7)	106(2)	123(2)	89(2)	57(2)	40(2)	54(2)
C(8)	90(2)	134(2)	70(2)	36(2)	28(1)	44(2)
C(9)	73(1)	100(2)	62(1)	18(1)	31(1)	25(1)
C(10)	82(2)	112(2)	72(2)	5(2)	28(1)	16(2)
C(11)	95(2)	85(2)	86(2)	-4(1)	44(2)	6(2)
C(12)	87(2)	67(1)	82(2)	11(1)	47(1)	17(1)
C(13)	65(1)	65(1)	64(1)	16(1)	39(1)	19(1)
C(14)	62(1)	74(1)	61(1)	21(1)	36(1)	23(1)
C(15)	63(1)	69(1)	71(1)	29(1)	34(1)	29(1)
O(2)	80(2)	65(1)	107(2)	45(1)	64(2)	39(1)
C(16)	84(2)	65(2)	76(2)	24(2)	49(2)	23(2)
C(17)	89(2)	70(2)	113(2)	43(2)	74(2)	40(2)
C(18)	133(4)	81(2)	106(4)	45(2)	78(3)	34(2)
C(19)	101(2)	147(4)	76(2)	15(2)	31(2)	21(2)
C(20)	158(4)	74(2)	164(4)	40(2)	125(3)	48(2)
C(21)	62(2)	152(4)	135(3)	68(3)	56(2)	38(2)

O(2X)	83(12)	58(6)	90(9)	28(5)	55(9)	26(6)
C(16X)	124(12)	64(9)	102(8)	27(7)	81(8)	27(8)
C(17X)	149(10)	74(9)	129(9)	43(6)	108(7)	42(7)
C(18X)	89(12)	75(11)	96(18)	53(11)	63(11)	43(8)
C(19X)	135(13)	140(20)	104(10)	38(11)	69(9)	43(12)
C(20X)	210(20)	71(11)	133(10)	29(8)	113(10)	40(12)
C(21X)	158(4)	74(2)	164(4)	40(2)	125(3)	48(2)

Table 5. Hydrogen coordinates (x 10^4) and isotropic displacement parameters ($Å^2$x 10 ^{3}) for $C_{21}H_{28}B_2N_2O_2$.

	x	y	z	U(eq)
H(1N)	6940(20)	530(20)	5500(20)	72
H(2N)	7240(20)	4240(20)	5610(20)	73
H(1A)	5429	2546	840	196
H(1B)	3959	1288	-262	196
H(2)	4075	272	1223	123
H(3A)	6560	2645	2994	74
H(3B)	6730	1205	3085	74
H(1X1)	3924	703	-143	398
H(1X2)	2471	-605	-553	398
H(2X)	3285	-489	1513	192
H(3X1)	5385	2078	1918	174
H(3X2)	6244	997	2357	174
H(4)	4740(20)	820(20)	3622(19)	74
H(6)	8609	-95	7304	98
H(7)	10770	614	9324	121
H(8)	12044	2831	10341	118
H(10)	12311	5231	10334	116
H(11)	11373	6766	9389	115
H(12)	9155	6088	7397	94
H(15A)	3380	2303	2787	77

H(15B)	4795	3586	3757	77
H(18A)	2014	1708	7290	143
H(18B)	1315	792	5831	143
H(18C)	2903	735	6909	143
H(19A)	4458	3570	8231	175
H(19B)	5265	2560	7772	175
H(19C)	5225	3882	7327	175
H(20A)	1855	4300	7159	166
H(20B)	3404	5077	7183	166
H(20C)	1778	5092	6127	166
H(21A)	9	2275	5260	162
H(21B)	41	3147	4309	162
H(21C)	480	1779	4152	162
H(18D)	1524	1391	6737	109
H(18E)	987	939	5216	109
H(18F)	2215	355	6153	109
H(19D)	4586	2616	8219	182
H(19E)	4778	1425	7308	182
H(19F)	5512	2939	7430	182
H(20D)	3064	4419	7957	191
H(20E)	4656	4866	7907	191
H(20F)	3317	5514	7254	191
H(21D)	629	3268	5913	166
H(21E)	1067	4382	5290	166
H(21F)	736	2841	4591	166

Table 6. Torsion angles [º] for $C_{21}H_{28}B_2N_2O_2$.

C(5)-N(1)-B(1)-N(2)	-0.3(3)
C(5)-N(1)-B(1)-C(4)	177.63(17)
C(13)-N(2)-B(1)-N(1)	3.0(3)
C(13)-N(2)-B(1)-C(4)	-174.87(17)
C(16)-O(1)-B(2)-O(2)	-13.7(3)
C(16)-O(1)-B(2)-C(15)	168.9(2)

C(1)-C(2)-C(3)-C(4)	128.2(4)
C(2)-C(3)-C(4)-C(15)	-61.5(3)
C(2)-C(3)-C(4)-B(1)	172.8(3)
N(1)-B(1)-C(4)-C(3)	-91.1(2)
N(2)-B(1)-C(4)-C(3)	86.7(2)
N(1)-B(1)-C(4)-C(15)	143.38(19)
N(2)-B(1)-C(4)-C(15)	-38.8(3)
B(1)-N(1)-C(5)-C(6)	177.7(2)
B(1)-N(1)-C(5)-C(14)	-2.5(3)
N(1)-C(5)-C(6)-C(7)	178.3(2)
C(14)-C(5)-C(6)-C(7)	-1.4(3)
C(5)-C(6)-C(7)-C(8)	0.2(4)
C(6)-C(7)-C(8)-C(9)	0.0(4)
C(7)-C(8)-C(9)-C(10)	179.7(3)
C(7)-C(8)-C(9)-C(14)	0.9(4)
C(8)-C(9)-C(10)-C(11)	-177.2(3)
C(14)-C(9)-C(10)-C(11)	1.5(4)
C(9)-C(10)-C(11)-C(12)	-0.6(4)
C(10)-C(11)-C(12)-C(13)	-0.8(4)
C(11)-C(12)-C(13)-N(2)	-178.90(19)
C(11)-C(12)-C(13)-C(14)	1.2(3)
B(1)-N(2)-C(13)-C(12)	177.31(19)
B(1)-N(2)-C(13)-C(14)	-2.7(3)
C(6)-C(5)-C(14)-C(13)	-177.37(19)
N(1)-C(5)-C(14)-C(13)	2.8(3)
C(6)-C(5)-C(14)-C(9)	2.4(3)
N(1)-C(5)-C(14)-C(9)	-177.38(17)
C(12)-C(13)-C(14)-C(5)	179.62(18)
N(2)-C(13)-C(14)-C(5)	-0.3(3)
C(12)-C(13)-C(14)-C(9)	-0.2(3)
N(2)-C(13)-C(14)-C(9)	179.89(17)
C(10)-C(9)-C(14)-C(5)	179.1(2)
C(8)-C(9)-C(14)-C(5)	-2.1(3)
C(10)-C(9)-C(14)-C(13)	-1.2(3)
C(8)-C(9)-C(14)-C(13)	177.6(2)

C(3)-C(4)-C(15)-B(2)	-179.8(2)
B(1)-C(4)-C(15)-B(2)	-56.5(2)
O(2)-B(2)-C(15)-C(4)	160.7(2)
O(1)-B(2)-C(15)-C(4)	-22.2(3)
O(1)-B(2)-O(2)-C(17)	-6.9(3)
C(15)-B(2)-O(2)-C(17)	170.5(2)
B(2)-O(1)-C(16)-C(18)	151.4(3)
B(2)-O(1)-C(16)-C(17)	27.1(3)
B(2)-O(1)-C(16)-C(19)	-90.1(3)
B(2)-O(2)-C(17)-C(20)	149.0(3)
B(2)-O(2)-C(17)-C(16)	23.6(3)
B(2)-O(2)-C(17)-C(21)	-93.4(3)
O(1)-C(16)-C(17)-O(2)	-30.0(3)
C(18)-C(16)-C(17)-O(2)	-150.0(4)
C(19)-C(16)-C(17)-O(2)	82.7(4)
O(1)-C(16)-C(17)-C(20)	-149.6(3)
C(18)-C(16)-C(17)-C(20)	90.3(4)
C(19)-C(16)-C(17)-C(20)	-36.9(5)
O(1)-C(16)-C(17)-C(21)	83.6(3)
C(18)-C(16)-C(17)-C(21)	-36.4(5)
C(19)-C(16)-C(17)-C(21)	-163.7(3)

Symmetry transformations used to generate equivalent atoms:

Table 7. Hydrogen bonds for $C_{21}H_{28}B_2N_2O_2$ [Å and º].

D-H...A	d(D-H)	d(H...A)	d(D...A)	<(DHA)
N(1)-H(1N)...O(1)#1	0.86(2)	2.42(2)	3.256(2)	165.4(19)
N(2)-H(2N)...O(2)#2	0.83(2)	2.40(2)	3.213(3)	167(2)

Symmetry transformations used to generate equivalent atoms:
#1 -x+1,-y,-z+1 #2 -x+1,-y+1,-z+1

■ **NMR Spectra**

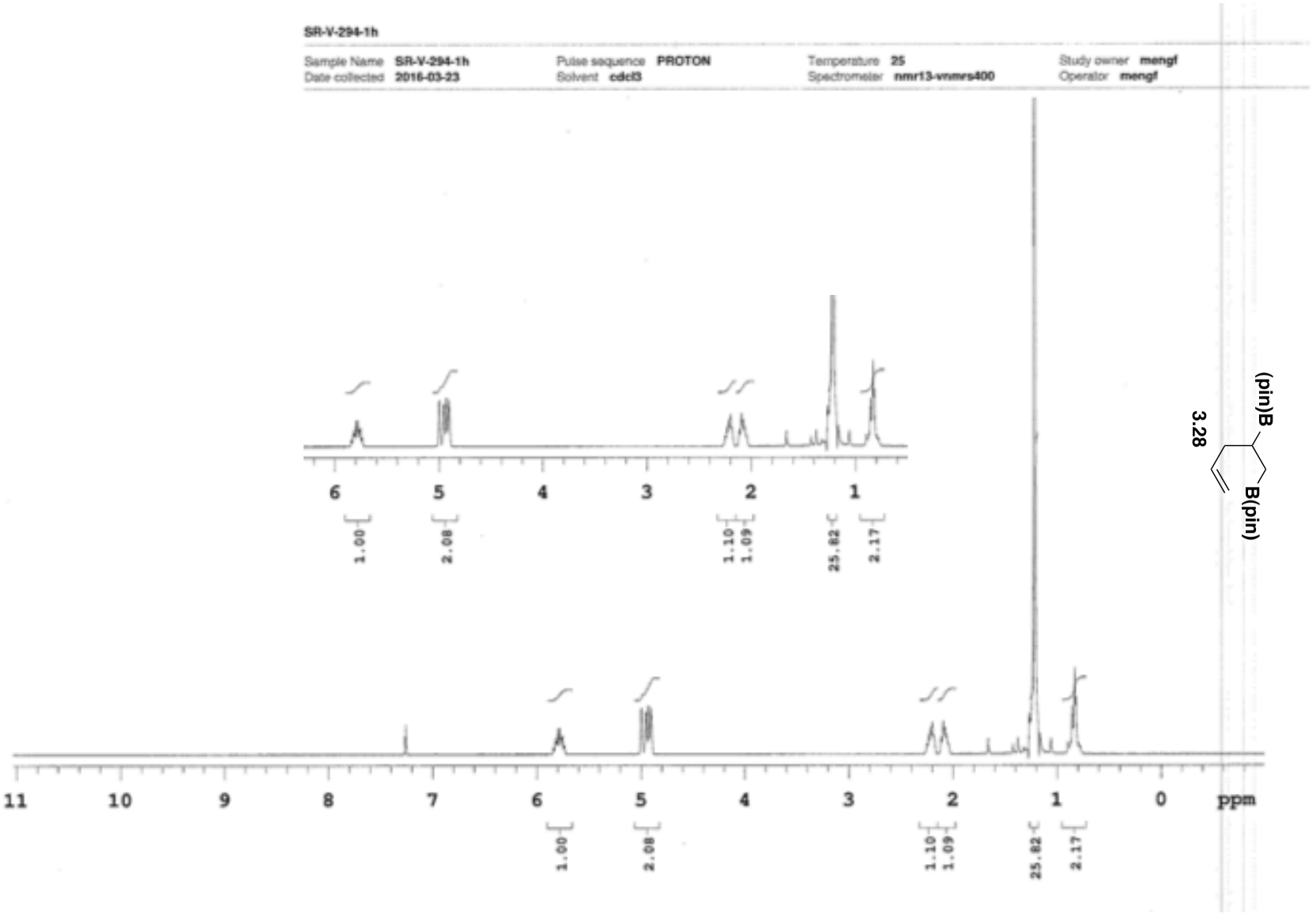
SR-V-294-1h
Sample Name SR-V-294-1h
Date collected 2016-03-23
Pulse sequence PROTON
Solvent cdcl3
Temperature 25
Spectrometer nmr13-vnmrs400
Study owner mengf
Operator mengf
3.28
(pin)B
B(pin)
11
10
9
8
7
6
5
4
3
2
1
0
ppm
1.00
2.08
1.10
1.09
25.82
2.17

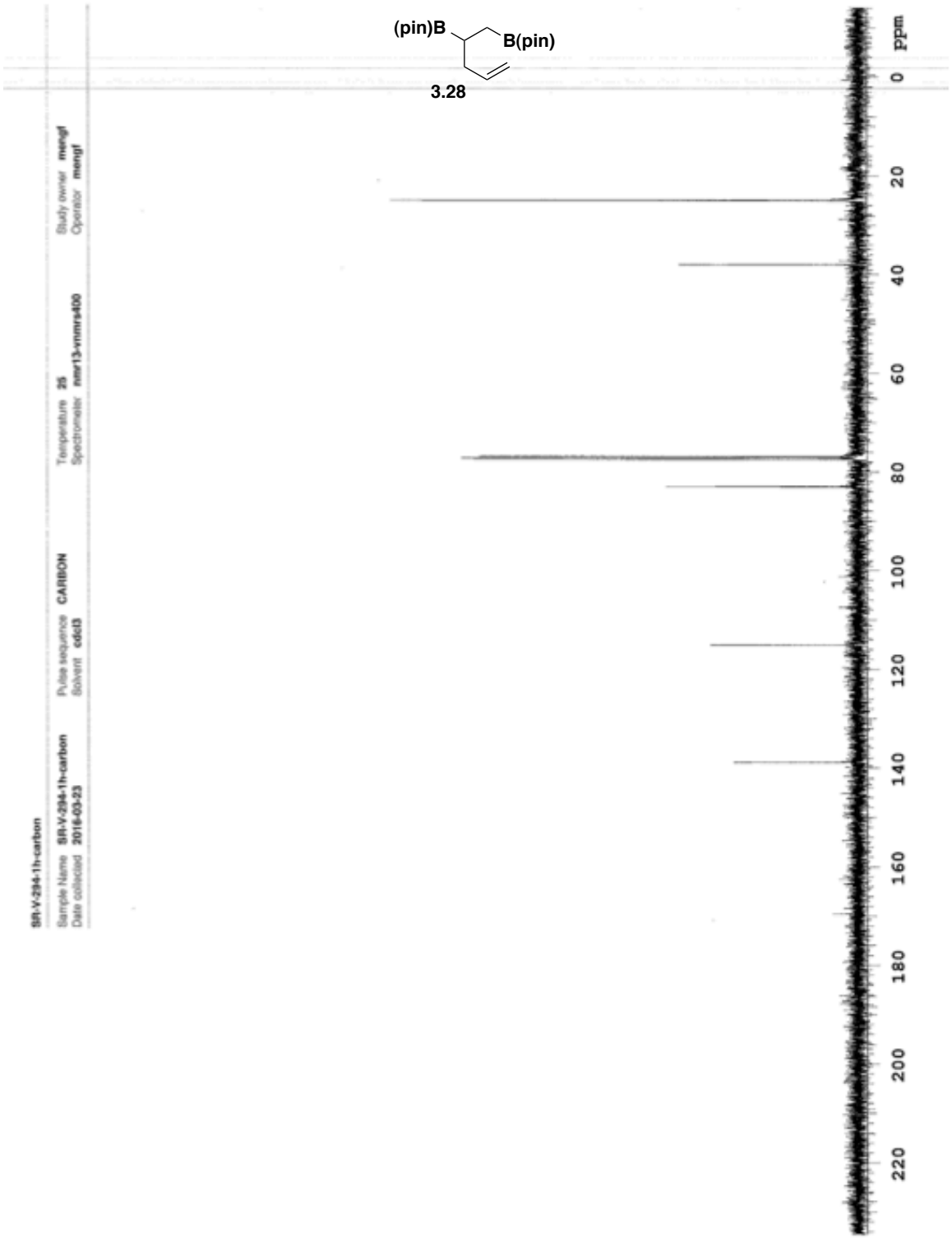
SR-V-294-1h-carbon
Sample Name SR-V-294-1h-carbon
Date collected 2016-03-23
Pulse sequence CARBON
Solvent cdcl3
Temperature 25
Spectrometer nmr13-vnmrs400
Study owner mengf
Operator mengf
(pin)B
B(pin)
3.28
ppm
0
20
40
60
80
100
120
140
160
180
200
220

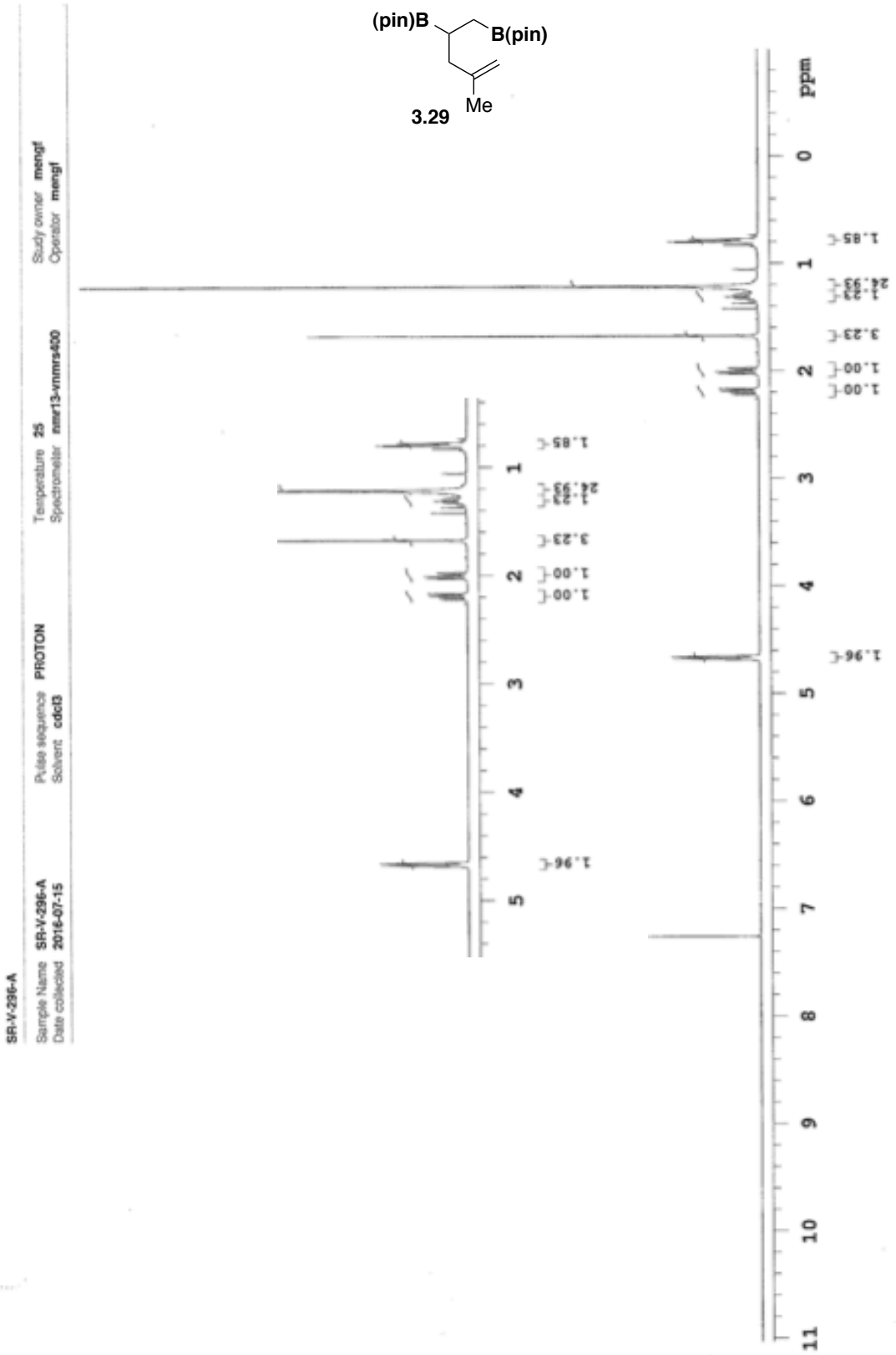
(pin)B
B(pin)
Me
3.29
SR-V-296-A
Sample Name SR-V-296-A
Date collected 2016-07-15
Pulse sequence PROTON
Solvent cdcl3
Temperature 25
Spectrometer nmr13-vnmrs400
Study owner mengf
Operator mengf
1.85
2.00
2.23
1.00
1.00
1.96
ppm

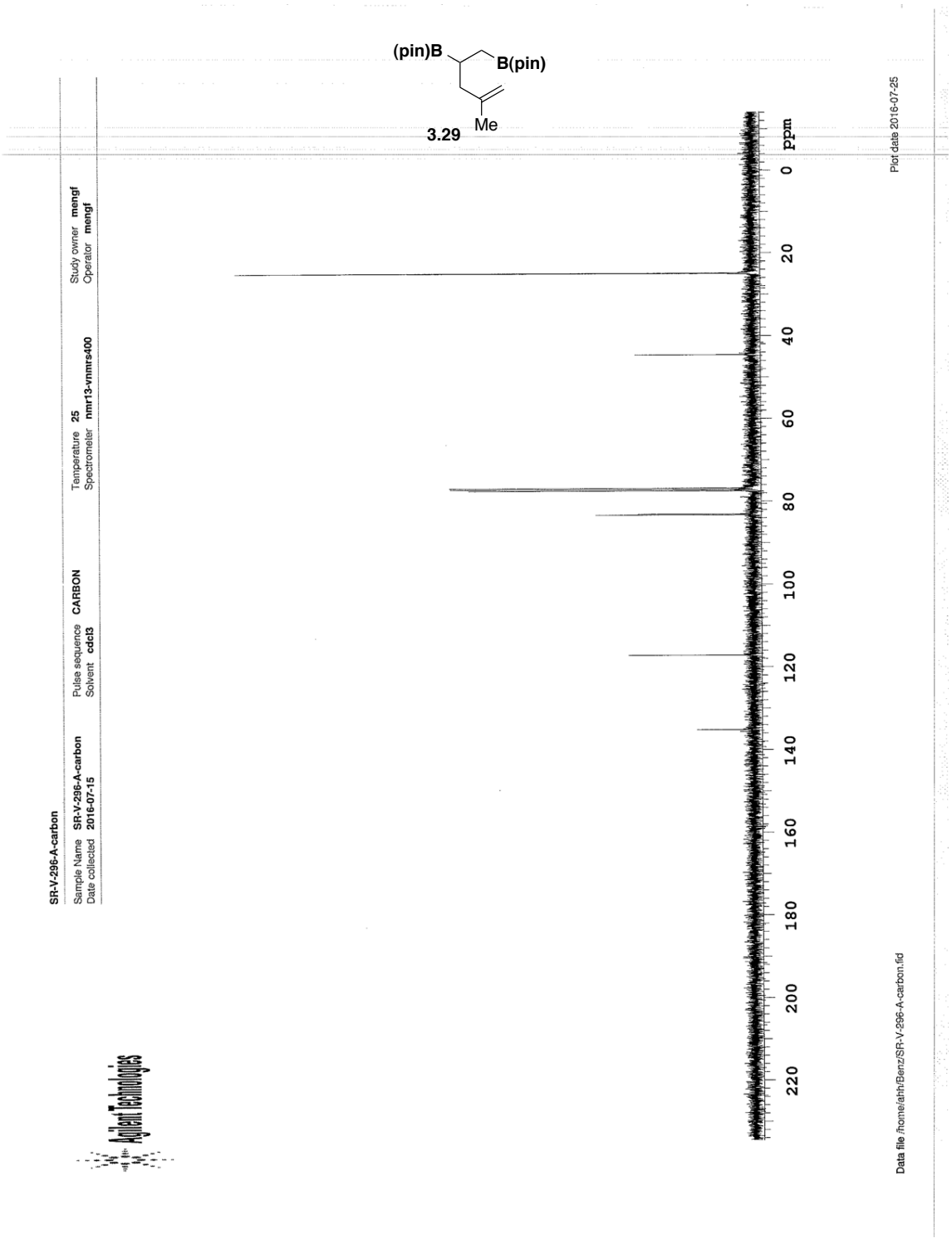
SR-V-296-A-carbon
Sample Name SR-V-296-A-carbon
Date collected 2016-07-15
Pulse sequence CARBON
Solvent cdcl3
Temperature 25
Spectrometer nmr13-vnmrs400
Study owner mengf
Operator mengf
(pin)B
B(pin)
Me
3.29
ppm
Plot date 2016-07-25
Data file /home/ahh/Benz/SR-V-296-A-carbon.fid
Agilent Technologies

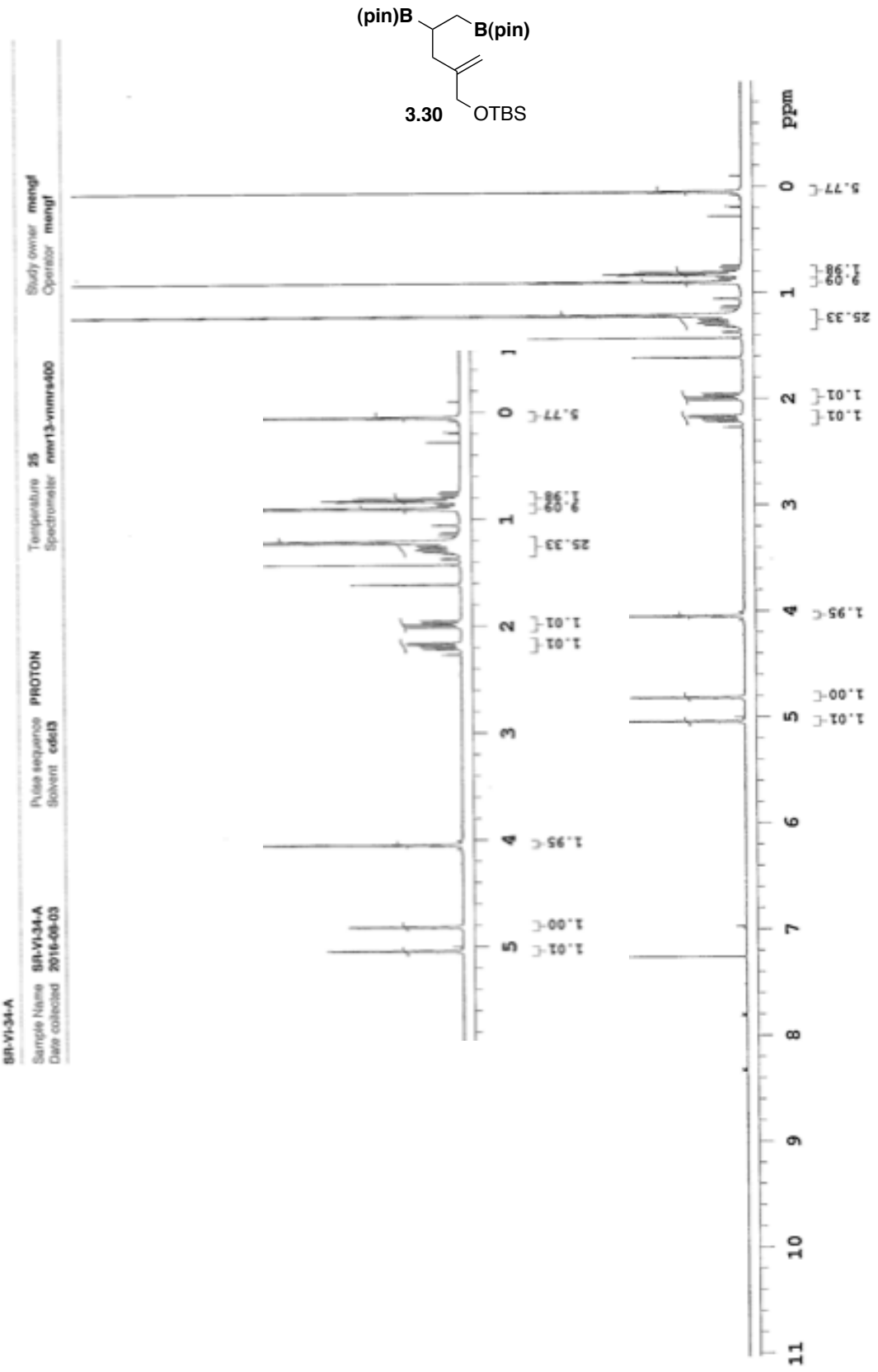
(pin)B
B(pin)
3.30
OTBS
BR-VI-34-A
Sample Name BR-VI-34-A
Date collected 2016-08-03
Pulse sequence PROTON
Solvent cdcl3
Temperature 25
Spectrometer nmr13-vnmrs400
Study owner mengf
Operator mengf
5.77
2.09
1.98
25.33
1.01
1.01
1.95
1.00
1.01
ppm

SR-VI-34-A-carbon
Sample Name SR-VI-34-A-carbon
Date collected 2016-08-03
Pulse sequence CARBON
Solvent cdcl3
Temperature 25
Spectrometer nmr13-vnmrs400
Study owner mengf
Operator mengf
(pin)B
B(pin)
3.30
OTBS
ppm
0
20
40
60
80
100
120
140
160
180
200

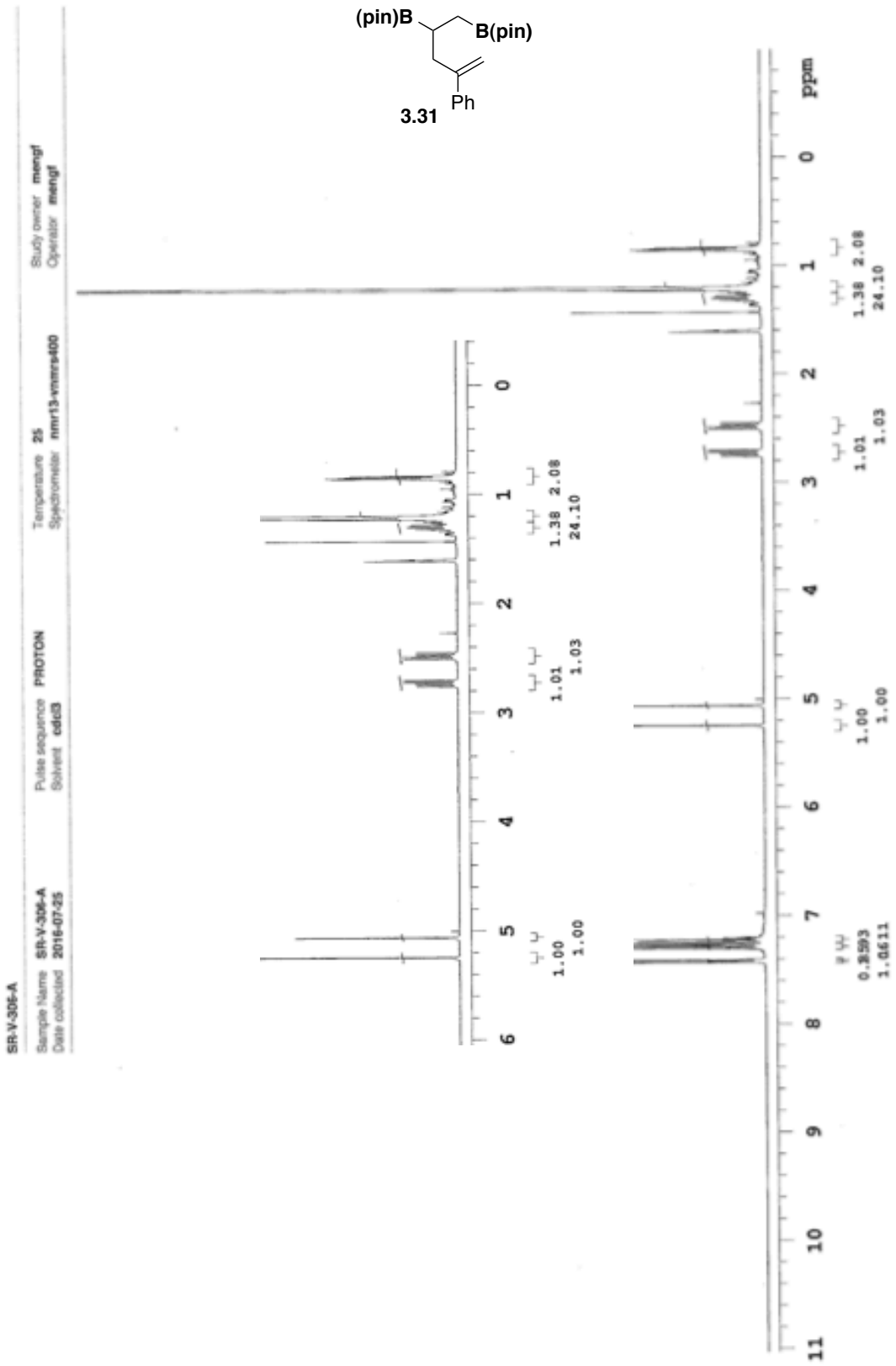
(pin)B
B(pin)
Ph
3.31
SR-V-306-A
Sample Name SR-V-306-A
Date collected 2016-07-25
Pulse sequence PROTON
Solvent cdcl3
Temperature 25
Spectrometer nmr13-vnmrs400
Study owner mengf
Operator mengf
ppm

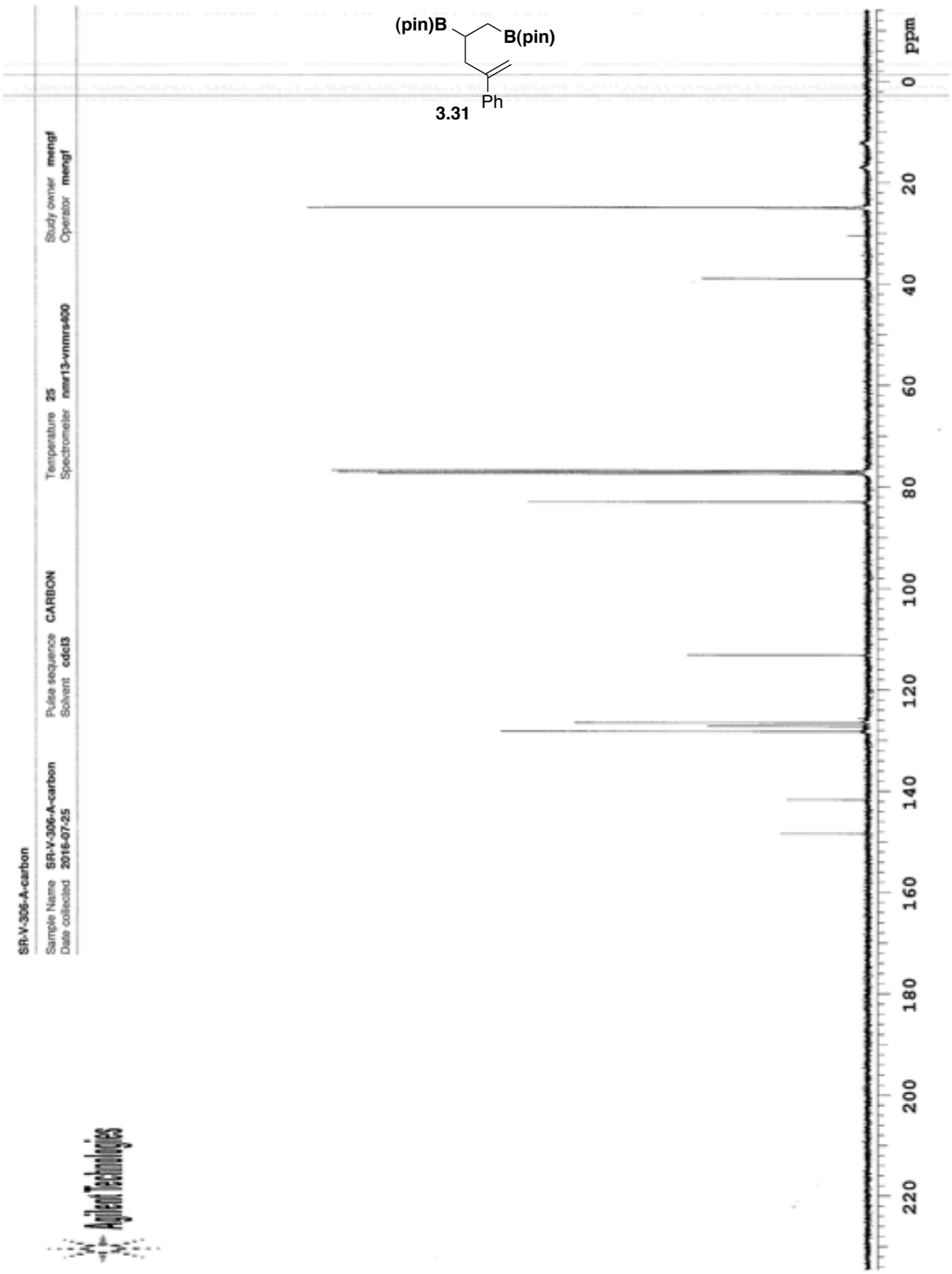
SR-V-306-A-carbon
Sample Name SR-V-306-A-carbon
Date collected 2016-07-25
Pulse sequence CARBON
Solvent cdcl3
Temperature 25
Spectrometer nmr13-vnmrs400
Study owner mengf
Operator mengf
(pin)B
B(pin)
Ph
3.31
ppm
0
20
40
60
80
100
120
140
160
180
200
220

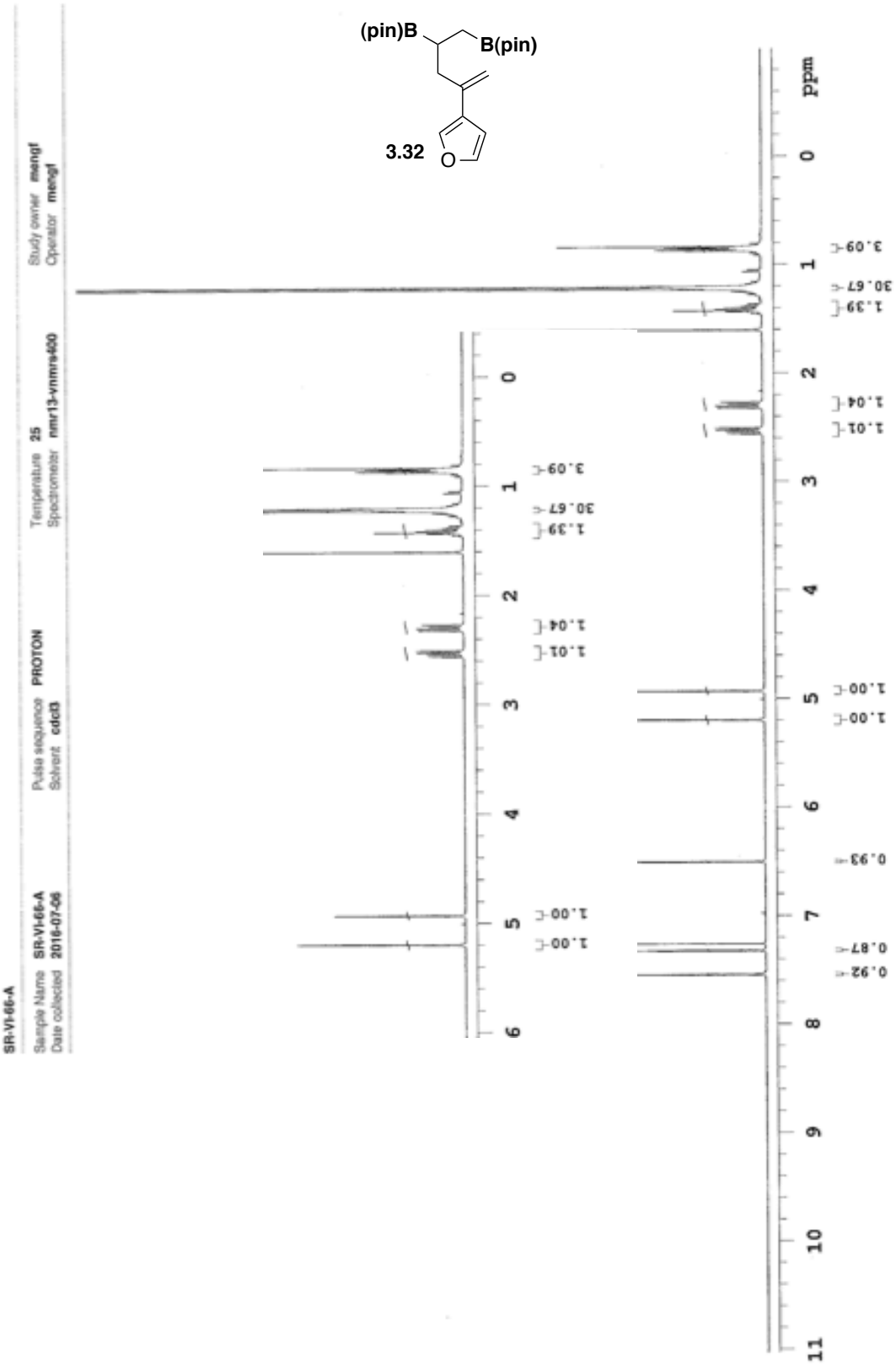
(pin)B
B(pin)
3.32
O
SR-VI-66-A
Sample Name SR-VI-66-A
Date collected 2016-07-06
Pulse sequence PROTON
Solvent cdcl3
Temperature 25
Spectrometer nmr13-vnmrs400
Study owner mengf
Operator mengf
3.09
30.67
1.39
1.04
1.01
1.00
1.00
0.93
0.87
0.92
ppm

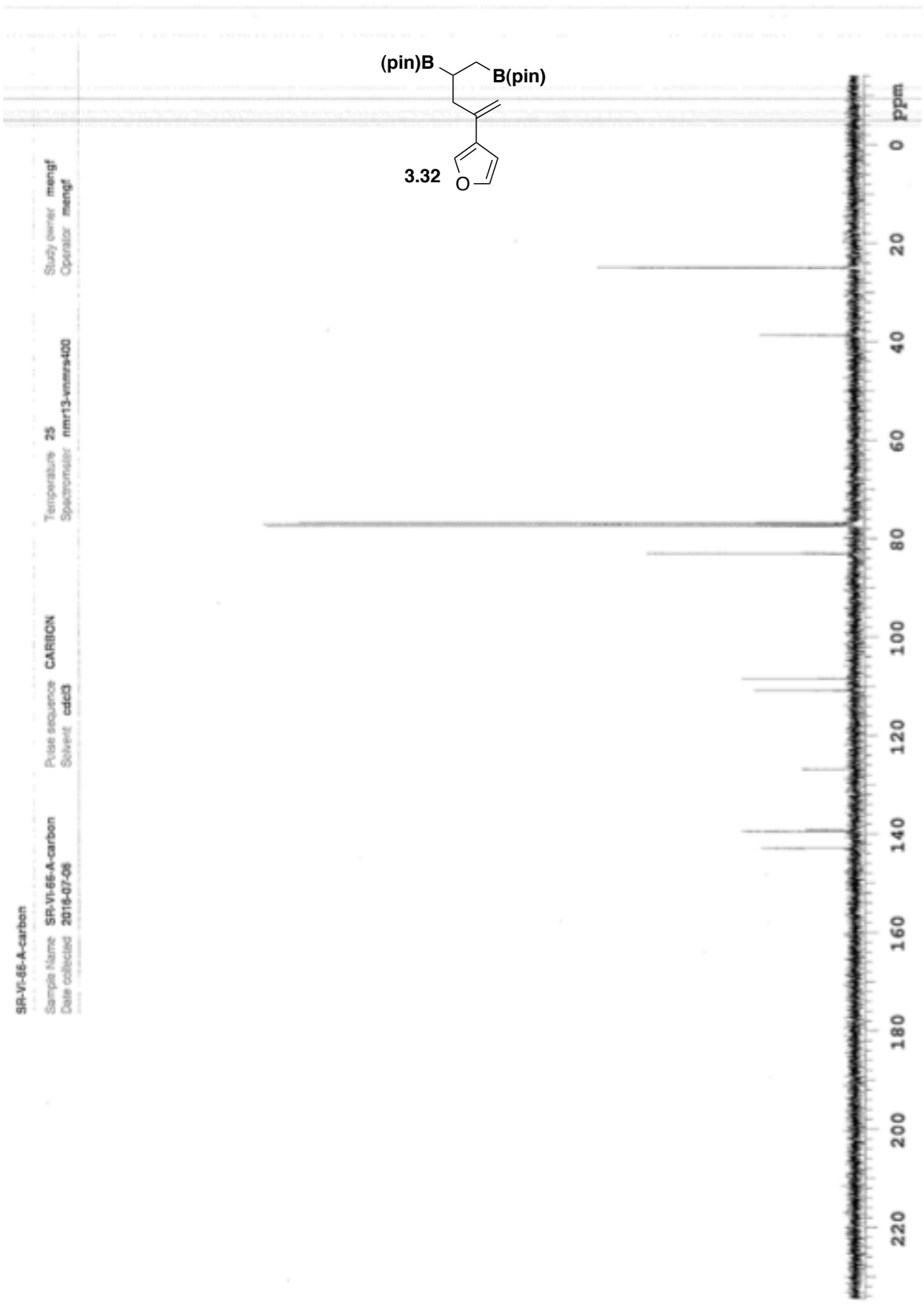
(pin)B
B(pin)
3.32
O
SR-VI-66-A-carbon
Sample Name SR-VI-66-A-carbon
Date collected 2016-07-08
Pulse sequence CARBON
Solvent cdcl3
Temperature 25
Spectrometer nmr13-vnmrs400
Study owner mengf
Operator mengf
ppm
0
20
40
60
80
100
120
140
160
180
200
220

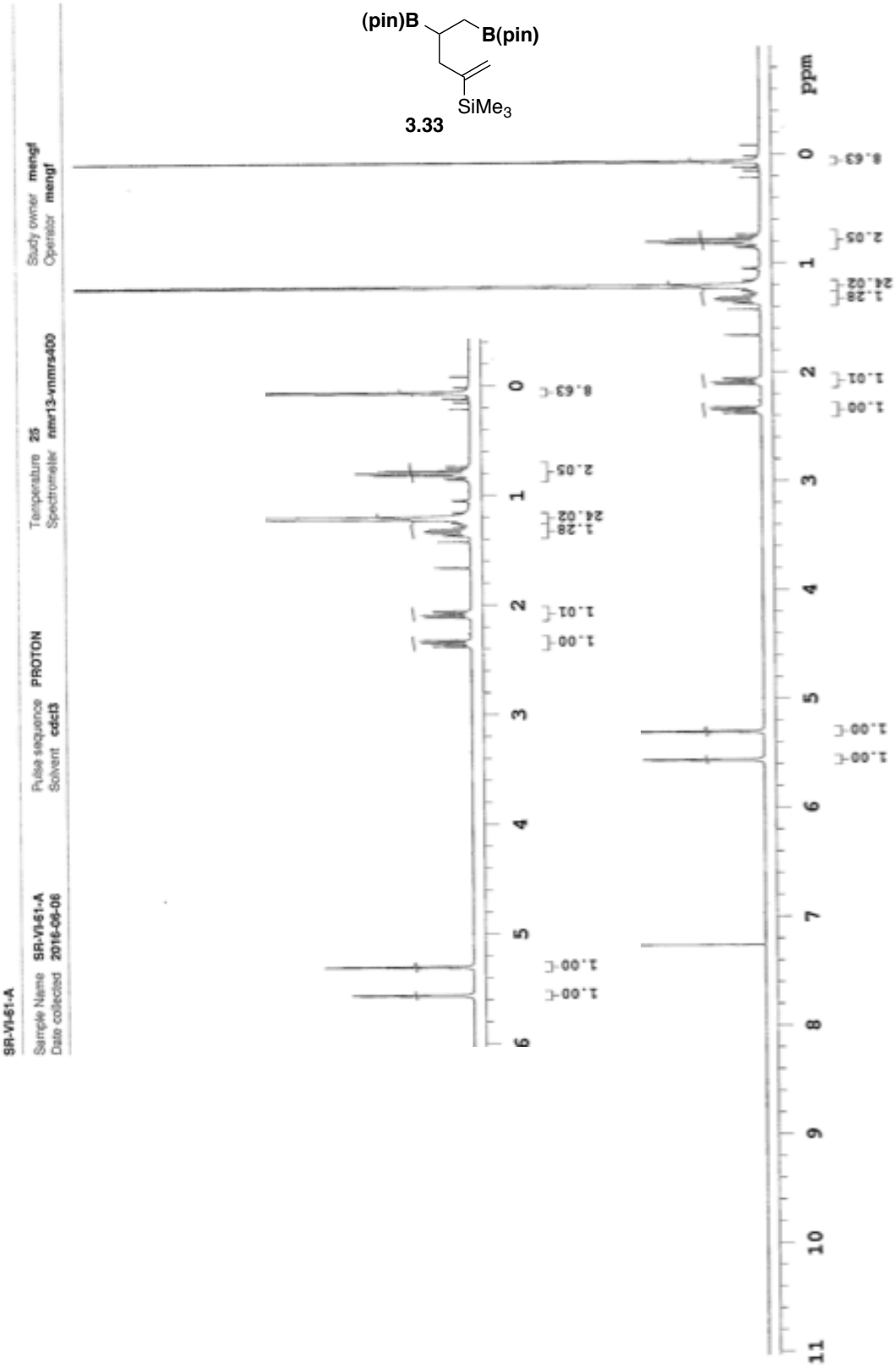
(pin)B
B(pin)
SiMe3
3.33
SR-VI-61-A
Sample Name SR-VI-61-A
Date collected 2016-06-06
Pulse sequence PROTON
Solvent cdcl3
Temperature 25
Spectrometer nmr13-vnmrs400
Study owner mengf
Operator mengf
ppm

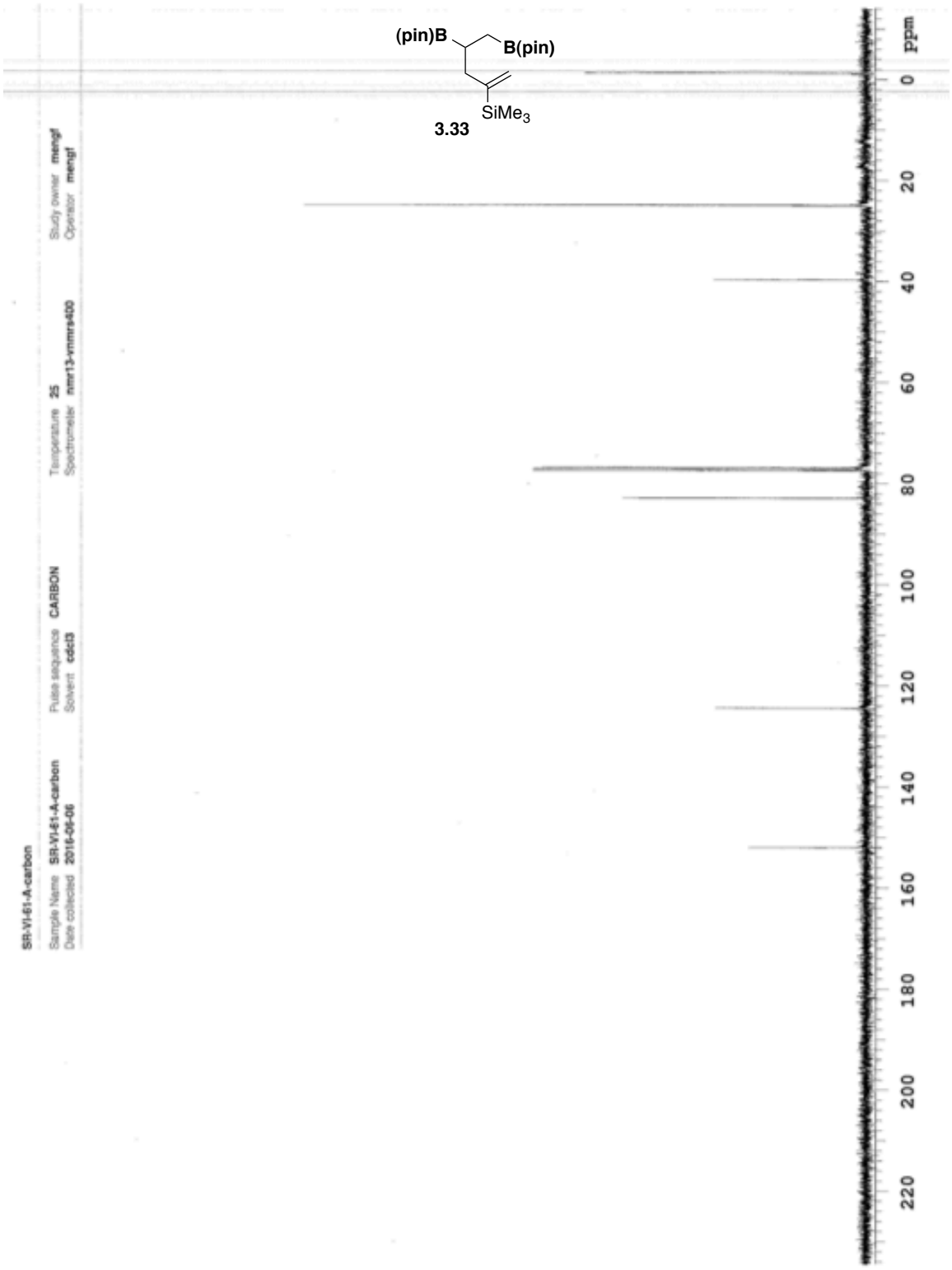
(pin)B
B(pin)
SiMe3
3.33
SR-VI-61-A-carbon
Sample Name SR-VI-61-A-carbon
Date collected 2016-06-06
Pulse sequence CARBON
Solvent cdcl3
Temperature 25
Spectrometer nmr13-vmrs400
Study owner mengf
Operator mengf
ppm
0
20
40
60
80
100
120
140
160
180
200
220

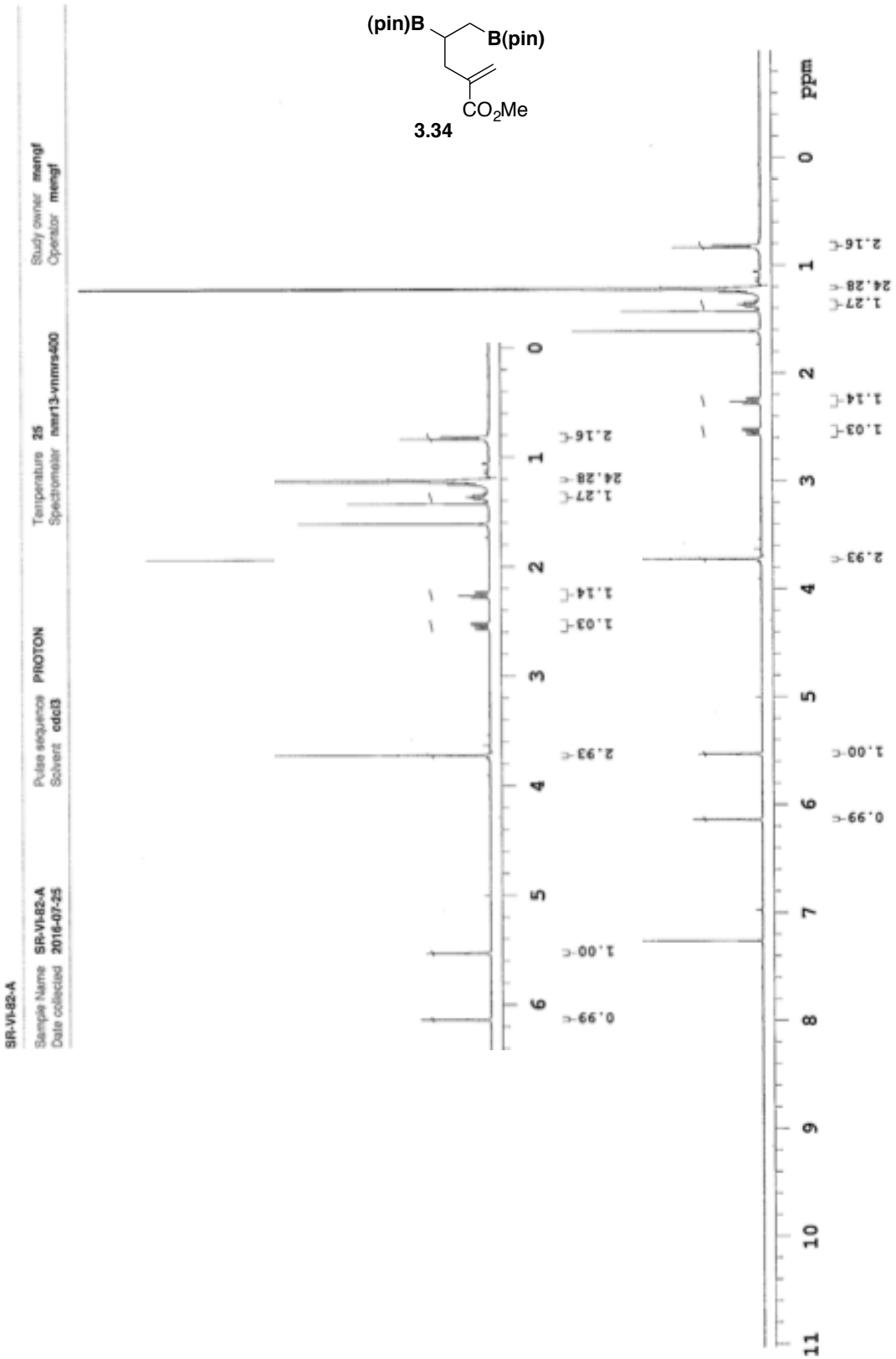
(pin)B
B(pin)
CO2Me
3.34
SR-VI-82-A
Sample Name SR-VI-82-A
Date collected 2016-07-25
Pulse sequence PROTON
Solvent cdcl3
Temperature 25
Spectrometer nmr13-vnmrs400
Study owner mengf
Operator mengf
2.16
24.28
1.27
1.14
1.03
2.93
1.00
0.99
ppm

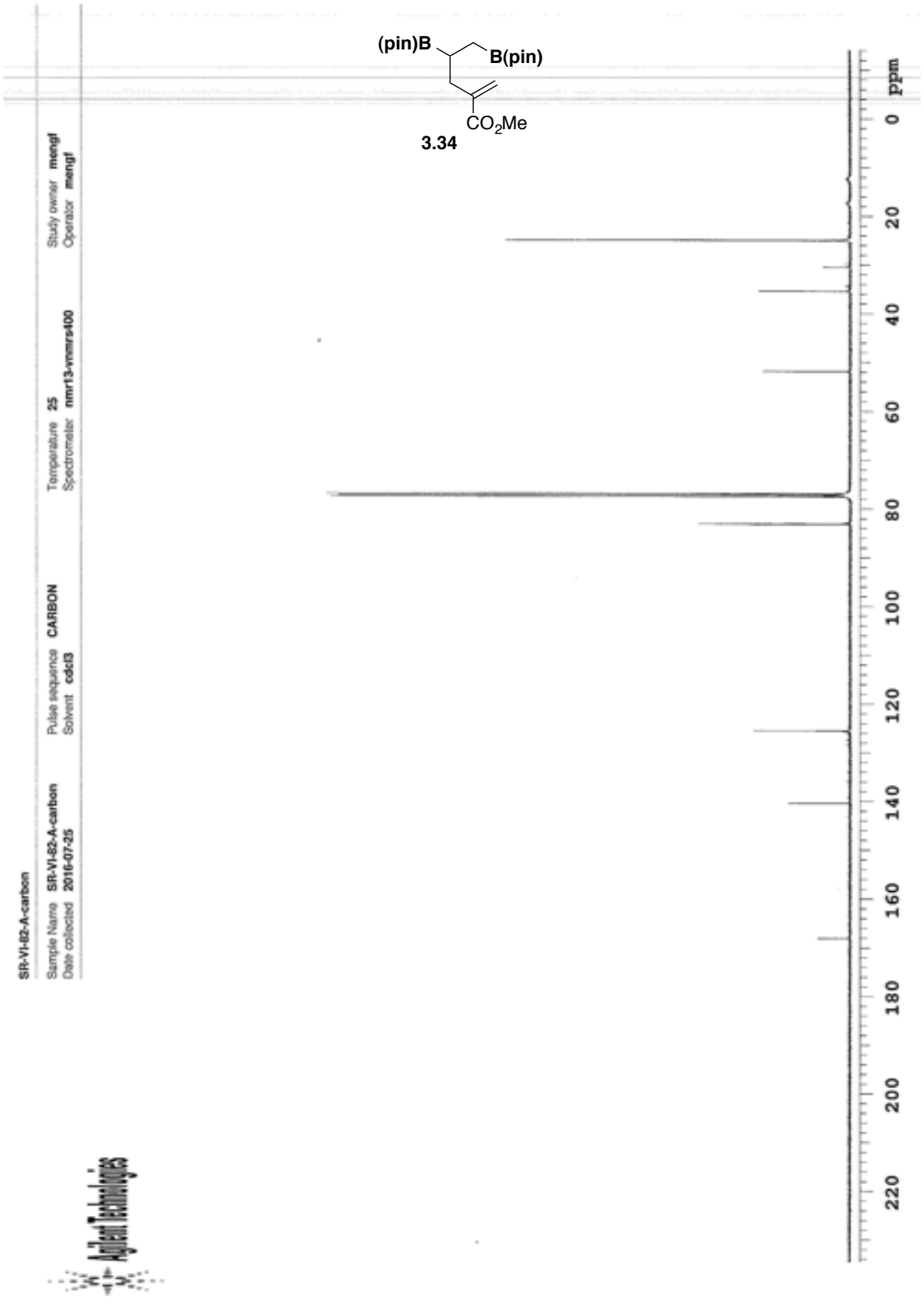
SR-VI-82-A-carbon
Sample Name SR-VI-82-A-carbon
Date collected 2016-07-25
Pulse sequence CARBON
Solvent cdcl3
Temperature 25
Spectrometer nmr13-vnmrs400
Study owner mengf
Operator mengf
(pin)B
B(pin)
CO2Me
3.34
ppm
0
20
40
60
80
100
120
140
160
180
200
220
Agilent Technologies

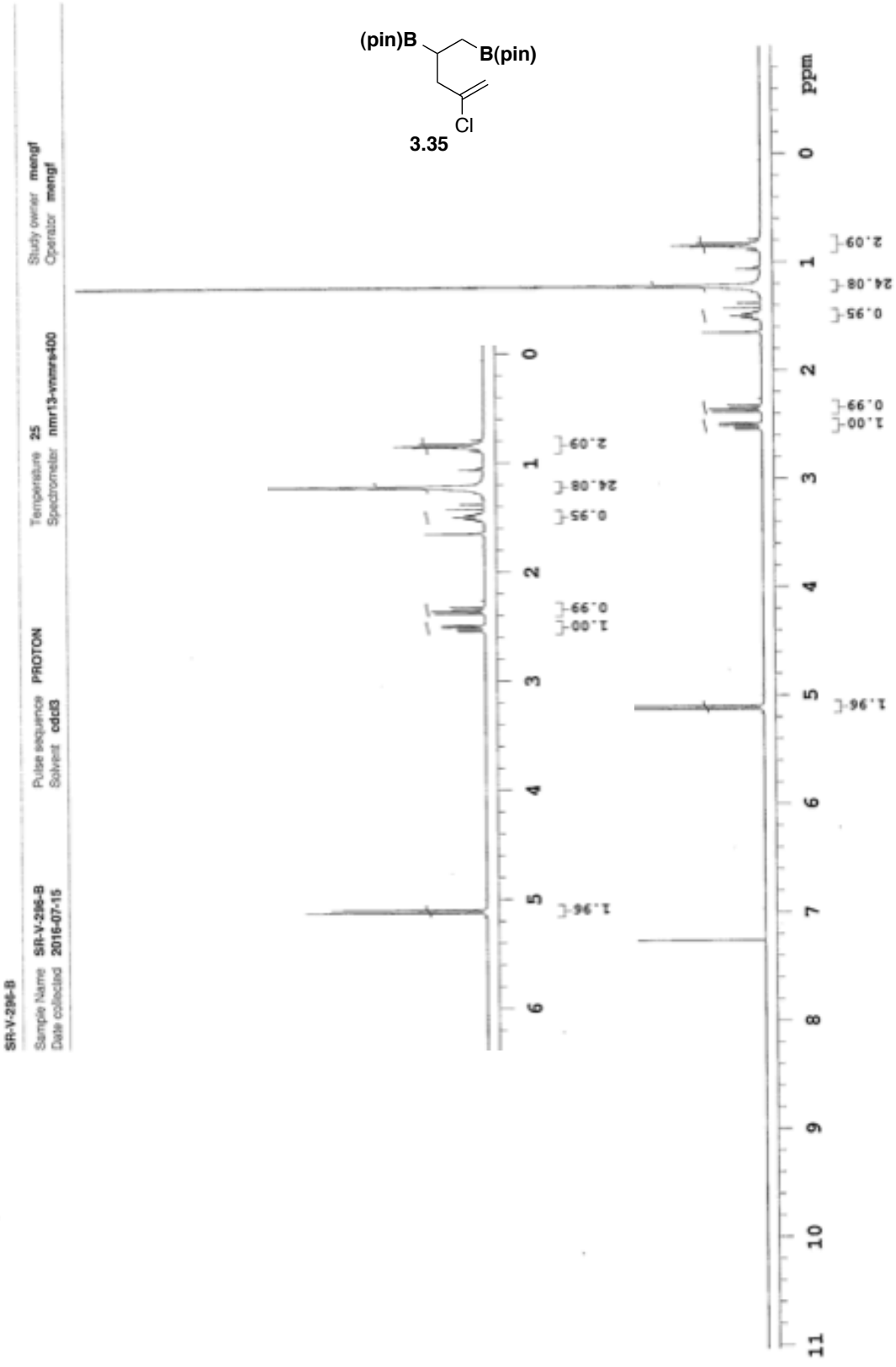
(pin)B
B(pin)
Cl
3.35
SR-V-296-B
Sample Name SR-V-296-B
Date collected 2016-07-15
Pulse sequence PROTON
Solvent cdcl3
Temperature 25
Spectrometer nmr13-vnmrs400
Study owner mengf
Operator mengf
2.09
24.08
0.95
1.00
0.99
1.96
ppm

SR-V-296-B-carbon
Sample Name SR-V-296-B-carbon
Date collected 2016-07-15
Pulse sequence CARBON
Solvent cdcl3
Temperature 25
Spectrometer nmr13-vnmrs400
Study owner mengf
Operator mengf
(pin)B
B(pin)
Cl
3.35
ppm
0
20
40
60
80
100
120
140
160
180
200
220

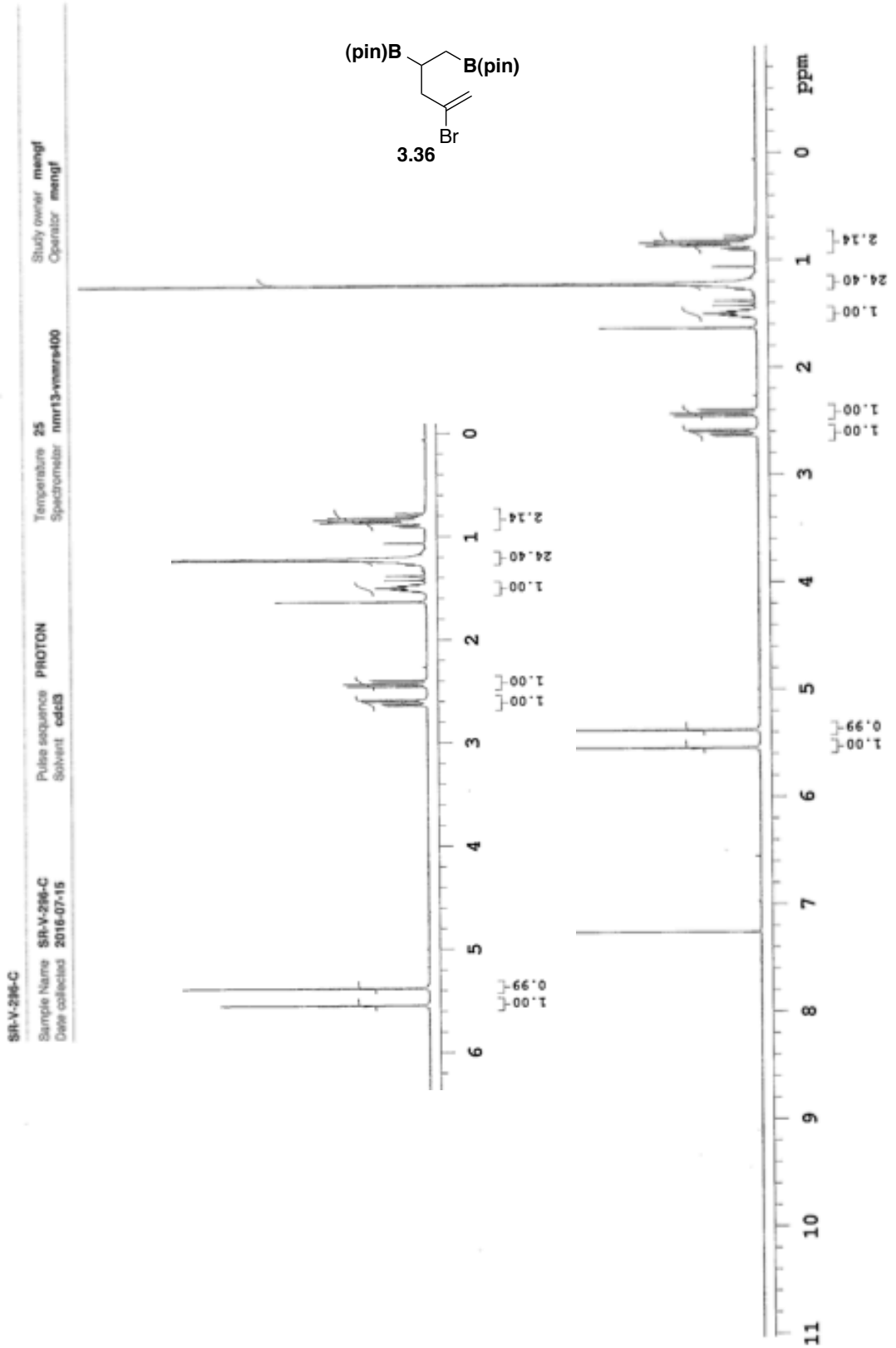
(pin)B
B(pin)
Br
3.36
SR-V-286-C
Sample Name SR-V-286-C
Date collected 2016-07-15
Pulse sequence PROTON
Solvent cdcl3
Temperature 25
Spectrometer nmr13-vnmrs400
Study owner mengf
Operator mengf
ppm
2.34
24.40
1.00
1.00
1.00
1.00
0.99
1.00

SR-V-296-C-carbon
Sample Name SR-V-296-C-carbon
Date collected 2016-07-15
Pulse sequence CARBON
Solvent cdcl3
Temperature 25
Spectrometer nmr13-vnmrs400
Study owner mengf
Operator mengf
(pin)B
B(pin)
Br
3.36
ppm
0
20
40
60
80
100
120
140
160
180
200
220

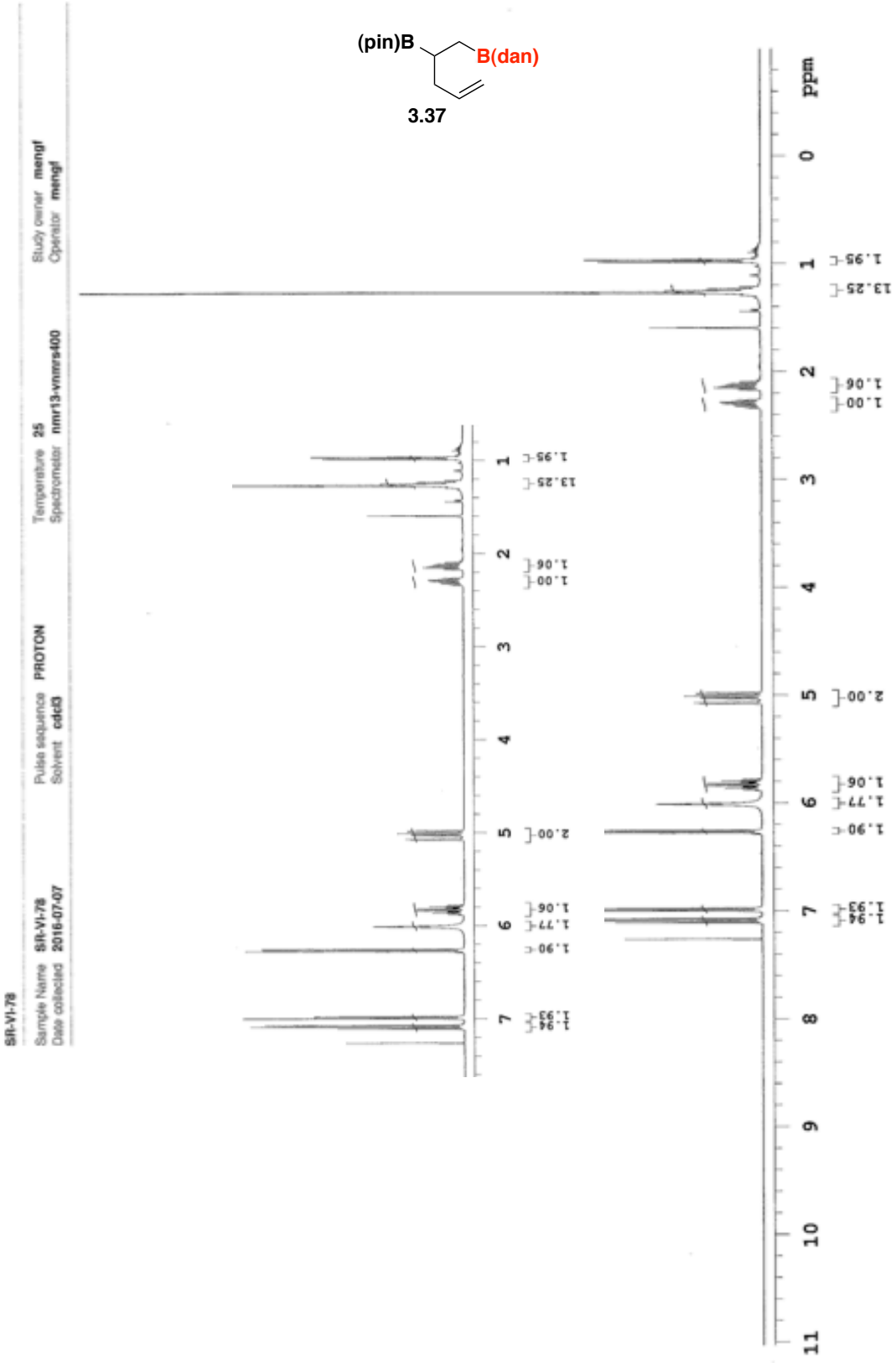
(pin)B
B(dan)
3.37
SR-VI-78
Sample Name SR-VI-78
Date collected 2016-07-07
Pulse sequence PROTON
Solvent cdcl3
Temperature 25
Spectrometer nmr13-vnmrs400
Study owner mengf
Operator mengf
ppm

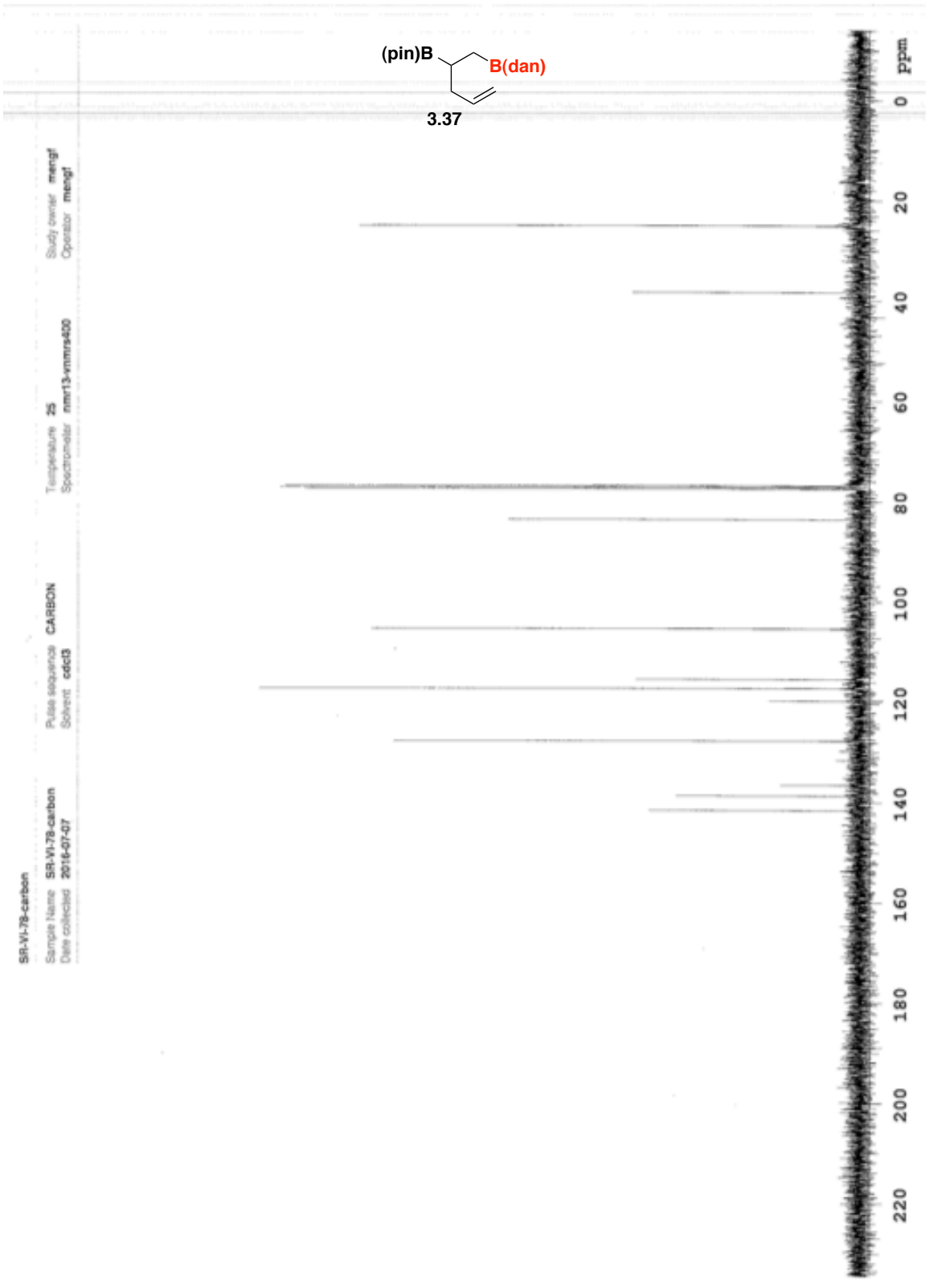
(pin)B
B(dan)
3.37
SR-VI-78-carbon
Sample Name SR-VI-78-carbon
Date collected 2016-07-07
Pulse sequence CARBON
Solvent cdcl3
Temperature 25
Spectrometer nmr13-vnmrs400
Study owner mengf
Operator mengf
ppm
0
20
40
60
80
100
120
140
160
180
200
220

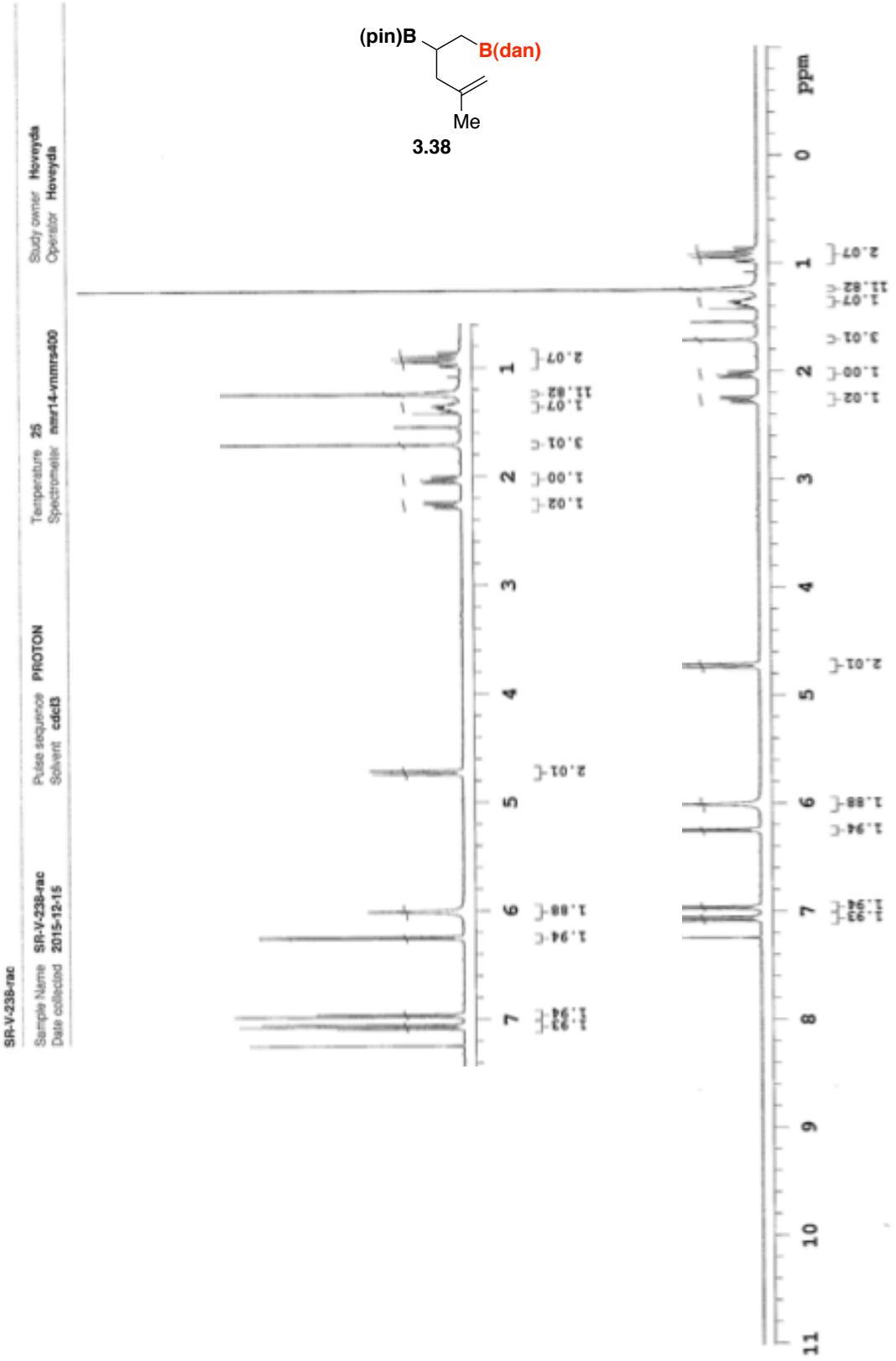
(pin)B
B(dan)
Me
3.38
SR-V-238-rac
Sample Name SR-V-238-rac
Date collected 2015-12-15
Pulse sequence PROTON
Solvent cdcl3
Temperature 25
Spectrometer nmr14-vnmrs400
Study owner Hoveyda
Operator Hoveyda
PPM
2.07
11.82
1.07
3.01
1.00
1.02
2.01
1.88
1.94

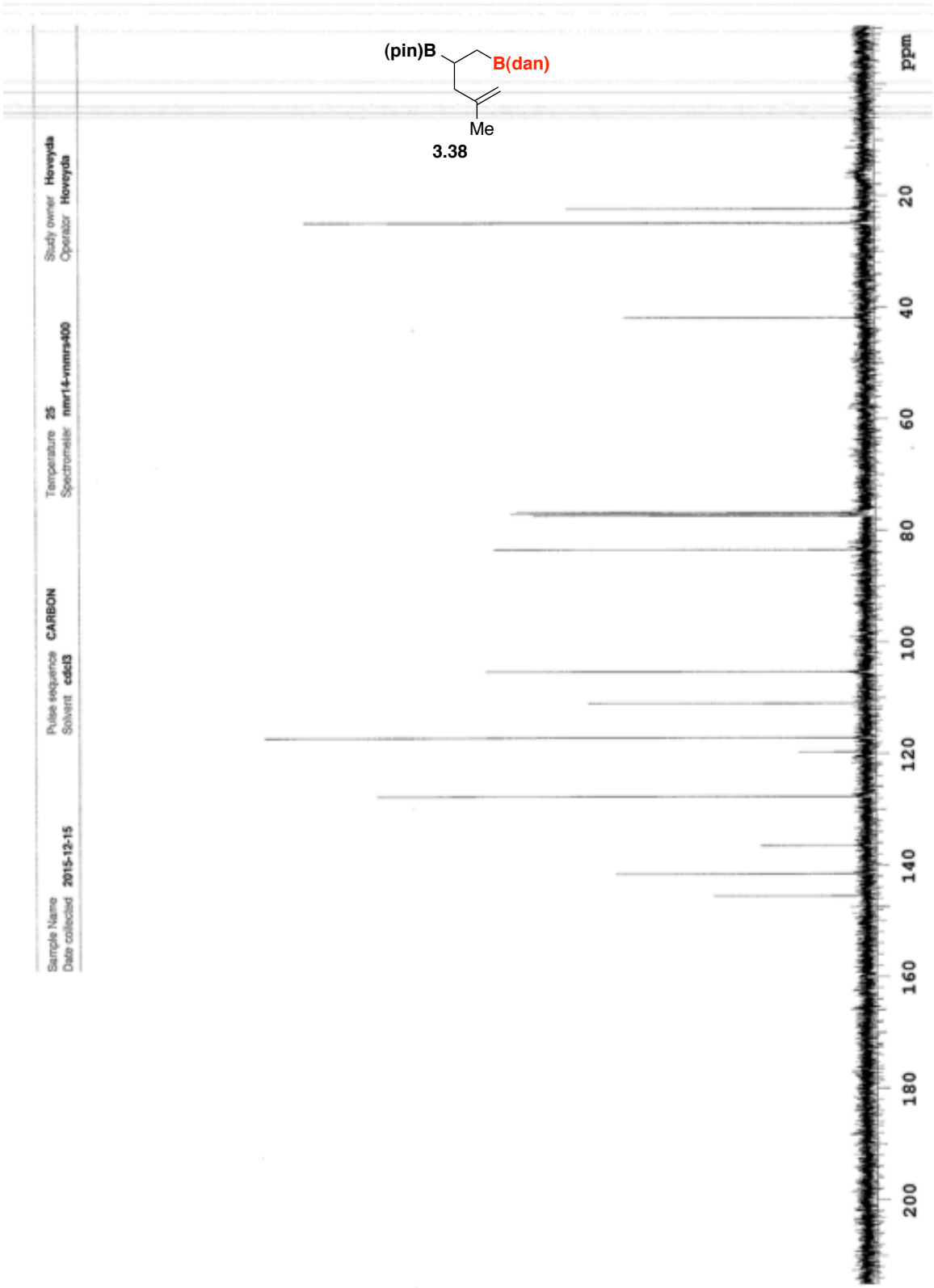
(pin)B
B(dan)
Me
3.38
Sample Name
Date collected 2015-12-15
Pulse sequence CARBON
Solvent cdcl3
Temperature 25
Spectrometer nmr14-vnmrs400
Study owner Hoveyda
Operator Hoveyda
ppm
200
180
160
140
120
100
80
60
40
20

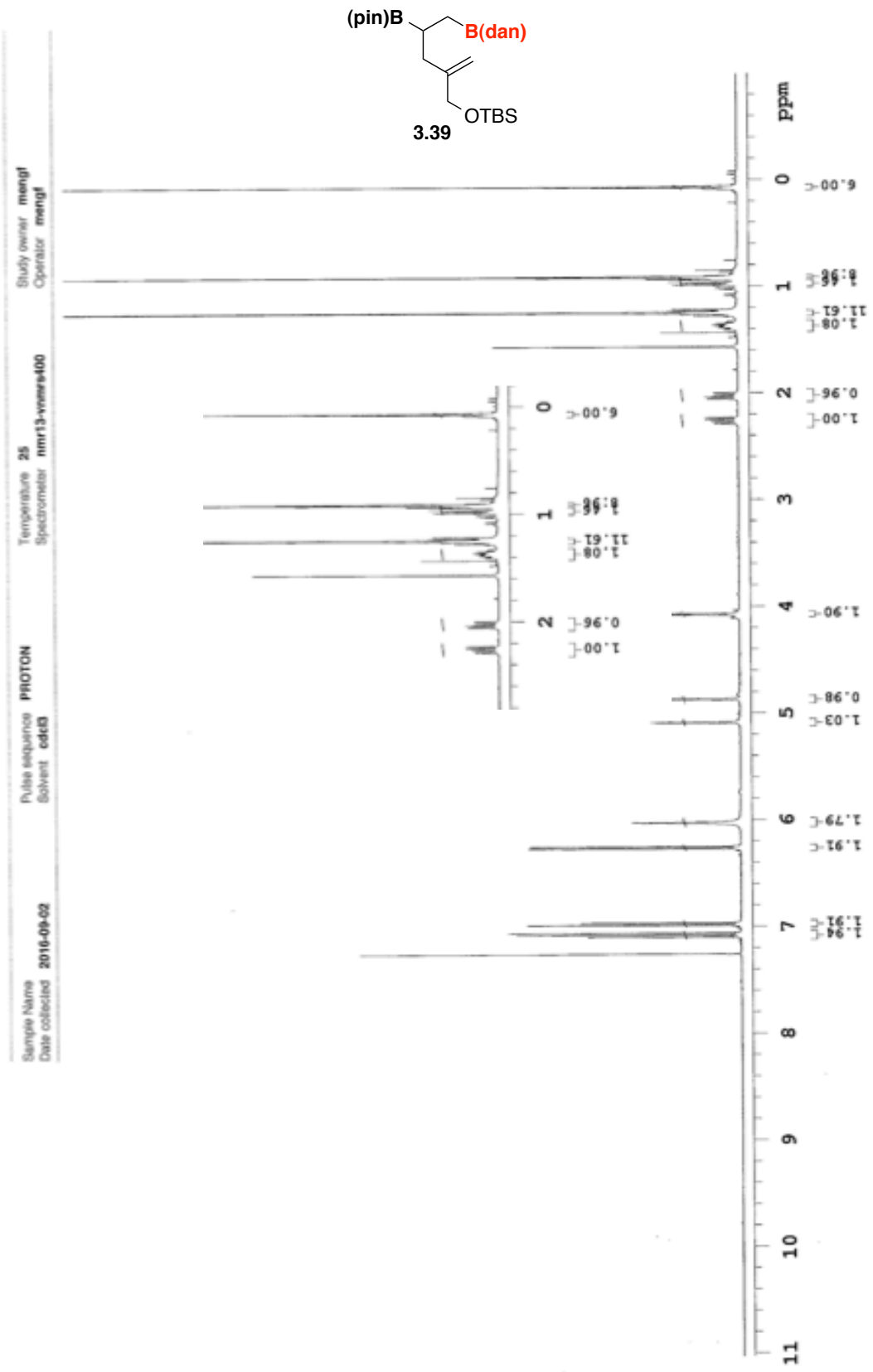
(pin)B
B(dan)
OTBS
3.39
Sample Name
Date collected 2016-09-02
Pulse sequence PROTON
Solvent cdcl3
Temperature 25
Spectrometer nmr13-vnmrs400
Study owner mengf
Operator mengf
ppm

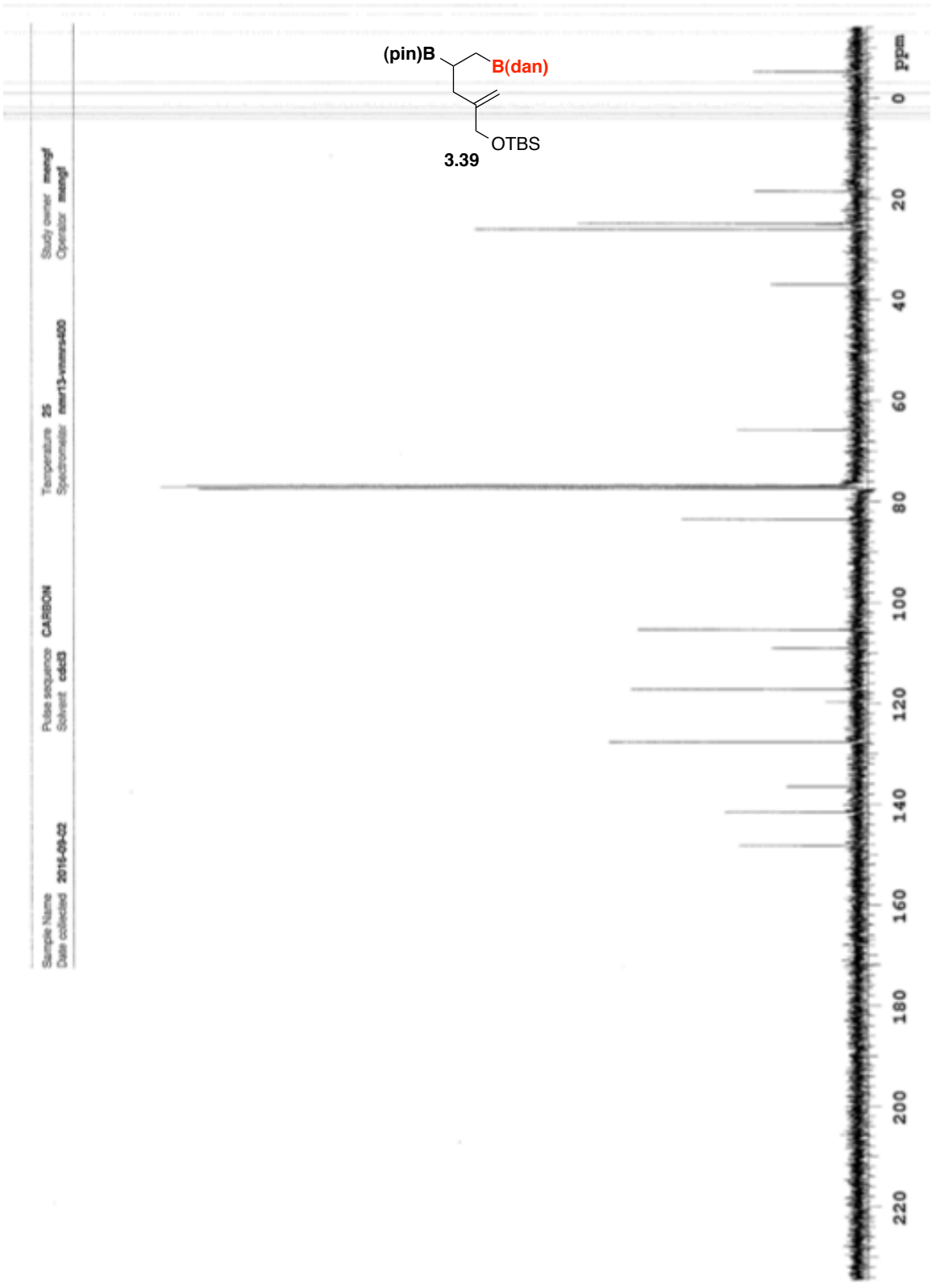
(pin)B
B(dan)
OTBS
3.39
Sample Name
Date collected 2016-09-02
Pulse sequence CARBON
Solvent cdcl3
Temperature 25
Spectrometer nmr13-vnmrs400
Study owner mengf
Operator mengf
ppm
0
20
40
60
80
100
120
140
160
180
200
220

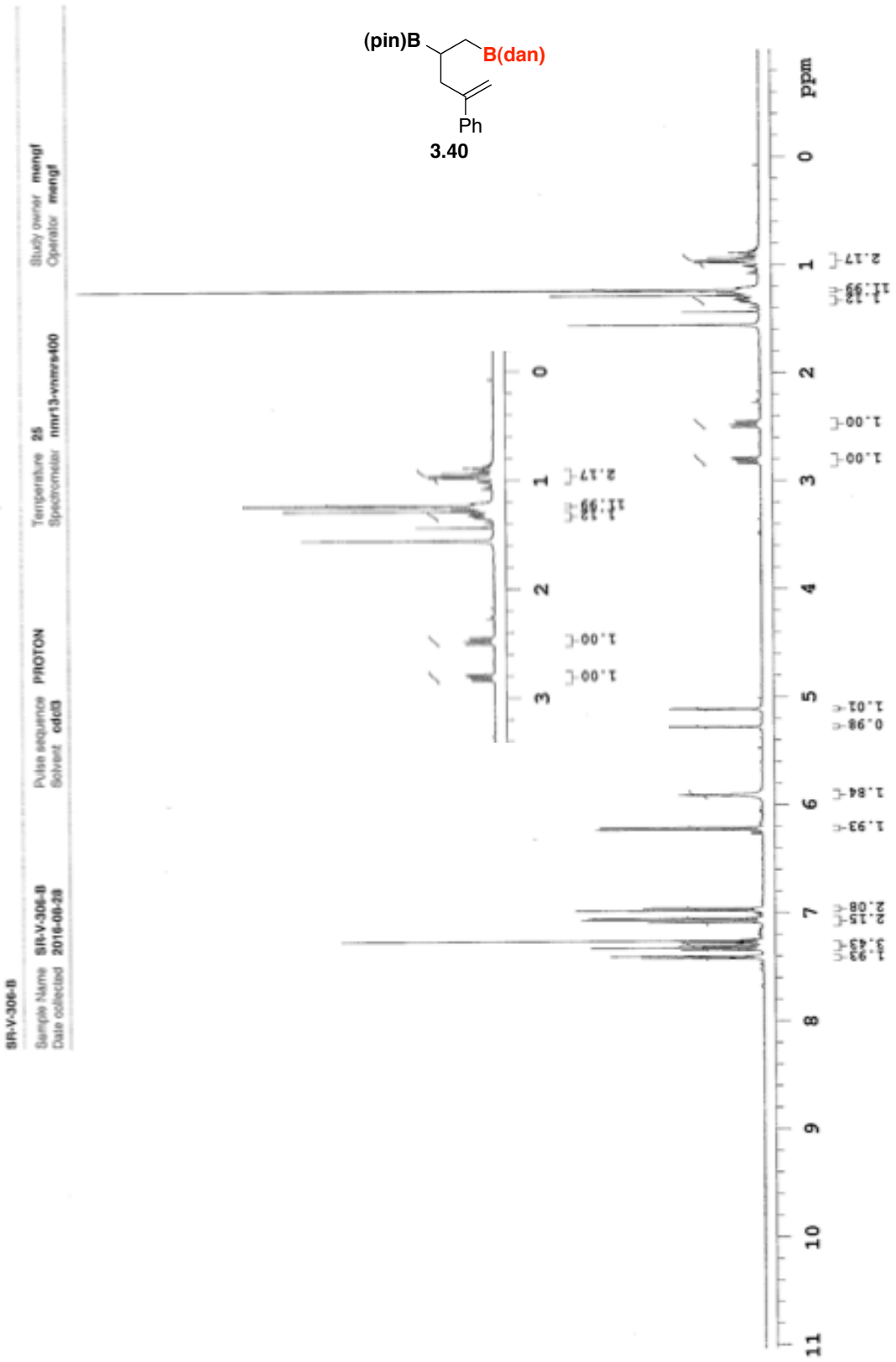
(pin)B
B(dan)
Ph
3.40
SR-V-306-B
Sample Name SR-V-306-B
Date collected 2016-08-28
Pulse sequence PROTON
Solvent cdcl3
Temperature 25
Spectrometer nmr13-vnmrs400
Study owner mengf
Operator mengf
ppm

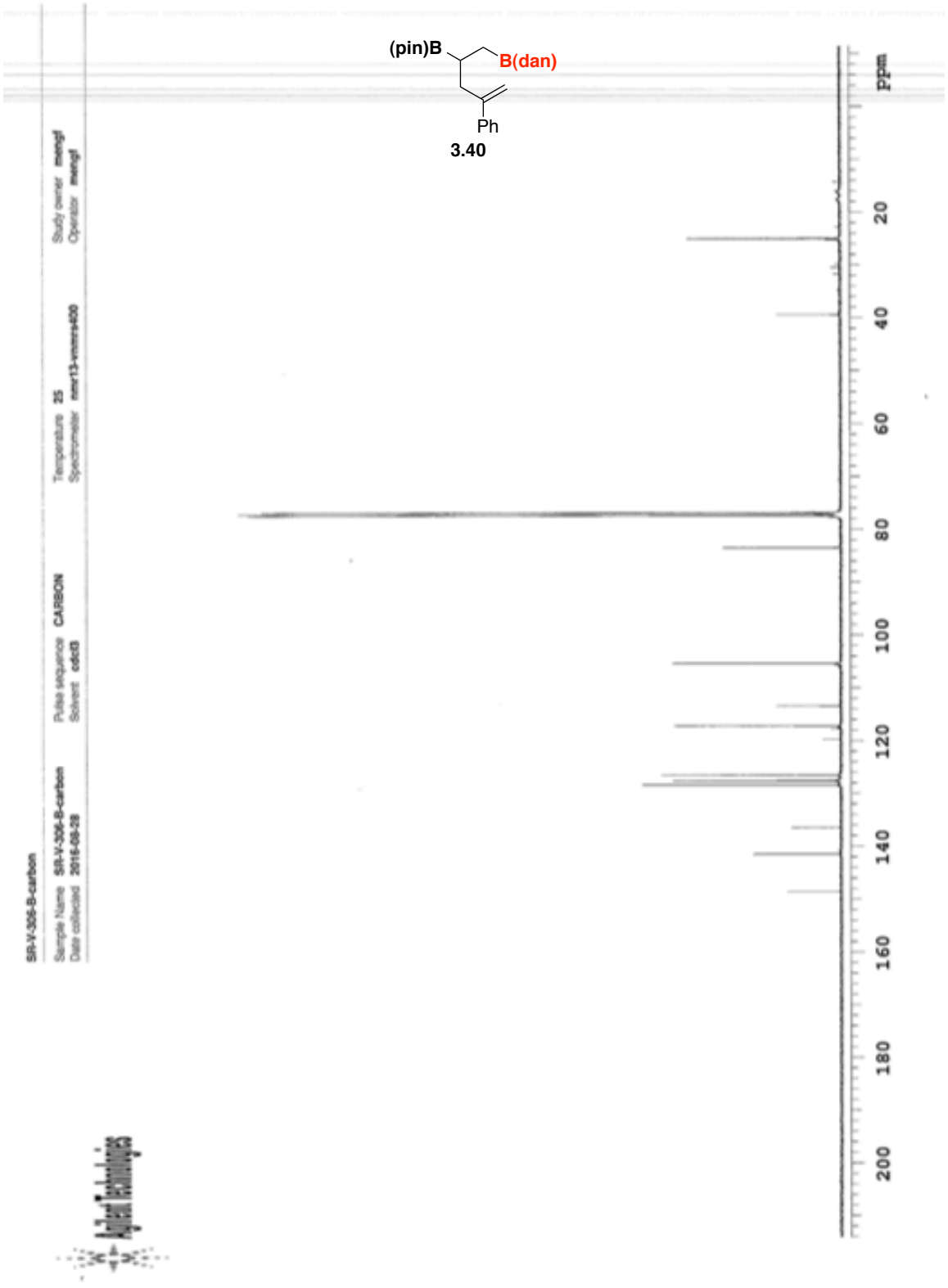
(pin)B
B(dan)
Ph
3.40
SR-V-306-B-carbon
Sample Name SR-V-306-B-carbon
Date collected 2016-08-28
Pulse sequence CARBON
Solvent cdcl3
Temperature 25
Spectrometer nmr13-vnmrs400
Study owner mengf
Operator mengf
ppm
20
40
60
80
100
120
140
160
180
200

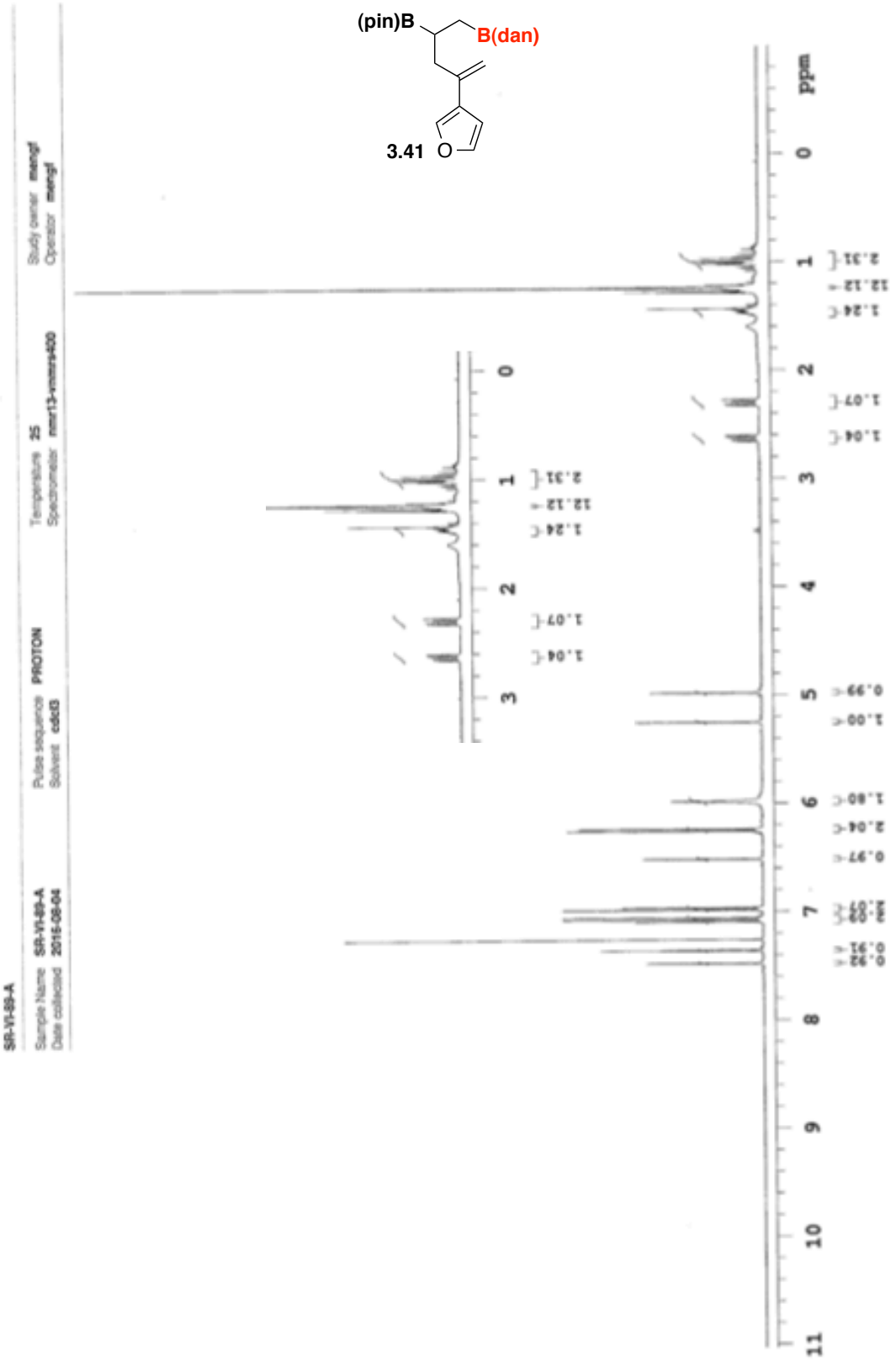
(pin)B
B(dan)
3.41
O
SR-VI-89-A
Sample Name SR-VI-89-A
Date collected 2015-06-04
Pulse sequence PROTON
Solvent cdcl3
Temperature 25
Spectrometer nmr13-vnmrs400
Study owner mengf
Operator mengf
ppm
2.31
12.12
1.24
1.07
1.04
0.99
1.00
1.80
2.04
0.97
1.09
1.09
0.92
0.91

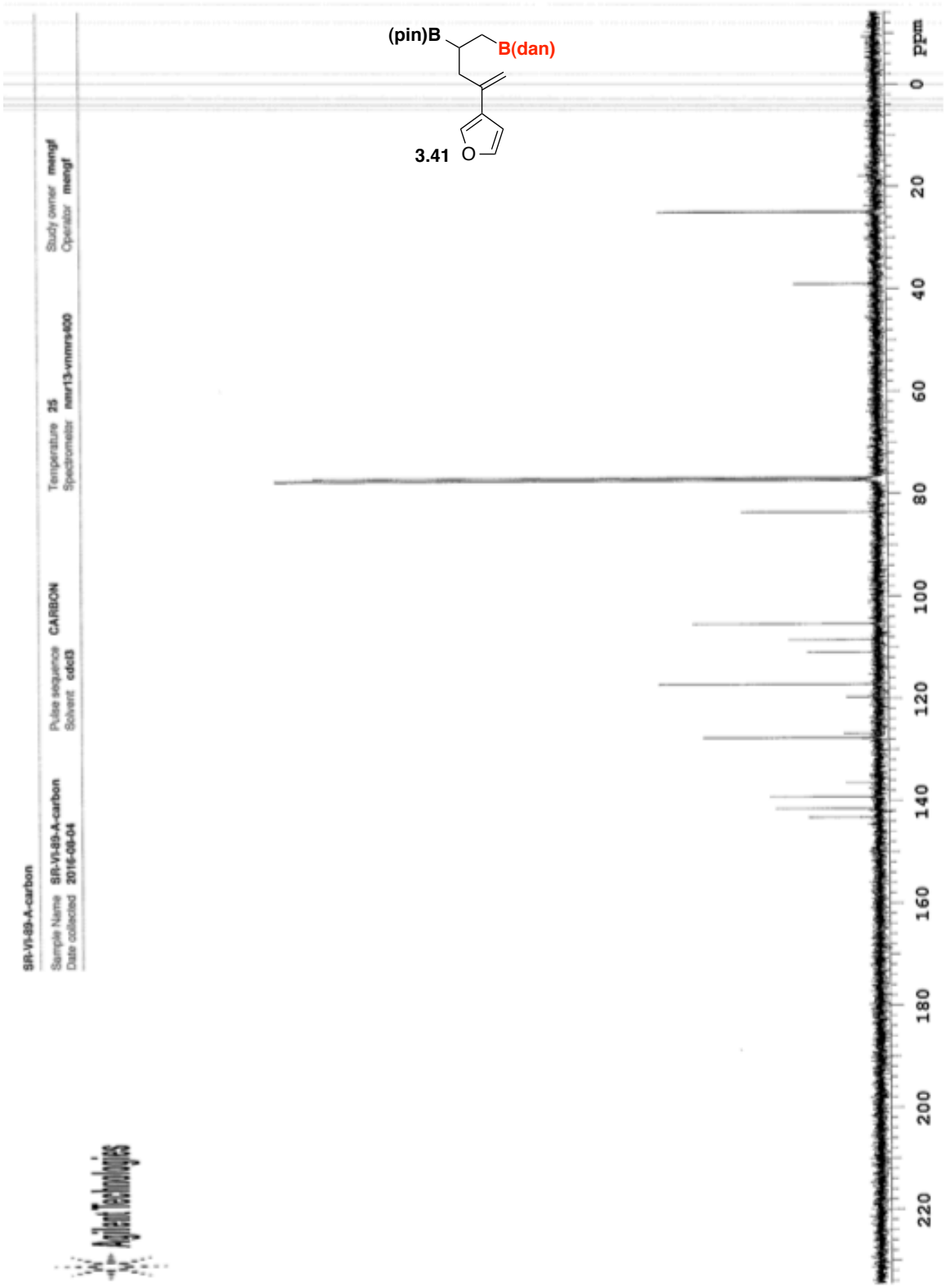
SR-VI-89-A-carbon
Sample Name SR-VI-89-A-carbon
Date collected 2016-08-04
Pulse sequence CARBON
Solvent cdcl3
Temperature 25
Spectrometer nmr13-vnmrs400
Study owner mengf
Operator mengf
(pin)B
B(dan)
3.41
O
ppm
0
20
40
60
80
100
120
140
160
180
200
220

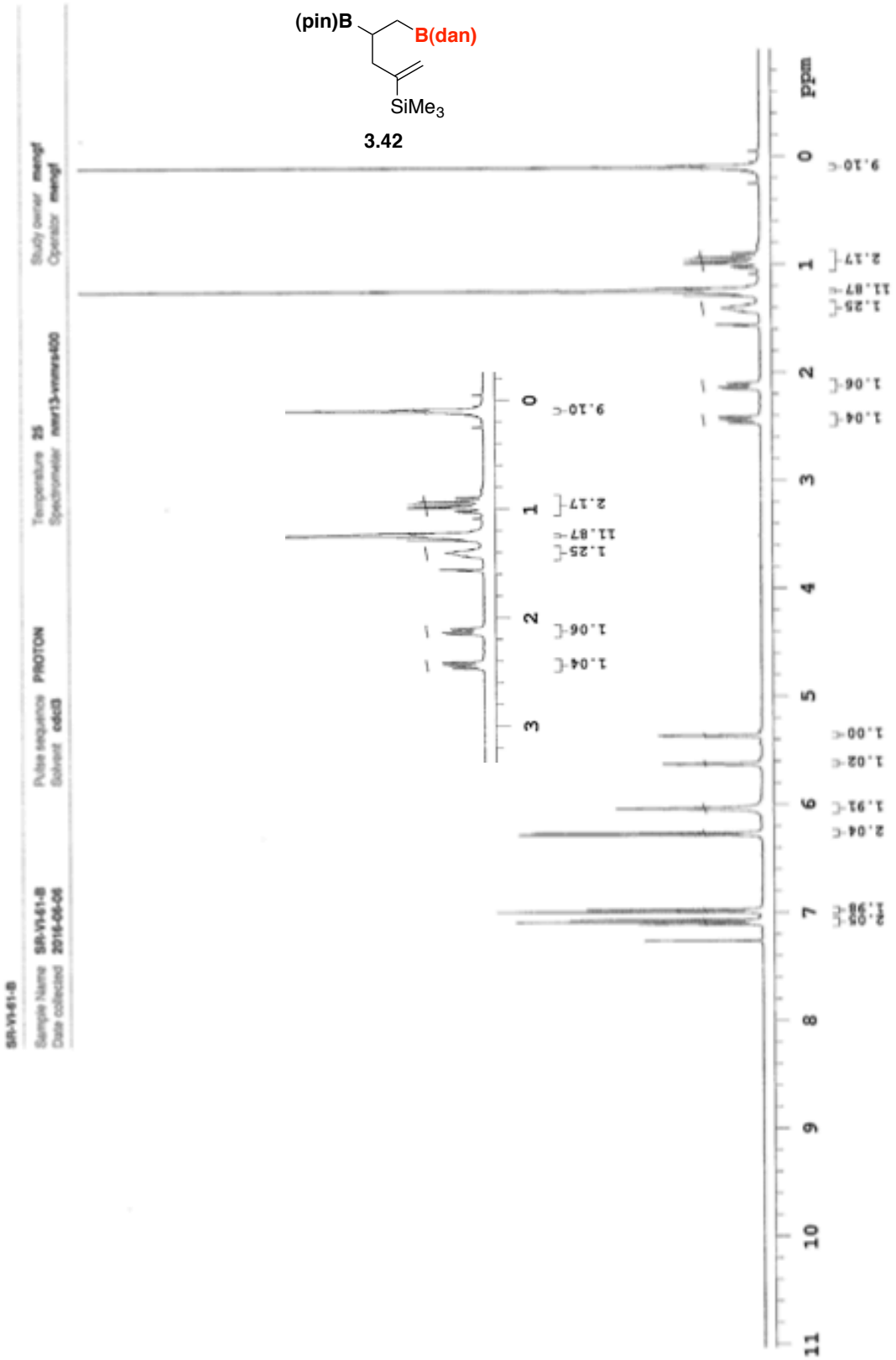
(pin)B
B(dan)
SiMe3
3.42
SR-V1-61-B
Sample Name SR-V1-61-B
Date collected 2016-06-06
Pulse sequence PROTON
Solvent cdcl3
Temperature 25
Spectrometer nmr13-vnmrs400
Study owner mengf
Operator mengf
ppm
9.10
2.17
11.87
1.25
1.06
1.04
1.00
1.02
1.91
2.04
1.98
1.93

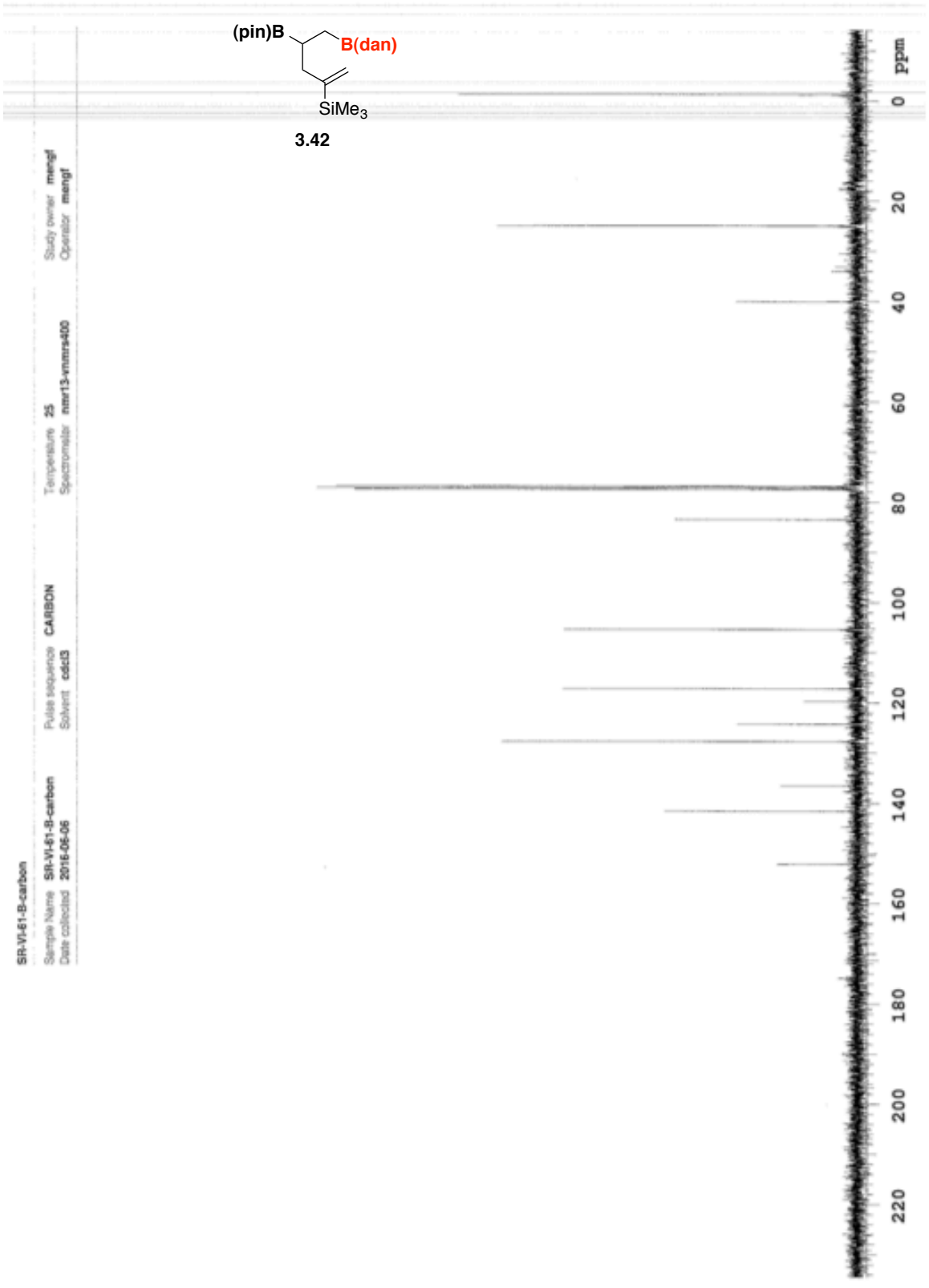
(pin)B
B(dan)
SiMe3
3.42
SR-VI-61-B-carbon
Sample Name SR-VI-61-B-carbon
Date collected 2016-06-06
Pulse sequence CARBON
Solvent cdcl3
Temperature 25
Spectrometer nmr13-vnmrs400
Study owner mengf
Operator mengf
ppm
0
20
40
60
80
100
120
140
160
180
200
220

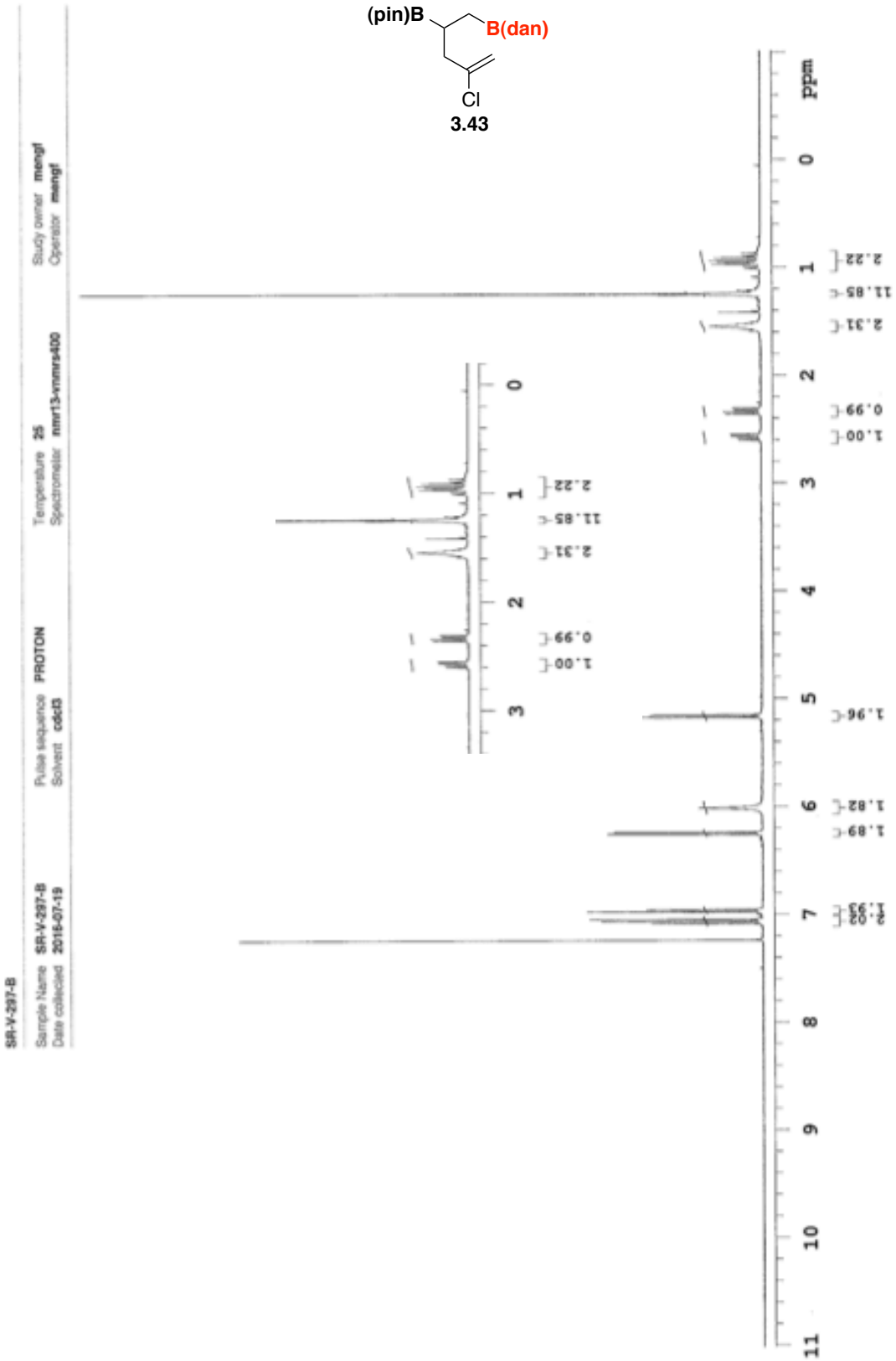
(pin)B
B(dan)
Cl
3.43
SR-V-297-B
Sample Name SR-V-297-B
Date collected 2016-07-19
Pulse sequence PROTON
Solvent cdcl3
Temperature 25
Spectrometer nmr13-vmmrs400
Study owner mengf
Operator mengf
ppm
2.22
11.85
2.31
0.99
1.00
1.96
1.82
1.89
2.02
1.93

(pin)B
B(dan)
Cl
3.43
SR-V-297-B-carbon
Sample Name SR-V-297-B-carbon
Date collected 2016-07-19
Pulse sequence CARBON
Solvent cdcl3
Temperature 25
Spectrometer nmr13-vnmrs400
Study owner mengf
Operator mengf
Agilent Technologies
ppm
0
20
40
60
80
100
120
140
160
180
200
220

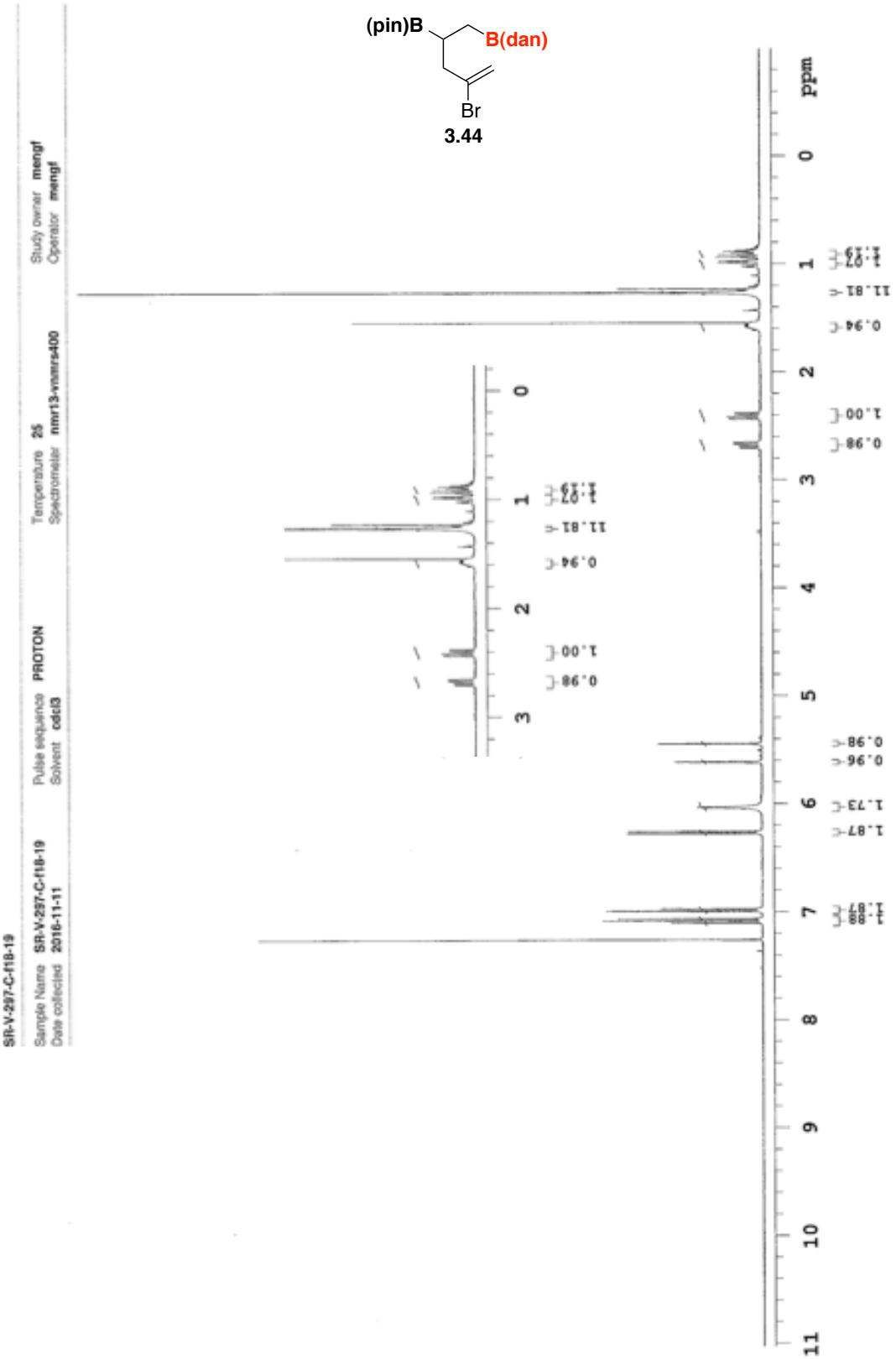
(pin)B
B(dan)
Br
3.44
SR-V-297-C-f18-19
Sample Name SR-V-297-C-f18-19
Date collected 2016-11-11
Pulse sequence PROTON
Solvent cdcl3
Temperature 25
Spectrometer nmr13-vnmrs400
Study owner mengf
Operator mengf
ppm
11.81
0.94
1.00
0.98
0.96
1.73
1.87

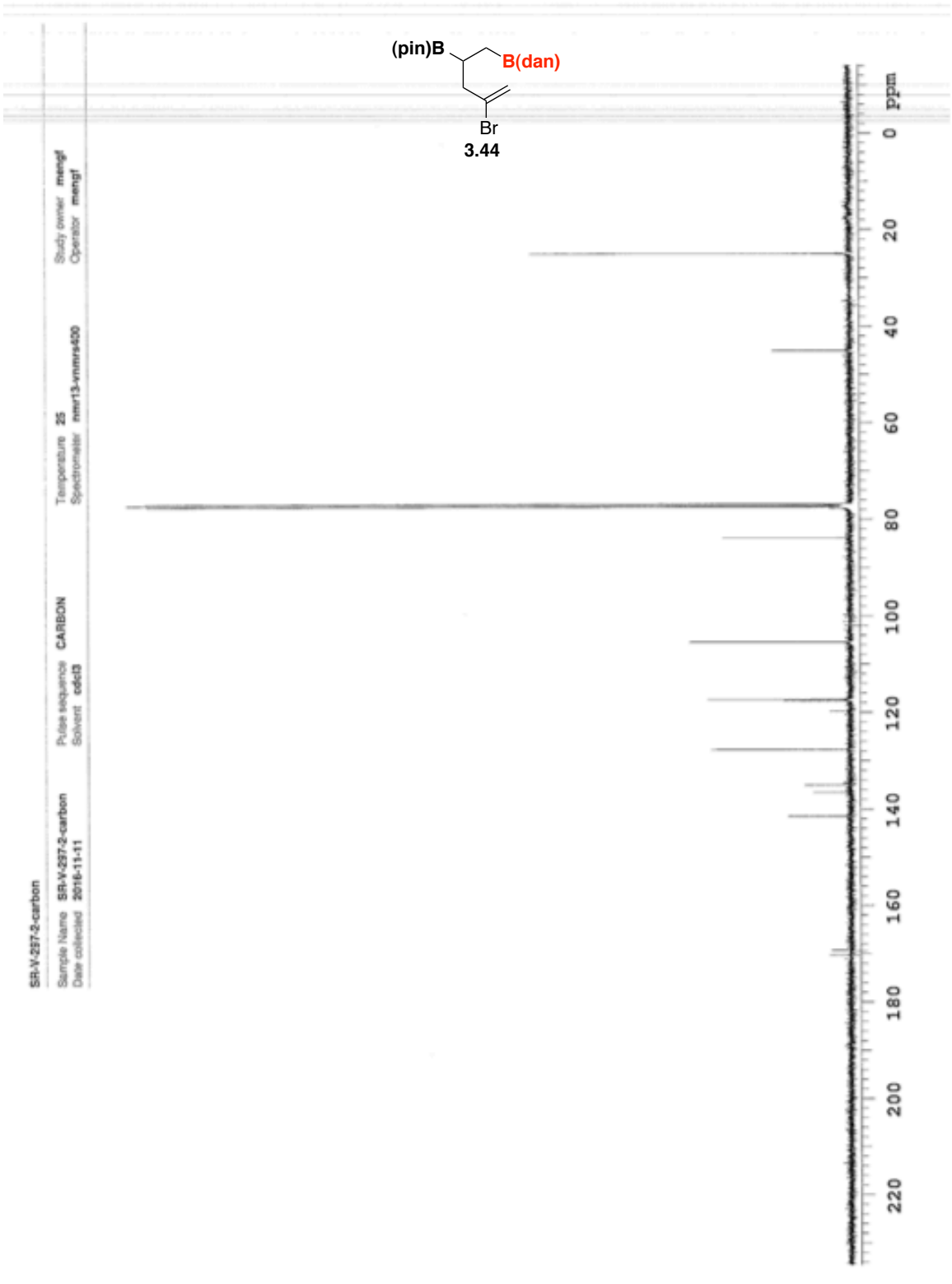
(pin)B
B(dan)
Br
3.44
SR-V-237-2-carbon
Sample Name SR-V-237-2-carbon
Date collected 2016-11-11
Pulse sequence CARBON
Solvent cdcl3
Temperature 25
Spectrometer nmr13-vnmrs400
Study owner mengf
Operator mengf
ppm
0
20
40
60
80
100
120
140
160
180
200
220

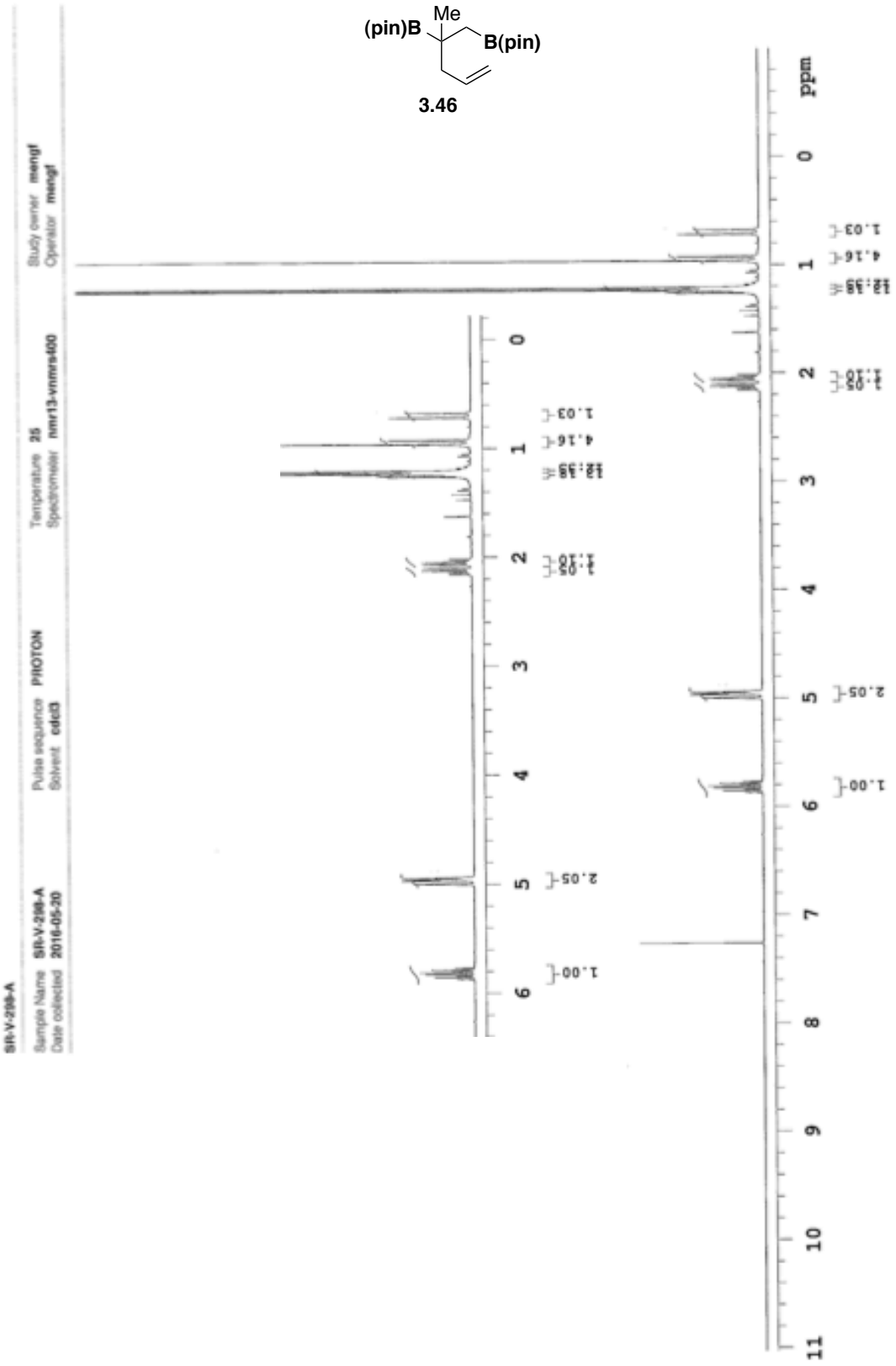
(pin)B
Me
B(pin)
3.46
SR-V-298-A
Sample Name SR-V-298-A
Date collected 2016-05-20
Pulse sequence PHOTON
Solvent cdcl3
Temperature 25
Spectrometer nmr13-vnmrs400
Study owner mengf
Operator mengf
ppm
1.03
4.16
12.38
2.05
1.00

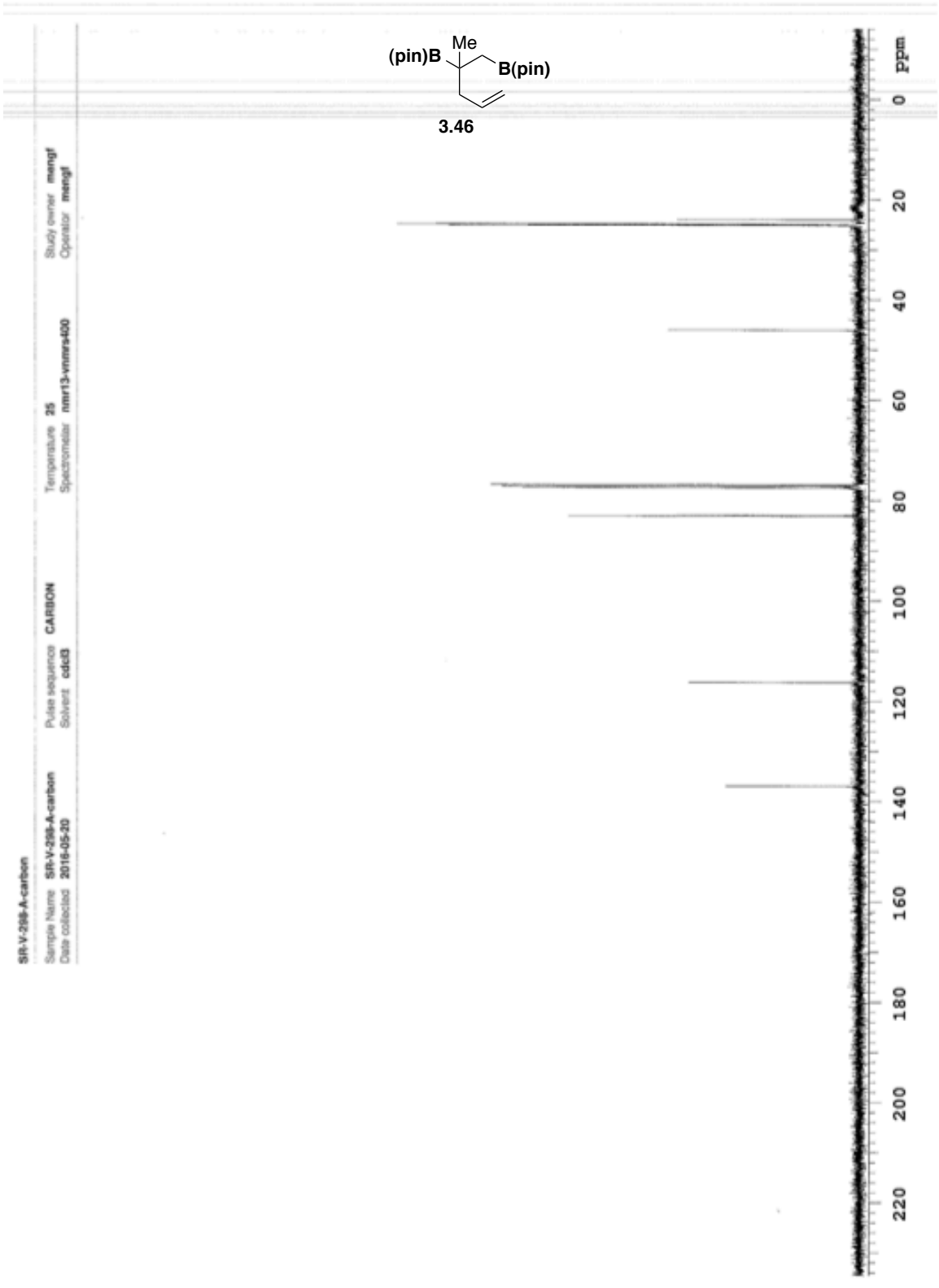
SR-V-298-A-carbon
Sample Name SR-V-298-A-carbon
Date collected 2016-05-20
Pulse sequence CARBON
Solvent cdcl3
Temperature 25
Spectrometer nmr13-vnmrs400
Study owner mangf
Operator mangf
(pin)B
Me
B(pin)
3.46
ppm
0
20
40
60
80
100
120
140
160
180
200
220

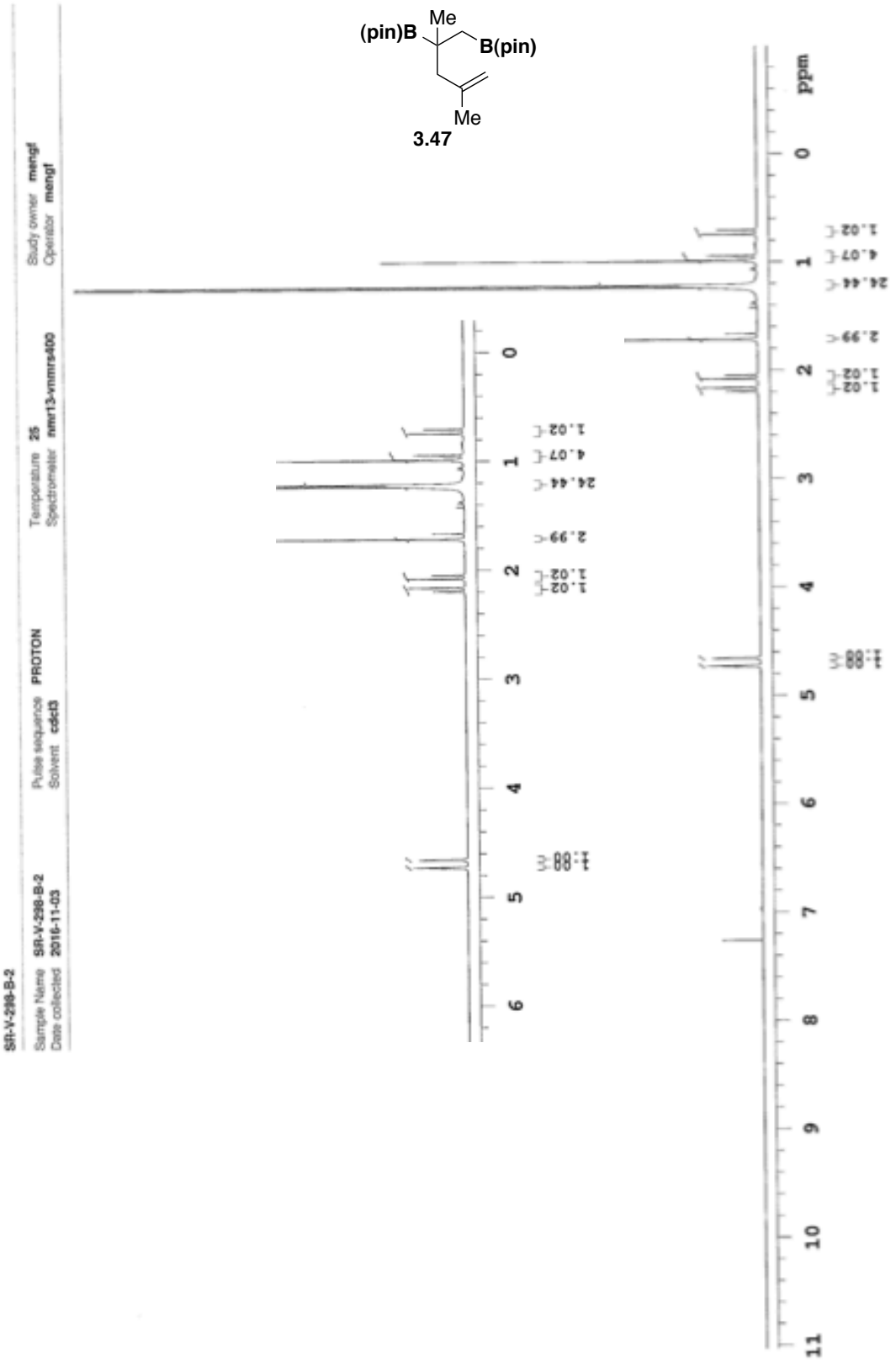
(pin)B
Me
B(pin)
Me
3.47
SR-V-298-B-2
Sample Name SR-V-298-B-2
Date collected 2016-11-03
Pulse sequence PROTON
Solvent cdcl3
Temperature 25
Spectrometer nmr13-vnmrs400
Study owner mengf
Operator mengf
1.02
4.07
24.44
2.99
1.02
1.02
4.88
4.88
ppm

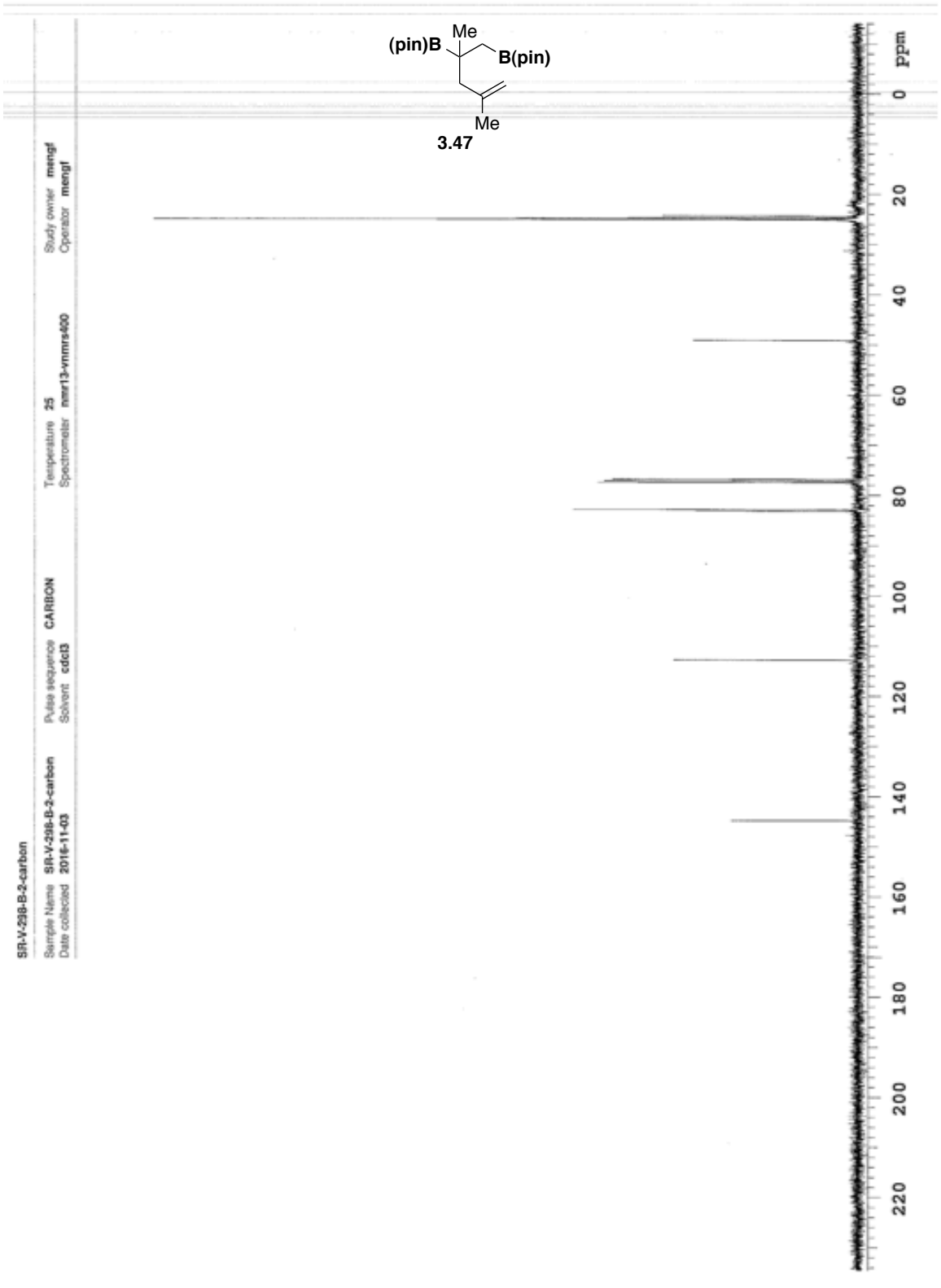
SR-V-298-B-2-carbon
Sample Name SR-V-298-B-2-carbon
Date collected 2016-11-03
Pulse sequence CARBON
Solvent cdcl3
Temperature 25
Spectrometer nmr13-vnmrs400
Study owner mengf
Operator mengf
(pin)B
Me
B(pin)
Me
3.47
ppm
0
20
40
60
80
100
120
140
160
180
200
220

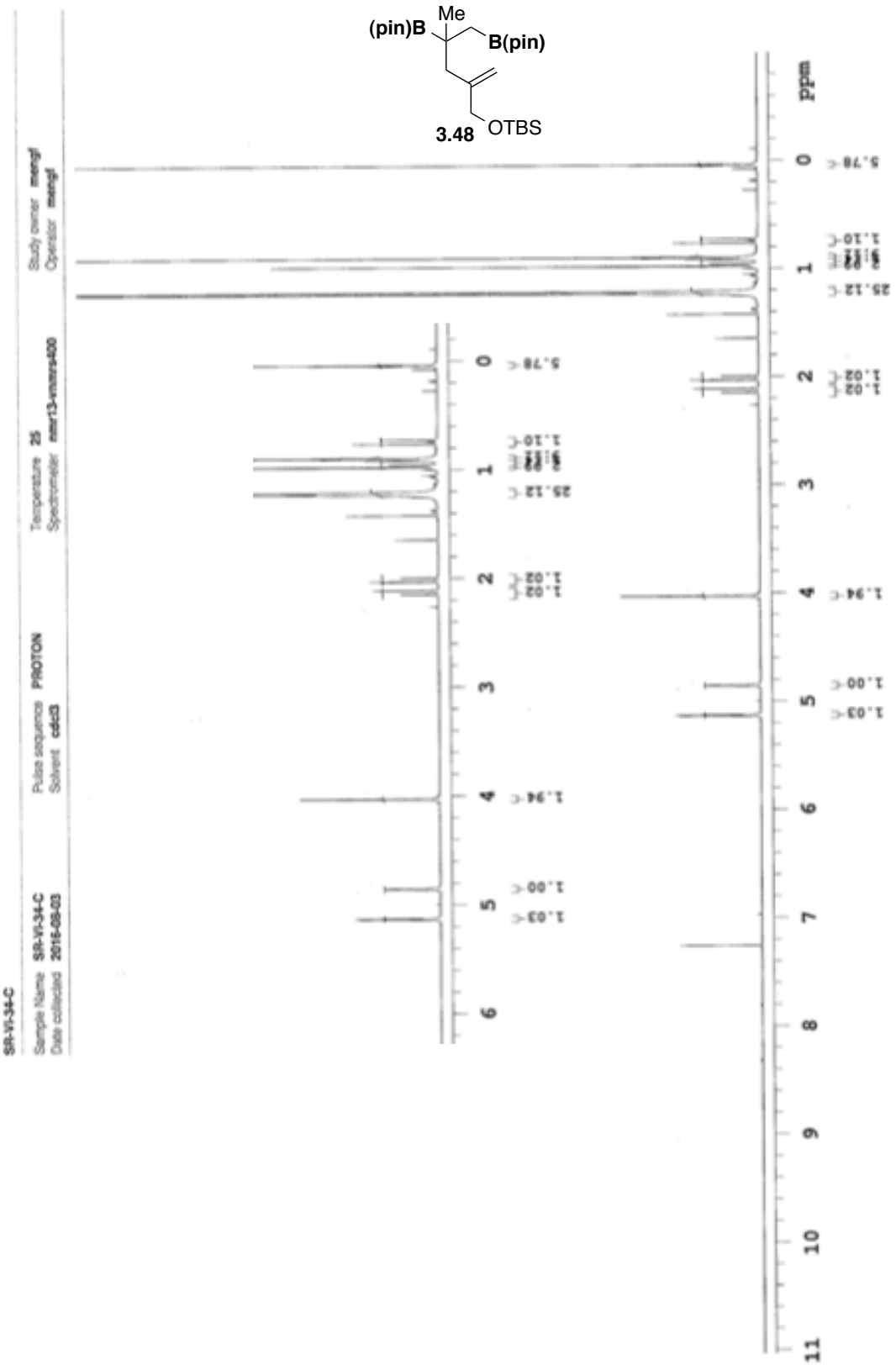
(pin)B
Me
B(pin)
OTBS
3.48
SR-VI-34-C
Sample Name SR-VI-34-C
Date collected 2016-08-03
Pulse sequence PROTON
Solvent cdcl3
Temperature 25
Spectrometer mer13-vnmrs400
Study owner mengf
Operator mengf
ppm

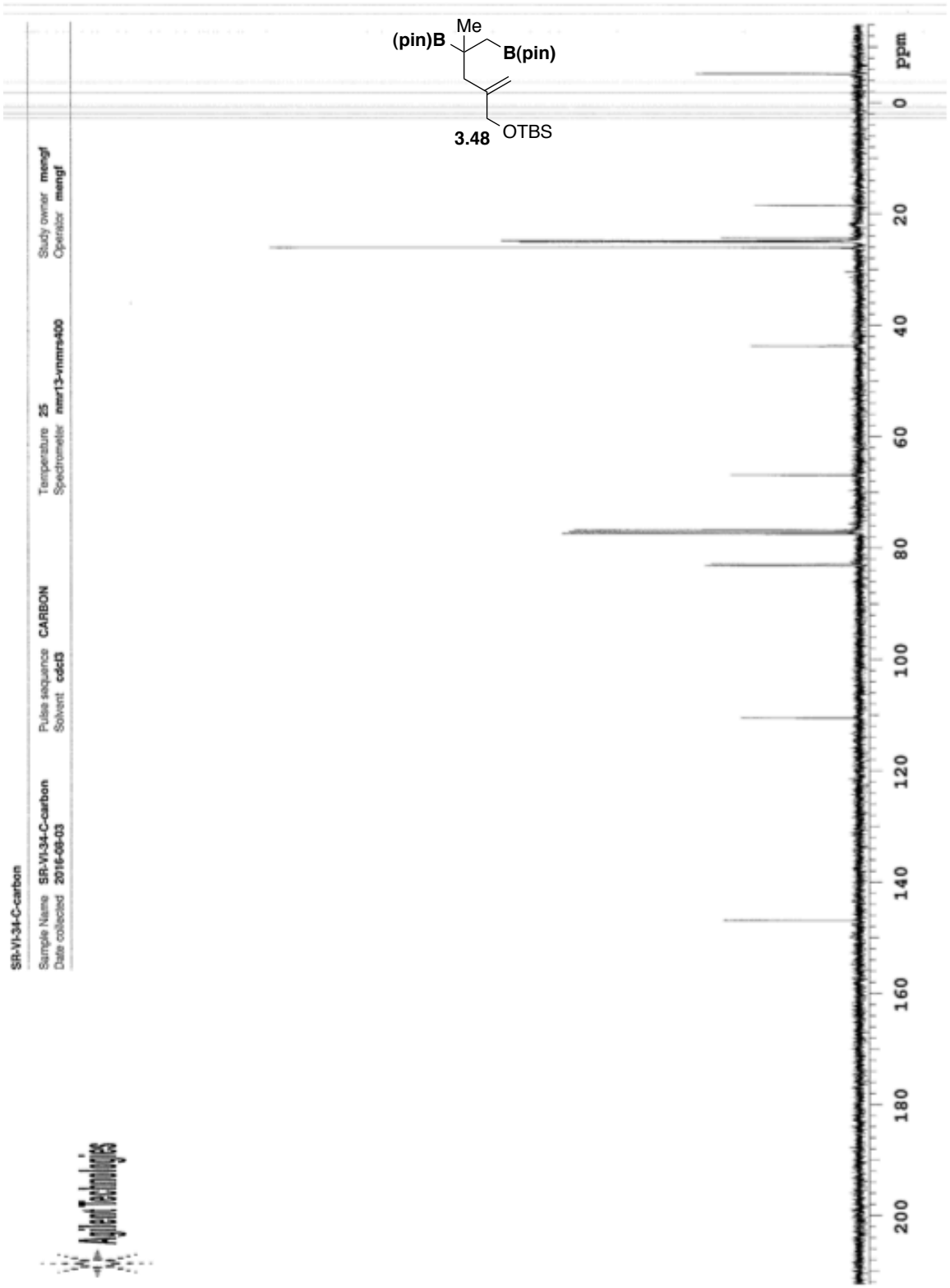
SR-VI-34-C-carbon
Sample Name SR-VI-34-C-carbon
Date collected 2016-08-03
Pulse sequence CARBON
Solvent cdcl3
Temperature 25
Spectrometer nmr13-vnmrs400
Study owner mengf
Operator mengf
Me
(pin)B
B(pin)
3.48
OTBS
ppm
0
20
40
60
80
100
120
140
160
180
200

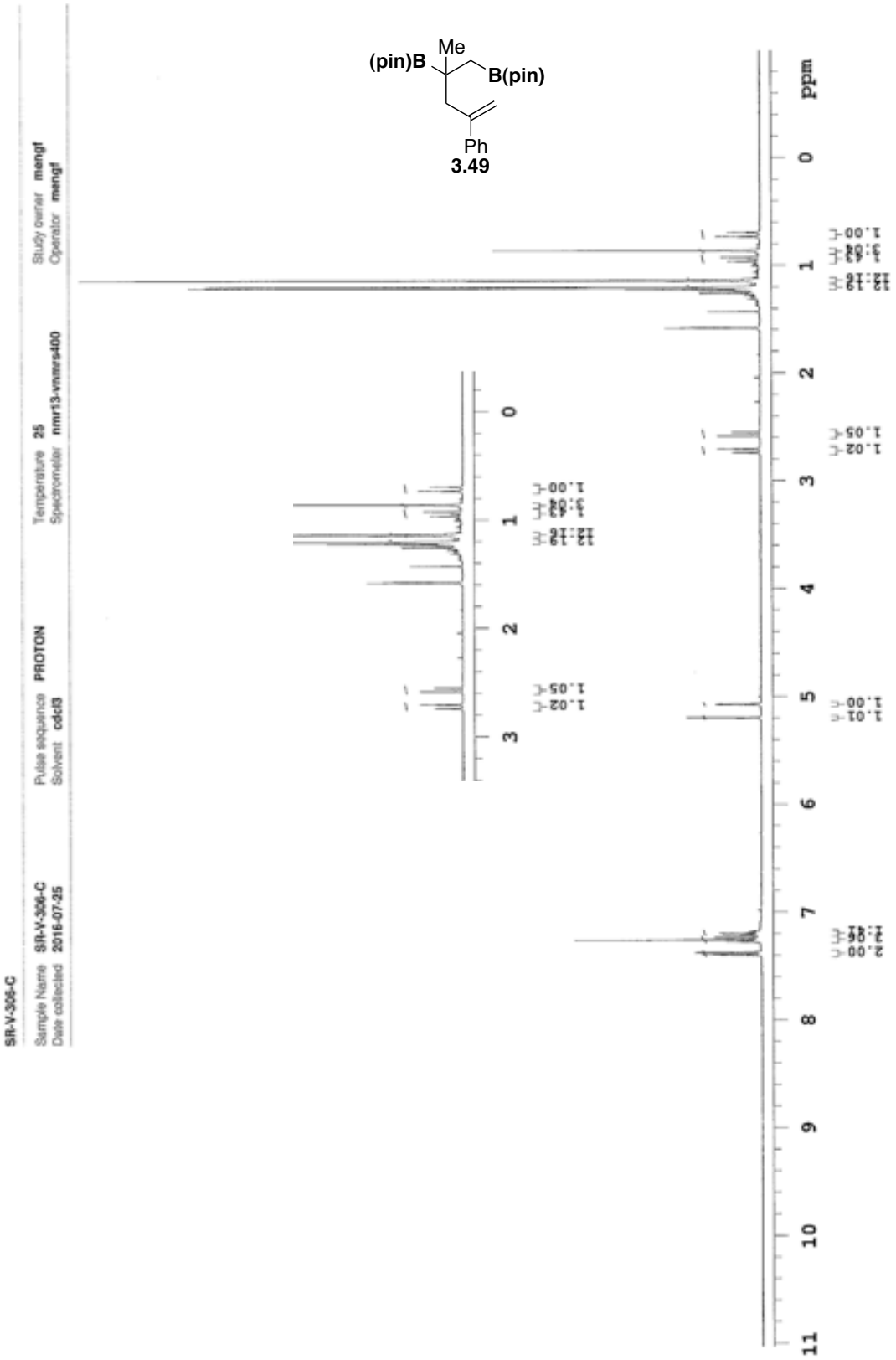
SR-V-306-C
Sample Name SR-V-306-C
Date collected 2016-07-25
Pulse sequence PROTON
Solvent cdcl3
Temperature 25
Spectrometer nmr13-vnmrs400
Study owner mengf
Operator mengf
(pin)B
Me
B(pin)
Ph
3.49
ppm

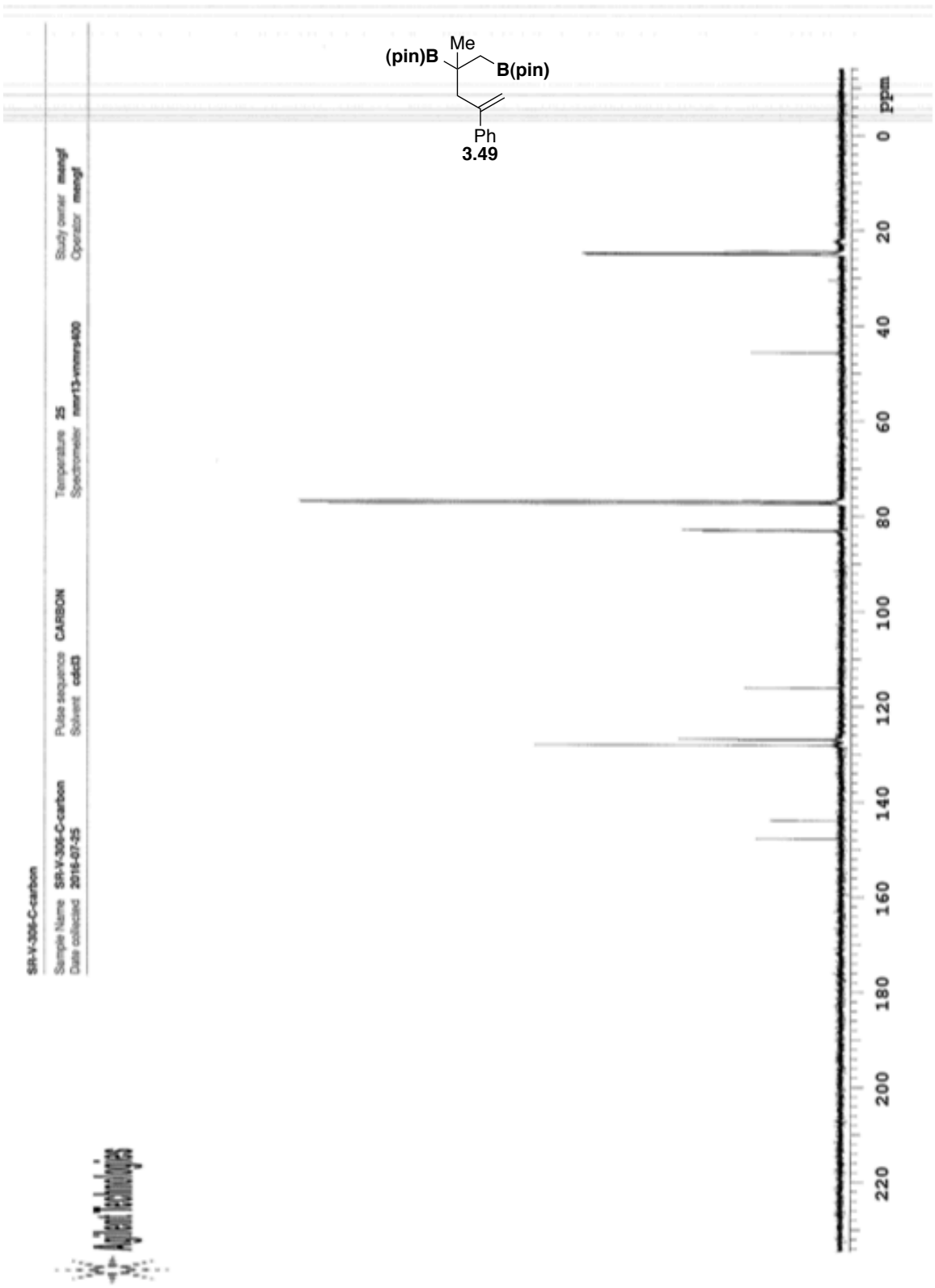
(pin)B
Me
B(pin)
Ph
3.49
SR-V-306-C-carbon
Sample Name SR-V-306-C-carbon
Date collected 2016-07-25
Pulse sequence CARBON
Solvent cdcl3
Temperature 25
Spectrometer nmr13-vnmrs400
Study owner mengf
Operator mengf
ppm
0
20
40
60
80
100
120
140
160
180
200
220

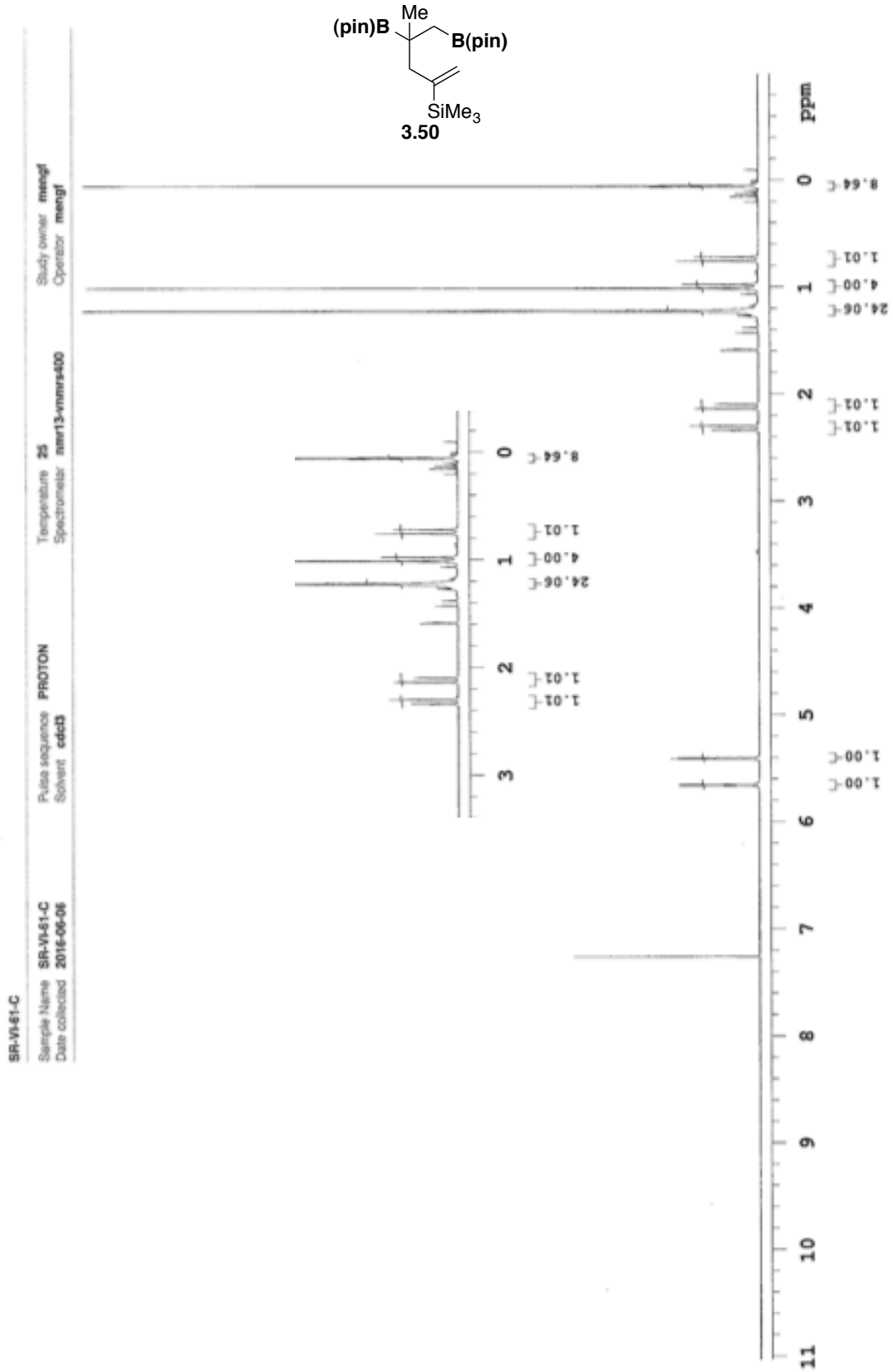
(pin)B
Me
B(pin)
SiMe3
3.50
SR-VI-61-C
Sample Name SR-VI-61-C
Date collected 2016-06-06
Pulse sequence PROTON
Solvent cdcl3
Temperature 25
Spectrometer nmr13-vnmrs400
Study owner mengf
Operator mengf
ppm
8.64
1.01
4.00
24.06
1.01
1.01
1.00
1.00

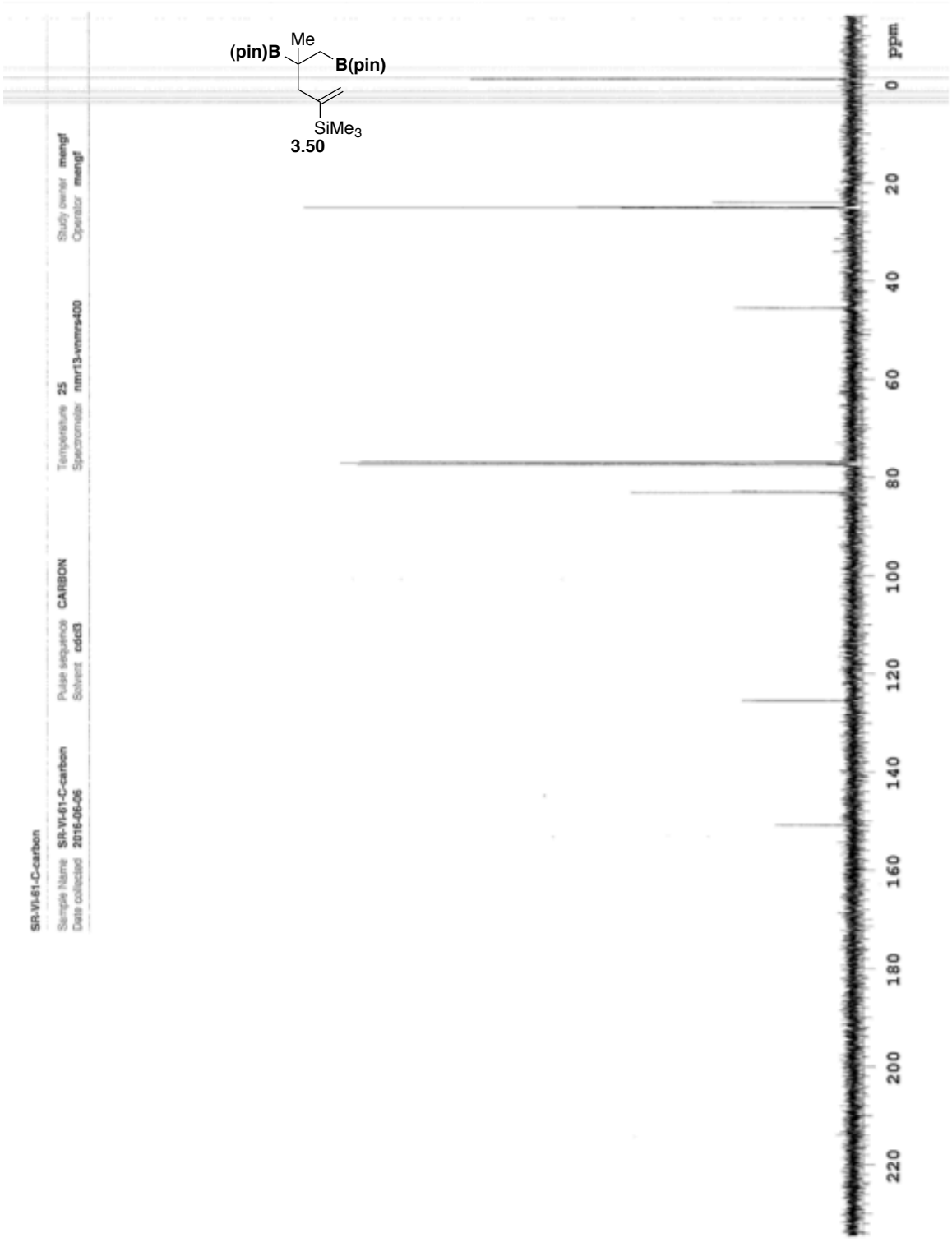
(pin)B
Me
B(pin)
SiMe3
3.50
SR-VI-61-C-carbon
Sample Name SR-VI-61-C-carbon
Date collected 2016-06-06
Pulse sequence CARBON
Solvent cdcl3
Temperature 25
Spectrometer nmr13-vnmrs400
Study owner mengf
Operator mengf
ppm
0
20
40
60
80
100
120
140
160
180
200
220

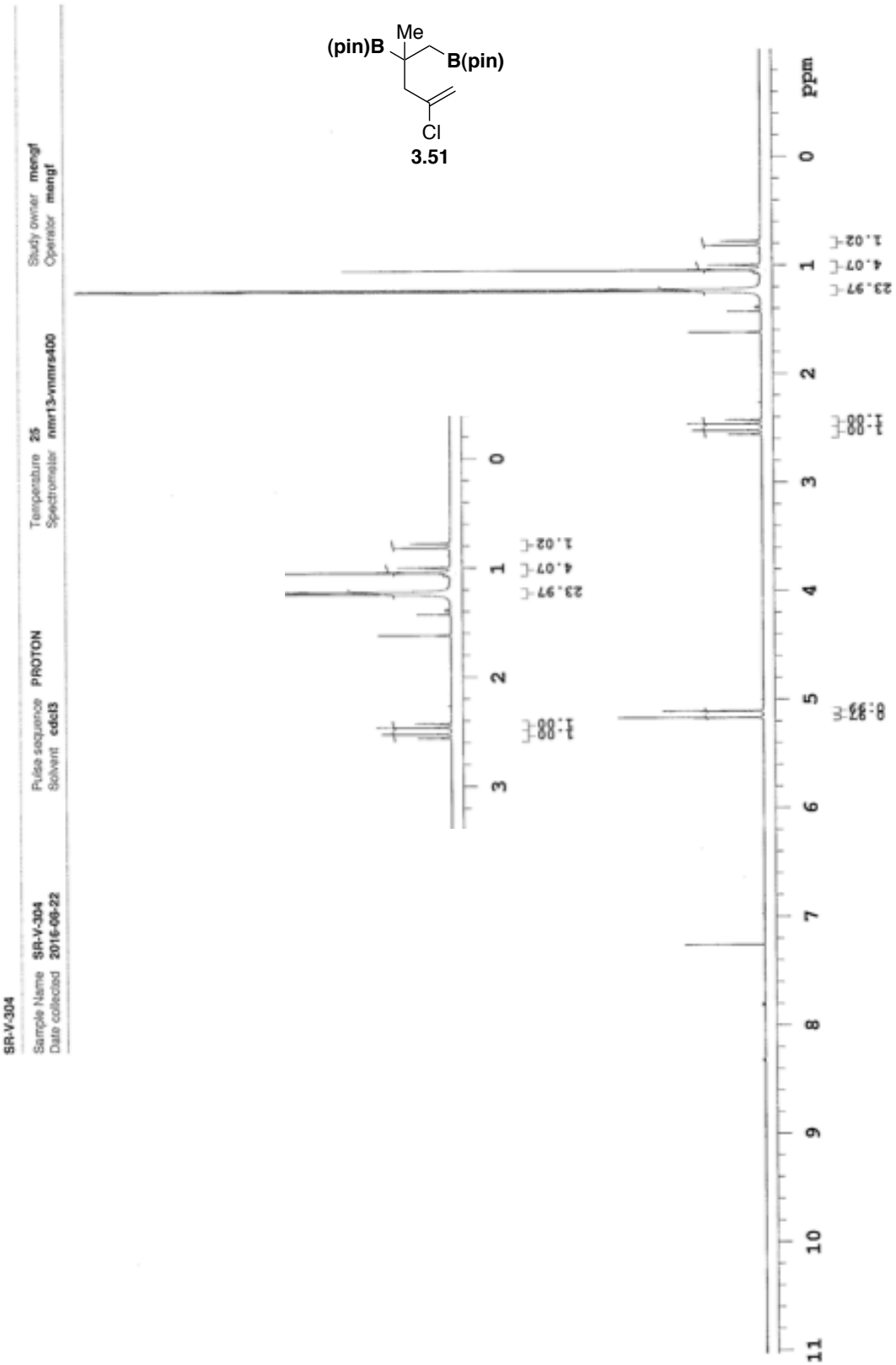
SR-V-304
Sample Name SR-V-304
Date collected 2016-06-22
Pulse sequence PROTON
Solvent cdcl3
Temperature 25
Spectrometer nmr13-vnmrs400
Study owner mengf
Operator mengf
(pin)B
Me
B(pin)
Cl
3.51
ppm
1.02
4.07
23.97
1.00
0.99

SR-V-304-carbon
Sample Name SR-V-304-carbon
Date collected 2016-08-22
Pulse sequence CARBON
Solvent cdcl3
Temperature 25
Spectrometer nmr13-vnmrs400
Study owner mengf
Operator mengf
(pin)B
Me
B(pin)
Cl
3.51
ppm
0
20
40
60
80
100
120
140
160
180
200
220

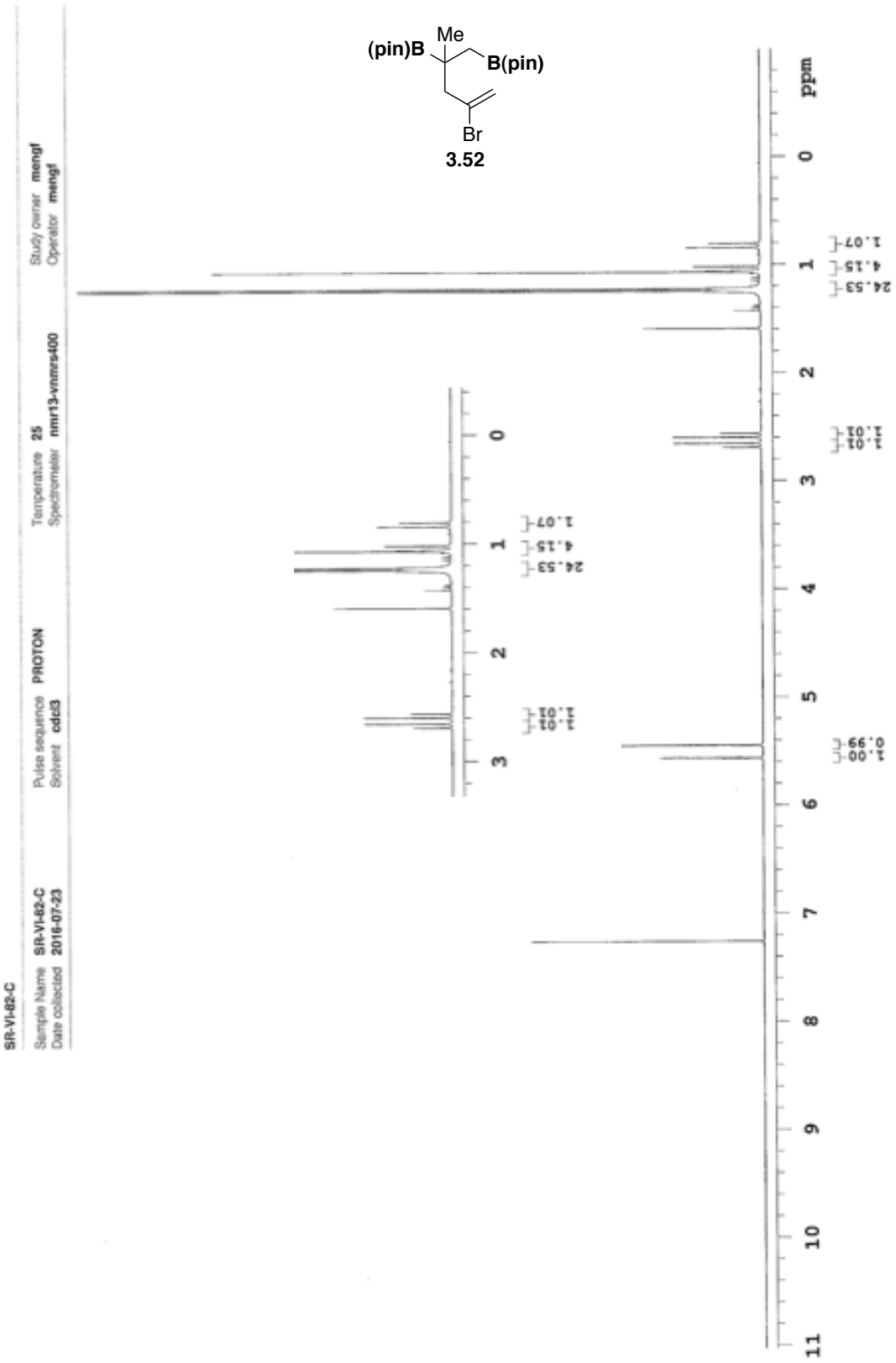
SR-VI-82-C
Sample Name SR-VI-82-C
Date collected 2016-07-23
Pulse sequence PROTON
Solvent cdcl3
Temperature 25
Spectrometer nmr13-vnmrs400
Study owner mengf
Operator mengf
(pin)B
Me
B(pin)
Br
3.52
ppm
1.07
4.15
24.53
11.01
11.01
1.00
0.99

Me
(pin)B
B(pin)
Br
3.52
Sfr-VI-82-C-carbon
Sample Name Sfr-VI-82-C-carbon
Date collected 2016-07-23
Pulse sequence CARBON
Solvent cdcl3
Temperature 25
Spectrometer nmr13-vnmrs400
Study owner mengf
Operator mengf
Agilent Technologies
220
200
180
160
140
120
100
80
60
40
20
0
ppm

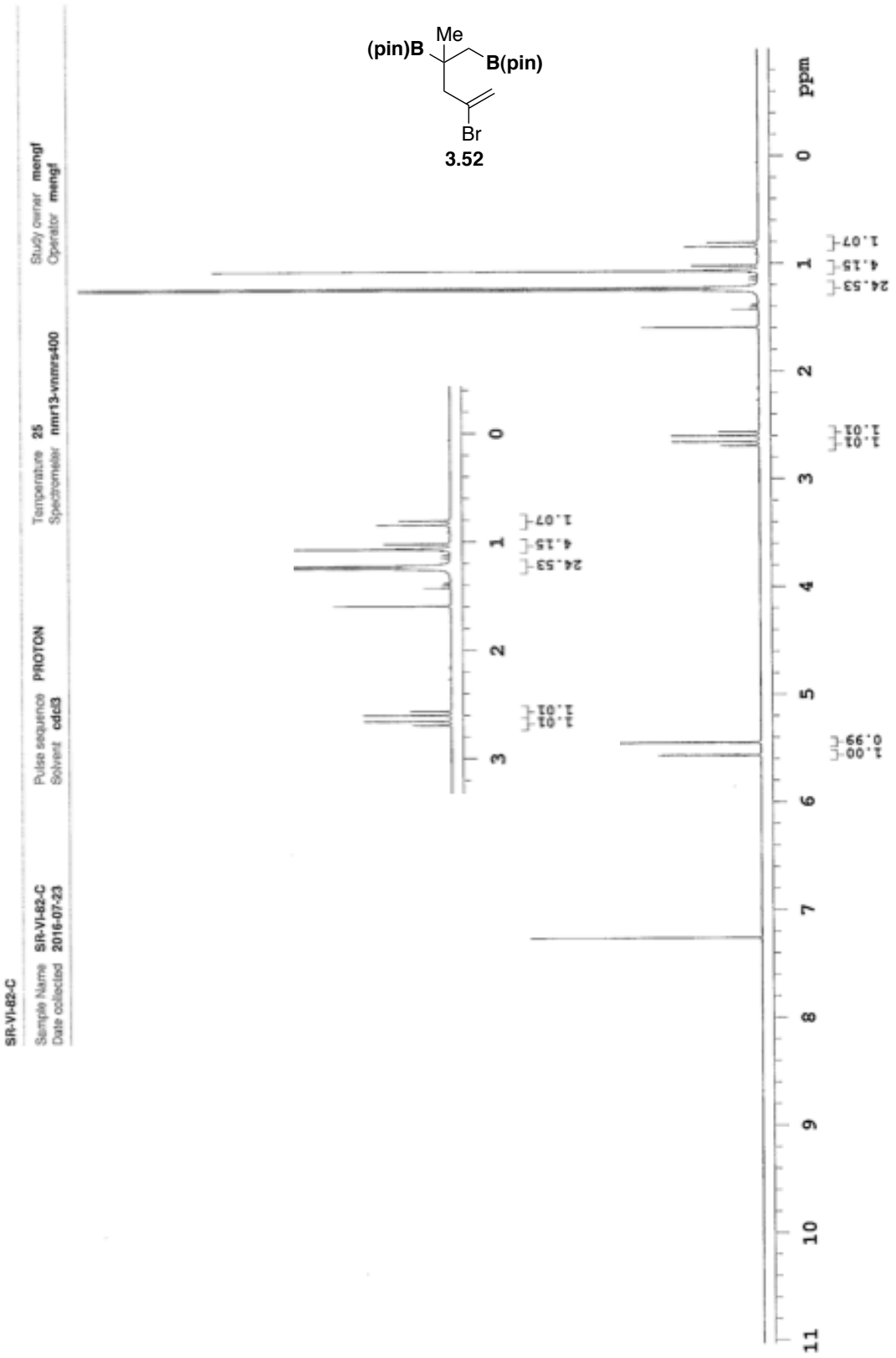
SR-VI-82-C
Sample Name SR-VI-82-C
Date collected 2016-07-23
Pulse sequence PROTON
Solvent cdcl3
Temperature 25
Spectrometer nmr13-vnmrs400
Study owner mengf
Operator mengf
(pin)B
Me
B(pin)
Br
3.52
ppm
1.07
4.15
24.53
11.01
11.01
1.00
0.99

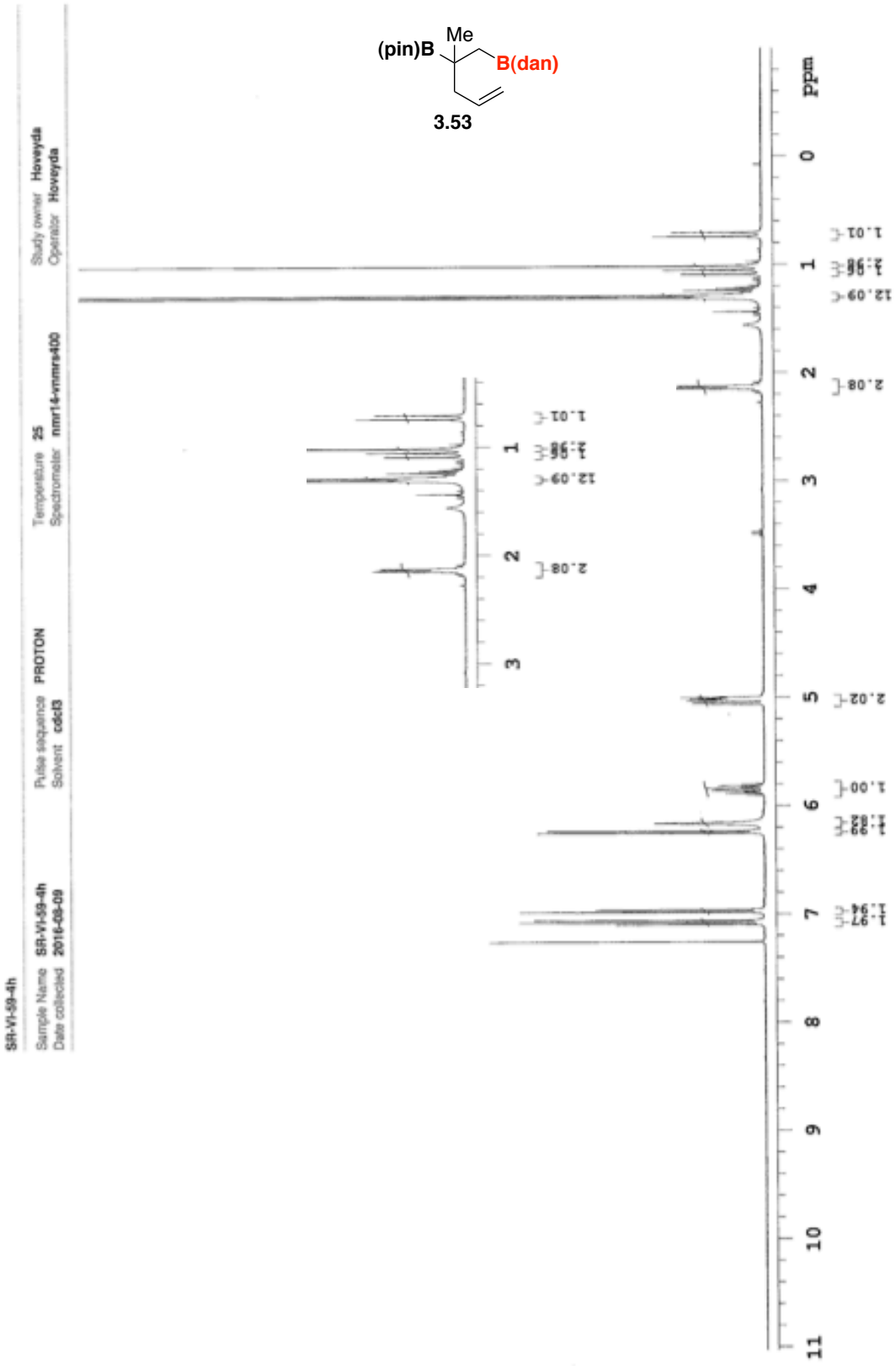
(pin)B
Me
B(dan)
3.53
SR-VI-59-4h
Sample Name SR-VI-59-4h
Date collected 2016-08-09
Pulse sequence PROTON
Solvent cdcl3
Temperature 25
Spectrometer nmr14-vnmrs400
Study owner Hoveyda
Operator Hoveyda
ppm
1.01
3.98
3.95
12.09
2.08
2.02
1.00
1.89
1.82
1.97
1.94

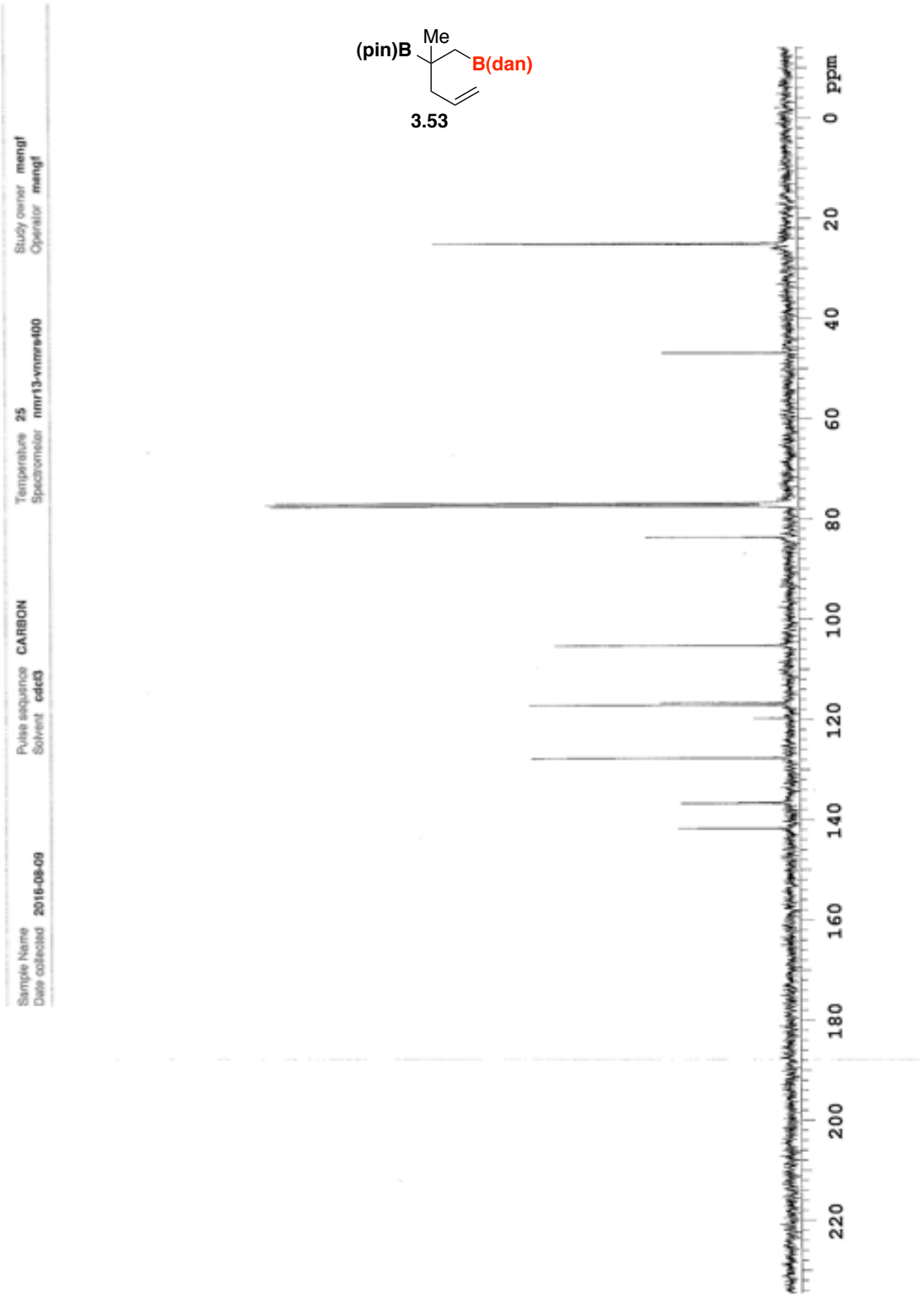
Sample Name
Date collected 2016-08-09
Pulse sequence CARBON
Solvent cdcl3
Temperature 25
Spectrometer nmr13-vnmrs400
Study owner mengf
Operator mengf
(pin)B
Me
B(dan)
3.53
ppm
0
20
40
60
80
100
120
140
160
180
200
220

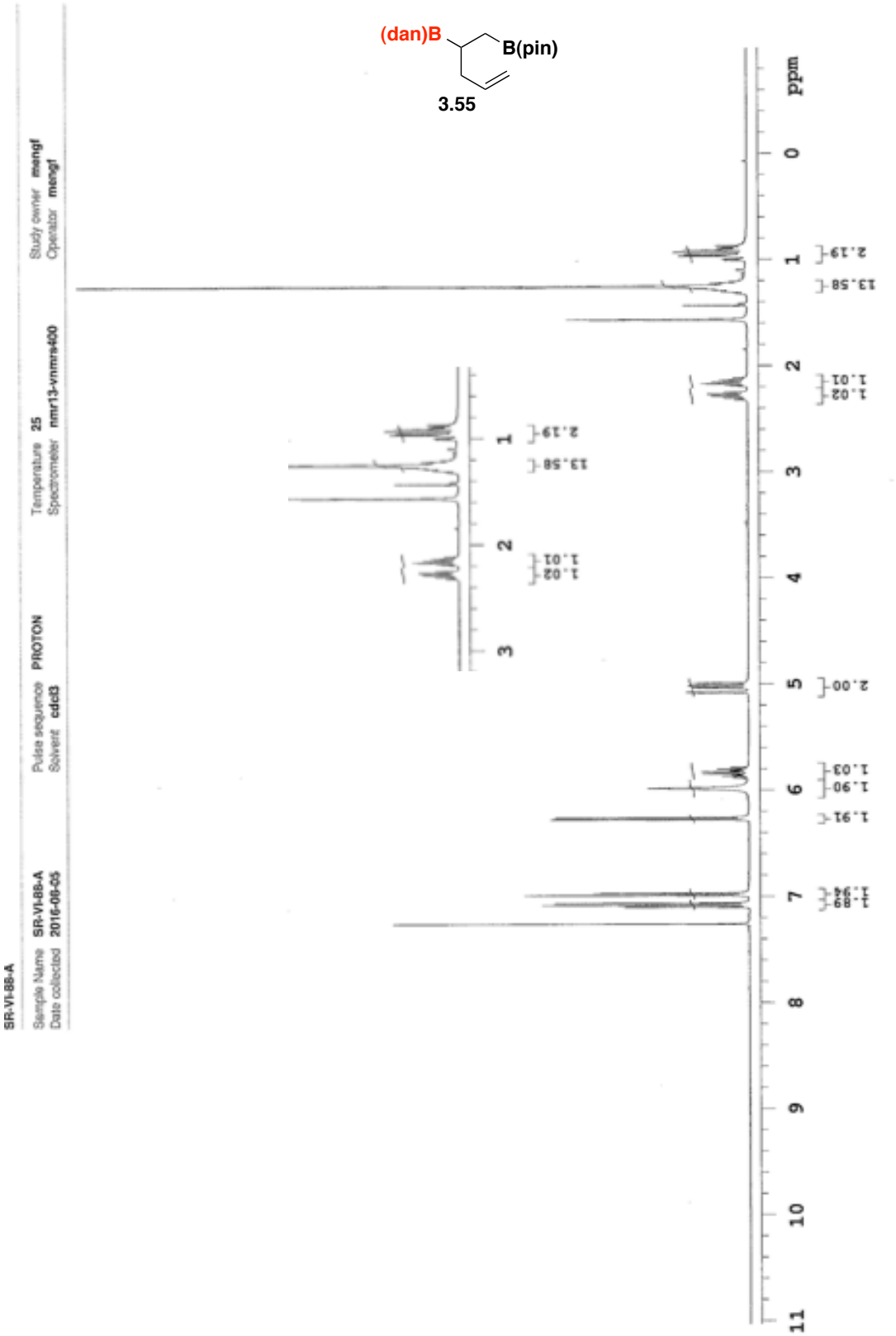
SR-VI-88-A
Sample Name SR-VI-88-A
Date collected 2016-09-05
Pulse sequence PROTON
Solvent cdcl3
Temperature 25
Spectrometer nmr13-vnmrs400
Study owner mengf
Operator mengf
(dan)B
B(pin)
3.55
ppm
2.19
13.58
1.02
1.01
2.00
1.03
1.90
1.91
1.89
1.84

(dan)B
B(pin)
3.55
Sample Name:
SR-V-164-carbon
Data Collected on:
vnmrj3-vnmrs408
Archive directory:
Sample directory:
Fidfile: CARBON
Pulse Sequence: CARBON (s2pul)
Solvent: cdcl3
Data collected on: Aug 12 2015
ppm
0
20
40
60
80
100
120
140
160
180
200
220